TARGETING THE IMMUNE SYSTEM TO TREAT HEPATITIS B VIRUS INFECTION

EDITED BY: Mengji Lu, Zhongji Meng, Jia Liu and Anna D. Kosinska
PUBLISHED IN: Frontiers in Immunology

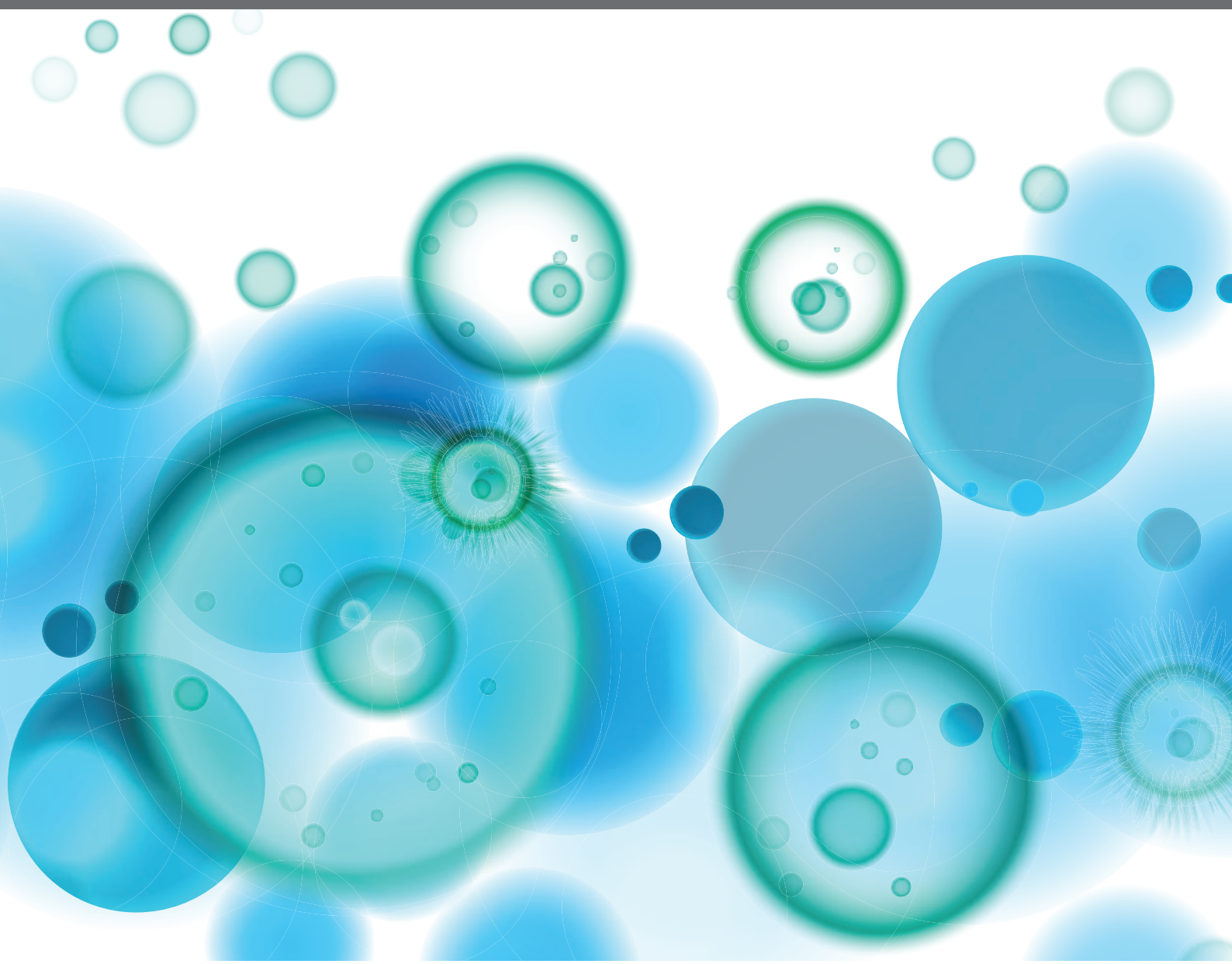

frontiers Research Topics

ISSN 1664-8714
ISBN 978-2-88974-856-3
DOI 10.3389/978-2-88974-856-3

About Frontiers

Frontiers is more than just an open-access publisher of scholarly articles: it is a pioneering approach to the world of academia, radically improving the way scholarly research is managed. The grand vision of Frontiers is a world where all people have an equal opportunity to seek, share and generate knowledge. Frontiers provides immediate and permanent online open access to all its publications, but this alone is not enough to realize our grand goals.

Frontiers Journal Series

The Frontiers Journal Series is a multi-tier and interdisciplinary set of open-access, online journals, promising a paradigm shift from the current review, selection and dissemination processes in academic publishing. All Frontiers journals are driven by researchers for researchers; therefore, they constitute a service to the scholarly community. At the same time, the Frontiers Journal Series operates on a revolutionary invention, the tiered publishing system, initially addressing specific communities of scholars, and gradually climbing up to broader public understanding, thus serving the interests of the lay society, too.

Dedication to Quality

Each Frontiers article is a landmark of the highest quality, thanks to genuinely collaborative interactions between authors and review editors, who include some of the world's best academicians. Research must be certified by peers before entering a stream of knowledge that may eventually reach the public - and shape society; therefore, Frontiers only applies the most rigorous and unbiased reviews.
Frontiers revolutionizes research publishing by freely delivering the most outstanding research, evaluated with no bias from both the academic and social point of view. By applying the most advanced information technologies, Frontiers is catapulting scholarly publishing into a new generation.

What are Frontiers Research Topics?

Frontiers Research Topics are very popular trademarks of the Frontiers Journals Series: they are collections of at least ten articles, all centered on a particular subject. With their unique mix of varied contributions from Original Research to Review Articles, Frontiers Research Topics unify the most influential researchers, the latest key findings and historical advances in a hot research area! Find out more on how to host your own Frontiers Research Topic or contribute to one as an author by contacting the Frontiers Editorial Office: frontiersin.org/about/contact

TARGETING THE IMMUNE SYSTEM TO TREAT HEPATITIS B VIRUS INFECTION

Topic Editors:
Mengji Lu, Essen University Hospital, Germany
Zhongji Meng, Hubei University of Medicine, China
Jia Liu, Huazhong University of Science and Technology, China
Anna D. Kosinska, Helmholtz Center München, Helmholtz Association of German Research Centres (HZ)Germany

Citation: Lu, M., Meng, Z., Liu, J., Kosinska, A. D., eds. (2022). Targeting the Immune System to Treat Hepatitis B Virus Infection. Lausanne: Frontiers Media SA.
doi: 10.3389/978-2-88974-856-3

Table of Contents

frontiers in Immunology

EDITORIAL
published: 15 March 2022
doi: 10.3389/fimmu.2022.868616

Editorial: Targeting the Immune System to Treat Hepatitis B Virus Infection

Zhongji Meng[1], *Jia Liu*[2], *Anna D. Kosinska*[3,5] *and Mengji Lu*[4*]

[1] Institute of Biomedical Research, Hubei Clinical Research Center for Precise Diagnosis and Therapy of Liver Cancer, Taihe Hospital, Hubei University of Medicine, Shiyan, China, [2] Department of Infectious Diseases, Union Hospital, Tongji Medical College, Huazhong University of Science and Technology, Wuhan, China, [3] Institute of Virology, Technische Universität München/Helmholtz Zentrum München, Munich, Germany, [4] Institute of Virology, University Hospital of Essen, University of Duisburg-Essen, Essen, Germany, [5] German Center for Infection Research (DZIF), Munich Partner Site, Munich, Germany

Keywords: hepatitis B Virus, Immune response, immune tolerance, immunotherapy, T cell therapy, innate immunity, therapeutic vaccine

Editorial on the Research Topic

Targeting the Immune System to Treat Hepatitis B Virus Infection

The dysfunctional immune responses play an essential role in persistent hepatitis B virus (HBV) infection as well as in liver inflammation. Modulation of the host immunity to strengthen specific cellular immune responses might help control HBV infection. Various strategies to restore and enhance innate and HBV-specific adaptive immune responses have been tested in preclinical studies and clinical trials and some with significant antiviral effects. However, the molecular mechanisms accounting for HBV persistence are still not fully elucidated despite of great progress in the research field. The current Research Topic issue covers a wide range of subjects in the immunopathogenesis and immune regulation in chronic HBV infection.

Interferons (IFNs) play diverse crucial roles in both innate and adaptive immune responses due to its ability to exert direct antiviral and immune regulatory functions. IFN-α or pegylated IFN-α has been widely used in the treatment of chronic hepatitis B (CHB) with the potential of functional cure, especially in patients with low level of HBsAg and viral loads. Ye and Chen summarize the status and unique advantages of IFN therapy against CHB, including the mechanisms of IFN-α action and factors affecting IFN response, and the options for improvement of IFN-based therapy and the rationale of combinations with other antiviral agents to achieve an HBV cure. Sajid et al. showed in their study that the overexpression of an IFN-α inducible gene IFI6 could inhibit HBV replication and gene expression in hepatoma cells and in the hydrodynamic injection (HDI) mouse model. The study added a new piece to the molecular mechanism of IFN-mediated antiviral functions.

Pathogen recognition receptors (PRRs) are key components in the host immunity through recognizing various conserved molecular patterns of pathogens and activating innate and adaptive immune responses. Immune modulation targeting innate immunity for the treatment of CHB has attract attentions in recent years. Suresh et al. investigated the expression kinetics of receptors from various PRR families (RLRs, NLRs, TLRs, CDSs, and inflammasomes) during acute, self-limited woodchuck hepatitis virus (WHV) infection. The study demonstrated differential intrahepatic

OPEN ACCESS

Edited and reviewed by:
Pei-Hui Wang,
Shandong University, China

****Correspondence:***
Mengji Lu
mengji.lu@uni-due.de

Specialty section:
This article was submitted to Viral Immunology, a section of the journal Frontiers in Immunology

Received: *03 February 2022*
Accepted: *25 February 2022*
Published: *15 March 2022*

Citation:
Meng Z, Liu J, Kosinska AD and Lu M (2022) Editorial: Targeting the Immune System to Treat Hepatitis B Virus Infection. Front. Immunol. 13:868616. doi: 10.3389/fimmu.2022.868616

expression of PRRs and immune cell markers during acute self-limiting infection and the progression to persistent WHV infection. Their results suggested that a weak innate immune response, most likely by type-I IFN production via activated viral DNA and selected RNA sensing receptor pathways, occurred in woodchucks with the progression to chronic infection, while the adaptive immune response was largely absent. In another paper, Suresh et al. demonstrated that, liver-targeted delivery of poly (dA:dT) induced the intrahepatic expression of ZBP1/DAI and AIM2 receptors and their effector cytokines, IFN-β and interleukins 1β and 18. The antiviral effect on WHV replication and production following *in vitro* activation of IFI16, ZBP1/DAI, and AIM2 receptor pathways was improved by targeting more than one cytosolic DNA receptor. The liver-targeted delivery of PRR agonists may improve the therapeutic efficacy against HBV. Ayithan et al. reported the effect of TLR8 agonism on supporting cytokines and follicular helper T (T_{FH}) and B cells in their recent study. Their results demonstrated that triggering TLR8 could induce IL-12 production in monocytes, which in turn leads to differentiation of CD4+ T cells into IL-21 producing T_{FH} in peripheral blood samples from CHB patients. Accordingly, co-culture of these differentiated T_{FH} with autologous B cells resulted in B cell differentiation into plasma cells and promoted IgG production. Finally, improved HBsAg-specific T_{FH} and B cell responses were observed in a fraction of CHB patients treated with a selective TLR8 agonist. The study suggested that TLR8 signaling has potential to repair a critical defect in T-B interaction that is necessary for robust B cell response.

Chronic HBV infection is characterized by quantitatively and qualitatively weak HBV-specific CD8+ T cell responses. To define the mechanisms of HBV-Specific CD8+ T cell dysfunction, Baudi et al. summarized data about the HBV-specific CD8+ T-cell tolerance in the liver, including immunoregulatory mediators in liver tolerance, negative signaling mechanisms, metabolic dysregulation in T cells, and intrahepatic antigen recognition. The elucidation of the key pathways and processes underline HBV-specific CD8+ T cell dysfunction will facilitate the development of effective HBV immunotherapies. Wang et al. reported in their recent work that, CXCR3+CXCR6+ γδT cells produced high levels of IFN-γ during acute HBV infection. An adoptive transfer of CXCR3 +CXCR6+ γδT cells into acute HBV infected TCRδ-/- mice led to reduced HBsAg and HBeAg expression. Their work suggested that liver resident CXCR3+CXCR6+ γδT cells play a protective role during acute HBV infection. The role of CXCR3+CXCR6+ γδT cells in immunotherapy for chronic HBV infection needs further study.

Identification of immunogenic targets against HBV-encoded proteins will provide crucial advances in developing potential antibody therapies. Gu et al. performed a screening on B-cell linear epitopes with sera from patients in different phases of the natural history of chronic HBV infection. Their study found that dominant linear B-cell epitopes are expanded in CHB. The proportion of dysfunctional atypical memory B cells was decreased in patients who achieved HBsAg loss and associated with successful treatment withdrawal. In this study, 7 dominant epitopes were recognized by antibodies from patients with HBsAg loss. The baseline of antibodies to a specific HBsAg epitope was found to be associated with a favorable treatment response to telbivudine therapy. Future studies are needed to confirm the diagnostic values of antibodies to linear epitopes of HBV proteins.

A functional cure for chronic HBV infection could be achieved by boosting HBV-specific immunity. HBV-specific chimeric antigen receptor T (CAR-T)/T-cell receptor T (TCR-T) cells are promising therapeutic approaches for treatment of CHB, but with potential risks of inducing cytokine release syndrome or hepatotoxicity. Klopp et al. generated an inducible caspase 9 (iC9) as a safety switch to control HBV-specific S-CART or TCR-T. *In vivo*, induction of iC9 in S-CAR T cells resulted in a strong and fast depletion of transferred T cells, leading to the loss of antiviral efficacy and preventing liver toxicity and cytokine release at the same time. Ferrando-Martinez et al. found that PD-L1 blockade could enhance the HBV-specific CD8 T cell response only in patients with lower frequencies of functionally exhausted HBV-specific CD8 T cells as indicated by a phenotype of LAG3+ TIM3+PD-1+. Higher levels of functionally exhausted HBV-specific CD8 T cells in CHB patients are associated with a lack of response to the anti-PD-L1 antibodies. Thus, blocking the PD-1:PD-L1 axis as a monotherapy may only have limited clinical effectiveness. Combination strategies with antibodies to other anti-inhibitory receptors like LAG-3, will likely be required to elicit a functional cure for patients with high levels of functionally exhausted HBV-specific CD8 T cells.

The NF-κB signaling pathway plays a key role in the development and function of host immune system and in inflammation and viral infection. Lu et al. summarized the knowledge about the interplay between non-canonical NF-κB signaling and HBV infection. They came to a conclusion that the non-canonical NF-κB signaling pathway plays also an important role in triggering inflammation in HBV-related diseases, while the mechanism of the interplay between HBV and non-canonical NF-κB signaling is largely unknown and needs further in-depth investigation.

The cellular mechanisms underlying the non-responsiveness of HBV vaccination are still poorly understood. Körber et al. reported significantly higher frequencies of $CD24^{high}CD38^{high}$ regulatory B cells (Breg) in parallel with significantly lower IL-10 expression levels of $CD24^{+}CD27^{+}$ and $CD24^{high}CD38^{high}$ Breg in 2^{nd} HBvac non-responders compared to 2^{nd} HBvac responders. Anti-HBs seroconversion accompanied by a decrease of Breg numbers after booster immunization with a third-generation HBV vaccine, which indicates a positive effect of third-generation HBV vaccines on Breg-mediated immunomodulation in HBV vaccine non-responders.

The level of serum HBcAb has been demonstrated as a new marker of the responsiveness to antiviral treatment in CHB patients. Lou et al. showed that lower pre-transplantation level of HBcAb in patients undergoing liver transplantation is associated with HBV re-infection, suggesting that the baseline concentration of HBcAb may be a promising predictor for HBV recurrence in liver transplantation.

HBV mouse models have been widely used in studies on infection, immune responses, pathogenesis, and antiviral therapies. Du et al. summarized the currently available mouse models for HBV research. The HDI model is extensively used in various studies investigating immune responses to HBV, viral clearance, and evaluating novel antiviral agents. The AAV transduction-mediated replicon delivery model can be used in evaluating antiviral compounds, while controversial in the role in investigating HBV immunology. HBV transgenic mouse models are highly useful in elucidating the molecular virus-host interactions and HBV-related immunology and pathogenesis. Compared to other HBV mouse models, human liver chimeric mouse models possess obvious advantages, however, is limited due to the high cost and technical difficulties.

Taken together, the papers collected in this Research Topic covered a wide range of subjects in HBV research including the functional status of innate immunity, especially the PRRs, and HBV-specific T-B cells, IFN-based therapies, HBV-specific CAR-T/TCR-T, and target activation of PRRs, as well as the animal models for HBV infection. This collection reflects the current activities in a very important research field about the immunopathogenesis and immunotherapy of chronic HBV infection.

AUTHOR CONTRIBUTIONS

MZ was a guest associate editor of the Research Topic and wrote the paper text. LJ was a guest associate editor of the Research Topic and edited the text, and acted as a coauthor or one paper in the Research Topic. AK is a guest associate editor of the Research Topic and edited the text, and acted as a coauthor of one paper in the Research Topic. LM was a guest associate editor of the Research Topic and edited the text, and acted as corresponding author for one paper in the Research Topic. All authors contributed to the article and approved the submitted version.

FUNDING

MZ is supported by the National Science and Technology Major Project (2018ZX10723203, 2018ZX10302206, and 2017ZX10202202), the Foundation for Innovative Research Groups of Hubei Provincial Natural Science Foundation (2018CFA031), and Hubei Province's Outstanding Medical Academic Leader Program. LJ is funded by the National Natural Science Foundation of China (82172256, 92169105, 81861138044 and 91742114). ADK is funded by the German Center for Infection research (DZIF) *via* project TTU05.803 "HBV Cure".

ACKNOWLEDGMENTS

We thank authors of the papers published in this research topic for their valuable contributions and the referees for their rigorous review. We also thank the editorial board of the Viral Immunology section, especially Mirko Santello (SM), and the Frontiers specialists, for their support.

Conflict of Interest: The authors declare that the research was conducted in the absence of any commercial or financial relationships that could be construed as a potential conflict of interest.

frontiers in Immunology

ORIGINAL RESEARCH
published: 01 April 2021
doi: 10.3389/fimmu.2021.634937

The Functional and Antiviral Activity of Interferon Alpha-Inducible IFI6 Against Hepatitis B Virus Replication and Gene Expression

Muhammad Sajid[1†], *Hafiz Ullah*[1†], *Kun Yan*[1†], *Miao He*[1,2], *Jiangpeng Feng*[1], *Muhammad Adnan Shereen*[1], *Ruidong Hao*[1], *Qiaohong Li*[3], *Deyin Guo*[2], *Yu Chen*[1] *and Li Zhou*[1,3*]

[1] State Key Laboratory of Virology, Modern Virology Research Center, College of Life Sciences, Wuhan University, Wuhan, China, [2] Ministry of Education Key Laboratory of Tropical Disease Control, The Infection and Immunity Center (TIIC), School of Medicine, Sun Yat-sen University, Shenzhen, China, [3] Animal Biosafety Level III Laboratory at Center for Animal Experiment, Wuhan University, Wuhan, China

Hepatitis B virus is an enveloped DNA virus, that infects more than three hundred and sixty million people worldwide and leads to severe chronic liver diseases. Interferon-alpha inducible protein 6 (IFI6) is an IFN-stimulated gene (ISG) whose expression is highly regulated by the stimulation of type I IFN-alpha that restricts various kinds of virus infections by targeting different stages of the viral life cycle. This study aims to investigate the antiviral activity of IFI6 against HBV replication and gene expression. The IFI6 was highly induced by the stimulation of IFN-α in hepatoma cells. The overexpression of IFI6 inhibited while knockdown of IFI6 elevated replication and gene expression of HBV in HepG2 cells. Further study determined that IFI6 inhibited HBV replication by reducing EnhII/Cp of the HBV without affecting liver enriched transcription factors that have significant importance in regulating HBV enhancer activity. Furthermore, deletion mutation of EnhII/Cp and CHIP analysis revealed 100 bps (1715-1815 nt) putative sites involved in IFI6 mediated inhibition of HBV. Detailed analysis with EMSA demonstrated that 1715-1770 nt of EnhII/Cp was specifically involved in binding with IFI6 and restricted EnhII/Cp promoter activity. Moreover, IFI6 was localized mainly inside the nucleus to involve in the anti-HBV activity of IFI6. *In vivo* analysis based on the hydrodynamic injection of IFI6 expression plasmid along with HBV revealed significant inhibition of HBV DNA replication and gene expression. Overall, our results suggested a novel mechanism of IFI6 mediated HBV regulation that could develop potential therapeutics for efficient HBV infection treatment.

Keywords: HBV, interferon-stimulated genes, antiviral activity, CHIP, EMSA, IFI6

OPEN ACCESS

Edited by:
Zhongji Meng,
Hubei University of Medicine, China

Reviewed by:
Qiang Deng,
Fudan University, China
Barbara Testoni,
Institut National de la Santé et de la Recherche Médicale (INSERM), France

***Correspondence:**
Li Zhou
zhouli_jerry@whu.edu.cn

[†]These authors have contributed equally to this work

Specialty section:
This article was submitted to Viral Immunology, a section of the journal Frontiers in Immunology

Received: *29 November 2020*
Accepted: *15 March 2021*
Published: *01 April 2021*

Citation:
Sajid M, Ullah H, Yan K, He M, Feng J, Shereen MA, Hao R, Li Q, Guo D, Chen Y and Zhou L (2021) The Functional and Antiviral Activity of Interferon Alpha-Inducible IFI6 Against Hepatitis B Virus Replication and Gene Expression. Front. Immunol. 12:634937. doi: 10.3389/fimmu.2021.634937

INTRODUCTION

The infection of the Hepatitis B virus (HBV) has a significant community health concern for the past few decades (1–3). About three hundred and sixty million people are chronically infected with severe liver diseases due to HBV (4, 5). Current treatment for chronic HBV infection is restricted to pegylated type 1 IFN and nucleotides/nucleosides analogs (6). However, current treatment for chronic HBV could only suppress HBV replication but unable to cure the disease due to the presence of minichromosomal cccDNA (7).

HBV is a noncytopathic and hepatocytotropic enveloped DNA virus that belongs to *Hepadnaviridae* family (8). The genome of HBV contains a greatly condensed genetic structure comprised of 3.2-kb partially closed relaxed circular double-stranded DNA (rcDNA). Upon hepatocytic infection through high-affinity binding with sodium taurocholate cotransported polypeptide (NTCP) receptor, rcDNA is converted into long-lived minichromosomal cccDNA by different host cellular enzymes in the nucleus and acts as a template for the transcription of HBV RNAs that serves as the primary transcript for the regulation and synthesis of all viral transcripts (Pregenomic, Precore, preS1, preS2, and X RNA transcript) (9, 10). Seven different HBV proteins are translated from these transcripts: HBeAg (hepatitis B e antigen), HBc (core protein), HBV polymerase (pol), the small (S), medium (M), large (L) envelope glycoprotein, and HBx protein (11, 12). The transcriptional activity of HBV RNAs is regulated by four HBV specific promoters (core, preS1, preS2, and X), two enhancer elements (EnhI and EnhII), and a negative regulatory cis-acting element (13). The cytokines and host nuclear factors are key elements to regulate the transcriptional activities of HBV promoters including STAT1 (signal transducer and activator of transcription), RXR (retinoid X receptor), and HNF-4 (hepatocyte nuclear factor 4) (14).

The type I IFN (IFN-α, β, and ε) is considered as the potent antiviral cytokine in vertebrates and has been widely used in the treatment of chronic HBV. Upon viral infection, the type I IFN induction carried out through binding of its type I IFN receptor (IFNAR1 and IFNRA2), subsequently activation of the cascade of JAK/STAT signaling pathway, leading to the induction of about 300 IFN-stimulated genes in the host nucleus that acts as an antiviral function, inhibits different stages of viral replication, transcription and post-transcriptional events (15–17). Since IFN-α therapy has some side effects or limitations ranging from mild clinical symptoms to significant mortality and morbidity (18), it is urgent to develop IFN- α related therapy that has the anti-HBV effect without significant limitations and clinical side effects.

IFN α inducible protein 6 (IFI6) is an IFN-stimulated gene, belongs to the FAM14 family of the gene that maps to chromosome 1P35 (19–21). *In Silico* analysis has identified four FAM14 genes in humans (IFI6, IFI27, ISG12*b*, and ISG12*c*) and three in mice (ISG12*a*, ISG12*b1*, and ISG12*b2*) (20). However, the function of these genes has not been fully characterized, and their physiological role is still elusive. Based on a sequence homology induced by type I IFN, the FAM14 family contains two prominent genes, IFI6 and IFI27, both are considered to be a mitochondrial proteins with a different function in apoptosis but the precise localization is still not clear. Both IFI6 and IFI27 are small hydrophobic protein shared 36% overall amino acid sequence. The IFI6 stabilizes the mitochondrial function that leads to discontinuation of apoptosis whereas the expression of IFI27 destabilizes the mitochondrial function and leads to apoptosis (22). The IFI6 is a 13 kDa protein of 130 amino acids that plays a critical role in immunomodulation and an antiapoptotic function by activation of JAK/STAT signaling pathway that subsequently blocks the mitochondrial release of cytochrome c and discontinues the apoptosis (23).IFI6 is a pro-survival protein that antagonizes the TRAIL (tumor necrosis factor related apoptosis inducing ligand) induced apoptosis in human myeloma cell through inhibiting the intrinsic apoptotic pathway (24). These studies demonstrated that the FAM14 family has diverse biological function, depending on the cell/tissue type they reside. The type I IFN is highly induced the expression of IFI6. A study based on the interaction of hepatoma cells with HBV suggested that the downregulation of HBV in hepatoma cells with siRNA changed the expression profile of some of the IFN-stimulated genes (IFI6, MDA5, IFI27, STAT1, IFIT1, ISGF3G, IFITM1, OAS1, and G1P2). These genes might be responsible for the interaction of HBV with host cells (25). A previous study on IFI6 indicates the association of IFI6 polymorphism with the chronicity of the chronic liver disease. These polymorphisms in IFI6 lead to modulate the IFI6 expression level and delay the release of cytochrome c that eventually block the apoptotic signal through HBV specific CD8+ T cells. After escaping from antigen-induced apoptosis, CD8+ T cells proliferate and differentiate into activated CD8+ T cells to clear HBV infection (26). However, only a few studies have been conducted to demonstrate the antiviral activity of IFI6. Emerging evidence on IFI6 strongly proposed its association with the immune system but the functional and antiviral role of IFI6 is not fully elucidated in HBV replication and gene expression.

In this study, we hypothesized the functional and antiviral role of IFI6 against HBV replication and gene expression. The overexpression and knockdown inhibit and enhances HBV replication and transcription, respectively. The *in vitro* study of IFI6 indicates a putative binding site of HBV that could restrict HBV EnhII/Cp promoter activity while *in vivo* study demonstrated a substantial reduction of HBV replication and gene expression.

MATERIALS AND METHODS

Ethics Statement

All mice were kept in a pathogen-free animal facility at Wuhan University. All experiments were performed per the instructions of the of Health National Institutes Guide for the Care and Use of Laboratory Animals. The protocol was approved by the Institutional Animal Care and Use Committee of Wuhan University (Project License WDSKY0201302 and WDSKY0201802).

Plasmids Construction

The pHBV1.3 plasmid (HBV, genotype D, GenBank accession number V01460.1) and the reporter plasmids were constructed as previously described (27). Briefly, the EnhI/Xp-Luc (950-1375 nt), EnhII/Cp-Luc (1415-1815 nt), SP1-Luc (2707-2849 nt), and SP2-Luc (2937-3182 nt) DNA fragments and their truncation mutants were amplified by PCR and cloned into pGL3-Basic (Promega, Madison, WI) at the HindIII and SacI restriction sites. The HA-tagged IFI6 (N-terminally tagged) fragment was amplified by PCR and introduced in the pCAGGS vector (Invitrogen, Carlsbad, CA). The pLKO.1 vector was used for insertion of Control short hairpin RNA (shRNAs) targeting GFP (enhanced green fluorescence protein) and Two IFI6 short hairpin RNAs. The shRNAs target sequence is shRNA (cont.) 5'- GCAGAAGAACGGCATCAAG-3', shIFI6-1 5'- CCTCCCA AGTAGGATTA-3', and shIFI6-2 5'- TCCAGAACTTT GTCTAT-3'.

Cell Culture and Transfection

HepG2, Huh7, and HEK293T cells were maintained in DMEM (Dulbecco's modified Eagle's medium) supplemented with 10% fetal bovine serum, 100 μg/ml streptomycin, and 100 U/ml penicillin. Transfection of HepG2 cells was carried out with Lipofectamine 3000 (Invitrogen) according to the manufacturer's instructions.

Lentiviral Production

The production of lentivirus for short hairpin RNAs was performed as described previously (28). Briefly, HEK293T cells (in a 10-cm cell culture dish) were cotransfected with 2 μg shRNA (cont.) shIFI6-1 and shIFI6-2 (cloned into pLKO.1 shRNAs vector), 1.5 μg pMD2.G, and 1.5 μg psPAX with neofect transfection reagents (Neofect Biotech, Beijing, China) according to manufacturer instructions. Supernatant from cells was collected at 48 hours and 72 hours post-transfection, and the lentivirus was centrifuged, filtered, and subsequently preserved at -80°C. Lentiviruses were used to infect HepG2 cells twice to increase transduction efficiency. The 2 μg/ml puromycin (NIH3T3) was added to cultivate knockdown cell lines.

Enzyme-Linked Immunosorbent Assay (ELISA)

Secreted proteins (HBsAg and HBeAg) from cell culture supernatant and mice serum were detected by ELISA kit (Kehua Bio-Engineering, Shanghai, China) according to manufacturer instructions at indicated time points. The activity of β-galactosidase was used to normalize the values in cell lysates and measured by a Beta-Glo kit (Promega).

Western Blot

Cells were washed with cold PBS, lysed with lysis buffer containing 25 mM tris-HCL (pH 7.5), 150 mM NaCl, 1 mM EDTA, 1% Triton X-100, mixed with 5% SDS loading buffer, and heated for 5 minutes. The samples were electrophoresed with SDS PAGE and subsequently transferred to nitrocellulose membrane (GE healthcare). The membrane was blocked with 5% skim milk having Tween 20 (0.1%) and probed overnight with antibodies IFI6 (Abclonal, Cat No, A6157), HA-tag (abcam, Cat No. ab9110), beta-actin (abClonal, Cat No, AC028). The signals were detected with an enhanced chemiluminescence (ECL) substrate (Millipore, Billerica, MA).

Cell Cytotoxicity Assay

HepG2 cells were seeded in 96 well cell culture plates for 24 hours and co-transfected with the indicated amount of plasmids. The shRNA mediated knockdown cells stably expressing shGFP, shIFI6-1 and shIFI6-2 were seeded in 96 well cell culture plate for 24 hours and transfected with pHBV1.3 (80 ng) and pSV-β-gal (20 ng). Cell toxicity was measured after 48 hours of transfection with the CCK8 kit (Dojindo) according to the manufacturer's instructions.

Nuclear and Cytoplasmic Protein Extraction

A nuclear and cytoplasmic protein extraction kit (Applygen) was used for the extraction of nuclear and cytoplasmic IFI6 protein according to the manufacturer's instructions.

RNA Extraction From Cells and Liver Tissue of Mice

Total RNA from cells and tissue from mice liver was extracted by Trizol reagent according to the manufacturer's instructions. Reverse transcription (RT-PCR) of total RNA into cDNA was performed with the PrimeScript RT reagent kit (Takara). The qRT-PCR was performed to amplify cDNA using SYBR Green Fast qPCR Master Mix (Cat No. 11201-11203: Yeasen, China). To standardize the samples with human and mouse GAPDH, the ΔΔCt method was used, and the primer sequence is mentioned in **Supplementary Table 1**.

HBV Transcripts Analysis With Northern Blot

HBV transcripts were analyzed by northern blot as previously described (27). Briefly, HBV RNA from transfected cells was extracted and purified with Trizol Reagent (Invitrogen) according to manufacturer instructions. The 4 μg from purified RNA were resolved on a 1.5% MOPS agarose gel containing 2.2 M formaldehyde, transferred onto a nylon membrane (GE Healthcare), immobilized with UV crosslinking, HBV transcripts corresponding to nucleotides 1072-2171 of HBV genome were detected with a DIG-labeled RNA probe. Dig Northern Starter Kit (Roche Diagnostics) was used for the preparation of probe and membrane detection. The quantity of 18S and 28S rRNAs were used as internal loading controls.

Analysis of Reporter Activity With Dual-Luciferase Reporter Assay

Dual-Luciferase Assay was carried out to determine HBV reporter activity in HepG2 cells as previously described (27). Cells were seeded in 24 well cell culture plates, and after 24 hours of seeding, cells were transfected with HBV reporters (200 ng) along with an indicated quantity of control vector (pCAGGS) or

IFI6 expression plasmid (250 ng). The pRL-TK (50 ng) plasmid was added as a transfection efficiency control. After 48 hours of transfection, the cells were washed and lysed with PLB (passive lysis buffer) and subjected to luciferase activity assay using the Dual-Glo system (Promega, Madison, WI).

Extracellular Encapsidated and Core Associated HBV DNA Analysis

The extracellular encapsidated DNA from the supernatant and mice sera were extracted and purified as previously described (29). Briefly, 80 µl of supernatant and 10 µl of mice sera were digested with 10 mM MgCl and DNase I to remove plasmid and free DNA. The enzymes were inactivated with 10 mM EDTA for 15 min at 70°C, and the samples were transferred into a lysis buffer containing 20 mM Tris-HCl, 50 mM NaCl, 20 mM EDTA, and 0.5% sodium dodecyl sulfate (SDS) containing 27 µg proteinase K, followed by overnight incubation at 65°C. Extraction of HBV DNA was performed with traditional phenol-chloroform extraction, followed by ethanol precipitation.

To extract core associated HBV DNA, the HepG2 cells were transfected with pSV-β-gal, pHBV1.3, and control vector (pCAGGS) or IFI6 in the indicated amount. After 96 hours of transfection, cells were washed and lysed in NP-40 lysis buffer containing 50 mM Tris-HCl (pH 7.4), 1 mM EDTA, and 1% NP-40 at 4°C for 30 min and centrifuged. The β-galactosidase activity assay was carried out as a transfection efficiency control in the same lysate. After centrifugation, the supernatants were collected and digested at 37°C for 1 hour with DNase I (Thermoscientific) then the enzymes were inactivated with 10 mM EDTA for 15 min at 70°C. The core-associated HBV DNA was purified with proteinase K digestion followed by traditional phenol-chloroform extraction and ethanol precipitation. The extracted DNA was subjected to qPCR using the primer RCCCS (nt 256-274) and RCCCAS (nt 421-404) (30). The primer sequence is mentioned in the **Supplementary Table 1**.

ChIP Assay

ChIP assay was carried out as described previously (31) with a ChIP Assay kit (Beyotime, catalog number P2078) according to the manufacturer's instructions. Briefly, HepG2 cells were seeded into a 10 cm cell culture dish and transfected with pHBV1.3 (5 µg) with IFI6 (5 µg) or control vector (pCAGGS, 5 µg). At 48 hours post-transfection, cells were crossed linked with 1% formaldehyde at 37°C for 10 minutes, neutralized with glycine (125 mM) followed by lysis with SDS lysis buffer containing 50 mM Tris-HCl, (pH 8.0), 150 mM NaCl, 10 mM EDTA, 1% SDS along with PIC (proteinase inhibitor cocktail) on ice. The lysate was subjected to sonication on ice with three pulses for 15s at 30% power to generate a genome size of 200-1000 bp. Chromatin was precipitated with HA-IFI6 antibody (abcam, Cat No, ab9110) at 4°C overnight along with Anti-RNA Polymerase II and normal mouse IgG separately as a positive and negative control, respectively. The precipitate was then washed, and immunoprecipitated DNA fragments were extracted with phenol-chloroform extraction. The DNA fragments were amplified with PCR using EnhII/Cp 1715-1815 nt primers mentioned in **Supplementary Table 1**.

Recombinant IFI6 Protein Purification

Escherichia coli BL21 (Invitrogen) was used to express GST-IFI6 protein at 16°C. The protein expression was induced in 0.7 mM IPTG (isopropyl-β D thiogalactopyranoside) and cells were collected after 12 hours of induction. Lysis buffer containing 50 mM Tris-HCl (pH 7.6), 1 mM EDTA, 150 mM NaCl, 0.1 mg/ml lysozyme, 1 mM DTT (dithiothreitol), and 0.05% NP-40 were used to lyse the cells. The recombinant protein was purified with GST-Fast Flow according to the manufacturer's instructions. The recombinant protein was quantified and stored in glycine at -80°C.

Electrophoretic Mobility Shift Assay

The GST-IFI6 protein was mixed in a binding buffer containing 400 mM Tris-HCl [pH 8.0], 50 mM DTT) and incubated for 30 minutes on ice as previously described (31). The CY5-labeled probe of the HBV EnhII 1715-1770 nt and non-competitive sequence (probe sequence is shown in **Supplementary Table 2**) was added to the protein mix and incubated for 30 minutes at room temperature. The samples were electrophoresed in 1% agarose gel for 1 hour at 130V and exposed to the gel for analysis with Typhoon FLA9500 (GE).

In Vivo Transfection

Hydrodynamic based tail vein injection in mice was used to transfect plasmids. Briefly, pSV-β-Gal (5µg) and pHBV 1.3 (10 µg) along with control vector (20 µg) or IFI6 (20 µg) mixed in saline solution and introduced into the tail vein of eight weeks old C57BL/6 male mice (5 mice in each group) within 5-8 seconds in a volume of saline equivalent to 10% body weight of the mouse. Five days post-injection, mice were slaughtered, and serum was collected to analyze HBV DNA, HBsAg, and HBeAg. For analysis of IFI6 and HA-tag protein, western blot was performed with a small piece of mice liver, homogenized in RIPA lysis buffer along with a phosphatase inhibitor cocktail (PIC). The 10 µg of protein samples were resolved in SDS-PAGE and analyzed with enhanced chemiluminescence (ECL) substrate (Millipore, Billerica, MA). For HBV RNA analysis, a small slice of mice liver was homogenized in Trizol reagent and extracted and purified total RNA. Reverse transcription (RT-PCR) of total RNA into cDNA was performed with the PrimeScript RT reagent kit (Takara). SYBR Green Fast qPCR Master Mix (Cat No. 11201-11203: Yeasen, China) was used to amplify cDNA, and qRT–PCR was performed. The primers for qRT–PCR, qPCR, and mice GAPDH are mentioned in **Supplementary Table 1**.

Statistical Analysis

All experiments were performed at least three times and the results were measured as a mean ± SD. An independent Student's *t*-test was used to measure the statistical differences between normally distributed samples (**Figures 1A**, **3C, D, F**, **4A–D**, **6B–E**) and non-parametric Student's *t*-test was used for non-normally distributed samples (**Figures 1B**, **2C–F**, **3E**, **5B**) by using GraphPad Prism 6.01 (GraphPad Software Inc, USA). A $p < 0.05$ was considered statistically significant.

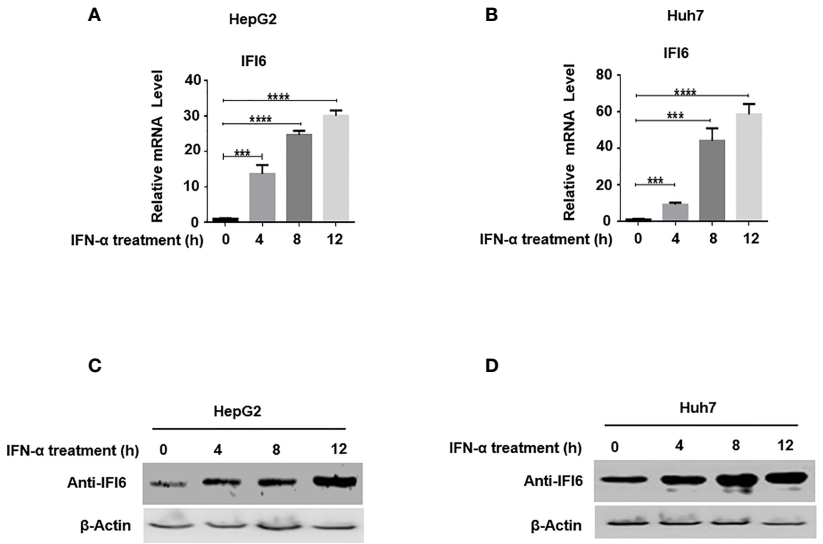

FIGURE 1 | Expression level of IFI6 is significantly induced by IFN-α in Hepatocytes. HepG2 and Huh7 cells were seeded in 12 well cell culture plates. After 24 hours, cells were treated with human IFN-α (100 ng/ml). Samples were collected at 0, 4, 8, and 12 hours after IFN-α treatment and total RNA was purified and subjected to qRT-PCR **(A, B)** and western blot for protein detection **(C, D).** The anti-IFI6 antibody was used to determine the protein level of IF6. Expression of β-actin was used as a loading control. The data are averages of three independent experiments; the results were measured as a mean ± SD and statistically analyzed. ***$P < 0.001$, ****$P < 0.0001$.

RESULTS

Expression of IFI6 Is Induced by IFN-α in Hepatocytes

IFN-α activates a cascade of the JAK/STAT pathway upon binding to the IFN receptors and subsequently triggers hundreds of IFN-stimulated genes (ISGs). IFI6 is one of the IFN stimulated genes (32). We first determined the IFI6 expression level by inducing the cells with IFN-α and assessed the mRNA level of IFI6 by qRT-PCR. The IFI6 expression was upregulated in a dose-dependent manner in HepG2 and Huh7 cells by the induction of IFN-α (**Figures 1A, B**). Furthermore, IFI6 protein was highly expressed in both types of cell lines by IFN-α stimulation (**Figures 1C, D**). The expression level of IFI6 by stimulation of IFN-α indicates a unique role of IFI6 against foreign invaders in terms of host defense strategy in hepatocytes.

IFI6 Overexpression Inhibits HBV Replication and Gene Expression

As the function of IFI6 on HBV replication and gene expression was not reported previously, we initially evaluated the role and function of IFI6 in HBV replication and gene expression in the HepG2 cell line. HA-tagged IFI6 or control vector (pCAGGS) at different concentrations was transiently transfected along with β-gal and pHBV1.3 in HepG2 cells. The mRNA and protein levels of IFI6 were detected with qRT-PCR and western blot, respectively. The IFI6 was highly expressed in a dose-dependent manner in HepG2 cells (**Figure 2A**). As the transcription of HBV RNA is controlled by core promoter and EnhII, we further evaluated the level of HBV RNA transcripts (3.5 kb, 2.4 kb, and 2.1 kb) by northern blot. The results indicated that the steady-state level of 3.5 kb pgRNA along with 2.4 kb, and 2.1 kb RNA transcripts were decreased in a dose-dependent manner (**Figure 2B**). Consistent with decreased HBV transcripts, the qRT-PCR analysis indicated the reduction of 3.5 kb HBV RNA level by overexpression of IFI6 (**Figure 2C**). As 3.5 kb HBV RNA acts as a template for HBV DNA replication, we further confirmed the HBV DNA replication inhibition in HepG2 cells and measured the level of HBV intracellular core-associated and extracellular encapsidated DNA level by q-PCR. The intracellular core-associated and extracellular HBV DNA replication significantly reduced upon overexpression of IFI6 (**Figures 2D,E**). To determine the HBV secreted proteins (HBsAg and HBeAg) level in supernatant of transfected cells, ELISA was performed, and the level of HBsAg and HBeAg in cell supernatant was highly reduced, indicating the inhibitory role of IFI6 (**Figure 2F**). Furthermore, we determined the cytotoxicity of transfected HepG2 cells with CCk8 assay. These results demonstrated that transfection of HepG2 cells with IFI6 plasmid has no cytotoxic effect in our experimental system (**Figure 2G**). Taken together, we conclude that IFI6 overexpression inhibits HBV replication and gene expression in HepG2 cells.

Knockdown of IFI6 Enhances HBV Replication and Gene Expression

The above data indicate that overexpression of IFI6 inhibits the replication of HBV and gene expression. To further evaluate the antiviral activity of IFI6 against HBV, we investigated whether downregulating the activity of IFI6 could enhance HBV gene expression. We used short hairpin RNA targeting two different regions of IFI6 and inserted it into the cell genome by lentivirus

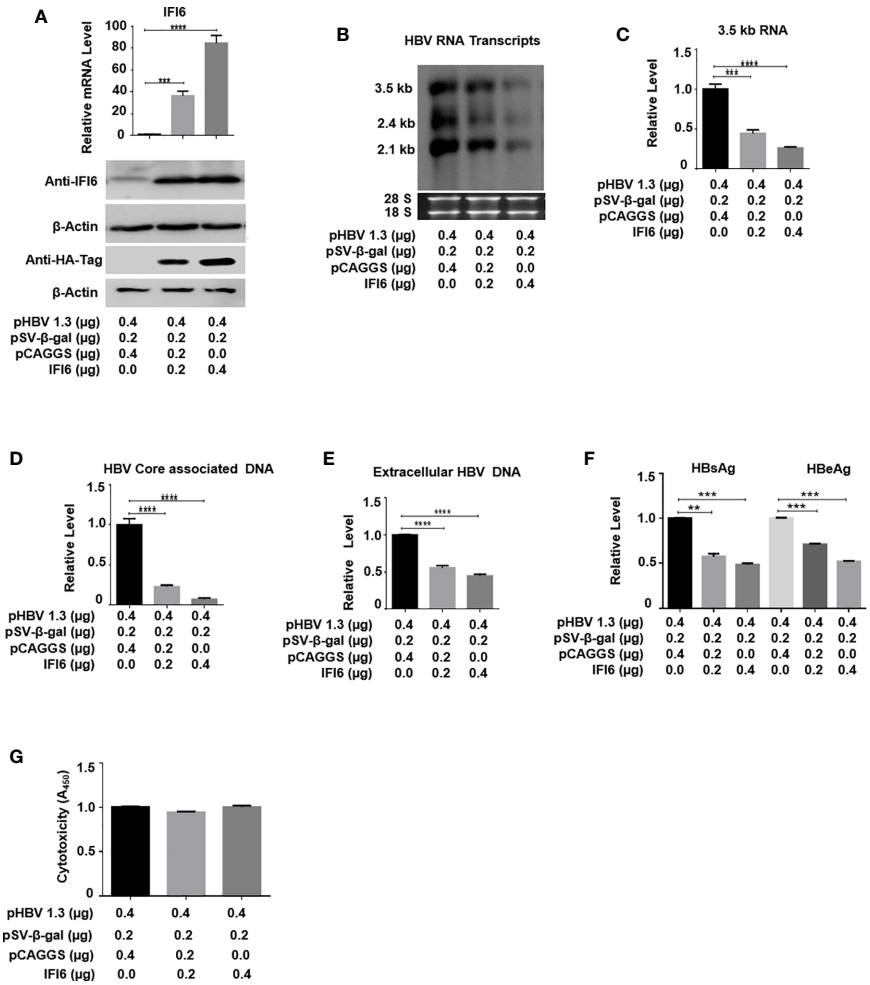

FIGURE 2 | IFI6 overexpression inhibits HBV replication and gene expression. HepG2 cells were seeded in 12 well cell culture plates and transfected with indicated amounts of the plasmid. Cells were harvested after 48 h posttransfection **(A, B, C, F, G)** or 96 hours post-transfection **(D, E). (A)** The expression of IFI6 mRNA and protein was measured by qRT-PCR and western blot, respectively. The anti-IFI6 and anti-HA-tag antibodies were used to determine the protein level of IF6 and HA-tag, respectively. The β-actin was used as a loading control. **(B)** HBV RNA transcripts (3.5 kb, 2.4 kb, and 2.1 kb) were determined with northern blot. The amount of 28S and 18S rRNAs was used as a loading control. **(C)** The level of HBV 3.5 kb RNA was measured with qRT-PCR. The GAPDH level was used as an internal control. HBV core associated **(D)** and extracellular DNA **(E)** was determined by qPCR. **(F)** The level of secreted HBsAg and HBeAg from transfected cell supernatant was measured with ELISA. **(G)** The cytotoxicity of transfected HepG2 was determined with a CCK8 kit after 48 hours of transfection with the indicated amount of plasmids. The data are averages of three independent experiments; the results were measured as a mean ± SD and were statistically measured. *** $P < 0.001$, **** $P < 0.0001$.

infection. We generated three stable HepG2 cell lines expressing control (shRNA) and two different target regions of IFI6 (named shIFI6-1 and shIFI6-2). The downregulating efficiency of stable cell lines was measured by qRT-PCR and western blot, respectively. The level of IFI6 mRNA and protein was significantly reduced as compared with control (**Figure 3A**). To further confirm the activity of stable IFI6 cell lines with HBV gene expression, pHBV1.3 and β-gal were transiently transfected and measured the level of HBV transcripts (3.5 kb, 2.4 kb, and 2.1 kb) by northern blot. The steady-state level of HBV RNA transcripts (3.5 kb, 2.4 kb, and 2.1 kb) was enhanced significantly by the downregulation of IFI6 activity (**Figure 3B**). Accordingly, the qRT-PCR analysis indicated the elevated level of 3.5 kb HBV RNA by IFI6 knockdown (**Figure 3C**). Consistent with the increased HBV RNA transcripts level, the level of HBV intracellular core associated and extracellular DNA level was measured with q-PCR, and the replication of HBV DNA was increased potently (**Figures 3D, E**). Moreover, the level of secreted HBsAg and HBeAg in the cell culture supernatant was significantly increased (**Figure 3F**). However, to determine the side effect of shRNA on HepG2 cells, cytotoxicity assay was performed with CCK8 kit, indicating no side effect of shRNA on growth condition of stable knockdown cell lines (**Figure 3G**). These results showed that the HBV gene expression increased by downregulating the activity of IFI6.

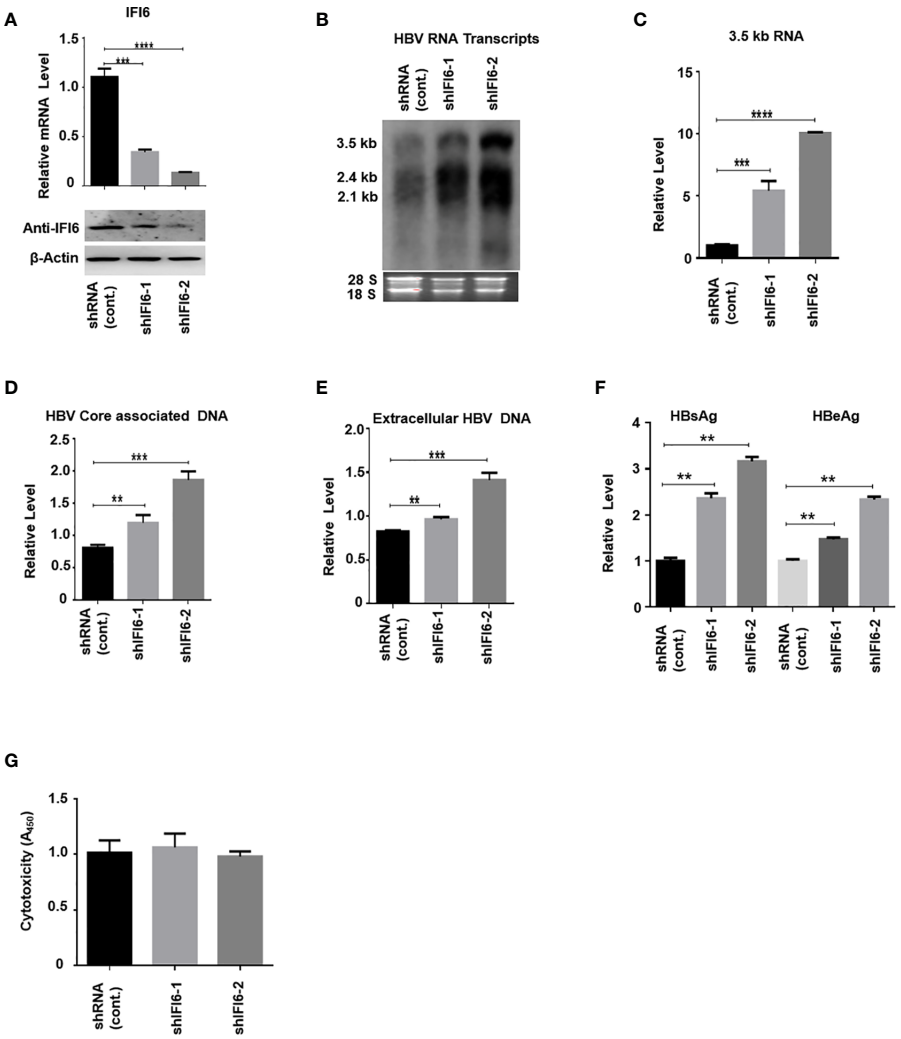

FIGURE 3 | Knockdown of IFI6 enhances HBV replication and gene expression. Stable HepG2 cell lines expressing shRNA (control), shIFI6-1, and shIFI6-2 were seeded in 12 well cell culture plate and transfected after 24 hours with pHBV1.3 (800 ng) and β-Gal (200 ng) and cells were harvested 48 hours posttransfection **(A, B, C, F, G)** or 96 hours posttransfection **(D, E)**. **(A)** The IFI6 mRNA and the protein expression level were measured by qRT-PCR and western blot, respectively. The anti-IFI6 antibody was used to determine the protein level of IF6. The β-actin was used as a loading control. **(B)** HBV RNA transcripts were determined with northern blot. The amount of 28S and 18S rRNAs was used as a loading control. **(C)** The level of HBV 3.5 kb RNA was measured with qRT-PCR. The GAPDH level was used as an internal control. **(D)** HBV core associated DNA and extracellular DNA **(E)** was determined with qPCR. **(F)** The level of secreted HBsAg and HBeAg from transfected cell supernatant was measured with ELISA. **(G)** The cytotoxicity of the stable knockdown cell line was determined with CCK8 kit after 48 hours of transfection with pHBV (800 ng) and β-Gal (200 ng). The data are averages of three independent experiments; the results were measured as a mean ± SD and were statistically measured. ** $P < 0.01$, *** $P < 0.001$, **** $P < 0.0001$.

IFI6 Downregulate HBV Gene Expression by Suppressing ENHII/Cp Promoter Activity

The HBV transcription is controlled by different promoters EnhI, EnhII, Sp1, and Sp2. To further evaluate the molecular mechanism of IFI6 mediated HBV suppression and measured the HBV promoters activity, the EnhI, EnhII, Sp1, and Sp2 were cloned into pGL3 basic vector to construct four reporter plasmids. HepG2 cells along with IFI6 expression plasmid or control plasmid was transiently transfected with four reporter plasmids and measured the dual-luciferase activity. The EnhII/Cp was significantly suppressed by overexpression of IFI6 (**Figure 4A**) while all other promoters were not affected by IFI6 overexpression. To further clarify that whether inhibition of EnhII/Cp is specifically due to overexpression of IFI6, we replaced EnhII/Cp with pCMV (cytomegalovirus promoter) and HepG2 cells along with IFI6 expression plasmid or control plasmid were transiently transfected with pCMV construct and measured the dual-luciferase activity. Interestingly, IFI6 does not change the activity of the pCMV promoter, indicating the specificity of IFI6 mediated inhibition of EnhII/Cp (**Figure 4B**). Moreover, dose-dependent of IFI6 significantly

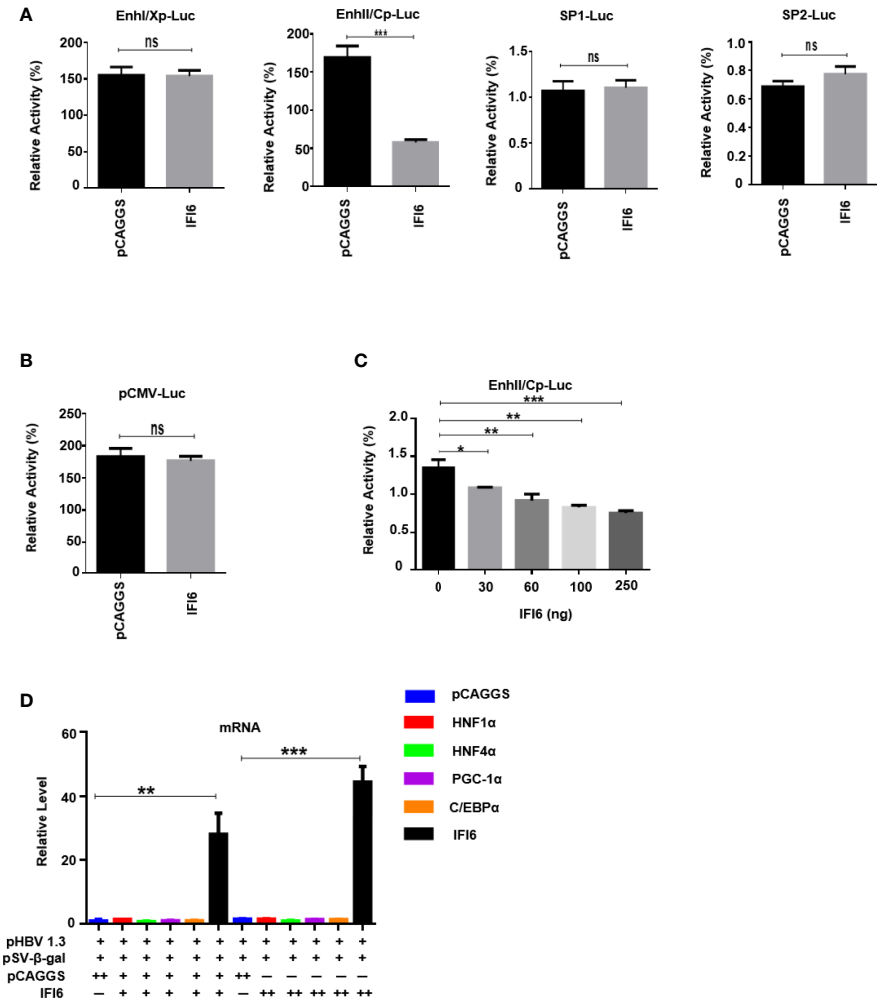

FIGURE 4 | IFI6 downregulate HBV gene expression by suppressing EnhII/Cp promoter activity. HepG2 cells, along with IFI6 expression plasmid or control plasmid (250 ng) was transiently transfected with four reporter plasmids (200 ng) in 24 well cell culture plates and harvested the cells after 48 hours of transfection and subjected to Dual-Luciferase assay. **(A)** The activity of four promoters was measured, and the pRL-TK (50 ng) was used as a transfection efficiency control. **(B)** The activity of the pCMV promoter (200 ng) was measured with a Dual-Luciferase assay. **(C)** The activity of EnhII/Cp was measured in the indicated dose. **(D)** The level of different liver enriched transcription factors was measured by qRT-PCR. The + in pHBV1.3 showing 0.4 μg concentration, the + in pSV-β-gal showing 0.2 μg concentration, the + and ++ in pCAGGS and IFI6 indicate 0.2 and 0.4 μg concentration of pCAGGS and IFI6, respectively, and - in pCAGGS and IFI6 panel is showing zero concentration of pCAGGS and IFI6. The data are averages of three independent experiments; the results were measured as a mean ± SD and were statistically measured. *p < 0.05, **p < 0.01, ***P < 0.001, ns, non-significant.

decreased the activity of EnhII/Cp promoter (**Figure 4C**). These results indicated that IFI6 downregulates HBV at the transcriptional level. Several previous studies revealed that liver enriched transcription factors such as HNF1α, HNF4α, PGC-1α, and C/EBPα are responsible for regulating the Enhancer activity of HBV (33–36). As the IFI6 inhibits the activity of EnhII/Cp, we further investigated the role of these liver enriched transcription factors and analyzed their activity by qRT-PCR. The overexpression of IFI6 did not alter the activity of these transcription factors (**Figure 4D**) suggesting that IFI6 has a direct influence on HBV EnhII/Cp activity. Taken together, our results indicated that IFI6 directly suppresses EnhII/Cp activity

IFI6 Suppresses HBV Replication by Binding to 1715-1770 nt of EnhII/Cp Promoter

As IFI6 directly suppresses the EnhII/Cp promoter activity, we further evaluated the specific binding site of the EnhII/Cp promoter. To investigate the specific binding site of EnhII/Cp promoter, a series of EnhII/Cp deletion mutant was generated and cloned into pGL3 basic vector to construct five reporters (**Figure 5A**). HepG2 cells along with IFI6 expression plasmid or control plasmid was transiently transfected with five reporters and dual-luciferase activity was measured. The IFI6 reduced the activity of EnhII/Cp 1715-1815 bp (100 bps) (**Figure 5B**). To

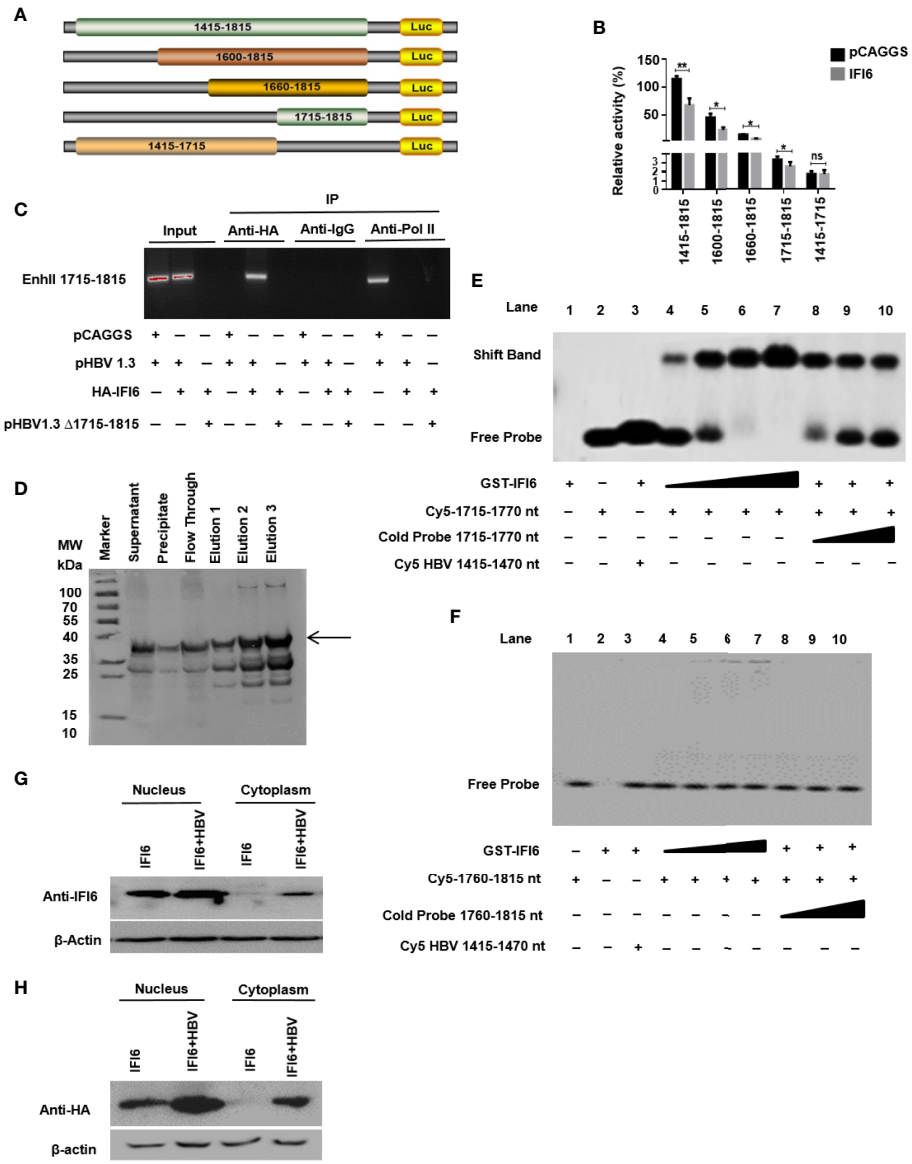

FIGURE 5 | IFI6 suppresses HBV replication by binding to 1715-1770 nt of EnhII/Cp promoter. **(A)** Schematic diagram of EnhII/Cp promoters and its truncated mutants. **(B)** The mutants were subcloned into pGL3 basic plasmid and transfected in HepG2 cells. Cells were harvested after 48 h of transfection, and Dual-luciferase activity was measured. **(C)** HepG2 cells were seeded in a 10 cm dish and transfected with pHBV1.3 (5 μg) with IFI6 (5 μg) or control plasmid (pCAGGS, 5 μg), after 48 hours of transfection, cells were harvested, immunoprecipitate was extracted with overnight incubation of Anti-Polymerase II, mouse IgG, and Anti-HA-Tag antibody to analyze the binding ability of EnhII 1715-1815. The protein-bound EnhII 1715-1815 DNA was extracted, amplified with PCR, and detected with agarose gel electrophoresis. **(D)** Expression and purification of recombinant GST-IFI6 protein were performed from *E.coli*. The western blot was performed to measure the size of the GST-tagged IFI6 protein. The arrow indicated the expected band size of protein, and elution 3 was used for subsequent EMSA experiments. **(E)** EMSA was performed to determine the specific binding of IFI6 with EnhII/Cp 1715-1770 region. Lane 1, GST IFI6 protein alone, Lane 2, Cy5 labeled probe (1715-1770 nt) alone, Lane 3, Cy5 labeled probe (1715-1770 nt) incubated with non-specific competitor probe (Cy5 1415-1470), Lane 4-7, Cy5 labeled probe (1715-1770 nt) incubated with different concentrations of GST IFI6 protein, Lane 8-10, a competition of Cy5 labeled probe (1715-1770 nt) with different concentrations of an unlabeled cold probe (1715-1770 nt). **(F)** EMSA was used to determine the binding of IFI6 with EnhII/Cp 1760-1815 region. Lane 1, Cy5 labeled probe (1760-1815) alone, Lane 2, GST IFI6 protein alone, Lane 3, Cy5 labeled probe (1760-1815 nt) incubated with non-specific competitor probe (Cy5 1415-1470), Lane 4-7, Cy5 labeled probe (1760-1815 nt) incubated with different concentrations of GST IFI6 protein, Lane 8-10, a competition of Cy5 labeled probe (1760-1815 nt) with different concentrations of an unlabeled cold probe (1760-1815 nt). **(G)** HepG2 cells were seeded in 12 well cell culture plates and transfected after 24 hours with IFI6 (1 μg) alone or co-transfected with pHBV1.3 (0.5 μg). Cells were harvested after 48 h posttransfection. Nuclear and cytoplasmic protein was extracted and subjected to western blot. The anti-IFI6 and **(H)** anti-HA-tag antibodies were used to determine the protein level of IF6 and HA-tag respectively from nuclear and cytoplasmic extracted protein. The β-actin was used as a loading control. The data shown in the graph are averages of three independent experiments; the results were measured as a mean ± SD and were statistically measured. * $P < 0.05$, ** $P < 0.01$, ns, non-significant.

further identify the 100 bp binding site of EnhII/Cp, chromatin immunoprecipitation assay (ChIP) was performed. ChIP assay indicated that IFI6 specifically binds to 1715-1815 nt of EnhII/Cp, however, no binding was observed between IFI6 and EnhII/Cp Δ1715-1815 nt when 1715-1815 bp were deleted (**Figure 5C**). To further identify the specific binding site of EnhII/Cp 1715-1815 bp, we generated two 55 base pairs long overlapped Cy5 labeled probes (1715-1770 bp, 1760-1815 bp) to identify the specific binding sites by Electrophoretic mobility shift assay. Recombinant GST-IFI6 protein was expressed and purified from *E.coli* (**Figure 5D**) and EMSA was performed to detect the binding of IFI6 with EnhII/Cp 1715-1815 bp. The results indicated that IFI6 could directly bind to the EnhII/Cp 1715-1770 bp (**Figure 5E**) while no binding was observed between the IFI6 protein and EnhII/Cp 1760-1815 bp (**Figure 5F**). Taken together, our results revealed that EnhII/Cp 1715-1770 bp of HBV is involved in IFI6 mediated HBV inhibition.

IFI6 Is Localized Mainly Inside the Nucleus

Previous studies demonstrated that IFI6 localized in mitochondria or endoplasmic reticulum inside the cells (21). As we indicated that IFI6 inhibits HBV replication and gene replication inside the nucleus (**Figures 5G, H**). We asked to evaluate the localization of IFI6. To this extent, HepG2 cells were transfected with HAtagged IFI6 alone or with pHBV1.3. After 48 hours of transfection, the nuclear and cytoplasmic protein was extracted and subjected to western blot. It is demonstrated that IFI6 is highly expressed in the nucleus rather than the cytoplasm (**Figure 5G**). Moreover, the IFI6 protein expresses more in the presence of HBV inside the nucleus indicating the expression of endogenous IFI6 as well. To further confirm this localization, a western blot was performed using HAtag antibody. **Figure 5H** shows the same localization found inside the nucleus rather than in the cytoplasm. These results clearly support our hypothesis of inhibition of HBV inside the nucleus.

IFI6 Inhibits Replication of HBV and Gene Expression in Mice

As *in vitro* results indicate that the IFI6 inhibits replication of HBV and gene expression, we further evaluated IFI6 mediated HBV inhibition in a mouse model. The IFI6 overexpression plasmid and pHBV1.3 together with its control vector were hydrodynamically injected into the tail vein of mice. After five days of injection, mice were slaughtered, liver and blood were collected. The western blot was performed to determined IFI6 and HA-tag protein levels. The results indicated a high expression of IFI6 protein level in mice liver (**Figure 6A**). To further verify the *in vivo* HBV transcription, 3.5 kb HBV RNA level was measured by qRT-PCR (**Figure 6B**), which indicated the inhibition of 3.5 kb HBV RNA which is a template of HBV transcription that subsequently leads to the inhibition of HBV DNA level (**Figure 6C**). Consistent with *in vitro* results, the level of HBV secreted HBsAg and HBeAg were significantly reduced in the mouse model (**Figures 6D, E**). To further confirm the *in vivo* inhibition of HBV, immunohistochemical staining was performed to evaluate the HBcAg level. **Figure 6F** clearly showed the reduced level of HBcAg expression level in mice liver. Taken together, our results revealed that IFI6 could inhibit the replication of HBV and gene expression *in vivo* that is consistent with *in vitro* results. Overall, our results demonstrate that induction of IFI6 inhibits HBV replication and gene expression inside the nucleus that specifically bind with the EnhII/Cp 1715-1770 nt and directly suppress the replication of HBV (**Figure 7**).

DISCUSSION

As HBV infection is a significant public health concern worldwide and the mechanism of HBV pathogenesis is mostly unclear. This study aims to assess the mechanism underlying the regulation of anti-HBV activity of IF6. This study identified a new horizon of a previously unidentified mechanism by which IFI6 inhibits HBV replication through specifically bind with EnhII/Cp region. The interaction between liver innate immunity and HBV infection has an essential role in HBV disease progression. During acute HBV infection, a noncytolytic mechanism triggers host T-cell responses to eliminate the virus from hepatocytes, which produces infiltrating TNF-α and IFN-γ that acts as proinflammatory antiviral cytokines (37). However, the role of IFI6 in the regulation of acute and chronic HBV infection has not been reported previously. Here we first time provide the evidence that IFI6 restricts HBV replication in *in vitro* and *in vivo*.

IFN is extensively prescribed to treat chronic HBV in clinical settings for the last couple of decades. For chronic HBV treatment, the only available immunotherapy to date is primarily based on pegylated IFN-α. However, the administration of pegylated IFN-α for HBV chronic treatment has only 20-40% seroconversion of HBeAg (38). The intracellular activity of IFN-α is primarily mediated by an array of transcription of around 300 IFN-stimulated genes (ISGs) (39). ISGs also show a tremendous antiviral effect by targeting different steps of the viral life cycle. Many of these ISG's inhibit replication of the hepatitis C virus (40), while some of the ISG's such as USP 18 and ISG15 enhanced HCV replication (41, 42). IFI6 is one of the IFN-stimulated genes and its antiviral mechanism and function are not fully elucidated in HBV replication. In this study, we hypothesized the functional and antiviral mechanism of the IFI6 gene against HBV gene expression and replication. In examining intrahepatic IFN-stimulated genes and evaluating the functional role of IFI6 in the context of HBV immune response, we determined the expression level of IFI6 by inducing hepatoma cell lines with IFN-α that significantly induces IFI6 expression (**Figure 1**). The overexpression of IFI6 reduced the HBV RNA transcripts and protein level, while the knocking down of IFI6 enhanced the activity of HBV gene expression and replication (**Figures 2** and **3**). A previous study based on ISG20 inhibited HBV replication in mouse hepatocytic cell lines and involved IFN-mediated HBV inhibition (43). Consistent with this study, our results of overexpression and knockdown of IFI6 significantly

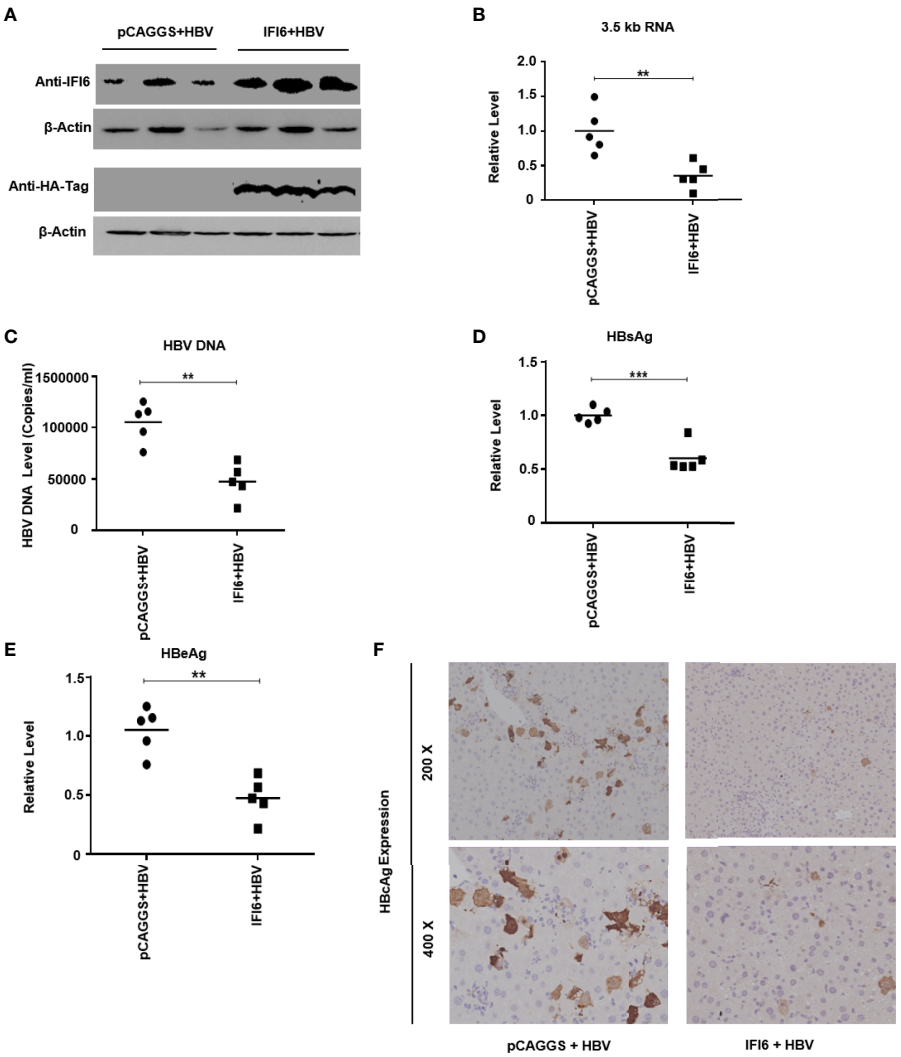

FIGURE 6 | IFI6 inhibits replication of HBV and gene expression in mice. The IFI6 (20 μg) or its control vector (pCAGGS, 20 μg) and pHBV1.3 (10 μg) plasmid were hydrodynamically injected in eight weeks old male C57BL/6 mice. After 5 days post-injection, mice sera and liver were collected. **(A)** The protein was extracted from mice liver and expression of IFI6 and HA-tag protein was determined with western blot using anti-IFI6 and anti-HA-tag antibody. The β-actin was used as a loading control. **(B)** The level of 3.5 kb HBV RNA was measured by qRT-PCR. The level of mice GAPDH was used as an internal control. **(C)** The HBV DNA was extracted from mice serum, and the level was determined by qPCR. The secreted HBsAg **(D)** and HBeAg **(E)** were determined with the ELISA. **(F)** The immunohistochemical staining of HBcAg from mice liver. The data are averages of three independent experiments; the results were measured as a mean ± SD and were statistically measured. ** $P < 0.01$, *** $P < 0.001$.

inhibit and elevated the replication of HBV and gene expression in HepG2 cells, respectively.

The HBV transcription is controlled by two enhancers (EnhI/Xp and EnhII/Cp) and four promoters' elements. Previous studies revealed that IFN-α influences different steps in the HBV life cycle, including DNA replication, the formation of the core particle, transcription and degradation, and the export of viral RNAs (44–47). As the EnhII is positioned adjacent to the core promoter and regulates the transcriptional activity of precore/preS1 and preS2 promoters in an orientation independent manner. Various other cellular and transcription factors, including HNF4α, Prox1, FOXO1 bind with EnhII and promote the HBV regulation. Previous reports postulated that an ISG TRIM22 significantly suppresses HBV gene expression by targeting EnhII/Cp promoter (48). In this study, we demonstrated that IFI6 influenced the activity of EnhII/Cp while there was no effect of IFI6 on other regulatory elements of HBV (Sp1, Sp2, and EnhI) (**Figure 4A**).

HBV transcription inhibition is involved in numerous molecules of cytokines. TNF-α and IFN-γ induced IL-32 in primary human hepatocytes and hepatoma cells that regulate the transcription of HBV core promoter by downregulating HNF1-α and HNF4-α. Similarly, IFN-γ-mediated anti-HBV activity is contributed by hepatocystin that downregulates viral

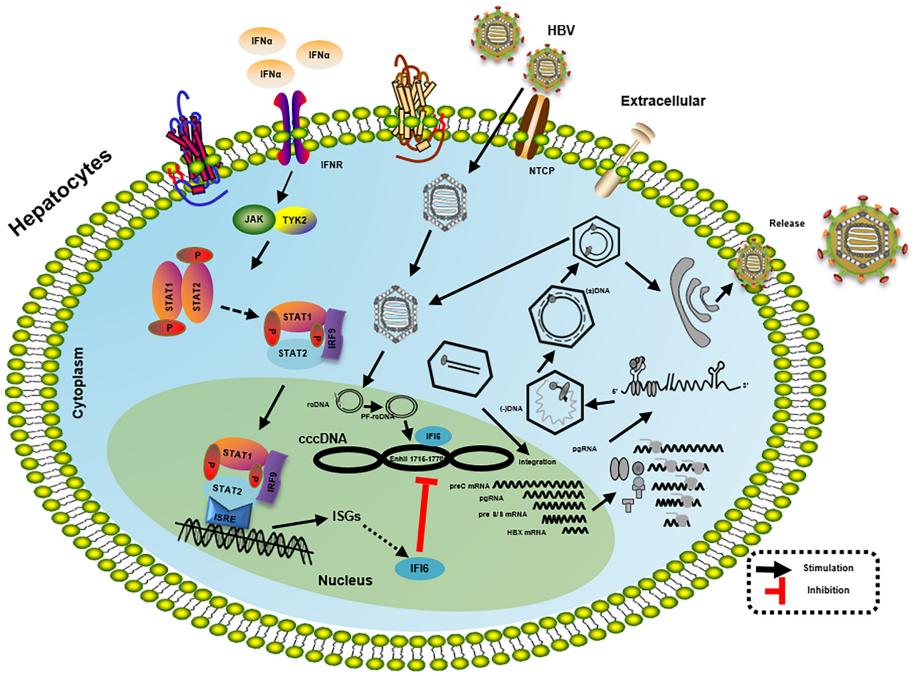

FIGURE 7 | Mechanism of IFI6 mediated inhibition of HBV replication and gene expression. The type I IFN binds to the cell receptor and induces the JAK-STAT signaling pathway that subsequently induces transcription of ISGs. IFI6 is one of the IFN-stimulated genes that inhibit the transcription of 3.5 kb, 2.4 kb, and 2.1 kb RNA of HBV that subsequently inhibit the translation of different HBV proteins.

enhancer activity by overexpression of HNF4-α (31–34, 47, 48). According to this context, our results indicate that IFI6 inhibit HBV replication by interacting with EnhII/Cp region without dysregulation of various liver enriched transcription factors, including HNF1α, HNF4α, PGC-1α, and C/EBPα (**Figure 4C**) (34). We speculate that overexpression of IFI6 inhibits the EnhII activity but does not affect the expression level of these transcription factors. There may be some other transcription factors that could bind to the EnhII region. However, we cannot exclude the recruitments of these transcription factors in the regulation of the EnhII with IFI6 overexpression. Their activity may be changed after IFI6 binding with the EnhII. Further study will be needed to clarify this mechanism.

The regulation of HBV is determined by *cis*-acting factors within HBV mRNA and *trans*-acting factors in the host cell. We further mapped the specific sequence binding site of HBV EnhII/Cp and identified the EnhII/Cp 1715-1770 nt specific cis-acting factors in IFI6 mediated HBV inhibition in EMSA assay with a detailed mechanism (**Figure 5E**). As the overexpression and knockdown clearly indicate the anti-HBV effect of IFI6 but the level of HBsAg dramatically increased which is not under the regulation of EnhII (49). This decrease might be due to transcriptional inhibition or some other liver transcriptional factors involved. Also, the function and role of HBV were elucidated *in vivo* indicated that overexpression of IFI6 markedly inhibited the replication of HBV DNA and gene expression in mouse sera and liver (**Figure 6**).

In conclusion, our study demonstrated the functional role and antiviral effect of IFI6 on the replication of HBV DNA and gene expression *in vitro* and *in vivo*. Furthermore, we showed that IFI6 is mainly localized inside the nucleus. Collectively, our findings also provide an understanding of the antiviral mechanism of IFI6. However, the study is limited to IF6 mediated inhibition of HBV on RNA level and results are generated from *in vitro* and *in vivo* experiments where no stable cccDNA pool is detected. Further study is needed to understand the detailed mechanism and to control HBV at the cccDNA level.

DATA AVAILABILITY STATEMENT

The original contributions presented in the study are included in the article/supplementary material. Further inquiries can be directed to the corresponding author.

AUTHOR CONTRIBUTIONS

YC, LZ, and MS conceived the study and designed the experiments. MS, HU, and KY performed the experiments. MH, JF, MAS, RH, and QL assisted with the experiments. MS and HU analyzed the data. MS wrote the initial draft of the

manuscript. DG and YC provided technical discussion. LZ revised the manuscript. All authors contributed to the article and approved the submitted version.

FUNDING

This work was supported by the Fundamental Research Funds of Health Planning Committee of Hubei Province (WJ2019Q040) to LZ and China NSFC projects (81672008), Hubei Natural Science Foundation (2018CFA035) and Basic Scientific Research Foundation of Central Universities (2042019gf0026) to YC.

ACKNOWLEDGMENTS

We are grateful to Ms. Chanjuan Zhou and Prof. Ying Zhu for providing plasmids and cell lines. We thank Prof. Yuchen Xia for the meaningful discussion. We are thankful to Zhang Hui and all the lab members for their valuable comments and technical support.

SUPPLEMENTARY MATERIAL

The Supplementary Material for this article can be found online at: https://www.frontiersin.org/articles/10.3389/fimmu.2021.634937/full#supplementary-material

REFERENCES

1. Hayes CN, Chayama K. HBV culture and infectious systems. *Hepatol Int* (2016) 10:559–66. doi: 10.1007/s12072-016-9712-y
2. Pollicino T, Cacciola I, Saffioti F, Raimondo G. Hepatitis B virus PreS/S gene variants: pathobiology and clinical implications. *J Hepatol* (2014) 61:408–17. doi: 10.1016/j.jhep.2014.04.041
3. Chabrolles H, Auclair H, Vegna S, Lahlali T, Pons C, Michelet M, et al. Hepatitis B virus Core protein nuclear interactome identifies SRSF10 as a host RNA-binding protein restricting HBV RNA production. *PLoS Pathog* (2020) 16(11):1–28. doi: 10.1101/2020.05.04.076646
4. Li J, Lin S, Chen Q, Peng L, Zhai J, Liu Y, et al. Inhibition of hepatitis B virus replication by MyD88 involves accelerated degradation of pregenomic RNA and nuclear retention of pre-S/S RNAs. *J Virol* (2010) 84:6387–99. doi: 10.1128/JVI.00236-10
5. Liaw Y-F, Chu C-M. Hepatitis B virus infection. *Lancet* (2009) 373:582–92. doi: 10.1016/S0140-6736(09)60207-5
6. Liu J, Kosinska A, Lu M, Roggendorf M. New therapeutic vaccination strategies for the treatment of chronic hepatitis B. *Virol Sin* (2014) 29:10–6. doi: 10.1007/s12250-014-3410-5
7. Hong X, Kim ES, Guo H. Epigenetic regulation of hepatitis B virus covalently closed circular DNA: implications for epigenetic therapy against chronic hepatitis B. *Hepatology* (2017) 66:2066–77. doi: 10.1002/hep.29479
8. Yang Q, Zhang Q, Zhang X, You L, Wang W, Liu W, et al. HoxA10 facilitates SHP-1-catalyzed dephosphorylation of p38 MAPK/STAT3 to repress hepatitis B virus replication by a feedback regulatory mechanism. *J Virol* (2019) 93:1–18. doi: 10.1128/JVI.01607-18
9. Yan H, Zhong G, Xu G, He W, Jing Z, Gao Z, et al. Sodium taurocholate cotransporting polypeptide is a functional receptor for human hepatitis B and D virus. *Elife* (2012) 1:e00049. doi: 10.7554/eLife.00049
10. Ezzikouri S, Ozawa M, Kohara M, Elmdaghri N, Benjelloun S, Tsukiyama-Kohara K. Recent insights into hepatitis B virus–host interactions. *J Med Virol* (2014) 86:925–32. doi: 10.1002/jmv.23916
11. Seeger C, Mason WS. Molecular biology of hepatitis B virus infection. *Virology* (2015) 479:672–86. doi: 10.1016/j.virol.2015.02.031
12. Lahlali T, Berke JM, Vergauwen K, Foca A, Vandyck K, Pauwels F, et al. Novel potent capsid assembly modulators regulate multiple steps of the hepatitis B virus life cycle. *Antimicrob Agents Chemother* (2018) 62:1–15. doi: 10.1128/AAC.00835-18
13. Nishitsuji H, Ujino S, Harada K, Shimotohno K. TIP60 complex inhibits hepatitis B virus transcription. *J Virol* (2018) 92:1–12. doi: 10.1128/JVI.01788-17
14. Waris G, Siddiqui A. Interaction between STAT-3 and HNF-3 leads to the activation of liver-specific hepatitis B virus enhancer 1 function. *J Virol* (2002) 76:2721–9. doi: 10.1128/JVI.76.6.2721-2729.2002
15. Hayes CN, Chayama K. Interferon stimulated genes and innate immune activation following infection with hepatitis B and C viruses. *J Med Virol* (2017) 89:388–96. doi: 10.1002/jmv.24659
16. Ivashkiv LB, Donlin LT. Regulation of type I interferon responses. *Nat Rev Immunol* (2014) 14:36–49. doi: 10.1038/nri3581
17. Liu S-Y, Aliyari R, Chikere K, Li G, Marsden MD, Smith JK, et al. Interferon-inducible cholesterol-25-hydroxylase broadly inhibits viral entry by production of 25-hydroxycholesterol. *Immunity* (2013) 38:92–105. doi: 10.1016/j.immuni.2012.11.005
18. Woo ASJ, Kwok R, Ahmed T. Alpha-interferon treatment in hepatitis B. *Ann Transl Med* (2017) 5:1–9. doi: 10.21037/atm.2017.03.69
19. Cheriyath V, Kuhns MA, Jacobs BS, Evangelista P, Elson P, Downs-Kelly E, et al. G1P3, an interferon-and estrogen-induced survival protein contributes to hyperplasia, tamoxifen resistance and poor outcomes in breast cancer. *Oncogene* (2012) 31:2222–36. doi: 10.1038/onc.2011.393
20. Parker N, Porter ACG. Identification of a novel gene family that includes the interferon-inducible human genes 6–16 and ISG12. *BMC Genomics* (2004) 5:8. doi: 10.1186/1471-2164-5-8
21. Cheriyath V, Kaur J, Davenport A, Khalel A, Chowdhury N, Gaddipati L. G1P3 (IFI6), a mitochondrial localised antiapoptotic protein, promotes metastatic potential of breast cancer cells through mtROS. *Br J Cancer* (2018) 119:52–64. doi: 10.1038/s41416-018-0137-3
22. Cheriyath V, Leaman DW, Borden EC. Emerging roles of FAM14 family members (G1P3/ISG 6–16 and ISG12/IFI27) in innate immunity and cancer. *J Interf Cytokine Res* (2011) 31:173–81. doi: 10.1089/jir.2010.0105
23. Porter AC, Chernajovsky Y, Dale TC, Gilbert CS, Stark GR, Kerr IM. Interferon response element of the human gene 6-16. *EMBO J* (1988) 7:85–92. doi: 10.1002/j.1460-2075.1988.tb02786.x
24. Cheriyath V, Glaser KB, Waring JF, Baz R, Hussein MA, Borden EC. G1P3, an IFN-induced survival factor, antagonizes TRAIL-induced apoptosis in human myeloma cells. *J Clin Invest* (2007) 117:3107–17. doi: 10.1172/JCI31122
25. Guo Y, Guo H, Zhang L, Xie H, Zhao X, Wang F, et al. Genomic analysis of anti-hepatitis B virus (HBV) activity by small interfering RNA and lamivudine in stable HBV-producing cells. *J Virol* (2005) 79:14392–403. doi: 10.1128/JVI.79.22.14392-14403.2005
26. Park G-H, Kim K-Y, Cho SW, Cheong JY, Im Yu G, Shin DH, et al. Association between interferon-inducible protein 6 (IFI6) polymorphisms and hepatitis B virus clearance. *Genomics Inform* (2013) 11:15. doi: 10.5808/GI.2013.11.1.15
27. Hao R, He J, Liu X, Gao G, Liu D, Cui L, et al. Inhibition of hepatitis B virus gene expression and replication by hepatocyte nuclear factor 6. *J Virol* (2015) 89:4345–55. doi: 10.1128/JVI.03094-14
28. Ji Y, Cao L, Zeng L, Zhang Z, Xiao Q, Guan P, et al. The N-terminal ubiquitin-associated domain of Cezanne is crucial for its function to suppress NF-κB pathway. *J Cell Biochem* (2018) 119:1979–91. doi: 10.1002/jcb.26359
29. Tian Y, Chen W, Ou JJ. Effects of interferon-α/β on HBV replication determined by viral load. *PloS Pathog* (2011) 7:e1002159. doi: 10.1371/journal.ppat.1002159
30. Liu X, Hao R, Chen S, Guo D, Chen Y. Inhibition of hepatitis B virus by the CRISPR/Cas9 system via targeting the conserved regions of the viral genome. *J Gen Virol* (2015) 96:2252–61. doi: 10.1099/vir.0.000159
31. Cao L, Ji Y, Zeng L, Liu Q, Zhang Z, Guo S, et al. P200 family protein IFI204 negatively regulates type I interferon responses by targeting IRF7 in nucleus. *PloS Pathog* (2019) 15:e1008079. doi: 10.1371/journal.ppat.1008079
32. Chen S, Li S, Chen L. Interferon-inducible Protein 6-16 (IFI-6-16, ISG16) promotes Hepatitis C virus replication in vitro. *J Med Virol* (2016) 88:109–14. doi: 10.1002/jmv.24302

33. López-Cabrera M, Letovsky J, Hu K-Q, Siddiqui A. Multiple liver-specific factors bind to the hepatitis B virus core/pregenomic promoter: trans-activation and repression by CCAAT/enhancer binding protein. *Proc Natl Acad Sci* (1990) 87:5069–73. doi: 10.1073/pnas.87.13.5069
34. Zheng Y, Li J, Ou J. Regulation of hepatitis B virus core promoter by transcription factors HNF1 and HNF4 and the viral X protein. *J Virol* (2004) 78:6908–14. doi: 10.1128/JVI.78.13.6908-6914.2004
35. Shlomai A, Paran N, Shaul Y. PGC-1α controls hepatitis B virus through nutritional signals. *Proc Natl Acad Sci* (2006) 103:16003–8. doi: 10.1073/pnas.0607837103
36. Tang H, McLachlan A. Transcriptional regulation of hepatitis B virus by nuclear hormone receptors is a critical determinant of viral tropism. *Proc Natl Acad Sci* (2001) 98:1841–6. doi: 10.1073/pnas.98.4.1841
37. Chisari FV, Isogawa M, Wieland SF. Pathogenesis of hepatitis B virus infection. *Pathol Biol* (2010) 58:258–66. doi: 10.1016/j.patbio.2009.11.001
38. Lau GKK, Piratvisuth T, Luo KX, Marcellin P, Thongsawat S, Cooksley G, et al. Peginterferon Alfa-2a, lamivudine, and the combination for HBeAg-positive chronic hepatitis B. *N Engl J Med* (2005) 352:2682–95. doi: 10.1056/NEJMoa043470
39. Dunn C, Peppa D, Khanna P, Nebbia G, Jones M, Brendish N, et al. Temporal analysis of early immune responses in patients with acute hepatitis B virus infection. *Gastroenterology* (2009) 137:1289–300. doi: 10.1053/j.gastro.2009.06.054
40. Itsui Y, Sakamoto N, Kurosaki M, Kanazawa N, Tanabe Y, Koyama T, et al. Expressional screening of interferon-stimulated genes for antiviral activity against hepatitis C virus replication. *J Viral Hepat* (2006) 13:690–700. doi: 10.1111/j.1365-2893.2006.00732.x
41. Randall G, Chen L, Panis M, Fischer AK, Lindenbach BD, Sun J, et al. Silencing of USP18 potentiates the antiviral activity of interferon against hepatitis C virus infection. *Gastroenterology* (2006) 131:1584–91. doi: 10.1053/j.gastro.2006.08.043
42. Chen L, Sun J, Meng L, Heathcote J, Edwards AM, McGilvray ID. ISG15, a ubiquitin-like interferon-stimulated gene, promotes hepatitis C virus production in vitro: Implications for chronic infection and response to treatment. *J Gen Virol* (2010) 91(2):382–8. doi: 10.1099/vir.0.015388-0
43. Wieland SF, Vega RG, Müller R, Evans CF, Hilbush B, Guidotti LG, et al. Searching for interferon-induced genes that inhibit hepatitis B virus replication in transgenic mouse hepatocytes. *J Virol* (2003) 77:1227–36. doi: 10.1128/JVI.77.2.1227-1236.2003
44. Wieland SF, Eustaquio A, Whitten-Bauer C, Boyd B, Chisari FV. Interferon prevents formation of replication-competent hepatitis B virus RNA-containing nucleocapsids. *Proc Natl Acad Sci* (2005) 102:9913–7. doi: 10.1073/pnas.0504273102
45. Romero R, Lavine JE. Cytokine inhibition of the hepatitis B virus core promoter. *Hepatology* (1996) 23:17–23. doi: 10.1002/hep.510230103
46. Gordien E, Rosmorduc O, Peltekian C, Garreau F, Bréchot C, Kremsdorf D. Inhibition of hepatitis B virus replication by the interferon-inducible MxA protein. *J Virol* (2001) 75:2684–91. doi: 10.1128/JVI.75.6.2684-2691.2001
47. Rang A, Günther S, Will H. Effect of interferon alpha on hepatitis B virus replication and gene expression in transiently transfected human hepatoma cells. *J Hepatol* (1999) 31:791–9. doi: 10.1016/S0168-8278(99)80279-7
48. Gao B, Duan Z, Xu W, Xiong S. Tripartite motif-containing 22 inhibits the activity of hepatitis B virus core promoter, which is dependent on nuclear-located RING domain. *Hepatology* (2009) 50:424–33. doi: 10.1002/hep.23011
49. Park YK, Lee SY, Lee AR, Kim K, Kim K, Kim K, et al. Antiviral activity of interferon-stimulated gene 20, as a putative repressor binding to hepatitis B virus enhancer II and core promoter. *J Gastroenterol Hepatol* (2020) 35:1426–36. doi: 10.1111/jgh.14986

Conflict of Interest: The authors declare that the research was conducted in the absence of any commercial or financial relationships that could be construed as a potential conflict of interest.

frontiers in Immunology

ORIGINAL RESEARCH
published: 22 July 2021
doi: 10.3389/fimmu.2021.713420

Involvement of Innate Immune Receptors in the Resolution of Acute Hepatitis B in Woodchucks

Manasa Suresh[1], *Bin Li*[1], *Marta G. Murreddu*[1], *Severin O. Gudima*[2] *and Stephan Menne*[1]*

[1] Department of Microbiology & Immunology, Georgetown University Medical Center, Washington, DC, United States,
[2] Department of Microbiology, Molecular Genetics & Immunology, University of Kansas Medical Center, Kansas City, KS, United States

The antiviral property of small agonist compounds activating pattern recognition receptors (PRRs), including toll-like and RIG-I receptors, have been preclinically evaluated and are currently tested in clinical trials against chronic hepatitis B (CHB). The involvement of other PRRs in modulating hepatitis B virus infection is less known. Thus, woodchucks with resolving acute hepatitis B (AHB) after infection with woodchuck hepatitis virus (WHV) were characterized as animals with normal or delayed resolution based on their kinetics of viremia and antigenemia, and the presence and expression of various PRRs were determined in both outcomes. While PRR expression was unchanged immediately after infection, most receptors were strongly upregulated during resolution in liver but not in blood. Besides well-known PRRs, including TLR7/8/9 and RIG-I, other less-characterized receptors, such as IFI16, ZBP1/DAI, AIM2, and NLRP3, displayed comparable or even higher expression. Compared to normal resolution, a 3–4-week lag in peak receptor expression and WHV-specific B- and T-cell responses were noted during delayed resolution. This suggested that PRR upregulation in woodchuck liver occurs when the mounting WHV replication reaches a certain level, and that multiple receptors are involved in the subsequent induction of antiviral immune responses. Liver enzyme elevations occurred early during normal resolution, indicating a faster induction of cytolytic mechanisms than in delayed resolution, and correlated with an increased expression of NK-cell and CD8 markers and cytolytic effector molecules. The peak liver enzyme level, however, was lower during delayed resolution, but hepatic inflammation was more pronounced and associated with a higher expression of cytolytic markers. Further comparison of PRR expression revealed that most receptors were significantly reduced in woodchucks with established and progressing CHB, and several RNA sensors more so than DNA sensors. This correlated with a lower expression of receptor adaptor and effector molecules, suggesting that persistent, high-level WHV replication interferes with PRR activation and is associated with a diminished antiviral immunity based on the

OPEN ACCESS

Edited by:
Anna D. Kosinska, Helmholtz-Gemeinschaft Deutscher Forschungszentren (HZ), Germany

Reviewed by:
Michael Roggendorf, Technical University of Munich, Germany
Xiaoyong Zhang, Southern Medical University, China

***Correspondence:**
Stephan Menne
Stephan.Menne@georgetown.edu

Specialty section:
This article was submitted to Viral Immunology, a section of the journal Frontiers in Immunology

Received: *22 May 2021*
Accepted: *05 July 2021*
Published: *22 July 2021*

Citation:
Suresh M, Li B, Murreddu MG, Gudima SO and Menne S (2021) Involvement of Innate Immune Receptors in the Resolution of Acute Hepatitis B in Woodchucks. Front. Immunol. 12:713420. doi: 10.3389/fimmu.2021.713420

reduced expression of immune cell markers, and absent WHV-specific B- and T-cell responses. Overall, the differential expression of PRRs during resolution and persistence of WHV infection emphasizes their importance in the ultimate viral control during AHB that is impaired during CHB.

Keywords: pattern recognition receptors, hepatitis B virus, acute hepatitis B, innate immune response, woodchuck, chronic hepatitis B

INTRODUCTION

The host innate immunity recognizes viral infections and activates appropriate defense mechanisms. An important part of this response is mediated by germline-encoded receptors, also called pathogen recognition receptors (PRRs) that bind pathogen-associated molecular patterns (PAMPs), ranging from viral nucleic acids to their encoded glycoproteins (1). Subsequent activation of PRRs triggers their downstream signaling pathways, involving adaptor molecules, transcription factors, and type-I interferons (IFNs) or pro-inflammatory cytokines, leading to cell intrinsic and antiviral immune responses (2). The known PRR families include toll-like receptors (TLRs), retinoic acid-inducible gene I (RIG-I) like receptors (RLRs), nucleotide-binding oligomerization domain (NOD) like receptors (NLRs), cytosolic DNA sensors (CDSs), and inflammasomes. The subcellular localization of these PRRs in immune and/or non-immune cells is either on plasma and endosomal membranes or within the cytoplasm and nucleus.

Hepatitis B virus (HBV) is a serious global health issue, with 257 million chronic carriers who are at high risk of developing chronic hepatitis B (CHB), liver cirrhosis, and hepatocellular carcinoma (3, July 8). HBV infection in adults usually leads to acute hepatitis B (AHB) and is often self-limited *via* the control by a strong antiviral immune response, with only a 5% chance of progressing to chronicity (4). However, HBV infection acquired at birth by mother-to-child transfer results in CHB in 95% of cases (5). CHB is associated with an inadequate antiviral immune response, which is responsible for the progression of liver disease. The surge in and the continuous presence of viral proteins during HBV replication interferes with many functions of the innate and adaptive immunity (6). These immunodeficiencies present in CHB have shifted the focus of drug development to immunomodulation as a therapeutic strategy for reviving the impaired immune response in patients with chronic HBV infection (7). The underlying reason is that current treatment options for CHB, including nucleos(t)ide analogs and (pegylated) IFN-α, rarely lead to immunological control of HBV infection (i.e., functional cure) and are further associated with adverse effects and viral relapse upon treatment discontinuation.

Small agonist molecules targeting selected PRRs have been recently developed, with several compounds tested in preclinical animal models of HBV and subsequently in patients with CHB (8). These includes compounds activating TLR3, TLR7, TLR8, TLR9, stimulator of interferon genes (STING), and RIG-I. In woodchucks infected with the HBV-like woodchuck hepatitis virus (WHV), several of these agonist molecules suppressed viral replication and mediated sustained antiviral effects. These studies have highlighted the important role of innate immune receptors in facilitating a coordinated adaptive immune response and hence are suitable targets for immune modulation.

Besides the above PRRs, the involvement of other viral nucleic acid sensing receptors in HBV infection, and especially in AHB resolution, remains unknown. Main reasons are that studying the early phase of HBV infection in patients is challenging due to its asymptomatic nature and that obtaining frequent liver biopsies from patients is limited. The Eastern woodchuck (*Marmota monax*) infected with WHV is a fully immunocompetent animal model that has been extensively used for investigating HBV-associated pathogenesis during the resolved *versus* chronic outcome of infection. Similar to HBV infection in humans, almost all adult woodchucks resolve WHV infection, whereas neonatal woodchucks infected shortly after birth mainly progress to CHB (9). Thus, woodchucks are an excellent animal model for studying the early events of host immune response to the virus following experimental WHV infection and for testing the safety and antiviral efficacy of novel drugs for the treatment of CHB. In our previous work on acute, self-limited WHV infection in adult woodchucks, we found that the coordinated interplay of innate and adaptive immune responses mediates resolution of AHB, with an initial viral control by natural killer- (NK-) cell associated IFN-γ production (10). In the present study, we investigated the kinetics of viral nucleic acid sensing PRRs in the liver and periphery of adult woodchucks with resolving WHV infection. Comparing the intrahepatic peak upregulation of important receptors during AHB to their expression and presence in the setting of established and progressing CHB revealed an involvement of viral DNA sensors in the control of WHV infection, and much more so than viral RNA sensors.

MATERIALS AND METHODS

Ethics Statement

The animal protocol entitled "Super-infection and virus spread during chronic hepadnaviral infection" and all procedures involving woodchucks were approved by the IACUC of Northeastern Wildlife, Inc. (Harrison, ID) on January 3, 2012, and adhered to the national guidelines of the NIH Guide for the Care and Use of Laboratory Animals. Woodchuck were anesthetized by intramuscular injection of ketamine (50 mg/kg) and xylazine (5 mg/kg) for blood collection and percutaneous liver biopsy. Prior to euthanasia, woodchucks were anesthetized as described above and euthanized by an overdose of

pentobarbital (80-100 mg/kg) administered by intracardiac injection, followed by bilateral intercostal thoracotomy.

Woodchucks and WHV Parameters

The ten adult woodchucks investigated were part of an animal cohort that was experimentally infected with an equal number of genome equivalents (GE) of WHV (11, 12). Animals were selected based on the duration of AHB resolution that allowed studying PRR expression in detail during the early stages of WHV infection. Woodchucks were further characterized as animals with normal or delayed resolution based on the individual kinetics of viremia and antigenemia in serum and liver. Following WHV inoculation, all woodchucks were monitored for approximately 14 to 18 weeks. Serum, blood, and liver samples were collected prior to inoculation (pre-inoculation or Pre) and again at the end of the study (EOS). In addition, serum was collected weekly, blood was obtained weekly or biweekly, and additional liver biopsies were taken at weeks +5/6, +9, and +12/13. Serum viral load, intrahepatic WHV replication, and innate and adaptive immune responses in some of these animals were reported recently (10–12). For woodchucks with established CHB, viremia and antigenemia in serum and liver, as well as antibody and T-cell responses in the periphery, were determined as described for animals resolving AHB. Liver tissues were further examined for sinusoidal and portal hepatitis and a composite score was obtained on a scale of 0-6, where 0 indicated absent, >0-2 indicated mild, >2-4 indicated moderate, and >4 indicated severe/marked inflammation.

Intrahepatic and Peripheral PRR Expression

Total RNA from liver biopsy samples was isolated using the RNeasy Mini kit (Qiagen, Redwood City, CA) by following the manufacture's protocol. Total RNA from whole blood collected in PAXgene blood tubes (Qiagen) was isolated using the PAXgene Blood miRNA kit (Qiagen) with on-column DNase I digestion using RNase-free DNase according to the manufacturer's instructions. RNA concentrations were measured using a Nano Drop 8000 spectrophotometer (Thermo Scientific, Waltham, MA). Liver and blood derived mRNA samples were then reverse transcribed using random primers and the High Capacity cDNA Reverse Transcription kit (Applied Biosystems, Foster City, CA). Changes in the transcript level of various PRRs, adaptor molecules, transcription factors, and effector molecules and cytokines (**Supplementary Table S1**) in the liver and blood during the course of acute WHV infection were determined using real-time PCR and woodchuck-specific primers and probes (**Supplementary Table S2**), as described previously (10). A fold-change of ≥2.1 from the pre-inoculation baseline was considered a positive result for increased molecule expression. Expression results for the above molecules in woodchuck liver are provided in **Supplementary Tables S3** and **S4**.

Immunohistochemistry

Liver tissues were stained with cross-reactive antibodies to selected PRRs, including RIG-I (Origene Technologies, Rockville, MD), TLR7 (Abcam, Cambridge, MA), TLR8 (Bioss, Woburn, MA), ZBP1 (Bioss), and NLRP3 (Bioss). Whole slide images were obtained using an Aperio Scanner GT450 (Leica Biosystems, Buffalo Grove, IL) and analyzed by QuPath, a quantitative pathology and bioimaging software developed at the University of Edinburg, UK (13). Five random areas of similar size were selected in each of the images and a set of same parameters was applied to each area for the detection of positively stained cells. The output results included the total number of immune and non-immune cells detected and the number of cells that stained positively. The percentage of stained cells in each whole slide image is presented as an average of the five areas. The number of positively stained immune cells in the same five areas was obtained by manual counting, a percentage was calculated based on the total number of cells detected and then averaged.

PRR Presence in Woodchucks With AHB and CHB and in WHV-Uninfected Controls

For comparing PRR expression during the acute and chronic outcomes of WHV infection, the following sample sets were used: (i) the pre-inoculation and peak expression levels of each receptor in the liver of the ten woodchucks with resolving WHV infection served as samples for the uninfected control or peak AHB, respectively; and (ii) receptor expression in historical liver tissues of ten age- and gender-matched, treatment-naïve, established chronic WHV carrier woodchucks were used as samples for progressing CHB. For each sample set, the PRR expression was averaged, and the percentage of increase or decrease in receptor transcript level during AHB and CHB was calculated relative to the uninfected control. A similar comparison was performed for innate and adaptive immune cell markers in each sample set. Furthermore, for comparing PRR presence at the protein level, liver tissues from each sample set were stained for selected receptors using the above-described cross-reactive antibodies.

Statistical Analysis

Statistical comparisons were performed using unpaired Student's *t*-test with equal variance for the intrahepatic expression of PRRs, adaptor molecules, interferon-stimulated genes (ISGs), and immune cell markers between woodchucks with AHB and CHB.

RESULTS

Course of WHV Infection in Woodchucks

The ten adult woodchucks investigated in this study were part of an animal cohort that was inoculated with WHV and then followed for 14 to 18 weeks (11, 12). The course of acute WHV infection in individual animals has been described previously (10–12), including serum viremia, antigenemia, antibody response, intrahepatic WHV replication and antigen expression, and liver enzyme levels. Overall, the increases and subsequent declines of the above infection parameters indicated

AHB in all animals, which eventually resolved. Based on the kinetics of viremia and antigenemia, these adult woodchucks were separated into animals with normal or delayed resolution, with five animals in each group. For comparison with progressing chronic infection, serum, blood, and liver samples obtained from five woodchucks with established CHB over a period of 18 weeks were included. The average changes in WHV relaxed circular (rc) DNA and surface antigen (WHsAg) loads, anti-WHsAg antibody (anti-WHs) titer, sorbitol dehydrogenase (SDH) liver enzyme level, and liver inflammation are provided in **Figure 1** for depicting differences in the course of AHB between woodchucks with normal and delayed resolution, as well as animals with CHB progression. For comparing the immune responses associated with liver inflammation in the setting of normal and delayed AHB resolution, the intrahepatic expression kinetics of NK-cell and cytotoxic CD8+ T-cell (CTL) markers and of cytolytic effector molecules are shown in **Figure 2**. These included natural cytotoxicity triggering receptor 1 (NCR1/NKp46), neural cell adhesion molecule (NCAM/CD56), IFN-γ, cluster of differentiation (CD) 8, perforin (PRF), granzyme B (GZMB), and apoptosis-inducing FAS ligand (FASL) and receptor (FASR). The changes in WHV rc-DNA levels are further used in the following figures for correlating the expression of PRRs and other immune response markers with acute and chronic WHV infection.

During normal resolution (**Figure 1**), the peak in serum WHV rc-DNA in woodchucks was observed at week 5. WHsAg and anti-WHs antibodies were detectable as early as weeks 2 or 3, respectively. The SDH level increased at week 8 and was maximal at week 12, which coincided with moderate liver inflammation and the peak in WHcAg- and WHsAg-specific T-cell responses. The peak expression of NK-cell and CTL markers (fold-change: NKp46, 4.0; NCAM, 2.9; IFN-γ, 34.1; CD8, 3.9) and of cytolytic effector molecules (fold-change: PRF, 7.6; FASL, 2.6) was almost always observed at week 9 (**Figure 2**). The average expression of GZMB and FASR revealed no increases that were considered positive (i.e., ≥2.1-fold from the pre-inoculation baseline). In animals with delayed resolution (**Figure 1**), there was a 3–4-week lag in the peak serum viremia and in the detection of antigenemia and antibodies (WHV rc-DNA at week 9, WHsAg at week 5 and anti-WHs at week 7). Similarly, the increase and peak in SDH level was observed later at week 12, with concentrations lower than during normal resolution. Liver inflammation, however, was often more pronounced in individual animals, ranging from moderate to severe hepatitis between week 12/13 and the EOS. This was further associated with a higher expression of NK-cell and CTL markers (fold-change: NKp46, 4.2; NCAM, 7.1; IFN-γ, 45.1; CD8, 6.2) and cytolytic effector molecules (fold-change: PRF, 8.0; GZMB, 2.4; FASL, 4.2) at week 12/13, except for NCAM with a maximum at week 9 (**Figure 2**). FASR expression again remained close to the baseline. Furthermore, the peak in WHV-specific T-cell responses was also noted later at week 18. In contrast to woodchucks with AHB, animals with established

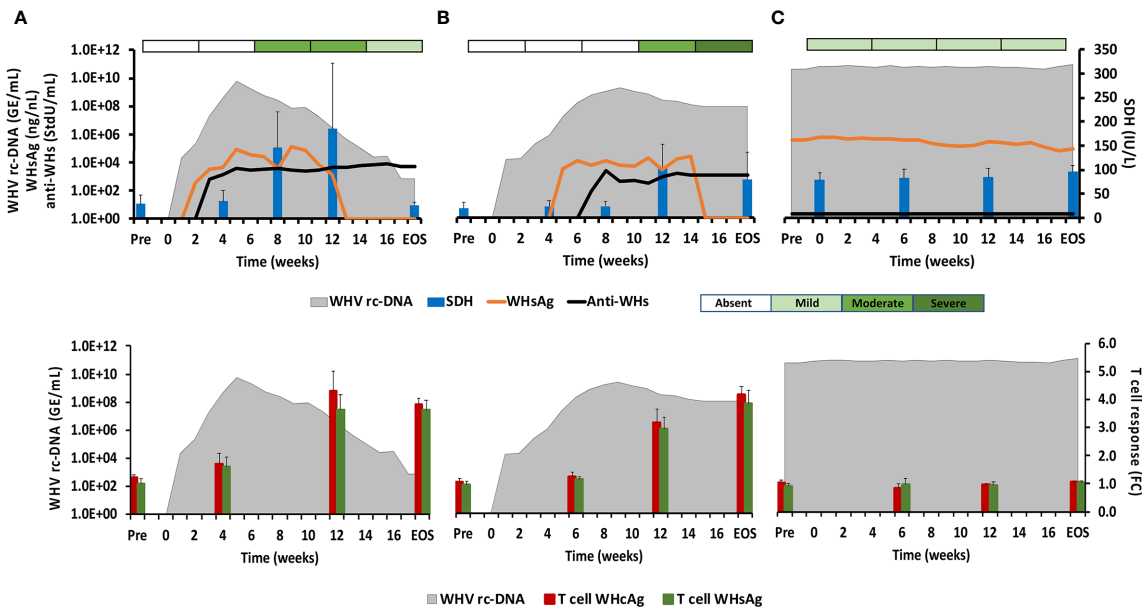

FIGURE 1 | Course of WHV infection in the periphery. Kinetics of serum viremia [WHV rc-DNA, as already reported (11, 12)] and antigenemia (WHsAg), antibody response (anti-WHs antibodies), liver enzyme (SDH) activity, and liver inflammation (top panels) and of blood T-cell response (specific to WHcAg and WHsAg) with WHV rc-DNA kinetics (bottom panels) in woodchucks during **(A)** AHB with normal resolution (n=5), **(B)** AHB with delayed resolution (n=5), and **(C)** CHB progression (n=5). Changes in WHV rc-DNA, WHsAg, and anti-WHs antibodies are plotted on the left y-axes, while changes in SDH and WHcAg- and WHsAg-specific T-cell responses are plotted on the right y-axes. Horizontal bars represent the standard error of the mean. The composite score for sinusoidal and portal hepatitis is represented as a scale bar, indicating absent, mild, moderate, or severe/marked liver inflammation. GE, genomic equivalents; IU, international unit; FC, fold-change in T-cell proliferation from unstimulated controls; Pre, pre-inoculation for AHB and start of study for CHB; EOS, end of study.

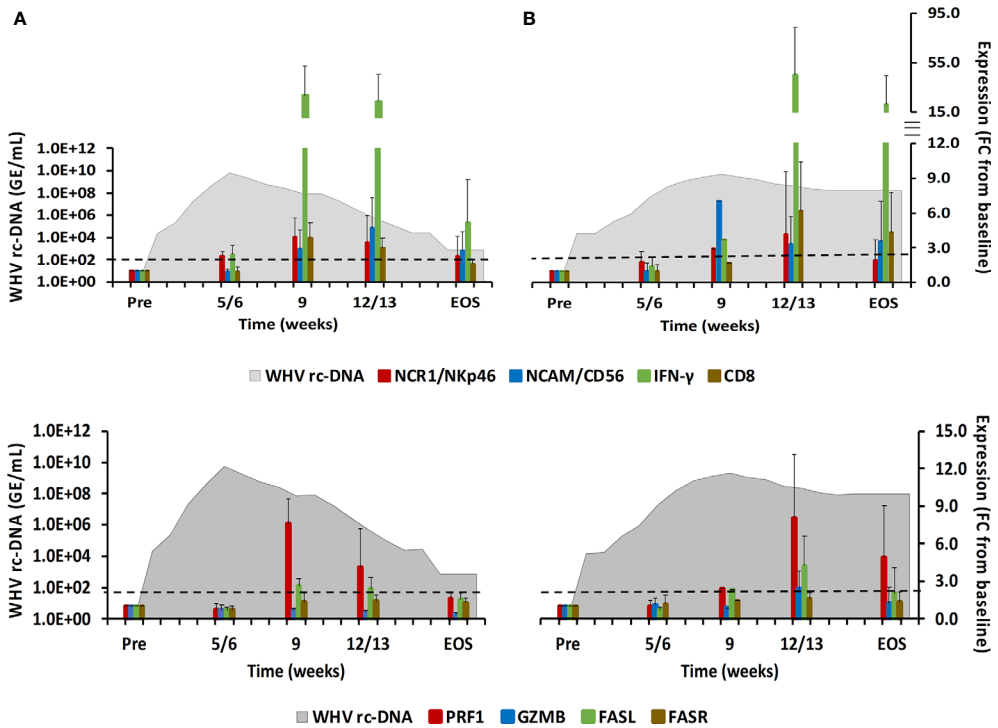

FIGURE 2 | Intrahepatic immune cell marker and cytolytic effector molecule expression. Expression changes of NK-cell and CTL markers (top-panels) and of the cytolytic effector molecules PRF, GZMB, FASL, and FASR (bottom panels) in liver with WHV rc-DNA kinetics of woodchucks during AHB with **(A)** normal resolution (n=5) and **(B)** delayed resolution (n=5). The fold-changes in immune cell marker and cytolytic effector molecule transcript level is plotted on the right y-axis, while serum WHV rc-DNA loads are plotted on the left y-axis. The horizontal, dotted line indicates the cutoff for positive expression (i.e., ≥2.1-fold increase from the pre-inoculation baseline). Horizontal bars represent the standard error of the mean. Pre, pre-inoculation for AHB; EOS, end of study; FC, fold-change.

and progressing CHB had nearly unchanged serum WHV rc-DNA and WHsAg levels at high concentrations during the 18-week period, with undetectable anti-WHs antibodies, rather uniform SDH levels, mild liver inflammation, and absent WHV-specific T-cell responses.

Intrahepatic PRR Presence During AHB Resolution and CHB Progression

PRRs sensing viral nucleic acids and then triggering downstream signaling pathways for the induction of an antiviral immune response include diverse families of receptors, such as RLRs, NLRs, TLRs, CDSs, and inflammasomes. For investigating the presence and upregulation of these PRRs during resolution of acute WHV infection or progression of chronic WHV infection, their expression in woodchuck liver and blood was determined prior to and following WHV inoculation (14). Complete liver data sets are presented from all ten woodchucks with AHB, and nearly complete blood data sets are available from three woodchucks each with normal or delayed resolution. Intrahepatic expression of PRRs in three animals with progressing CHB was determined as well but remained close to the baseline and did not show pronounced changes for most receptors. Blood expression of PRRs in animals with CHB was not determined.

RLRs

This PRR family includes RIG-I, melanoma differentiation-associated protein 5 (MDA5), and laboratory of genetics and physiology 2 (LGP2), which are mainly expressed in the cytosol of non-immune cells, including hepatocytes, but are sometimes also expressed in immune cells, and that sense viral single-stranded (ss) RNA (RIG-I and MDA5) or double-stranded (ds) RNA (LGP2) (15). Upon binding of their PAMP, the caspase recruitment domain (CARD) of RIG-I and MDA5 interacts with the CARD domain of the adaptor molecule, mitochondrial antiviral signaling protein (MAVS). This interaction then activates the downstream signaling pathway involving nuclear factor kappa-light-chain-enhancer of activated B-cells (NF-κB) and IFN-regulating factor (IRF) 3 and 7 as transcription factors to produce type-I IFNs, especially IFN-α (16, 17). LGP2 is a less-characterized receptor and is mainly considered a negative regulator of RIG-I and MDA5. In woodchuck liver (**Figure 3**), the average RIG-I expression during normal and delayed resolution revealed no increases over time. MDA5 and LGP2 expression also remained unchanged during normal resolution but was increased and/or peaked between week 12/13 and the EOS during delayed resolution (fold-change: MDA5, 2.4; LGP2, 3.4). LGP2 was the only receptor in animals with progressing CHB with somewhat increased expression at the EOS (fold-

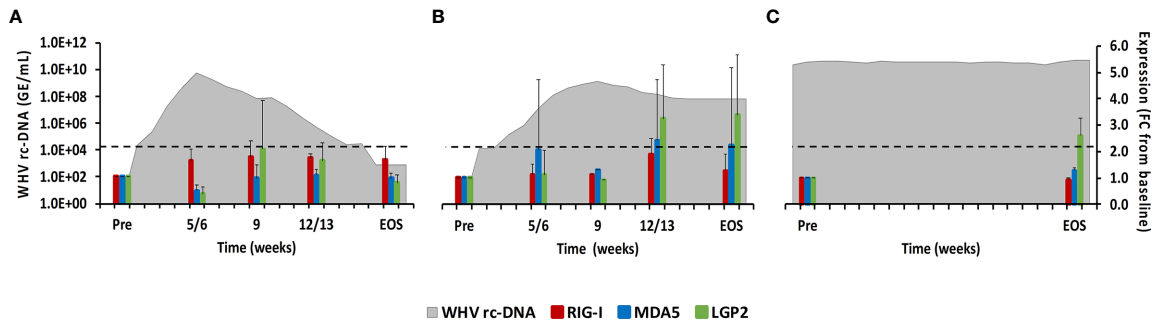

FIGURE 3 | Intrahepatic RLR expression. Expression changes of RIG-I, MDA5, and LGP2 in liver with WHV rc-DNA kinetics of woodchucks during **(A)** AHB with normal resolution (n=5), **(B)** AHB with delayed resolution (n=5), and **(C)** CHB progression (n=3). The fold-changes in receptor transcript level are plotted on the right y-axis, while serum WHV rc-DNA loads are plotted on the left y-axis. The horizontal, dotted line indicates the cutoff for positive expression (i.e., ≥2.1-fold increase from the pre-inoculation baseline). Horizontal bars represent the standard error of the mean. Pre, pre-inoculation for AHB and start of study for CHB; EOS, end of study; FC, fold-change.

change: LGP2, 2.6). In woodchuck blood (**Supplementary Figure 1**), increased RLR expression was observed for LGP2 at week 12 during delayed resolution (fold-change: 2.4), but not for RIG-1 and MDA5.

NLRs

This PRR family is characterized by a tandem CARD domain at the amino-terminal end, followed by the conserved NOD domain and leucine-rich repeat (LRR) motifs at the carboxy-terminal end that bind PAMPs (18, 19). Most NLRs are located within the cytosol of immune and non-immune cells, except for NOD-like receptor family CARD domain containing 5 (NLRC5) that also translocates into the nucleus (18). Family members include NOD2, NLRC5, and NOD-like pyrin domain-containing 3 (NLRP3), which is described later with the inflammasomes. NOD2 senses ssRNA and induces type-I IFNs *via* the MAVS-IRF3 signaling pathway (18). NLRC5 is a receptor inducible by IFN-α and IFN-γ (18). In woodchuck liver (**Figure 4**), an increase in NOD2 expression was only observed during delayed resolution, with a peak expression at week 12/13 (fold-change: 2.4). Maximum NLRC5 expression was noted at week 9 during normal resolution (fold-change: 7.8) and at week 12/13 during delayed resolution (fold-change: 14.0). In woodchuck blood (**Supplementary Figure 2**), NOD2 expression was unchanged in both resolution outcomes. NLRC5 expression was maximal at the EOS during normal resolution (fold-change: 2.2) and at weeks 4 and 12 during delayed resolution (fold-change: 2.5-3.5).

TLRs

TLRs have been widely studied in regard to HBV, since their function can be inhibited by viral proteins, but also activated by small agonist molecules for bringing out antiviral effects (8, 20). TLRs are usually expressed in immune cells on the surface or within the endosome (21). TLR2 and TLR4 are expressed on the cell surface and recognize viral proteins. TLR3 (senses ss/dsRNA), TLR7/8 (sense ssRNA), and TLR9 (usually senses unmethylated dsDNA containing cytosine and guanine triphosphate deoxynucleotide (CpG) motifs) are located on endosomal membranes and produce mainly IFN-α *via* the

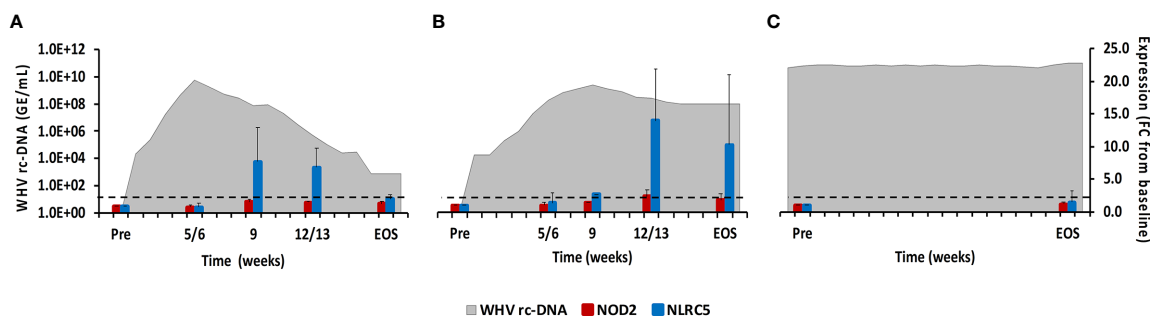

FIGURE 4 | Intrahepatic NLR expression. Expression changes of NOD2 and NLRC5 in liver with WHV rc-DNA kinetics of woodchucks during **(A)** AHB with normal resolution (n=5), **(B)** AHB with delayed resolution (n=5), and **(C)** CHB progression (n=3). The fold-changes in receptor transcript level are plotted on the right y-axis, while serum WHV rc-DNA loads are plotted on the left y-axis. The horizontal, dotted line indicates the cutoff for positive expression (i.e., ≥2.1-fold increase from the pre-inoculation baseline). Horizontal bars represent the standard error of the mean. Pre, pre-inoculation for AHB and start of study for CHB; EOS, end of study; FC, fold-change.

myeloid differentiation primary-response protein 88 (MyD88) adaptor molecule and the IRF3/5/7 downstream pathways (17, 21). In woodchuck liver (**Figure 5**), peak expression of TLR8 and TLR9 was observed at week 9 during normal resolution (fold-change: 3.4 or 9.6, respectively), and at week 12/13 for TLR2 and TLR7 (fold-change:2.7 or 3.0, respectively). Expression of TLR3 and TLR4 remained close to the baseline. During delayed resolution, peak expression of all TLRs, except TLR3, was noted at week 12/13 (fold-change: TLR2, 6.5; TLR4, 3.6; TLR7, 6.2; TLR8, 4.0; and TLR9, 7.2). In woodchuck blood (**Supplementary Figure 3**), expression increases were only observed for TLR3 at the EOS during normal resolution (fold-change: 3.0) and for TLR3 and TLR4 at week 4 and 12, respectively, during delayed resolution (fold-change: TLR3, 2.1; TLR4, 2.6).

CDSs

Molecules located within the cytosol of immune and non-immune cells have been identified that sense dsDNA and induce type-I IFNs, especially IFN-β (22). The downstream signaling pathway of these PRRs apparently involves STING as the adaptor molecule and TANK-binding kinase 1 (TBK1) and IRF3 for type-I IFN production. Family members include ZBP1/DAI, IFI16, cyclic GMP-AMP synthase (cGAS), DExH-box helicase 9 (DHX9), and DEAH-box helicase 36 (DHX36). In woodchuck liver (**Figure 6**), peak expression of IFI16 and ZBP1/DAI was noted at week 9 during normal resolution (fold-change: 3.1 or 7.4, respectively) and at week 12/13 during delayed resolution (fold-change: 3.3 or 4.2, respectively). An increase in cGAS expression was only observed during delayed resolution at week 12/13 (fold-change: 2.3). DHX9 and DHX36 expression was unchanged in the liver of all woodchucks and in blood of most animals (data not shown). In woodchuck blood (**Supplementary Figure 4**), the expression of IFI16 and ZBP1/DAI was rather unchanged, except for an increase at week 4 during normal resolution (fold-change: ZBP1/DAI, 3.3). cGAS expression in blood was not determined due to insufficient RNA amounts.

Inflammasomes

Cytosolic nucleic acids produced during viral replication or as damage-associated molecular patterns are sensed by PRRs, which triggers the formation of multiprotein complexes called inflammasomes that are located in the cytoplasm and/or nucleus of immune and non-immune cells (23). Inflammasomes present in liver include Absent in Melanoma 2 (AIM2) and NLRP3. After binding of their PAMP, both inflammasomes interact with apoptosis-associated speck-like protein containing CARD (ASC) as the adaptor molecule. This activates caspase-1 and results in the production of the inflammatory cytokines IL-1β and IL-18 (23). In woodchuck liver (**Figure 7**), peak expression of both inflammasomes was observed at week 9 during normal resolution and at week 12/13 during delayed resolution (fold-change: AIM2, 3.6 or 5.0; NLRP3, 3.3 or 12.0, respectively). In woodchuck blood (**Supplementary Figure 5**), however, inflammasome expression was not apparent, except for NLRP3 at the EOS during normal resolution (fold-change: 2.3).

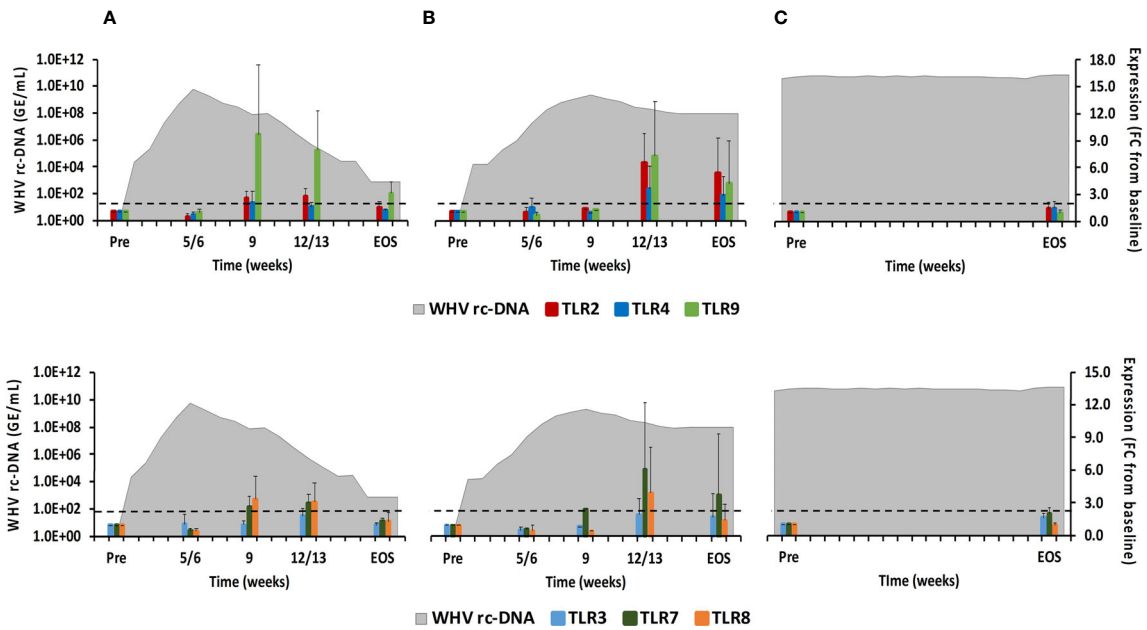

FIGURE 5 | Intrahepatic TLR expression. Expression changes of TLR2/4/9 (top panels) and TLR3/7/8 (bottom panels) in liver with WHV rc-DNA kinetics of woodchucks during **(A)** AHB with normal resolution (n=5), **(B)** AHB with delayed resolution (n=5), and **(C)** CHB progression (n=3). The fold-changes in receptor transcript level are plotted on the right y-axis, while serum WHV rc-DNA loads are plotted on the left y-axis. The horizontal, dotted line indicates the cutoff for positive expression (i.e., ≥2.1-fold increase from the pre-inoculation baseline). Horizontal bars represent the standard error of the mean. Pre, pre-inoculation for AHB and start of study for CHB; EOS, end of study; FC, fold-change.

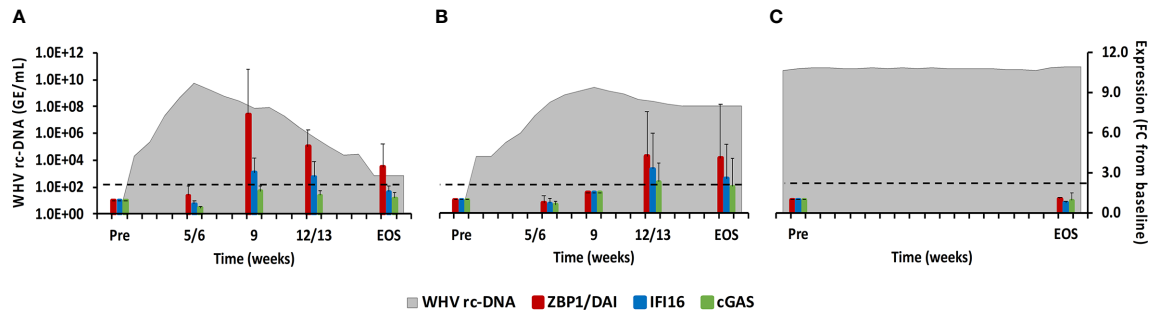

FIGURE 6 | Intrahepatic CDS expression. Expression changes of ZBP1/DA1, IFI16, and cGAS in liver with WHV rc-DNA kinetics of woodchucks during **(A)** AHB with normal resolution (n=5), **(B)** AHB with delayed resolution (n=5), and **(C)** CHB progression (n=3). The fold-changes in receptor transcript level are plotted on the right y-axis, while serum WHV rc-DNA loads are plotted on the left y-axis. The horizontal, dotted line indicates the cutoff for positive expression (i.e., ≥2.1-fold increase from the pre-inoculation baseline). Horizontal bars represent the standard error of the mean. Pre, pre-inoculation for AHB and start of study for CHB; EOS, end of study; FC, fold-change.

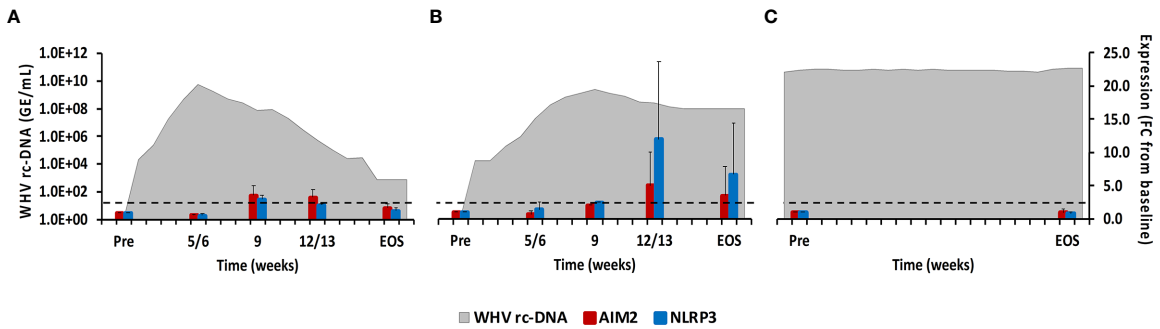

FIGURE 7 | Intrahepatic inflammasome expression. Expression changes of AIM2 and NLRP3 in liver with WHV rc-DNA kinetics of woodchucks during **(A)** AHB with normal resolution (n=5), **(B)** AHB with delayed resolution (n=5), and **(C)** CHB progression (n=3). The fold-changes in receptor transcript level are plotted on the right y-axis, while serum WHV rc-DNA loads are plotted on the left y-axis. The horizontal, dotted line indicates the cutoff for positive expression (i.e., ≥2.1-fold increase from the pre-inoculation baseline). Horizontal bars represent the standard error of the mean. Pre, pre-inoculation for AHB and start of study for CHB; EOS, end of study; FC, fold-change.

Adaptor Molecules and Transcription Factors

As described above, PRRs initiate downstream signaling *via* receptor-specific adaptor molecules following PAMP binding, including MyD88, MAVS, STING, TBK1, and ASC (24). This leads to the activation of common transcription factors, such as IRF3/5/7, or the formation of inflammasomes, which ultimately mediates the production of type-I IFNs and pro-inflammatory cytokines (1). In woodchuck liver (**Figure 8**), the expression of MAVS and TBK1 did not increase during resolution. MyD88 and ASC expression remained close to the baseline during normal resolution but showed peak expression at week 12/13 during delayed resolution (fold-change: MyD88, 2.3; ASC, 6.3). The peak in STING expression was noted at weeks 9 or 12/13, respectively, during normal and delayed resolution (fold-change: 3.0 or 4.5, respectively). Expression of IRF3 and IRF7 remained unchanged during normal resolution but was maximal increased at week 12/13 during delayed resolution (fold-change: IRF3, 2.8; IRF7, 6.8). Similar to PRRs, changes in the expression of adaptor molecules and transcription factors were not noted in animals with CHB progression. Expression of adaptor molecules and transcription factors in blood was not tested due to insufficient RNA amounts.

For verifying the upregulation of selected PRRs during AHB at the protein level, liver tissues from one representative woodchuck with normal (M7392) or delayed resolution (M7249) were stained by immunohistochemistry (IHC) for RIG-I, TLR7, TLR8, ZBP1/DAI, and NLRP3 using cross-reactive antibodies (**Supplementary Figures 6A–E** and **Figure 9**). PRR staining in the liver of both animals was then compared to the respective intrahepatic receptor expression. This revealed that the changes in the percentage of positively stained cells for these receptors followed an almost similar kinetic as observed at the transcript level, with peaks at week 9 during normal resolution (RIG-I, 21.8%; TLR7, 13.8%; TLR8, 34.2%; ZBP1/DAI, 24.0%; NLRP3, 26.7%) and at week 12/13 during delayed resolution (RIG-I, 29.0%; TLR7, 16.7%; TLR8,

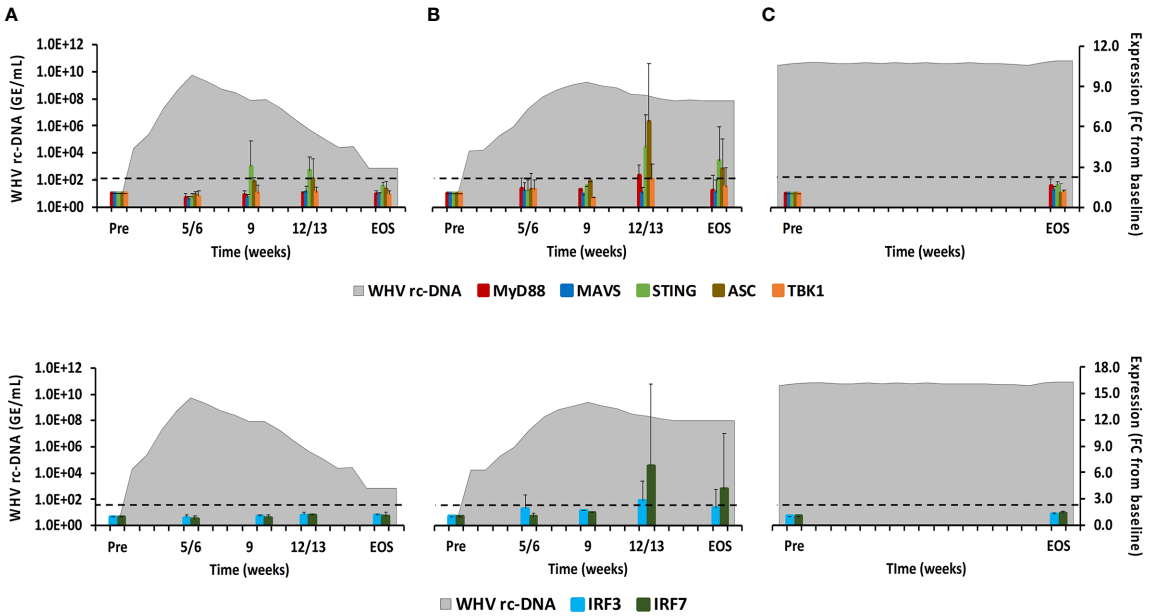

FIGURE 8 | Intrahepatic adaptor molecule and transcription factor expression. Expression changes of adaptor molecules MyD88, MAVS, STING, ASC, and TBK1 (top panels) and transcription factors IRF3 and IRF7 (bottom panels) in liver with WHV rc-DNA kinetics of woodchucks during **(A)** AHB with normal resolution (n=5), **(B)** AHB with delayed resolution (n=5), and **(C)** CHB progression (n=3). The fold-changes in adaptor molecule and transcription factor transcript level are plotted on the right y-axis, while serum WHV rc-DNA loads are plotted on the left y-axis. The horizontal, dotted line indicates the cutoff for positive expression (i.e., ≥2.1-fold increase from the pre-inoculation baseline). Horizontal bars represent the standard error of the mean. Pre, pre-inoculation for AHB and start of study for CHB; EOS, end of study; FC, fold-change.

17.3%; ZBP1/DAI, 10.0%; NLRP3, 11.4%). Since PRR expression was determined in whole liver biopsy samples, the transcription analysis could not discriminate between cell subsets expressing these receptors. However, based on the IHC results (**Figure 9**), RIG-I, TLR7, TLR8, and NLRP3 were present in both immune and non-immune cells, while ZBP1/DAI was only observed in hepatocytes, but not in monocytes and macrophages. The subcellular localization of RIG-I, ZBP1/DAI and NLRP3 was cytoplasmic, while those of TLR7 and TLR8 was endosomal, based on the more granular staining. The peak in the percentage of infiltrating immune cells positively stained for RIG-I and NLRP3 remained less than 1% of all cells during normal and delayed resolution. Contrary, the peak percentage of immune cells positive for TLR7 and TLR8 staining ranged between 6.1 and 8.1% and between 2.1 and 4.0% of all cells during normal or delayed resolution, respectively.

Differential Intrahepatic Presence of PRRs and Immune Cells Markers During AHB Resolution and CHB Progression

Since the intrahepatic kinetics of PRRs and their adaptor molecules during normal and delayed resolution were comparable and mainly differed in regard to the timepoint of peek expression, the upregulation of various PRRs in the liver of adult woodchuck during the course of acute WHV infection suggested their involvement in AHB resolution. In the setting of human CHB, *in vitro* studies have shown that the high amounts of HBV antigens interfere with the function of selected PRRs (25, 26).

For determining *in vivo* differences in PRR expression that may depend on the antigenemia level present during acute and chronic WHV infection (i.e., relatively low *versus* high WHV surface and e antigen loads), the peek expression of important receptors during AHB resolution and CHB progression was compared to their baseline expression in WHV-uninfected controls (i.e., in the liver of the ten animals with AHB prior to WHV inoculation). This comparison (**Figure 10**) revealed that the expression of certain viral RNA sensors, including MDA5, TLR3, and TLR8, was upregulated in woodchucks during AHB resolution, but downregulated in animals with CHB progression (percentage-change: AHB, +33.1 to +319.9%; CHB, -14.3 to -52.4%). Other RNA sensing receptors, such as RIG-I, NOD2, and TLR7, were upregulated in both settings, but to a much lesser extent during CHB progression (percentage-change: AHB, +85.7 to +283.9%; CHB, +17.0 to +66.7%). Similarly, the expression of viral DNA sensors, including TLR9, ZBP1/DAI, IFI16, cGAS, AIM2, and NLRP3, was upregulated during AHB resolution, and also during CHB progression, although to a lesser degree (percentage-change: AHB, +116.9 to +646.1%; CHB, +8.1 to +115.7%).

The comparison of IHC results for selected PPRs in liver tissues from two woodchucks each with AHB resolution or CHB progression with two uninfected controls (**Supplementary Figure 7**) confirmed the receptor expression at the transcript level. The percentage of stained immune and non-immune cells during CHB progression was always lower than during the peak of AHB resolution (RIG-I, AHB, 21.8 to 29.0%, CHB, 4.2 to 6.1%; TLR7, AHB, 13.8 to 16.7%, CHB, 3.6 to 5.2%; TLR8, AHB, 17.3

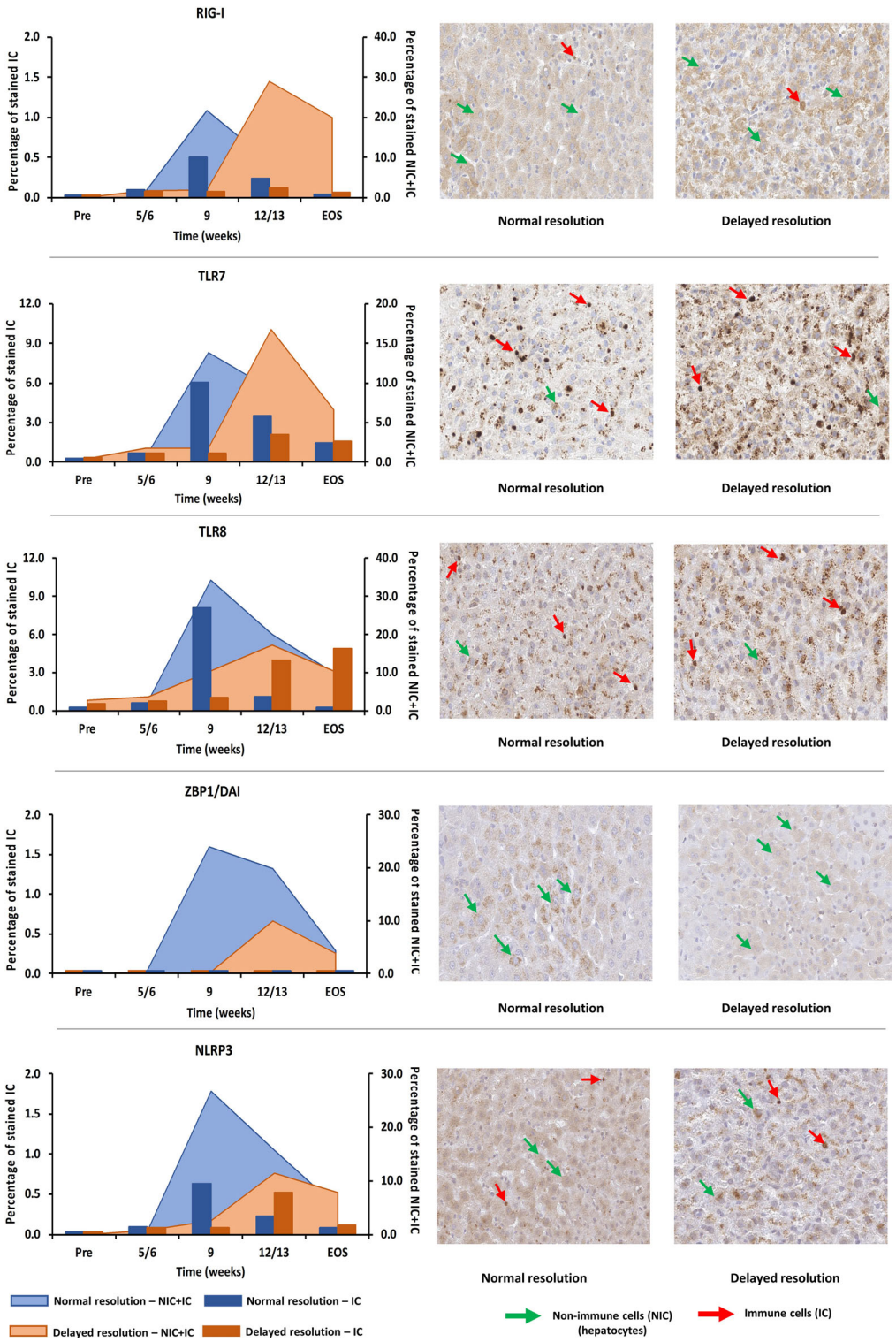

FIGURE 9 | Intrahepatic presence of selected PRRs. Liver tissues from one representative woodchuck each during AHB with normal (M7392) or delayed resolution (M7249) were stained for viral RNA (RIG-I, TLR7, and TLR8) and viral DNA sensing receptors (ZBP1/DAI and NLRP3) using cross-reactive antibodies. The kinetics in the percentage of positively stained cells are presented (left panels). The percentage of stained immune and non-immune cells is plotted on the right y-axis, while the percentage of stained immune cells is plotted on the left y-axis. Representative staining images for the cellular and sub-cellular localization of receptors are shown (right panels). Pre, pre-inoculation; EOS, end of study; NIC, non-immune cells; IC, immune cells.

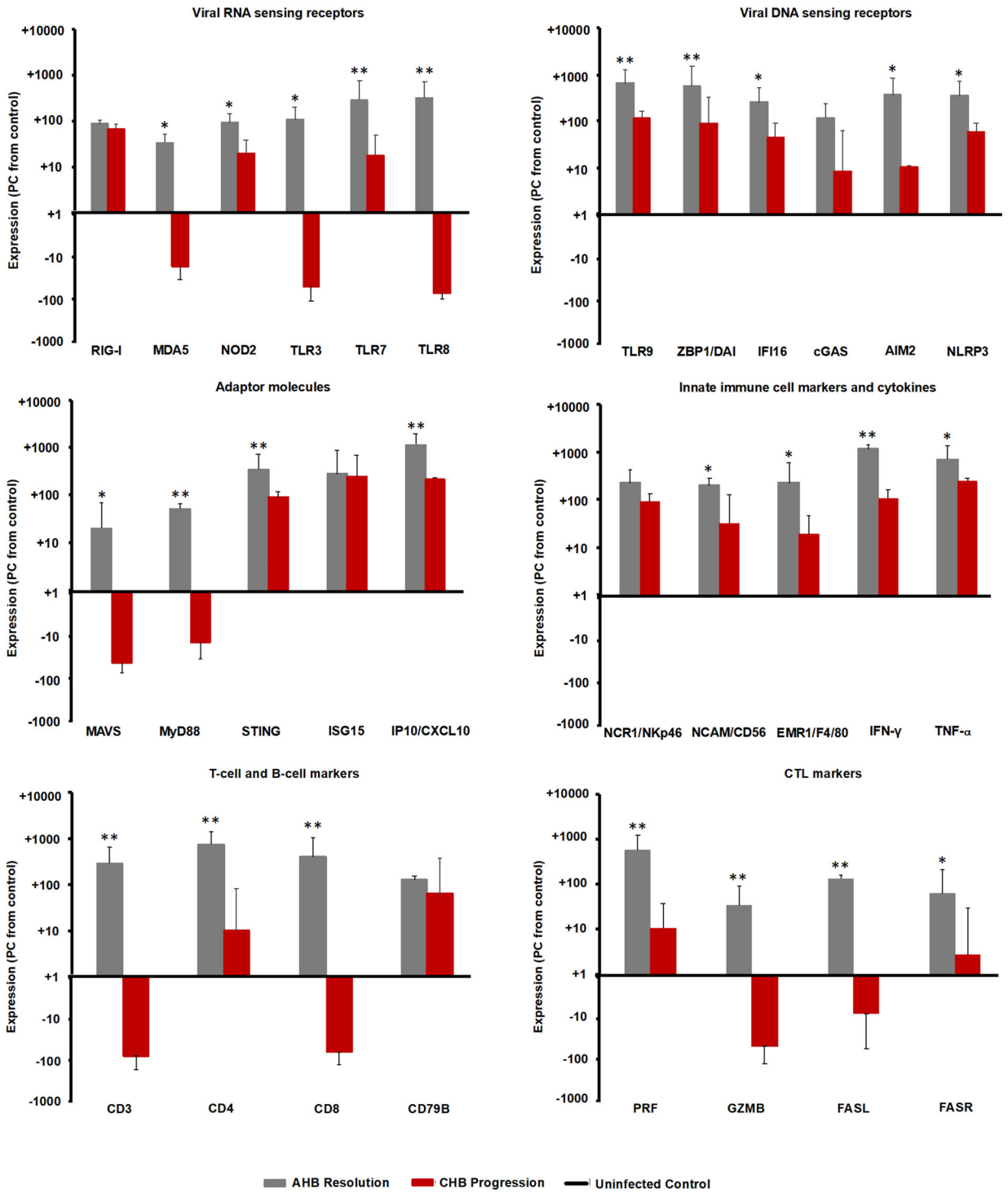

FIGURE 10 | Comparison of intrahepatic expression of PRRs, adaptor molecules, ISGs, innate and adaptive immune cell markers, and cytokines during the resolved and chronic outcomes of WHV infection. Liver expression of important viral RNA and DNA sensing receptors, adaptor molecules, ISGs, innate and adaptive immune cell markers, and cytokines in ten woodchucks each with AHB resolution or CHB progression was compared to their expression in WHV-uninfected controls (i.e., in the liver obtained from the ten woodchucks with normal or delayed AHB resolution prior to WHV inoculation). The marker expression was averaged for each setting (i.e., peak AHB, CHB, and uninfected control). The percentage increase or decrease in expression relative to the uninfected control is presented. Horizontal bars represent the standard error of the mean. *P* values representing statistical significance during AHB resolution compared to CHB progression are shown as * for <0.05 and ** for <0.01. PC, percentage-change.

to 34.2%, CHB, 3.2 to 3.6%; ZBP1, AHB, 10.0 to 24.0%, CHB, 1.1 to 2.2%; NLRP3, AHB, 11.4 to 26.7%, CHB, 2.4 to 2.6%).

Consistent with the above findings, the expression of MAVS and MyD88 adaptor molecules (**Figure 10**), both of which are involved in RNA receptor pathways, was downregulated during CHB progression when compared to AHB resolution (percentage-change: AHB, +20.0 to 51.5%; CHB, -10.0 to -26.0%), while the expression of the STING adaptor molecule that is utilized in DNA receptor pathways was upregulated (percentage-change: AHB, +345.9%; CHB, +88.4%). Upregulation was also noted for common ISGs, such as ISG15 and IFN-gamma-induced protein 10 (IP-10/CXCL10), but like STING, their expression was lower than during AHB resolution (percentage-change: AHB, +282.7 to +1,156.7%; CHB, +218.7 to +246.0%).

For determining if the upregulated expression of viral DNA sensing receptors and of half of the viral RNA sensing receptors tested is associated with an immune response during CHB progression, selected immune cell markers and cytokines were analyzed (**Figure 10**). Regarding innate immunity, the expression of NK-cell markers, including NCR1/NKp46 and NCAM/CD56, IFN-γ, and tumor necrosis factor-alpha (TNF-α) was upregulated during CHB progression, when compared to their expression in the uninfected control, but always lower than during AHB resolution (percentage-change: AHB, NKp46, +224.8%, NCAM, +193.0%, IFN-γ, +1,137.0%, TNF-α, +703.0%; CHB, NKp46, +89.6%, NCAM, +31.8%, IFN-γ, +106.5%, TNF-α, +246.12%). Since the expression of the macrophage marker EGF-like module-containing mucin-like hormone receptor like-1 (EMR1/F4/80) was reduced during CHB progression when compared to AHB resolution (percentage-change: AHB, +345.9%; CHB, +88.4%), this may indicate that macrophages/Kupffer cells are a less likely cell source for upregulated expression of viral RNA and DNA sensors and TNF-α. Adaptive immune cell markers, including CD3, CD4, and CD8 for T helper cells and CTLs, CD79B for B-cells, and effector molecules produced mainly by CTLs, such as PRF, GZMB, as well as FASR and FASL, displayed a reduced or even downregulated expression during CHB progression, when compared to AHB resolution and the uninfected control (percentage-change: AHB, CD3, +286.2%, CD4, +735.0%, CD8, +389.6%, CD79B, +125.9%, PRF, +556.4%, GZMB, +33.8%, FASL, +132.0%, FASR, +63.8%; CHB, CD3, -75.8%, CD4, +10.2%, CD8, -61.3%, CD79B, +62.7%, PRF, +10.7%, GZMB, -48.0%, FASL, -7.5%, FASR, +2.7%). These results could indicate an immune response during CHB progression, which is mainly mediated by NK-cells *via* IFN-γ for non-cytolytic viral control and *via* TNF-α for apoptosis and necroptosis of most likely virus-infected hepatocytes. Compared to the innate immunity, the adaptive immune response apparently was less present during CHB progression based on the reduced or downregulated expression of T-cell subset markers and cytolytic effector cytokines. This overall suggested an underlying weak innate immune response in woodchucks with CHB progression, most likely by type-I IFN production *via* activated viral DNA and selected RNA sensing receptor pathways, while the adaptive immune response was largely absent.

DISCUSSION

PRRs recognize viral nucleic acids and initiate an antiviral immune response *via* their downstream signaling pathways (24). Activation of PRRs further shapes the adaptive immune response against viral infections, including HBV (27–29). The antiviral properties of selected PRRs after activation by agonist molecules have been preclinically evaluated for possible treatment of patients with CHB (8, 30, 31). GS-9620, the first-in-class oral TLR7 agonist developed for the treatment of CHB generated CTL and NK-cell responses following the induction of IFN-α and ISGs in HBV-infected chimpanzees and in WHV-infected woodchucks (32, 33). APR002, another TLR7 agonist, produced elevated expression of ISGs and induced a functional cure in a subset of woodchucks, when administered together with Entecavir (ETV) (34). GS-9688, a TLR8 agonist, also mediated sustained antiviral effects in a subset of woodchucks (35). AIC649, an inactivated parapoxvirus ovis particle preparation that activates antigen-presenting cells (APCs) mainly *via* TLR9, suppressed viral replication in woodchucks as a single agent; however, the combination of AIC649 and ETV produced superior antiviral effects (31). Likewise, CpG 21798, a synthetic oligodeoxynucleotide containing CpG motifs for the activation of TLR9, modulated WHV replication and delayed viral relapse after treatment discontinuation, but only when provided together with ETV to woodchucks (36). Apart from TLR stimulators, the RIG-I agonist, SB9200, mediated antiviral immunity and direct antiviral activity *in vivo* (37, 38), and activation of the immune response by this compound before additional viral suppression with ETV resulted in pronounced antiviral effects in woodchucks (39). Besides these receptors, the activation of other PPRs during HBV infection and their contribution to viral control is less known. In the present study, the expression kinetics of receptors from various PRR families were investigated during acute, self-limited WHV infection in ten adult woodchucks.

For a better delineation of events during different stages of WHV infection, these woodchucks were separated into five animals each with normal and delayed WHV resolution, based on the individual kinetics of viremia and antigenemia. Compared to normal resolution, the detection of and the peeks in serum viremia and antigenemia lagged by approximately 4 weeks in animals with delayed resolution. Although a few PRRs appeared sporadically upregulated in the blood of 1 to 2 woodchucks, the average peripheral and intrahepatic expression of the 16 receptors tested did not increase during the initial 5/6 or 9 weeks of WHV infection in animals with normal or delayed resolution, respectively. The unchanged PRR expression was present despite the detection of WHV rc-DNA in serum during the first week after inoculation and a subsequent peak in viremia 4 to 8 weeks later. This is comparable to the acute HBV infection in three adult chimpanzees, during which a correlation between increasing HBV rc-DNA loads and upregulated expression of virus-induced host genes and immune response-related genes in the liver was not observed during the initial 6 weeks post-inoculation (40). The study on AHB resolution in chimpanzees,

however, was unable to address the expression of various PRRs, except for IFI16, as most receptors were identified more recently. The peak expression of IFI16 in chimpanzee liver was observed at weeks 13/14 post-inoculation during the ongoing HBV clearance phase (40), which is similar to the peak expression of this and most other PPRs in the liver of woodchucks, especially in animals with delayed AHB resolution. Based on the intrahepatic PRR presence at the transcript level in woodchucks, this pointed to a stealth-like behavior of WHV, as described for HBV (8, 40–43). These studies showed that HBV and WHV fail to induce an innate immune response mediated by type-I IFNs and antiviral ISGs immediately after infection, which was also observed recently for five woodchucks of this study (10). Furthermore, in chimpanzees with AHB resolution, the kinetics of HBV-specific T-cell response and the expression of T-cell derived IFN-γ regulated genes demonstrated the importance of the adaptive immune response in viral control (40), as also shown in the current study and reported previously for woodchucks with AHB resolution (10, 41, 44).

The stealth-like behavior of hepadnaviruses, however, is currently being revisited due to recent *in vitro* findings, while the underlying mechanism of initial viral escape from the innate immune response still remains poorly understood. A few studies reported that DNA receptor pathways in primary human hepatocytes (PHHs) are sometimes less activatable by agonists due to a lower receptor presence, when compared to human blood-derived macrophages and woodchuck fibroblastoma cells (45, 46). This is in contrast to studies in which naked HBV DNA, covalently-closed circular DNA, and pre-genomic RNA were sensed in PHHs and human hepatoma cells by sufficient levels of cytoplasmic cGAS, nuclear IFI16, or nuclear and cytoplasmic RIG-I, respectively, leading to a pathway activation of the respective receptors (47–49). Furthermore, HBV virions are sensed by PHHs *via* TLR2 and induce a receptor-mediated expression of pro-inflammatory cytokines in these cells, but without activating IFNs and ISGs (50). In support of the latter studies, activation of an innate immune response in liver as early as 6 hours after experimental WHV infection was shown in adult woodchucks (44). Increased expression of IFN-γ and interleukin 12 was followed by an elevated transcription of several APC and NK- and NKT-cell markers 48 to 72 hours later, all of which was associated with a partial suppression of WHV replication although the infection was able to expand further and to reach a peak thereafter. Since this study did not test for changes in PRR expression, it is unknown if receptors were upregulated as well immediately after WHV infection. Considering the results of the current study, it appears that there is a lack phase of continued innate immune response activation in woodchuck liver and that WHV replication needs to reach a certain level in regard to viral DNA, RNA, and/or antigen loads in hepatocytes before PPRs become strongly upregulated and/or activated again. Interestingly, this marked PPR upregulation occurred after the induction of an anti-WHs antibody response that most likely modulated the levels of intracellular WHsAg and of circulating subviral particles and infectious virions, possibly indicating a role of WHV nucleic acids in PRR activation. Thus, differing from several *in vitro* findings, the average expression of all PRRs investigated in the current study was unchanged during the initial 5/6 to 9 weeks of WHV infection, but the expression of most receptors increased thereafter, and became maximal elevated at weeks 9 and 12/13 during normal or delayed resolution, respectively. Of note is that individual woodchucks with delayed resolution had a notable increase in the percentage of TLR8+ cells already at week 9, possibly indicating a difference at the transcript and protein level of this particular receptor and/or between the two resolution outcomes. At the transcript level, however, the kinetics of intrahepatic PRR expression were comparable between normal and delayed resolution, but receptor upregulation and peak expression were deferred by 3 to 4 weeks during the latter outcome. The peak expression of most PRRs was often higher in woodchuck with delayed than with normal resolution, while the presence of selected receptors sometimes differed at the protein level, with lower numbers of TLR8+ and NLRP3+ cells in the liver during delayed resolution. The underlying reason for this observation is unknown but may depend on the timing of the liver biopsies and/or different sensitivities of the PCR assay and IHC. The staining results for selected PRRs overall confirmed the differential kinetics of receptor expression between the two resolution outcomes. Taken together, the PRR results of the present study likely indicated an involvement and coordinated activation of several viral RNA (i.e., TLR7/8 and NLRC5) and DNA sensing receptors (i.e., TLR9, IFI16, ZBP1/DAI, AIM2, and NLRP3) in the successful viral control during WHV resolution. Other viral RNA and DNA sensors, such as RIG-I, NOD2, TLR3, cGAS, DHX9 and DHX36 did not show pronounced and/or prolonged expression increases during resolution. Peak receptor and pathway upregulation in the liver correlated with the induction and maximum of innate and adaptive immune responses (10), including NK-cell and CTL markers and cytolytic effector molecules, and with a decline in WHV replication in both resolution outcomes (10–12). The longer lasting viremic phase during delayed resolution apparently required more induction of CTL response and likely included additional NK-cell help for cytolytic and non-cytolytic control of the infection, based on a lower level of SDH secreted by killed WHV-infected hepatocytes and a more pronounced liver inflammation. PRR expression in the blood of three animals each with normal or delayed resolution, when detectable, was usually lower and showed different kinetics than in the liver, suggesting a preferential receptor presence and/or upregulation in the liver, the organ of viral replication and disease. However, since changes in PRR presence and expression but not in function were tested, direct receptor activation by WHV nucleic acids was undistinguishable from indirect receptor upregulation by type-I IFNs produced by already activated receptors, such as presumably TLR8 during delayed resolution. This differentiation may be important, since systemic IFN-α administration to woodchucks with CHB induced several of the investigated PRRs in the liver (51).

The inefficiency of the antiviral immune response present during chronic HBV infection in patients has been described

extensively, especially for the adaptive arm (30, 52), but less is known regarding the innate arm. In the present study, the intrahepatic PRR expression in ten woodchucks each with AHB resolution or CHB progression was compared to those of WHV-uninfected controls. A similar comparison was performed for two animals each at the protein level for selected receptors. Both viral RNA and DNA sensors were clearly reduced during CHB progression, when compared to their peak expression and presence during AHB resolution. Furthermore, at the transcript but not at the protein level, several DNA receptors showed comparable or even higher upregulation than RNA receptors in the CHB setting. However, compared to the uninfected control, the expression of several RNA receptors, including MDA5, TLR3, and TLR8 was downregulated during CHB progression, while those of other RNA receptors, such as RIG-I, NOD2, TLR7, and of all DNA receptors, was upregulated, but to a lesser extent than during the peak of AHB resolution. This difference was also noted for RIG-I, TLR7, ZBP1/DAI, and NLRP3 at the protein level and to some degree for TLR8, with a receptor presence that was comparable between uninfected control and CHB progression. Upregulation of DNA receptors (i.e., CDS) during AHB resolution and CHB progression correlated with increased transcript levels of the adaptor molecule STING, as well as antiviral ISGs (i.e., ISG15 and IP-10/CXCL10). The observed ISG15 induction during CHB progression when compared to the uninfected control differs from the comparable levels in cultured liver biopsy samples from control individuals with mainly alcohol-induced liver disease and patients with CHB (43). Nevertheless, CDS and inflammasome upregulation during CHB progression correlated further with expression increases in IFN-γ and TNF-α most likely produced by NK-cells, as macrophage and T-cell markers and cytolytic effector molecules were reduced or downregulated when compared to the uninfected control or peak AHB resolution, all of which is consistent with previous reports on immune response in woodchucks with CHB (41, 53, 54). Overall, this indicated an underlying but weak innate immune response and a deficient adaptive immune response during CHB progression, both of which are apparently insufficient for controlling WHV infection, when compared to the strong immune response during AHB resolution observed in the current study and described recently (10). The cause of this impaired innate immune response is unknown but may involve a lack of WHV RNA recognition by several PRRs and/or subsequent activation of RNA receptor pathways, as suggested by the downregulated transcript levels of their MyD88 and MAVS adaptor molecules and the reduced expression of IRF3/7 transcription factors. In cell cultures and the HBV humanized mouse model (25, 55), it was shown that HBV infection and viral proteins affect type-I IFN production by inhibiting adaptor molecule and transcription factor functions of PRRs. Thus, it is conceivable that the prolonged presence and/or the higher levels of WHV surface and e antigens in woodchucks with CHB progression than during AHB resolution interfere more with the activation of RNA than DNA receptor pathways. This is further supported by the antiviral effects mediated by RNA receptor agonism *in vitro* (TLR3) and *in vivo* (TLR3/7/8/9 or RIG-I), with the latter often resulting in reduced or undetectable viremia and antigenemia levels, and antibody seroconversion in at least subsets of animals (31, 33, 35, 39, 56). Future studies should focus on understanding how HBV/WHV in the setting of CHB progression avoids efficient detection by PRRs and the induction of an innate immune response that is different to the receptor pathway activation and strong immune response induction during AHB resolution. The above studies could not differentiate between the PRR location in WHV-infected or uninfected hepatocytes. However, the IHC results for selected PRRs in the current study identified their presence in only hepatocytes (i.e., ZBP1/DAI) and in both hepatocytes and infiltrating immune cells (i.e., RIG-I and NLRP3 and more so TLR7 and TLR8). The subcellular localization of these receptors was either cytoplasmic (RIG-I, ZBP1/DAI and NLRP3) or endosomal (TLR7 and TLR8). This agrees with the described localization of these receptors in other studies (15, 21–23). The IHC results did not reveal a nuclear localization of RIG-I in woodchuck hepatocytes, as described in a recent *in vitro* study in which HBV pre-genomic RNA was sensed by a nucleus-specific RIG-I in human hepatoma cells (in addition to its more potent cytoplasmic counterpart) and resulted in the induction of type-III IFNs (47).

In summary, the present study investigated in great detail the previously unknown kinetics of receptors from different PRR families in liver and blood during AHB resolution in the woodchuck model of HBV, including the less explored receptors ZBP1/DAI, IFI16, AIM2, and NLRP3. Separation of woodchucks with different kinetics of AHB resolution did not show differences in PRR expression and presence during the early weeks after infection but revealed a correlation between the decline in viremia and antigenemia and the peak upregulation of these receptors in hepatocytes and infiltrating immune cells. The difference in PRR expression and presence during peak AHB resolution and CHB progression, as well as the correlation with immune response marker expression, indicated the involvement of these receptors in the control of WHV infection during resolution and the lack thereof during persistence. This observation supports the concept of PRR agonism that is currently explored for the induction of functional cure in patients with CHB. However, mirroring the situation in AHB resolution, parallel activation of multiple endosomal and cytosolic PRRs in hepatocytes and immune cells during CHB progression, and especially of viral RNA receptors, may be beneficial or required for inducing HBV cure.

DATA AVAILABILITY STATEMENT

The original contributions presented in the study are included in the article/**Supplementary Material**. Further inquiries can be directed to the corresponding author.

ETHICS STATEMENT

The animal study was reviewed and approved by the Institutional Animal Care and Use Committee (IACUC) of Northeastern Wildlife, Inc. (Harrison, ID).

AUTHOR CONTRIBUTIONS

MS, BL, MM, SG, and SM contributed to the conception and design of the study. MS, BL, MM, and SM performed the experiments. MS performed the statistical analysis. MS wrote the first draft of the manuscript. All authors contributed to the article and approved the submitted version.

FUNDING

MS, MM, SG, and SM were supported in part by grant R01CA166213 of the National Institutes of Health (NIH)/ National Cancer Institute (NCI). The funders had no role in the design of the study, in the collection, analyses, or interpretation of data, in the writing of the manuscript, or in the decision to publish the results.

ACKNOWLEDGMENTS

The authors gratefully acknowledge Dr. Aaron Rozeboom, Enoch Adekola, Supti Sen, and Vinona Muralidaran of the Histopathology and Tissue Shared Resources (HTSR) at Georgetown University Medical Center for their excellent assistance with the immunohistochemistry of woodchuck liver tissues and the training in QuPath software. The HTSR is partially supported by NIH/NCI grant P30 CA051008. The authors further gratefully acknowledge Dr. Bhaskar V. Kallakury, Department of Pathology at Georgetown University Medical Center for his excellent assistance with the evaluation of hepatic inflammation in woodchuck liver tissues. Partial data from the five animals presented in this manuscript were previously included in the thesis document of MS (14).

SUPPLEMENTARY MATERIAL

The Supplementary Material for this article can be found online at: https://www.frontiersin.org/articles/10.3389/fimmu.2021.713420/full#supplementary-material

Supplementary Figure 1 | Peripheral RLR expression. Expression changes of RIG-I, MDA5, and LGP2 in blood with WHV rc-DNA kinetics of woodchucks during AHB with **(A)** normal resolution (n=3) and **(B)** delayed resolution (n=3). The fold-changes in receptor transcript level are plotted on the right y-axis, while serum WHV rc-DNA loads are plotted on the left y-axis. The horizontal, dotted line indicates the cutoff for positive expression (i.e., ≥2.1-fold increase from the pre-inoculation baseline). Pre, pre-inoculation; EOS, end of study; FC, fold-change.

Supplementary Figure 2 | Peripheral NLR expression. Expression changes of NOD2 and NLRC5 in blood with WHV rc-DNA kinetics of woodchucks during AHB with **(A)** normal resolution (n=3) and **(B)** delayed resolution (n=3). The fold-changes in receptor transcript level are plotted on the right y-axis, while serum WHV rc-DNA loads are plotted on the left y-axis. The horizontal, dotted line indicates the cutoff for positive expression (i.e., ≥2.1-fold increase from the pre-inoculation baseline). Pre, pre-inoculation; EOS, end of study; FC, fold-change.

Supplementary Figure 3 | Peripheral TLR expression. Expression changes of TLR 2/4/9 (top panels) and TLR 3/7/8 (bottom panels) in blood with WHV rc-DNA kinetics of woodchucks during AHB with **(A)** normal resolution (n=3) and **(B)** delayed resolution (n=3). The fold-changes in receptor transcript level are plotted on the right y-axis, while serum WHV rc-DNA loads are plotted on the left y-axis. The horizontal, dotted line indicates the cutoff for positive expression (i.e., ≥2.1-fold increase from the pre-inoculation baseline). Pre, pre-inoculation; EOS, end of study; FC, fold-change.

Supplementary Figure 4 | Peripheral CDS expression. Expression changes of ZBP1/DAI and IFI16 in blood with WHV rc-DNA kinetics of woodchucks during AHB with **(A)** normal resolution (n=3) and **(B)** delayed resolution (n=3). The fold-changes in receptor transcript level are plotted on the right y-axis, while serum WHV rc-DNA loads are plotted on the left y-axis. The horizontal, dotted line indicates the cutoff for positive expression (i.e., ≥2.1-fold increase from the pre-inoculation baseline). Pre, pre-inoculation; EOS, end of study; FC, fold-change.

Supplementary Figure 5 | Peripheral inflammasome expression. Expression changes of AIM2 and NLRP3 in blood with WHV rc-DNA kinetics of woodchucks during AHB with **(A)** normal resolution and **(B)** delayed resolution. The fold-changes in receptor transcript level are plotted on the right y-axis, while serum WHV rc-DNA loads are plotted on the left y-axis. The horizontal, dotted line indicates the cutoff for positive expression (i.e., ≥2.1-fold increase from the pre-inoculation baseline). Pre, pre-inoculation; EOS, end of study; FC, fold-change.

Supplementary Figure 6 | Liver tissues from one woodchuck each during AHB with normal (M7392; top panels) or delayed resolution (M7249; bottom panels) was collected at the indicated timepoints and stained for RIG-I, TLR7, TLR8, ZBP1/DAI, and NLRP3 using cross-reactive antibodies. One representative image is shown for each timepoint and the corresponding changes at the RNA (fold-change from baseline) and protein level (percentage of positively stained immune and non-immune cells) are provided below each image.

Supplementary Figure 7 | Comparison of intrahepatic presence of selected PPRs during the resolved and chronic outcomes of WHV infection. Liver tissues from two woodchucks each prior to WHV inoculation (uninfected control), during peak AHB resolution, or during CHB progression were stained for RIG-I, TLR7, TLR8, ZBP1/DAI, and NLRP3 using cross-reactive antibodies. One representative image is shown for each setting and the percentage range of positively stained immune and non-immune cells is provided below each image.

REFERENCES

1. Chan YK, Gack MU. Viral Evasion of Intracellular DNA and RNA Sensing. *Nat Rev Microbiol* (2016) 14(6):360–73. doi: 10.1038/nrmicro.2016.45
2. Junt T, Barchet W. Translating Nucleic Acid-Sensing Pathways Into Therapies. *Nat Rev Immunol* (2015) 15(9):529–44. doi: 10.1038/nri3875
3. World Health Organization, W. *Hepatitis B* (2019). Available at: https://www.who.int/en/news-room/fact-sheets/detail/hepatitis-b.
4. Chang JJ, Lewin SR. Immunopathogenesis of Hepatitis B Virus Infection. *Immunol Cell Biol* (2007) 85(1):16–23. doi: 10.1038/sj.icb.7100009
5. Yuen MF, Chen DS, Dusheiko GM, Janssen HLA, Lau DTY, Locarnini SA, et al. Hepatitis B Virus Infection. *Nat Rev Dis Primers* (2018) 4:18035. doi: 10.1038/nrdp.2018.35
6. Tan A, Koh S, Bertoletti A. Immune Response in Hepatitis B Virus Infection. *Cold Spring Harb Perspect Med* (2015) 5(8):a021428. doi: 10.1101/cshperspect.a021428

7. Fanning GC, Zoulim F, Hou J, Bertoletti A. Therapeutic Strategies for Hepatitis B Virus Infection: Towards a Cure. *Nat Rev Drug Discov* (2019) 18(11):827–44. doi: 10.1038/s41573-019-0037-0
8. Suslov A, Wieland S, Menne S. Modulators of Innate Immunity as Novel Therapeutics for Treatment of Chronic Hepatitis B. *Curr Opin Virol* (2018b) 30:9–17. doi: 10.1016/j.coviro.2018.01.008
9. Cote PJ, Korba BE, Miller RH, Jacob JR, Baldwin BH, Hornbuckle WE, et al. Effects of Age and Viral Determinants on Chronicity as an Outcome of Experimental Woodchuck Hepatitis Virus Infection. *Hepatology* (2000) 31 (1):190–200. doi: 10.1002/hep.510310128
10. Suresh M, Czerwinski S, Murreddu MG, Kallakury BV, Ramesh A, Gudima SO, et al. Innate and Adaptive Immunity Associated With Resolution of Acute Woodchuck Hepatitis Virus Infection in Adult Woodchucks. *PloS Pathog* (2019) 15(12):e1008248. doi: 10.1371/journal.ppat.1008248
11. Freitas N, Lukash T, Dudek M, Litwin S, Menne S, Gudima SO. Capacity of a Natural Strain of Woodchuck Hepatitis Virus, WHVNY, to Induce Acute Infection in Naive Adult Woodchucks. *Virus Res* (2015a) 205:12–21. doi: 10.1016/j.virusres.2015.05.003
12. Freitas N, Lukash T, Rodrigues L, Litwin S, Kallakury BV, Menne S, et al. Infection Patterns Induced in Naive Adult Woodchucks by Virions of Woodchuck Hepatitis Virus Collected During Either the Acute or Chronic Phase of Infection. *J Virol* (2015b) 89(17):8749–63. doi: 10.1128/JVI.00984-15
13. Bankhead P, Loughrey MB, Fernandez JA, Dombrowski Y, McArt DG, Dunne PD, et al. Qupath: Open Source Software for Digital Pathology Image Analysis. *Sci Rep* (2017) 7(1):16878. doi: 10.1038/s41598-017-17204-5
14. Suresh M. Immune Responses During Resolution of Acute Hepatitis B in Woodchucks and Their Modulation for Treatment of Chronic Hepatitis B (2020). Washington, DC: Georgetown University Dissertation Document.
15. Rehwinkel J, Gack MU. RIG-I-like Receptors: Their Regulation and Roles in RNA Sensing. *Nat Rev Immunol* (2020) 20(9):537–51. doi: 10.1038/s41577-020-0288-3
16. Kato H, Takeuchi O, Sato S, Yoneyama M, Yamamoto M, Matsui K, et al. Differential Roles of MDA5 and RIG-I Helicases in the Recognition of RNA Viruses. *Nature* (2006) 441(7089):101–5. doi: 10.1038/nature04734
17. Liu G, Gack MU. Distinct and Orchestrated Functions of RNA Sensors in Innate Immunity. *Immunity* (2020) 53(1):26–42. doi: 10.1016/j.immuni.2020.03.017
18. Kanneganti TD. Central Roles of NLRs and Inflammasomes in Viral Infection. *Nat Rev Immunol* (2010) 10(10):688–98. doi: 10.1038/nri2851
19. Correa RG, Milutinovic S, Reed JC. Roles of NOD1 (NLRC1) and NOD2 (NLRC2) in Innate Immunity and Inflammatory Diseases. *Biosci Rep* (2012) 32(6):597–608. doi: 10.1042/BSR20120055
20. Lucifora J, Bonnin M, Aillot L, Fusil F, Maadadi S, Dimier L, et al. Direct Antiviral Properties of TLR Ligands Against HBV Replication in Immune-Competent Hepatocytes. *Sci Rep* (2018) 8(1):5390. doi: 10.1038/s41598-018-23525-w
21. O'Neill LA, Golenbock D, Bowie AG. The History of Toll-like Receptors - Redefining Innate Immunity. *Nat Rev Immunol* (2013) 13(6):453–60. doi: 10.1038/nri3446
22. Broz P, Monack DM. Newly Described Pattern Recognition Receptors Team Up Against Intracellular Pathogens. *Nat Rev Immunol* (2013) 13(8):551–65. doi: 10.1038/nri3479
23. Lupfer C, Malik A, Kanneganti TD. Inflammasome Control of Viral Infection. *Curr Opin Virol* (2015) 12:38–46. doi: 10.1016/j.coviro.2015.02.007
24. Schlee M, Hartmann G. Discriminating Self From Non-Self in Nucleic Acid Sensing. *Nat Rev Immunol* (2016) 16(9):566–80. doi: 10.1038/nri.2016.78
25. Revill P, Yuan Z. New Insights Into How HBV Manipulates the Innate Immune Response to Establish Acute and Persistent Infection. *Antivir Ther* (2013) 18(1):1–15. doi: 10.3851/IMP2542
26. Zou ZQ, Wang L, Wang K, Yu JG. Innate Immune Targets of Hepatitis B Virus Infection. *World J Hepatol* (2016) 8(17):716–25. doi: 10.4254/wjh.v8.i17.716
27. Palm NW, Medzhitov R. Pattern Recognition Receptors and Control of Adaptive Immunity. *Immunol Rev* (2009) 227(1):221–33. doi: 10.1111/j.1600-065X.2008.00731.x
28. Maini MK, Gehring AJ. The Role of Innate Immunity in the Immunopathology and Treatment of HBV Infection. *J Hepatol* (2016) 64(1 Suppl):S60–70. doi: 10.1016/j.jhep.2016.01.028
29. Gehring AJ, Protzer U. Targeting Innate and Adaptive Immune Responses to Cure Chronic HBV Infection. *Gastroenterology* (2019) 156(2):325–37. doi: 10.1053/j.gastro.2018.10.032
30. Meng Z, Chen Y, Lu M. Advances in Targeting the Innate and Adaptive Immune Systems to Cure Chronic Hepatitis B Virus Infection. *Front Immunol* (2019) 10:3127. doi: 10.3389/fimmu.2019.03127
31. Korolowicz KE, Suresh M, Li B, Huang X, Yon C, Leng X, et al. Treatment With the Immunomodulator AIC649 in Combination With Entecavir Produces Antiviral Efficacy in the Woodchuck Model of Chronic Hepatitis B. *Viruses* (2021) 13(4):648. doi: 10.3390/v13040648
32. Lanford RE, Guerra B, Chavez D, Giavedoni L, Hodara VL, Brasky KM, et al. GS-9620, an Oral Agonist of Toll-like receptor-7, Induces Prolonged Suppression of Hepatitis B Virus in Chronically Infected Chimpanzees. *Gastroenterology* (2013) 144(7):1508–17.e1501–10. doi: 10.1053/j.gastro.2013.02.003
33. Menne S, Tumas DB, Liu KH, Thampi L, AlDeghaither D, Baldwin BH, et al. Sustained Efficacy and Seroconversion With the Toll-Like Receptor 7 Agonist GS-9620 in the Woodchuck Model of Chronic Hepatitis B. *J Hepatol* (2015) 62 (6):1237–45. doi: 10.1016/j.jhep.2014.12.026
34. Korolowizc KE, Li B, Huang X, Yon C, Rodrigo E, Corpuz M, et al. Liver-Targeted Toll-Like Receptor 7 Agonist Combined With Entecavir Promotes a Functional Cure in the Woodchuck Model of Hepatitis B Virus. *Hepatol Commun* (2019) 3(10):1296–310. doi: 10.1002/hep4.1397
35. Daffis S, Balsitis S, Chamberlain J, Zheng J, Santos R, Rowe W, et al. Toll-Like Receptor 8 Agonist GS-9688 Induces Sustained Efficacy in the Woodchuck Model of Chronic Hepatitis B. *Hepatology* (2020) 73(1):53–67. doi: 10.1002/hep.31255
36. Meng Z, Zhang X, Pei R, Zhang E, Kemper T, Vollmer J, et al. Combination Therapy Including CpG Oligodeoxynucleotides and Entecavir Induces Early Viral Response and Enhanced Inhibition of Viral Replication in a Woodchuck Model of Chronic Hepadnaviral Infection. *Antiviral Res* (2016) 125:14–24. doi: 10.1016/j.antiviral.2015.11.001
37. Iyer RP, Roland A, Jin Y, Mounir S, Korba B, Julander JG, et al. Anti-Hepatitis B Virus Activity of ORI-9020, a Novel Phosphorothioate Dinucleotide, in a Transgenic Mouse Model. *Antimicrob Agents Chemother* (2004) 48(6):2318–20. doi: 10.1128/AAC.48.6.2318-2320.2004
38. Korolowicz KE, Iyer RP, Czerwinski S, Suresh M, Yang J, Padmanabhan S, et al. Antiviral Efficacy and Host Innate Immunity Associated With SB 9200 Treatment in the Woodchuck Model of Chronic Hepatitis B. *PloS One* (2016) 11(8):e0161313. doi: 10.1371/journal.pone.0161313
39. Suresh M, Korolowicz KE, Balarezo M, Iyer RP, Padmanabhan S, Cleary D, et al. Antiviral Efficacy and Host Immune Response Induction During Sequential Treatment With SB 9200 Followed by Entecavir in Woodchucks. *PloS One* (2017) 12(1):e0169631. doi: 10.1371/journal.pone.0169631
40. Wieland S, Thimme R, Purcell RH, Chisari FV. Genomic Analysis of the Host Response to Hepatitis B Virus Infection. *Proc Natl Acad Sci U S A* (2004) 101 (17):6669–74. doi: 10.1073/pnas.0401771101
41. Fletcher SP, Chin DJ, Cheng DT, Ravindran P, Bitter H, Gruenbaum L, et al. Identification of an Intrahepatic Transcriptional Signature Associated With Self-Limiting Infection in the Woodchuck Model of Hepatitis B. *Hepatology* (2013) 57(1):13–22. doi: 10.1002/hep.25954
42. Mutz P, Metz P, Lempp FA, Bender S, Qu B, Schoneweis K, et al. HBV Bypasses the Innate Immune Response and Does Not Protect HCV From Antiviral Activity of Interferon. *Gastroenterology* (2018) 154(6):1791–1804 e1722. doi: 10.1053/j.gastro.2018.01.044
43. Suslov A, Boldanova T, Wang X, Wieland S, Heim MH. Hepatitis B Virus Does Not Interfere With Innate Immune Responses in the Human Liver. *Gastroenterology* (2018a) 154(6):1778–90. doi: 10.1053/j.gastro.2018.01.034
44. Guy CS, Mulrooney-Cousins PM, Churchill ND, Michalak TI. Intrahepatic Expression of Genes Affiliated With Innate and Adaptive Immune Responses Immediately After Invasion and During Acute Infection With Woodchuck Hepadnavirus. *J Virol* (2008) 82(17):8579–91. doi: 10.1128/JVI.01022-08
45. Yan Q, Li M, Liu Q, Li F, Zhu B, Wang J, et al. Molecular Characterization of Woodchuck IFI16 and AIM2 and Their Expression in Woodchucks Infected With Woodchuck Hepatitis Virus (WHV). *Sci Rep* (2016) 6:28776. doi: 10.1038/srep28776
46. Cheng X, Xia Y, Serti E, Block PD, Chung M, Chayama K, et al. Hepatitis B Virus Evades Innate Immunity of Hepatocytes But Activates Cytokine Production by Macrophages. *Hepatology* (2017) 66(6):1779–93. doi: 10.1002/hep.29348

47. Liu G, Lu Y, Thulasi Raman SN, Xu F, Wu Q, Li Z, et al. Nuclear-Resident RIG-I Senses Viral Replication Inducing Antiviral Immunity. *Nat Commun* (2018) 9(1):3199. doi: 10.1038/s41467-018-05745-w
48. Lauterbach-Riviere L, Bergez M, Monch S, Qu B, Riess M, Vondran FWR, et al. Hepatitis B Virus DNA Is a Substrate for the cGAS/STING Pathway But Is Not Sensed in Infected Hepatocytes. *Viruses* (2020) 12(6):592. doi: 10.3390/v12060592
49. Yang Y, Zhao X, Wang Z, Shu W, Li L, Li Y, et al. Nuclear Sensor Interferon-Inducible Protein 16 Inhibits the Function of Hepatitis B Virus Covalently Closed Circular DNA by Integrating Innate Immune Activation and Epigenetic Suppression. *Hepatology* (2020) 71(4):1154–69. doi: 10.1002/hep.30897
50. Zhang Z, Trippler M, Real CI, Werner M, Luo X, Schefczyk S, et al. Hepatitis B Virus Particles Activate Toll-Like Receptor 2 Signaling Initial Upon Infection of Primary Human Hepatocytes. *Hepatology* (2020) 72(3):829–44. doi: 10.1002/hep.31112
51. Fletcher SP, Chin DJ, Gruenbaum L, Bitter H, Rasmussen E, Ravindran P, et al. Intrahepatic Transcriptional Signature Associated With Response to Interferon-alpha Treatment in the Woodchuck Model of Chronic Hepatitis B. *PloS Pathog* (2015) 11(9):e1005103. doi: 10.1371/journal.ppat.1005103
52. Bertoletti A, Gehring A. Immune Response and Tolerance During Chronic Hepatitis B Virus Infection. *Hepatol Res* (2007) 37(Suppl 3):S331–8. doi: 10.1111/j.1872-034X.2007.00221.x
53. Wang Y, Menne S, Jacob JR, Tennant BC, Gerin JL, Cote PJ. Role of Type 1 *Versus* Type 2 Immune Responses in Liver During the Onset of Chronic Woodchuck Hepatitis Virus Infection. *Hepatology* (2003) 37(4):771–80. doi: 10.1053/jhep.2003.50154
54. Fletcher SP, Chin DJ, Ji Y, Iniguez AL, Taillon B, Swinney DC, et al. Transcriptomic Analysis of the Woodchuck Model of Chronic Hepatitis B. *Hepatology* (2012) 56(3):820–30. doi: 10.1002/hep.25730
55. Luangsay S, Gruffaz M, Isorce N, Testoni B, Michelet M, Faure-Dupuy S, et al. Early Inhibition of Hepatocyte Innate Responses by Hepatitis B Virus. *J Hepatol* (2015) 63(6):1314–22. doi: 10.1016/j.jhep.2015.07.014
56. Wu J, Huang S, Zhao X, Chen M, Lin Y, Xia Y, et al. Poly(I:C) Treatment Leads to Interferon-Dependent Clearance of Hepatitis B Virus in a Hydrodynamic Injection Mouse Model. *J Virol* (2014) 88(18):10421–31. doi: 10.1128/JVI.00996-14

Conflict of Interest: SM serves occasionally as a paid scientific consultant to Northeastern Wildlife, Inc. (Harris, ID, USA), the only commercial source for woodchucks within the United States, from which the animals of the current study were purchased.

The remaining authors declare that the research was conducted in the absence of any commercial or financial relationships that could be construed as a potential conflict of interest.

frontiers in Immunology

MINI REVIEW
published: 06 August 2021
doi: 10.3389/fimmu.2021.721975

HBV-Specific CD8+ T-Cell Tolerance in the Liver

Ian Baudi[1], *Keigo Kawashima*[1] *and Masanori Isogawa*[2]*

[1] Department of Virology and Liver Unit, Nagoya City University Graduate School of Medical Sciences, Nagoya, Japan,
[2] Research Center for Drug and Vaccine Development, National Institute of Infectious Diseases, Tokyo, Japan

Hepatitis B virus (HBV) remains a leading cause of liver-related morbidity and mortality through chronic hepatitis that may progress to liver cirrhosis and cancer. The central role played by HBV-specific CD8+ T cells in the clearance of acute HBV infection, and HBV-related liver injury is now well established. Vigorous, multifunctional CD8+ T cell responses are usually induced in most adult-onset HBV infections, while chronic hepatitis B (CHB) is characterized by quantitatively and qualitatively weak HBV-specific CD8+ T cell responses. The molecular basis of this dichotomy is poorly understood. Genomic analysis of dysfunctional HBV-specific CD8+ T cells in CHB patients and various mouse models suggest that multifaceted mechanisms including negative signaling and metabolic abnormalities cooperatively establish CD8+ T cell dysfunction. Immunoregulatory cell populations in the liver, including liver resident dendritic cells (DCs), hepatic stellate cells (HSCs), myeloid-derived suppressor cells (MDSCs), may contribute to intrahepatic CD8+ T cell dysfunction through the production of soluble mediators, such as arginase, indoleamine 2,3-dioxygenase (IDO) and suppressive cytokines and the expression of co-inhibitory molecules. A series of recent studies with mouse models of HBV infection suggest that genetic and epigenetic changes in dysfunctional CD8+ T cells are the manifestation of prolonged antigenic stimulation, as well as the absence of co-stimulatory or cytokine signaling. These new findings may provide potential new targets for immunotherapy aiming at invigorating HBV-specific CD8+ T cells, which hopefully cures CHB.

Keywords: T cell exhaustion, liver tolerance, co-inhibitory signaling, metabolic regulation, intrahepatic antigen recognition, interferon signaling, hepatitis B virus

OPEN ACCESS

Edited by:
Jia Liu,
Huazhong University of Science and Technology, China

Reviewed by:
Sachiyo Yoshio,
National Center For Global Health and Medicine, Japan
Yongyin Li,
Southern Medical University, China
Zhiyong Ma,
Wuhan University, China

***Correspondence:**
Masanori Isogawa
nisogawa@niid.go.jp

Specialty section:
This article was submitted to Viral Immunology, a section of the journal Frontiers in Immunology

Received: *08 June 2021*
Accepted: *13 July 2021*
Published: *06 August 2021*

Citation:
Baudi I, Kawashima K and Isogawa M (2021) HBV-Specific CD8+ T-Cell Tolerance in the Liver. Front. Immunol. 12:721975. doi: 10.3389/fimmu.2021.721975

INTRODUCTION

Hepatitis B virus (HBV) chronically infects more than 250 million people worldwide, which is more than seven times the number of the human immunodeficiency virus (HIV) (1). Chronic hepatitis B (CHB) accounted for over 800,000 deaths in 2015, rivaling HIV (2). Of the estimated 250 million chronic HBV (CHB) carriers worldwide, treatment is indicated in just a small fraction (10-30%) (1). Moreover, although current HBV therapies like nucleos(t)ide analogs (NAs) can effectively suppress viral replication, they are incapable of directly targeting the stable episomal HBV reservoir, the covalently closed circular DNA (cccDNA) (2). CHB patients remain at risk of developing liver

cirrhosis and cancer despite available potentially life-long and non-curative treatment (3, 4). This situation justifies an urgent need for more effective HBV therapies.

The central role played by T cell responses in the control of HBV infection is now well recognized (5–7). Immunocompetent human adults readily clear acute HBV infection, up to 95% of the time (8). T cell responses behind the transient, self-limited infections are often described as strong and polyclonal (9–11). In experimentally infected chimpanzees, depletion of CD8+ T cells at the peak of viremia delays viral clearance until the T cells return, providing the most definitive evidence that HBV clearance is largely mediated by virus-specific CD8+ T cells. Meanwhile, CD4+ T cells aid the activation and maintenance of the CD8+ T cell responses in addition to triggering HBV-specific humoral responses that prevent viral dissemination (12, 13). In CHB patients, T cell responses are quantitively weak, and if present, functionally impaired (9, 14). It has become evident that multiple factors contribute to T cell dysfunction, but immunological events in the liver appear particularly important to establish T cell tolerance to HBV. The liver environment has generally been considered tolerogenic, plausibly to avoid detrimental immune reaction to gut-derived microorganisms and xenobiotics (15, 16). The cellular and molecular immunoregulatory mechanisms behind this long-standing notion, and especially its implications on HBV clinical outcomes, are beginning to be understood.

In this mini-review, we summarize the current understanding of immunological factors deemed to contribute to T cell dysfunction in the liver. A full appreciation of the mechanisms behind intrahepatic T cell dysfunction is essential to develop a 'cure' for CHB and liver cancer by immune reinvigoration.

T CELL DYSFUNCTION DURING HBV INFECTION

Several human and animal studies have sought to define the frequency, phenotype, and function of HBV-specific CD8+ T cells to compare and contrast these features between acute HBV resolvers and CHB patients (11, 14, 17–20). There is consensus that in CHB, effector CD8+ T cells show multiple levels of an 'exhausted' phenotype, i.e., markedly reduced capacity to proliferate, produce IFNγ, IL-2, TNFα, granzymes, or perforins (9, 11, 18, 21). Characteristically low frequencies of HBV-specific CD8+ T cells are often recorded in CHB patients than in acute resolvers (14, 17, 18). Low CD8+ T cell numbers could be due to either poor expansion or increased clonal deletion. Frequency alone may not be of absolute importance over the function and breadth of the T cell population (11, 14, 20). A higher frequency of functional but partially exhausted CD8+ T cell with a CD127+ PD1+ phenotype was previously described in inactive CHB carriers. A subset showing more profound exhaustion displayed the CD127- PD1+ phenotype (20). Recently, acute resolvers were shown to have a multi-specific T cell repertoire covering HBV core, polymerase, and envelope epitopes in all the study participants. By contrast, a fraction of the CHB patients in the same study had T cells against HBV core and polymerase, with none against the HBV envelope (11). Similarly, HBV core and polymerase but not envelope specific CD8+ T cells were found in peripheral circulation in CHB patients in an independent study (20). The absence of envelope-specific CD8+ T cells is thought to reflect clonal deletion, as envelope-specific CD8+ T cells presumably become hyper-responsive to the relatively abundant hepatitis B surface antigen (HBsAg). However, caution should be exercised in interpreting these findings since only a few CD8+ T cell epitopes have been tested for each antigen. Besides the quantities of the cognate antigen, differences in antigen processing in the liver may also affect the qualitative and quantitative features of HBV-specific CD8+ T cells.

MECHANISMS OF HBV-SPECIFIC CD8+ T CELL DYSFUNCTION

Potential mechanisms of HBV-specific CD8+ T cell dysfunction are summarized in **Figure 1**, and discussed below.

Immunoregulatory Mediators in Liver Tolerance

Early studies on MHC mismatched liver transplants in animal models established the liver as a tolerogenic organ (15). Furthermore, studies in the 1970s already showed that soluble human and rat liver extracts inhibit T cell activation and DNA synthesis (22, 23). These extracts are now known to have been arginase whose high expression levels in the liver and peripheral blood have been associated with antigen nonspecific impairment of T cells in both acute and chronic HBV patients (24, 25). Hepatic necroinflammation may exacerbate the release of these enzymes by hepatic cytolysis. Plausibly, the observed high arginase levels during acute HBV infection serve as part of a regulatory feedback loop to minimize liver damage (24). Similar immunosuppressive enzymes that deplete metabolites required for the proliferation and maintenance of functional T cells, such as the tryptophan-depleting indoleamine-2-3deoxygenase (IDO) have also since been identified (15, 25, 26). These enzymes are secreted by various myeloid immune cells, including monocytic and granulocytic myeloid-derived suppressor cells (MDSCs) that have been found to be enriched in CHB patients (26–28). Interestingly, a recent study by Yang et al. reported that monocytic MDSCs (mMDSCs) were differentially upregulated in HBeAg-positive CHB patients. HBeAg was then shown to trigger mMDSC expansion that led to the IDO-mediated suppression of CD8+ T cell responses *in vitro* (28). Although the mechanism of HBeAg-induced mMDSCs expansion remains to be elucidated, this report, supplementary to the previous reports on HBeAg tolerogenicity (29, 30), suggests a novel targetable way by which HBV exploits nonspecific immunosuppressive effects to maintain liver persistence.

Other liver cell populations such as dendritic cells (DCs), liver sinusoidal endothelial cells (LSECs) hepatic stellate cells (HSCs) may also contribute towards T cell tolerance in the liver by several mechanisms that include: (i) IFNγ-dependent production

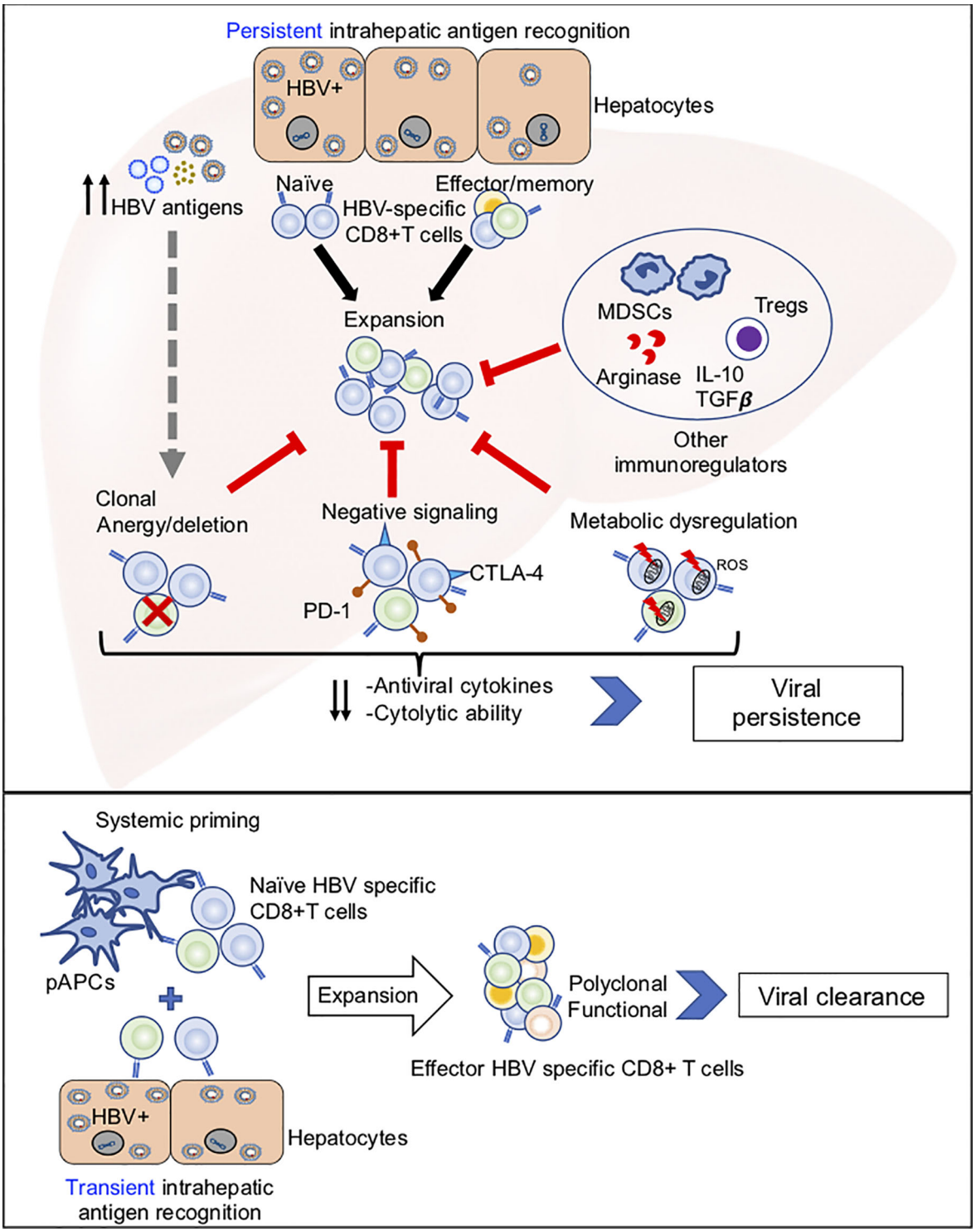

FIGURE 1 | Potential mechanisms of HBV-specific CD8+ T cell dysfunction. Top panel: Illustration of how persistent antigen recognition, predominantly by HBV infected hepatocytes, results in dysfunctional HBV-specific CD8+ T cells that fail to clear infection. Bottom panel: Illustration of how systemic and hepatic antigen recognition may cooperatively trigger robust HBV-specific CD8+ T cell responses that result in viral clearance.

of the soluble factors like IDO, arginase (31) (ii) activation of T regulatory cells (Tregs) *via* the expression of anti-inflammatory cytokines such as interleukin-10 (IL10) and transforming growth factor-beta (TGFβ) (15, 16, 32), (iii) upregulation of co-inhibitory receptor ligands, particularly PD-L1 that leads to T cell exhaustion in a positive feedback cycle with IL10 and TGFβ1 (32, 33) (iv) Expression of cell killing ligands like FasL and TRAIL (34). Notably, liver DCs have been described as immature and dysfunctional compared to peripheral DCs (35). However, this remains controversial in CHB because some studies don't report any such difference (36).

Negative Signaling Mechanisms

Exhausted CD8+ T cells exhibit reduced effector function often in association with upregulation of co-inhibitory receptors such as PD-1, cytotoxic T-lymphocyte associated antigen 4 (CTLA-4), T-cell immunoglobulin and mucin domain-containing protein (Tim-3) (37–41). Of these, PD1-PD-L1 interactions have so far received the greatest attention as a target for tumor immune therapy. Ligation of PD-L1 to PD-1 receptors on T cells impairs downstream TCR signaling to inhibit their immune activation (33). A brief overview of how PD-1 expression is regulated in general is given by Bally et al. (42). The role of PD-1-PD-L1 in HBV-specific CD8+ T cell dysfunction (37, 38, 43–46) has been intensively investigated. Sustained PD-1upregulation is correlated with HBV-specific T cell dysfunction during CHB (18, 43) and PD-L1 expression on peripheral blood was shown to be upregulated in CHB patients (47). PD-L1 expression could also be induced on hepatocytes by type I and type II interferons (48). Anti-PD-L1 treatment on CHB patient-derived peripheral and intrahepatic HBV-specific CD8+ T cells enhanced IFNγ expression *in vitro* (38, 44), suggesting the immune restoration potential of PD-1 blockade. However, promising results of the *in vitro* studies do not necessarily assure therapeutic value *in vivo*. In HBV transgenic mice, antibody blockade, as well as genetic removal of PD-1 signaling, increased the frequency of HBV-specific CD8+ T cells, but the majority of HBV-specific CD8+ T cells remained dysfunctional (37). Importantly, a recent clinical study by Gane et al. showed that treatment of HBeAg negative CHB patients with a single dose of the PD-1 antibody Nivolumab resulted in modest HBsAg reduction within 24 weeks without any adverse events (46), and only one out of 10 patients exhibited HBsAg seroconversion and strong induction of HBV-specific CD8+ T cell responses. While the results were encouraging, the therapeutic impact of PD-1 signaling blockade was rather marginal. The data raises the possibility that other yet unknown co-regulatory molecules are present to suppress HBV-specific CD8+ T cell responses. Simultaneous blockade of multiple inhibitory receptors seems to improve therapeutic potential. In vivo co-blockade of PD-1/LAG-3 and PD-1/Tim-3 during LCMV infection synergistically enhanced CD8+ T cell responses (49, 50). Dual PD-1/CTLA-4 pathway blockade showed similar synergism in partially reversing HBV-specific CD8+ T cell exhaustion *in vitro* (51) There is a paucity of data on the impact of multiple target blockade in CHB, and the nature and extent of negative regulatory molecules' co-regulation and expression may differ between patients. Personalized T cell characterization may be required for optimized treatment to reverse T cell exhaustion.

Metabolic Dysregulation in T Cells

Metabolic reprogramming after priming is important for T cell differentiation because energy demand largely differs between naïve, effector, and memory T cells (52–54), and mitochondrial plasticity is directly linked to T cell metabolism (55). Metabolic abnormalities, such as reduced glycolysis and oxidative phosphorylation, were observed in exhausted virus-specific CD8+ T cells during the early phase of chronic lymphocytic choriomeningitis virus (LCMV) infection (56). PD-1 high HBV-specific CD8+ T cells in CHB patients were also shown to highly express the glucose transporter, Glut1, and dependent on glucose supplies (57). These changes were accompanied by increased mitochondrial size and lower mitochondrial potential. Recently, Fisicaro et al. reported extensive mitochondrial dysfunction, such as mitochondrial membrane potential depolarization and reactive oxygen species (ROS) elevation in association with upregulation of co-inhibitory receptor genes in the CD8+ T cells from CHB patients (58). More importantly, mitochondrial antioxidant treatment using mitoquinone and a piperidine-nitroxide could modestly enhance IFNγ production by HBV-core specific CD8+ T cells from these patients (58), indicating a potential role for ROS in CD8+ T cell exhaustion. Coordinated protein catabolism by the ubiquitin-proteasome and autophagy-lysosome systems is also essential for CD8+ T cell survival, proliferation, and memory formation (59–61). In addition, autophagy was recently shown to enable HBV-specific effector memory CD8+ T cells to reside in the liver and resist mitochondrial depolarization (62). Importantly, genes associated with ubiquitin-proteasome and autophagy-lysosome systems were also markedly downregulated in exhausted HBV-specific CD8+ T cells in CHB patients (59, 63). In vitro treatment of exhausted HBV-specific CD8+ T cells with polyphenols, such as resveratrol and oleuropein, improved autophagic influx and antiviral CD8+ T cell function (64). More recently, p53, a known negative regulator of glycolysis and an enhancer of oxidative phosphorylation (OXPHOS), was shown to be upregulated in exhausted HCV-specific CD8+ T cells from chronic HCV patients (65). Its relevance to chronic HBV infection remains to be determined because p53 was thought to be upregulated by type I interferon (IFN-I) response, which is largely absent during HBV infections. Overall, these results characterize CD8+ T cell exhaustion as a state of metabolic insufficiencies with suppressed mitochondrial respiration, glycolysis, protein degradation. These abnormalities are reminiscent of functional defects previously associated with CD8+ T cell senescence, although exhaustion and senescence are distinctly different in terms of generation, development, and metabolic and molecular regulation (63, 66).

Intrahepatic Antigen Recognition

The tolerogenic environment in the liver likely contributes to imprinting the genetic and epigenetic signatures in the dysfunctional HBV-specific CD8+ T cells during CHB. It is important to keep it in mind, however, that efficient HBV-specific CD8+ T cell responses are induced in the majority of

adult-onset HBV infections, resulting in viral clearance. Factors that determine the dichotomy presumably include traditional factors such as T cell receptor (TCR) signaling (signal 1), co-stimulatory signaling (signal 2), and cytokine signaling (signal 3).

A strong antigenic stimulus is necessary for effective CD8+ T cell responses (67). We have shown recently that the magnitude of HBV-specific CD8+ T cell responses was directly correlated with the level of early antigen expression in an animal model of transient HBV infection, i.e., hydrodynamic transfection of HBV plasmid (67). Suppression of HBV by siRNA also inhibited the expansion of HBV-specific CD8+ T cells (67), indicating the importance of strong antigen recognition for the induction of HBV-specific CD8+ T cell responses. Paradoxically, the same antigenic stimulus becomes extremely detrimental for T cell responses if it is prolonged (68–70). Indeed, HBV-specific effector memory CD8+ T cells that were generated by DNA-prime, vaccinia-boost immunization produced a large amount of IFNγ upon antigen recognition in the liver, but they lost the IFNγ producing ability almost completely within three days during which they continuously recognized antigen and express PD-1 (71). Slow blood flow in the liver sinusoid, as well as tightly packed microanatomy of the hepatic parenchyma, facilitate prolonged interaction between HBV infected hepatocytes and HBV-specific CD8+ T cells (72). Intravital imaging analysis revealed that HBV-specific CD8+ T cells were able to recognize HBV expressing hepatocytes while they were still in the sinusoid (73). Prolonged antigen recognition appears to inhibit TCR signaling partially through PD-1 signaling (74).

Antigen presentation by hepatocytes alone is probably insufficient for priming of functional HBV-specific CD8+ T cell responses. We have previously shown that HBV-specific naïve CD8+ T cells are primed by HBV-expressing hepatocytes (75). Although hepatocyte-primed naïve and memory HBV-specific CD8+ T can expand rapidly, they produce very little to no IFNγ and Granzyme B (75–77). The lack of functional differentiation presumably reflects the absence of co-stimulatory signaling (i.e., signal 2) as hepatocytes do not express ligands for co-stimulatory molecules. Indeed, activation of dendritic cells appears to facilitate functional differentiation of intrahepatically primed CD8+ T cells (75, 76). In addition, expression of a co-stimulatory molecule OX40 expression by CD4 T cells and its ligand OX40L by hepatic innate immune cells were shown to be pivotal in determining HBV immunity in an HBsAg transgenic mouse model (78).

Recently, we and others characterized genetic signatures of intrahepatic T cell priming. Similar to HBV-specific CD8+ T cells in CHB patients, the intrahepatically primed, dysfunctional CD8+ T cells showed upregulation of inhibitory molecules PD-1, Lag 3, and Tim-3, together with enrichment in binding sites for the transcription factors AP-1, NFAT, NR4A, OCT, TCF, and EGR (79). Interestingly, NR4A has been implicated in T cell exhaustion that limits CAR-T cell-based immunotherapy in solid tumors and LCMV infection (80, 81). In stark contrast to exhausted CD8+ T cells during LCMV infection, genes related to IFN-I signaling activation were downregulated in intrahepatically primed T cells. Importantly, strong stimulation of IFN-I signaling in the liver enhanced T cell responses (82), suggesting that IFN-Is indeed provide the third signal (signal 3) that complements the TCR signal (signal 1) and co-stimulatory signal (signal 2). It should be noted, however, that the same IFN-I signaling could suppress HBV-specific CD8+ T cell responses by reducing antigen expression levels during the early phase of T cell priming (67), a phenomenon recently highlighted in the development of RNA vaccines (83).

PERSPECTIVES

Recent advances in unbiased deep sequencing and other genetic analysis methods have accelerated the delineation of CD8+ T cell dysfunction in the liver, providing numerous targets to test for novel immunotherapies against CHB. It would be now important to determine whether the functionalities of highly exhausted T cells are reversible. Even more crucial is to establish an ideal animal model for evaluating the therapeutic value of each target. Several mouse models have been used to study HBV-specific CD8+ T cell responses during transient and persistent antigen expression. The advantages and disadvantages of each mouse model have been described elsewhere (84, 85). While these models provided useful information on T cell responses, none of them mimics a bona fide HBV infection. It is therefore essentially impossible to assess the extent to which chronically infected individuals can tolerate the restoration of HBV-specific CD8+ T cell responses, as the expansion of functional CD8+ T cells likely cause hepatitis. In this regard, antigen suppression should be incorporated in the immune restoration approach to mitigate the risk of uncontrolled T cell expansion.

CONCLUSION

Given the stability of cccDNA, invigoration of HBV-specific CD8+ T cells remains one of the most viable approaches to cure CHB. Therefore, delineation of the key pathways and processes that underline HBV-specific CD8+ T cell dysfunction T cell is an important research goal to develop effective HBV immunotherapies.

AUTHOR CONTRIBUTIONS

MI conceived the outline of the manuscript. IB and MI wrote the original manuscript. IB and MI selected the references. IB prepared the Figure. KK reviewed the manuscript. All authors contributed to the article and approved the submitted version.

FUNDING

This work was supported by grants-in-aid from the Ministry of Education, Cultures, Sports, Science, and Technology, Japan: From Japan Society for Promotion of Science (KAKENHI) under

grants 20K08313 (to MI); and from the Research Program on Hepatitis from the Japan Agency for Medical Research and Development (AMED) under grants 21fk0310106s0405 (to MI), 21fk0310101h1205 (to MI), and 21fk0310103j8005 (to MI).

ACKNOWLEDGMENTS

The authors like to thank Drs. Francis V. Chisari, Tatsuya Kanto, and Yasuhito Tanaka for continuous guidance and support.

REFERENCES

1. Thomas DL. Global Elimination of Chronic Hepatitis. *N Engl J Med* (2019) 380:2041–50. doi: 10.1056/nejmra1810477
2. Lok AS, Zoulim F, Dusheiko G, Ghany MG. Hepatitis B Cure: From Discovery to Regulatory Approval. *Hepatology* (2017) 66:1296–313. doi: 10.1002/hep.29323
3. World Health Organization (WHO). *Global Hepatitis Report* (2017). Available at: https://www.who.int/publications/i/item/global-hepatitis-report-2017.
4. Arbuthnot P, Kew M. Hepatitis B Virus and Hepatocellular Carcinoma. *Int J Exp Pathol* (2001) 82:77–100. doi: 10.1186/1750-9378-7-2
5. Thimme R, Wieland S, Steiger C, Ghrayeb J, Reimann KA, Purcell RH, et al. CD8+ T Cells Mediate Viral Clearance and Disease Pathogenesis During Acute Hepatitis B Virus Infection. *J Virol* (2003) 77:68–76. doi: 10.1128/jvi.77.1.68-76.2003
6. Guidotti LG, Ishikawa T, Hobbs MV, Matzke B, Schreiber R, Chisari FV. Intracellular Inactivation of the Hepatitis B Virus by Cytotoxic T Lymphocytes. *Immunity* (1996) 4:25–36. doi: 10.1016/S1074-7613(00)80295-2
7. Guidotti LG, Isogawa M, Chisari FV. Host-Virus Interactions in Hepatitis B Virus Infection. *Curr Opin Immunol* (2015) 36:61–6. doi: 10.1016/j.coi.2015.06.016
8. Terrault NA, Lok ASF, McMahon BJ, Chang KM, Hwang JP, Jonas MM, et al. Update on Prevention, Diagnosis, and Treatment of Chronic Hepatitis B: AASLD 2018 Hepatitis B Guidance. *Clin Liver Dis* (2018) 12:33–4. doi: 10.1002/cld.728
9. Chisari FVV, Isogawa M, Wieland SF, Wieland SF. Pathogenesis of Hepatitis B Virus Infection. *Pathol Biol* (2010) 58:258–66. doi: 10.1016/j.patbio.2009.11.001
10. Maini MK, Boni C, Ogg GS, King AS, Reignat S, Chun KL, et al. Direct Ex Vivo Analysis of Hepatitis B Virus-Specific CD8+ T Cells Associated With the Control of Infection. *Gastroenterology* (1999) 117:1386–96. doi: 10.1016/S0016-5085(99)70289-1
11. Hoogeveen RC, Robidoux MP, Schwarz T, Heydmann L, Cheney JA, Kvistad D, et al. Phenotype and Function of HBV-Specific T Cells Is Determined by the Targeted Epitope in Addition to the Stage of Infection. *Gut* (2019) 68:893–904. doi: 10.1136/gutjnl-2018-316644
12. Asabe S, Wieland SF, Chattopadhyay PK, Roederer M, Engle RE, Purcell RH, et al. The Size of the Viral Inoculum Contributes to the Outcome of Hepatitis B Virus Infection. *J Virol* (2009) 83:9652–62. doi: 10.1128/jvi.00867-09
13. Yang PL, Althage A, Chung J, Maier H, Wieland S, Isogawa M, et al. Immune Effectors Required for Hepatitis B Virus Clearance. *Proc Natl Acad Sci USA* (2010) 107:798–802. doi: 10.1073/pnas.0913498107
14. Webster GJM, Reignat S, Brown D, Ogg GS, Jones L, Seneviratne SL, et al. Longitudinal Analysis of CD8+ T Cells Specific for Structural and Nonstructural Hepatitis B Virus Proteins in Patients With Chronic Hepatitis B: Implications for Immunotherapy. *J Virol* (2004) 78:5707–19. doi: 10.1128/jvi.78.11.5707-5719.2004
15. Crispe IN. Immune Tolerance in Liver Disease. *Hepatology* (2014) 60:2109–17. doi: 10.1002/hep.27254
16. Knolle PA, Thimme R. Hepatic Immune Regulation and Its Involvement in Viral Hepatitis Infection. *Gastroenterology* (2014) 146:1193–207. doi: 10.1053/j.gastro.2013.12.036
17. Sobao Y, Tomiyama H, Sugi K, Tokunaga M, Ueno T, Saito S, et al. The Role of Hepatitis B Virus-Specific Memory CD8 T Cells in the Control of Viral Replication. *J Hepatol* (2002) 36:105–15. doi: 10.1016/S0168-8278(01)00264-1
18. Boni C, Fisicaro P, Valdatta C, Amadei B, Di Vincenzo P, Giuberti T, et al. Characterization of Hepatitis B Virus (HBV)-Specific T-Cell Dysfunction in Chronic HBV Infection. *J Virol* (2007) 81:4215–25. doi: 10.1128/jvi.02844-06
19. Das A, Hoare M, Davies N, Lopes AR, Dunn C, Kennedy PTF, et al. Functional Skewing of the Global CD8 T Cell Population in Chronic Hepatitis B Virus Infection. *J Exp Med* (2008) 205:2111–24. doi: 10.1084/jem.20072076
20. Schuch A, Salimi Alizei E, Heim K, Wieland D, Kiraithe MM, Kemming J, et al. Phenotypic and Functional Differences of HBV Core-Specific Versus HBV Polymerase-Specific CD8+ T Cells in Chronically HBV-Infected Patients With Low Viral Load. *Gut* (2019) 68:905–15. doi: 10.1136/gutjnl-2018-316641
21. Park JJ, Wong DK, Wahed AS, Lee WM, Feld JJ, Terrault N, et al. Hepatitis B Virus-Specific and Global T-Cell Dysfunction in Chronic Hepatitis B. *Gastroenterology* (2016) 150:684–95. doi: 10.1053/j.gastro.2015.11.050
22. Chisari FV. Regulation of Human Lymphocyte Function by a Soluble Extract From Normal Human Liver. *J Immunol* (1978) 121:1279–86.
23. Pizzo C, Lee D, Chisari FV. Suppression of Lymphocyte Activation by a Protein Released From Isolated Perfused Rat Liver. *Hepatology* (2007) 2:295S–303S. doi: 10.1002/hep.1840020302
24. Sandalova E, Laccabue D, Boni C, Watanabe T, Tan A, Zong HZ, et al. Increased Levels of Arginase in Patients With Acute Hepatitis B Suppress Antiviral T Cells. *Gastroenterology* (2012) 143:78–87.e3. doi: 10.1053/j.gastro.2012.03.041
25. Pallett LJ, Gill US, Quaglia A, Sinclair LV, Jover-Cobos M, Schurich A, et al. Metabolic Regulation of Hepatitis B Immunopathology by Myeloid-Derived Suppressor Cells. *Nat Med* (2015) 21:591–600. doi: 10.1038/nm.3856
26. Molinier-Frenkel V, Castellano F. Immunosuppressive Enzymes in the Tumor Microenvironment. *FEBS Lett* (2017) 591:3135–57. doi: 10.1002/1873-3468.12784
27. Huang A, Zhang B, Yan W, Wang B, Wei H, Zhang F, et al. Myeloid-Derived Suppressor Cells Regulate Immune Response in Patients With Chronic Hepatitis B Virus Infection Through PD-1–Induced IL-10. *J Immunol* (2014) 193:5461–9. doi: 10.4049/jimmunol.1400849
28. Yang F, Yu X, Zhou C, Mao R, Zhu M, Zhu H, et al. Hepatitis B E Antigen Induces the Expansion of Monocytic Myeloid-Derived Suppressor Cells to Dampen T-Cell Function in Chronic Hepatitis B Virus Infection. *PloS Pathog* (2019) 15:e1007690. doi: 10.1371/journal.ppat.1007690
29. Ferrando-Martinez S, Huang K, Bennett AS, Sterba P, Yu L, Suzich JA, et al. HBeAg Seroconversion Is Associated With a More Effective PD-L1 Blockade During Chronic Hepatitis B Infection. *JHEP Rep* (2019) 1:170–8. doi: 10.1016/j.jhepr.2019.06.001
30. Tian Y, Kuo C, Akbari O, Ou J-HJ. Maternal-Derived Hepatitis B Virus E Antigen Alters Macrophage Function in Offspring to Drive Viral Persistence After Vertical Transmission. *Immunity* (2016) 44:1204–14. doi: 10.1016/j.immuni.2016.04.008
31. Mondanelli G, Bianchi R, Pallotta MT, Orabona C, Albini E, Iacono A, et al. A Relay Pathway Between Arginine and Tryptophan Metabolism Confers Immunosuppressive Properties on Dendritic Cells. *Immunity* (2017) 46:233–44. doi: 10.1016/j.immuni.2017.01.005
32. Li H, Zhai N, Wang Z, Song H, Yang Y, Cui A, et al. Regulatory NK Cells Mediated Between Immunosuppressive Monocytes and Dysfunctional T Cells in Chronic HBV Infection. *Gut* (2018) 67:2035–44. doi: 10.1136/gutjnl-2017-314098
33. Okazaki T, Honjo T. The PD-1-PD-L Pathway in Immunological Tolerance. *Trends Immunol* (2006) 27:195–201. doi: 10.1016/j.it.2006.02.001
34. Peppa D, Gil US, Reynolds G, Easom NJW, Pallett LJ, Schurich A, et al. Up-Regulation of a Death Receptor Renders Antiviral T Cells Susceptible to NK Cell–Mediated Deletion. *J Exp Med* (2013) 210:99–114. doi: 10.1084/jem.20121172
35. Fisicaro P, Barili V, Rossi M, Montali I, Vecchi A, Acerbi G, et al. Pathogenetic Mechanisms of T Cell Dysfunction in Chronic HBV Infection and Related Therapeutic Approaches. *Front Immunol* (2020) 11:849. doi: 10.3389/fimmu.2020.00849
36. Gehring AJ, D'Angelo JA. Dissecting the Dendritic Cell Controversy in Chronic Hepatitis B Virus Infection. *Cell Mol Immunol* (2015) 12:283–91. doi: 10.1038/cmi.2014.95
37. Maier H, Isogawa M, Freeman GJ, Chisari FV. PD-1:PD-L1 Interactions Contribute to the Functional Suppression of Virus-Specific CD8 + T Lymphocytes in the Liver. *J Immunol* (2007) 178:2714–20. doi: 10.4049/jimmunol.178.5.2714

38. Bengsch B, Martin B, Thimme R. Restoration of HBV-Specific CD8+ T Cell Function by PD-1 Blockade in Inactive Carrier Patients Is Linked to T Cell Differentiation. *J Hepatol* (2014) 61:1212–9. doi: 10.1016/j.jhep.2014.07.005
39. Wykes MN, Lewin SR. Immune Checkpoint Blockade in Infectious Diseases. *Nat Rev Immunol* (2018) 18:91–104. doi: 10.1038/nri.2017.112
40. Barber DL, Wherry EJ, Masopust D, Zhu B, Allison JP, Sharpe AH, et al. Restoring Function in Exhausted CD8 T Cells During Chronic Viral Infection. *Nature* (2006) 439:682–7. doi: 10.1038/nature04444
41. Isogawa M, Tanaka Y. Immunobiology of Hepatitis B Virus Infection. *Hepatol Res* (2015) 45:179–89. doi: 10.1111/hepr.12439
42. Bally APR, Austin JW, Boss JM. Genetic and Epigenetic Regulation of PD-1 Expression. *J Immunol* (2016) 196:2431–7. doi: 10.4049/jimmunol.1502643
43. Peng G, Li S, Wu W, Tan X, Chen Y, Chen Z. PD-1 Upregulation Is Associated With HBV-Specific T Cell Dysfunction in Chronic Hepatitis B Patients. *Mol Immunol* (2008) 45:963–70. doi: 10.1016/j.molimm.2007.07.038
44. Fisicaro P, Valdatta C, Massari M, Loggi E, Ravanetti L, Urbani S, et al. Combined Blockade of Programmed Death-1 and Activation of CD137 Increase Responses of Human Liver T Cells Against HBV, But Not HCV. *Gastroenterology* (2012) 143:1576–85.e4. doi: 10.1053/j.gastro.2012.08.041
45. Jacobi FJ, Wild K, Smits M, Zoldan K, Csernalabics B, Flecken T, et al. OX40 Stimulation and PD-L1 Blockade Synergistically Augment HBV-Specific CD4 T Cells in Patients With HBeAg-Negative Infection. *J Hepatol* (2019) 70:1103–13. doi: 10.1016/j.jhep.2019.02.016
46. Gane E, Verdon DJ, Brooks AE, Gaggar A, Nguyen AH, Subramanian GM, et al. Anti-PD-1 Blockade With Nivolumab With and Without Therapeutic Vaccination for Virally Suppressed Chronic Hepatitis B: A Pilot Study. *J Hepatol* (2019) 71:900–7. doi: 10.1016/j.jhep.2019.06.028
47. Chen J, Wang X-M, Wu X-J, Wang Y, Zhao H, Shen B, et al. Intrahepatic Levels of PD-1/PD-L Correlate With Liver Inflammation in Chronic Hepatitis B. *Inflammation Res* (2011) 60:47–53. doi: 10.1007/s00011-010-0233-1
48. Mühlbauer M, Fleck M, Schütz C, Weiss T, Froh M, Blank C, et al. PD-L1 Is Induced in Hepatocytes by Viral Infection and by Interferon-Alpha and -Gamma and Mediates T Cell Apoptosis. *J Hepatol* (2006) 45:520–8. doi: 10.1016/j.jhep.2006.05.007
49. Blackburn SD, Shin H, Haining WN, Zou T, Workman CJ, Polley A, et al. Coregulation of CD8+ T Cell Exhaustion by Multiple Inhibitory Receptors During Chronic Viral Infection. *Nat Immunol* (2009) 10:29–37. doi: 10.1038/ni.1679
50. Jin HTH-T, Anderson AC, Tan WG, West EE, Ha SJS-J, Araki K, et al. Cooperation of Tim-3 and PD-1 in CD8 T-Cell Exhaustion During Chronic Viral Infection. *Proc Natl Acad Sci USA* (2010) 107:14733–8. doi: 10.1073/pnas.1009731107
51. Schurich A, Khanna P, Lopes AR, Han KJ, Peppa D, Micco L, et al. Role of the Coinhibitory Receptor Cytotoxic T Lymphocyte Antigen-4 on Apoptosis-Prone CD8 T Cells in Persistent Hepatitis B Virus Infection. *Hepatology* (2011) 53:1494–503. doi: 10.1002/hep.24249
52. Chang JT, Wherry EJ, Goldrath AW. Molecular Regulation of Effector and Memory T Cell Differentiation. *Nat Immunol* (2014) 15:1104–15. doi: 10.1038/ni.3031
53. MacIver NJ, Michalek RD, Rathmell JC. Metabolic Regulation of T Lymphocytes. *Annu Rev Immunol* (2013) 31:259–83. doi: 10.1146/annurev-immunol-032712-095956
54. Chang C-H, Curtis JD, Maggi LB, Faubert B, Villarino AV, O'Sullivan D, et al. Posttranscriptional Control of T Cell Effector Function by Aerobic Glycolysis. *Cell* (2013) 153:1239–51. doi: 10.1016/j.cell.2013.05.016
55. Franco F, Jaccard A, Romero P, Yu Y-R, Ho P-C. Metabolic and Epigenetic Regulation of T-Cell Exhaustion. *Nat Metab* (2020) 2:1001–12. doi: 10.1038/s42255-020-00280-9
56. Bengsch B, Johnson AL, Kurachi M, Odorizzi PM, Pauken KE, Attanasio J, et al. Bioenergetic Insufficiencies Due to Metabolic Alterations Regulated by the Inhibitory Receptor PD-1 Are an Early Driver of CD8+ T Cell Exhaustion. *Immunity* (2016) 45:358–73. doi: 10.1016/j.immuni.2016.07.008
57. Schurich A, Pallett LJ, Jajbhay D, Wijngaarden J, Otano I, Gill US, et al. Distinct Metabolic Requirements of Exhausted and Functional Virus-Specific CD8 T Cells in the Same Host. *Cell Rep* (2016) 16:1243–52. doi: 10.1016/j.celrep.2016.06.078
58. Fisicaro P, Barili V, Montanini B, Acerbi G, Ferracin M, Guerrieri F, et al. Targeting Mitochondrial Dysfunction can Restore Antiviral Activity of Exhausted HBV-Specific CD8 T Cells in Chronic Hepatitis B. *Nat Med* (2017) 23:327–36. doi: 10.1038/nm.4275
59. Kovacs JR, Li C, Yang Q, Li G, Garcia IG, Ju S, et al. Autophagy Promotes T-Cell Survival Through Degradation of Proteins of the Cell Death Machinery. *Cell Death Differ* (2012) 19:144–52. doi: 10.1038/cdd.2011.78
60. Xu X, Araki K, Li S, Han J-H, Ye L, Tan WG, et al. Autophagy Is Essential for Effector CD8+ T Cell Survival and Memory Formation. *Nat Immunol* (2014) 15:1152–61. doi: 10.1038/ni.3025
61. Widjaja CE, Olvera JG, Metz PJ, Phan AT, Savas JN, de Bruin G, et al. Proteasome Activity Regulates CD8+ T Lymphocyte Metabolism and Fate Specification. *J Clin Invest* (2017) 127:3609–23. doi: 10.1172/JCI90895
62. Swadling L, Pallett LJ, Diniz MO, Baker JM, Amin OE, Stegmann KA, et al. Human Liver Memory CD8+ T Cells Use Autophagy for Tissue Residence. *Cell Rep* (2020) 30:687–98. doi: 10.1016/j.celrep.2019.12.050
63. Akbar AN, Henson SM. Are Senescence and Exhaustion Intertwined or Unrelated Processes That Compromise Immunity? *Nat Rev Immunol* (2011) 11:289–95. doi: 10.1038/nri2959
64. Acerbi G, Montali I, Ferrigno GD, Barili V, Schivazappa S, Alfieri A, et al. Functional Reconstitution of HBV-Specific CD8 T Cells by *In Vitro* Polyphenol Treatment in Chronic Hepatitis B. *J Hepatol* (2021) 74:783–93. doi: 10.1016/j.jhep.2020.10.034
65. Barili V, Fisicaro P, Montanini B, Acerbi G, Filippi A, Forleo G, et al. Targeting P53 and Histone Methyltransferases Restores Exhausted CD8+ T Cells in HCV Infection. *Nat Commun* (2020) 11:604. doi: 10.1038/s41467-019-14137-7
66. Zhao Y, Shao Q, Peng G. Exhaustion and Senescence: Two Crucial Dysfunctional States of T Cells in the Tumor Microenvironment. *Cell Mol Immunol* (2020) 17:27–35. doi: 10.1038/s41423-019-0344-8
67. Kawashima K, Isogawa M, Hamada-Tsutsumi S, Baudi I, Saito S, Nakajima A, et al. Type I Interferon Signaling Prevents Hepatitis B Virus-Specific T Cell Responses by Reducing Antigen Expression. *J Virol* (2018) 92:1–13. doi: 10.1128/jvi.01099-18
68. Wherry EJ, Blattman JN, Murali-Krishna K, van der Most R, Ahmed R. Viral Persistence Alters CD8 T-Cell Immunodominance and Tissue Distribution and Results in Distinct Stages of Functional Impairment. *J Virol* (2003) 77:4911–27. doi: 10.1128/JVI.77.8.4911-4927.2003
69. Michler T, Kosinska AD, Festag J, Bunse T, Su J, Ringelhan M, et al. Knockdown of Virus Antigen Expression Increases Therapeutic Vaccine Efficacy in High-Titer Hepatitis B Virus Carrier Mice. *Gastroenterology* (2020) 158:1762–1775.e9. doi: 10.1053/j.gastro.2020.01.032
70. Mueller SN, Ahmed R. High Antigen Levels are the Cause of T Cell Exhaustion During Chronic Viral Infection. *Proc Natl Acad Sci USA* (2009) 106:8623–8. doi: 10.1073/pnas.0809818106
71. Isogawa M, Furuichi Y, Chisari FV. Oscillating CD8(+) T Cell Effector Functions After Antigen Recognition in the Liver. *Immunity* (2005) 23:53–63. doi: 10.1016/j.immuni.2005.05.005
72. Crispe IN. Hepatic T Cells and Liver Tolerance. *Nat Rev Immunol* (2003) 3:51–62. doi: 10.1038/nri981
73. Guidotti LG, Inverso D, Sironi L, Di Lucia P, Fioravanti J, Ganzer L, et al. Immunosurveillance of the Liver by Intravascular Effector CD8+ T Cells. *Cell* (2015) 161:486–500. doi: 10.1016/j.cell.2015.03.005
74. Sandu I, Cerletti D, Claassen M, Oxenius A. Exhausted CD8+ T Cells Exhibit Low and Strongly Inhibited TCR Signaling During Chronic LCMV Infection. *Nat Commun* (2020) 11:1–11. doi: 10.1038/s41467-020-18256-4
75. Isogawa M, Chung J, Murata Y, Kakimi K, Chisari FV. CD40 Activation Rescues Antiviral CD8+ T Cells From PD-1-Mediated Exhaustion. *PloS Pathog* (2013) 9:1–16. doi: 10.1371/journal.ppat.1003490
76. Murata Y, Kawashima K, Sheikh K, Tanaka Y, Isogawa M. Intrahepatic Cross-Presentation and Hepatocellular Antigen Presentation Play Distinct Roles in the Induction of Hepatitis B Virus-Specific CD8 + T Cell Responses. *J Virol* (2018) 92:1–14. doi: 10.1128/jvi.00920-18
77. Isogawa M, Kakimi K, Kamamoto H, Protzer U, Chisari FV. Differential Dynamics of the Peripheral and Intrahepatic Cytotoxic T Lymphocyte Response to Hepatitis B Surface Antigen. *Virology* (2005) 333:293–300. doi: 10.1016/j.virol.2005.01.004
78. Publicover J, Gaggar A, Jespersen JM, Halac U, Johnson AJ, Goodsell A, et al. An OX40/OX40L Interaction Directs Successful Immunity to Hepatitis B Virus. *Sci Transl Med* (2018) 10:eaah5766. doi: 10.1126/scitranslmed.aah5766

79. Bénéchet AP, De Simone G, Di Lucia P, Cilenti F, Barbiera G, Le Bert N, et al. Dynamics and Genomic Landscape of CD8+ T Cells Undergoing Hepatic Priming. *Nature* (2019) 574:200–5. doi: 10.1038/s41586-019-1620-6
80. Chen J, López-Moyado IF, Seo H, Lio C-WJ, Hempleman LJ, Sekiya T, et al. Genome-Wide Analysis Identifies NR4A1 as a Key Mediator of T Cell Dysfunction. *Nature* (2019) 567:530–4. doi: 10.1038/s41586-019-0985-x
81. Chen J, López-Moyado IF, Seo H, Lio C-WJ, Hempleman LJ, Sekiya T, et al. NR4A Transcription Factors Limit CAR T Cell Function in Solid Tumours. *Nature* (2019) 567:530–4. doi: 10.1038/s41586-019-0985-x
82. Kawashima K, Isogawa M, Onishi M, Baudi I, Saito S, Nakajima A, et al. Restoration of Type I Interferon Signaling in Intrahepatically Primed CD8+ T Cells Promotes Functional Differentiation. *JCI Insight* (2021) 6(3):e145761. doi: 10.1172/jci.insight.145761
83. Van Hoecke L, Roose K, Ballegeer M, Zhong Z, Sanders NN, De Koker S, et al. The Opposing Effect of Type I IFN on the T Cell Response by Non-Modified mRNA-Lipoplex Vaccines Is Determined by the Route of Administration. *Mol Ther - Nucleic Acids* (2020) 22:373–81. doi: 10.1016/j.omtn.2020.09.004
84. Iannacone M, Guidotti LG. Mouse Models of Hepatitis B Virus Pathogenesis. *Cold Spring Harb Perspect Med* (2015) 5:1–11. doi: 10.1101/cshperspect.a021477
85. Inuzuka T, Takahashi K, Chiba T, Marusawa H. Mouse Models of Hepatitis B Virus Infection Comprising Host-Virus Immunologic Interactions. *Pathog (Basel Switzerland)* (2014) 3:377–89. doi: 10.3390/pathogens3020377

Conflict of Interest: The authors declare that the research was conducted in the absence of any commercial or financial relationships that could be construed as a potential conflict of interest.

Publisher's Note: All claims expressed in this article are solely those of the authors and do not necessarily represent those of their affiliated organizations, or those of the publisher, the editors and the reviewers. Any product that may be evaluated in this article, or claim that may be made by its manufacturer, is not guaranteed or endorsed by the publisher.

frontiers in Immunology

ORIGINAL RESEARCH
published: 26 August 2021
doi: 10.3389/fimmu.2021.735913

Follicular Helper T (T_{FH}) Cell Targeting by TLR8 Signaling For Improving HBsAg-Specific B Cell Response In Chronic Hepatitis B Patients

*Natarajan Ayithan[1], Lydia Tang[1], Susanna K. Tan[2], Diana Chen[2], Jeffrey J. Wallin[2], Simon P. Fletcher[2], Shyam Kottilil[1] and Bhawna Poonia[1]**

[1] Division of Clinical Care and Research, Institute of Human Virology, University of Maryland School of Medicine, Baltimore, MD, United States, [2] Clinical Research, Gilead Sciences Inc., Foster City, CA, United States

OPEN ACCESS

Edited by:
Jia Liu,
Huazhong University of Science and Technology, China

Reviewed by:
Martyn Andrew French, University of Western Australia, Australia
Kartika Padhan, National Institutes of Health (NIH), United States

***Correspondence:**
Bhawna Poonia
bpoonia@ihv.umaryland.edu

Specialty section:
This article was submitted to Viral Immunology, a section of the journal Frontiers in Immunology

Received: *03 July 2021*
Accepted: *11 August 2021*
Published: *26 August 2021*

Citation:
Ayithan N, Tang L, Tan SK, Chen D, Wallin JJ, Fletcher SP, Kottilil S and Poonia B (2021) Follicular Helper T (T_{FH}) Cell Targeting by TLR8 Signaling For Improving HBsAg-Specific B Cell Response In Chronic Hepatitis B Patients. Front. Immunol. 12:735913. doi: 10.3389/fimmu.2021.735913

Identifying signaling pathways that induce B cell response can aid functional cure strategies for chronic hepatitis B infection (CHB). TLR8 activation with ssRNA was shown to enhance follicular helper T cell (T_{FH}) function leading to improved B cell responses *in vitro*. We investigated whether this mechanism can rescue an exhausted immune response in CHB infection. Effect of TLR8 agonism on supporting cytokines and T_{FH} and B cells were evaluated using *ex vivo* and *in vitro* assays. The ability of an oral TLR8 agonist to promote T_{FH} and B cell response was tested in samples from phase 1b clinical trial. TLR8 agonism induced T_{FH} polarizing cytokine IL-12 in monocytes. Treatment of peripheral blood mononuclear cells (PBMCs) from CHB patients with TLR8 agonists induced cytokine IL-21 by T_{FH} cells with enhanced IL-21$^+$BCL-6$^+$ and ICOS$^+$BCL-6$^+$ co-expression. Mechanistically, incubation of isolated naïve CD4$^+$ T cells with TLR8 triggered monocytes resulted in their differentiation into IL-21$^+$ICOS$^+$BCL-6$^+$ T_{FH} in an IL-12 dependent manner. Furthermore, co-culture of these IL-21 producing T_{FH} with autologous naïve B cells led to enhanced memory (CD19$^+$CD27$^+$) and plasma B cell generation (CD19$^+$CD27^{++}CD38$^+$) and IgG production. Importantly, in T_{FH} from CHB patients treated with an oral TLR8 agonist, HBsAg-specific BCL-6, ICOS, IL-21 and CD40L expression and rescue of defective activation induced marker (AIM) response along with partial restoration of HBsAg-specific B cell ELISPOT response was evident. TLR8 agonism can thus enhance HBV-specific B cell responses in CHB patients by improving monocyte-mediated T_{FH} function and may play a role in achieving HBV functional cure.

Keywords: toll-like receptor 8, chronic hepatitis B, selgantolimod (SLGN), follicular helper T cell, B cell, HBsAg-specific B cell response, inflammatory cytokine, activation induced marker (AIM)

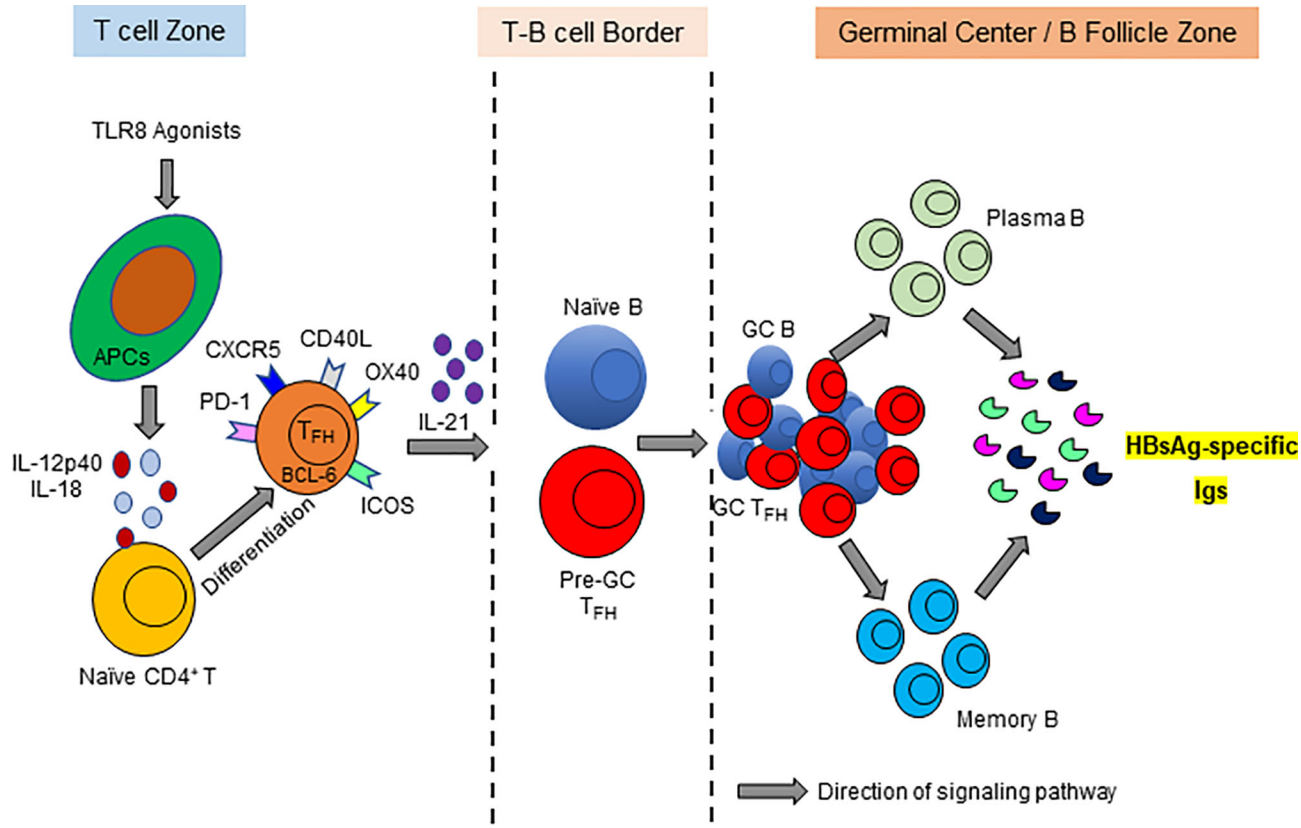

TLR8 pathway promotes GC T_{FH} differentiation and enhance B cell responses in CHB patients

GRAPHICAL ABSTRACT |

INTRODUCTION

Hepatitis B virus (HBV) infection remains a major global health burden with over 257 million people worldwide chronically infected. A major barrier to HBV cure with standard nucleos/tide analog (NUC) therapy is the persistent dysfunction of the antiviral (HBV) immune response despite therapy induced viral suppression (1, 2). As such identifying immunomodulatory strategies that aid HBs antigen loss/seroconversion, which defines functional cure of infection, is of high significance in HBV cure research (3).

In the past years, HBs antigen (HBsAg)-specific B cells have received attention and several laboratories including ours identified dysfunction in antigen-specific B cell response (4–6). These B cells have upregulated inhibitory receptor expression and impaired HBsAg-specific IgG production *ex vivo*. Dysfunctional B cell response can be attributed to intrinsic B cell defects along with insufficient help from $CD4^+$ T cells. T follicular helper (T_{FH}) cells are the $CD4^+$ T cells that provide signals for antigen specific B cell maturation into a plasma cell, making them essential for the generation of most isotype switched and affinity matured antibodies. Coordinated T_{FH} and B cell response determines acquisition and maintenance of antibody response to prophylactic

Abbreviations: CHB, chronic hepatitis B; HBV, hepatitis B virus; T_{FH}, follicular helper T cells; cT_{FH}, circulating follicular helper T cells; PBMCs, peripheral blood mononuclear cells; APCs, antigen-presenting cells; TLR8, toll-like receptor 8; HC, healthy control; GC, germinal center; HBsAg, hepatitis B surface antigen; ssRNA40, single stranded RNA40; mg, milligram; Kg, kilogram; PBS, phosphate-buffered saline, FBS, fetal bovine serum; AIM assay, activation induced marker assay; SEB, staphylococcal enterotoxin B; ELISPOT, enzyme-linked immune absorbent spot; ASC, antigen-specific antibody secreting cell; IL, interleukin; LPS, lipopolysaccharide; IMQ, imiquimod; TNF-α, tumor-necrosis factor alpha; MB, memory B; PB, plasma B; PCs, plasma cells; PBs, plasmablasts; NBs, naïve B; RMBs, resting memory B; AMBs, activated memory B; ATMBs, atypical memory B; PMA, phorbol-12-myristat-13-acetate; Ion, ionomycin; LEP, large envelop protein; Stim- stimulation; FACS, fluorescence-activated cell sorting; ICS, intracellular staining; UT, untreated; BL, baseline; IgG, immunoglobulin G; ELISA, enzyme-linked immunosorbent assay; HBV Pep; hepatitis B virus peptide; ANOVA, analysis of variance.

HBsAg based vaccine (7). This response is defective during CHB infection, where an accumulation of activated and phenotypically abnormal T_{FH} dysregulates cytokine profiles (8, 9). Dysfunctional antigen-specific T_{FH} response was shown to promote persistence of HBV in a mouse model (9). In samples from CHB patients, impaired T_{FH} response was shown to be due to IL-21 suppression mediated by CTLA-expressing Tregs, which could be restored by inhibiting Tregs with an antibody against CTLA-4 (9). We showed that abnormal T_{FH} persist even in long-term NUC treated CHB patients, possibly explaining the low incidence of anti-HBs seroconversion in these patients (6). Thus, we believe this impaired T_{FH} response is a critical defect associated with hepatitis B virus persistence and resolving the dysfunction will be of significance in resolution of CHB.

Among the immunomodulatory strategies, toll-like receptors are a promising way to correct immune deficiencies. Human liver derived monocytes respond strongly to TLR8 agonism, producing IL-12 and IL-18 (10). IL-12 induced by TLR8 signaling has a potential impact on anti-viral CD8 T cell response (11). Importantly, IL-12 was shown to aid T_{FH} differentiation that led to plasma cell generation in individuals vaccinated with a live attenuated vaccine (12). We investigated whether similar mechanism can restore dysfunctional T_{FH} response and aid exhausted HBsAg-specific B cell response (4–6) present in chronic HBV infection. Here we demonstrate that TLR8 signaling induces differentiation of T_{FH} cells into efficient B cell helpers with potential to promote plasma cell generation and an HBsAg-specific B cell response.

MATERIALS AND METHODS

Patients and Samples

For investigating *in vitro* effects of TLR8 stimulation, peripheral blood samples were available from CHB patients or HBV vaccinated healthy volunteers enrolled in HOPE cohort at University of Maryland, Baltimore. The study protocol was approved by the institutional ethical committee, and all subjects gave written, informed consent. Demographic and clinical details of patients are provided in **Table 1**.

TABLE 1 | Demographic and clinical characteristics of chronic hepatitis B patients.

Clinical Characteristics	Chronic Hepatitis B (CHB) Patients
Subjects	n=29
HBV DNA (copies/mL)	UND (11), <20 (9), >7906 (9)
Hgb (gm/dL)	14.4
Platelet (10^9/L)	212
Creatinine (mg/dL)	0.8
ALT (U/L)	30
AST (U/L)	26
Albumin (g/dL)	4.6 (14), ND (15)
HBsAg IU	UND (2), 11974 (18), ND (9)
HBeAg	positive (8), negative (20)
HBsAg	positive (27), negative (2)
HBeAb	positive (20), negative (8), ND (1)
Anti-HBs	negative (27), ND (2)

Values are presented as median. ALT, Alanine aminotransferase; AST, Aspartate aminotransferase; UND, Undetected; ND, Not Detected.

For investigating *in vivo* effects of TLR8 agonism, peripheral blood samples from previously completed phase 1b clinical trial (ACTRN identifier: 12617000235303) of a selective-TLR8 agonist (Selgantolimod (SLGN), GS-9688) in CHB patients (N=14) and in healthy subjects (13, 14) were available courtesy of Gilead Sciences. Paired samples from baseline (BL) and TLR8 single oral dose treatment (8 hours-post SLGN, 1.5 or 3 mg) time-points were used here.

TLR Agonists Stimulation of PBMCs

The following TLR ligands (InvivoGen, each 1 μg/mL) were added into wells of 24-well plate containing 1-2 x 10^6 PBMCs: Poly(I:C) HMW (TLR3), LPS-EK Ultrapure (lipopolysaccharide, TLR4), Imiquimod (IMQ) (R837, TLR7), Resiquimod (R848, TLR7/8), TL8-506 (TLR8), ssRNA40/LyoVec (TLR8) and CpG-ODN (TLR9). The concentration of 1 μg/mL is within the range of manufacturer recommendation and induced maximum cytokine response (not shown) (10, 12). Golgi plug (1 μl/mL, BD Biosciences) was added to block the cytokines release and cell culture continued for 18h. For some experiments, PBMCs were stimulated with agonists alone or in combination with recombinant human HBsAg subtype adw (10 μg/mL, Fitzgerld) (15) and PepMix HBV (LEP) Ultra (2 μg/mL, JPT) and cultured for 5 days at 37°C incubator. In experiments for transcription factor induction, cells were re-stimulated with Phorbol-12-myristat-13-acetate (PMA, 50ng/mL) and Ionomycin (Ion, 1 μg/mL) on day 4.

Flow Cytometry (FACS) and Intracellular Cytokine Staining (ICS)

PBMCs were stained and analyzed by flow cytometry using standard methods (panels listed in **Supplementary Table 1**). Cells were acquired on a Cytek Aurora multi-color FACS machine and data analysis done by Flow Jo software (Tree Star, San Carlos, California, USA).

Activation Induced Markers (AIM) Assay

For examination of contribution of TLR8 signaling in HBV antigen-specific germinal center like (GC) T_{FH} induction, a cytokine-independent approach was followed (16, 17). It is known that formulation of antigen can influence the type and extent of activation markers induced in $CD4^+$ T cells (18). To capture multiple activation markers induced in T_{FH} with TLR8 signaling, here we used combination of HBsAg intact protein and peptide, as is described for other antigens (16, 17). Approximately 1-2 x 10^6 PBMCs were aliquoted into 24-well plate and stimulated with HBV envelope peptide (2 μg/mL, JPT) and recombinant human HBsAg subtype adw (10 μg/mL, Fitzgerald). Intact protein antigens or antigenic peptides are used for stimulating antigen specific CD4 T cell response. Staphylococcal enterotoxin B (SEB 1 μg/mL, Toxins Technology) served as positive control and AIM-V medium alone served as untreated negative control (UT). CXCR5-BV605 and CXCR3-PeCy7 antibodies (Biolegend, 1 μl each) were added directly into the cell culture well and also included in the staining panel. After 18h stimulation, PBMCs cultures were washed twice with 1X PBS and followed the FACS staining protocol as stated in the above method using AIM assay panel

flow antibodies provided in **Supplementary Table 1**. Cells were washed, fixed with 1% paraformaldehyde and acquired on the same day.

Follicular Helper T Cells (T_{FH}) Differentiation

To examine TLR8-mediated differentiation of T_{FH} cells, $CD14^+$ monocytes and naïve $CD4^+$ T cells were isolated from autologous human PBMCs of CHB patients (n=4) by negative selection (Miltenyi Biotec). The following co-culture experiments were adopted from previously published methods (12). First, purified $CD14^+$ monocytes (1 x 10^6 cells/mL) were left untreated or treated with TLR8-specific agonists ssRNA40/Lyovec (1 μg/mL, InvivoGen) or TL8-506 (1 μg/mL, InvivoGen) for 1.5 h. Isolated autologous naïve $CD4^+$ T cells were directly added into the culture at a ratio of 2:1 (monocyte:$CD4^+$) along with SEB (1 μg/mL, Toxins Technology). After 6 days, cells were either processed for T_{FH} cell sorting for further downstream study or re-stimulated overnight (O/N) with PMA (phorbol-12-myristat-13-acetate, 50 ng/mL, Sigma) and ionomycin (Ion 1 μg/mL, Sigma) as positive control to effectively activate T_{FH} cells. After 3-4h, Golgi plug (1 μl/mL, Invitrogen) was added and culture continued for additional 18h to investigate T_{FH} cell proliferation and differentiation related markers by flow cytometry. The culture supernatants were recovered and tested for IL-12p40, IL-18 and IL-21 cytokine quantifications by Luminex multiplex immunoassay.

T_{FH} Cells Sorting and Naïve B Cells Co-Culture

For T_{FH} sorting, cells recovered after 6 days of monocyte-naïve CD4 co-culture (n=4) were stained with anti-human PD-1-BV421, ICOS-BV510, CXCR5-BV605, CXCR3-PeCy7 and CD4-APC antibodies. T_{FH} cell sorting was carried out on BD FACS Aria III.

For naïve B-T_{FH} co-culture, naïve B cells were isolated (Miltenyi Biotec) from autologous PBMCs of CHB patients (n=4) and co-cultured with sorted T_{FH} cells (from above) at 2:1 (B:T_{FH}) in the presence of SEB (1 μg/mL) for 7 days after which T_{FH}-mediated differentiation of B cells into various subsets was analyzed by flow cytometry.

Neutralization (Ab Blocking) and Recombinant Protein Addition

Purified $CD14^+$ monocytes (1 x 10^6 cells/mL) (N=4) were pre-treated with LEAF purified mouse IgG1, k isotype control, Ultra-LEAF purified anti-human IL-12p40 or Ultra-LEAF purified anti-human IL-18 neutralizing antibodies (each 10 μg/mL, Biolegend) for 2h at 37°C humidified incubator (19), followed by stimulation with TL8-506 or ssRNA40/Lyovec for 1.5h. For recombinant protein stimulation assay, isolated autologous naïve $CD4^+$ T cells were treated with recombinant human IL-12 or recombinant human IL-18 (each 20 ng/mL, Biolegend) followed by co-culture experiments as described above.

B Cell ELISPOT Assay

PBMC from CHB patients obtained at baseline (BL, pre-TLR8) and TLR8 (8h post-Selgantolimod) single oral dose were tested. To examine HBsAg-specific antibody secreting B cells, cells were stimulated with polyclonal stimuli R848 (1 μg/mL, Mabtech) and recombinant human IL-2 (10 ng/mL, Mabtech) and cultured for 5 days to effectively induce memory B cell proliferation. B cell ELISPOT assay was conducted as previously described (6).

Luminex Multiplex Immunoassay

Quantification of IL-12p40, IL-18 and IL-21 in cell culture supernatants collected from co-culture experiments was analyzed by Luminex multiplex immunoassay (Luminex LX200 multianalyte system, Bio-Rad Corporation) according to manufacturer protocol.

Enzyme-Linked Immunosorbent Assay (ELISA)

Quantification of human class-switched immunoglobulin (IgG) was made in cell culture supernatants collected from naïve B-T_{FH} cell co-cultures using high sensitivity ELISA kit according to manufacturer's protocol (XpressBio, Express Biotech International).

Statistical Analyses

Statistical analyses were performed using one-way analysis of variance (ANOVA) or Kruskal-Wallis with Dunn's multiple comparisons test. Paired samples between BL (pre) and TLR8 (8h-post) were analyzed by two-tailed paired, or the Wilcoxon signed-rank Student's t test or non-parametric Mann-Whitney U test for comparisons between treatments. A p value of <0.05 was considered significant. Levels of significance are indicated by *: *$p \leq 0.05$, **$p \leq 0.01$, ***$p \leq 0.001$, ****$p \leq 0.0001$ and ns (no significance).

RESULTS

In Vitro TLR8 Stimulation Induces Proinflammatory Cytokines in Monocytes From CHB Patients

TLR8 signaling induces IL-12 in monocytes, which supports T_{FH} differentiation in healthy individuals (12). We tested whether this pathway induces T_{FH} polarizing cytokines in samples from CHB patients. PBMCs isolated from CHB patients were stimulated with various TLR agonists for 18-24h or with medium alone (UT) as negative control. The ligation of TLR8 in monocytes by synthetic agonists, single stranded RNA40 (ssRNA40/LyoVec), TL8-506 and TLR7/8 ligand R848 induced proinflammatory cytokines IL-6, IL-12p40, IL-18, TNF-α in $CD14^+HLA\text{-}DR^+$ activated monocytes (**Figures 1A–D**) as analyzed by intracellular cytokine staining using flow cytometry. TLR8 agonist ssRNA40 significantly enhanced the production of cytokines IL-12p40 and IL-18 when compared with other TLR agonists. LPS stimulation induced cytokines IL-6, IL-1β and IL-23p19. Relative frequencies of $CD14^+HLA\text{-}DR^+$ monocytes producing

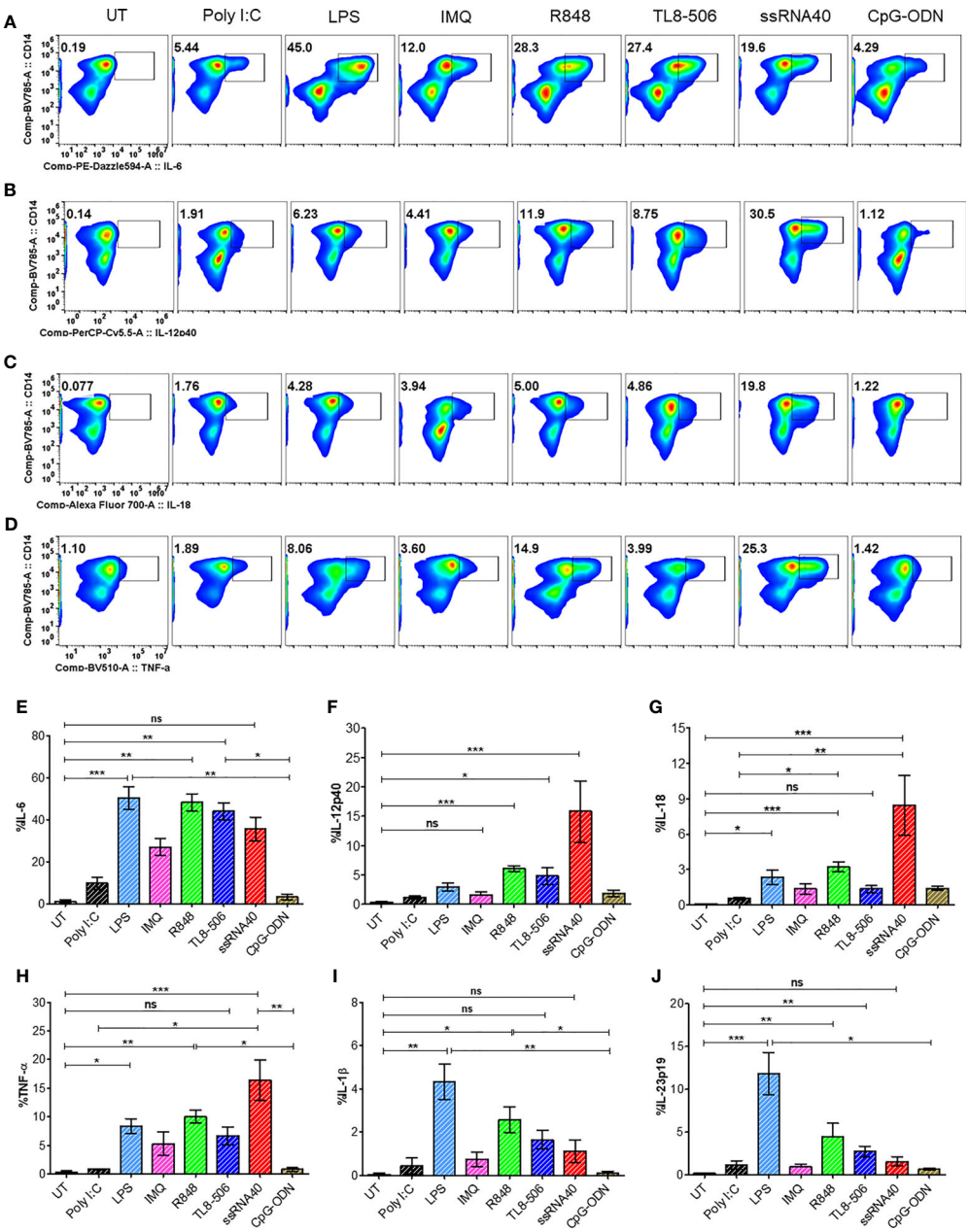

FIGURE 1 | *In vitro* TLR8 stimulation augments proinflammatory cytokines in monocytes. PBMCs from CHB patients (n=6) stimulated with various TLR agonists as indicated to evaluate T_{FH} polarizing pro-inflammatory cytokine induction in monocytes. Representative pseudo color flow plots show intracellular expression of T_{FH} skewing pro-inflammatory cytokines **(A)** IL-6, **(B)** IL-12p40, **(C)** IL-18 and **(D)** TNFα, gated on $CD14^+HLA\text{-}DR^+$ monocytes. Numbers inside the box indicate percentages of $CD14^+HLA\text{-}DR^+$ monocytes secreting pro-inflammatory cytokine events compared between untreated (UT) negative control and different TLR agonists treated PBMCs. Frequencies shown in **(E)** IL-6, **(F)** IL-12p40, **(G)** IL-18, **(H)** TNFα, **(I)** IL-1β and **(J)** IL-23p19 as percentage of cytokine positive $CD14^+HLA\text{-}DR^+$ cells. Error bar on the graph represents the standard error of mean calculated from 6 individual donors. Differences between stimulations calculated by one-way analysis of variance (ANOVA) or Kruskal-Wallis test for multiple comparisons. P values ≤0.05*, 0.01**, 0.001*** indicate statistical significance levels. ns, no significance; IMQ, imiquimod; LPS, lipopolysaccharide.

these proinflammatory cytokines in response to various TLRs engagement are shown (**Figures 1E–J**). The frequencies of $CD14^+HLA\text{-}DR^+$ monocytes or the expression levels of the TLR8 receptor in $CD14^+HLA\text{-}DR^+$ monocytes did not change with any of the TLR agonist treatments (**Supplementary Figures 1A–C**). TGF-β1 was induced only by TL8-506 and no significant induction of IL-27p28 was observed (**Supplementary Figures 1D, E**). These data demonstrate that cytokines IL-12 and IL-18 are induced in monocytes from CHB patients when stimulated with TLR8 agonists.

TLR8 Agonism Induces T_{FH} Cells Differentiation

Having shown potent induction of T_{FH} polarizing cytokine IL-12p40 (12) in monocytes from CHB samples, we next examined the impact of TLR8 agonism on T_{FH} phenotypes. Circulating $CD4^+CXCR5^+$ cells in peripheral blood share characteristics and functional phenotypes with GC-like T_{FH} cells (20). The expression of signature cytokine IL-21, BCL-6 (a master regulator of T_{FH} cells programing and differentiation) and CD40 ligand (CD40L) in T_{FH} cells provide signals to B cells that are required for Ig class-switching recombination and high affinity antibody productions (21). The expression of inducible co-stimulatory molecule (ICOS) indicates T_{FH} development, migration and their active state (22). We asked whether TLR8-induced cytokines modulate these immunophenotypic profiles of circulating T_{FH} cells (cT_{FH}). CHB patient samples were stimulated with TLR8-specific agonists ssRNA40 or TL8-506 in the presence or absence of mitogenic stimulation using PMA/Ion (required for induction of BCL-6 and ICOS). The sequential gating strategy for T_{FH} cell panel is presented in **Supplementary Figure 2A**. Flow plots (**Figure 2A**) show that the frequency of IL-21 producing cT_{FH} cells ($IL\text{-}21^+CXCR5^+$) gated on $CD4^+$ T cells was significantly increased in conditions with ssRNA40 or TL8-506. The data represented for ssRNA40 stim or TL8-506 stim are response found in TLR8 agoniost+PMA/Ion re-stimulated response subtracted with PMA/Ion alone response (**Figures 2A–F**). The co-expression of GC-like T_{FH} markers $IL\text{-}21^+BCL\text{-}6^+$ and $ICOS^+BCL\text{-}6^+$ were significantly increased in ssRNA40 stim or TL8-506 stim conditions (**Figures 2B–F**). Since proinflammatory cytokines IL-12p40 and IL-18 were induced in monocytes in response to TLR8 agonism (**Figure 1**), we measured levels of these cytokines in the PBMC culture supernatants. As expected, cultures incubated with TLR8-specific agonists ssRNA40 or TL8-506 markedly induced the secretion of both these cytokines (**Figures 2G, H**).

Next, we asked whether TLR8-specific signaling modulates subsets of circulating T_{FH} cells in CHB patients. When compared with untreated negative control, PBMCs in conditions with ssRNA40 or TL8-506 had significantly increased frequencies of cT_{FH} subsets $cT_{FH}1$ ($CXCR3^+CCR6^-$) and $T_{FH}1/17$ ($CXCR3^+CCR6^+$) (**Supplementary Figures 2B, D, G**), while no differences were observed for global cT_{FH} ($CXCR5^+CD4^+$ gated on $CD3^+$ T lymphocytes) cells, subsets $cT_{FH}2$ ($CXCR3^-CCR6^-$) and $cT_{FH}17$ ($CXCR3^-CCR6^+$) (**Supplementary Figures 2C, E, F**). It has been previously reported that $cT_{FH}1$ and $cT_{FH}1/17$ are the source for IL-21 and IFNγ, whereas $cT_{FH}2$ and $cT_{FH}17$ are source for anti-inflammatory cytokines IL-4, IL-10 and IL-17A. These results collectively suggest that TLR8-specific signaling induces IL-21 producing T_{FH} subsets in the setting of CHB.

Selgantolimod Treatment Enhanced T_{FH} Differentiation and Rescued Defective Antigen-Specific Activation of T_{FH} Cells

After *in vitro* demonstration of T_{FH} differentiation with TLR8 agonism, we tested samples from CHB patients given a single oral dose of Selgantolimod. Surprisingly, in post-Selgantolimod treated samples that had been obtained only 8 hours after dosing, a significant induction of GC-like signature T_{FH} factors $IL\text{-}21^+BCL\text{-}6^+$, $ICOS^+BCL\text{-}6^+$ and $ICOS^+CD40L^+$ cells were observed (**Supplementary Figures 3A–H**).

Next, we employed a cytokine-independent method for detection of HBsAg-specific T_{FH} cell activation by measuring the upregulation of activation induced markers (AIM) CD69, CD25, OX40, PD-L1 and CD40L (16, 17). Both frequencies of $CD3^+CD4^+CXCR5^+CXCR3^-PD\text{-}1^+$ T_{FH} and their activation, indicated by surface expression of $OX40^+CD25^+$, $PD\text{-}L1^+CD25^+$ and $CD69^+CD40L^+$, was increased in vaccinated individuals upon *in vitro* stimulation with HBV antigens or SEB compared to the negative control (**Figures 3A–F**, **Supplementary Figure 4**). Expectedly, baseline samples from CHB patients displayed low HBV specific activation of T_{FH} indicating defective response. Importantly, a significant increase in AIM response was evident in 8 hour samples, which was comparable to HBV vaccinated samples (**Figures 3A–F**). Additionally, the frequencies of $PD\text{-}1^+CXCR3^-$ cT_{FH} cells, but not total $CXCR5^+$ cT_{FH} cells, were significantly higher in samples collected at post-TLR8 time-point (**Supplementary Figures 4B, C**). These data demonstrate that TLR8-specific signaling can normalize defective antigen specific T_{FH} response.

TLR8 Signaling Increased Memory B, Plasma B, and Modulated B Cell Subsets

To determine whether the activation of TLR8 pathway and resulting T_{FH} differentiation impacts B cell populations in CHB infection, frequencies of various B cell subsets were examined after incubation of PBMC with ssRNA40, TL8-506 or R848 in presence or absence of HBV antigens for 5 days. Frequencies of $CD19^+$ B cells did not change with these treatments (**Supplementary Figures 5A–C**). Activation of TLR8 pathway with ssRNA40 or of TLR7/8 with R848 significantly expanded the frequencies of memory B cells ($CD19^+CD27^+$), plasma B cells ($CD19^+CD27^{++}CD38^+$), plasmablasts ($CD19^+CD27^{++}CD38^+CD138^-$) and plasma cells ($CD19^-CD138^+$) (**Figures 4A–E** and **Supplementary Figures 5D, E**). While TL8-506 treatment did not result in significant changes in frequencies of these populations, it increased naïve B ($CD19^+CD27^-CD21^+$) and long-lived plasma ($CD19^-CD138^+$) cells (**Figure 4F** and **Supplementary Figure 5D**). Addition of HBV antigens in addition to TLR8 agonism didn't alter naïve B ($CD19^+CD27^-CD21^+$), resting memory B ($CD19^+CD27^+CD21^+$) or activated memory B cells $CD19^+CD27^+CD21^-$) (**Figures 4A–I** and **Supplementary Figures 5D, E**).

Previously we reported that atypical memory B cells that expressed high levels of FcRL family receptors were expanded in CHB patients and this sub-population lacks HBsAg-specific B cell response (6). Here we observed that TLR8 stimulation expanded memory B cells with an atypical phenotypic signature ($CD19^+CD21^-CD27^-$) (**Figure 4C, I**). We believe that this subset lacking CD21 and CD27 that is expanded in response

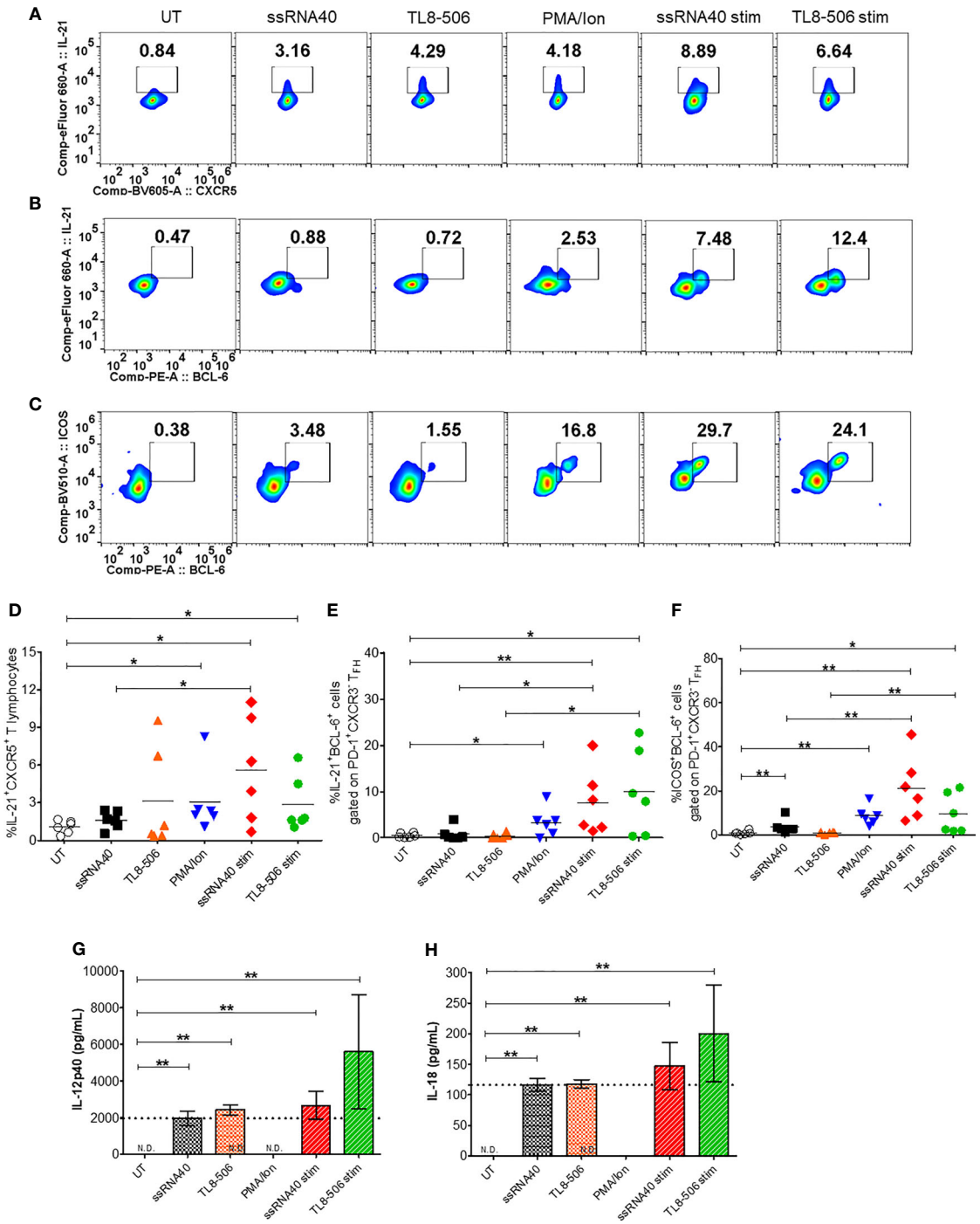

FIGURE 2 | TLR8 agonism induces T_{FH} differentiation. PBMCs from CHB patients (n=6) were left untreated (UT) or treated with TLR8 agonists ssRNA40 or TL8-506 for 5 days. ssRNA40 stim and TL8-506 stim indicates subtraction of overnight PMA/Ion stimulations from the respective values of TLR8 + PMA/Ion re-stimulations. Illustrative flow plots show **(A)** intracellular expression of T_{FH} signature cytokine IL-21 gated on cT_{FH} ($CD4^+CXCR5^+CD3^+$ T lymphocytes) cells, co-expression of GC-like T_{FH} development factors **(B)** IL-21^+BCL-6^+ and **(C)** $ICOS^+$BCL-6^+ gated on PD-1^+CXCR3^- T_{FH} cells upon treatment with TLR8-specific ligands. Frequencies are shown for **(D)** IL-21^+CXCR5^+, **(E)** IL-21^+BCL-6^+ and **(F)** $ICOS^+$BCL-6^+ cells. Pro-inflammatory cytokines secreted in the supernatants collected from indicated conditions of PBMC cultures quantified by Luminex multiplex immunoassay. Bar graphs depict mean levels of cytokines **(G)** IL-12p40 (pg/mL) and **(H)** IL-18 (pg/mL) upregulated by TLR8-specific agonists. Dotted line indicates comparison between TLR8 stimulations. The differences between stimulations were evaluated by one-way ANOVA or Kruskal-Wallis test for multiple comparisons. P values ≤0.05*, 0.01** indicate statistical significance levels. N.D., not detected; $cT_{FH,}$ circulating follicular helper T cells; GC-like $T_{FH,}$ germinal center-like T_{FH}; PMA, phorbol-12-myristat-13-acetate; Ion, ionomycin; Stim, stimulation.

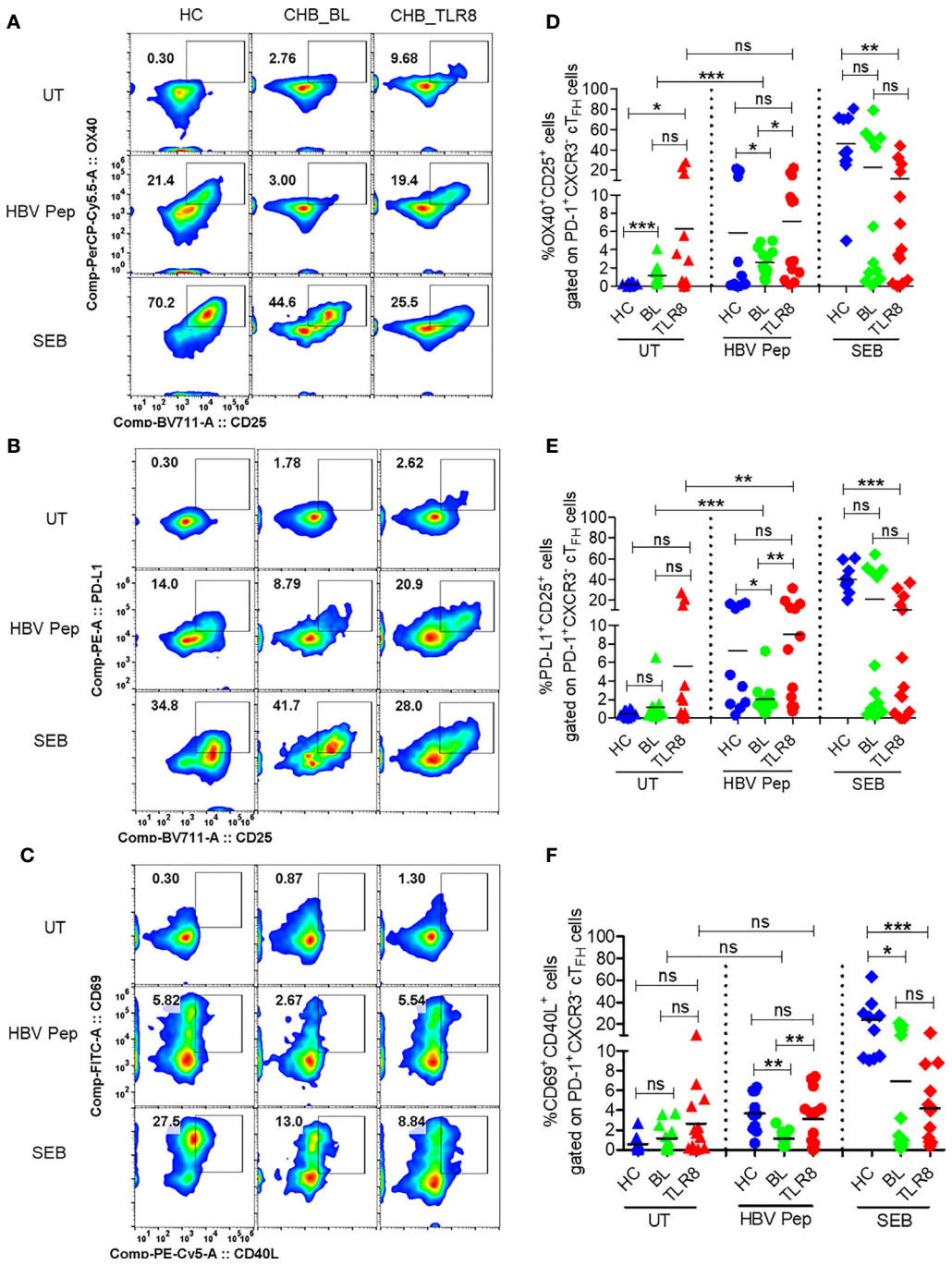

FIGURE 3 | Selgantolimod treatment rescued defective antigen-specific activation of T_{FH} cells. PBMCs isolated from HBV vaccinated healthy controls (HC, n=10) and paired samples from CHB patients at baseline (BL) or 8h post-TLR8 agonist (single oral dose of 1.5-3 mg/Kg, Selgantolimod) administration (CHB_TLR8) (n=10-14) were stimulated with combination of HBsAg and HBV peptides pool for 18-24h. Staphylococcal enterotoxin B (SEB, T cell antigen receptor stimulus) and AIM-V medium alone (UT) served as positive and negative controls, respectively. Flow cytometry analysis was performed using AIM assay panel antibodies (**Supplementary Table 1**). Flow plots represent co-expression of HBV-specific activation induced T_{FH} markers (AIM). Representative pseudo color plots show comparative co-expression of **(A)** $OX40^+CD25^+$, **(B)** $PD\text{-}L1^+CD25^+$ and **(C)** $CD69^+CD40L^+$ cells gated on GC-like T_{FH} ($PD\text{-}1^+$ $CXCR3^-$ cT_{FH}) cells in HC and CHB (BL and TLR8) samples. Numbers shown inside the flow box indicate percentage of events. Relative frequencies of GC-like T_{FH} markers shown in graph as percentage of cells expressing **(D)** $OX40^+CD25^+$, **(E)** $PD\text{-}L1^+CD25^+$ and **(F)** $CD69^+CD40L^+$. Each symbol in the graph shows individual donors and the dotted line distinguishes the data between stimulations. A two-tailed unpaired or paired, non-parametric or the Wilcoxon signed-rank Student's t test were conducted to evaluate the differences between HC, BL and 8h post-TLR8 treated samples. P values of ≤0.05*, 0.01**, 0.001*** indicate statistical significance. HC, vaccinated healthy control; CHB, chronic hepatitis B; HBV Pep, HBsAg/HBV peptides pool; ns, no significance.

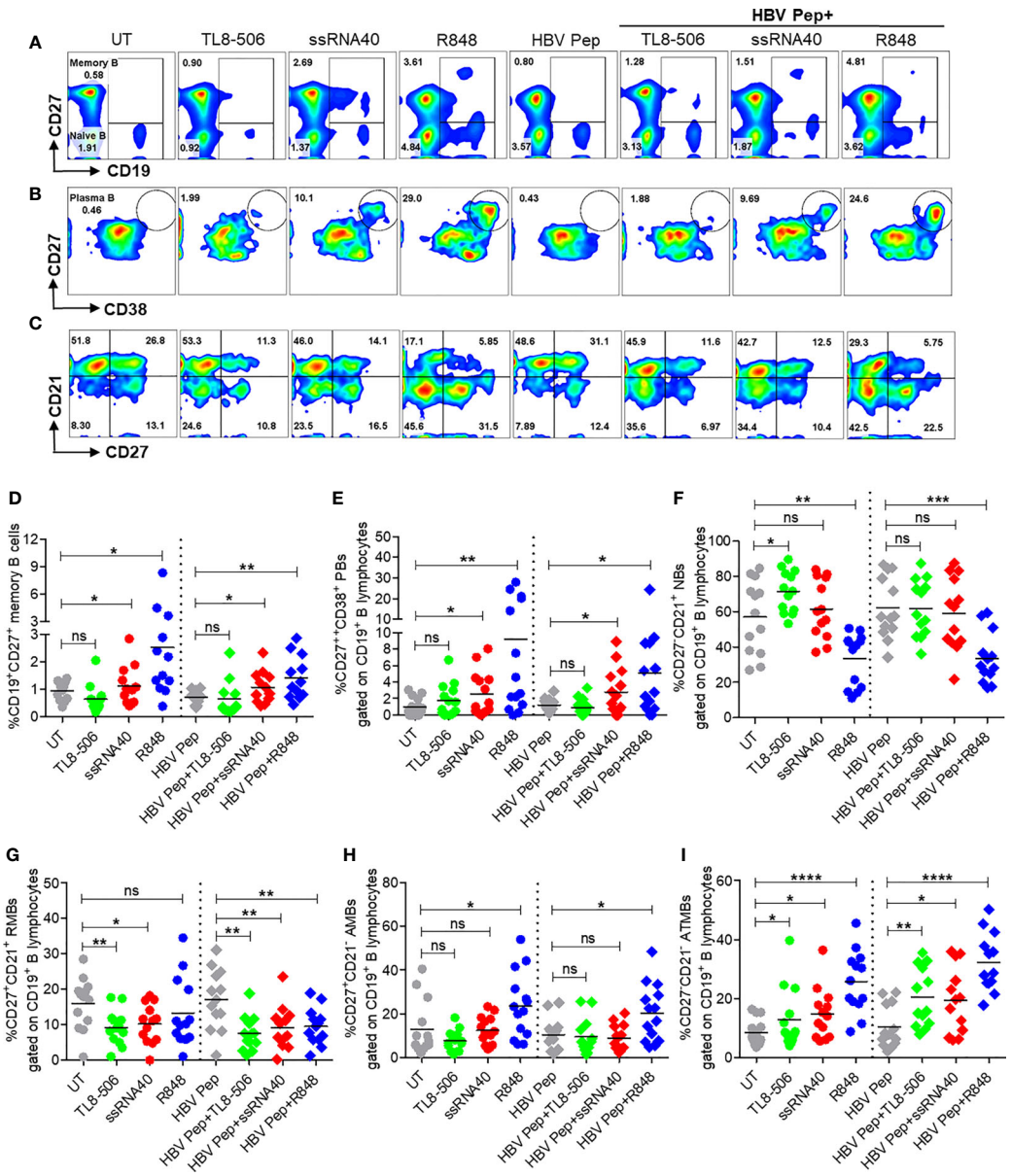

FIGURE 4 | Activation of TLR8 pathway increased memory B, plasma B, and modulated B cell subsets. PBMCs collected from CHB infected patients (n=10-14), were left untreated (UT) or treated with specific TLR8 ligands TL8-506, ssRNA40 or TLR7/8 ligand R848 along with or without HBsAg and HBV Pep and cultured for 5 days. Flow cytometry evaluation of B cell subsets at the end of culture for **(A)** MB ($CD27^+$), **(B)** plasma B ($CD27^{++}CD38^+$) and **(C)** B cell subsets defined by CD27 and CD21 expressions, gated on $CD19^+$ B lymphocytes. Dot plots show the frequencies of **(D)** MB ($CD19^+CD27^+$), **(E)** plasma B ($CD19^+CD27^{++}CD38^+$), **(F)** NBs ($CD19^+CD27^-CD21^+$), **(G)** RMBs ($CD19^+CD27^+CD21^+$), **(H)** AMBs ($CD19^+CD27^+CD21^-$) and **(I)** ATMBs ($CD19^+CD27^-CD21^-$). Numbers inside the quadrants represent percentage of subsets. Dotted lines distinguish TLR8 without or with HBV Pep treatment conditions. Statistical significance determined by two-tailed, non-parametric or the Wilcoxon signed-rank Student's t test for comparison between stimulations. P values ≤0.05*, 0.01**, 0.001***, 0.0001**** indicate statistical significance. ns, no significance; MB, memory B; PB, plasma B; NBs, naïve B; RMBs, resting memory B; AMBs, activated memory B; ATMBs, atypical memory B cells.

to TLR7/8 stimulation does not represent an elevation of dysfunctional cells. R848 is typically used to increase memory B cells for measuring B cell responses with ELISPOTs for chronic HBV infection (9, 23). It is also known that during malaria, B cells with similar 'atypical' phenotype are in fact functional and produce neutralizing antibodies (24).

TLR8 Signaling Promotes IL-12-Dependent GC-Like T_{FH} Cell Differentiation and Improved IL-21 Production

In order to discern the mechanism behind TLR8-mediated differentiation and proliferation of T_{FH} cells, we performed co-culture experiments of isolated monocytes and $CD4^+$ T cells. $CD14^+$

monocytes were treated with ssRNA40 or TL8-506, in presence of isotype control IgG or anti-human IL-12 or anti-human IL-18 neutralizing (blocking) antibodies followed by co-culture with autologous naïve $CD4^+$ T cells for 6 days. Monocytes stimulated with TLR8-specific agonists induced T_{FH} cell markers on $CD4^+$ T cells ($CD4^+CXCR5^+IL\text{-}21^+$, $IL\text{-}21^+ICOS^+$ and $ICOS^+PD\text{-}1^+$) in samples from healthy individuals and CHB patients. Untreated monocytes co-cultured with autologous naïve $CD4^+$ T cells failed to induce IL-21 and other differentiation factors (**Figures 5A–C** and **Supplementary Figures 6A–C**).

In humans, TLR8 pathway-specific secretion of proinflammatory cytokine IL-12 sends the signal responsible for IL-21 production and drives the T_{FH} cell differentiation (12, 25). In CHB patients, T_{FH} cell frequencies are high due to hyperactivation and these cells lack IL-21 cytokine production. We therefore explored whether TLR8-specific cytokine induction will promote circulating T_{FH} cell differentiation and recover defective IL-21 production in PBMCs of CHB patients. IL-12p40 and IL-18 secretion in monocytes and IL-21 production from newly generated T_{FH} cells were quantitatively analyzed in supernatants of co-culture experiments and naïve $CD4^+$ T cell culture by Luminex multiplex immunoassay. As expected, IL-12 neutralization (ssRNA40+α-IL-12 and more clearly TL8-506+α-IL-12) in $CD14^+$ monocytes-naïve $CD4^+$ T cells co-culture significantly decreased IL-21 production as well as the co-expression of GC-like T_{FH} markers $IL\text{-}21^+ICOS^+$ and $ICOS^+PD\text{-}1^+$, on cT_{FH} cells ($CD3^+CD4^+CXCR5^+$); IL-18 neutralization (ssRNA40+α-IL-18 or TL8-506+α-IL-18) did not have similar effect (**Figures 5A–C** and **Supplementary Figures 6A–C**). Correspondingly, the secretion of cytokine IL-21 was significantly reduced in co-cultures pre-treated with IL-12 neutralizing antibody (ssRNA40+α-IL-12 and more notably with TL8-506+α-IL-12). IL-18 blocking again did not have an effect on IL-21 production in either ssRNA40+α-IL-18 or TL8-506+α-IL-18 antibody treatment conditions (**Figures 5D–F**). IL-18 production remained intact with α-IL-12 treatments. To further justify that TLR8-specific IL-12 cytokine-dependent signal is responsible for T_{FH} cell differentiation and IL-21 cytokine production, we tested naïve CD4+ T cells isolated from PBMCs of HC and CHB patients that were left untreated or directly incubated with recombinant human IL-12 or IL-18 and cultured for 5 days in the absence of $CD14^+$ monocytes. The frequency of IL-21 producing T_{FH} cells was significantly increased when incubated with rhIL-12, but not with rhIL-18 (**Figures 5A–F** and **Supplementary Figure 6F**). It is important to note here that effect of TLR8 was not specific to $CXCR5^+$ T_{FH} and the agonist activated $CD4^+$ T cells including $CXCR5^-$ cells in an IL-12 dependent manner (**Supplementary Figures 6D, E**). Taken together, these data demonstrate that TLR8-specific IL-12-induction in monocytes plays a critical role in the T_{FH} cells differentiation, which can restore the deficient IL-21 production in CHB.

T_{FH} Cells Differentiated by TLR8 Agonists Support The Generation of Memory B and Plasma B Cells

To evaluate the utility of newly generated T_{FH} cells as true helpers of B cells, we sorted $CD4^+CXCR5^+CXCR3^-PD\text{-}1^+ICOS^+$ T_{FH} generated with UT, ssRNA40 or TL8-506 pre-exposed $CD14^+$ monocytes and assessed their ability to promote plasma B cell differentiation after co-culture with autologous naïve B cells for 7 days. T_{FH} generated from TLR8 primed monocytes enhanced the differentiation of global memory B ($CD27^+$), plasma B ($CD27^{++}CD38^+$), long-lived antibody-producing plasma cells ($CD27^{++}CD38^-CD138^+$) and plasmablasts (PBs) ($CD27^{++}CD38^+CD138^-$), whereas T_{FH} derived from UT or naïve $CD4^+$ T cells co-cultured with B cells failed to induce memory, plasma B and long-live plasma cell differentiation (**Figures 6A–J**).

Additionally, significantly higher frequencies of IgG^+ ($CD19^+CD27^+$) memory B cells and robust IgG production in TL8-506 primed T_{FH}-naïve B co-culture condition compared to naïve B without or with naïve $CD4^+$ T or UT_T_{FH} co-culture conditions was present (**Figures 6I, J**). Flow plot in **Figure 6D** shows ssRNA40 and TL8-506-primed T_{FH}-naïve B co-culture conditions resulted in a reduction in naïve B ($CD19^+CD21^+CD27^-$) and increase in resting memory B ($CD19^+CD21^+CD27^+$), activated memory B ($CD19^+CD21^-CD27^+$) and atypical memory B ($CD19^+CD21^-CD27^-$) cell populations, relative to non-TLR8 conditions. Thus T_{FH} differentiated with TLR8-treatment support the generation of memory B cells and their subsets in CHB samples.

Selgantolimod Treatment Enhanced B Cell Responses

To assess whether this mechanism of enhancing T_{FH} response impacts B cell response *in vivo*, we next examined the effect of Selgantolimod oral treatment in paired samples from before and 8 hours after treatment. For this experiment, in addition to phase 1b clinical samples, clinical samples from phase 1a trial in CHB negative healthy subjects with known positive HBV vaccination status were tested for HBsAg-specific IgG and total IgG with ELISPOT assays. We defined responders as those who exhibited an increase of ≥1.5-fold SFU/ml after Selgantolimod administration. Using this as criteria, there were 4/11 responders for HBs specific and 6/13 responders for total IgG response among phase 1a samples (**Figures 7A–C**). In samples from CHB patients (phase 1b), HBs specific IgG spots increased in 6/17 subjects and total IgG in 5/18 subjects (**Figures 7D–F**). Most subjects that showed improvement in spots had lower baseline IgG response, though there was no clear cutoff for determining responders. These outcomes suggest that TLR8 treatment has potential to augment memory B cell response in a subset of CHB subjects. It will be important to identify characteristics of responders or non-responders; however, here we did not see positive correlation between T_{FH} response and ELISPOT response in the small number of responders.

DISCUSSION

In this investigation we demonstrated that triggering of TLR8 induces IL-12 production from monocytes, which in turn leads to differentiation of $CD4^+$ T cells into IL-21 producing T_{FH} in peripheral blood samples from CHB patients. Accordingly, co-

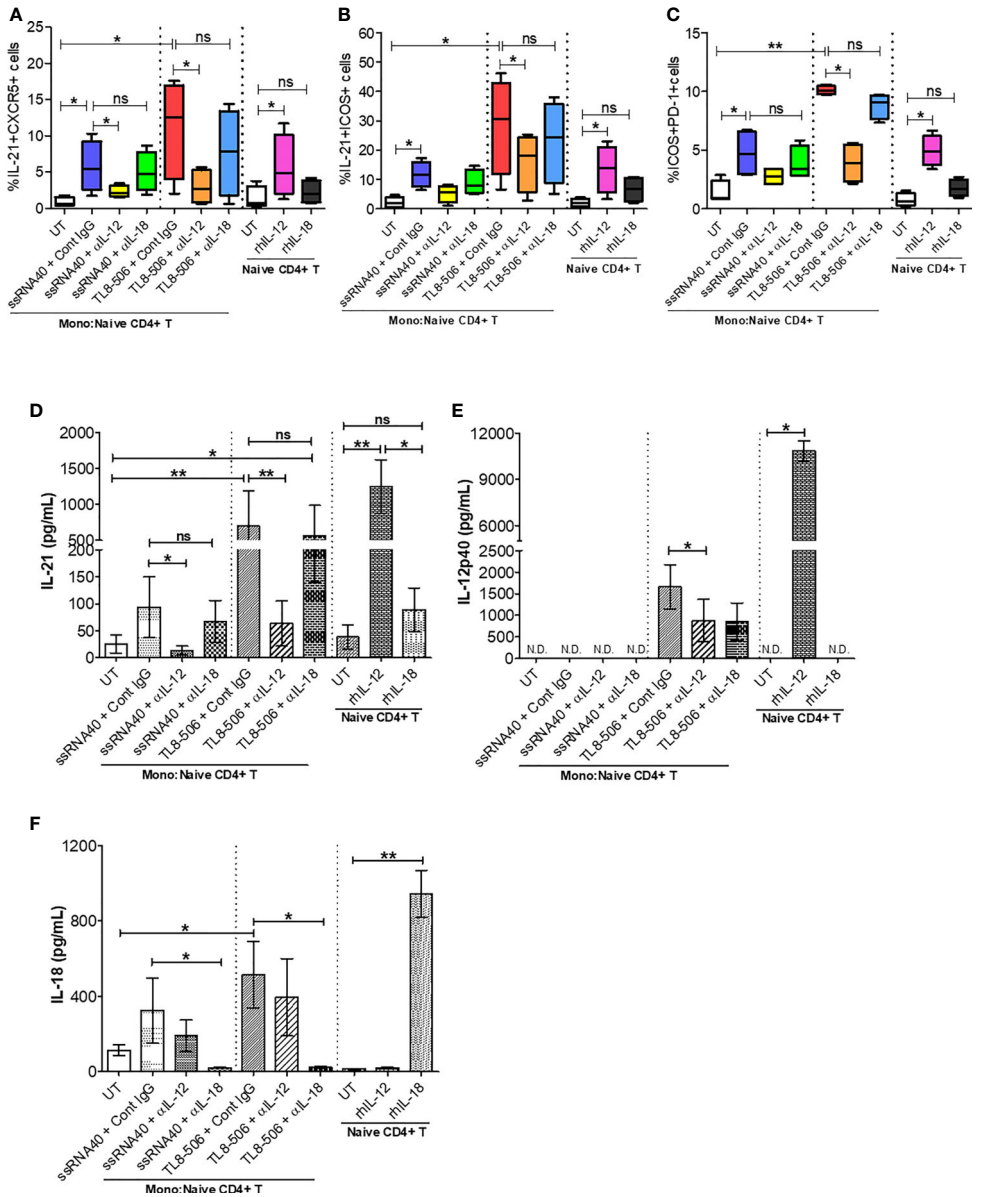

FIGURE 5 | TLR8 signaling promotes IL-12-dependent GC-like T_{FH} cell differentiation and improved IL-21 production. Autologous naïve $CD4^+$ T cells were isolated from PBMCs of HC (n=2) and CHB patients (n=2) and co-cultured with $CD14^+$ enriched monocytes (as APCs, 2:1 ratio) previously stimulated with medium (UT, negative control), TLR8-specific ligands ssRNA40 or TL8-506 along with isotype control IgG, anti-IL-12 or anti-IL-18 neutralizing (blocking) Ab and cultured for 6 days in the presence of SEB followed by re-stimulation with PMA/Ion to activate T_{FH} cells. Flow cytometry was carried out and the frequencies of cells co-expressing T_{FH} markers are shown for **(A)** $IL\text{-}21^+CXCR5^+$, **(B)** $IL\text{-}21^+ICOS^+$ and **(C)** $ICOS^+PD\text{-}1^+$. Cytokine levels were quantified in the supernatants collected from monocyte-naïve $CD4^+$ T co-cultures as well as naïve $CD4^+$ T cell culture by Luminex multiplex immunoassay. Bar graph depicts the levels of **(D)** IL-21 (pg/mL), **(E)** IL-12p40 (pg/mL) and **(F)** IL-18 (pg/mL) secretion in response to TLR8-specific agonists and blocked by anti-IL-12, anti-IL-18 neutralizing Abs or upon incubation with human recombinant proteins IL-12 or IL-18. Statistical significance calculated by one-way ANOVA or Kruskal-Wallis test for comparison between stimulation conditions. P values ≤0.05*, 0.01** considered significant, ns, no significance; APCs, antigen-presenting cells; SEB, staphylococcal enterotoxin B; rhIL-12/IL-18, recombinant human protein IL-12/IL-18; Cont. IgG, isotype control IgG; N.D., not detected.

culture of these differentiated T_{FH} with autologous B cells resulted in B cell differentiation into plasma cells and promoted IgG production. Finally, in a fraction of CHB patients treated with a selective TLR8 agonist, improved HBsAg-specific T_{FH} and B cell responses were observed. Therefore, our study established that TLR8 signaling has potential to restore a critical defect in T-B interaction that is necessary for robust B cell response.

Humoral immunity requires interaction between B cells and specialized populations of $CD4^+$ T cells, the $CD4^+CXCR5^+$

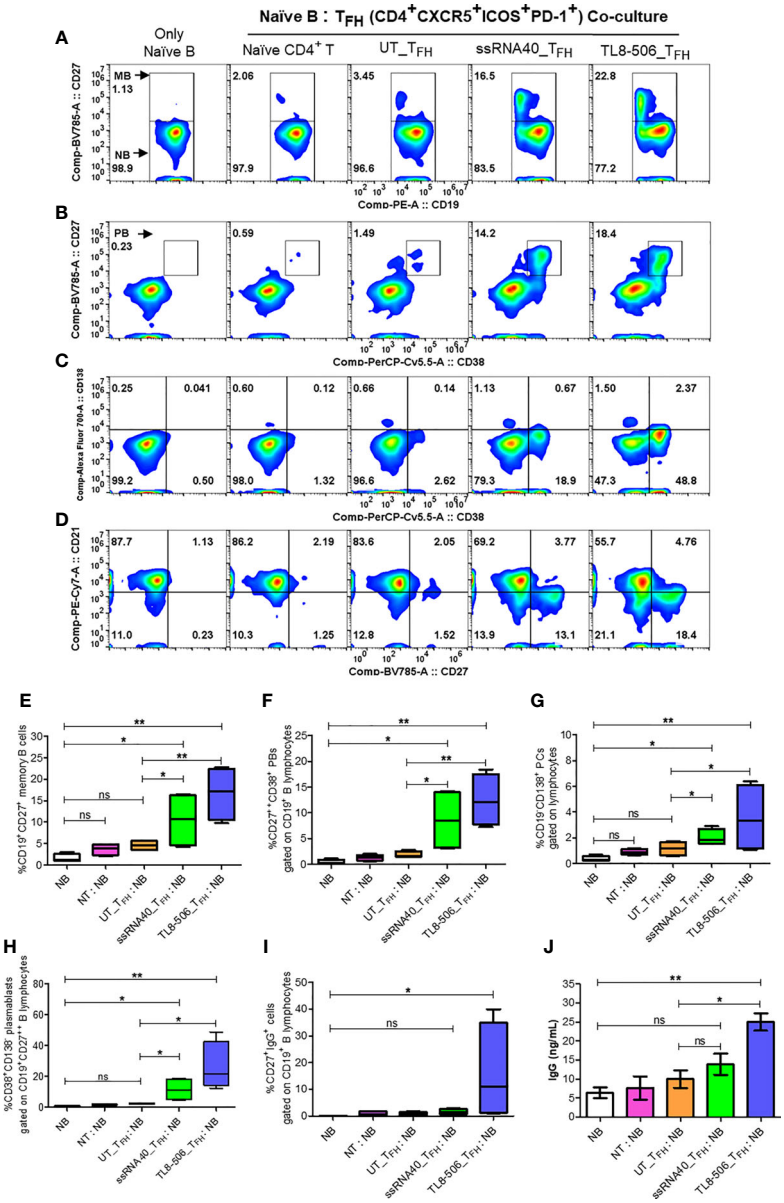

FIGURE 6 | T_{FH} cells differentiated by TLR8 pathway support the generation of memory B and plasma B cells. GC-like T_{FH} cells (PD-1$^+$CXCR3$^-$ cT_{FH}) differentiated with TLR8 agonists were sorted and co-cultured with autologous naïve B cells from healthy donors (n=2) and CHB patients (n=2) at T_{FH}:naïve B ratio of 1:2 in the presence of staphylococcal enterotoxin and generated B cell subsets and IgG examined. Flow cytometry analysis carried out using B cell panel antibodies show pseudo color flow plot of **(A)** Memory B (CD27$^+$), **(B)** Plasma B (CD27^{++}CD38$^+$), **(C)** PCs (CD27^{++}CD38$^-$CD138$^+$), PBs (CD27^{++}CD38$^+$CD138$^-$) and **(D)** B cell subsets NBs (CD27$^-$CD21$^+$), RMBs (CD27$^+$CD21$^+$), AMBs (CD27$^+$CD21$^-$), ATMBs (CD27$^-$CD21$^-$), gated on CD19$^+$ B lymphocytes. Numbers inside the quadrant represents the percentage of events. The frequencies of different B cell subsets are presented in the bar graphs **(E–H)**, as indicated. **(I)** frequencies of IgG$^+$ cells, gated on CD19$^+$CD27$^+$ memory B cells. **(J)** IgG levels (ng/mL) secreted by memory B cells in the supernatants recovered from naïve B-T_{FH} co-culture experiments detected by high sensitivity ELISA assay. Statistical analyses done by one-way ANOVA or Kruskal-Wallis test for comparison between cell culture conditions. P values ≤0.05*, 0.01** represent statistical significance. NBs, naïve B; NT, Naïve CD4$^+$ T; PCs, plasma cells; PBs, plasmablasts; RMBs, resting memory B; AMBs, activated memory B; ATMBs, atypical memory B cells; ns, no significance.

follicular helper (T_{FH}) cells, the latter help generate memory B cells and long-lived plasma cells (26); both these immune cell types are dysfunctional in CHB patients. Since HBcAg-specific antibodies are generated during infection, this defect is selective to HBsAg-specific cells, potentially due to high levels of circulating HBsAg present in patients (27). Indeed, HBs specific but not HBc specific B cells show characteristics of impaired cells characterized by atypical memory phenotype and poor differentiation into antibody secreting cells (5, 6, 28, 29). At the same time, T_{FH} have dysregulated response to HBsAg

that associates with HBV persistence (30). Our results also demonstrate that HBsAg-specific T_{FH} response is defective in CHB patients relative to HBV vaccinated controls. We show here that IL-12 induction by monocytes in response to TLR8 signaling was able to rescue these defective T_{FH}. Specifically, signaling through TLR8 resulted in differentiation of T_{FH} into phenotypes consistent with bona fide helpers of B cells i.e., PD-1^+BCL-6^+ICOS$^+$IL-21^+, in samples from CHB patients. *In vitro* use of Selgantolimod resulted in a similar increase in frequency of circulating PD-1^+ T_{FH} in another study (31). We have only studied peripheral T_{FH} here due to limitations in access to lymphoid cells from patients. As such this may not entirely reflect the impact on antibody generation process, which occurs in secondary lymphoid organs, specifically in structures called germinal centers. However, specific subsets of circulating T_{FH} are identified which share similar phenotypes, transcriptional and

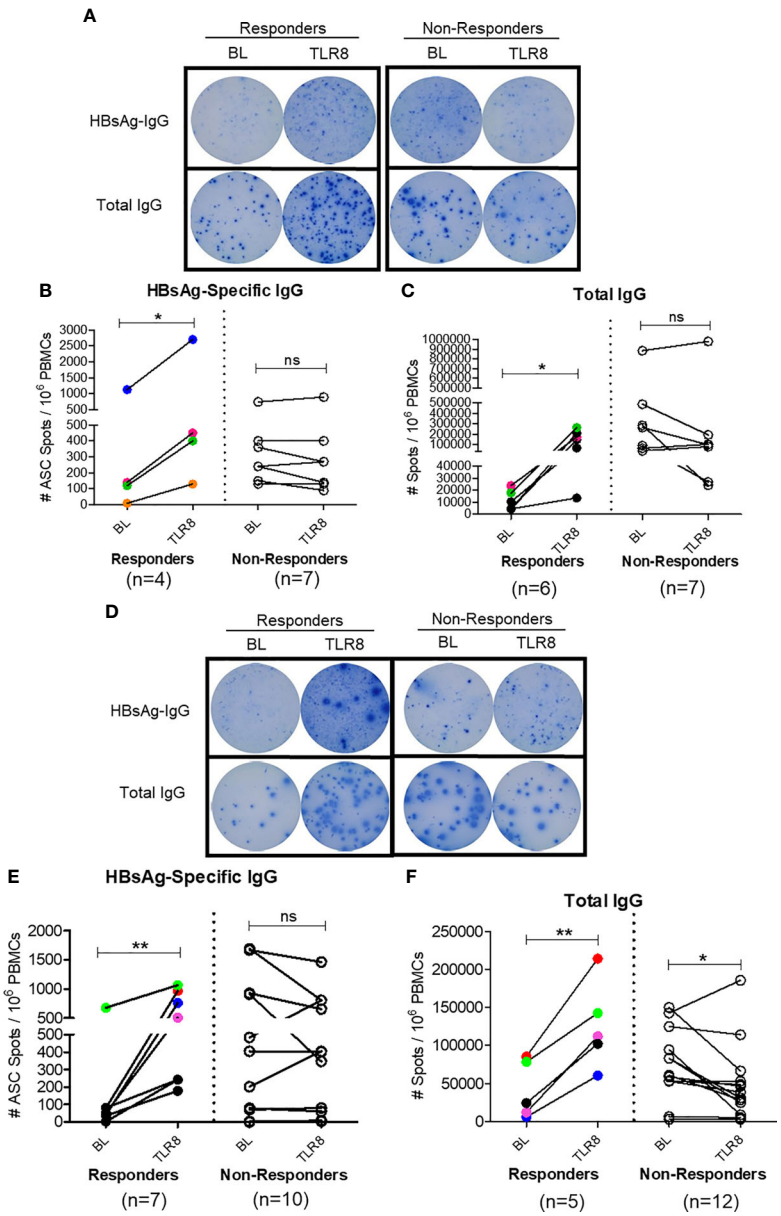

FIGURE 7 | Selgantolimod treatment enhanced B cell responses. PBMCs from BL or Selgantolimod (TLR8) administered HC (phase 1a **A–C**) and CHB (phase 1b, **D–F**) samples were stimulated as detailed in methods to effectively induce memory B cells proliferation. **(A, D)** Representative ELISPOT results show IgG spots in responders and non-responders, **(B, E)** HBsAg-specific IgG and **(C, F)** total IgG secreting B cells from phase 1a and phase 1b samples. Statistical significance calculated by two-tailed paired Student's t test or the Wilcoxon signed-rank. Color-coded symbols in responders group indicate same clinical sample tested for HBs-IgG and total IgG. Responder defined as subject with >=1.5-fold improvement in SFU in TLR8 compared with BL time-point. P value of ≤0.05*, 0.01** indicate statistical significance. ns, no significance. BL- baseline; TLR8- toll-like receptor 8; IgG, immunoglobulin; n, number of paired samples.

functional characteristics with germinal center T_{FH} cells (20); this peripheral population allows an easily accessible means to examine phenotypic and functional state of these cells during diseases and to investigate effects of interventions on them (21). Canonical T_{FH} differentiation starts with dendritic cell priming of naïve $CD4^+$ T cell whereupon receiving cytokine signals, expression of CXCR5 on $CD4^+$ T cell allows early T_{FH} to migrate to T-B cell border and undergo further differentiation. Among DC derived cytokines, IL-12 and TGF-β1 are most efficient at inducing human naïve $CD4^+$ T cells to express T_{FH} molecules CXCR5, ICOS, IL-21 and BCL-6 (32–36). Recently, it was discovered that TLR8 signaling results in differentiation of functional T_{FH}; the intact ssRNA in attenuated vaccines triggers TLR8 on monocytes, inducing IL-12 production, which in turn differentiates naïve $CD4^+$ T cells into functional T_{FH}. These T_{FH} cells support plasma cell generation and IgG production from B cells (12).

CHB infection is associated with significant immune dysregulation, whether TLR8 agonism will lead to TFH differentiation and subsequent B cell help was therefore not a given. Reports have shown both functional (10) and defective TLR8 response (37) in CHB. However, *in vitro* testing of Selgantolimod showed comparable levels of cytokines in PBMC from healthy and CHB subjects (31). In clinical trial of this agonist in healthy subjects, we previously showed IL-12p40, IL-12p70, IL-1RA and IL-18 induction in serum (14), here we show T_{FH} polarizing cytokines, IL-12 is induced with the agonist in monocytes from CHB patients which led to naïve $CD4^+$ T cells to differentiated into $CXCR5^+BCL\text{-}6^+ICOS^+IL\text{-}21^+$ T_{FH}. A significant finding here is demonstration of HBsAg-specific T_{FH} response ($ICOS^+BCL\text{-}6^+$ T_{FH} and upregulation of AIM markers) in CHB patients treated with a single dose of Selgantolimod. IL-12p40 and IL-12-p70 are induced within 4 hours after oral administration of this agonist (14); we hypothesize that IL-12p70 provided requisite signal to naïve $CD4^+$ T cells in treated patients, which was manifested by the expression of T_{FH}-specific growth factors when PBMC were tested in our *in vitro* culture assays. Mechanistically, TLR8 agonism induced T_{FH} with phenotypes bona fide helpers which aided plasma cell generation and IgG response. In our study this was reflected in results from naïve B-T_{FH} co-culture and B cell ELISPOT assays, which demonstrated enhanced total IgG and HBsAg-specific B cell responses after TLR8 agonist treatment. It may seem surprising that an improvement in B cell response was present in an acute treatment setting (8 hours) with a single dose of Selgantolimod. However, it is important to note that these B cell responses were not measured *ex vivo*, rather the ELISPOT assay measures memory B cell responses generated after short-term cultures of 5 days. We believe that Selgantolimod treatment generated favorable conditions, such as effective T_{FH} response and cytokine IL-21, which aided these improved B cell responses *in vitro*.

These finding have significance for use of TLR8 agonism for hepatotropic HBV; liver derived cells respond to TLR8 agonism by inducing IL-12 and IL-18 (10). In a woodchuck model of chronic HBV, this same TLR8 agonist resulted in sustained antiviral response and loss of HBs antigen (38). This model uses a surrogate virus and the translatability of these findings to CHB in humans is uncertain, however, the same agonist resulted in similar induction of cytokines IL-12p40, IL-12p70, IL-1β, IL-6, IL-18 and TNF-α *in vivo* in humans (14, 13, 38) and in cultures (here). In a separate study, IL-12, IL-1β and IFN-β induced by ssRNA were shown critical for T_{FH} differentiation, this effect was mediated by TLR signaling adaptor TRIF (39).

There are certain limitations of our study. For more precise evaluation of antigen specific T_{FH} and B cells, use of class II tetramers and HBsAg specific B cell probes, respectively, is needed. It is out of the scope for this investigation due to limited availability of frozen PBMC from these previously completed clinical trials for further experiments. It is also important to show whether an increase in the IgG secreting B cells (ASCs) observed in ELISPOT from some patients correlates with enhanced monocytic IL-12 production or with expression of GC-like T_{FH} growth factors ($IL\text{-}21^+BCL\text{-}6^+$, $IL\text{-}21^+CD40L^+$ and $ICOS^+BCL\text{-}6^+$) or B cell phenotypes. However, due to small sample size it was not possible to perform such correlation analyses in 'responders' and 'non-responders' to TLR8 agonism. A focus on peripheral examination of T-B responses with lack of any investigation into tissue or lymph node responses is another limitation here. T_{FH}-B cell responses will be studied in the ongoing Phase 2 clinical trial, which could establish the true nature of T_{FH}-B cell interactions in restoring clinically relevant anti-HBs response in CHB patients.

Our data has significance for our understanding of impaired HBV-specific protective immunity in CHB patients. Strategies to achieve a functional cure are focused on restoring HBs-antibody responses in CHB patients. HBs antigen-based vaccine candidates have shown mixed results when tested in clinical trials in chronically infected patients (40). Our data support further testing of TLR8 agonism in HBV functional cure approaches that include a combination of antiviral and immune modulatory agents.

DATA AVAILABILITY STATEMENT

The original data presented in the study are included in the article and **Supplementary Material**. Further inquiries can be directed to the corresponding author.

ETHICS STATEMENT

The studies involving human participants were reviewed and approved by University of Maryland, Baltimore. The patients/participants provided their written informed consent to participate in this study.

AUTHOR CONTRIBUTIONS

NA designed methods, performed the experiments, analyzed data and prepared results. LT provided clinical expertise and

provided CHB samples. SKT, DC, JW, and SF provided samples from Selgantolimod clinical trials and critically edited the manuscript. SK participated in study design, critically edited the manuscript and provided resources. BP designed the study, analyzed and interpreted the results, wrote the manuscript and provided funding. All authors contributed to the article and approved the submitted version.

FUNDING

The study was financially supported by Gilead Sciences, Foster City, CA and IHV, University of Maryland school of Medicine, Baltimore, MD.

ACKNOWLEDGMENTS

The authors acknowledge Dr. Xiaoxuan Fan and iLab flowcore facility, University of Maryland School of Medicine for support with Cytek Aurora multi-color FACS panel designs, acquisition and technical advice. We also thank IHV, flowcore facility for sorting on BD FACS Aria III machine.

SUPPLEMENTARY MATERIAL

The Supplementary Material for this article can be found online at: https://www.frontiersin.org/articles/10.3389/fimmu.2021.735913/full#supplementary-material

REFERENCES

1. Maini MK, Bertoletti A. HBV in 2016: Global and Immunotherapeutic Insights Into Hepatitis B. *Nat Rev Gastroenterol Hepatol* (2017) 14(2):71–2. doi: 10.1038/nrgastro.2016.196
2. Revill PA, Chisari FV, Block JM, Dandri M, Gehring AJ, Guo H, et al. A Global Scientific Strategy to Cure Hepatitis B. *Lancet Gastroenterol Hepatol* (2019) 4(7):545–58. doi: 10.1016/S2468-1253(19)30119-0
3. Fanning GC, Zoulim F, Hou J, Bertoletti A. Therapeutic Strategies for Hepatitis B Virus Infection: Towards a Cure. *Nat Rev Drug Discov* (2019) 18(11):827–44. doi: 10.1038/s41573-019-0037-0
4. Burton AR, Pallett LJ, McCoy LE, Suveizdyte K, Amin OE, Swadling L, et al. Circulating and Intrahepatic Antiviral B Cells Are Defective in Hepatitis B. *J Clin Invest* (2018) 128(10):4588–603. doi: 10.1172/JCI121960
5. Salimzadeh L, Le Bert N, Dutertre CA, Gill US, Newell EW, Frey C, et al. PD-1 Blockade Partially Recovers Dysfunctional Virus-Specific B Cells in Chronic Hepatitis B Infection. *J Clin Invest* (2018) 128(10):4573–87. doi: 10.1172/JCI121957
6. Poonia B, Ayithan N, Nandi M, Masur H, Kottilil S. HBV Induces Inhibitory FcRL Receptor on B Cells and Dysregulates B Cell-T Follicular Helper Cell Axis. *Sci Rep* (2018) 8(1):15296. doi: 10.1038/s41598-018-33719-x
7. Doi H, Yoshio S, Yoneyama K, Kawai H, Sakamoto Y, Shimagaki T, et al. Immune Determinants in the Acquisition and Maintenance of Antibody to Hepatitis B Surface Antigen in Adults After First-Time Hepatitis B Vaccination. *Hepatol Commun* (2019) 3(6):812–24. doi: 10.1002/hep4.1357
8. Hu TT, Song XF, Lei Y, Hu HD, Ren H, Hu P. Expansion of Circulating TFH Cells and Their Associated Molecules: Involvement in the Immune Landscape in Patients With Chronic HBV Infection. *Virol J* (2014) 11:54. doi: 10.1186/1743-422X-11-54
9. Tian C, Chen Y, Liu Y, Wang S, Li Y, Wang G, et al. Use of ELISpot Assay to Study HBs-Specific B Cell Responses in Vaccinated and HBV Infected Humans. *Emerg Microbes Infect* (2018) 7(1):16. doi: 10.1038/s41426-018-0034-0
10. Jo J, Tan AT, Ussher JE, Sandalova E, Tang XZ, Tan-Garcia A, et al. Toll-Like Receptor 8 Agonist and Bacteria Trigger Potent Activation of Innate Immune Cells in Human Liver. *PLoS Pathog* (2014) 10(6):e1004210. doi: 10.1371/journal.ppat.1004210
11. Schurich A, Pallett LJ, Lubowiecki M, Singh HD, Gill US, Kennedy PT, et al. The Third Signal Cytokine IL-12 Rescues the Anti-Viral Function of Exhausted HBV-Specific CD8 T Cells. *PLoS Pathog* (2013) 9(3):e1003208. doi: 10.1371/journal.ppat.1003208
12. Ugolini M, Gerhard J, Burkert S, Jensen KJ, Georg P, Ebner F, et al. Recognition of Microbial Viability *via* TLR8 Drives TFH Cell Differentiation and Vaccine Responses. *Nat Immunol* (2018) 19(4):386–96. doi: 10.1038/s41590-018-0068-4
13. Mackman RL, Mish M, Chin G, Perry JK, Appleby T, Aktoudianakis V, et al. Discovery of GS-9688 (Selgantolimod) as a Potent and Selective Oral Toll-Like Receptor 8 Agonist for the Treatment of Chronic Hepatitis B. *J Med Chem* (2020). doi: 10.1021/acs.jmedchem.0c00100
14. Reyes M, Lutz JD, Lau AH, Gaggar A, Grant EP, Joshi A, et al. Safety, Pharmacokinetics and Pharmacodynamics of Selgantolimod, an Oral Toll-Like Receptor 8 Agonist: A Phase Ia Study in Healthy Subjects. *Antivir Ther* (2020). doi: 10.3851/IMP3363
15. Boltjes A, Groothuismink ZM, van Oord GW, Janssen HL, Woltman AM, Boonstra A. Monocytes From Chronic HBV Patients React *In Vitro* to HBsAg and TLR by Producing Cytokines Irrespective of Stage of Disease. *PLoS One* (2014) 9(5):e97006. doi: 10.1371/journal.pone.0097006
16. Reiss S, Baxter AE, Cirelli KM, Dan JM, Morou A, Daigneault A, et al. Comparative Analysis of Activation Induced Marker (AIM) Assays for Sensitive Identification of Antigen-Specific CD4 T Cells. *PLoS One* (2017) 12(10):e0186998. doi: 10.1371/journal.pone.0186998
17. Dan JM, Lindestam Arlehamn CS, Weiskopf D, da Silva Antunes R, Havenar-Daughton C, Reiss SM, et al. A Cytokine-Independent Approach To Identify Antigen-Specific Human Germinal Center T Follicular Helper Cells and Rare Antigen-Specific CD4+ T Cells in Blood. *J Immunol* (2016) 197(3):983–93. doi: 10.4049/jimmunol.1600318
18. Sun L, Paschall AV, Middleton DR, Ishihara M, Ozdilek A, Wantuch PL, et al. Glycopeptide Epitope Facilitates HIV-1 Envelope Specific Humoral Immune Responses by Eliciting T Cell Help. *Nat Commun* (2020) 11(1):2550. doi: 10.1038/s41467-020-16319-0
19. Goodier MR, Londei M. Lipopolysaccharide Stimulates the Proliferation of Human CD56+CD3- NK Cells: A Regulatory Role of Monocytes and IL-10. *J Immunol* (2000) 165(1):139–47. doi: 10.4049/jimmunol.165.1.139
20. Morita R, Schmitt N, Bentebibel SE, Ranganathan R, Bourdery L, Zurawski G, et al. Human Blood CXCR5(+)CD4(+) T Cells are Counterparts of T Follicular Cells and Contain Specific Subsets That Differentially Support Antibody Secretion. *Immunity* (2011) 34(1):108–21. doi: 10.1016/j.immuni.2010.12.012
21. Crotty S. A Brief History of T Cell Help to B Cells. *Nat Rev Immunol* (2015) 15(3):185–9. doi: 10.1038/nri3803
22. Ise W, Fujii K, Shiroguchi K, Ito A, Kometani K, Takeda K, et al. T Follicular Helper Cell-Germinal Center B Cell Interaction Strength Regulates Entry Into Plasma Cell or Recycling Germinal Center Cell Fate. *Immunity* (2018) 48(4):702–15.e704. doi: 10.1016/j.immuni.2018.03.027
23. Crotty S, Aubert RD, Glidewell J, Ahmed R. Tracking Human Antigen-Specific Memory B Cells: A Sensitive and Generalized ELISPOT System. *J Immunol Methods* (2004) 286(1-2):111–22. doi: 10.1016/j.jim.2003.12.015
24. Muellenbeck MF, Ueberheide B, Amulic B, Epp A, Fenyo D, Busse CE, et al. Atypical and Classical Memory B Cells Produce Plasmodium Falciparum Neutralizing Antibodies. *J Exp Med* (2013) 210(2):389–99. doi: 10.1084/jem.20121970
25. Vinuesa CG, Linterman MA, Yu D, MacLennan IC. Follicular Helper T Cells. *Annu Rev Immunol* (2016) 34:335–68. doi: 10.1146/annurev-immunol-041015-055605

26. Nutt SL, Tarlinton DM. Germinal Center B and Follicular Helper T Cells: Siblings, Cousins or Just Good Friends? *Nat Immunol* (2011) 12(6):472–7. doi: 10.1038/ni.2019
27. Kim JH, Ghosh A, Ayithan N, Romani S, Khanam A, Park JJ, et al. Circulating Serum HBsAg Level Is a Biomarker for HBV-Specific T and B Cell Responses in Chronic Hepatitis B Patients. *Sci Rep* (2020) 10(1):1835. doi: 10.1038/s41598-020-58870-2
28. Le Bert N, Salimzadeh L, Gill US, Dutertre CA, Facchetti F, Tan A, et al. Comparative Characterization of B Cells Specific for HBV Nucleocapsid and Envelope Proteins in Patients With Chronic Hepatitis B. *J Hepatol* (2020) 72 (1):34–44. doi: 10.1016/j.jhep.2019.07.015
29. Vanwolleghem T, Groothuismink ZMA, Kreefft K, Hung M, Novikov N, Boonstra A. Hepatitis B Core-Specific Memory B Cell Responses Associate With Clinical Parameters in Patients With Chronic HBV. *J Hepatol* (2020) 73 (1):52–61. doi: 10.1016/j.jhep.2020.01.024
30. Wang X, Dong Q, Li Q, Li Y, Zhao D, Sun J, et al. Dysregulated Response of Follicular Helper T Cells to Hepatitis B Surface Antigen Promotes HBV Persistence in Mice and Associates With Outcomes of Patients. *Gastroenterology* (2018) 154(8):2222–36. doi: 10.1053/j.gastro.2018.03.021
31. Amin OE, Colbeck EJ, Daffis S, Khan S, Ramakrishnan D, Pattabiraman D, et al. Therapeutic Potential of TLR8 Agonist GS-9688 (Selgantolimod) in Chronic Hepatitis B: Re-Modelling of Antiviral and Regulatory Mediators. *Hepatology* (2020). doi: 10.1002/hep.31695
32. Ma CS, Suryani S, Avery DT, Chan A, Nanan R, Santner-Nanan B, et al. Early Commitment of Naive Human CD4(+) T Cells to the T Follicular Helper (T (FH)) Cell Lineage is Induced by IL-12. *Immunol Cell Biol* (2009) 87(8):590–600. doi: 10.1038/icb.2009.64
33. Schmitt N, Liu Y, Bentebibel SE, Munagala I, Bourdery L, Venuprasad K, et al. The Cytokine TGF-Beta Co-Opts Signaling *via* STAT3-STAT4 to Promote the Differentiation of Human TFH Cells. *Nat Immunol* (2014) 15(9):856–65. doi: 10.1038/ni.2947
34. Schmitt N, Liu Y, Bentebibel SE, Ueno H. Molecular Mechanisms Regulating T Helper 1 Versus T Follicular Helper Cell Differentiation in Humans. *Cell Rep* (2016) 16(4):1082–95. doi: 10.1016/j.celrep.2016.06.063
35. Schmitt N, Morita R, Bourdery L, Bentebibel SE, Zurawski SM, Banchereau J, et al. Human Dendritic Cells Induce the Differentiation of Interleukin-21-Producing T Follicular Helper-Like Cells Through Interleukin-12. *Immunity* (2009) 31(1):158–69. doi: 10.1016/j.immuni.2009.04.016
36. Powell MD, Read KA, Sreekumar BK, Jones DM, Oestreich KJ. IL-12 Signaling Drives the Differentiation and Function of a TH1-Derived TFH1-Like Cell Population. *Sci Rep* (2019) 9(1):13991. doi: 10.1038/s41598-019-50614-1
37. Deng G, Ge J, Liu C, Pang J, Huang Z, Peng J, et al. Impaired Expression and Function of TLR8 in Chronic HBV Infection and its Association With Treatment Responses During Peg-IFN-Alpha-2a Antiviral Therapy. *Clin Res Hepatol Gastroenterol* (2017) 41(4):386–98. doi: 10.1016/j.clinre.2016.12.006
38. Daffis S, Balsitis S, Chamberlain J, Zheng J, Santos R, Rowe W, et al. Toll-Like Receptor 8 Agonist GS-9688 Induces Sustained Efficacy in the Woodchuck Model of Chronic Hepatitis B. *Hepatology* (2020). doi: 10.1002/hep.31255
39. Barbet G, Sander LE, Geswell M, Leonardi I, Cerutti A, Iliev I, et al. Sensing Microbial Viability Through Bacterial RNA Augments T Follicular Helper Cell and Antibody Responses. *Immunity* (2018) 48(3):584–98.e585. doi: 10.1016/j.immuni.2018.02.015
40. Stasi C, Silvestri C, Voller F. Hepatitis B Vaccination and Immunotherapies: An Update. *Clin Exp Vaccine Res* (2020) 9(1):1–7. doi: 10.7774/cevr.2020.9.1.1

Conflict of Interest: SKT, DC, JJW and SPF were employed by Gilead Sciences Inc. BP received financial support paid to University of Maryland from Gilead Sciences. The authors also declare that this study received funding from Gilead Sciences. The funder had the following involvement with the study: interpretation of data/editing of manuscript.

frontiers in Immunology

REVIEW
published: 07 September 2021
doi: 10.3389/fimmu.2021.733364

Interferon and Hepatitis B: Current and Future Perspectives

Jianyu Ye[1] *and Jieliang Chen*[1,2*]

[1] Key Laboratory of Medical Molecular Virology (MOE/NHC/CAMS), School of Basic Medical Sciences, Shanghai Medical College, Fudan University, Shanghai, China, [2] Research Unit of Cure of Chronic Hepatitis B Virus Infection, Chinese Academy of Medical Sciences, Shanghai, China

Chronic hepatitis B virus (HBV) infection remains a major health burden worldwide for which there is still no effective curative treatment. Interferon (IFN) consists of a group of cytokines with antiviral activity and immunoregulatory and antitumor effects, that play crucial roles in both innate and adaptive immune responses. IFN-α and its pegylated form have been used for over thirty years to treat chronic hepatitis B (CHB) with advantages of finite treatment duration and sustained virologic response, however, the efficacy is limited and side effects are common. Here, we summarize the status and unique advantages of IFN therapy against CHB, review the mechanisms of IFN-α action and factors affecting IFN response, and discuss the possible improvement of IFN-based therapy and the rationale of combinations with other antiviral agents in seeking an HBV cure.

Keywords: IFN, HBV, chronic hepatitis B, cccDNA, innate immunity, antiviral therapy, immunotherapy, biomarker

OPEN ACCESS

Edited by:
Jia Liu,
Huazhong University of Science and Technology, China

Reviewed by:
Yuchen Xia,
Wuhan University, China
Kyun-Hwan Kim,
Sungkyunkwan University, South Korea

***Correspondence:**
Jieliang Chen
jieliangchen@fudan.edu.cn

Specialty section:
This article was submitted to Viral Immunology, a section of the journal Frontiers in Immunology

Received: *30 June 2021*
Accepted: *17 August 2021*
Published: *07 September 2021*

Citation:
Ye J and Chen J (2021) Interferon and Hepatitis B: Current and Future Perspectives. Front. Immunol. 12:733364. doi: 10.3389/fimmu.2021.733364

INTRODUCTION

Hepatitis B virus (HBV) leads to acute and chronic liver diseases that cause over 780000 deaths yearly worldwide and, currently, there are still more than 250 million chronically infected individuals (1). Chronic hepatitis B (CHB) can progress to cirrhosis in up to 40% of untreated patients, and there is an associated risk of decompensated cirrhosis and hepatocellular carcinoma (HCC) (2). There are two main antiviral therapies: nucleos(t)ide analogs (NAs) and pegylated interferon (IFN) α (PEG-IFN-α). NAs effectively control HBV replication but functional cure is rare. PEG-IFN has a limited treatment course and the responders to IFN therapy may maintain a virologic response after drug withdrawal, but its efficacy is still not satisfactory.

IFNs, a group of cytokines firstly described in 1957, are crucial modulators of the immune response against various viruses as well as carcinoma. IFNs are grouped into three types: I (α, β, ϵ, κ, ω), II (γ), and III (λ), based on the types of IFN receptors through which they signal. In humans, IFN-α can be further categorized into 13 different IFN-α subtypes, which all signal through a shared type I IFN heterodimeric receptor complex comprising two IFN-α receptor subunits (IFNAR1 and IFNAR2), and these IFNAR receptor subunits are present on nearly all nucleated cells (3). The IFN-IFNAR complex then activates the JAK-STAT pathway, resulting in the expression of dozens of interferon-simulating genes (ISGs), that function as downstream effectors to control viral replication and regulate immune responses. Here, we summarize the status of IFN-α-based therapy in CHB patients, review the mechanisms of IFN action and factors affecting responsiveness, and discuss the possible improvements in IFN therapy leading toward an HBV cure.

ADVANTAGES AND MECHANISMS OF IFN-α TREATMENT AGAINST CHB

For CHB patients, standard PEG-IFN monotherapy is administered once weekly as a subcutaneous injection for 48 weeks, with advantages of finite treatment duration and sustained virologic response. PEG-IFN resulted in a sustained loss of hepatitis B e antigen (HBeAg) and nondetectable hepatitis in 30% of patients (4). In HBeAg-negative CHB, combination NAs plus PEG-IFN for 48 weeks is safe and could result in greater treatment efficacy than NAs monotherapy (5–7). For patients who achieve virologic suppression with NAs, such as entecavir (ETV), switching to a finite course of PEG-IFN significantly increases rates of HBsAg seroclearance to 20% of those with baseline HBsAg < 1500 IU/ml (8). In contrast, HBsAg seroclearance during NAs monotherapy is low (0-3% after 1 year) (9). Once the HBV genome was inactivated ("inactivate carriers"), HBsAg seroclearance occurred in 40% of those receiving PEG-IFN therapy (10, 11). In addition, treatment by PEG-IFN has been suggested to be associated with a lower incidence of HCC than NAs treatment in chronic HBV infection (12).

IFN-α treatment can induce an antiviral state in hepatocytes by regulating gene expression and protein translation, which exert non-cytolytic antiviral effects in several stages of the HBV life cycle.

First, HBV replicates its DNA genome through reverse transcription of its viral pregenomic RNA (pgRNA), and pgRNA is exported into the cytoplasm. In this process, the expression of APOBEC3 cytidine deaminases can be strongly enhanced by IFN-α simulation to induce extensive G-to-A hypermutations and block HBV DNA replication (13, 14). MX2, which is induced by IFN-α reduces HBV RNA levels by downregulating synthesis of viral RNA (15). IFN-α can also induce TRIM22, which binds to the HBV core promoter region to inhibit its transcription (16). In addition, IFN-α simulates ISG20, which binds to the HBV RNA terminal redundant region to degrade pgRNA (17, 18). IFN-α can also induce MyD88 to accelerate the degradation of pgRNA and promote the expression of MxA to impede HBV RNA nuclear export (19). Of note, HBV infection itself does not induce a significant ISG-mediated response in the liver. Liver biopsy samples from patients with HBV infection do not have higher levels of ISG expressions than those from patients without HBV infection (20). Moreover, recent *in vitro* studies suggested that HBV does not affect the pattern of ISG expressions induced by polyinosinic: polycytidylic acid (poly I:C) and Sendai virus (21). From this perspective, exogenous IFN-α may play unique roles in activating endogenous antiviral immune responses against HBV.

Second, once HBV delivers its 3.2kb rcDNA genome into the nuclei of hepatocyte, rcDNA can be repaired into the fully double-stranded covalently closed circular DNA (cccDNA) (22), which serves as the template for transcription of all viral mRNA. The HBV cccDNA is organized as a minichromosome in the nuclei of infected hepatocytes with various host and viral proteins, such as histone proteins and HBx (23, 24), and the intrahepatic cccDNA pool is not homogenous but exists as a heterogeneous population of viral minichromosomes (25). Accumulating evidence suggests that cccDNA transcriptional activity is regulated by epigenetic mechanisms (26, 27). HBx binds to the cccDNA and modifies the epigenetic landscape of cccDNA. The cccDNA without HBx expression transcribes significantly less pgRNA (28). Administration of IFN-α resulted in cccDNA-bound histone hypoacetylation as well as active recruitment to the cccDNA of transcriptional corepressors, which included reduction of acetylated histone H3 lysine 9 (H3K9) and 27 (H3K27) and increase in HDAC1 and Sirt1 in cccDNA minichromosomes. IFN-α treatment also reduced the binding of the STAT1 and STAT2 transcription factors to active cccDNA (29, 30). These modifications are associated with reduced transcription of pgRNA and subgenomic RNAs from the cccDNA minichromosome. In addition to regulating cccDNA transcription, recent studies suggested that IFN may induce degradation of cccDNA by inducing APOBEC3A and ISG20 (31, 32). However, it remains unclear how efficient such a mechanism is in the liver and whether cccDNAs in distinct epigenetic states are similar or differ in their sensitivity to IFN and IFN-induced antiviral factors. It is more certain that IFN-α affects cccDNA epigenetic modifications and represses cccDNA transcription, which in turn reduces the replenishment of the cccDNA pool. From this perspective, IFN-α can indirectly lead to subsequent reduction of the cccDNA pool (33). In addition, IFN-α treatment reduces the expression levels of HBx, which has been demonstrated to promote the degradation of the SMC5/6 complex to enhance HBV replication (34, 35), and thus can restore SMC5/6 expression, resulting in sustained cccDNA silence in HBV-infected human liver chimeric mice (36).

HBV-related protein translation and HBV virion secretion are two other processes that can be inhibited by certain ISGs. In the Huh-7 cell-based HBV transfection model (the double-stranded RNA (dsRNA)-dependent protein kinase) was induced by IFN-α treatment and then, reduced the replication-competent viral capsids, whereas the HBV transcripts, including pgRNA, were not affected (37). In addition, the IFN-inducible factor BST-2/tetherin was able to restrict HBV virion secretion. Knockdown of tetherin attenuated the IFN-α-mediated reduction of HBV virion release (38).

Beyond the scope of a single cell, cell-to-cell transmission of viral resistance is also a mechanism for amplifying IFN-α-induced antiviral response. IFN-α can induce the transfer of resistance to HBV from nonpermissive liver nonparenchymal cells (LNPCs) to hepatocytes *via* exosomes (39–41). Exosomes from IFN-α-treated LNPCs are rich in molecules with antiviral activity. Further studies suggest that macrophage exosomes depend on T cell immunoglobulin and mucin receptor 1 (TIM-1), a hepatitis A virus receptor, to enter hepatocytes for delivering IFN induced anti-HBV activity. Hepatocytes could utilize two primary virus infection endocytic routes (clathrin-mediated endocytosis (CME) and micropinocytosis) and lysobisphosphatidic acid (LBPA) to permit exosome entry and uncoating (42).

In addition to the direct anti-HBV effects, IFNs shape the landscape of the immune system to coordinate various immune cells. IFNs activated macrophages, natural killer cells, dendritic cells (DCs), and T cells. All these activated immune cells secrete a variety of cytokines, such as IL-1β, IL-6, TNF-α, and IFN-γ. Among them, IL-6, IL-12, and IL-15 by DCs were partially induced by IFN-α/β and then modulated B and T cell differentiation (Th1 polarization) and activation (43). IFN-I signaling in plasmacytoid dendritic cells (pDCs) led to altered CD69 and sphingosine-1-phosphate 4 (S1P4) receptor expression, which, in turn, affected pDCs retention in lymph nodes (44). IFN-α/β also enhance the antigen presenting capacity of the APC by increasing MHC class II, CD86, and CD40 expression. Moreover, IFN-α/β help neutrophil survival and strengthen phagocytosis of macrophage and neutrophil. HBV-specific $CD8^+$ T cell are then propagated into the liver, and destructed the infected hepatocytes by perforin-granzymes or surface death receptors such as FAS/FASL, or both (45). This is called "cytopathic mechanism".

Notably, HBV infection in immunocompetent adults is usually self-limited and transient. Over 90% of adults achieve viral control with strong, polyclonal, and multi-specific adaptive immune responses, such as specific $CD8^+$ and $CD4^+$ T cells, against HBV components (46). During acute HBV infection, most hepatocytes were reported to be infected by HBV. Assuming most infected hepatocytes are destroyed through the cytopathic mechanism, patients will have severe liver trauma, which is rarely seen in the clinic. Thus, "non-cytopathic mechanism" has been proposed to explain this (47). It is believed that non-cytopathic mechanisms allow infected hepatocytes to purge HBV replicative intermediates from the cytoplasm and cccDNA from the nucleus without being killed. Some clues support this notion. First, HBsAg-specific class I-restricted cytotoxic T lymphocytes (CTLs) profoundly suppress hepatocellular HBV gene expression in HBV transgenic mice by a noncytolytic process. This regulatory effect of the CTLs is initially mediated by IFN-α/β, IFN-γ, and TNF-α, which greatly exceeds their cytopathic effects in magnitude and duration (47, 48). Second, in acutely infected chimpanzees, HBV DNA was shown to largely disappear from the liver and the blood long before the peak of T cell infiltration (49). When knocking out one of these key components (T cell, NK cell, Fas, IFN-γ, IFN-α/β, and TNF-α) in the mouse model, hydrodynamically injected HBV-expressing plasmid persisted for at least 60 days, indicating that each of these effectors contributes to eliminate HBV components (50). In addition, proinflammatory cytokines such as IL-6, IL-1β, IL-4, and TGF-β, which could be induced by IFN show antiviral effects in different stages of HBV replication (51). Nonetheless, the non-cytopathic mechanism has not been adequately revealed because of the complexity of the liver immune microenvironment and the lack of an appropriate animal model.

In IFN-mediated control and clearance of HBV infection, it is still uncertain to what extent the direct anti-HBV effects and indirect immunomodulatory effects contribute to the IFN-α-mediated antiviral action. In the HBV-infected humanized uPA/SCID mice model, PEG-IFN-α treatment can induce sustained responsiveness in HBV-infected hepatocytes and trigger substantial HBV antigen decline without the involvement of immune cell response (52). Notably, a poor restoration of immune cell functions was observed in the early phases of IFN treatment (53), but changes in the inflammatory environment in the liver take a long time to develop and cytotoxic CD8+ T cells can be more readily expanded in the blood of treatment responders than nonresponders, indicating the importance of immune cells in HBV control and supporting a role of IFN-based therapy in restoration of the immune system.

One study indicated that the absolute number of $CD8^+$ T cells were strikingly reduced, including CMV-specific CD8 T cells, while $CD56^{bright}$ NK cells were potently expanded in a cohort of HBeAg negative patients receiving PEG-IFN-α therapy. Depleting $CD8^+$ T cells may limit the efficacy of PEG-IFN-α, on the other hand, $CD56^{bright}$ NK cells could enhance anti-HBV efficacy (54). More understanding of the mechanisms of IFN-α action will assist in the improvement of antiviral efficacy.

FACTORS THAT INFLUENCE IFN RESPONSE

HBV has been called a 'stealth' virus since it does not induce a significant IFN response in the liver. Besides, sustained off-treatment response to exogenous IFN-α therapy can be achieved only in a minority of CHB patients. Both host and viral factors influence the IFN response during HBV infection and IFN-α therapy (**Table 1**), some of which could be used as predictors to improve the cost-effectiveness of IFN-α therapy.

VIRAL FACTORS

Low HBV viral and antigen load is important predictor favoring IFN therapy. The viral load could influence both innate and adaptive immune response pathways, which impairs the response to IFN. In untreated CHB patients, intrahepatic gene expression profiling showed a strong downregulation of the antiviral effector, interferon stimulated genes, and pathogen recognition receptor pathway compared with non-infected controls (92). Although it remains controversial whether the host could detect the virion and express innate and IFN genes during HBV infection (20, 21, 93–97), HBV has developed strategies to counteract the innate and IFN system. HBV particles readily inhibit host innate immune responses upon virion/cell interaction (98, 99). HBV polymerase (Pol) and HBx could block multiple critical innate immune response pathways in hepatocytes, including RIG-I, STING, TRIM22, and IRF (64, 65, 100). HBsAg could inhibit the induction of IFN-α and proinflammatory cytokines such as IL-12, and HBeAg could target and suppress activation of the TLR and related signaling pathway (61, 62, 72). In addition, prolonged exposure of T cells to high quantities of HBV-related antigen, especially HBsAg, is

TABLE 1 | Viral and host factors that affect IFN response during HBV infection and IFN therapy.

Viral and host factors			Role in modulating IFN response	Ref
Viral Factors	Viral load		Lower viral load and antigen levels associate with higher responsiveness to IFN-α therapy	(55, 56)
	Genotype and mutants		Gt A and B associates with better response to IFN treatment than gt D and C, respectively Precore and core promoter mutants limits the probability of response to IFN in HBeAg-positive CHB	(57–60)
	Viral Counteractions	HBsAg	Inhibits with TLRs signaling and IFN-α induction in pDCs, and interfers with immune cell functions.	(61–63)
		Pol	Inhibits RIG-I/TLR3/STING-IRF-IFN-I and IFN-I-JAK/STAT signaling in hepatocytes	(64–66)
		HBx	Inhibits RIG-I/MAVS signaling	(67–69)
		HBc	Inhibits IFN-inducible MxA and IFITM1	(70, 71)
		HBeAg	Inhibits TLR2 and TIR intracellular form and IFN signaling	(72–74)
		HBSP	Inhibits IFN-I signaling	(75)
Host Factors	ALT		Higher baseline ALT levels are predictive of better IFN responsiveness	(56, 76)
	Age and gender		Younger age and female are predictive of better IFN responsiveness	(77, 78)
	Genetic polymorphisms		SNPs of IL28B(IFN-λ3), STAT4 and UBE2L3 could be associated with IFN response	(79–87)
	Liver stage and intrinsic sensitivity to IFN		Staging of liver fibrosis, presence of liver steatosis may affect the IFN response	(55, 78)
	Anti-IFN antibodies		May associate with non-response to IFN-α therapy	(88–91)

HBSP, hepatitis B spliced protein; IFITM1, interferon induced transmembrane protein 1; MxA, myxovirus resistance protein; RIG-I, retinoic acid-inducible gene I; TIR, Toll/IL-1 receptor; STING, stimulator of interferon genes; IRF, interferon regulatory factor; MAVS, mitochondrial antiviral-signaling protein.

the most likely reason for defective T-cell function in CHB patients (101). The decline of viral load is beneficial for the antigen removal, which allows T cells to rest from antigenic stimulation and might be necessary for reconstitution of functional T-cell responses (102, 103). Moreover, higher HBV replication levels lead to a lower sensitivity of HBV to IFN-α in PHH culture models (55), corresponding to the clinical observation that higher viral load is associated with poor response to IFN-α. In this regard, IFN-based therapy may contribute to the restoration of the immune system by directly suppressing antigen production in infected hepatocytes, in addition to its immunomodulatory effect. On the other hand, the magnitude of HBV-specific CD8+ T cell response is primarily regulated by the initial antigen expression level, and a recent study using the HBV hydrodynamic transduction model suggests that IFN-I signaling may negatively regulated HBV-specific CD8+ T cell responses by reducing early HBV antigen expression (104). Notably, although HBV *per se* does not activate IFN-I signaling during natural HBV infection, recent studies in chimpanzees and humanized mouse models indicate that IFN-I signaling induced by HCV infection could contribute to HBV control (105, 106).

HBV genotype has been shown to influence the therapeutic response to IFN-α therapy. In HBeAg-positive patients, the SVR was significantly better in genotypes A and B patients than for genotypes C and D that were treated with standard IFN-α (7). In HBeAg-positive Asian populations, HBV genotype B patients are more responsive to IFN-based therapy, whether PEG-IFN-α or standard IFN-α therapy, whereas genotype C patients have a higher likelihood of response to PEG-IFN-α compared to standard IFN-α (107). In HBeAg-negative patients, PEG-IFN-α was less effective in genotypes D and E with an SVR of around 20%. It should be noted that the prevalence of HBV genotypes varies geographically. Although genotypes A to J have been found (108), genotypes A, B, and C are most prevalent in North America (109). Genotypes B and C are the dominant types in East Asia (110). The above clinical statistical conclusions may be influenced by other factors, such as race, lifestyle, and, even, infected period. For instance, genotype A2 was mostly adult acquired whereas genotypes B and C were transmitted at birth or in very early childhood in a large proportion of Asian patients. The differential IFN response observed among these patients might be in part a reflection of transmission-related immune tolerance or host genetic polymorphisms, rather than the viral genotypes. Nonetheless, HBV genotyping is useful in patients being considered for IFN-α therapy (111). Since HBV population in the host usually consists of remarkable genetic heterogeneity and persists in the form of quasispecies, a number of studies have indicated that HBV mutations at baseline might affect IFN response (112, 113).

HOST FACTORS

A series of host factors have been identified as independent predictors of response to IFN therapy including younger age, female gender in HBeAg-negative CHB patients, and high serum alanine transaminase (ALT) levels (≥2-5 upper limit of normal) in both HBeAg-negative and positive patients (56, 76). Although high serum ALT levels may indicate active immune status and eradication of HBV, the mechanism behind its association with response to IFN is worth exploring.

Host genetics is an important aspect affecting the responsiveness to treatments. Interleukin (IL)28B polymorphisms were reported to be associated with IFN-α treatment response in CHB patients. The relationship between IL28B polymorphisms and response to PEG-IFN-α therapy has also been investigated. Among HBeAg-positive patients, three different single nucleotide polymorphisms (SNP) in IL28B were investigated separately: rs8099917, rs12980275, and rs8099917 (94–96). The polymorphisms in rs8099917 showed no difference in response to PEG-IFN-α, while rs12980275 and rs8099917 polymorphisms showed a difference in HBeAg seroconversion rate. Among HBeAg-negative patients, one study enrolled 101 patients treated with PEG-IFN-α therapy for a median of 23 months (79). Most patients were middle-aged men with HBV genotype D, average serum HBV DNA 6.0 log cp/mL, ALT

136 IU/L, and 42% with cirrhosis. The proportion of patients with CC, CT, and TT genotypes for IL28B rs12979860 were 47%, 42%, and 11%, respectively. The rate of serum HBsAg clearance was 29% in CC compared to 13% in non-CC. The C allele of rs12979860 was associated with a higher rate of response in HBeAg-negative patients with genotype D of HBV treated with PEG-IFN-α. However, the power of IL28B polymorphisms to predict the outcomes of IFN therapy remains limited because of various SNPs, patients' conditions, and duration of treatment.

Given that STAT4 is an important part of the JAK-STAT pathway, SNPs in STAT4 could also be candidates that predict the outcome of IFN-α therapy. Multiple genomic loci, rs7574865, rs4274624, rs11889341, rs10168266, and rs8179673, were shown to be associated with the risk of HBV infections or predictors of PEG-IFN-α therapy (80). For instance, in HBeAg-positive patients, the rs7574865 GG genotype was significantly associated with a reduced sustained virologic response (SVR, defined as HBeAg seroconversion and HBV DNA level < 1000 cp/ml) compared with the GT/TT genotype in patients receiving PEG-IFN-α (18.0% *versus* 41.2%, $P = 9.74\times10^{-5}$) or IFN-α (21.1% *versus* 37.2%, P = 0.01) therapy (81). However, meta-analysis cannot validate the correlation between STAT4 rs7574865 and HBV susceptibility or natural clearance (82, 83). To sum up, transferring these genomic approaches to clinical practice to improve pretreatment patient selection is still challenging.

The occurrence of endogenous anti-IFN antibodies is another factor that may be associated with non-response to IFN-α therapy. During IFN therapy, IFN neutralizing antibodies appeared in the serum of 7%~39% CHB patients (88–90). Anti-IFN antibodies lowered the levels of serum IFN bioactivity and may reduce downstream IFN signaling pathways. For patients relapsing during or after IFN treatment, the appearance of anti-IFN antibodies is likely to occur prior to or at the same time as serum HBV DNA loss (88). However, a study retrospectively suggested that the presence of anti-IFN antibodies was not associated with non-response to PEG-IFN-α therapy in CHB patients (91). In this regard, more studies are required to identify the role of anti-IFN antibodies in the process of HBV chronic infection. In addition, since IFN-α can be divided into different subtypes, it would be interesting to know whether the anti-IFN-α antibodies have subtype bias.

Several cell culture systems have been used to study HBV and IFN interaction. For liver cell culture models, there are mainly four types of systems: hepatoma cell lines (such as HepG2 and Huh7) and related strains (such as HepG2-NTCP and HepAD38), bi-potent liver progenitor cell line (HepaRG), primary human hepatocytes (PHH) (114), and induced human hepatocyte-like cells (such as HepLPCs and iHeps) (115–117). Notably, the responses of IFN differ a lot among these models. Among them, PHH is still regarded as the gold standard for hepatic *in vitro* culture models and is more sensitive to IFN-α than most hepatoma cell lines such as HepG2 or HepG2-NTCP. The expression of ISGs after IFN-α stimulation is partially incompetent in hepatoma cell lines. ISGs including GBP5, GBP1, WARS, and CXCL10, which have been reported to be associated with the IFN-α response in patients (118, 119), are either absent or weakly expressed in HepG2-NTCP cells treated by IFN-α (55).

STRATEGIES TO IMPROVE THE EFFICACY OF IFN-BASED THERAPY

Given the unique advantages of but relatively low response rates to IFN therapy, there is an urgent need to improve its efficacy (**Figure 1**).

Massive and persistent transcription of cccDNA contribute to the inhibition of both innate and adaptive immune responses of IFN. This may explain why the decrease in HBV viremia is not seen earlier than 3-4 weeks into IFN therapy and takes several months to reach its maximum (120). Thus, reduction of the viral load before IFN therapy, including HBV DNA and antigen, could be beneficial. Earlier studies showed that concomitant administration of PEG-IFN and NAs resulted in higher rates of on-treatment virologic response but had no advantage on post-therapy response compared with PEG-IFN monotherapy (57). Nonetheless, the addition of PEG-IFN to ongoing NAs therapy or switching from NAs therapy to PEG-IFN monotherapy in virally suppressed patients has shown better outcomes. A prospective study in CHB patients with HBV DNA fully suppressed by long-term NAs treatment showed that the addition of PEG-IFN for a maximum of 96 weeks led to HBsAg loss and cessation of NAs treatment in 6 of 10 patients, with no relapse for 12-18 months of follow up (121). A matched-pair study in HBeAg-positive patients who did not achieve HBeAg seroconversion after NA monotherapy showed that PEG-IFN combined with NA for another 48 weeks achieved more HBeAg seroconversion than continuing NA monotherapy (44% *versus* 6%) (122). In a randomized open-label trial, switching to a finite course of PEG-IFN significantly increased rates of HBeAg seroconversion and HBsAg loss among patients who achieved virologic suppression with NA therapy (8). Such a treatment concept can provide limited but reliable optimization in current IFN therapy.

Criteria identifying CHB patients who are suitable for IFN therapy is another critical aspect of optimization. Simple and clear guidance is needed to select specific groups of patients. At present, the natural history of CHB has been schematically divided into several phases, mainly focusing on the presence of HBeAg, HBsAg, HBV DNA levels, ALT values, and eventually the presence or absence of liver inflammation. Among them, baseline high ALT and low HBV DNA are the IFN pretreatment predictors of IFN response. Other than these classical biomarkers, novel host factors may potentially help to predict IFN treatment efficacy. For example, baseline quantitative anti-HBc titer has been shown to be a predictor of Peg-IFN efficacy in HBeAg-positive CHB patients (123). In another study, a simplified scoring model composed of miR-210, miR-22, and ALT was used to predict the virologic response of IFN therapy in CHB (124). Environmental factors and individual differences could cause a severe bias towards the accuracy of prediction.

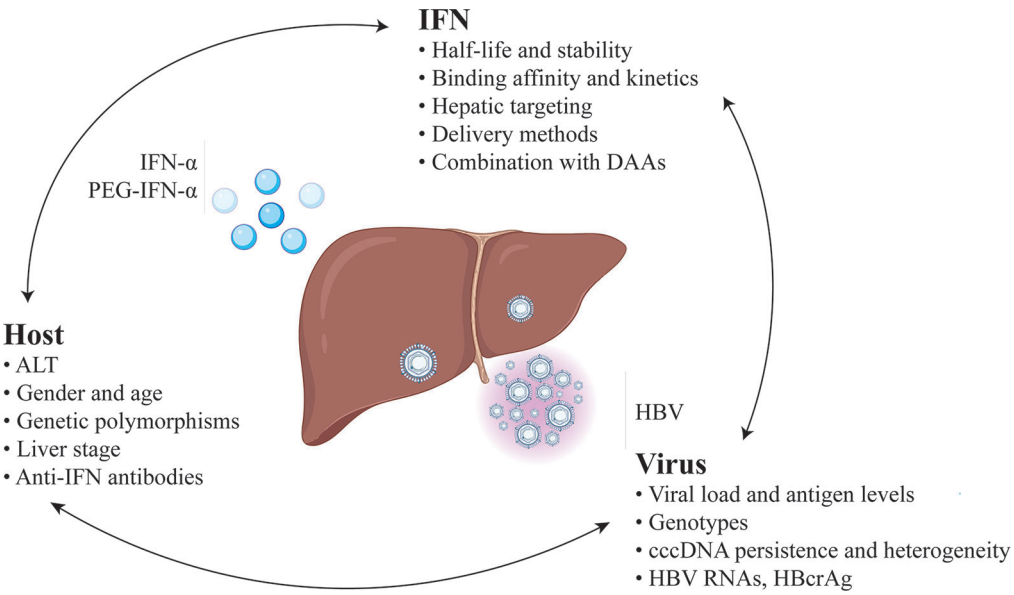

FIGURE 1 | Predictors and strategies for improvement of the efficacy of IFN-based therapy for chronic hepatitis B.

Moreover, some commonly used biomarkers, such as HBV DNA and ALT, are time-dependent and the immune states of CHB patients can hardly be reflected in a single test. For those falling into an indeterminate gray area, an explicit decision is difficult. In recent years, several studies indicate that some novel viral parameters have a statistical relationship with the response of IFN therapy, including serum HBV RNA (125, 126), hepatitis B core-related antigen (HBcrAg) (127), and spliced HBV variants (75), which are worthy of further studies in larger cohorts.

Optimization of IFN itself may, as well, be beneficial for improving therapeutic effects (128, 129). PEG-IFN-α2 is one of the most successful modified protein drugs to date. Grafting IFN-α with PEG attenuates renal filtration, and thus, decreases the rate of IFN clearance from serum. Compared with IFN-α2, PEG-IFN-α2 not only reduces the number of injections but also slightly improves the patient compliance and response rates (130). It is worth noting that poly amino acids are a group of unstructured repetitive segments of hydrophilic amino acids whose biophysical properties are similar to PEG including PAS polypeptides and elastin-like polypeptide. They have been widely considered as potential alternatives to PEG for IFN modification because of their excellent biodegradability and relatively simple preparation procedures compared with pegylation (131, 132). Apart from half-life extension, another modification aspect is the reduction of severe side-effects of IFN-α by targeting hepatocytes precisely because IFN-α acts on almost all human nucleated cells evoking a complex reaction pattern when administered systemically. Novel delivery methods that can improve targeting are of particular interest. One strategy is utilizing the metabolic characteristics of the liver by linking moieties with liver tropism to IFN-α. For instance, high-density lipoproteins (HDLs) are generated in the liver and remove cholesterol from peripheral tissues for delivery to hepatocytes. Anchoring IFN-α to ApoA-I, the main protein component of HDLs, promoted targeting to the liver, and therefore, showed increased immunostimulatory properties and lower hematological toxicity (133). In addition, orally administrable low molecular weight agent which can mimic IFN activity has been shown to suppress HBV replication and reduce cccDNA levels (134).

Increasing binding affinity between IFN-α and IFNAR has proved to be an alternative direction to improve the IFN-α biological efficacy. The key point is that a change in the affinity for IFNAR translates differently among pleiotropic activities induced by IFN-α, including antiproliferative, antiviral, and immunomodulatory activities, which means higher therapeutic effects and lower side effects compared with wild type IFN-α (135). Patten and colleagues constructed the IFN-B9X series consisting of 15 mutants by gene shuffling and point mutation (136). All 15 mutants displayed increased antiviral potency without obvious change in antiproliferative activity compared with IFN-α2. A four-residue motif (FLFY) that overlapped with the IFNAR1 binding site greatly improved the binding affinity between IFN-B9X and IFNAR1 contributed significantly to this phenotype (136). The pegylated form of IFN-B9X, which is called IFN-R7025, has exhibited ~50-fold higher anti-HCV activity compared to PEG-IFN-α2a, but only 2- to 10-fold greater antiproliferative activity *in vitro* (137). However, increasing binding affinity by gene shuffling or point mutation may generate new potential T cell epitopes, which can eventually hinder clinical transformation once it happens (138). IFN-β has the highest binding affinities for both IFNAR1 and IFNAR2. However, IFN-β is more toxic in patients, probably because of its high antiproliferative activity (139), and thus might have a low risk/benefit ratio. Among 13 human IFN-α subtypes, IFN-α2 is

most widely applied in clinical investigation and treatment. However, there are studies revealing that other IFN-α subtypes with higher binding affinity towards IFNAR1 may exert better therapeutic effects in treating certain types of virus compared with IFN-α2 (140). IFN-α subtype 14, one of the naturally engineered variants, has been identified as the most potent subtype against HBV. By comparing the regions between IFN-α2 and IFN-α14 that account for the binding of IFN to IFNAR1, a variant comprised of mutations D83E, T87I, Y90F, and R121K (IFN-α2-EIFK), was constructed, which exhibited potent activity in reducing HBs and HBeAg like IFN-α14. Moreover, a concerted IFN-α and -γ response in liver, which could be efficiently elicited by IFN-α14, is associated with potent HBV suppression (141).

In addition to type I IFN, type III IFNs, consisting of four IFN-λ subtypes (IFN-λ1, IFN-λ2, IFN-λ3, and IFN-λ4), has been considered as an alternative in treatment of CHB (142). IFN-III signals through a heterodimeric receptor composed of IFN-λ receptor-1 (IFNLR1) and interleukin-10 receptor subunit beta (IL10RB) (143). IFNLR1 is expressed primarily on epithelial cells, such as hepatocytes, and on select immune cells, including pDCs and some B-lymphocytes, which may indicate better cell-type specific activity (144, 145). One of the most impactful findings about IFN-λ is the strong association of IFN-λ polymorphisms with chronic HCV clearance during the acute stage of infection and of achieving HCV cure with IFN-I-based therapy in chronic infection (146). Unfortunately, the similar association cannot be identified in HBV patients with high confidence and good reproducibility among various studies (147, 148). Although IFN-λ can activate IFN signaling pathways and lower HBV viral load, pegylated IFN-λ1 was less efficient than PEG-IFN-α2 24 weeks post-treatment because fewer patients achieved HBeAg seroconversion (149).

PERSPECTIVE

All CHB patients are at risk of progression to cirrhosis and HCC. Because of HBV cccDNA persistence and HBV DNA integration into the host genome, it has not yet been possible to eradicate HBV completely with available antiviral agents. Serum HBV DNA and HBsAg loss and sustained intrahepatic cccDNA silencing could significantly reduce the risk of the above hepatic diseases, which can be achieved in a few CHB patients receiving IFN therapy. Given that chronic HBV infection leads to immune injury and tolerance, IFN therapy, as an immune-based approach, has unique mechanistic advantages, compared with NAs, in antiviral immune modulation and may disrupt immune tolerant states. Despite a variety of direct-acting antiviral agents (DAA) targeting various steps of the HBV life cycle are underway, such as HBV entry inhibitor, viral gene expression inhibitor, capsid assembly modifiers, it seems that none of them alone will effectively cure CHB patients in the foreseeable future (150–152). A combination of IFN with these new DAAs may have synergistic effects in CHB. Thus, as discussed above, IFN therapy needs more novel and reliable biomarkers to improve clinical management, and novel combination strategies, and optimization of IFN itself, such as new IFN subtypes and delivery methods, are anticipated to substantially increase the efficacy of treatment for chronic hepatitis B.

AUTHOR CONTRIBUTIONS

All authors listed have made a substantial, direct, and intellectual contribution to the work and approved it for publication.

FUNDING

This work was supported by National Natural Science Foundation of China (82022043, 81974304), the Shanghai Rising-Star Program (20QA1400700) and "Fuqing Scholar" Student Scientific Research Program of Shanghai Medical College, Fudan University (FQXZ202109B).

ACKNOWLEDGMENTS

The authors thank the funding agencies supporting the work.

REFERENCES

1. Martinez MG, Boyd A, Combe E, Testoni B, Zoulim F. Covalently Closed Circular DNA: The Ultimate Therapeutic Target for Curing Hepatitis B Virus Infections. *J Hepatol* (2021) 75(3):706–17. doi: 10.1016/j.jhep.2021.05.013
2. Tang LSY, Covert E, Wilson E, Kottilil S. Chronic Hepatitis B Infection A Review. *Jama-J Am Med Assoc* (2018) 319:1802–13. doi: 10.1001/jama.2018.3795
3. Hoffmann H-H, Schneider WM, Rice CM. Interferons and Viruses: An Evolutionary Arms Race of Molecular Interactions. *Trends Immunol* (2015) 36:124–38. doi: 10.1016/j.it.2015.01.004
4. Perrillo RP. Therapy of Hepatitis B – Viral Suppression or Eradication? *Hepatology* (2006) 43:S182–93. doi: 10.1002/hep.20970
5. Piccolo P, Lenci I, Demelia L, Bandiera F, Piras MR, Antonucci G, et al. A Randomized Controlled Trial of Pegylated Interferon-Alpha2a Plus Adefovir Dipivoxil for Hepatitis B E Antigen-Negative Chronic Hepatitis B. *Antivir Ther* (2009) 14:1165–74. doi: 10.3851/IMP1466
6. Bahardoust M, Mokhtare M, Barati M, Bagheri-Hosseinabadi Z, Behnagh AK, Keyvani H, et al. A Randomized Controlled Trial of Pegylated Interferon-Alpha With Tenofovir Disoproxil Fumarate for Hepatitis B E Antigen-Negative Chronic Hepatitis B: A 48-Week Follow-Up Study. *J Infect Chemother* (2020) 26:1265–71. doi: 10.1016/j.jiac.2020.07.005
7. Marcellin P, Ahn SH, Ma X, Caruntu FA, Tak WY, Elkashab M, et al. Combination of Tenofovir Disoproxil Fumarate and Peginterferon Alpha-2a Increases Loss of Hepatitis B Surface Antigen in Patients With Chronic Hepatitis B. *Gastroenterology* (2016) 150:134–44.e110. doi: 10.1053/j.gastro.2015.09.043
8. Ning Q, Han M, Sun Y, Jiang J, Tan D, Hou J, et al. Switching From Entecavir to PegIFN Alfa-2a in Patients With HBeAg-Positive Chronic Hepatitis B: A Randomised Open-Label Trial (OSST Trial). *J Hepatol* (2014) 61:777–84. doi: 10.1016/j.jhep.2014.05.044

9. Revill PA, Chisari FV, Block JM, Dandri M, Gehring AJ, Guo H, et al. A Global Scientific Strategy to Cure Hepatitis B. *Lancet Gastroenterol Hepatol* (2019) 4:545–58. doi: 10.1016/S2468-1253(19)30119-0
10. Woo ASJ, Kwok R, Ahmed T. Alpha-Interferon Treatment in Hepatitis B. *Ann Transl Med* (2017) 5:159. doi: 10.21037/atm.2017.03.69
11. Cao Z, Liu Y, Ma L, Lu J, Jin Y, Ren S, et al A Potent Hepatitis B Surface Antigen Response in Subjects With Inactive Hepatitis B Surface Antigen Carrier Treated With Pegylated-Interferon Alpha. *Hepatology* (2017) 66 (4):1058–66. doi: 10.1002/hep.29213
12. Liang KH, Hsu CW, Chang ML, Chen YC, Lai MW, Yeh CT. Peginterferon Is Superior to Nucleos(t)ide Analogues for Prevention of Hepatocellular Carcinoma in Chronic Hepatitis B. *J Infect Dis* (2016) 213:966–74. doi: 10.1093/infdis/jiv547
13. Bonvin M, Achermann F, Greeve I, Stroka D, Keogh A, Inderbitzin D, et al. Interferon-Inducible Expression of APOBEC3 Editing Enzymes in Human Hepatocytes and Inhibition of Hepatitis B Virus Replication. *Hepatology* (2006) 43:1364–74. doi: 10.1002/hep.21187
14. Nguyen DH, Gummuluru S, Hu J. Deamination-Independent Inhibition of Hepatitis B Virus Reverse Transcription by APOBEC3G. *J Virol* (2007) 81:4465–72. doi: 10.1128/JVI.02510-06
15. Wang YX, Niklasch M, Liu T, Wang Y, Shi B, Yuan W, et al. Interferon-Inducible MX2 Is a Host Restriction Factor of Hepatitis B Virus Replication. *J Hepatol* (2020) 72:865–76. doi: 10.1016/j.jhep.2019.12.009
16. Gao B, Duan Z, Xu W, Xiong S. Tripartite Motif-Containing 22 Inhibits the Activity of Hepatitis B Virus Core Promoter, Which is Dependent on Nuclear-Located RING Domain. *Hepatology* (2009) 50:424–33. doi: 10.1002/hep.23011
17. Liu Y, Nie H, Mao R, Mitra B, Cai D, Yan R, et al. Interferon-Inducible Ribonuclease ISG20 Inhibits Hepatitis B Virus Replication Through Directly Binding to the Epsilon Stem-Loop Structure of Viral RNA. *PloS Pathog* (2017) 13:e1006296. doi: 10.1371/journal.ppat.1006296
18. Imam H, Kim GW, Mir SA, Khan M, Siddiqui A. Interferon-Stimulated Gene 20 (ISG20) Selectively Degrades N6-Methyladenosine Modified Hepatitis B Virus Transcripts. *PloS Pathog* (2020) 16:e1008338. doi: 10.1371/journal.ppat.1008338
19. Gordien E, Rosmorduc O, Peltekian C, Garreau F, Brechot C, Kremsdorf D. Inhibition of Hepatitis B Virus Replication by the Interferon-Inducible MxA Protein. *J Virol* (2001) 75:2684–91. doi: 10.1128/JVI.75.6.2684-2691.2001
20. Suslov A, Boldanova T, Wang X, Wieland S, Heim MH. Hepatitis B Virus Does Not Interfere With Innate Immune Responses in the Human Liver. *Gastroenterology* (2018) 154:1778–90. doi: 10.1053/j.gastro.2018.01.034
21. Cheng X, Xia Y, Serti E, Block PD, Chung M, Chayama K, et al. Hepatitis B Virus Evades Innate Immunity of Hepatocytes But Activates Cytokine Production by Macrophages. *Hepatology* (2017) 66:1779–93. doi: 10.1002/hep.29348
22. Levrero M, Pollicino T, Petersen J, Belloni L, Raimondo G, Dandri M. Control of cccDNA Function in Hepatitis B Virus Infection. *J Hepatol* (2009) 51:581–92. doi: 10.1016/j.jhep.2009.05.022
23. Pollicino T, Belloni L, Raffa G, Pediconi N, Squadrito G, Raimondo G, et al. Hepatitis B Virus Replication is Regulated by the Acetylation Status of Hepatitis B Virus cccDNA-Bound H3 and H4 Histones. *Gastroenterology* (2006) 130:823–37. doi: 10.1053/j.gastro.2006.01.001
24. Yuan Y, Yuan HF, Yang G, Yun HL, Zhao M, Liu ZX, et al. IFN-Alpha Confers Epigenetic Regulation of HBV cccDNA Minichromosome by Modulating GCN5-Mediated Succinylation of Histone H3K79 to Clear HBV cccDNA. *Clin Epigenet* (2020) 12. doi: 10.1186/s13148-020-00928-z
25. Newbold JE, Xin H, Tencza M, Sherman G, Dean J, Bowden S, et al. The Covalently Closed Duplex Form of the Hepadnavirus Genome Exists In-Situ as a Heterogeneous Population of Viral Minichromosomes. *J Virol* (1995) 69:3350–7. doi: 10.1128/jvi.69.6.3350-3357.1995
26. Zhang W, Chen J, Wu M, Zhang X, Zhang M, Yue L, et al. PRMT5 Restricts Hepatitis B Virus Replication Through Epigenetic Repression of Covalently Closed Circular DNA Transcription and Interference With Pregenomic RNA Encapsidation. *Hepatology* (2017) 66:398–415. doi: 10.1002/hep.29133
27. Yang YY, Zhao XZ, Wang ZY, Shu WQ, Li LJ, Li YQ, et al. Nuclear Sensor Interferon-Inducible Protein 16 Inhibits the Function of Hepatitis B Virus Covalently Closed Circular DNA by Integrating Innate Immune Activation and Epigenetic Suppression. *Hepatology* (2020) 71:1154–69. doi: 10.1002/hep.30897
28. Belloni L, Pollicino T, De Nicola F, Guerrieri F, Raffa G, Fanciulli M, et al. Nuclear HBx Binds the HBV Minichromosome and Modifies the Epigenetic Regulation of cccDNA Function. *Proc Natl Acad Sci USA* (2009) 106:19975–9. doi: 10.1073/pnas.0908365106
29. Belloni L, Allweiss L, Guerrieri F, Pediconi N, Volz T, Pollicino T, et al. IFN-Alpha Inhibits HBV Transcription and Replication in Cell Culture and in Humanized Mice by Targeting the Epigenetic Regulation of the Nuclear cccDNA Minichromosome. *J Clin Invest* (2012) 122:529–37. doi: 10.1172/JCI58847
30. Liu F, Campagna M, Qi Y, Zhao X, Guo F, Xu C, et al. Alpha-Interferon Suppresses Hepadnavirus Transcription by Altering Epigenetic Modification of cccDNA Minichromosomes. *PloS Pathog* (2013) 9:e1003613. doi: 10.1371/journal.ppat.1003613
31. Lucifora J, Xia Y, Reisinger F, Zhang K, Stadler D, Cheng X, et al. Specific and Nonhepatotoxic Degradation of Nuclear Hepatitis B Virus cccDNA. *Science* (2014) 343:1221–8. doi: 10.1126/science.1243462
32. Stadler D, Kachele M, Jones AN, Hess J, Urban C, Schneider J, et al. Interferon-Induced Degradation of the Persistent Hepatitis B Virus cccDNA Form Depends on ISG20. *EMBO Rep* (2021) 22:e49568. doi: 10.15252/embr.201949568
33. Xia Y, Stadler D, Lucifora J, Reisinger F, Webb D, Hosel M, et al. Interferon-Gamma and Tumor Necrosis Factor-Alpha Produced by T Cells Reduce the HBV Persistence Form, cccDNA, Without Cytolysis. *Gastroenterology* (2016) 150:194–205. doi: 10.1053/j.gastro.2015.09.026
34. Decorsiere A, Mueller H, Van Breugel PC, Abdul F, Gerossier L, Beran RK, et al. Hepatitis B Virus X Protein Identifies the Smc5/6 Complex as a Host Restriction Factor. *Nature* (2016) 531:386–9. doi: 10.1038/nature17170
35. Murphy CM, Xu Y, Li F, Nio K, Reszka-Blanco N, Li X, et al. Hepatitis B Virus X Protein Promotes Degradation of SMC5/6 to Enhance HBV Replication. *Cell Rep* (2016) 16:2846–54. doi: 10.1016/j.celrep.2016.08.026
36. Allweiss L, Giersch K, Pirosu A, Volz T, Muench RC, Beran RK, et al. Therapeutic Shutdown of HBV Transcripts Promotes Reappearance of the SMC5/6 Complex and Silencing of the Viral Genome *In Vivo*. *Gut* (2021). doi: 10.1136/gutjnl-2020-322571
37. Park IH, Baek KW, Cho EY, Ahn BY. PKR-Dependent Mechanisms of Interferon-Alpha for Inhibiting Hepatitis B Virus Replication. *Mol Cells* (2011) 32:167–72. doi: 10.1007/s10059-011-1059-6
38. Yan R, Zhao X, Cai D, Liu Y, Block TM, Guo JT, et al. The Interferon-Inducible Protein Tetherin Inhibits Hepatitis B Virus Virion Secretion. *J Virol* (2015) 89:9200–12. doi: 10.1128/JVI.00933-15
39. Li J, Liu K, Liu Y, Xu Y, Zhang F, Yang H, et al. Exosomes Mediate the Cell-to-Cell Transmission of IFN-Alpha-Induced Antiviral Activity. *Nat Immunol* (2013) 14:793–803. doi: 10.1038/ni.2647
40. Wu W, Wu D, Yan W, Wang Y, You J, Wan X, et al. Interferon-Induced Macrophage-Derived Exosomes Mediate Antiviral Activity Against Hepatitis B Virus Through miR-574-5p. *J Infect Dis* (2021) 223(4):686–98. doi: 10.1093/infdis/jiaa399
41. Jia X, Chen J, Megger DA, Zhang X, Kozlowski M, Zhang L, et al. Label-free Proteomic Analysis of Exosomes Derived from Inducible Hepatitis B Virus-Replicating HepAD38 Cell Line. *Mol Cell Proteomics* (2017) 16(4 suppl 1): S144–60. doi: 10.1074/mcp.M116.063503
42. Yao Z, Qiao Y, Li X, Chen J, Ding J, Bai L, et al. Exosomes Exploit the Virus Entry Machinery and Pathway To Transmit Alpha Interferon-Induced Antiviral Activity. *J Virol* (2018) 92(24):e01578–18. doi: 10.1128/JVI.01578-18
43. Hervas-Stubbs S, Luis Perez-Gracia J, Rouzaut A, Sanmamed MF, Le Bon A, Melero I. Direct Effects of Type I Interferons on Cells of the Immune System. *Clin Cancer Res* (2011) 17:2619–27. doi: 10.1158/1078-0432.CCR-10-1114
44. Gao Y, Majchrzak-Kita B, Fish EN, Gommerman JL. Dynamic Accumulation of Plasmacytoid Dendritic Cells in Lymph Nodes is Regulated by Interferon-Beta. *Blood* (2009) 114:2623–31. doi: 10.1182/blood-2008-10-183301
45. Knolle PA, Thimme R. Hepatic Immune Regulation and Its Involvement in Viral Hepatitis Infection. *Gastroenterology* (2014) 146:1193–207. doi: 10.1053/j.gastro.2013.12.036
46. Guidotti LG, Chisari FV. Noncytolytic Control of Viral Infections by the Innate and Adaptive Immune Response. *Annu Rev Immunol* (2001) 19:65–91. doi: 10.1146/annurev.immunol.19.1.65

47. Guidotti LG, Ando K, Hobbs MV, Ishikawa T, Runkel L, Schreiber RD, et al. Cytotoxic T-Lymphocytes Inhibit Hepatitis-B Virus Gene-Expression By a Noncytolytic Mechanism In Transgenic Mice. *Proc Natl Acad Sci USA* (1994) 91:3764–8. doi: 10.1073/pnas.91.9.3764
48. McClary H, Koch R, Chisari FV, Guidotti LG. Relative Sensitivity of Hepatitis B Virus and Other Hepatotropic Viruses to the Antiviral Effects of Cytokines. *J Virol* (2000) 74:2255–64. doi: 10.1128/JVI.74.5.2255-2264.2000
49. Guidotti LG, Rochford R, Chung J, Shapiro M, Purcell R, Chisari FV. Viral Clearance Without Destruction of Infected Cells During Acute HBV Infection. *Science* (1999) 284:825–9. doi: 10.1126/science.284.5415.825
50. Yang PL, Althage A, Chung J, Maier H, Wieland S, Isogawa M, et al. Immune Effectors Required for Hepatitis B Virus Clearance. *Proc Natl Acad Sci USA* (2010) 107:798–802. doi: 10.1073/pnas.0913498107
51. Xia Y, Protzer U. Control of Hepatitis B Virus by Cytokines. *Viruses* (2017) 9 (1):18. doi: 10.3390/v9010018
52. Allweiss L, Volz T, Lutgehetmann M, Giersch K, Bornscheuer T, Lohse AW, et al. Immune Cell Responses Are Not Required to Induce Substantial Hepatitis B Virus Antigen Decline During Pegylated Interferon-Alpha Administration. *J Hepatol* (2014) 60:500–7. doi: 10.1016/j.jhep.2013.10.021
53. Penna A, Laccabue D, Libri I, Giuberti T, Schivazappa S, Alfieri A, et al. Peginterferon-Alpha Does Not Improve Early Peripheral Blood HBV-Specific T-Cell Responses in HBeAg-Negative Chronic Hepatitis. *J Hepatol* (2012) 56:1239–46. doi: 10.1016/j.jhep.2011.12.032
54. Micco L, Peppa D, Loggi E, Schurich A, Jefferson L, Cursaro C, et al. Differential Boosting of Innate and Adaptive Antiviral Responses During Pegylated-Interferon-Alpha Therapy of Chronic Hepatitis B. *J Hepatol* (2013) 58:225–33. doi: 10.1016/j.jhep.2012.09.029
55. Shen F, Li Y, Wang Y, Sozzi V, Revill PA, Liu J, et al. Hepatitis B Virus Sensitivity to Interferon-Alpha in Hepatocytes is More Associated With Cellular Interferon Response Than With Viral Genotype. *Hepatology* (2018) 67:1237–52. doi: 10.1002/hep.29609
56. Cooksley G, Manns M, Lau GKK, Liaw YF, Marcellin P, Chow WC, et al. Effect of Genotype and Other Baseline Factors on Response to Peginterferon Alpha-2a (40 kDa) (PEGASYS (R)) in HBeAg-POSITIVE Chronic Hepatitis B: Results From a Large, Randomised Study. *J Hepatol* (2005) 42:30–1. doi: 10.1016/S0168-8278(05)81483-7
57. Lau GKK, Piratvisuth T, Luo KX, Marcellin P, Thongsawat S, Cooksley G, et al. Peginterferon Alfa-2a, Lamivudine, and the Combination for HBeAg-Positive Chronic Hepatitis B. *New Engl J Med* (2005) 352:2682–95. doi: 10.1056/NEJMoa043470
58. Janssen HLA, van Zonneveld M, Senturk H, Zeuzem S, Akarca US, Cakaloglu Y, et al. Pegylated Interferon Alfa-2b Alone or in Combination With Lamivudine for HBeAg-Positive Chronic Hepatitis B: A Randomised. *Lancet* (2005) 365:123–9. doi: 10.1016/S0140-6736(05)17701-0
59. Wai CT, Chu CJ, Hussain M, Lok ASF. HBV Genotype B is Associated With Better Response to Interferon Therapy in HBeAg(+) Chronic Hepatitis Than Genotype C. *Hepatology* (2002) 36:1425–30.
60. Sonneveld MJ, Rijckborst V, Zeuzem S, Heathcote EJ, Simon K, Senturk H, et al. Presence of Precore and Core Promoter Mutants Limits the Probability of Response to Peginterferon in Hepatitis B E Antigen-Positive Chronic Hepatitis B. *Hepatology* (2012) 56:67–75. doi: 10.1002/hep.25636
61. Wang S, Chen Z, Hu C, Qian F, Cheng Y, Wu M, et al. Hepatitis B Virus Surface Antigen Selectively Inhibits TLR2 Ligand-Induced IL-12 Production in Monocytes/Macrophages by Interfering With JNK Activation. *J Immunol* (2013) 190:5142–51. doi: 10.4049/jimmunol.1201625
62. Xu Y, Hu Y, Shi B, Zhang X, Wang J, Zhang Z, et al. HBsAg Inhibits TLR9-Mediated Activation and IFN-Alpha Production in Plasmacytoid Dendritic Cells. *Mol Immunol* (2009) 46:2640–6. doi: 10.1016/j.molimm.2009.04.031
63. Tout I, Loureiro D, Mansouri A, Soumelis V, Boyer N, Asselah T. Hepatitis B Surface Antigen Seroclearance: Immune Mechanisms, Clinical Impact, Importance for Drug Development. *J Hepatol* (2020) 73:409–22. doi: 10.1016/j.jhep.2020.04.013
64. Wang H, Ryu WS. Hepatitis B Virus Polymerase Blocks Pattern Recognition Receptor Signaling *via* Interaction With DDX3: Implications for Immune Evasion. *PloS Pathog* (2010) 6:e1000986. doi: 10.1371/journal.ppat.1000986
65. Liu Y, Li J, Chen J, Li Y, Wang W, Du X, et al. Hepatitis B Virus Polymerase Disrupts K63-Linked Ubiquitination of STING to Block Innate Cytosolic DNA-Sensing Pathways. *J Virol* (2015) 89:2287–300. doi: 10.1128/JVI.02760-14
66. Yu S, Chen J, Wu M, Chen H, Kato N, Yuan Z. Hepatitis B Virus Polymerase Inhibits RIG-I- and Toll-Like Receptor 3-Mediated Beta Interferon Induction in Human Hepatocytes Through Interference With Interferon Regulatory Factor 3 Activation and Dampening of the Interaction Between TBK1/IKKepsilon and DDX3. *J Gen Virol* (2010) 91:2080–90. doi: 10.1099/vir.0.020552-0
67. Kumar M, Jung SY, Hodgson AJ, Madden CR, Qin J, Slagle BL. Hepatitis B Virus Regulatory HBx Protein Binds to Adaptor Protein IPS-1 and Inhibits the Activation of Beta Interferon. *J Virol* (2011) 85:987–95. doi: 10.1128/JVI.01825-10
68. Wei C, Ni C, Song T, Liu Y, Yang X, Zheng Z, et al. The Hepatitis B Virus X Protein Disrupts Innate Immunity by Downregulating Mitochondrial Antiviral Signaling Protein. *J Immunol* (2010) 185:1158–68. doi: 10.4049/jimmunol.0903874
69. Wang F, Shen F, Wang Y, Li Z, Chen J, Yuan Z. Residues Asn118 and Glu119 of Hepatitis B Virus X Protein Are Critical for HBx-Mediated Inhibition of RIG-I-MAVS Signaling. *Virology* (2020) 539:92–103. doi: 10.1016/j.virol.2019.10.009
70. Fernandez M, Quiroga JA, Carreno V. Hepatitis B Virus Downregulates the Human Interferon-Inducible MxA Promoter Through Direct Interaction of Precore/Core Proteins. *J Gen Virol* (2003) 84:2073–82. doi: 10.1099/vir.0.18966-0
71. Li T, Ke Z, Liu W, Xiong Y, Zhu Y, Liu Y. Human Hepatitis B Virus Core Protein Inhibits IFNalpha-Induced IFITM1 Expression by Interacting With BAF200. *Viruses* (2019) 11(5):427. doi: 10.3390/v11050427
72. Lang T, Lo C, Skinner N, Locarnini S, Visvanathan K, Mansell A. The Hepatitis B E Antigen (HBeAg) Targets and Suppresses Activation of the Toll-Like Receptor Signaling Pathway. *J Hepatol* (2011) 55:762–9. doi: 10.1016/j.jhep.2010.12.042
73. Visvanathan K, Skinner NA, Thompson AJ, Riordan SM, Sozzi V, Edwards R, et al. Regulation of Toll-Like Receptor-2 Expression in Chronic Hepatitis B by the Precore Protein. *Hepatology* (2007) 45:102–10. doi: 10.1002/hep.21482
74. Mitra B, Wang J, Kim ES, Mao R, Dong M, Liu Y, et al. Hepatitis B Virus Precore Protein P22 Inhibits Alpha Interferon Signaling by Blocking STAT Nuclear Translocation. *J Virol* (2019) 93(13):e00196–19. doi: 10.1128/JVI.00196-19
75. Chen J, Wu M, Wang F, Zhang W, Wang W, Zhang X, et al. Hepatitis B Virus Spliced Variants Are Associated With an Impaired Response to Interferon Therapy. *Sci Rep* (2015) 5:16459. doi: 10.1038/srep16459
76. European Association for the Study of the Liver. Electronic Address Eee, European Association for the Study of the L. EASL 2017 Clinical Practice Guidelines on the Management of Hepatitis B Virus Infection. *J Hepatol* (2017) 67:370–98. doi: 10.1016/j.jhep.2017.03.021
77. Bonino F, Marcellin P, Lau GKK, Hadziyannis S, Jin R, Piratvisuth T, et al. Predicting Response to Peginterferon Alpha-2a, Lamivudine and the Two Combined for HBeAg-Negative Chronic Hepatitis B. *Gut* (2007) 56:699–705. doi: 10.1136/gut.2005.089722
78. Kau A, Vermehren J, Sarrazin C. Treatment Predictors of a Sustained Virologic Response in Hepatitis B and C. *J Hepatol* (2008) 49:634–51. doi: 10.1016/j.jhep.2008.07.013
79. Lampertico P, Vigano M, Cheroni C, Facchetti F, Invernizzi F, Valveri V, et al. IL28B Polymorphisms Predict Interferon-Related Hepatitis B Surface Antigen Seroclearance in Genotype D Hepatitis B E Antigen-Negative Patients With Chronic Hepatitis B. *Hepatology* (2013) 57:890–6. doi: 10.1002/hep.25749
80. Jiang X, Su K, Tao J, Fan R, Xu Y, Han H, et al. Association of STAT4 Polymorphisms With Hepatitis B Virus Infection and Clearance in Chinese Han Population. *Amino Acids* (2016) 48:2589–98. doi: 10.1007/s00726-016-2283-3
81. Jiang DK, Wu X, Qian J, Ma XP, Yang J, Li Z, et al. Genetic Variation in STAT4 Predicts Response to Interferon-Alpha Therapy for Hepatitis B E Antigen-Positive Chronic Hepatitis B. *Hepatology* (2016) 63:1102–11. doi: 10.1002/hep.28423
82. Liao Y, Cai B, Li Y, Chen J, Tao C, Huang H, et al. Association of HLA-DP/DQ and STAT4 Polymorphisms With HBV Infection Outcomes and a Mini Meta-Analysis. *PloS One* (2014) 9(11):e111677. doi: 10.1371/journal.pone.0111677
83. Lee DH, Cho Y, Seo JY, Kwon JH, Cho EJ, Jang ES, et al. Polymorphisms Near Interleukin 28b Gene Are Not Associated With Hepatitis B Virus Clearance, Hepatitis B E Antigen Clearance and Hepatocellular Carcinoma Occurrence. *Intervirology* (2013) 56:84–90. doi: 10.1159/000342526

84. Tseng T-C, Yu M-L, Liu C-J, Lin C-L, Huang Y-W, Hsu C-S, et al. Effect of Host and Viral Factors on Hepatitis B E Antigen-Positive Chronic Hepatitis B Patients Receiving Pegylated Interferon-Alpha-2a Therapy. *Antiviral Ther* (2011) 16:629–37. doi: 10.3851/IMP1841
85. Sonneveld MJ, Wong VWS, Woltman AM, Wong GLH, Cakaloglu Y, Zeuzem S, et al. Polymorphisms Near IL28B and Serologic Response to Peginterferon in HBeAg-Positive Patients With Chronic Hepatitis B. *Gastroenterology* (2012) 142:513–U165. doi: 10.1053/j.gastro.2011.11.025
86. Wu X, Xin Z, Zhu X, Pan L, Li Z, Li H, et al. Evaluation of Susceptibility Locus for Response to Interferon-Alpha Based Therapy in Chronic Hepatitis B Patients in Chinese. *Antiviral Res* (2012) 93:297–300. doi: 10.1016/j.antiviral.2011.12.009
87. Zhou L, Ren J-H, Cheng S-T, Xu H-M, Chen W-X, Chen D-P, et al. A Functional Variant in Ubiquitin Conjugating Enzyme E2 L3 Contributes to Hepatitis B Virus Infection and Maintains Covalently Closed Circular DNA Stability by Inducing Degradation of Apolipoprotein B mRNA Editing Enzyme Catalytic Subunit 3a. *Hepatology* (2019) 69:1885–902. doi: 10.1002/hep.30497
88. Porres JC, Carreno V, Ruiz M, Marron JA, Bartolome J. Interferon Antibodies In Patients With Chronic HBV Infection Treated With Recombinant Interferon. *J Hepatol* (1989) 8:351–7. doi: 10.1016/0168-8278(89)90034-2
89. Lok ASF, Lai CL, Leung EKY. Interferon Antibodies May Negate The Antiviral Effects Of Recombinant Alpha-Interferon Treatment In Patients With Chronic Hepatitis-B Virus-Infection. *Hepatology* (1990) 12:1266–70. doi: 10.1002/hep.1840120603
90. Brook MG, McDonald JA, Karayiannis P, Caruso L, Forster G, Harris JRW, et al. Randomized Controlled Trial Of Interferon-Alfa-2a (RBE) (ROFERON-A) For The Treatment Of Chronic Hepatitis-B Virus (HBV) Infection - Factors That Influence Response. *Gut* (1989) 30:1116–22. doi: 10.1136/gut.30.8.1116
91. Arends P, van der Eijk AA, Sonneveld MJ, Hansen BE, Janssen HL, Haagmans BL. Presence of Anti-Interferon Antibodies is Not Associated With Non-Response to Pegylated Interferon Treatment in Chronic Hepatitis B. *Antivir Ther* (2014) 19:423–7. doi: 10.3851/IMP2711
92. Lebosse F, Testoni B, Fresquet J, Facchetti F, Galmozzi E, Fournier M, et al. Intrahepatic Innate Immune Response Pathways Are Downregulated in Untreated Chronic Hepatitis B. *J Hepatol* (2017) 66:897–909. doi: 10.1016/j.jhep.2016.12.024
93. Durantel D, Zoulim F. Innate Response to Hepatitis B Virus Infection: Observations Challenging the Concept of a Stealth Virus. *Hepatology* (2009) 50:1692–5. doi: 10.1002/hep.23361
94. Mutz P, Metz P, Lempp FA, Bender S, Qu B, Schoeneweis K, et al. HBV Bypasses the Innate Immune Response and Does Not Protect HCV From Antiviral Activity of Interferon. *Gastroenterology* (2018) 154:1791–804. doi: 10.1053/j.gastro.2018.01.044
95. Zhang Z, Trippler M, Real CI, Werner M, Luo X, Schefczyk S, et al. Hepatitis B Virus Particles Activate Toll-Like Receptor 2 Signaling Initially Upon Infection of Primary Human Hepatocytes. *Hepatology* (2020) 72:829–44. doi: 10.1002/hep.31112
96. Verrier ER, Yim SA, Heydmann L, El Saghire H, Bach C, Turon-Lagot V, et al. Hepatitis B Virus Evasion From Cyclic Guanosine Monophosphate-Adenosine Monophosphate Synthase Sensing in Human Hepatocytes. *Hepatology* (2018) 68:1695–709. doi: 10.1002/hep.30054
97. Sato S, Li K, Kameyama T, Hayashi T, Ishida Y, Murakami S, et al. The RNA Sensor RIG-I Dually Functions as an Innate Sensor and Direct Antiviral Factor for Hepatitis B Virus. *Immunity* (2015) 42:123–32. doi: 10.1016/j.immuni.2014.12.016
98. Luangsay S, Gruffaz M, Isorce N, Testoni B, Michelet M, Faure-Dupuy S, et al. Early Inhibition of Hepatocyte Innate Responses by Hepatitis B Virus. *J Hepatol* (2015) 63(6):1314–22. doi: 10.1016/j.jhep.2015.07.014
99. Zhou L, He R, Fang P, Li M, Yu H, Wang Q, et al. Hepatitis B Virus Rigs the Cellular Metabolome to Avoid Innate Immune Recognition. *Nat Commun* (2021) 12(1):98. doi: 10.1038/s41467-020-20316-8
100. Lim KH, Park ES, Kim DH, Cho KC, Kim KP, Park YK, et al. Suppression of Interferon-Mediated Anti-HBV Response by Single CpG Methylation in the 5'-UTR of TRIM22. *Gut* (2018) 67:166–78. doi: 10.1136/gutjnl-2016-312742
101. Fang Z, Li J, Yu X, Zhang D, Ren G, Shi B, et al. Polarization of Monocytic Myeloid-Derived Suppressor Cells by Hepatitis B Surface Antigen Is Mediated *via* ERK/IL-6/STAT3 Signaling Feedback and Restrains the Activation of T Cells in Chronic Hepatitis B Virus Infection. *J Immunol* (2015) 195:4873–83. doi: 10.4049/jimmunol.1501362
102. Boni C, Laccabue D, Lampertico P, Giuberti T, Vigano M, Schivazappa S, et al. Restored Function of HBV-Specific T Cells After Long-Term Effective Therapy With Nucleos(T)Ide Analogues. *Gastroenterology* (2012) 143:963–73.e969. doi: 10.1053/j.gastro.2012.07.014
103. Wherry EJ, Ahmed R. Memory CD8 T-Cell Differentiation During Viral Infection. *J Virol* (2004) 78:5535–45. doi: 10.1128/JVI.78.11.5535-5545.2004
104. Kawashima K, Isogawa M, Hamada-Tsutsumi S, Baudi I, Saito S, Nakajima A, et al. Type I Interferon Signaling Prevents Hepatitis B Virus-Specific T Cell Responses by Reducing Antigen Expression. *J Virol* (2018) 92(23): e01099–18. doi: 10.1128/JVI.01099-18
105. Cheng X, Uchida T, Xia Y, Umarova R, Liu CJ, Chen PJ, et al. Diminished Hepatic IFN Response Following HCV Clearance Triggers HBV Reactivation in Coinfection. *J Clin Invest* (2020) 130:3205–20. doi: 10.1172/JCI135616
106. Wieland SF, Asabe S, Engle RE, Purcell RH, Chisari FV. Limited Hepatitis B Virus Replication Space in the Chronically Hepatitis C Virus-Infected Liver. *J Virol* (2014) 88:5184–8. doi: 10.1128/JVI.03553-13
107. Lin C-L, Kao J-H. The Clinical Implications of Hepatitis B Virus Genotype: Recent Advances. *J Gastroenterol Hepatol* (2011) 26:123–30. doi: 10.1111/j.1440-1746.2010.06541.x
108. Yuen MF, Chen DS, Dusheiko GM, Janssen HLA, Lau DTY, Locarnini SA, et al. Hepatitis B Virus Infection. *Nat Rev Dis Primers* (2018) 4:18035. doi: 10.1038/nrdp.2018.35
109. Ghany MG, Perrillo R, Li R, Belle SH, Janssen HLA, Terrault NA, et al. Characteristics of Adults in the Hepatitis B Research Network in North America Reflect Their Country of Origin and Hepatitis B Virus Genotype. *Clin Gastroenterol Hepatol* (2015) 13:183–92. doi: 10.1016/j.cgh.2014.06.028
110. Yuan J, Zhou B, Tanaka Y, Kurbanov F, Orito E, Gong Z, et al. Hepatitis B Virus (HBV) Genotypes/Subgenotypes in China: Mutations in Core Promoter and Precore/Core and Their Clinical Implications. *J Clin Virol* (2007) 39:87–93. doi: 10.1016/j.jcv.2007.03.005
111. Terrault NA, Lok ASF, McMahon BJ, Chang KM, Hwang JP, Jonas MM, et al. Update on Prevention, Diagnosis, and Treatment of Chronic Hepatitis B: AASLD 2018 Hepatitis B Guidance. *Hepatology* (2018) 67:1560–99. doi: 10.1002/hep.29800
112. McNaughton AL, D'Arienzo V, Ansari MA, Lumley SF, Littlejohn M, Revill P, et al. Insights From Deep Sequencing of the HBV Genome-Unique, Tiny, and Misunderstood. *Gastroenterology* (2019) 156:384–99. doi: 10.1053/j.gastro.2018.07.058
113. Chuaypen N, Payungporn S, Poovorawan K, Chotiyaputta W, Piratvisuth T, Tangkijvanich P. Next Generation Sequencing Identifies Baseline Viral Mutants Associated With Treatment Response to Pegylated Interferon in HBeAg-Positive Chronic Hepatitis B. *Virus Genes* (2019) 55:610–8. doi: 10.1007/s11262-019-01689-5
114. Xiang C, Du Y, Meng G, Yi LS, Sun S, Song N, et al. Long-Term Functional Maintenance of Primary Human Hepatocytes In Vitro. *Science* (2019) 364 (6438):399–402. doi: 10.1126/science.aau7307
115. Fu GB, Huang WJ, Zeng M, Zhou X, Wu HP, Liu CC, et al. Expansion and Differentiation of Human Hepatocyte-Derived Liver Progenitor-Like Cells and Their Use for the Study of Hepatotropic Pathogens. *Cell Res* (2019) 29:8–22. doi: 10.1038/s41422-018-0103-x
116. Zeilinger K, Freyer N, Damm G, Seehofer D, Knospel F. Cell Sources for *In Vitro* Human Liver Cell Culture Models. *Exp Biol Med (Maywood)* (2016) 241:1684–98. doi: 10.1177/1535370216657448
117. Shlomai A, Schwartz RE, Ramanan V, Bhatta A, de Jong YP, Bhatia SN, et al. Modeling Host Interactions With Hepatitis B Virus Using Primary and Induced Pluripotent Stem Cell-Derived Hepatocellular Systems. *Proc Natl Acad Sci USA* (2014) 111:12193–8. doi: 10.1073/pnas.1412631111
118. Jansen L, de Niet A, Makowska Z, Dill MT, van Dort KA, Terpstra V, et al. An Intrahepatic Transcriptional Signature of Enhanced Immune Activity Predicts Response to Peginterferon in Chronic Hepatitis B. *Liver Int* (2015) 35:1824–32. doi: 10.1111/liv.12768
119. Wu H-L, Hsiao T-H, Chen P-J, Wong S-H, Kao J-H, Chen D-S, et al. Liver Gene Expression Profiles Correlate With Virus Infection and Response to Interferon Therapy in Chronic Hepatitis B Patients. *Sci Rep* (2016) 6:31349. doi: 10.1038/srep31349
120. Marcellin P, Lau GKK, Bonino F, Farci P, Hadziyannis S, Jin R, et al. Peginterferon Alfa-2a Alone, Lamivudine Alone, and the Two in Combination in Patients With HBeAg-Negative Chronic Hepatitis B. *N Engl J Med* (2004) 351:1206–17. doi: 10.1056/NEJMoa040431

121. Ouzan D, Penaranda G, Joly H, Khiri H, Pironti A, Halfon P. Add-On Peg-Interferon Leads to Loss of HBsAg in Patients With HBeAg-Negative Chronic Hepatitis and HBV DNA Fully Suppressed by Long-Term Nucleotide Analogs. *J Clin Virol* (2013) 58:713–7. doi: 10.1016/j.jcv.2013.09.020
122. Li G-J, Yu Y-Q, Chen S-L, Fan P, Shao L-Y, Chen J-Z, et al. Sequential Combination Therapy With Pegylated Interferon Leads to Loss of Hepatitis B Surface Antigen and Hepatitis B E Antigen (HBeAg) Seroconversion in HBeAg-Positive Chronic Hepatitis B Patients Receiving Long-Term Entecavir Treatment. *Antimicrob Agents Chemother* (2015) 59:4121–8. doi: 10.1128/AAC.00249-15
123. Fan R, Sun J, Yuan Q, Xie Q, Bai X, Ning Q, et al. Baseline Quantitative Hepatitis B Core Antibody Titre Alone Strongly Predicts HBeAg Seroconversion Across Chronic Hepatitis B Patients Treated With Peginterferon or Nucleos(T)Ide Analogues. *Gut* (2016) 65:313–20. doi: 10.1136/gutjnl-2014-308546
124. Li J, Zhang X, Chen L, Zhang Z, Zhang J, Wang W, et al. Circulating miR-210 and miR-22 Combined With ALT Predict the Virological Response to Interferon-Alpha Therapy of CHB Patients. *Sci Rep* (2017) 7:15658. doi: 10.1038/s41598-017-15594-0
125. van Bommel F, van Bommel A, Krauel A, Wat C, Pavlovic V, Yang L, et al. Serum HBV RNA as a Predictor of Peginterferon Alfa-2a Response in Patients With HBeAg-Positive Chronic Hepatitis B. *J Infect Dis* (2018) 218:1066–74. doi: 10.1093/infdis/jiy270
126. Farag MS, van Campenhout MJH, Pfefferkorn M, Fischer J, Deichsel D, Boonstra A, et al. Hepatitis B Virus RNA as Early Predictor for Response to Pegylated Interferon Alpha in HBeAg-Negative Chronic Hepatitis B. *Clin Infect Dis* (2021) 72:202–11. doi: 10.1093/cid/ciaa013
127. Chuaypen N, Posuwan N, Payungporn S, Tanaka Y, Shinkai N, Poovorawan Y, et al. Serum Hepatitis B Core-Related Antigen as a Treatment Predictor of Pegylated Interferon in Patients With HBeAg-Positive Chronic Hepatitis B. *Liver Int* (2016) 36:827–36. doi: 10.1111/liv.13046
128. Mendoza JL, Escalante NK, Jude KM, Sotolongo Bellon J, Su L, Horton TM, et al. Structure of the IFNgamma Receptor Complex Guides Design of Biased Agonists. *Nature* (2019) 567:56–60. doi: 10.1038/s41586-019-0988-7
129. Spangler JB, Moraga I, Mendoza JL, Garcia KC. Insights Into Cytokine-Receptor Interactions From Cytokine Engineering. *Annu Rev Immunol* (2015) 33:139–67. doi: 10.1146/annurev-immunol-032713-120211
130. Heathcote EJ, Shiffman ML, Cooksley WGE, Dusheiko GM, Lee SS, Balart L, et al. Peginterferon Alfa-2a in Patients With Chronic Hepatitis C and Cirrhosis. *New Engl J Med* (2000) 343:1673–80. doi: 10.1056/NEJM200012073432302
131. Hu J, Wang G, Liu X, Gao W. Enhancing Pharmacokinetics, Tumor Accumulation, and Antitumor Efficacy by Elastin-Like Polypeptide Fusion of Interferon Alpha. *Adv Mater* (2015) 27:7320–4. doi: 10.1002/adma.201503440
132. Xia Y, Schlapschy M, Morath V, Roeder N, Vogt EI, Stadler D, et al. PASylated Interferon Alpha Efficiently Suppresses Hepatitis B Virus and Induces Anti-HBs Seroconversion in HBV-Transgenic Mice. *Antiviral Res* (2019) 161:134–43. doi: 10.1016/j.antiviral.2018.11.003
133. Fioravanti J, Gonzalez I, Medina-Echeverz J, Larrea E, Ardaiz N, Gonzalez-Aseguinolaza G, et al. Anchoring Interferon Alpha to Apolipoprotein A-I Reduces Hematological Toxicity While Enhancing Immunostimulatory Properties. *Hepatology* (2011) 53:1864–73. doi: 10.1002/hep.24306
134. Furutani Y, Toguchi M, Shiozaki-Sato Y, Qin XY, Ebisui E, Higuchi S, et al. An Interferon-Like Small Chemical Compound CDM-3008 Suppresses Hepatitis B Virus Through Induction of Interferon-Stimulated Genes. *PloS One* (2019) 14:e0216139. doi: 10.1371/journal.pone.0216139
135. Kalie E, Jaitin DA, Abramovich R, Schreiber G. An Interferon Alpha2 Mutant Optimized by Phage Display for IFNAR1 Binding Confers Specifically Enhanced Antitumor Activities. *J Biol Chem* (2007) 282:11602–11. doi: 10.1074/jbc.M610115200
136. Brideau-Andersen AD, Huang X, Sun S-CC, Chen TT, Stark D, Sas IJ, et al. Directed Evolution of Gene-Shuffled IFN-Alpha Molecules With Activity Profiles Tailored for Treatment of Chronic Viral Diseases. *Proc Natl Acad Sci USA* (2007) 104:8269–74. doi: 10.1073/pnas.0609001104
137. Symons J, Brideau-Andersen AD, Huang J, Huang X, Vogt A, Sun S-CC, et al. In Vitro and *In Vivo* Characterization of R7025, a Novel Pegylated Human Interferon Alpha Molecule, Generated by DNA Shuffling for the Treatment of Chronic Hepatitis C. *Hepatology* (2007) 46:853A–4A.
138. Pereira AA, Jacobson IM. New and Experimental Therapies for HCV. *Nat Rev Gastroenterol Hepatol* (2009) 6:403–11. doi: 10.1038/nrgastro.2009.92
139. Schreiber G, Piehler J. The Molecular Basis for Functional Plasticity in Type I Interferon Signaling. *Trends Immunol* (2015) 36:139–49. doi: 10.1016/j.it.2015.01.002
140. Lavoie TB, Kalie E, Crisafulli-Cabatu S, Abramovich R, DiGioia G, Moolchan K, et al. Binding and Activity of All Human Alpha Interferon Subtypes. *Cytokine* (2011) 56:282–9. doi: 10.1016/j.cyto.2011.07.019
141. Chen J, Li Y, Lai F, Wang Y, Sutter K, Dittmer U, et al. Functional Comparison of IFN-Alpha Subtypes Reveals Potent HBV Suppression by a Concerted Action of IFN-Alpha and -Gamma Signaling. *Hepatology* (2021) 73(2):486–502. doi: 10.1002/hep.31282
142. Novotny LA, Evans JG, Su L, Guo H, Meissner EG. Review of Lambda Interferons in Hepatitis B Virus Infection: Outcomes and Therapeutic Strategies. *Viruses* (2021) 13(6):1090. doi: 10.3390/v13061090
143. Sheppard P, Kindsvogel W, Xu WF, Henderson K, Schlutsmeyer S, Whitmore TE, et al. IL-28, IL-29 and Their Class II Cytokine Receptor IL-28r. *Nat Immunol* (2003) 4:63–8. doi: 10.1038/ni873
144. Doyle SE, Schreckhise H, Khuu-Duong K, Henderson K, Rosler R, Storey H, et al. Interleukin-29 Uses a Type 1 Interferon-Like Program to Promote Antiviral Responses in Human Hepatocytes. *Hepatology* (2006) 44:896–906. doi: 10.1002/hep.21312
145. Ye L, Schnepf D, Staeheli P. Interferon-Lambda Orchestrates Innate and Adaptive Mucosal Immune Responses. *Nat Rev Immunol* (2019) 19:614–25. doi: 10.1038/s41577-019-0182-z
146. Ge D, Fellay J, Thompson AJ, Simon JS, Shianna KV, Urban TJ, et al. Genetic Variation in IL28B Predicts Hepatitis C Treatment-Induced Viral Clearance. *Nature* (2009) 461:399–401. doi: 10.1038/nature08309
147. Seto W-K, Wong DK-H, Kopaniszen M, Proitsi P, Sham P-C, Hung IF-N, et al. HLA-DP and IL28B Polymorphisms: Influence of Host Genome on Hepatitis B Surface Antigen Seroclearance in Chronic Hepatitis B. *Clin Infect Dis* (2013) 56:1695–703. doi: 10.1093/cid/cit121
148. Karatayli SC, Bozdayi M, Karatayli E, Ozturk T, Husseini AA, Albayrak R, et al. Interleukin-28 Gene Polymorphisms may Contribute to HBsAg Persistence and the Development of HBeAg-Negative Chronic Hepatitis B. *Liver Int* (2015) 35:846–53. doi: 10.1111/liv.12595
149. Chan HLY, Ahn SH, Chang T-T, Peng C-Y, Wong D, Coffin CS, et al. Peginterferon Lambda for the Treatment of HBeAg-Positive Chronic Hepatitis B: A Randomized Phase 2b Study (LIRA-B). *J Hepatol* (2016) 64:1011–9. doi: 10.1016/j.jhep.2015.12.018
150. Naggie S, Lok AS. New Therapeutics for Hepatitis B: The Road to Cure. *Annu Rev Med* (2021) 72:93–105. doi: 10.1146/annurev-med-080119-103356
151. Klumpp K, Shimada T, Allweiss L, Volz T, Luetgehetmann M, Hartman G, et al. Efficacy of NVR 3-778, Alone and In Combination With Pegylated Interferon, *vs* Entecavir In uPA/SCID Mice With Humanized Livers and HBV Infection. *Gastroenterology* (2018) 154:652–62. doi: 10.1053/j.gastro.2017.10.017
152. Zoulim F. Inhibition of Hepatitis B Virus Gene Expression: A Step Towards Functional Cure. *J Hepatol* (2018) 68:386–8. doi: 10.1016/j.jhep.2017.11.036

Conflict of Interest: The authors declare that the research was conducted in the absence of any commercial or financial relationships that could be construed as a potential conflict of interest.

frontiers in Immunology

ORIGINAL RESEARCH
published: 10 September 2021
doi: 10.3389/fimmu.2021.713351

Hepatitis B Vaccine Non-Responders Show Higher Frequencies of $CD24^{high}CD38^{high}$ Regulatory B Cells and Lower Levels of IL-10 Expression Compared to Responders

Nina Körber[1,2], Laureen Pohl[1], Birgit Weinberger[3], Beatrix Grubeck-Loebenstein[3], Andrea Wawer[4], Percy A. Knolle[2,5], Hedwig Roggendorf[2,5], Ulrike Protzer[1,2,6] and Tanja Bauer[1,2]*

[1] Institute of Virology, Helmholtz Zentrum München, Munich, Germany, [2] German Center for Infection Research (DZIF), Munich, Germany, [3] Institute for Biomedical Aging Research, Universität Innsbruck, Innsbruck, Austria, [4] Occupational Health Unit, School of Medicine, Technical University of Munich (TUM), Munich, Germany, [5] Institute of Molecular Immunology and Experimental Oncology, School of Medicine, Technical University of Munich (TUM), Munich, Germany, [6] Institute of Virology, School of Medicine, Technical University of Munich (TUM), Munich, Germany

OPEN ACCESS

Edited by:
Zhongji Meng, Hubei University of Medicine, China

Reviewed by:
Kathrin Sutter, University of Duisburg-Essen, Germany
Salvatore Leonardi, University of Catania, Italy

***Correspondence:**
Nina Körber
nina.koerber@helmholtz-muenchen.de

Specialty section:
This article was submitted to Vaccines and Molecular Therapeutics, a section of the journal Frontiers in Immunology

Received: *22 May 2021*
Accepted: *25 August 2021*
Published: *10 September 2021*

Citation:
Körber N, Pohl L, Weinberger B, Grubeck-Loebenstein B, Wawer A, Knolle PA, Roggendorf H, Protzer U and Bauer T (2021) Hepatitis B Vaccine Non-Responders Show Higher Frequencies of $CD24^{high}CD38^{high}$ Regulatory B Cells and Lower Levels of IL-10 Expression Compared to Responders. Front. Immunol. 12:713351. doi: 10.3389/fimmu.2021.713351

Background: The cellular mechanisms involved in the lack of protective antibody response after hepatitis B vaccination are still rather unclear. Regulatory B cells (Breg) known as modulators of B-and T-cell responses may contribute to poor vaccine responsiveness. The current study aimed to investigate the role of regulatory B cells (Breg) in hepatitis B vaccine non-responsiveness after immunization with second- or third-generation hepatitis B vaccines.

Method: We performed comparative phenotypic and frequency analysis of Breg subsets ($CD24^{+}CD27^{+}$ and $CD24^{high}CD38^{high}$ Breg) in second-generation hepatitis B vaccine non-responders (2^{nd} HBvac NR, n = 11) and responders (2^{nd} HBvac R, n = 8) before (d0), on day 7 (d7), and 28 (d28) after booster vaccination. Cryopreserved peripheral blood mononuclear cells were stimulated *ex vivo* with a combination of CpG, PMA, and Ionomycin (CpG+P/I) and analyzed for numbers and IL-10 expression levels of Breg by flow cytometry-based analyses.

Results: Flow cytometry-based analyses revealed elevated frequencies of $CD24^{+}CD27^{+}$ Breg at all time points and significantly higher frequencies of $CD24^{high}CD38^{high}$ Breg on d0 ($p = 0.004$) and 28 ($p = 0.012$) in 2^{nd} HBvac NR compared to 2^{nd} HBvac R. In parallel, we observed significantly lower levels of CpG+P/I-induced IL-10 expression levels of $CD24^{+}CD27^{+}$ and $CD24^{high}CD38^{high}$ Breg (d0: $p < 0.0001$; d7: $p = 0.0004$; d28: $p = 0.0003$ and d0: $p = 0.016$; d7: $p = 0.016$, respectively) in 2^{nd} HBvac NR compared to 2^{nd} HBvac R before and after booster immunization. Frequencies of $CD24^{+}CD27^{+}$ and $CD24^{high}CD38^{high}$ Breg significantly decreased after third-generation hepatitis B booster vaccination (d7: $p = 0.014$; d28: $p = 0.032$ and d7: $p = 0.045$, respectively), whereas IL-10 expression levels of both Breg subsets remained stable.

Conclusion: Here we report significantly higher frequencies of $CD24^{high}CD38^{high}$ Breg in parallel with significantly lower IL-10 expression levels of $CD24^{+}CD27^{+}$ and $CD24^{high}CD38^{high}$ Breg in 2nd HBvac NR compared to 2nd HBvac R. Anti-HBs seroconversion accompanied by a decrease of Breg numbers after booster immunization with a third-generation hepatitis B vaccine could indicate a positive effect of third-generation hepatitis B vaccines on Breg-mediated immunomodulation in hepatitis B vaccine non-responders.

Keywords: regulatory B cells, IL-10 expression, vaccine non-responsiveness, hepatitis B vaccination, $B10^{+}$ cells

1 INTRODUCTION

According to the WHO 260 million people are chronically infected with HBV and 887,000 people are dying each year due to hepatitis B virus (HBV) infection (1). Second-generation hepatitis B vaccines composed of the small HBV envelope protein (hepatitis B surface antigen; HBsAg) are currently used for universal vaccination and reduce the overall incidence of both hepatitis B and the associated long-term consequences such as chronic hepatitis B and liver cirrhosis (2, 3).

Vaccination with recombinant HBsAg triggers the production of anti-HBs with an anti-HBs titer of > 10 IU/L being a very reliable surrogate marker for vaccine-induced protective immunity (4). Approximately 5-10% of vaccinees are defined as "non-responders", i.e. they do not develop a protective anti-HBs titer after completing a full primary series of the hepatitis B vaccine (5–8). Third-generation hepatitis B vaccines containing additional HBV envelope proteins (pre-S1 and pre-S2) are known to be more immunogenic and superior in inducing protective antibody titers also in non-responders to the conventional vaccines (9). Despite the success of universal immunization programs leading to high regional vaccination coverage rates in most Western countries, non-responsiveness to hepatitis B vaccination is a major problem, especially for health care workers for whom successful hepatitis B vaccination is mandatory (10, 11). Genetically determined resistance, advanced age, gender, obesity, smoking, chronic/systemic disease, and immunosuppressive therapies are known factors contributing to non-response to immunization (6, 12–18). Several aspects like failure of antigen presentation or costimulatory signals, defects in the generation of HBsAg-specific CD4 T helper (Th) cells and insufficient production of Th1 and Th2 cytokines upon hepatitis B vaccination have been discussed, but the exact underlying immunological and molecular mechanisms contributing to hepatitis B vaccine non-responsiveness remain largely unclear (10, 19–24). Further studies investigating immune cells and immunological mechanisms involved in non-responsiveness to vaccines are urgently needed and will help to improve immunogenicity of existing or the development of new vaccines to overcome non-responsiveness to hepatitis B vaccines.

In the last years, studies revealed that regulatory B cells (Breg) have an immunosuppressive capacity and help to maintain immunological homeostasis (25, 26). Breg suppress immunopathology by skewing T-cell differentiation, induction and maintenance of regulatory T cells, as well as suppression of pro-inflammatory cells, mainly mediated through regulatory cytokines IL-10, TGF-ß, and IL-35 (25–29). There is an ongoing debate on the phenotypic characterization of different Breg subsets, specific Breg markers, and the question whether all B cells can acquire suppressive function in response to environmental triggers, or whether Breg represent a distinct lineage (28, 30–32). $CD24^{+/high}CD27^{+}$ and $CD24^{high}CD38^{high}$ Breg have been described as distinct Breg subpopulations and investigated in different disease entities like autoimmune diseases (e.g. multiple sclerosis, rheumatoid arthritis, systemic lupus erythematosus, etc.) and cancer (25, 30, 33–35). For both, $CD24^{+/high}CD27^{+}$ and $CD24^{high}CD38^{high}$ Breg it is known that they can suppress effector CD4 T cells and dendritic cells, and $CD24^{high}CD38^{high}$ Breg can additionally induce regulatory T cells (Treg) and suppress virus-specific CD8 T cells (30, 33, 36).

Rosser et al. (37) postulated three potential mechanism for Breg-mediated suppression of antibody responses, which could also play a role in the case of hepatitis B vaccine non-responsiveness: (i) Breg may alter the cytokine microenvironment in which plasma cell maturation takes place; (ii) Breg could suppress CD4 Th cells, which leads to a diminished maturation of B cells into antibody producing plasma cells; (iii) Breg could induce Treg which may contribute to an indirect suppression of antibody production (25, 37).

In the last years, some studies investigated the role of Breg in hepatitis B vaccine non-responsiveness, but findings were

Abbreviations: aa, amino acid; ANOVA, analysis of variance; anti-HBs, antibody to hepatitis B surface antigen; APC, antigen presenting cells; BMI, body mass index; Breg, regulatory B cells; CD, cluster of differentiation; CpG, Cytosine and Guanine oligonucleotides; CpG+P/I, CpG+PMA and Ionomycin; DMSO, dimethyl sulfoxide; FCS, fetal calf serum; FSC, forward scatter; HBsAg, hepatitis B surface antigen; HBV, hepatitis B virus; ICS, intracellular cytokine staining; IFN, interferon; IL, interleukin; MFI, median fluorescence intensity; MHC, major histocompatibility complex; PBMC, peripheral blood mononuclear cells; PBS, phosphate buffered saline; PMA, Phorbol-12-myristat-13-acetat; RPMI, Roswell Park Memorial Institute; RT, room temperature; TBE, tick-borne encephalitis; TGF-ß, Transforming growth factor beta; Th cells, T helper cells; TNF, tumor necrosis factor Treg, regulatory T cells; WHO, World Health Organization; 2nd HBvac NR, second-generation hepatitis B vaccine non-responder; 2nd HBvac R, second-generation hepatitis B vaccine responder; 3rd HBvac HR, third-generation hepatitis B vaccine high-responder; 3rd HBvac LR, third-generation hepatitis B vaccine low-responder.

contradictory and in-depth analyses remain elusive (12, 38, 39). Bolther et al. concluded that levels of regulatory B cells do not predict serological responses to hepatitis B vaccination (38). In contrast, Garner-Spitzer et al. reported clearly elevated frequencies of $CD24^{high}CD38^{high}$ Breg in hepatitis B vaccine non-responders which might contribute to the increased baseline levels of IL-10 in these individuals and also lead to an induction of regulatory T cells (39).

The current study aimed to investigate different Breg subpopulations in hepatitis B vaccine responders and non-responders before and after booster vaccination with a second- *versus* a third-generation hepatitis B vaccine.

2 MATERIALS AND METHODS

2.1 Study Cohorts

Two groups of hepatitis B vaccinated individuals were enrolled in this study. The first group comprised eleven non-responders to second-generation hepatitis B vaccine (2^{nd} HBvac NR) (9 women, 2 men; average age of 25.7 years) (**Table 1**). All 2^{nd} HBvac NR subjects received a full primary series of hepatitis B vaccine and were repeatedly vaccinated with Engerix® or Twinrix® in the past, without developing protective anti-HBs levels (> 10 IU/L). The second group consists of eight responders to second-generation hepatitis B vaccine (2^{nd} HBvac R) (6 women, 2 men; average age: 30.0 years), who received a full series of Twinrix® vaccination more than ten years in the past (**Table 1**). On day 0, group 1 (2^{nd} HBvac NR) received a booster vaccination with the third-generation recombinant hepatitis B vaccine Sci-B-Vac™ (VBI Vaccines Inc., Rehovot, Israel), whereas group 2 (2^{nd} HBvac R) was revaccinated with the second-generation recombinant hepatitis B vaccine Twinrix® (Glaxo Smith Kline, Brentford, UK). Peripheral blood was taken by venipuncture at baseline (day 0), and on day 7, and 28 after vaccination with the approval of the local ethic committees (School of Medicine, Technical University of Munich and Innsbruck Medical University). Data on age, weight, and height (BMI (body mass index) measurement), smoking status, alcohol consumption, medical co-morbidities, and medication were collected at baseline (**Table 1**). Informed consent was obtained from all participating individuals prior to their inclusion.

TABLE 1 | Characteristics of study cohorts.

Cohorts (Number of participants)	Hepatitis B vaccine non-responders (n = 11)	Hepatitis B vaccine responders (n = 8)
Gender		
Female	n = 9	n = 6
Male	n = 2	n = 2
Mean age at 1. Visit (years)	25.7 (20.0 – 38.0)	30.0 (23.0 – 38.0)
Mean BMI (range)	24.7 (18.7 – 37.9)	24.6 (19.8 – 32.7)
Smoking (%)	18.2	not known
History of co-morbidities (%)	27.3	not known
Allergies (%)	54.5	not known

2.2 Determination of Serum Anti-HBs Levels

Serum levels of HBsAg-specific antibodies (anti-HBs) were quantified using the Architect® chemiluminescence microparticle immunoassay (Abbott Diagnostics, Wiesbaden, Germany). The detection limit was 10 IU/mL.

2.3 Isolation and Cryoconservation of PBMC

Within 4 h after collection of heparinized whole blood human peripheral blood mononuclear cells (PBMC) were separated by Ficoll density gradient (human Pancoll, PAN-BIOTECH, Aidenbach, Germany) as described previously (40). PBMC were frozen in aliquots of 5 x 10^6 PBMC per vial in 1.8 mL cryotubes (Thermo Scientific, Roskilde, Denmark) in a concentration of 1 x 10^7 PBMC per 1 mL freezing medium (fetal calf serum (FCS) (Life Technologies, Darmstadt, Germany) supplemented with 10% DMSO (Sigma-Aldrich, Steinheim, Germany) in a freezing container (Mr. Frosty, Thermo Scientific, Roskilde, Denmark) and put on -80°C. After 48 h PBMC were stored in the vapor phase of a liquid nitrogen tank until further use.

2.4 Thawing and Resting of PBMC

PBMC were thawed at 37°C using CTL Anti-Aggregate Wash™ 20x Solution (Cellular Technology Limited (CTL) Europe, Bonn, Germany) diluted in RPMI-1640 medium (Life Technologies, Darmstadt, Germany) (1:20). Cells were counted with an automated cell counter (Vi-cell XR, Beckman Coulter, Krefeld, Germany) in CTL-Test™ Medium (Cellular Technology Limited (CTL) Europe, Bonn, Germany). The median cell recovery after thawing was 4.4 x 10^6 PBMC per vial with a median viability of 92%. For a standard resting procedure PBMC were incubated for 18 h at 37°C in a humidified atmosphere at 5% CO_2 in a concentration of 2 x 10^6 PBMC/mL CTL-Test™ medium supplemented with 10% FCS and 1% penicillin–streptomycin (PenStrep, Life Technologies, Invitrogen, Darmstadt, Germany) (abbr.: RPMI-10) RPMI-10. The median cell recovery after resting was 4.2 x 10^6 PBMC per vial with a median viability of 94%.

2.5 Flow Cytometry-Based Analysis of Cell Frequencies and Cytokine Production

2.5.1 *Ex Vivo* Stimulation of PBMC

2 x 10^6 overnight rested PBMC were seeded in polypropylene U-bottom 96-well microtiter plates (Fisher Scientific, Hampton, USA) with CTL-Test™ Medium and either stimulated with CpG oligodeoxynucleotides (10 µg/mL) (InvivoGen, Toulouse, France), PMA (Phorbol-12-myristat-13-acetat) (30 ng/mL) (Sigma-Aldrich, St. Louis, USA), and Ionomycin (1 µg/mL) (Sigma-Aldrich, St. Louis, USA) (referred to as "CpG+P/I") or left unstimulated as a medium control to define background activity. After 1 h of incubation at 37°C in 5% CO_2, 10 µg/mL of

secretion blocker Brefeldin A (Sigma-Aldrich, St. Louis, USA) in a total volume of 50 µL CTL-Test™ medium was added to each well. Stimulation was stopped after 4 h by transferring the plates to 4°C overnight.

2.5.2 Surface Marker and Intracellular Cytokine Staining

After a centrifugation step (560g, 5 min, 4°C), PBMC were resuspended in 100 µL of eBioscience™ Flow Cytometry Staining Buffer (Life Technologies, Invitrogen, Darmstadt, Germany) and a Fc block (Human TruStain FcX™, BioLegend, San Diego, USA, 1:20) was added followed by incubation for 10 min at RT. Next, PBMC were stained with 100 µL of UV Live/Dead working solution (1:100 LIVE/DEAD™ Fixable Blue Dead Cell Stain Kit (Life Technologies, Invitrogen, Darmstadt, Germany) for 30 min on ice in the dark followed by two washing steps with 200 µL eBioscience™ Flow Cytometry Staining Buffer (Life Technologies, Invitrogen, Darmstadt, Germany). For a combined intracellular and surface staining, PBMC were fixed for 20 min on ice in the dark using 100 µL/well eBioscience™ Intracellular Fixation buffer (Life Technologies, Invitrogen, Darmstadt, Germany) and afterwards centrifuged (710g, 5 min, 4°C) and washed in permeabilization buffer eBioscience (10X) (Life Technologies, Invitrogen, Darmstadt, Germany) for three times. PBMC were stained with the antibodies listed in Additional file 1: **Table S1** in a total volume of 100 µL antibody staining solution (1:2) (Permeabilization Buffer and Brilliant Stain Buffer (BD Biosciences, Franklin Lakes, USA) for 30 min on ice in the dark. Cells were washed twice with 200 µL/well Permeabilization Buffer and finally re-suspended in 300 µL Staining Buffer and Permeabilization Buffer (1:2) for acquisition. For compensation, UltraComp eBeads™ Compensation Beads (Life Technologies, Invitrogen, Darmstadt, Germany) and ArC™ Amine Reactive Compensation Bead Kit (Life Technologies, Invitrogen, Darmstadt, Germany) were stained with antibodies and live/dead discriminating dyes without fixation steps and finally re-suspended in 300 µL Staining and Permeabilization buffer (1:2) for acquisition. Cells were stored cold and in the dark until acquisition.

2.5.3 Data Acquisition

Acquisition of samples was performed within 4 h after staining using a BD LSR Fortessa flow cytometer (Becton Dickinson, Franklin Lakes, USA) equipped with a 96-well plate reader and FACSDiva Software V.6.0 (Becton Dickinson, Heidelberg, Germany). On a weekly basis, the flow cytometer's performance was checked and settings were configured with Cytometer, Setup & Tracking beads (Becton Dickinson, Franklin Lakes, USA). Photomultiplier voltages were adjusted with the help of unstained cells for all parameters.

2.5.4 Gating Strategy

Flow cytometry-based analysis was performed on at least 1.0 x 10^5 living lymphocytes using the software FlowJo version 10 (FlowJo LLC, BD, Ashland, USA). Gating strategy for analysis of *ex vivo* re-stimulated PBMC is shown in the supplementary information (Additional file 2: **Figure S1**). Each gate was set in the negative control sample and then adjusted to the antigen stimulated samples. In detail, we firstly set a broad forward-side scatter gate to prevent excluding cells of interest, followed by an exclusion of dead cells. Using a FSC-W against FSC-A plot, we excluded doublets. Next, we gated on $CD3^-CD14^-$ cells and $CD19^+$ B cells. Within the $CD19^+$ cells, we gated on $CD24^+CD27^+$ and $CD24^{high}CD38^{high}$ Breg, respectively. FMO controls were used to gate on $CD24^+$, $CD27^+$, and $CD38^+$ cells, respectively. For functional analysis, we gated on IL-10, IL-35, and TGF-ß expression in the $CD19^+$ B cell, $CD24^+CD27^+$, and $CD24^{high}CD38^{high}$ Breg population. Two independent audits were performed to control the gating.

2.5.5 Data Interpretation

We detected significantly higher levels of IL-10, IL-35, and TGF-ß expression of $CD24^+CD27^+$ and/or $CD24^{high}CD38^{high}$ Breg upon CpG+P/I re-stimulation compared to unstimulated PBMC in both cohorts. In line with this, we used CpG+P/I induced frequencies for further analysis without further background subtraction. Detected frequencies of cytokine expressing Breg which derived from rare events (< 20 events) were excluded from further analysis to avoid misleading interpretations. The median fluorescence intensity (MFI) of $CD24^+CD27^+IL\text{-}10^+$, $CD24^+CD27^+IL\text{-}35^+$, $CD24^+CD27^+TGF\text{-}ß^+$ and $CD24^{high}CD38^{high}IL\text{-}10^+$ Breg of second-generation hepatitis B vaccine non-responders and responders before (day 0) and 7, and 28 days after vaccination with a third-generation hepatitis B vaccine are shown in Additional file 3: **Figure S2**.

2.6 Statistical Analysis

All results were included in the analysis, as no attempt was made to exclude outliers. All tests were two-sided and conducted on exploratory 5% significance levels. Effect measures are presented with 95% confidence intervals. Nonparametric statistical tests were applied in all cases. Unpaired Mann-Whitney U test was used to define significance of values between the 2nd HBvac NR and 2nd HBvac R group. One-Way ANOVA (Friedman test) was applied for analyses within the two groups for the different time points. In case of resulting p-values < 0.05, paired Wilcoxon signed rank tests were performed to assess significance of change in values within the 2nd HBvac NR and 2nd HBvac R group, respectively. The software Graph Pad Prism 9.1.0 (GraphPad Software, La Jolla, California, USA) was used for statistical analyses. Interpretation of Spearman`s correlation coefficient was performed according to Cohen (41).

3 RESULTS

3.1 Vaccination With Third-Generation Hepatitis B Vaccine Sci-B-Vac Overcomes Non-Responsiveness to Second-Generation Hepatitis B Vaccination

First, we examined anti-HBs (antibody to hepatitis B surface antigen) levels of second-generation hepatitis B vaccine non-responders (n = 11) (referred to as "2nd HBvac NR") before (day

0) and after vaccination (day 28 and 56) with the third-generation hepatitis B vaccine Sci-B-Vac. Sci-B-Vac vaccination led to anti-HBs seroconversion (anti-HBs levels >Partner Site Munich 10 IU/L) in 10/11 (90.9%) 2nd HBvac NR. In detail, we detected median anti-HBs levels of 3.97 IU/L (0Partner Site Munich - 8.46 IU/L) on day 0 and 72.44 IU/L (0 - >1000 IU/L) on day 28 after Sci-B-Vac vaccination (p = 0.002) (**Figure 1**). Three of six Sci-B-Vac vaccination non-(anti-HBs levels < 10) or low (anti-HBs levels < 100) -responder subjects (42) received a second Sci-B-Vac vaccination on day 30, resulting in anti-HBs levels of 0, 33.0, and 634.2 IU/L at day 56, respectively (**Figure 1**).

Comparison of the characteristics of Sci-B-Vac vaccine low- ("3rd HBvac LR"; anti-HBs < 100 IU/L; n = 5) and high- ("3rd HBvac HR"; anti-HBs > 100 IU/L; n = 5) responders revealed no differences in age (mean: 25.6 (range 21-31) and 23.4 (range 21-30) years, respectively) (p = 0.524), gender (4 female, 1 male in each cohort), smoking habits (one smoker in the 3rd HBvac HR group), and in history of comorbidities (one person with comorbidities per group) and medication (none in each group).

The only one remaining non-responder from study group 1 (2nd and 3rd HBvac NR) had risk factors (smoking, obesity, hypertension) known to impair vaccine efficacy.

3.2 Vaccine Non-Responders Showed Higher Numbers of CD24^{high}CD38^{high} Breg And Lower Breg-Derived IL-10 Expression Compared to Vaccine Responders

High levels of immunomodulatory lymphocytes and related cytokines such as regulatory B cells (Breg) and IL-10 have been associated with serological non-response to hepatitis B vaccination. To investigate this, we analyzed frequencies of two populations of Breg (CD24$^+$CD27$^+$ and CD24^{high}CD38^{high} Breg) and respective IL-10 levels in a cohort of 2nd HBvac NR (n = 11) at baseline visit and on day 7 and 28 post Sci-B-Vac booster vaccination. For comparative analysis, we additionally determined frequencies of Breg and IL-10 expression levels on day 0, 7, and 28 also in a cohort of second-generation hepatitis B vaccine responders (referred to as "2nd HBvac R"; n = 8) receiving a second-generation hepatitis B booster vaccination.

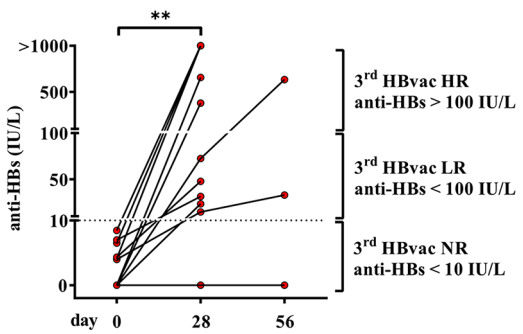

FIGURE 1 | Anti-HBs levels of second-generation hepatitis B vaccine non-responders before and after vaccination with third-generation hepatitis B vaccine Sci-B-Vac™. Depicted are anti-HBs levels (IU/L) of second-generation hepatitis B vaccine non-responders (2nd HBvac NR, n = 11) before (day 0), after primary (day 28), and second (day 56, n = 3) Sci-B-Vac™ vaccination. The dashed line indicates the threshold for protective anti-HBs levels (> 10 IU/L). The interconnected lines link the respective data points of each subject at each time point. Statistics are based on paired Wilcoxon signed rank tests. **p < 0.01.

Frequencies of CD24$^+$CD27$^+$ Breg tend to be higher in 2nd HBvac NR compared to 2nd HBvac R at all three time points (d0: p = 0.062; d7: p = 0.059; d28: p = 0.109) (**Figure 2A**). In parallel, we observed significantly higher frequencies of CD24^{high}CD38^{high} Breg in the 2nd HBvac NR compared to the 2nd HBvac R group on day 0 (p = 0.004) and day 28 (p = 0.012), but not on day 7 (p = 0.051) (**Figure 2B** and **Table 2**).

Comparison of CpG- and PMA/Ionomycin (CpG+P/I)-induced IL-10 expression levels of Breg between both cohorts showed significantly lower frequencies of CD24$^+$CD27$^+$IL-10$^+$ Breg in the 2nd HBvac NR group at all time points (d0: p < 0.0001; d7: p = 0.0004; d28: p = 0.0003) (**Figure 2C**). Frequencies of CD24^{high}CD38^{high}IL-10$^+$ Breg were also significantly lower in 2nd HBvac NR compared to 2nd HBvac R on day 0 and 7, but not on day 28 (d0: p = 0.016; d7: p = 0.016; d28: p = 0.111) (**Figure 2D** and **Table 2**).

Besides IL-10, other cytokines like IL-35 and TGF-ß could mediate immunosuppressive function of Breg. CD24$^+$CD27$^+$IL-35$^+$ Breg were detectable in nine 2nd HBvac NR and three 2nd HBvac R (**Figure 3A**). Median frequencies of CD24$^+$CD27$^+$IL-35$^+$ Breg were comparable between both groups and time points, but reactivity rates in the 2nd HBvac R group were too low for statistical analysis (**Figure 3A** and **Table 1**). CD24^{high}CD38^{high}IL-35$^+$ Breg were largely undetectable in both groups (1/11 2nd HBvac NR and 0/8 2nd HBvac R; data not shown). Regarding TGF-ß expression, we detected CD24$^+$CD27$^+$TGF-ß$^+$ Breg in ten 2nd HBvac NR but only one 2nd HBvac R (**Figure 3B** and **Table 2**). CD24^{high}CD38^{high}TGF-ß$^+$ Breg were detectable in six 2nd HBvac NR subjects with comparable frequencies at all time points, but in none of the 2nd HBvac R subjects (**Table 2**).

Correlation analysis revealed no correlation of pre-vaccination levels of CD24$^+$CD27$^+$IL-10$^+$ Breg and anti-HBs levels on day 28 (r_s = 0.083), but a moderate correlation of pre-vaccination levels of CD24^{high}CD38^{high}IL-10$^+$ Breg and anti-HBs levels on day 28 (r_s = 0.300) (Additional file 4: **Figures S3A, B**).

3.3 Significant Lower Frequencies of B10$^+$ Cells in Vaccine Non-Responders Compared to Responders

We further analyzed CpG+P/I-induced IL-10 expression levels of CD19$^+$ B cells (B10$^+$ cells), since IL-10 plays an active role in B-cell differentiation into antibody secreting plasmablasts and B10$^+$ cells. We determined significantly lower frequencies of B10$^+$ cells in 2nd HBvac NR compared to 2nd HBvac R at baseline (day 0) (p < 0.0001), and also on day 7 (p = 0.0005), and day 28 (p = 0.0001) post vaccinations (**Figure 4**). In detail, we detected median frequencies of B10$^+$ cells of 0.70% (0.28 – 1.51%) and 2.24% (1.29 – 4.40%) on day 0, 0.66% (0.23 – 2.01%), and 2.13% (1.53 – 3.67%) on day 7, and 0.77% (0.24 – 1.75%) and 2.18%

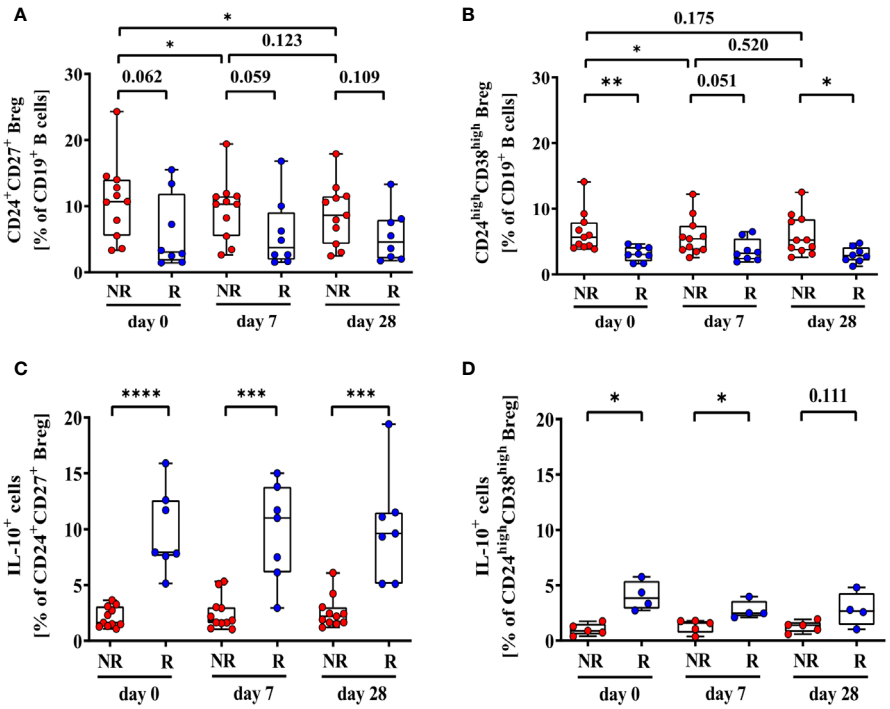

FIGURE 2 | Frequencies of $CD24^+CD27^+$ **(A)**, $CD24^{high}CD38^{high}$ **(B)**, $CD24^+CD27^+IL\text{-}10^+$ **(C)**, and $CD24^{high}CD38^{high}IL\text{-}10^+$ Breg **(D)** of second-generation hepatitis B vaccine non-responders and responders. Depicted are (CpG+P/I)-induced frequencies of $CD24^+CD27^+$ **(A)**, $CD24^{high}CD38^{high}$ **(B)**, $CD24^+CD27^+IL\text{-}10^+$ **(C)**, and $CD24^{high}CD38^{high}IL\text{-}10^+$ Breg **(D)** of second-generation hepatitis B vaccine non-responders (NR, red circles, n = 11) and second-generation hepatitis B vaccine responders (R, blue circles, n = 8) before (day 0) and 7, and 28 days after vaccination with a third- (NR group) or second- (R group) generation hepatitis B vaccine, respectively. The boxes show the median and the 25th and 75th percentile. Whiskers indicate the highest and lowest values. Statistical analyses are based either on unpaired Mann-Whitney U tests for the analysis of the NR *vs.* the R group or on Friedman tests with post Wilcoxon signed rank testing for analysis of the impact of third- and second-generation hepatitis B vaccines within the NR or R group. *$p < 0.05$; **$p < 0.01$; ***$p < 0.001$; ****$p < 0.0001$.

TABLE 2 | Frequencies and cytokine expression levels of $CD24^+CD27^+$ and $CD24^{high}CD38^{high}$ Breg and $B10^+$ cells.

Cell population	Time point	2nd HBvac NR; Median (min-max) (%)	2nd HBvac R; Median (min-max) (%)	*p*-value
$CD24^+CD27^+$ Breg	d0	10.70 (3.33 – 24.3)	3.07 (1.44 – 15.50)	0.062
	d7	10.30 (2.62– 19.40)	3.75 (1.52 – 16.80)	0.059
	d28	8.62 (2.47 – 17.90)	4.56 (1.75 – 13.30)	0.109
$CD24^{high}CD38^{high}$ Breg	d0	5.67 (3.84 – 14.10)	3.04 (1.63 – 4.63)	0.004
	d7	5.42 (2.54 – 12.20)	3.22 (1.88 – 6.48)	0.051
	d28	5.20 (2.59 – 12.50)	2.84 (1.23 – 4.75)	0.012
$CD24^+CD27^+IL\text{-}10^+$ Breg	d0	1.63 (1.08 – 3.63)	7.92 (5.14 – 15.90)	<0.0001
	d7	1.84 (1.04 – 5.31)	11.0 (2.95 – 15.0)	0.0004
	d28	2.19 (1.20 – 6.08)	9.61 (5.10 – 19.40)	0.0003
$CD24^{high}CD38^{high}IL\text{-}10^+$ Breg	d0	0.89 (0.39 – 1.75)	3.85 (2.73 – 5.75)	0.016
	d7	1.59 (0.36 – 1.79)	2.48 (2.11 – 3.97)	0.016
	d28	1.39 (0.58 – 1.93)	2.68 (1.03 – 4.80)	0.111
$CD24^+CD27^+IL\text{-}35^+$ Breg	d0	1.68 (0.48 – 2.14)	1.19 (0.76 – 2.54)	ND
	d7	1.39 (0.73 – 3.06)	1.05 (0.71 – 2.73)	ND
	d28	1.23 (0.52 – 3.94)	1.76 (0.70 – 2.34)	ND
$CD24^+CD27^+TGF\text{-}ß^+$ Breg	d0	1.49 (0.78 – 3.20)	0.31	ND
	d7	1.34 (0.89 – 2.09)	0.66	ND
	d28	1.31 (0.79 – 3.21)	0.38	ND
$CD24^{high}CD38^{high}TGF\text{-}ß^+$ Breg	d0	1.44 (0.77 – 1.85)	U	ND
	d7	1.07 (0.72 – 2.20)	U	ND
	d28	1.18 (0.60 - 2.44)	U	ND
$B10^+$ cells	d0	0.70 (0.28 – 1.51)	2.24 (1.29 – 4.40)	<0.0001
	d7	0.66 (0.23 – 2.01)	2.13 (1.53 – 3.67)	0.0005
	d28	0.77 (0.24 – 1.75)	2.18 (1.21 – 3.92)	0.0001

U, undetectable; ND, not done.

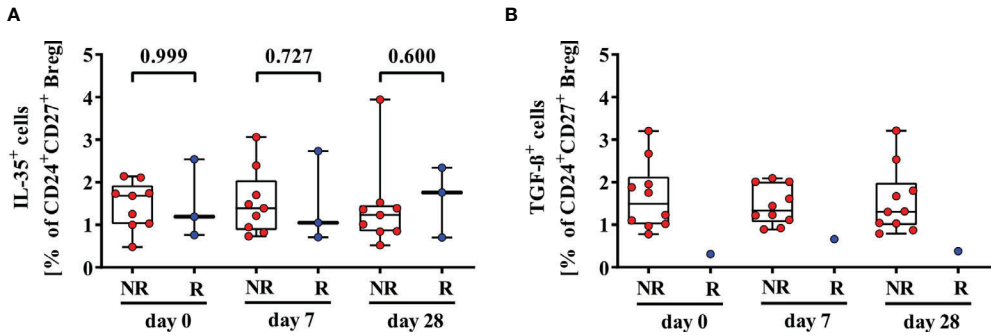

FIGURE 3 | Comparison of frequencies of $CD24^+CD27^+IL\text{-}35^+$ **(A)** and $CD24^+CD27^+TGF\text{-}ß^+$ **(B)** Breg of second-generation hepatitis B vaccine non-responders and responders. Depicted are (CpG+P/I)-induced frequencies of $CD24^+CD27^+IL\text{-}35^+$ **(A)** and $CD24^+CD27^+TGF\text{-}ß^+$ **(B)** Breg of second-generation hepatitis B vaccine non-responders (NR, red circles) and second-generation hepatitis B vaccine responders (R, blue circles) before (day 0) and 7, and 28 days after vaccination with a third- (NR group) or second- (R group) generation hepatitis B vaccine, respectively. The boxes show the median and the 25th and 75th percentile. Whiskers indicate the highest and lowest values. Statistical analyses were done with unpaired Mann-Whitney U tests.

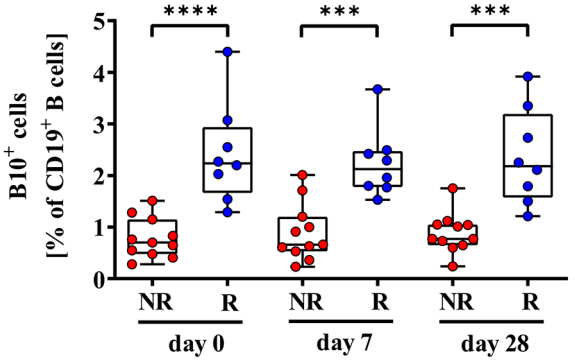

FIGURE 4 | Comparison of frequencies of $CD19^+IL\text{-}10^+$ B ($B10^+$) cells of second-generation hepatitis B vaccine non-responders and responders. Depicted are frequencies of $B10^+$ cells of second-generation hepatitis B vaccine non-responders (NR, red circles) and second-generation hepatitis B vaccine responders (R, blue circles) before (day 0) and 7, and 28 days after vaccination with a third- (NR group) or second- (R group) generation hepatitis B vaccine, respectively. The boxes show the median and the 25th and 75th percentile. Whiskers indicate the highest and lowest values. Statistical analyses are based either on unpaired Mann-Whitney U tests for the analysis of the NR *vs*. the R group or on Friedman tests with post Wilcoxon signed rank testing for analysis of the impact of third- and second-generation hepatitis B vaccines within the NR or R group. ***$p < 0.001$; ****$p < 0.0001$.

(1.21 – 3.92%) on day 28 in 2nd HBvac NR compared to 2nd HBvac R, respectively (**Figure 4** and **Table 2**).

3.4 Frequencies of $CD24^+CD27^+$ and $CD24^{high}CD38^{high}$ Breg Decreased Upon Booster Vaccination With Third-Generation Vaccine but Remained Stable Upon Second-Generation Vaccine Booster Immunization

Next, we assessed the impact of booster vaccination with second- (2nd HBvac R group) and third- (2nd HBvac NR group) generation hepatitis B vaccines on Breg and $B10^+$ cell frequencies as well as Breg-derived IL-10 expression

Upon booster vaccination with the third-generation vaccine (2nd HBvac NR group), we observed significantly higher frequencies of $CD24^+CD27^+$ Breg prior (d0) compared to day 7 ($p = 0.014$) and day 28 ($p = 0.032$) post vaccination, but no difference between day 7 and 28 ($p = 0.123$) (**Figure 2A**). Frequencies of $CD24^{high}CD38^{high}$ Breg were also significantly higher prior vaccination (d0) compared to day 7 post vaccination ($p = 0.045$), but comparable between the other time points (d0 *vs*. d28: $p = 0.175$; d7 *vs*. d28: $p = 0.520$) (**Figure 2B**).

After booster vaccination with a second-generation vaccine (2nd HBvac R group), frequencies of $CD24^+CD27^+$ and $CD24^{high}CD38^{high}$ Breg were comparable across time points ($p = 0.531$ and $p = 0.236$, respectively) (**Figures 2A, B**).

Analysis of $CD24^+CD27^+IL\text{-}10^+$ and $CD24^{high}CD38^{high}IL\text{-}10^+$ Breg numbers revealed no significant differences between the different booster vaccines and time points (2nd HBvac NR: $p = 0.643$ and $p = 0.124$, respectively; 2nd HBvac R: $p = 0.423$ and $p = 0.125$, respectively) (**Figures 2C, D**).

We also observed no significant differences in frequencies of $B10^+$ cells between the different booster vaccines and time points (2nd HBvac NR: $p = 0.256$ and 2nd HBvac R: $p = 0.967$) (**Figure 4**).

3.5 Third-Generation Hepatitis B Vaccine Low- and High-Responders Showed Different Frequencies of $CD24^+CD27^+$ And $CD24^{high}CD38^{high}$ Breg Before and One Week After Booster Vaccination

Finally, we analyzed differences in frequencies of Breg and $B10^+$ cells between third-generation hepatitis B vaccine low- (3rd HBvac LR) and high-responders (3rd HBvac HR) (n = 5, respectively). Frequencies of $CD24^+CD27^+$ Breg were significantly higher in the 3rd HBvac LR compared to the 3rd HBvac HR group on day 0 and day 7, but not on day 28 (d0: $p = 0.032$; d7: $p = 0.024$, and d28: $p = 0.548$, respectively) (**Figure 5A**

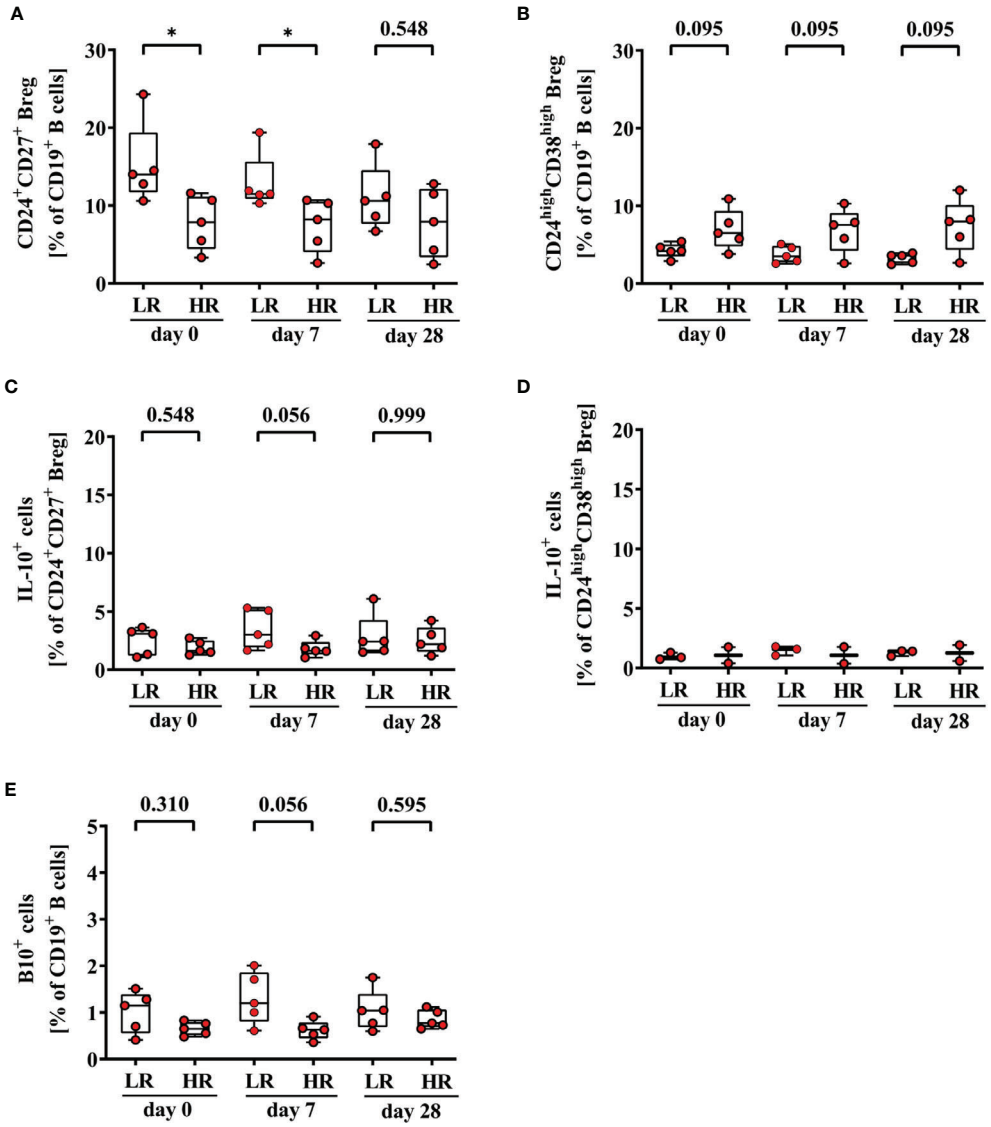

FIGURE 5 | Frequencies of $CD24^+CD27^+$ **(A)**, $CD24^{high}CD38^{high}$ **(B)**, $CD24^+CD27^+IL\text{-}10^+$ **(C)**, $CD24^{high}CD38^{high}IL\text{-}10^+$ Breg **(D)**, and $CD19^+IL\text{-}10^+$ B ($B10^+$) cells **(E)** of third-generation hepatitis B vaccine low- and high-responders. Depicted are (CpG+P/I)-induced frequencies of $CD24^+CD27^+$ **(A)**, $CD24^{high}CD38^{high}$ **(B)**, $CD24^+CD27^+IL\text{-}10^+$ **(C)**, $CD24^{high}CD38^{high}IL\text{-}10^+$ Breg **(D)** and $CD19^+IL\text{-}10^+$ B ($B10^+$) cells **(E)** of third-generation hepatitis B vaccine low- (LR) and high-responders (HR) (red circles, n = 5, respectively) before (day 0) and 7, and 28 days after vaccination with a third-generation hepatitis B vaccine. The boxes show the median and the 25th and 75th percentile. Whiskers indicate the highest and lowest values. Statistical analyses are based on unpaired Mann-Whitney U tests. *$p < 0.05$.

and **Table 3**). In contrast, we observed a tendency of lower frequencies of $CD24^{high}CD38^{high}$ Breg in the 3rd HBvac LR compared to the HR group at all three time points ($p = 0.095$, respectively) (**Figure 5B** and **Table 3**).

Regarding IL-10 expression levels, we observed a tendency of higher frequencies of $B10^+$ cells (d0: $p = 0.310$; d7: $p = 0.056$; d28 $p = 0.595$) and $CD24^+CD27^+IL\text{-}10^+$ Breg (d0: $p = 0.548$, d7: $p = 0.056$, d28: $p = 0.999$) in the 3rd HBvac LR compared to the HR group at all three time points, respectively (**Figures 5C, E** and **Table 3**). Since $CD24^{high}CD38^{high}IL\text{-}10^+$ Breg were only detectable in three 3rd HBvac LR and two HR at all three time points, we could not conduct reliable statistical analyses between the two groups (**Figure 5D** and **Table 3**). One of the eleven 2nd HBvac NR failed to produce protective anti-HBs levels even after vaccination with a third-generation hepatitis B vaccine. This 3rd HBvac NR showed low frequencies of $CD24^+CD27^+$ and $CD24^+CD27^+IL\text{-}10^+$ Breg (d0: 3.58%; d7: 3.44%; d28: 3.02% and d0: 1.49%; d7: 1.12%; d28: 1.65%, respectively). The frequencies of $CD24^{high}CD38^{high}$ Breg of the 3rd HBvac NR subject were in the median range of all 2nd HBvac NR subjects (d0: 5.67%; d7: 5.42%; d28: 5.20%). Noteworthy, the 3rd HBvac NR subject showed the highest frequencies of $CD19^+$ B cells

TABLE 3 | Frequencies and cytokine expression levels of $CD24^+CD27^+$ and $CD24^{high}CD38^{high}$ Breg and $B10^+$ cells of 3rd HBvac LR and 3rd HBvac HR.

Cell population	Time point	3rd HBvac LR; Median (min-max) (%)	3rd HBvac HR; Median (min-max) (%)	*p*-value
$CD24^+CD27^+$ Breg	d0	14.0 (10.60 – 24.30)	7.86 (3.33 – 11.60)	0.032
	d7	11.50 (10.30 – 19.40)	8.22 (2.62 – 10.70)	0.024
	d28	10.60 (6.72 – 17.90)	7.92 (2.47 – 12.80)	0.548
$CD24^{high}CD38^{high}$ Breg	d0	4.20 (2.90 – 5.42)	6.50 (3.81 – 10.90)	0.095
	d7	3.51 (2.57 – 5.09)	7.56 (2.61 – 10.30)	0.095
	d28	3.60 (2.46 – 3.93)	7.98 (2.66 – 12.0)	0.095
$CD24^+CD27^+$IL-10^+ Breg	d0	3.09 (1.08 – 3.63)	1.63 (1.27 – 2.73)	0.548
	d7	3.02 (1.66 – 5.31)	1.63 (1.04 – 2.93)	0.056
	d28	2.42 (1.51 – 6.08)	2.19 (1.20 – 4.22)	0.999
$CD24^{high}CD38^{high}$IL-10^+ Breg	d0	0.89 (0.73 – 1.29)	1.07 (0.39 – 1.75)	ND
	d7	1.59 (1.05 – 1.79)	1.07 (0.36 – 1.77)	ND
	d28	1.39 (0.99 – 1.42)	1.26 (0.58 – 1.93)	ND
$B10^+$ cells	d0	1.15 (0.41 – 1.51)	0.65 (0.48 – 0.83)	0.310
	d7	1.20 (0.61 – 2.01)	0.63 (0.36 – 0.91)	0.056
	d28	1.04 (0.60 – 1.75)	0.77 (0.65 – 1.12)	0.595

ND, not done.

within the 2nd HBvac NR group, but the lowest frequencies of $B10^+$ cells of all 2nd HBvac NR and 2nd HBvac R subjects (d0: 0.28%; d7: 0.23%; d28: 0.24%).

4 DISCUSSION

Although several potential immunological mechanisms associated with hepatitis B vaccine non-responsiveness, like failure of antigen presentation or costimulatory signals, impact of certain HLA class II alleles, or lack of specific CD4 Th cells have been investigated, the decisive underlying immunological mechanisms remain unclear (10, 19, 20, 39, 43). In the current study, we asked whether non-responsiveness to hepatitis B vaccine is associated with a dysregulation of certain Breg subpopulations and analyzed their frequency and function in relation to second- *versus* third-generation hepatitis B vaccine induced immunity

Breg known to mediate immunosuppressive functions and the effect of different hepatitis B vaccine formulations on their frequency and function have not yet been investigated in parallel as possible factors involved in vaccine non-responsiveness. We performed comparative phenotypic and frequency analysis of $CD24^+CD27^+$ and $CD24^{high}CD38^{high}$ Breg in 2nd HBvac NR and R before and after booster vaccination to investigate whether non-responsiveness to hepatitis B vaccination is associated with alterations of Breg frequencies and their cytokine expression levels.

One of our main findings was the detection of higher frequencies of $CD24^+CD27^+$ and $CD24^{high}CD38^{high}$ Breg accompanied by lower levels of IL-10 expression in 2nd HBvac NR compared to R. So far, very few studies investigated the association of Breg frequencies and IL-10 expression levels with non-responsiveness to hepatitis B vaccination (12, 38, 39). In contrast to our results, Bolther et al. observed no significant differences in frequencies of $CD24^{high}CD38^{high}$ Breg between 2nd HBvac non-/low-responder and high-responder (38). But since the authors combined non- and low-responder in one group, the finding of comparable frequencies of $CD24^{high}CD38^{high}$ Breg in non-/low *versus* high-responder group could be biased by the very low number of non-responder subject included (38). Correlation analysis revealed no significant correlation of anti-HBs levels and frequencies of IL-$10^+CD24^{high}CD38^{high}$ Breg, which is in line with our results (38).

In a study cohort of hepatitis B and tick-borne encephalitis (TBE) vaccine non-responders Garner-Spitzer et al. investigated, whether non-responsiveness is an antigen and/or vaccine-specific phenomenon. In line with our observations, Garner-Spitzer et al. reported clearly elevated frequencies of $CD24^{high}CD38^{high}$ Breg in HBvac NR pre- and post-booster TBE vaccination compared to TBE non- or high-responders (39). Since HBvac NR developed sufficient anti-TBE titers (neutralization test (NT) titers ≥ 1:10) and Breg frequencies did not decline post TBE booster vaccination, they concluded that the underlying immunological mechanisms of non-responsiveness rather depend on the applied vaccine antigen and host-related genetic predispositions (39).

Interestingly, TBE non- and high responders had comparable median frequencies of $CD24^{high}CD38^{high}$ Breg pre-booster which only increased in the non-responder group after TBE booster vaccination. In our study, we observed a decline of both, $CD24^+CD27^+$ and $CD24^{high}CD38^{high}$ Breg frequencies, post third-generation booster vaccination in 2nd HBvac NR, which could indicate a positive effect of third-generation hepatitis B vaccines on Breg-mediated immunomodulation in HBvac NR. Interestingly we did not observe decreased numbers of $CD24^+CD27^+$ and $CD24^{high}CD38^{high}$ Breg post-boost with the second-generation hepatitis B vaccine.

Breg modulate immune responses predominantly, although not exclusively, *via* IL-10, therefore IL-10 expression is often used as a marker for Breg function (25). IL-10, a pleiotropic cytokine, is known to act as an immunoregulatory molecule which inhibits the production of inflammatory cytokines by T cells and monocytes and suppresses antigen-presentation e.g. by downregulation of MHC II expression (12, 44), but it is also known to promote B-cell differentiation into antibody secreting plasmablasts (12, 44–46). Several subsets of B cells produce

IL-10, including $B10^+$ cells, $CD24^+CD27^+$ and $CD24^{high}CD38^{high}$ Breg (30, 34). Within our study cohorts, we observed significantly lower IL-10 expression levels of $CD24^+CD27^+$ and $CD24^{high}CD38^{high}$ Breg and $CD19^+$ $B10^+$ cells in HBvac NR compared to HBvac R pre-booster.

Heine et al. reported that genes associated with the differentiation into antibody-secreting cells are upregulated in IL-10-secreting B cells and concluded that autocrine and paracrine IL-10 signaling contributes to differentiation of B cells into antibody secreting cells (45). Therefore, low IL-10 expression levels may additionally favor non-responsiveness to hepatitis B vaccination.

The fact, that we observed significantly lower IL-10 expression levels of $CD24^+CD27^+$ and $CD24^{high}CD38^{high}$ Breg and $B10^+$ cells in 2nd HBvac NR support the hypothesis that IL-10 may contribute to B-cell differentiation into anti-HBs secreting plasma cells (12). Of note, also the HBvac NR who was the only individual without protective anti-HBs titer even after booster with third-generation hepatitis B vaccine had very low frequencies of IL-10 expressing $CD24^+CD27^+$ and $CD24^{high}CD38^{high}$ Breg and $B10^+$ cells. However, we could not observe a significant increase in IL-10 expression levels of $CD24^+CD27^+$ and $CD24^{high}CD38^{high}$ Breg in 2nd HBvac NR who seroconverted after third-generation booster vaccination.

Although the immunoregulatory role of Breg is predominantly driven by IL-10, other cytokines, like IL-35 and TGF-ß are known to impact responsiveness to hepatitis B vaccination (10, 26–29). Breg-derived TGF-β can lead to an expansion of Treg linked with impaired antibody production (26, 35). In line with reports of Jarrosson et al. (10), we observed robust frequencies of IL-35 and TGF-ß expressing $CD24^+CD27^+$ Breg in the 2nd HBvac NR whereas in 2nd HBvac R group, these Breg were mostly undetectable.

Another important result of our study was the high seroconversion rate of HBvac NR after booster vaccination with a third-generation hepatitis B vaccine which was also observed in previous studies, using Sci-B-Vac™ (9, 47–49). Commonly used hepatitis B vaccines belong to the second-generation vaccines and are composed of the yeast-derived recombinant non-glycosylated small (S) HBV envelope protein (HBsAg) (3), whereas third-generation hepatitis B vaccines like Sci-B-Vac™, consist of glycosylated and non-glycosylated pre-S1, pre-S2, and S proteins produced in mammalian cells (48). Differences in glycosylation patterns and physical properties of these vaccine antigens might result in higher immunogenicity and successful induction of protective anti-HBs titers (9, 47, 49–51). The exact underlying immunological mechanisms of higher anti-HBs seroconversion rates in formerly non-responders are still unclear, but it is assumed that the additional pre-S1 and pre-S2 domains increase immunogenicity and may evade genetic non-responsiveness to the S antigen (52, 53).

As postulated by Garner-Spitzer et al., non-responder status does probably not reflect a basic defect in antibody production, as HBV-NR respond well to TBE and influenza vaccine. Our data support this hypothesis since ten of eleven 2nd HBvac NR showed a seroconversion after vaccination with Sci-B-Vac™. There are reports suggesting that a real hepatitis B non-responder status is quite rare and that most non-responders are indeed low-responders where higher vaccine doses, intradermal vaccine application or repeated vaccinations could overcome the NR status (54, 55). At least for our study cohort this does not apply, as most study participants already received several booster vaccinations with second-generation vaccines without showing seroconversion. The fact, that vaccination with a third-generation hepatitis B vaccine lead to anti-HBs seroconversion in more than 90% of our study participants also argues against an overall defect in the priming and generation of vaccine-induced memory B cells. Valats et al. reported that 2nd HBvac NR showed substantial numbers of HBsAg-specific memory B cells able to differentiate into anti-HBs secreting plasma cells upon *in vitro* re-stimulation (54). Since production of anti-HBs is known to be Th cell-dependent (19, 56–59) also a dysfunction in T-cell help mediating hepatitis B vaccine non-responsiveness was discussed (60, 61). But this is contradicted by the fact that several studies reported vaccine-induced, HBs-Ag-specific T cells being detectable in second-generation hepatitis B vaccine non-responders (10, 62). We have not investigated Th cell function or immunoregulatory T-cell subsets in our study cohorts as our main focus was the possible involvement of Breg on vaccine non-responsiveness. It remains to be investigated whether and how Breg-mediated effects described here interact with other immunoregulatory mechanisms (e.g. a vaccine-induced, dysfunctional T-cell response) which might synergistically favor hepatitis B vaccine non-responsiveness.

In summary, we report significantly higher frequencies of $CD24^{high}CD38^{high}$ Breg in parallel with significantly lower IL-10 expression levels of $CD24^+CD27^+$ and $CD24^{high}CD38^{high}$ Breg in 2nd HBvac NR compared to 2nd HBvac R. Anti-HBs seroconversion accompanied by a decrease of Breg numbers after booster immunization with a third-generation hepatitis B vaccine could indicate a positive effect of third-generation hepatitis B vaccines on Breg-mediated immunomodulation in hepatitis B vaccine non-responders. Further studies investigating Breg-mediated mechanisms involved in non-responsiveness to vaccines also during primary series of hepatitis B vaccination may help to further improve immunogenicity of existing or the development of new vaccines to overcome non-responsiveness to hepatitis B vaccines.

DATA AVAILABILITY STATEMENT

The raw data supporting the conclusions of this article will be made available by the authors, without undue reservation.

ETHICS STATEMENT

The studies involving human participants were reviewed and approved by ethic committees: School of Medicine, Technical University of Munich and Innsbruck Medical University. The

patients/participants provided their written informed consent to participate in this study.

AUTHOR CONTRIBUTIONS

NK, TB, and UP conceived and designed the experiments. BW and BG-L provided blood samples. NK and LP performed the experiments and acquired the data. NK, LP, and TB analyzed the data. NK, LP, BW, BG-L, PK, HR, UP, and TB interpreted the data. NK, LP, and TB drafted the manuscript. All authors contributed to the article and approved the submitted version.

FUNDING

This study was supported by Helmholtz Initiative for Personalized Medicine (iMed, project title: "Molecular basis and early predictors of non-responsiveness to hepatitis B vaccination").

The research leading to these results has received funding from the European Union's Seventh Framework Programme [FP7/2007-2013] under Grant Agreement No: 280873 ADITEC.

ACKNOWLEDGMENTS

We thank Manuela Laumer, Christoph Richter (both: Institute of Virology, Helmholtz Zentrum München, Munich, Germany) and Dominik Diem (Institute of Molecular Immunology and Experimental Oncology, School of Medicine, Technical University of Munich (TUM), Munich) for technical support.

SUPPLEMENTARY MATERIAL

The Supplementary Material for this article can be found online at: https://www.frontiersin.org/articles/10.3389/fimmu.2021.713351/full#supplementary-material

REFERENCES

1. WHO. *WHO Global Hepatitis Report* (2017). Available at: https://www.who.int/hepatitis/publications/global-hepatitis-report2017/en/.
2. Shepard CW, Simard EP, Finelli L, Fiore AE, Bell BP. Hepatitis B Virus Infection: Epidemiology and Vaccination. *Epidemiol Rev* (2006) 28:112–25. doi: 10.1093/epirev/mxj009
3. Zanetti AR, Van Damme P, Shouval D. The Global Impact of Vaccination Against Hepatitis B: A Historical Overview. *Vaccine* (2008) 26(49):6266–73. doi: 10.1016/j.vaccine.2008.09.056
4. CDC. *Hepatitis B Questions and Answers for Health Professionals* (2021). Available at: https://www.cdc.gov/hepatitis/hbv/hbvfaq.htm.
5. Cardell K, Akerlind B, Sallberg M, Fryden A. Excellent Response Rate to a Double Dose of the Combined Hepatitis A and B Vaccine in Previous Nonresponders to Hepatitis B Vaccine. *J Infect Dis* (2008) 198(3):299–304. doi: 10.1086/589722
6. Zuckerman JN. Protective Efficacy, Immunotherapeutic Potential, and Safety of Hepatitis B Vaccines. *J Med Virol* (2006) 78(2):169–77. doi: 10.1002/jmv.20524
7. Filippelli M, Lionetti E, Gennaro A, Lanzafame A, Arrigo T, Salpietro C, et al. Hepatitis B Vaccine by Intradermal Route in Non Responder Patients: An Update. *World J Gastroenterol* (2014) 20(30):10383–94. doi: 10.3748/wjg.v20.i30.10383
8. Ponde RAA. Expression and Detection of Anti-HBs Antibodies After Hepatitis B Virus Infection or Vaccination in the Context of Protective Immunity. *Arch Virol* (2019) 164(11):2645–58. doi: 10.1007/s00705-019-04369-9
9. Rendi-Wagner P, Shouval D, Genton B, Lurie Y, Rumke H, Boland G, et al. Comparative Immunogenicity of a PreS/S Hepatitis B Vaccine in Non- and Low Responders to Conventional Vaccine. *Vaccine* (2006) 24(15):2781–9. doi: 10.1016/j.vaccine.2006.01.007
10. Jarrosson L, Kolopp-Sarda MN, Aguilar P, Bene MC, Lepori ML, Vignaud MC, et al. Most Humoral non-Responders to Hepatitis B Vaccines Develop HBV-Specific Cellular Immune Responses. *Vaccine* (2004) 22(27-28):3789–96. doi: 10.1016/j.vaccine.2004.02.046
11. Gunson RN, Shouval D, Roggendorf M, Zaaijer H, Nicholas H, Holzmann H, et al. Hepatitis B Virus (HBV) and Hepatitis C Virus (HCV) Infections in Health Care Workers (HCWs): Guidelines for Prevention of Transmission of HBV and HCV From HCW to Patients. *J Clin Virol* (2003) 27(3):213–30. doi: 10.1016/s1386-6532(03)00087-8
12. Hohler T, Reuss E, Freitag CM, Schneider PM. A Functional Polymorphism in the IL-10 Promoter Influences the Response After Vaccination With HBsAg and Hepatitis A. *Hepatology* (2005) 42(1):72–6. doi: 10.1002/hep.20740
13. Van der Wielen M, Van Damme P, Chlibek R, Smetana J, von Sonnenburg F. Hepatitis a/B Vaccination of Adults Over 40 Years Old: Comparison of Three Vaccine Regimens and Effect of Influencing Factors. *Vaccine* (2006) 24(26):5509–15. doi: 10.1016/j.vaccine.2006.04.016
14. Hohler T, Reuss E, Evers N, Dietrich E, Rittner C, Freitag CM, et al. Differential Genetic Determination of Immune Responsiveness to Hepatitis B Surface Antigen and to Hepatitis A Virus: A Vaccination Study in Twins. *Lancet* (2002) 360(9338):991–5. doi: 10.1016/S0140-6736(02)11083-X
15. Kubba AK, Taylor P, Graneek B, Strobel S. Non-Responders to Hepatitis B Vaccination: A Review. *Commun Dis Public Health* (2003) 6(2):106–12.
16. Liu F, Guo Z, Dong C. Influences of Obesity on the Immunogenicity of Hepatitis B Vaccine. *Hum Vaccin Immunother* (2017) 13(5):1014–7. doi: 10.1080/21645515.2016.1274475
17. Yang S, Tian G, Cui Y, Ding C, Deng M, Yu C, et al. Factors Influencing Immunologic Response to Hepatitis B Vaccine in Adults. *Sci Rep* (2016) 6:27251. doi: 10.1038/srep27251
18. Young KM, Gray CM, Bekker LG. Is Obesity a Risk Factor for Vaccine Non-Responsiveness? *PloS One* (2013) 8(12):e82779. doi: 10.1371/journal.pone.0082779
19. Bocher WO, Herzog-Hauff S, Herr W, Heermann K, Gerken G, Meyer Zum Buschenfelde KH, et al. Regulation of the Neutralizing Anti-Hepatitis B Surface (HBs) Antibody Response *In Vitro* in HBs Vaccine Recipients and Patients With Acute or Chronic Hepatitis B Virus (HBV) Infection. *Clin Exp Immunol* (1996) 105(1):52–8. doi: 10.1046/j.1365-2249.1996.d01-732.x
20. Salazar M, Deulofeut H, Granja C, Deulofeut R, Yunis DE, Marcus-Bagley D, et al. Normal HBsAg Presentation and T-Cell Defect in the Immune Response of Nonresponders. *Immunogenetics* (1995) 41(6):366–74. doi: 10.1007/BF00163994
21. Avanzini MA, Belloni C, Soncini R, Ciardelli L, de Silvestri A, Pistorio A, et al. Increment of Recombinant Hepatitis B Surface Antigen-Specific T-Cell Precursors After Revaccination of Slow Responder Children. *Vaccine* (2001) 19(20-22):2819–24. doi: 10.1016/s0264-410x(01)00007-x
22. Chedid MG, Deulofeut H, Yunis DE, Lara-Marquez ML, Salazar M, Deulofeut R, et al. Defect in Th1-Like Cells of Nonresponders to Hepatitis B Vaccine. *Hum Immunol* (1997) 58(1):42–51. doi: 10.1016/s0198-8859(97)00209-7
23. Jafarzadeh A, Shokri F. The Antibody Response to HBs Antigen is Regulated by Coordinated Th1 and Th2 Cytokine Production in Healthy Neonates. *Clin Exp Immunol* (2003) 131(3):451–6. doi: 10.1046/j.1365-2249.2003.02093.x
24. Kardar GA, Jeddi-Tehrani M, Shokri F. Diminished Th1 and Th2 Cytokine Production in Healthy Adult Nonresponders to Recombinant Hepatitis B Vaccine. *Scand J Immunol* (2002) 55(3):311–4. doi: 10.1046/j.1365-3083.2002.01057.x

25. Chekol Abebe E, Asmamaw Dejenie T, Mengie Ayele T, Dagnew Baye N, Agegnehu Teshome A, Tilahun Muche Z. The Role of Regulatory B Cells in Health and Diseases: A Systemic Review. *J Inflamm Res* (2021) 14:75–84. doi: 10.2147/JIR.S286426
26. Sanaei MJ, Nahid-Samiei M, Abadi MSS, Arjmand MH, Ferns GA, Bashash D, et al. New Insights Into Regulatory B Cells Biology in Viral, Bacterial, and Parasitic Infections. *Infect Genet Evol* (2021) 89:104753. doi: 10.1016/j.meegid.2021.104753
27. Barsotti NS, Almeida RR, Costa PR, Barros MT, Kalil J, Kokron CM. IL-10-Producing Regulatory B Cells Are Decreased in Patients With Common Variable Immunodeficiency. *PloS One* (2016) 11(3):e0151761. doi: 10.1371/journal.pone.0151761
28. Esteve-Sole A, Teixido I, Deya-Martinez A, Yague J, Plaza-Martin AM, Juan M, et al. Characterization of the Highly Prevalent Regulatory CD24hiCD38hi B-Cell Population in Human Cord Blood. *Front Immunol* (2017) 8:201. doi: 10.3389/fimmu.2017.00201
29. Jansen K, Cevhertas L, Ma S, Satitsuksanoa P, Akdis M, van de Veen W. Regulatory B cells, A to Z. *Allergy* (2021) 76(9):2699–715. doi: 10.1111/all.14763
30. Rosser EC, Mauri C. Regulatory B Cells: Origin, Phenotype, and Function. *Immunity* (2015) 42(4):607–12. doi: 10.1016/j.immuni.2015.04.005
31. Ticha O, Moos L, Wajant H, Bekeredjian-Ding I. Expression of Tumor Necrosis Factor Receptor 2 Characterizes TLR9-Driven Formation of Interleukin-10-Producing B Cells. *Front Immunol* (2017) 8:1951. doi: 10.3389/fimmu.2017.01951
32. Wasik M, Nazimek K, Bryniarski K. Regulatory B Cell Phenotype and Mechanism of Action: The Impact of Stimulating Conditions. *Microbiol Immunol* (2018) 62(8):485–96. doi: 10.1111/1348-0421.12636
33. Iwata Y, Matsushita T, Horikawa M, Dilillo DJ, Yanaba K, Venturi GM, et al. Characterization of a Rare IL-10-Competent B-Cell Subset in Humans That Parallels Mouse Regulatory B10 Cells. *Blood* (2011) 117(2):530–41. doi: 10.1182/blood-2010-07-294249
34. Yang M, Du C, Wang Y, Liu J. Increased CD19+CD24+CD27+ B Regulatory Cells are Associated With Insulin Resistance in Patients With Type I Hashimoto's Thyroiditis. *Mol Med Rep* (2017) 15(6):4338–45. doi: 10.3892/mmr.2017.6507
35. Yang M, Rui K, Wang S, Lu L. Regulatory B Cells in Autoimmune Diseases. *Cell Mol Immunol* (2013) 10(2):122–32. doi: 10.1038/cmi.2012.60
36. Das A, Ellis G, Pallant C, Lopes AR, Khanna P, Peppa D, et al. IL-10-Producing Regulatory B Cells in the Pathogenesis of Chronic Hepatitis B Virus Infection. *J Immunol* (2012) 189(8):3925–35. doi: 10.4049/jimmunol.1103139
37. Rosser EC, Blair PA, Mauri C. Cellular Targets of Regulatory B Cell-Mediated Suppression. *Mol Immunol* (2014) 62(2):296–304. doi: 10.1016/j.molimm.2014.01.014
38. Bolther M, Andersen KLD, Tolstrup M, Visvanathan K, Woolley I, Skinner N, et al. Levels of Regulatory B Cells Do Not Predict Serological Responses to Hepatitis B Vaccine. *Hum Vaccin Immunother* (2018) 14(6):1–6. doi: 10.1080/21645515.2018.1441653
39. Garner-Spitzer E, Wagner A, Paulke-Korinek M, Kollaritsch H, Heinz FX, Redlberger-Fritz M, et al. Tick-Borne Encephalitis (TBE) and Hepatitis B Nonresponders Feature Different Immunologic Mechanisms in Response to TBE and Influenza Vaccination With Involvement of Regulatory T and B Cells and IL-10. *J Immunol* (2013) 191(5):2426–36. doi: 10.4049/jimmunol.1300293
40. Körber N, Behrends U, Hapfelmeier A, Protzer U, Bauer T. Validation of an IFNgamma/IL2 FluoroSpot Assay for Clinical Trial Monitoring. *J Transl Med* (2016) 14(1):175. doi: 10.1186/s12967-016-0932-7
41. Cohen J. *Statistical Power Analysis for the Behavioral Sciences. 2nd ed* Vol. 567. Hillsdale, NJ: Erlbaum (1988).
42. Harder T, Remschmidt C, Falkenhorst G, Zimmermann R, Hengel H, Ledig T, et al. Background Paper to the Revised Recommendation for Hepatitis B Vaccination of Persons at Particular Risk and for Hepatitis B Postexposure Prophylaxis in Germany. *Bundesgesundheitsblatt Gesundheitsforschung Gesundheitsschutz* (2013) 56(11):1565–76. doi: 10.1007/s00103-013-1845-8
43. McDermott AB, Cohen SB, Zuckerman JN, Madrigal JA. Human Leukocyte Antigens Influence the Immune Response to a Pre-s/S Hepatitis B Vaccine. *Vaccine* (1999) 17(4):330–9. doi: 10.1016/s0264-410x(98)00203-5
44. van de Veen W, Stanic B, Yaman G, Wawrzyniak M, Sollner S, Akdis DG, et al. IgG4 Production Is Confined to Human IL-10-Producing Regulatory B Cells That Suppress Antigen-Specific Immune Responses. *J Allergy Clin Immunol* (2013) 131(4):1204–12. doi: 10.1016/j.jaci.2013.01.014
45. Heine G, Drozdenko G, Grun JR, Chang HD, Radbruch A, Worm M. Autocrine IL-10 Promotes Human B-Cell Differentiation Into IgM- or IgG-Secreting Plasmablasts. *Eur J Immunol* (2014) 44(6):1615–21. doi: 10.1002/eji.201343822
46. Dang VD, Hilgenberg E, Ries S, Shen P, Fillatreau S. From the Regulatory Functions of B Cells to the Identification of Cytokine-Producing Plasma Cell Subsets. *Curr Opin Immunol* (2014) 28:77–83. doi: 10.1016/j.coi.2014.02.009
47. Shapira MY, Zeira E, Adler R, Shouval D. Rapid Seroprotection Against Hepatitis B Following the First Dose of a Pre-S1/Pre-S2/S Vaccine. *J Hepatol* (2001) 34(1):123–7. doi: 10.1016/s0168-8278(00)00082-9
48. Shouval D, Roggendorf H, Roggendorf M. Enhanced Immune Response to Hepatitis B Vaccination Through Immunization With a Pre-S1/Pre-S2/S Vaccine. *Med Microbiol Immunol* (2015) 204(1):57–68. doi: 10.1007/s00430-014-0374-x
49. Krawczyk A, Ludwig C, Jochum C, Fiedler M, Heinemann FM, Shouval D, et al. Induction of a Robust T- and B-Cell Immune Response in Non- and Low-Responders to Conventional Vaccination Against Hepatitis B by Using a Third Generation PreS/S Vaccine. *Vaccine* (2014) 32(39):5077–82. doi: 10.1016/j.vaccine.2014.06.076
50. Elhanan E, Boaz M, Schwartz I, Schwartz D, Chernin G, Soetendorp H, et al. A Randomized, Controlled Clinical Trial to Evaluate the Immunogenicity of a PreS/S Hepatitis B Vaccine Sci-B-Vac, as Compared to Engerix B((R)), Among Vaccine Naive and Vaccine Non-Responder Dialysis Patients. *Clin Exp Nephrol* (2018) 22(1):151–8. doi: 10.1007/s10157-017-1416-7
51. Coursaget P, Bringer L, Sarr G, Bourdil C, Fritzell B, Blondeau C, et al. Comparative Immunogenicity in Children of Mammalian Cell-Derived Recombinant Hepatitis B Vaccine and Plasma-Derived Hepatitis B Vaccine. *Vaccine* (1992) 10(6):379–82. doi: 10.1016/0264-410x(92)90067-t
52. McDermott AB, Zuckerman JN, Sabin CA, Marsh SG, Madrigal JA. Contribution of Human Leukocyte Antigens to the Antibody Response to Hepatitis B Vaccination. *Tissue Antigens* (1997) 50(1):8–14. doi: 10.1111/j.1399-0039.1997.tb02827.x
53. Zuckerman JN, Zuckerman AJ, Symington I, Du W, Williams A, Dickson B, et al. Evaluation of a New Hepatitis B Triple-Antigen Vaccine in Inadequate Responders to Current Vaccines. *Hepatology* (2001) 34(4 Pt 1):798–802. doi: 10.1053/jhep.2001.27564
54. Valats JC, Tuaillon E, Funakoshi N, Hoa D, Brabet MC, Bollore K, et al. Investigation of Memory B Cell Responses to Hepatitis B Surface Antigen in Health Care Workers Considered as non-Responders to Vaccination. *Vaccine* (2010) 28(39):6411–6. doi: 10.1016/j.vaccine.2010.07.058
55. Rahman F, Dahmen A, Herzog-Hauff S, Bocher WO, Galle PR, Lohr HF. Cellular and Humoral Immune Responses Induced by Intradermal or Intramuscular Vaccination With the Major Hepatitis B Surface Antigen. *Hepatology* (2000) 31(2):521–7. doi: 10.1002/hep.510310237
56. Chisari FV, Isogawa M, Wieland SF. Pathogenesis of Hepatitis B Virus Infection. *Pathol Biol (Paris)* (2010) 58(4):258–66. doi: 10.1016/j.patbio.2009.11.001
57. Mosmann TR, Coffman RL. TH1 and TH2 Cells: Different Patterns of Lymphokine Secretion Lead to Different Functional Properties. *Annu Rev Immunol* (1989) 7:145–73. doi: 10.1146/annurev.iy.07.040189.001045
58. Mosmann TR, Sad S. The Expanding Universe of T-Cell Subsets: Th1, Th2 and More. *Immunol Today* (1996) 17(3):138–46. doi: 10.1016/0167-5699(96)80606-2
59. Larsen CE, Xu J, Lee S, Dubey DP, Uko G, Yunis EJ, et al. Complex Cytokine Responses to Hepatitis B Surface Antigen and Tetanus Toxoid in Responders, Nonresponders and Subjects Naive to Hepatitis B Surface Antigen. *Vaccine* (2000) 18(26):3021–30. doi: 10.1016/s0264-410x(00)00084-0
60. Shokrgozar MA, Shokri F. Enumeration of Hepatitis B Surface Antigen-Specific B Lymphocytes in Responder and Non-Responder Normal Individuals Vaccinated With Recombinant Hepatitis B Surface Antigen. *Immunology* (2001) 104(1):75–9. doi: 10.1046/j.1365-2567.2001.01273.x
61. Goncalves L, Albarran B, Salmen S, Borges L, Fields H, Montes H, et al. The Nonresponse to Hepatitis B Vaccination Is Associated With Impaired Lymphocyte Activation. *Virology* (2004) 326(1):20–8. doi: 10.1016/j.virol.2004.04.042

62. Nystrom J, Cardell K, Bjornsdottir TB, Fryden A, Hultgren C, Sallberg M. Improved Cell Mediated Immune Responses After Successful Re-Vaccination of Non-Responders to the Hepatitis B Virus Surface Antigen (HBsAg) Vaccine Using the Combined Hepatitis A and B Vaccine. *Vaccine* (2008) 26 (47):5967–72. doi: 10.1016/j.vaccine.2008.08.054

Conflict of Interest: UP received funding for the project from the Helmholtz Association in context of the iMed initiative and the Helmholtz-Alberta-Initiative in Infectious Disease Research. UP serves as scientific advisor for Gilead, Leukocare, Abbvie, MSD, Arbutus, GSK, Vaccitech, Biontech, and Dicerna.

The remaining authors declare that the research was conducted in the absence of any commercial or financial relationships that could be construed as a potential conflict of interest.

frontiers in Immunology

ORIGINAL RESEARCH
published: 13 September 2021
doi: 10.3389/fimmu.2021.648420

Functional Exhaustion of HBV-Specific CD8 T Cells Impedes PD-L1 Blockade Efficacy in Chronic HBV Infection

Sara Ferrando-Martinez[1†], Angie Snell Bennett[1], Elisabete Lino[1], Adam J. Gehring[2,3], Jordan Feld[2], Harry L. A. Janssen[2] and Scott H. Robbins[4]*

[1] Microbial Sciences, Biopharmaceuticals R&D, AstraZeneca, Gaithersburg, MD, United States, [2] Toronto Center for Liver Disease, Toronto General Hospital, University Health Network, Toronto, ON, Canada, [3] Department of Immunology, University of Toronto, Toronto, ON, Canada, [4] Late Stage Oncology Development, Oncology R&D, AstraZeneca, Gaithersburg, MD, United States

OPEN ACCESS

Edited by:
Anna D. Kosinska, Helmholtz-Gemeinschaft Deutscher Forschungszentren (HZ), Germany

Reviewed by:
Bertram Bengsch, University of Freiburg Medical Center, Germany
Anna Schurich, King's College London, United Kingdom

***Correspondence:**
Sara Ferrando-Martinez
sfm@neoimmunetech.com

†Present address:
Sara Ferrando-Martinez, Translational Research Division NeoImmunetech, LLC, Rockville, MD, United States

Specialty section:
This article was submitted to Viral Immunology, a section of the journal Frontiers in Immunology

Received: *31 December 2020*
Accepted: *24 August 2021*
Published: *13 September 2021*

Citation:
Ferrando-Martinez S, Snell Bennett A, Lino E, Gehring AJ, Feld J, Janssen HLA and Robbins SH (2021) Functional Exhaustion of HBV-Specific CD8 T Cells Impedes PD-L1 Blockade Efficacy in Chronic HBV Infection. Front. Immunol. 12:648420. doi: 10.3389/fimmu.2021.648420

Background: A functional cure for chronic HBV could be achieved by boosting HBV-specific immunity. *In vitro* studies show that immunotherapy could be an effective strategy. However, these studies include strategies to enrich HBV-specific CD8 T cells, which could alter the expression of the anti-PD-1/anti-PD-L1 antibody targets. Our aim was to determine the efficacy of PD-L1 blockade *ex vivo*.

Methods: HBV-specific CD8 T cells were characterized *ex vivo* by flow cytometry for the simultaneous analysis of six immune populations and 14 activating and inhibitory receptors. *Ex vivo* functionality was quantified by ELISpot and by combining peptide pool stimulation, dextramers and intracellular flow cytometry staining.

Results: The functionality of HBV-specific CD8 T cells is associated with a higher frequency of cells with low exhaustion phenotype ($LAG3^-TIM3^-PD\text{-}1^+$), independently of the clinical parameters. The accumulation of HBV-specific CD8 T cells with a functionally exhausted phenotype ($LAG3^+TIM3^+PD\text{-}1^+$) is associated with lack of *ex vivo* functionality. PD-L1 blockade enhanced the HBV-specific CD8 T cell response only in patients with lower exhaustion levels, while response to PD-L1 blockade was abrogated in patients with higher frequencies of exhausted HBV-specific CD8 T cells.

Conclusion: Higher levels of functionally exhausted HBV-specific CD8 T cells are associated with a lack of response that cannot be restored by blocking the PD-1:PD-L1 axis. This suggests that the clinical effectiveness of blocking the PD-1:PD-L1 axis as a monotherapy may be restricted. Combination strategies, potentially including the combination of anti-LAG-3 with other anti-iR antibodies, will likely be required to elicit a functional cure for patients with high levels of functionally exhausted HBV-specific CD8 T cells.

Keywords: chronic HBV infection, PD-L1 blockade, LAG3, exhaustion, HBV cure

INTRODUCTION

Public health awareness for chronic hepatitis B (HBV) infection have progressively increased in the last decade. Despite a preventive vaccine being available, coverage is still under 40% and prevention strategies are insufficiently implemented (1). More than 257 million people, a striking 3.5% of the worldwide population, are living with chronic HBV infection. Persistent viral replication and continuous liver necroinflammation eventually leads to cirrhosis, end-stage liver disease, hepatic decompensation and hepatocellular carcinoma (HCC) (2, 3) which, annually, results in more than 850,000 deaths (1). Current antiviral therapies (PEGylated-IFNα and nucleos(t)ide reverse transcriptase inhibitors – NRTI), while they provide long-term benefits by suppressing HBV viremia and reducing hepatic necroinflammation, they do not eliminate the cumulative risk of developing HCC (4–6). Therefore, while mortality caused by other widespread chronic infectious diseases – like tuberculosis or HIV – has declined over time, HBV-related mortality has increased by 22% in the last decade, highlighting the need to find new therapeutic strategies able to elicit a functional cure for chronic HBV infection.

A functional cure, defined as persistently undetectable levels of HBsAg in the absence of antiviral therapy (AVT) (7), implies the complete suppression of intrahepatic HBV replication even at the subclinical level. This level of viral control is observed during self-resolving acute HBV infection, suggesting that enhancement of HBV-specific immune responses through immunotherapy strategies could be a successful approach. Self-resolving HBV infection relies on an effective CD4 T cell, CD8 T cell and B cell response that will result in non-cytolytic HBV clearance. The critical antiviral role of cytotoxic CD8 T cells during this process has been demonstrated in the chimpanzee model (8) and it's associated with vigorous, broad and polyclonal T cell responses (8–10). *In vitro* studies have shown that HBV-specific T cell-related production of IFNγ and TNF can effectively suppress viral replication (11). Critically, the immune system of liver transplant immune recipients is able to clear HBV infection (12, 13), proving that chronic HBV can be cured by a strong, broad and effective immune response.

In chronically infected patients a sufficient boost of HBV-specific immunity through immunotherapy can be challenging, due to both extremely low levels of HBV-specific T cells and weak T cell responses that are associated with immune exhaustion, immune dysregulation and inhibitory pathways of immune suppression [reviewed in (14)]. However, even with high exhaustion and low functionality there is an ongoing immune control during chronic HBV infection. This is highlighted by the fact that liver T cell infiltrates correlate with better viral control and less liver inflammation (15) and viral replication increases with immunosuppressive treatment (16). Thus, immunotherapies to boost both immune responses for chronic HBV infection hold promise and are being actively researched. It is worth noting that even if immunotherapy is now used in routine clinical practice and has even become the standard of care for some cancer indications [reviewed in (17)], the use of checkpoint inhibitors in the context of chronic viral infections is still controversial and in pre-clinical development stages [reviewed in (18)]. For HBV infection, most clinical data is in the context of HBV-induced HCC cancer treatment (19). Strong pre-clinical data clearly outlining whether the benefit of checkpoint blockade in chronic HBV-infected patients would outweigh the risk associated with this type of therapy is needed to encourage clinical trials aiming to a functional cure.

While immunotherapy strategies are intended to boost intrahepatic immunity, PBMCs are the most widely used proxy to study *in vitro* HBV-specific reactivity and efficacy of immunotherapies. In this approach, the scarcity of HBV-specific T cells within the PBMC compartment adds an additional challenge. To overcome this limitation, in our previous work (20) we developed a 5-day expansion protocol to increase sensitivity and we showed that PD-L1 blockade enhanced HBV-specific T cell reactivity. This approach, using expansion protocols to enrich on HBV-specific CD8 T cells prior to characterize their functionality, has been reported elsewhere (21, 22). Notwithstanding the relevance of this proof-of-concept, *in vitro* expansion and manipulation of the target cells can modify the expression of PD-1, PD-L1 and/or other activating (aR) or inhibitory (iR) receptors, affecting the *in vivo* translatability of the results. Thus, the aim of this study was to determine the efficacy of PD-L1 blockade *ex vivo* to increase the functionality of HBV-specific CD8 T cell responses.

RESULTS

HBV-Specific CD8 T Cell Response Types Evolve With Clinical Progression

To overcome the scarcity of HBV-specific CD8 T cells, in previous studies we (20), and others (21, 22), have used strategies focused on the expansion of HBV-specific T cells prior to PD-L1 blockade assessment. However, to avoid the modification of the expression patterns of the different inhibitory (iR) and activating (aR) receptors associated with expansion protocols, for this study we have optimized an *ex vivo* ELISpot strategy (**Figure 1A**). HBV-specific reactivity was analyzed using two different HBV peptide pools (HBVsp; Core and Pool). Reactivity to prevalent herpes infections (HERsp; CMV and EBV) was included for every sample as an example of chronic viral infections with effective immune control. Negative (Actin) and positive (CEFX) peptide pool controls were included for each sample. *Ex vivo* HBV-specific reactivity was detected in 36% and 33.7% of patients for Core and Pool, respectively (**Figure 1B**), with a combined HBV-specific response of 51.7% [HBVsp (+); 46/89; Core and/or Pool]. HERPES-specific reactivity [HERsp (+); 56/89; CMV and/or EBV] was detected at a slightly higher frequency (62.9%) but consistent with the prevalence of these infections on the general population in North America (23, 24). In addition, HBV-reactive samples showed a significantly lower magnitude of the response than HERPES-reactive samples (**Figure 1C**).

We then sought to analyze whether HBV-specific reactivity was associated with clinical parameters. Patients were

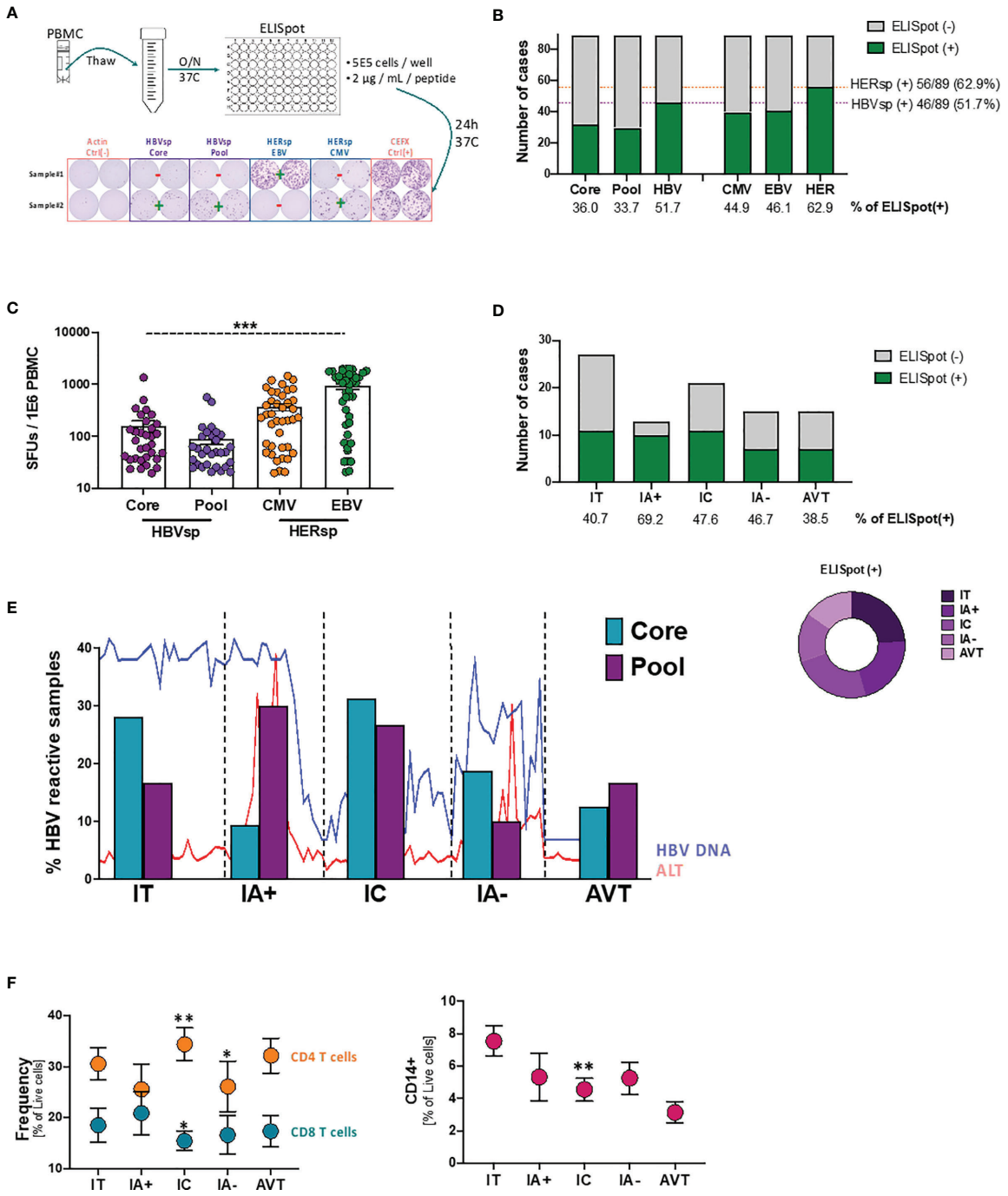

FIGURE 1 | *Ex vivo* HBV-specific response evolves with clinical progression. **(A)** Schematic representation of the *ex vivo* ELISpot workflow with representative example of the response levels. **(B)** Number of samples with *ex vivo* ELISpot reactivity. HBV number of cases shows CORE and/or POOL while HER (HERPES) number of cases shows EBV and/or CMV. **(C)** Magnitude of the Ag-specific response, as measured as spot-forming units (SFUs) per million PBMCs, among the different stimulations. ***$p < 0.0001$; Kruskal-Wallis one-way analysis of variance. **(D)** Number of samples with *ex vivo* HBV-specific (core and/or pool) reactivity among the different clinical groups. **(E)** Evolution of the individual HBV-specific stimulations (CORE and POOL) with clinical progression. Lines show the variability of HBV DNA and ALT levels within each group. **(F)** Frequency of T cells (left panel) and CD14+ monocytes (right panel) among the different clinical groups. *$p < 0.05$; **$p < 0.01$; Mann Whitney U test. IT, Immune Tolerant; IA+, HBeAg+ Immune Active; IC, Immune Control; IA-, HBeAg- Immune Active; AVT, Anti-Viral Therapy.

categorized in 5 different groups according to HBeAg serology and ALT levels (25). According to this clinical definition Immune Tolerant (IT) is defined as HBeAg positive and ALT ≤ 1.3X upper limit normal (ULN); HBeAg+ Immune Active Hepatitis (IA+) as HBeAg positive and ALT > 1.3X ULN; *Immune control* (IC) as HBeAg negative and ALT ≤ 1.3X ULN and HBeAg- Immune Active hepatitis (IA-) as HBeAg negative and ALT > 1.3X ULN. All patients under antiviral therapy where included in the AVT group. *Ex vivo* HBV-specific reactivity was distributed among all clinical groups (**Figure 1D**) and independently of HBeAg, HBsAg, ALT or HBV DNA levels (**Supplementary Figure 1**). Interestingly, the proportion of the two different HBV stimuli changed with clinical evolution (**Figure 1E**). Our results show that during the IT phase, where the adaptive immune response is not strong, reactivity towards the more conserved proteins of the core and capsid were more frequently detected. HBV reactivity for patients with HBeAg+ hepatitis (IA+), a clinical status normally associated with a strong adaptive immune response that will lead to the negativization of the HBeAg, favored a broader and more polyclonal T cell response. This broad response is associated with the partial control of the HBV viral replication during the **IC** phase while the failure to maintain a diverse T cell response could be responsible of the viral escape observed during HBeAg-hepatitis (IA-). Patients under AVT, despite being a more heterogeneous group, consistently had a more constrained frequency similar to the reactivity observed during the IA-phase. In line with these results, peripheral CD8 T cells were increased in IA+ samples but significantly decreased in IC phase while inflammation [as measured as frequency of CD14+ monocytes (26)] consistently declines (**Figure 1F**). However, after viral escape, IA- samples fail to increase CD8 T cells or inflammation again. Altogether, these results strongly suggest that exhaustion of the HBV-specific CD8 T cell population plays an active role on the clinical progression of chronic HBV infection.

General T Cell Exhaustion Is Not Detected in Chronic HBV Infection

To determine whether exhaustion had a main role in viral escape from CD8 T cell control, we quantified the expression of six different populations and 14 different iR and aR (full list of markers is shown in **Supplementary Table 2**). Representative examples of the gating strategy are shown in **Figure 2A** and **Supplementary Figure 2A**. Our data showed that neither the frequency of the different immune populations (CD11c DC, CD14 Monocytes, CD56 NK, CD20 B cells, CD4 T cells and CD8 T cells) nor iR and aR expression levels on bulk CD8 T cells was different between samples with or without *ex vivo* HBV-specific or HERPES-specific reactivity (data not shown). We then analyze expression patterns of six iR/aR strongly related with chronic HBV infection and PD-1/PD-L1 blockade immunotherapy (**Figure 2A**). Results showed that expression patterns of these selected markers were similar among samples with or without *ex vivo* HBV-specific or HERPES-specific reactivity (**Figure 2B**) and did not change with clinical progression (**Supplementary Figure 2B**). To confirm that exhaustion of bulk CD8 T cells was not associated with reactivity we quantified the frequency of CD8 T cells expressing a Low exhaustion (LAG3-TIM3-PD-1+), Intermediate exhaustion (LAG3-TIM3+PD-1+) or High exhaustion (LAG3+TIM3+PD-1+) phenotype, but no differences were observed between reactive or not reactive samples (**Figure 2C**). However, while the level of Low exhaustion remained unchanged among the different clinical groups (**Figure 2D**, left panel) we observed a significant decrease of CD8 T cells with Intermediate exhaustion phenotype (**Figure 2D**, middle panel) and a concomitant increase of Highly exhausted CD8 T cells (**Figure 2D**, right panel) associated with clinical progression. Any other immune population analyzed did not show changes associated with reactivity or clinical progression (data not shown), except for a significant increase of FAS-expressing CD11c DC during IA- phase (**Supplementary Figure 2C**). Increased sensitivity to cell death of antigen presenting cells like DC has been associated with failure to control chronic viral infections (27) and in this study was significantly associated with a lower frequency of peripheral CD8 T cells (**Supplementary Figure 2D**). This data suggests that even if exhaustion is related to longer times of infection and clinical progression and could be associated with the loss of HBV-specific reactivity leading to viral escape, antigen-specific CD8 T cells must be gathering most defects.

HBV-Specific CD8 T Cells Express a Higher Frequency of Exhaustion Markers

Dextramer positivity was tested for any sample with the alleles HLA-A*0201; B*3501 and B*5101 (n = 48). MHC I Dextramers® (Immundex) specific for HBV capsid, three different epitopes of HBV Protein S, CMV and EBV were used to detect Ag specific T cells. A gating example for Ag-specific CD8 T cells is shown in **Supplementary Figure 3A**. Fourteen individual patients had detectable HBV-specific CD8 T cells using this method. The positive samples were distributed equally among clinical groups (**Supplementary Figure 3B**) and independent of HBsAg levels (**Supplementary Figure 3C**). HBV DNA levels were slightly increased in the samples with detectable HBV-specific CD8 T cells (**Supplementary Figure 3C**). We then quantified the expression of iR and aR in dextramer-positive Ag-specific CD8 T cells (**Figure 3A** and **Supplementary Figure 3A**). Expression patterns of 6 different receptors (**Figure 3B**, 6+ markers PD-1+41BB+TIGIT+PD-L1+TIM3+LAG3+) showed that Ag-specific CD8 T cells, either HERPES-specific or HBV-specific, are significantly more exhausted than paired bulk CD8 T cells. In addition, HERPES-specific CD8 T cells, which are successfully controlling viral replication, are significantly less exhausted than the HBV-specific CD8 T cells (**Figure 3B**). While HERPES-specific CD8 T cells express mostly one or two of these iR at the same time (**Figure 3B**, 2+/1+ makers), most HBV-specific CD8 T cells simultaneously co-express 3 to 6 iR. In addition, the frequency of some receptors (**Supplementary Figure 3D**; CD127, 2B4, TIGIT, PD-L1 and PD-L2) is significantly different between bulk CD8 and Ag-specific CD8 T cells but similar between HERPES- and HBV-specific CD8 T cells.

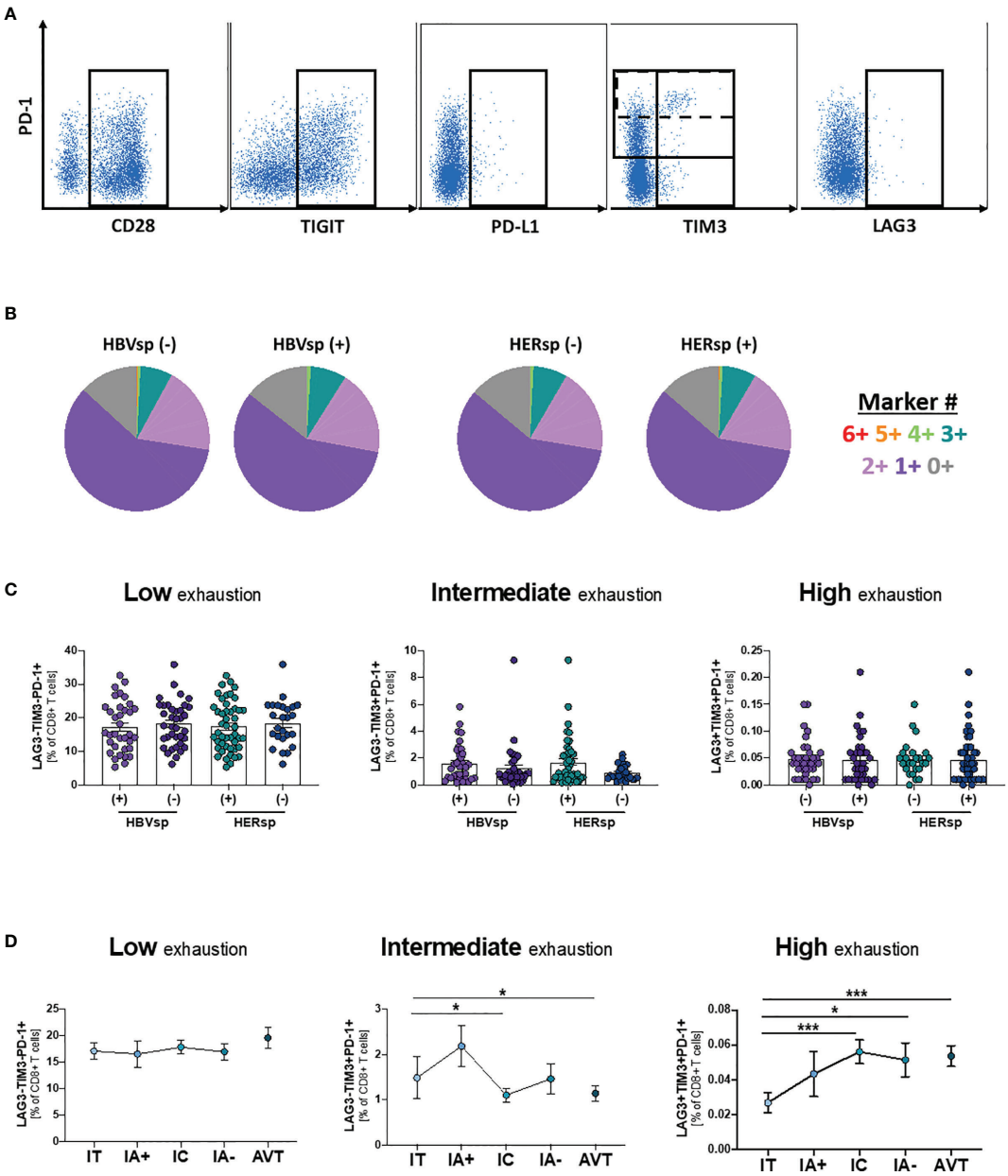

FIGURE 2 | *Ex-vivo* Ag-specific reactivity does not associate with bulk CD8 T cell exhaustion levels. **(A)** Representative flow plots showing expression levels, on bulk CD8 T cells, of inhibitory (iR) and activating (aR) receptors included in the SPICE analysis. **(B)** SPICE analysis showing the distribution of marker co-expression (*6+* markers for CD28+PD-1+TIGIT+PD-L1+TIM3+LAG3+) among patients with either HBV-specific reactivity (core and/or pool, left panel) or HERPES-specific reactivity (CMV and/or EBV, right panel). Frequency of CD8 T cells with phenotype consistent with low exhaustion (LAG3-TIM3-PD-1+, left panel), intermediate exhaustion (LAG3-TIM3+PD-1+, middle panel) or high exhaustion (LAG3+TIM3+PD-1+, right panel) **(C)** among patients with either HBV-specific reactivity (core and/or pool) or HERPES-specific reactivity (CMV and/or EBV) and **(D)** among the different clinical groups. IT, Immune Tolerant; IA+, HBeAg+ Immune Active; IC, Immune Control; IA-, HBeAg- Immune Active; AVT, Anti-Viral Therapy. *p < 0.05; ***p < 0.001.

However, HBV-specific CD8 T cells showed significantly higher expression of markers like 4-1BB, ICOS or PD-1^{hi} (**Figure 3C**).

When we focused on PD-1, TIM3 and LAG3 expression, hallmarks of functional exhaustion, the data showed a significant increase of Low exhaustion and Intermediate exhaustion HERPES-specific CD8 T cells (1+ markers; LAG3-TIM3-PD-1+ and 2+ markers; LAG3-TIM3+PD-1+), phenotypes consistent with an activated and functional response associated to viral control (**Figures 3D–F**). HBV-specific CD8 T cells, on the other hand, showed a significant increase of Intermediate exhaustion and High exhaustion (2+ markers; LAG3-TIM3+PD-1+ and 3+ markers; LAG3+TIM3+PD-1+), a phenotype consistent with

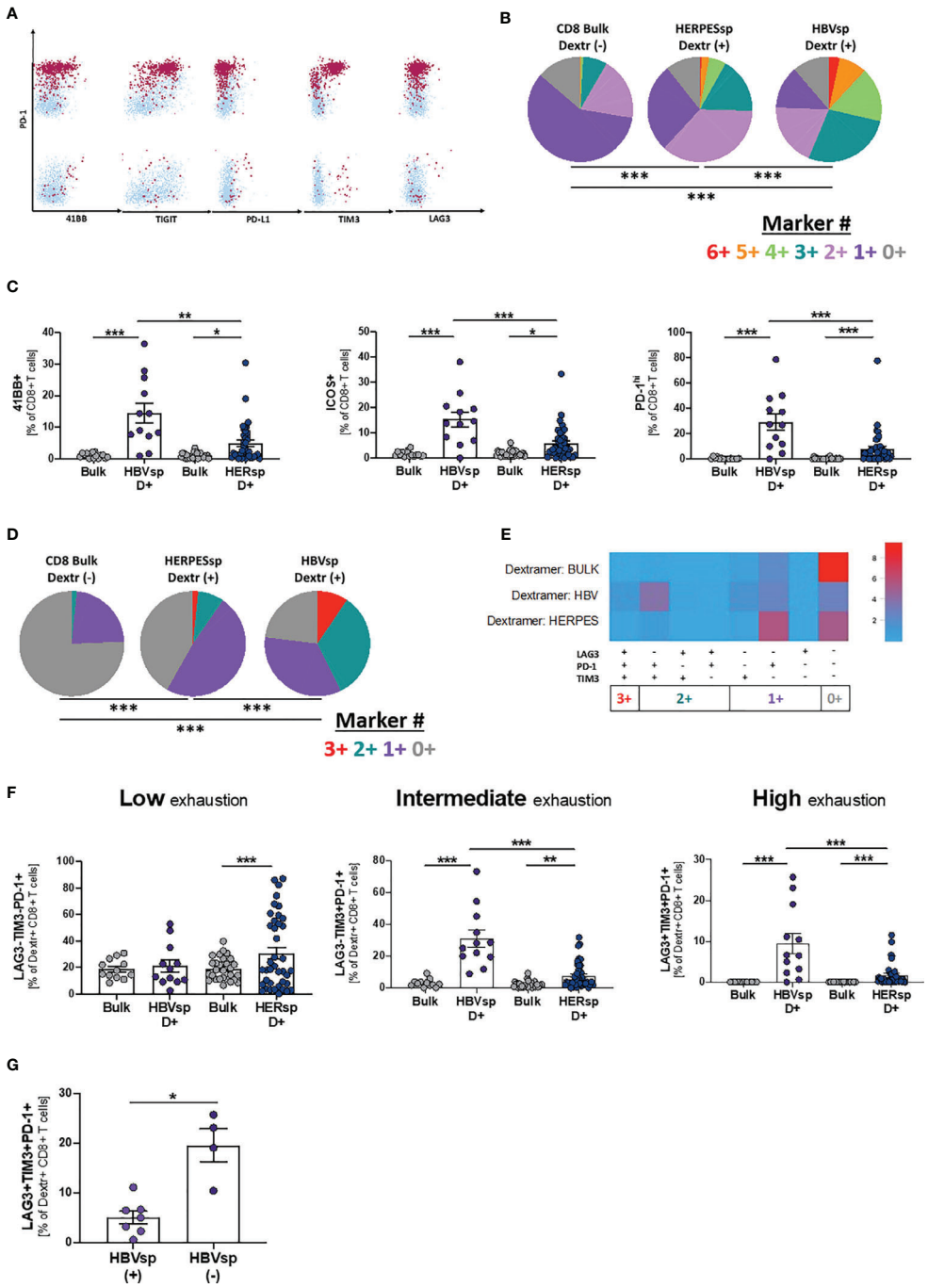

FIGURE 3 | HBV-specific CD8 T cells express high frequency of exhaustion markers. **(A)** Representative flow plots showing expression levels, on HBV-specific CD8 T cells, of inhibitory (iR) and activating (aR) receptors included in the SPICE analysis. Dextramer-positive HBV-specific CD8 T cells (maroon) are overlaid on bulk CD8 T cells (light blue). **(B)** SPICE analysis showing the distribution of inhibitory receptors (*6+* markers for 41BB+PD-1+TIGIT+PD-L1+TIM3+LAG3+) in bulk CD8 T cells (left pie), HERPES-specific CD8 T cells (CMV and/or EBV, *middle pie*) and HBV-specific CD8 T cells (core and/or pool, right pie). ***p < 0.0001; Permutation test. **(C)** Frequency of 41BB (*left panel*), ICOS (*middle panel*) and PD-1hi (right panel) expression in bulk, HBV-specific (core and/or pool) and HERPES-specific (CMV and/or EBV) CD8 T cells. *p < 0.05; **p < 0.001; ***p < 0.0001; Wilcoxon signed rank test (bulk *vs.* Ag-specific) and Mann-Whitney U (HBV-specific *vs.* HERPES-specific). Frequency of bulk, HBV-specific (core and/or pool) and HERPES-specific (CMV and/or EBV) CD8 T cells with phenotype consistent with low exhaustion (LAG3-TIM3-PD-1+, *1+* markers), intermediate exhaustion (LAG3-TIM3+PD-1+, *2+ markers*) or high exhaustion (LAG3+TIM3+PD-1+, *3+* markers) shown as **(D)** SPICE analysis; ***p < 0.0001; Permutation test, **(E)** SPICE CoolPlot and **(F)** pooled data; **p < 0.001; ***p < 0.0001; Wilcoxon signed rank test (bulk *vs.* Ag-specific) and Mann-Whitney U (HBV-specific *vs.* HERPES-specific). **(G)** Frequency of HBV-specific CD8 T cells with a high exhaustion phenotype (LAG3+TIM3+PD-1+) among patients with [HBVsp(+)] or without [HBVsp(-)] *ex vivo* HBV-specific reactivity (core and/or pool). *$p < 0.05$; Mann Whitney U test.

functional exhaustion and lack of viral control (**Figures 3D–F**). Despite the low number of samples, High exhaustion tends to increase with clinical progression (**Supplementary Figure 3E**). In line with these results, patients with *ex vivo* HBV reactivity [HBVsp(+)] have significantly lower amounts of highly exhausted HBV-specific CD8 T cells (**Figure 3G**).

We then sought to determine whether non-reactive, exhausted HBV-specific CD8 T cells retained the ability to proliferate. Samples with different levels of *ex vivo* HBV reactivity were incubated, in the presence of IL-2, with different HBV peptide pools and controls and proliferation levels were quantified on day 10 (**Figure 4A**). Samples with *ex*

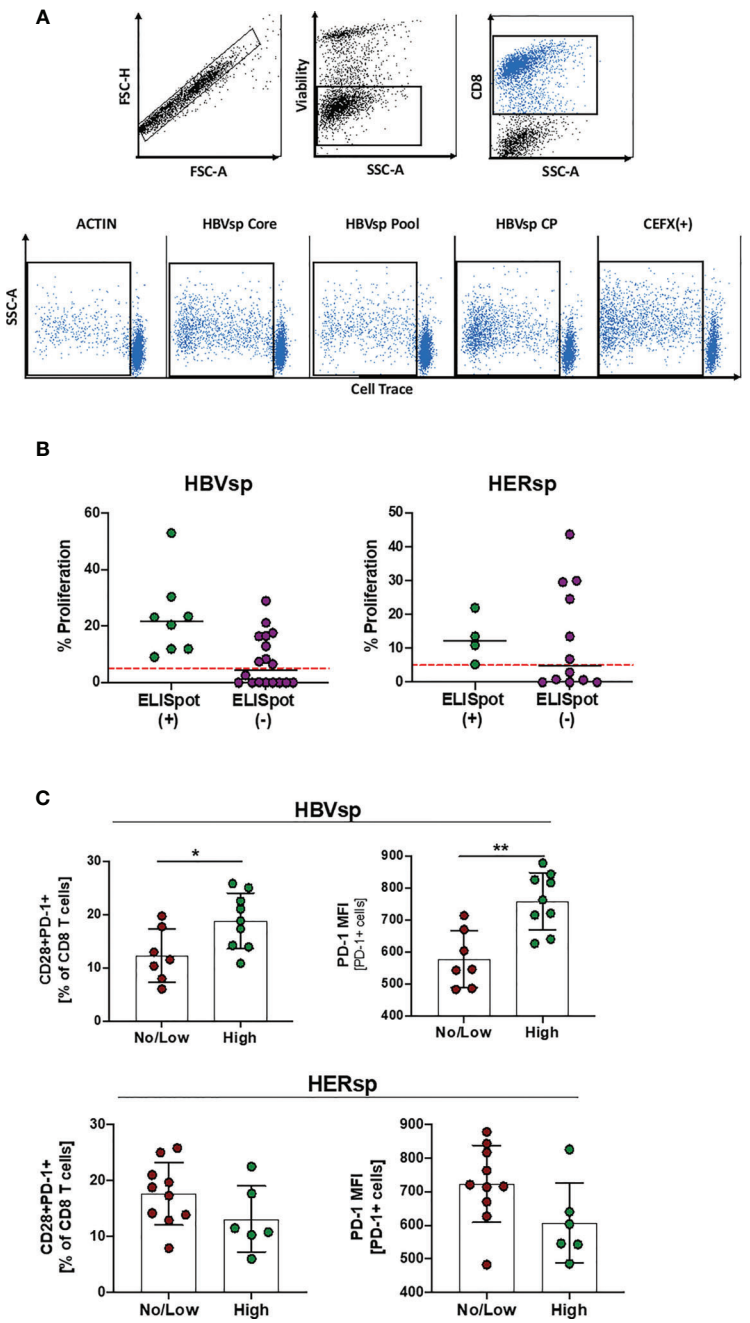

FIGURE 4 | T cell expansion unveils Ag-specific T cells in *ex vivo* not-reactive samples. **(A)** Representative flow plots showing the gating strategy for the cell trace dilution assay. **(B)** Frequency of CD8 proliferating cells among reactive and non-reactive samples for both HBV-specific (core and/or pool) and HERPES-specific (CMV and/or EBV) assays. **(C)** Baseline frequency of CD28+PD-1+ CD8 T cells and the mean fluorescence intensity (MFI) of the PD-1 marker on CD8 T cells among samples with low or high proliferation levels. *p < 0.05; **p < 0.001; Mann Whitney U.

vivo reactivity [ELISpot(+)] showed consistent proliferation for both HBV- and HERPES-specific stimulations (**Figure 4B**). Samples that did not show any *ex vivo* reactivity for the ELISpot assay were only partially recovered by proliferation (**Figure 4B**). Despite the lower limit of detection of the proliferation assay, some samples did not show any proliferative capability. High proliferation levels for HBV-specific T cell reactivity was associated with a higher baseline frequency of CD28+PD-1+ co-expression and higher expression of PD-1 per cell on bulk CD8 T cells (**Figure 4C** and **Supplementary Figure 4A**), suggesting that low exhaustion is a requisite for HBV-specific T cell proliferation, while this difference was not observed for HERPES-associated proliferation. Altogether, these results show that functional exhaustion of HBV-specific CD8 T cells plays a role in the clinical progression of chronic HBV infection and could be a barrier to successful immunotherapy strategies.

Lack of Response to PD-L1 Blockade Is Associated With Higher Frequency of Functionally Exhausted HBV-Specific T Cells

Ex vivo HBV-specific reactivity was assessed in the presence of MEDI2790, a PD-L1 inhibitor. Response to PD-L1 blockade was defined as increase of at least 10 SFUs in the *ex vivo* ELISpot when compared to the untreated control. We observed a 50% response to MEDI2790 [R(+)](**Figure 5A**). Response to PD-L1 blockade was independent of HBeAg, HBsAg, ALT or HBV DNA levels (**Supplementary Figures 5A, B**). Distribution patterns of the 6 iR (**Supplementary Figure 5C**, 6+ markers PD-1+41BB+TIGIT+PD-L1+TIM3+LAG3+) was also similar between responders and not responders. However, non-responders had a significantly higher frequency of functionally exhausted HBV-specific CD8 T cells (3+ markers, LAG3+TIM3+PD-1+), independently of the expression levels of PD-L1 (**Figures 5A–C**) while response to MEDI2790 was associated with a higher frequency of the phenotype TIM-3+PD-1+PD-L1+ in absence of LAG3 expression (**Figures 5A, C**). These results strongly suggest that LAG3 expression signifies a functionally exhausted status that cannot be recovered by PD-L1 blockade strategies.

Response to PD-L1 Blockade Increases HBV-Specific T Cell Functionality

Finally, we tried to determine the mechanisms underlying the increase of *ex vivo* HBV reactivity after PD-L1 blockade. However, proliferation levels were not increased in the presence of MEDI2790 (**Figure 6A**), MitoTempo, a mitochondrial-targeted antioxidant agent that has shown to restore T cell activation (28)IL-12, a third signal cytokine that regulates T cell responses and could rescue anti-viral activity of exhausted cells (29, 30), or the combination of all three agents (**Supplementary Figure 6A**). Then, we sought to determine whether PD-L1 blockade would affect cytokine production. HBV-specific CD8 T cells are present in such a low frequency that conventional approaches combining peptide pool stimulation and intracellular staining of bulk CD8 T cells often fail because the signal is under the threshold of detection. To overcome this limitation, we used an innovative approach to force the upregulation of the TCR to the cell surface that allowed us to combine dextramer staining, peptide pool stimulation and intracellular staining of HBV-specific CD8 T cells, greatly increasing the sensitivity of the flow cytometry-based approach. As shown in **Figure 6B**, overnight stimulation of PBMCs with the irrelevant peptide Actin and dasatinib treatment prior to the dextramer and intracellular staining did not detect cytokine production among HBV-specific CD8 T cells. However, when a relevant peptide (HBV Pool) was used for the stimulation (**Figure 6B**, right panel) we were able to detect a robust cytokine production by HBV-specific CD8 T cells. PD-L1 blockade significantly increased IFNγ production and cytotoxicity (IFNγ+GrzB+) for both HBV-specific and HERPES-specific CD8 T cells (**Figure 6C**, left and middle panels). IL-10 production was increased only for HBV-specific T cells (**Figure 6C**, right panel) while TNF, IL-2 and IFNγ+CD107a+ remained unchanged (**Supplementary Figure 6B**). In line with our previous results, the frequency of Ag-specific CD8 T cells with a functional response (cytokine production or cytotoxicity) is inversely associated with the frequency of functional exhaustion (**Figure 6D** and **Supplementary Figure 6C**).

DISCUSSION

In this study we show that a high frequency of functionally exhausted HBV-specific CD8 T cells (as determined by the simultaneous expression of LAG3+TIM3+PD-1+) is associated with both lack of *ex vivo* reactivity and unresponsiveness to PD-L1 blockade. These results could have implications in the design of immunotherapy strategies aiming to achieve a functional cure for chronic HBV infection.

Chronic HBV infection, besides the stigma and significant impact on quality of life (31, 32), is characterized by a 100-fold increase of the risk to develop hepatocellular carcinoma (HCC) (2, 33). A functional cure, defined as persistent absence of HBsAg in the absence of antiviral therapy, indicates complete immune control and viral suppression and is regarded as the optimal point of therapy (7). Current antiviral therapy (AVT) with different nucleos(t)ide reverse transcriptase inhibitors (NRTI) can provide long-term benefits by suppressing HBV viremia but they are still life-long treatments with negligible rates of HBsAg loss and patients maintain a 6% 8-years cumulative risk to develop HCC (4–6). Some patients can achieve functional cure after discontinuation of NRTI treatment (34, 35), but this is a minority and stopping NRTI's is not without risks as severe flares and liver decompensation may occur (36). PEGylated-IFNα is a finite but toxic therapy, given for 6-12 months as monotherapy or combined with NRTI, resulting in about 10% HBsAg loss after long-term follow-up. Thus, achieving HBsAg loss with finite therapy is a current need for chronic HBV infected patients.

The immune system is able to completely suppress intrahepatic HBV replication during self-resolving acute HBV infection and the critical antiviral role of adaptive immunity,

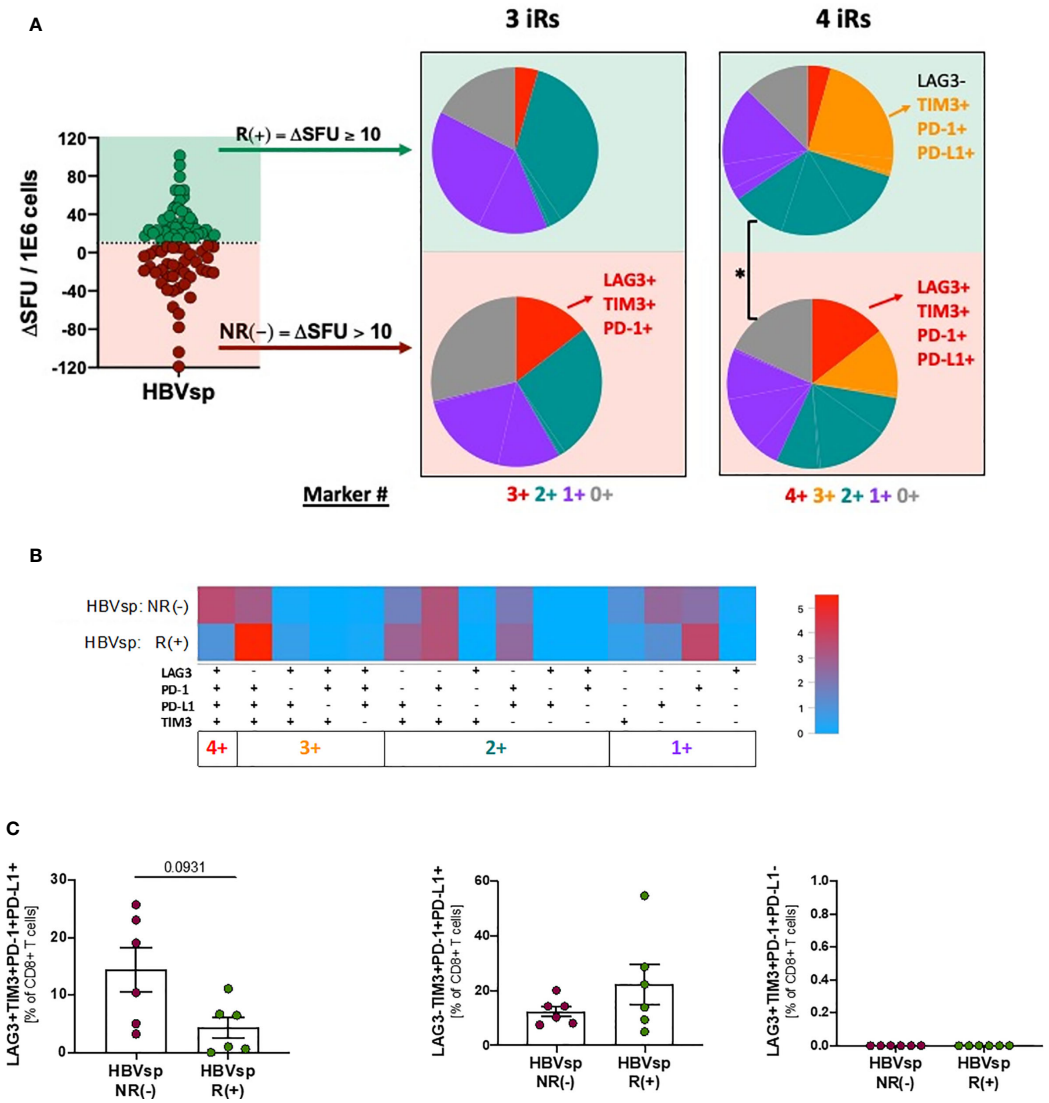

FIGURE 5 | Highly exhausted HBV-specific CD8 T cells do not respond to PD-L1 blockade. Frequency of HBV-specific (core and/or pool) CD8 T cells with phenotype consistent with low exhaustion (LAG3-TIM3-PD-1+PD-L1-; *1+* markers); intermediate exhaustion LAG3-TIM3+PD-1+PD-L1±; *2+/3+* markers) and high exhaustion (LAG3+TIM3+PD-1+PD-L1+; *4+* markers) between responders (R) and non-responders (NR) to PD-L1 blockade shown as **(A)** SPICE analysis. *$p < 0.05$; Permutation test, **(B)** SPICE CoolPlot and **(C)** pooled data. Mann Whitney U.

especially cytotoxic CD8 T cells, during the resolution of acute HBV infection has been clearly defined (8–10). In humans, liver transplant immune recipients are able to clear HBV infection in organs from chronically infected donors (12, 13), proving that chronic HBV infection can be functionally cured by an effective immune response. Direct disruption of the PD-1:PD-L1 axis with monoclonal antibodies has been successfully tested to restore functionality of CD8 T cell in both, cancer and infectious diseases (37–40). The combination of immunotherapy and therapeutic vaccine showed some promising results in a small clinical trial (41). In addition, we have previously shown that *in vitro* PD-L1 blockade with MEDI2790 increased by two-fold the HBV-specific T cell response in 97% of chronically infected patients with baseline T cell reactivity (20). However, due to the extremely low frequency of peripheral HBV-specific T cells, in our past study HBV-specific T cell were expanded prior to the PD-L1 blockade, serving as a proof-of-concept for the use of immunotherapy in chronic HBV infection.

To increase the translatability of this proof-of-concept, in this study we optimized an *ex vivo* approach to determine HBV-specific T cell reactivity and response to MEDI2790. Two different HBV peptide pools, a commercially available peptide pool containing 9 HLA-class-I restricted T cell epitopes known to be highly immunogenic and a custom-generated pool including 34 HLA-class-I restricted epitopes shared by all HBV genotypes, were used to maximize the level of response when

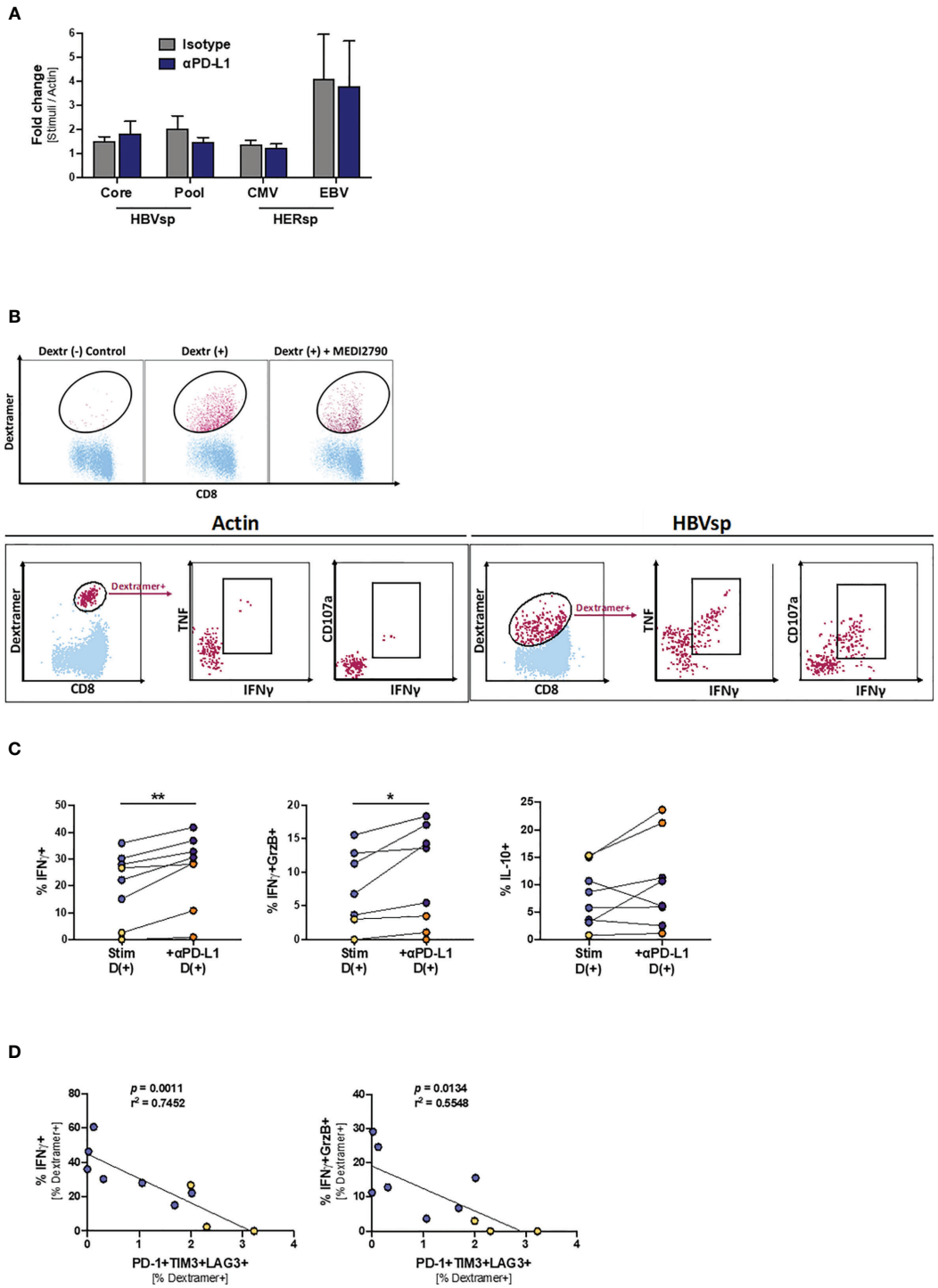

FIGURE 6 | PD-L1 blockade increases the frequency of IFNγ-producing Ag-specific CD8 T cells. **(A)** Effect of PD-L1 blockade on the proliferation levels of Ag-specific CD8 T cells. **(B)** Representative flow plots showing the gating strategy for intracellular cytokine staining of dasatinib-treated HBV-specific CD8 T cells. Dextramer-positive CD8 T cells (maroon) are overlaid on bulk CD8 T cells (light blue). While cytokines cannot be detected on samples stimulated with Actin negative control (left panel), dasatinib-treated stimulated HBV-specific T cells accumulate both cytokines and degranulation markers (right panel). **(C)** Effect of PD-L1 blockade in IFNγ (left panel), IFNγ+GrzB+ (middle panel) and IL-10 (right panel) production. Blue dots show HERPES-specific stimulations (CMV or EBV) while orange dots show HBV-specific stimulations (pool). *p < 0.05; **p < 0.001; Wilcoxon signed rank test. **(D)** Linear regression showing the negative correlation between Ag-specific IFNγ production and the frequency of highly exhausted (LAG3+TIM3+PD-1+) Ag-specific CD8 T cells. Blue dots show HERPES-specific stimulations (CMV or EBV) while orange dots show HBV-specific stimulations (pool).

using this *ex vivo* approach. HBsAg overlapping peptide pools were not included for *ex vivo* ELISpot analysis, since HBsAg immune responses are normally scarce and impaired during chronic HBV (22, 40, 42). As recently reported (43, 44), in this study we show that the immune response leading to the initial control of viral replication is broad and targets multiple HBV proteins while HBeAg- Immune Active hepatitis is characterized by a narrow and weak HBV-specific T cell response. In line with these results, we found that HBV-specific CD8 T cells are significantly more exhausted than herpes-specific CD8 T cells (CMV and/or EBV) in the same patients. It is worth noting that herpes infections are also chronically established but, in immunocompetent hosts, don't show a clinical progression due to complete control of replication by the immune system. Not surprisingly, high levels of functional exhaustion in the HBV-specific CD8 T cell population was associated to lack of *ex vivo* reactivity and failure to respond to MEDI2790 PD-L1 blockade.

We then developed a strategy to quantify cytokine production by HBV-specific CD8 T cell by flow cytometry. While MHCI dextramers have been widely used as a detection tool for *ex vivo* approaches, once antigen-specific CD8 T cells are activated the T cell receptor gets internalized and thus unavailable for dextramer-based staining. Due to this limitation, flow cytometry approaches to quantify cytokine production from antigen-specific T cells usually focus on the bulk CD8 subset, greatly limiting the sensitivity of the detection. This is especially problematic in chronic HBV infection where, due to the rare frequency of these cells, the frequency of cytokine-producing cells is rarely detected over the background noise. To overcome this limitation, we used dasatinib, a blocker of the Src kinase family (45–47), to force the re-expression of the TCR on the surface of antigen-specific CD8 T cells after peptide stimulation. Using this approach, we were able to determine that HBV-specific CD8 T cells with low level of exhaustion were indeed responding to PD-L1 blockade by increasing the production of IFNγ and IFNγ+GrzB+ cytotoxic responses. However, HBV-specific CD8 T cells with higher levels of exhaustion, mainly characterized by the expression of LAG3, are unable to respond to this immunotherapeutic approach.

Bengsch et al. (48) have previously shown that iR expression on HBV-specific CD8 T cells is hierarchical, with PD-1 being expressed the most and LAG-3 being the hardest iR to detect. Despite the comprehensive characterization of the different iR expression on HBV-specific CD8 T cells, they analyzed the response to PD-L1 blockade as the increase on proliferative capacity. Since this approach has a higher detection limit, they were not able to identify a specific phenotype associated with lack of response. In this study, we were able to determine that the co-expression of PD-1, TIM-3 and LAG-3 is associated with the lack of response to anti-PD-L1 antibodies. This result has direct translational implications. Foremost, it suggests that monotherapy strategies are not suitable to treat chronically infected HBV patients. In addition, since terminally exhausted CD8 T cells undergo epigenetic changes that prevents for this phenotype to be rescued (49, 50), finding the appropriate therapeutic window before HBV-specific T cells become functionally exhausted, may be necessary to successfully apply immunotherapy to cure chronic HBV infection. Finally, even if combination strategies may be still effective in selected or unselected HBV patients, targeting LAG-3 blockade (51, 52) may be essential to elicit a clinically effective response.

Altogether, our results suggest that while immunotherapeutic approaches aimed to boost HBV-specific T cell immunity could be a successful strategy to elicit a functional cure for chronic HBV infection, a monotherapy aiming to disrupt the PD-1:PD-L1 axis could have limited effectiveness. The high levels of functional exhaustion present in the HBV-specific CD8 T cell subset suggest that combination strategies, potentially including the combination of anti-LAG-3 with other anti-iR antibodies, should be explored and likely prioritized for unselected chronic HBV patients.

METHODS

Patients

One hundred adult patients with chronic HBV infection (female 38%; median age 48 years old) were included in this study. All patients were in follow up at the Toronto General Hospital Liver Centre, University Health Network in Toronto, Canada and willing to provide informed consent. All patients had confirmed chronic HBV infection, documented by the presence of HBsAg for at least 12 months prior to the inclusion of this study. The study protocol was approved by the Ethics Committee of the Toronto General Hospital, University Health Network. Exclusion criteria included acute HBV infection, acute flare or reactivation of HBV infection (defined as symptoms of acute hepatitis and recent elevation of ALT > 10xULN or bilirubin levels), treatment with interferon (IFN)-α, systemic corticosteroids or any other immune modulators or suppressive agents within 4 weeks of screening, cirrhosis, hepatocellular carcinoma, liver transplantation, known coinfection with HCV, HDV and/or HIV, need for renal dialysis and known active autoimmune disease, including autoimmune hepatitis. Informed consent was obtained from each individual at enrollment. Peripheral blood samples were obtained by venipuncture, anonymized and processed to obtain peripheral blood mononuclear cells (PBMC). All samples were cryopreserved until further use. Characteristics of the cohort are summarized in **Table 1**.

Ex Vivo ELISpot

PBMC samples from chronic hepatitis B (HBV) patients were thawed and washed in CTL Anti-Aggregate™ medium (Cellular Technology Limited, CTL) and rested overnight at 37°C in complete RPMI with 10% human serum. Duplicated wells containing 5E5 PBMC were incubated overnight with the appropriate peptide pools in CTL-Test™ Medium (Cellular Technology Limited, CTL), including negative and positive controls, in the presence of MEDI2790 or a control IgG isotype. Antigen-specific T cell responses were quantified using

TABLE 1 | Characteristics of the cohort.

	Flow cytometry	*Ex vivo* ELISpot	*p*
n	100	89	
Sex (% Female)	38/100 (38%)	44/89 (49.4%)	
Age	48 [35 - 57]	44 [33 – 54]	NS[1]
Race (% Asian)	81/100 (81%)	76/89 (85.4%)	
AVT[2]	21/100 (21%)	13/89 (14.6%)	
AVT (years)	5 [3.5 – 7.8]	5 [3.5 – 8.7]	NS
HBeAg (% Negative)			
AVT(-)	49/79 (62.0%)	36/76 (47.4%)	
AVT(+)	18/21 (85.7%)	10/13 (76.9%)	
ALT (U/mL)	30 [23 - 58]	29 [22 – 63]	NS
ULN[3] ≤ 1.3X			
AVT(-)	54/79 (68.4%)	49/76 (64.5%)	
AVT(+)	18/21 (85.7%)	13/13 (100%)	
Log HBV DNA	4.0 [1.3 – 8.0]	5.8 [2.3 – 8.2]	NS
HBsAg (IU/mL)	2803 [683 - 12176]	5181 [1023 – 45385]	NS
HBsAg (% ≤10)			
AVT(-)	6/68 (8.8%)	4/64 (6.3%)	
AVT(+)	1/20 (5.0%)	0/13 (0.0%)	
Clinical groups[4]			
Immune Tolerant (IT)	19/100 (19%)	27/89 (30.3%)	
HBeAg+ Immune Active (IA+)	12/100 (12%)	13/89 (14.6%)	
Immune Control (IC)	34/100 (34%)	21/89 (23.6%)	
HBeAg- Immune Active (IA-)	14/100 (14%)	15/89 (16.9%)	
Antiviral Therapy (AVT)	21/100 (21%)	13/89 (14.6%)	

[1]NS, Not significant; p > 0.1. [2]AVT, Antiviral Therapy. [3]ULN, ALT upper limit of normal. [4]All HBeAg-negative patients in this category spontaneously seroconvert. IT = HBeAg (+) and ULN ≤ 1.3X; HBeAg+ IA = HBeAg (+) and ULN > 1.3X; IC = HBeAg (-) and ULN ≤ 1.3X; HBeAg- IA = HBeAg (-) and ULN > 1.3X. Dichotomic variables are expressed as number/total number (frequency). Continuous variables are expressed as median [Interquartile range, IQR].

ELISpot PLUS IFNγ pre-coated plates (MabTech) and the ImmunoSpot® reader and software (Cellular Technology Limited, CTL). CORE, POOL, CMV, EBV and the negative control ACTIN pool were used at a concentration of 2 μg/peptide/mL. The positive control CEFX pool was used at 0.2 μg/peptide/mL. HBVsp refers to combined results from HBV CORE and HBV POOL stimulations. HERsp (HERPES) refers to combined results from CMV and EBV stimulations. Additional information, including specific peptides, of the peptide pools can be found in **Supplementary Table 1**.

One hundred samples were tested in this study. Samples with failed positive and/or negative controls after two independent attempts were discarded. A total of 89 ELISpot quantifications passed all quality controls and were included in the analysis for this study. All results are reported after background subtraction using each sample's actin control.

Polychromatic Flow Cytometry

Ex Vivo Analysis of Bulk CD8 T Cells

PBMC samples from the 100 chronic HBV patients were thawed, washed in CTL Anti-Aggregate™ medium (Cellular Technology Limited, CTL) and rested 2h in CTL Test™ medium (Cellular Technology Limited, CTL). Cells were then washed and stained in 96-well plates at 1E6 - 2E6 cells per well with titrated amounts of LIVE/DEAD™ Fixable Blue Dead Cell stain kit (Invitrogen). All surface markers were stained at a final volume of 100μL with titrated amounts of monoclonal antibodies, in the presence of Super Bright Staining Buffer (eBiosciences) for 45 min at room temperature. After the final wash cells were fixed with 1% PFA/PBS and acquired in a BDSymphony® flow cytometer. Analysis was performed with FlowJo v10.6.2. Further information about the antibodies can be found in **Supplementary Table 2**.

Ex Vivo Analysis of HBV-Specific CD8 T Cells

For a subset of patients with selected HLA alleles (HLA-A*0201, HLA-B*3501 and HLA-B*5101; n = 48) dextramer staining was included in the *ex vivo* analysis. Samples were incubated for 15 min, previous to the surface marker staining, with the appropriated dextramers depending on their HLA type. Negative controls were included for all samples. Further information of the dextramers can be found in **Supplementary Table 3**.

Functional Analysis by Intracellular Staining

Thirteen HLA-A*0201 samples, with HBV-specific dextramer frequency higher than 0.1% and sample availability were selected for a functional analysis. PBMC samples were thawed, washed in CTL Anti-Aggregate™ medium (Cellular Technology Limited, CTL) and rested 2h in CTL Test Plus™ medium (Cellular Technology Limited, CTL). PBMC were then washed and added to 48 well plates at a concentration of 2E6/mL on CTL Test Plus™ medium. Samples were stimulated with either HBV Pool (PX-HBV ThinkPeptide), CMV (PA-CMV-001, PanaTecs), EBV (PA-CMV-001, PanaTecs) or Actin control (PM-ACTS, JPT) at 2μg/peptide/mL for 12h in the presence of brefeldin A (BFA) and titrated amounts of CD107a antibody. Cells were then washed and incubated with Dasatinib 100mM (Sigma-Aldrich) in PBS for 1h at 37°C to favor the re-expression of the TCR in the cell surface (45–47). All further incubations and washed were done in the presence of 100mM Dasatinib (Sigma-Aldrich). This approach is a modification of a previously reported protocol (30, 53). After the incubation cells were stained with titrated amounts of LIVE/DEAD™ Fixable Blue Dead Cell stain kit (Invitrogen). After a blocking step, each actin control/peptide-stimulated pair was stained with the appropriate dextramers (Capsid or Protein S for Actin/HBV pool, CMV for Actin/CMV pool and EBV for Actin/EBV pool) for 15 minutes. Stimulated and dasatinib-treated samples stained with control dextramers were used to determine the gating strategy. All surface markers were then stained at a final volume of 100μL with titrated amounts of monoclonal antibodies in the presence of Super Bright Staining Buffer (eBiosciences). Cells were then permeabilized using a fixation/permeabilization kit (BD) according to the manufacturer's instructions and stained with titrated amounts of monoclonal antibodies for 45 min at 4°C. After the final washes cell were resuspended in 1% PFA/PBS and acquired in a BDSymphony® flow cytometer. Analysis was performed with FlowJo v10.6.2. Further information about the antibodies and dextramers can be found in **Supplementary Tables 2, 3**.

Proliferation Assay

Fifteen samples with available Leukopak where included for the proliferation assay. PBMCs were thawed, washed in CTL Anti-Aggregate™ medium (Cellular Technology Limited, CTL) and rested for 2h at 37°C in CTL Test Plus™ medium (Cellular

Technology Limited, CTL). After resting PBMCs were counted and transferred to 50mL conical tubes and resuspended at 1E6/mL in PBS with titrated amounts of Cell Trace™ Violet Cell proliferation (ThermoFisher Scientific). After a 20min incubation at 37°C the staining was stopped with PBS 10% FCS at 1:4 ratio. PBMCs stained with the Violet Cell Trace™ were cultured at 2E6/mL, in duplicate, in the presence of 20 IU of IL-2 and 2μg/peptide/mL of the appropriate stimuli (HBV Core, HBV Pool, HBV Capsid, CMV, EBV, Actin or CEFX peptide pools as described in the ELISpot section) in the presence of either 1) IgG control, 2) MEDI2790, 3) 0.1 μM Mitotempo (Sigma Aldrich), 4) 10 ng/mL IL-12 and 5) MEDI2790 + 0.1 μM Mitotempo (Sigma Aldrich) + 10 ng/mL IL-12. Media (with IL-2) was changed at day 5 and proliferation was assessed on day 10 by flow cytometry.

MEDI2790 Antibody Generation

MEDI2790 generation has been previously described (20, 54). Briefly, IgG2 and IgG4 XenoMouse animals were immunized with human PD-L1-Ig or CHO cells expressing human PD-L1. Hybridomas were established and supernatants screened for binding to human PD-L1-transfected HEX 293 cells and inhibition of PD-1 binding to PD-L1 expressing CHO cells. MEDI2790 was selected based on affinity, activity and specificity profile. The constant domain of the antibody was then exchanged for a human IgG1 triple-mutant domain containing three-point mutations that reduce binding to C1q and Fc gamma receptors, resulting in reduced antibody-dependent cellular cytotoxicity (ADCC) and complement-dependent cytotoxicity (CDC).

Statistical Analysis

GraphPad Prism (PRISM 8 for macOS v8.3.0) was used to perform statistical analyses and to create graphs. Data is shown as number of cases, individual points or bars depicting the mean ± standard error (SEM). Variables were analyzed using non-parametric tests as appropriate: Mann-Whitney U test for unpaired variables, Wilcoxon matched-pairs signed rank test for paired variables and Kruskal-Wallis one-way analysis of variance for the simultaneous comparison of 3 or more groups. Associations were analyzed by linear regression and 95% confident interval (CI). Analysis and graphical representation of the distribution of inhibitory (iR) and activating (aR) receptors on the different CD8 T cell populations was performed using the Simplified Presentation of Incredibly Complex Evaluations (SPICE v6) as previously described (55).

DATA AVAILABILITY STATEMENT

The original contributions presented in the study are included in the article/**Supplementary Material**. Further inquiries can be directed to the corresponding author.

AUTHOR CONTRIBUTIONS

SFM and SR designed the study. AG, JF and HJ provided and processed the samples. SFM, AS and EL performed the experiments. SFM and AS performed the analysis. SFM and SR wrote the manuscript. All authors contributed to the article and approved the submitted version.

FUNDING

The study was fully funded by AstraZeneca.

ACKNOWLEDGMENTS

The authors want to acknowledge all the personnel from the Toronto Center for Liver Disease involved in patient recruitment and sample handling. Special thanks to all patients involved; without their help this study would not be possible.

SUPPLEMENTARY MATERIAL

The Supplementary Material for this article can be found online at: https://www.frontiersin.org/articles/10.3389/fimmu.2021.648420/full#supplementary-material

REFERENCES

1. WHO. *Global Hepatitis Report 2017*. ISBN 978-92-4-156545-5. World Health Organization (2017). Available at: https://www.who.int/publications/i/item/global-hepatitis-report-2017.
2. Beasley RP. Hepatitis B Virus. The Major Etiology of Hepatocellular Carcinoma. *Cancer* (1988) 61(10):1942–56. doi: 10.1002/1097-0142(19880515)61:10>1942::aid-cncr2820611003<3.0.co;2-j
3. Stanaway JD, Flaxman AD, Naghavi M, Fitzmaurice C, Vos T, Abubakar I, et al. The Global Burden of Viral Hepatitis From 1990 to 2013: Findings From the Global Burden of Disease Study 2013. *Lancet* (2016) 388(10049):1081–8. doi: 10.1016/S0140-6736(16)30579-7
4. Chen JD, Yang HI, Iloeje UH, You SL, Lu SN, Wang LY, et al. Carriers of Inactive Hepatitis B Virus are Still at Risk for Hepatocellular Carcinoma and Liver-Related Death. *Gastroenterology* (2010) 138(5):1747–54. doi: 10.1053/j.gastro.2010.01.042
5. Kim GA, Lee HC, Kim MJ, Ha Y, Park EJ, An J, et al. Incidence of Hepatocellular Carcinoma After HBsAg Seroclearance in Chronic Hepatitis B Patients: A Need for Surveillance. *J Hepatol* (2015) 62(5):1092–9. doi: 10.1016/j.jhep.2014.11.031
6. Yip TC, Wong GL, Chan HL, Tse YK, Lam KL, Lui GC, et al. HBsAg Seroclearance Further Reduces Hepatocellular Carcinoma Risk After Complete Viral Suppression With Nucleos(T)Ide Analogues. *J Hepatol* (2019) 70(3):361–70. doi: 10.1016/j.jhep.2018.10.014
7. European Association for the Study of the Liver. Electronic Address Eee, and European Association for the Study of the L. EASL 2017 Clinical Practice Guidelines on the Management of Hepatitis B Virus Infection. *J Hepatol* (2017) 67(2):370–98. doi: 10.1016/j.jhep.2017.03.021
8. Thimme R, Wieland S, Steiger C, Ghrayeb J, Reimann KA, Purcell RH, et al. CD8+ T Cells Mediate Viral Clearance and Disease Pathogenesis During Acute Hepatitis B Virus Infection. *J Virol* (2003) 77(1):68–76. doi: 10.1128/JVI.77.1.68-76.2003
9. Maini MK, Boni C, Ogg GS, King AS, Reignat S, Lee CK, et al. Direct *Ex Vivo* Analysis of Hepatitis B Virus-Specific CD8(+) T Cells Associated With the Control of Infection. *Gastroenterology* (1999) 117(6):1386–96. doi: 10.1016/S0016-5085(99)70289-1

10. Rehermann B, Fowler P, Sidney J, Person J, Redeker A, Brown M, et al. The Cytotoxic T Lymphocyte Response to Multiple Hepatitis B Virus Polymerase Epitopes During and After Acute Viral Hepatitis. *J Exp Med* (1995) 181 (3):1047–58. doi: 10.1084/jem.181.3.1047
11. Xia Y, Stadler D, Lucifora J, Reisinger F, Webb D, Hosel M, et al. Interferon-Gamma and Tumor Necrosis Factor-Alpha Produced by T Cells Reduce the HBV Persistence Form, cccDNA, Without Cytolysis. *Gastroenterology* (2016) 150(1):194–205. doi: 10.1053/j.gastro.2015.09.026
12. Loggi E, Bihl F, Chisholm JV3rd, Biselli M, Bontadini A, Vitale G, et al. Anti-HBs Re-Seroconversion After Liver Transplantation in a Patient With Past HBV Infection Receiving a HBsAg Positive Graft. *J Hepatol* (2009) 50(3):625–30. doi: 10.1016/j.jhep.2008.08.026
13. Loggi E, Micco L, Ercolani G, Cucchetti A, Bihl FK, Grazi GL, et al. Liver Transplantation From Hepatitis B Surface Antigen Positive Donors: A Safe Way to Expand the Donor Pool. *J Hepatol* (2012) 56(3):579–85. doi: 10.1016/j.jhep.2011.09.016
14. Bertoletti A, Bert NL. Immunotherapy for Chronic Hepatitis B Virus Infection. *Gut Liver* (2018) 12(5):497–507. doi: 10.5009/gnl17233
15. Maini MK, Boni C, Lee CK, Larrubia JR, Reignat S, Ogg GS, et al. The Role of Virus-Specific CD8(+) Cells in Liver Damage and Viral Control During Persistent Hepatitis B Virus Infection. *J Exp Med* (2000) 191(8):1269–80. doi: 10.1084/jem.191.8.1269
16. Perrillo RP, Gish R, Falck-Ytter YT. American Gastroenterological Association Institute Technical Review on Prevention and Treatment of Hepatitis B Virus Reactivation During Immunosuppressive Drug Therapy. *Gastroenterology* (2015) 148(1):221–44.e3. doi: 10.1053/j.gastro.2014.10.038
17. Waldman AD, Fritz JM. And Lenardo MJ. A Guide to Cancer Immunotherapy: From T Cell Basic Science to Clinical Practice. *Nat Rev Immunol* (2020) 20(11):651–68. doi: 10.1038/s41577-020-0306-5
18. Gambichler T, Reuther J, Scheel CH, Becker JC. On the Use of Immune Checkpoint Inhibitors in Patients With Viral Infections Including COVID-19. *J Immunother Cancer* (2020) 8(2):e001145. doi: 10.1136/jitc-2020-001145
19. Ziogas DC, Kostantinou F, Cholongitas E, Anastasopoulou A, Diamantopoulos P, Haanen J, et al. Reconsidering the Management of Patients With Cancer With Viral Hepatitis in the Era of Immunotherapy. *J Immunother Cancer* (2020) 8(2):e000943. doi: 10.1136/jitc-2020-000943
20. Ferrando-Martinez S, Huang K, Bennett AS, Sterba P, Yu L, Suzich JA, et al. HBeAg Seroconversion is Associated With a More Effective PD-L1 Blockade During Chronic Hepatitis B Infection. *JHEP Rep* (2019) 1(3):170–8. doi: 10.1016/j.jhepr.2019.06.001
21. Kim JH, Ghosh A, Ayithan N, Romani S, Khanam A, Park JJ, et al. Circulating Serum HBsAg Level is a Biomarker for HBV-Specific T and B Cell Responses in Chronic Hepatitis B Patients. *Sci Rep* (2020) 10(1):1835. doi: 10.1038/s41598-020-58870-2
22. Le Bert N, Gill US, Hong M, Kunasegaran K, Tan DZM, Ahmad R, et al. Effects of Hepatitis B Surface Antigen on Virus-Specific and Global T Cells in Patients With Chronic Hepatitis B Virus Infection. *Gastroenterology* (2020) 159(2):652–64. doi: 10.1053/j.gastro.2020.04.019
23. Carvalho-Queiroz C, Johansson MA, Persson JO, Jortso E, Kjerstadius T, Nilsson C, et al. Associations Between EBV and CMV Seropositivity, Early Exposures, and Gut Microbiota in a Prospective Birth Cohort: A 10-Year Follow-Up. *Front Pediatr* (2016) 4:93. doi: 10.3389/fped.2016.00093
24. Smatti MK, Al-Sadeq DW, Ali NH, Pintus G, Abou-Saleh H, Nasrallah GK. Epstein-Barr Virus Epidemiology, Serology, and Genetic Variability of LMP-1 Oncogene Among Healthy Population: An Update. *Front Oncol* (2018) 8:211. doi: 10.3389/fonc.2018.00211
25. Terrault NA, Bzowej NH, Chang K-M, Hwang JP, Jonas MM, Murad MH. AASLD Guidelines for Treatment of Chronic Hepatitis B. *Hepatology* (2016) 63(1):261–83. doi: 10.1002/hep.28156
26. Kapellos TS, Bonaguro L, Gemund I, Reusch N, Saglam A, Hinkley ER, et al. Human Monocyte Subsets and Phenotypes in Major Chronic Inflammatory Diseases. *Front Immunol* (2019) 10:2035. doi: 10.3389/fimmu.2019.02035
27. Varanasi V, Khan AA, Chervonsky AV. Loss of the Death Receptor CD95 (Fas) Expression by Dendritic Cells Protects From a Chronic Viral Infection. *Proc Natl Acad Sci USA* (2014) 111(23):8559–64. doi: 10.1073/pnas.1401750111
28. Rinker F, Zimmer CL, Honer Zu Siederdissen C, Manns MP, Kraft ARM, Wedemeyer H, et al. Hepatitis B Virus-Specific T Cell Responses After Stopping Nucleos(T)Ide Analogue Therapy in HBeAg-Negative Chronic Hepatitis B. *J Hepatol* (2018) 69(3):584–93. doi: 10.1016/j.jhep.2018.05.004
29. Trinchieri G. Interleukin-12 and the Regulation of Innate Resistance and Adaptive Immunity. *Nat Rev Immunol* (2003) 3(2):133–46. doi: 10.1038/nri1001
30. Schurich A, Pallett LJ, Lubowiecki M, Singh HD, Gill US, Kennedy PT, et al. The Third Signal Cytokine IL-12 Rescues the Anti-Viral Function of Exhausted HBV-Specific CD8 T Cells. *PloS Pathog* (2013) 9(3):e1003208. doi: 10.1371/journal.ppat.1003208
31. Li G, Wang G, Hsu FC, Xu J, Pei X, Zhao B, et al. Effects of Depression, Anxiety, Stigma, and Disclosure on Health-Related Quality of Life Among Chronic Hepatitis B Patients in Dalian, China. *Am J Trop Med Hyg* (2020) 105 (5):988–94. doi: 10.4269/ajtmh.19-0007
32. Spiegel BM, Bolus R, Han S, Tong M, Esrailian E, Talley J, et al. Development and Validation of a Disease-Targeted Quality of Life Instrument in Chronic Hepatitis B: The Hepatitis B Quality of Life Instrument, Version 1.0. *Hepatology* (2007) 46(1):113–21. doi: 10.1002/hep.21692
33. Fattovich G, Pantalena M, Zagni I, Realdi G, Schalm SW, Christensen E, et al. Effect of Hepatitis B and C Virus Infections on the Natural History of Compensated Cirrhosis: A Cohort Study of 297 Patients. *Am J Gastroenterol* (2002) 97(11):2886–95. doi: 10.1111/j.1572-0241.2002.07057.x
34. Bayliss J, Yuen L, Rosenberg G, Wong D, Littlejohn M, Jackson K, et al. Deep Sequencing Shows That HBV Basal Core Promoter and Precore Variants Reduce the Likelihood of HBsAg Loss Following Tenofovir Disoproxil Fumarate Therapy in HBeAg-Positive Chronic Hepatitis B. *Gut* (2017) 66 (11):2013–23. doi: 10.1136/gutjnl-2015-309300
35. Huang J, Zhang K, Chen W, Liao J, Luo X, Chen R. Switching to PegIFNalpha-2b Leads to HBsAg Loss in Patients With Low HBsAg Levels and HBV DNA Suppressed by NAs. *Sci Rep* (2017) 7(1):13383. doi: 10.1038/s41598-017-13747-9
36. Liem KS, Gehring AJ, Feld JJ, Janssen HLA. Challenges With Stopping Long-Term Nucleos(t)ide Analogue Therapy in Patients With Chronic Hepatitis B. *Gastroenterology* (2020) 158(5):1185–90. doi: 10.1053/j.gastro.2019.10.050
37. Boni C, Fisicaro P, Valdatta C, Amadei B, Di Vincenzo P, Giuberti T, et al. Characterization of Hepatitis B Virus (HBV)-Specific T-Cell Dysfunction in Chronic HBV Infection. *J Virol* (2007) 81(8):4215–25. doi: 10.1128/JVI.02844-06
38. Fisicaro P, Valdatta C, Massari M, Loggi E, Biasini E, Sacchelli L, et al. Antiviral Intrahepatic T-Cell Responses can be Restored by Blocking Programmed Death-1 Pathway in Chronic Hepatitis B. *Gastroenterology* (2010) 138(2):682–93, 93.e1-4. doi: 10.1053/j.gastro.2009.09.052
39. Nishino M, Ramaiya NH, Hatabu H, Hodi FS. Monitoring Immune-Checkpoint Blockade: Response Evaluation and Biomarker Development. *Nat Rev Clin Oncol* (2017) 14(11):655–68. doi: 10.1038/nrclinonc.2017.88
40. Salimzadeh L, Le Bert N, Dutertre CA, Gill US, Newell EW, Frey C, et al. PD-1 Blockade Partially Recovers Dysfunctional Virus-Specific B Cells in Chronic Hepatitis B Infection. *J Clin Invest* (2018) 128(10):4573–87. doi: 10.1172/JCI121957
41. Gane E, Verdon DJ, Brooks AE, Gaggar A, Nguyen AH, Subramanian GM, et al. Anti-PD-1 Blockade With Nivolumab With and Without Therapeutic Vaccination for Virally Suppressed Chronic Hepatitis B: A Pilot Study. *J Hepatol* (2019) 71(5):900–7. doi: 10.1016/j.jhep.2019.06.028
42. Cornberg M, Wong VW, Locarnini S, Brunetto M, Janssen HLA, Chan HL. The Role of Quantitative Hepatitis B Surface Antigen Revisited. *J Hepatol* (2017) 66(2):398–411. doi: 10.1016/j.jhep.2016.08.009
43. Chua CG, Mehrotra A, Mazzulli T, Wong DK, Feld JJ, Janssen HLA, et al. Optimized *Ex Vivo* Stimulation Identifies Multi-Functional HBV-Specific T Cells in a Majority of Chronic Hepatitis B Patients. *Sci Rep* (2020) 10 (1):11344. doi: 10.1038/s41598-020-68226-5
44. Sung PS, Park DJ, Kim JH, Han JW, Lee EB, Lee GW, et al. *Ex Vivo* Detection and Characterization of Hepatitis B Virus-Specific CD8(+) T Cells in Patients Considered Immune Tolerant. *Front Immunol* (2019) 10:1319. doi: 10.3389/fimmu.2019.01319
45. Lissina A, Ladell K, Skowera A, Clement M, Edwards E, Seggewiss R, et al. Protein Kinase Inhibitors Substantially Improve the Physical Detection of T-Cells With Peptide-MHC Tetramers. *J Immunol Methods* (2009) 340(1):11–24. doi: 10.1016/j.jim.2008.09.014

46. Rius C, Attaf M, Tungatt K, Bianchi V, Legut M, Bovay A, et al. Peptide-MHC Class I Tetramers Can Fail To Detect Relevant Functional T Cell Clonotypes and Underestimate Antigen-Reactive T Cell Populations. *J Immunol* (2018) 200(7):2263–79. doi: 10.4049/jimmunol.1700242
47. Schade AE, Schieven GL, Townsend R, Jankowska AM, Susulic V, Zhang R, et al. Dasatinib, a Small-Molecule Protein Tyrosine Kinase Inhibitor, Inhibits T-Cell Activation and Proliferation. *Blood* (2008) 111(3):1366–77. doi: 10.1182/blood-2007-04-084814
48. Bengsch B, Martin B, Thimme R. Restoration of HBV-Specific CD8+ T Cell Function by PD-1 Blockade in Inactive Carrier Patients is Linked to T Cell Differentiation. *J Hepatol* (2014) 61(6):1212–9. doi: 10.1016/j.jhep.2014.07.005
49. Pauken KE, Sammons MA, Odorizzi PM, Manne S, Godec J, Khan O, et al. Epigenetic Stability of Exhausted T Cells Limits Durability of Reinvigoration by PD-1 Blockade. *Science* (2016) 354(6316):1160–5. doi: 10.1126/science.aaf2807
50. Philip M, Fairchild L, Sun L, Horste EL, Camara S, Shakiba M, et al. Chromatin States Define Tumour-Specific T Cell Dysfunction and Reprogramming. *Nature* (2017) 545(7655):452–6. doi: 10.1038/nature22367
51. Jiang H, Ni H, Zhang P, Guo X, Wu M, Shen H, et al. PD-L1/LAG-3 Bispecific Antibody Enhances Tumor-Specific Immunity. *Oncoimmunology* (2021) 10 (1):1943180. doi: 10.1080/2162402X.2021.1943180
52. Seidel L, Bengsch B. Shed it, and Help-LAG3 Cleavage Drives Conventional CD4(+) T Cells to Overcome Resistance to PD-1 Immunotherapy. *Sci Immunol* (2020) 5(49):eabc8644. doi: 10.1126/sciimmunol.abc8644
53. Appay V, Rowland-Jones SL. The Assessment of Antigen-Specific CD8+ T Cells Through the Combination of MHC Class I Tetramer and Intracellular Staining. *J Immunol Methods* (2002) 268(1):9–19. doi: 10.1016/S0022-1759 (02)00195-3
54. Stewart R, Morrow M, Hammond SA, Mulgrew K, Marcus D, Poon E, et al. Identification and Characterization of MEDI4736, an Antagonistic Anti-PD-L1 Monoclonal Antibody. *Cancer Immunol Res* (2015) 3(9):1052–62. doi: 10.1158/2326-6066.CIR-14-0191
55. Roederer M, Nozzi JL, Nason MC. SPICE: Exploration and Analysis of Post-Cytometric Complex Multivariate Datasets. *Cytometry A* (2011) 79(2):167–74. doi: 10.1002/cyto.a.21015

Conflict of Interest: Authors SFM, ASB, EL and SHR were employed by company AstraZeneca, involved in the development and production of MEDI2790.

The authors declare that this study was funded by AstraZeneca. The funder had the following involvement in the study: development and production of MEDI2790.

frontiers in Immunology

MINI REVIEW
published: 29 September 2021
doi: 10.3389/fimmu.2021.730684

Interplay Between Non-Canonical NF-κB Signaling and Hepatitis B Virus Infection

*Xinyu Lu, Qianhui Chen, Hongyan Liu and Xiaoyong Zhang**

State Key Laboratory of Organ Failure Research, Guangdong Provincial Key Laboratory of Viral Hepatitis Research, Department of Infectious Diseases, Nanfang Hospital, Southern Medical University, Guangzhou, China

The non-canonical nuclear factor kappa-light-chain-enhancer of activated B cells (NF-κB) signaling pathway is an important component of NF-κB transcription complex. Activation of this pathway mediates the development and function of host immune system involved in inflammation and viral infection. During hepatitis B virus (HBV) infection, there is a complex interaction between infected hepatocytes and the immune cells, which can hinder antiviral immune responses and is associated with pathological changes in liver tissue. Consistently, the host immune system is closely related to the severity of liver damage and the level of viral replication. Previous studies indicated that the non-canonical NF-κB signaling pathway was affected by HBV and might play an important regulatory role in the antiviral immunity. Therefore, systematically elucidating the interplay between HBV and non-canonical NF-κB signaling will contribute the discovery of more potential therapeutic targets and novel drugs to treat HBV infection.

Keywords: hepatitis B virus (HBV), non-canonical NF-κB signaling, antiviral immunity, NF-κB-inducing kinase (NIK), p100/p52 (NFKB2)

OPEN ACCESS

Edited by:
Mengji Lu,
Essen University Hospital, Germany

Reviewed by:
Yuchen Xia,
Wuhan University, China
En-Qiang Chen,
Sichuan University, China

***Correspondence:**
Xiaoyong Zhang
xiaoyzhang@smu.edu.cn

Specialty section:
This article was submitted to Viral Immunology, a section of the journal Frontiers in Immunology

Received: *25 June 2021*
Accepted: *13 September 2021*
Published: *29 September 2021*

Citation:
Lu X, Chen Q, Liu H and Zhang X (2021) Interplay Between Non-Canonical NF-κB Signaling and Hepatitis B Virus Infection. Front. Immunol. 12:730684. doi: 10.3389/fimmu.2021.730684

INTRODUCTION

Nuclear factor kappa-light-chain-enhancer of activated B cells (NF-κB) encompasses an important family of transcription factors, can regulate the expression of multiple genes, and has been implicated in diverse biological processes including innate and adaptive immunity, inflammation, stress, immune cell development, and lymphatic organ formation (1, 2). Based on the components of the signaling cascade, NF-κB signaling pathways can be categorized as canonical or non-canonical (3). The canonical NF-κB pathway is rapid and transient, and mainly stimulated by proinflammatory cytokines such as IL-1β, tumor necrosis factor (TNF)-α, antigen ligands, and toll-like receptors (TLRs). Activation of the canonical NF-κB pathway relies on phosphorylation and ubiquitination of IκB kinase α/β (IKKα/β) causing the degradation of κB inhibitory factors (IκBs) protein, thereby countering inhibition of the nuclear transcription factor heterodimer RelA/p50 by IκBs (4, 5). The non-canonical NF-κB signaling pathway is slow and persistent, and generally activated by ligands of the TNF receptor superfamily, including lymphotoxin beta (LTB), CD40, OX40, RANK, TWEAK and B cell-activating factor (BAFF). These ligands stimulation induces NF-κB-inducing kinase (NIK, also called MAP3K14) stabilization and accumulation, results in IKKα

phosphorylation. Activated IKKα subsequently phosphorylates p100, triggering K48 linked ubiquitination and degradation of p100, generating p52 (also known as NFKB2). The nuclear translocation of RelB-p52 heterodimer then initiates the expression of target genes (4, 5) (**Figure 1**). NIK is a key molecule for non-canonical NF-κB pathway activation, and this process requires both NIK expression and kinase activity (6, 7). Expression of human NIK-dominant inactivated mutant (NIKKA, KK429/430AA) results in the blockage of the non-canonical NF-κB pathway (8).

It was reported that the alymphoplasia (aly/aly) mice with loss-of-function mutation of NIK exhibited aberrant development of spleen architecture and lymph nodes, impaired B cell proliferation and maturation, no formation of germinal center or isotype antibody switching in antigen-specific immune responses, and disordered thymus structure, and autoimmune inflammation in multiple organs (9, 10). Moreover, the phenotype of NFKB2 KO mice was similar to that of the aly/aly mice, with defects in splenic architecture, lymph nodes, and peripheral B cell maturation, as well as impaired antibody responses (11, 12). The severe immunodeficiencies observed in these mice strains indicates that the non-canonical NF-κB signaling pathway plays an essential role in multiple important biological processes, including the initiation and regulation of B cell and T cell immunity (13).

Host antiviral immunity is an important defense mechanism with respect to preventing virus invasion, and effectively clearing viral infection. Many RNA and DNA viruses, can regulate the activation of the non-canonical NF-κB pathway *via* different adaptor proteins, leading to the regulation of antiviral immunity (14). In contrast, some viruses can evade antiviral immunity by affecting the non-canonical NF-κB pathway. For example, the RNA virus EV71 upregulated NIK, the key protein of the non-canonical NF-κB pathway, to promote the secretion of inflammatory cytokines and apoptosis of EV71-infected cells (14, 15). Epstein-Barr virus, human T-lymphotropic virus 1, and Kaposi's sarcoma associated herpesvirus could activate the non-canonical NF-κB pathway by encoding corresponding oncogenic proteins (16–18). Currently, increasing evidence suggests that the non-canonical NF-κB pathway also plays roles in host responses to hepatitis B virus (HBV) infection. In this review, we discussed the interplay between HBV and the non-canonical NF-κB pathway.

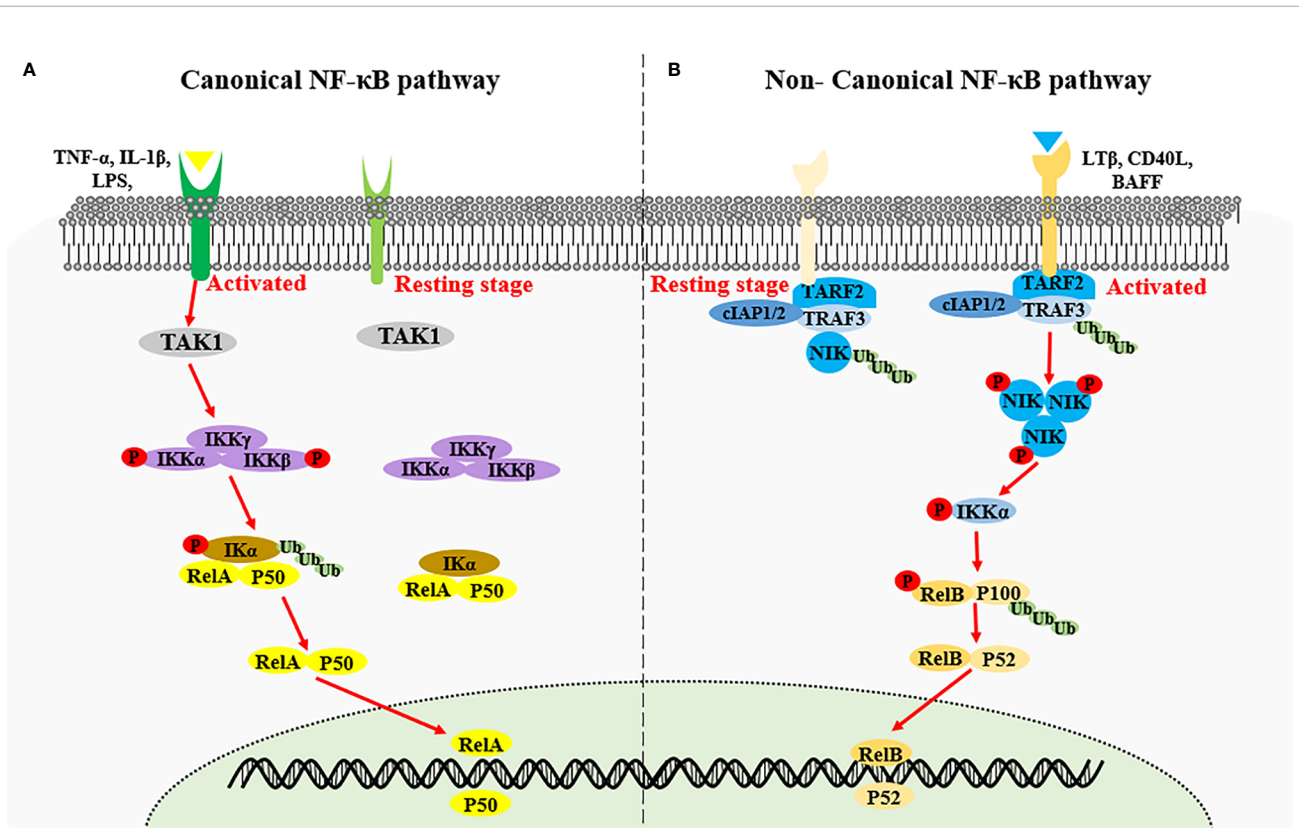

FIGURE 1 | Activation of canonical NF-κB signaling and non-canonical NF-κB signaling. **(A)** Canonical NF-κB signaling is stimulated by proinflammatory cytokines such as IL-1β, TNF-α and LPS, inducing the activation of IKK complex by TAK1. The IKK complex then phosphorylates the IκB kinase α/β (IKKα/β), causing the ubiquitin-dependent degradation of κB inhibitory factors (IκBs) protein, thereby triggering the nuclear transcription factor heterodimer RelA/p50. **(B)** Non-canonical NF-κB signaling is activated by the specific TNFR superfamily. Receptor activation induce the recruitment of TRAF3-TRAF2-cIAP1/2 receptor complex, followed by the degradation of TRAF3 *via* ubiquitination, resulting in the stabilization and accumulation of NIK. NIK phosphorylates IKKα which in turn phosphorate p100, triggering the ubiquitination and degradation of p100 to generate p52 and the nuclear transduction of RelB-p52 heterodimer.

REGULATION OF NON-CANONICAL NF-ΚB SIGNALING PATHWAY BY HBV INFECTION

HBV is a DNA virus that encodes multiple proteins that affect the activation of the non-canonical NF-κB pathway, thus enabling regulation of the host defense response. The type I interferon (IFN) system, an indispensable part of the innate immune response to HBV, is involved in an immediate antiviral response *via* the induction of numerous functional proteins against the viral life cycle, and activates the adaptive immune response (19). TBK1 can function as a positive and negative regulator of the non-canonical NF-κB pathway (20). HBV polymerase (Pol) can evidently inhibit the phosphorylation, dimerization, and nuclear translocation of IRF3, as well as IFN-β expression at the TBK1/IKKε level (19). Activating NIK promote phosphorylation of IRF3 to produce type I interferon (21, 22). Therefore, the mechanism by which HBV pol protein inhibits IFN-β production in human hepatocytes may also be associated with the level of non-canonical NF-κB pathway activation. Liu et al. (23) reported that Pol protein did not alter the level of NF-κB expression, but could prevent the activation of the non-canonical NF-κB pathway required for IFN-β activation by inhibiting the nuclear translocation of RelB/p52 and NF-κB subunits in hepatoma cells. These studies suggested that Pol protein could inhibit IFN-β production, which may be associated with the non-canonical NF-κB pathway in hepatocytes. However, additional studies showed some conflicting results. As observed in chronic HBV infection patients, the IFN-stimulated genes (ISGs) were not activated in liver tissues (24). In addition, results of the *in vitro* models of HBV-infected hepatocytes also found that HBV infection did not induce type I and III IFNs, and the downstream ISGs (25, 26), which further supported the inability of HBV to induce IFN response. Thus, the relationship between Pol protein, IFN signaling and non-canonical NF-κB pathway remains to be explored.

HBx protein plays a vital role in HBV replication, and is a potential inducer for hepatocellular carcinoma development (HCC) (27, 28). Previous studies indicate that HBx induced the phosphorylation and degradation of intracellular IkBα to activate the classical NF-κB pathway, accompanied with slight decrease in the level of p100 protein, suggesting that HBx may be involved in activation of the non-canonical NF-κB pathway (29, 30). Kim et al. (31) reported that HBx might disturb the activation of the non-canonical NF-κB pathway *via* a NIK-IKK-IkB-dependent mechanism in the liver, and result in the induction of inflammatory response or hepatic oncogenesis by stimulating hepatocyte proliferation. But whether the effect mediated by HBx is valid in the HBV infection need to be further studied.

HBV e antigen (HBeAg), a secreted protein and not required for viral replication, is thought to play an immunoregulatory role and promote viral persistence during viral infection. Researches by Wang et al. (32) has found that HBeAg can associate with NEMO, the regulatory subunit for IκB kinase (IKK) that controls the NF-κB signaling pathway, and thereby inhibited TRAF6-mediated K63-linked ubiquitination of NEMO induced by IL-1β, resulting in the downregulation of NF-κB activity and increased virus replication. HBeAg suppresses LPS-induced NLRP3 inflammasome activation, pro-IL-1β expression and IL-1β production in kuffer cells not only *via* inhibiting NF-κB phosphorylation but inhibiting ROS production (33). The roles of HBeAg in regulating the NF-κB pathway to affect host immune response are controversial during the infection of HBV. In addition, the HBeAg affected NEMO mainly functions in canonical NF-κB signaling pathway. Nevertheless, canonical and non-canonical NF-κB activation pathways are connected *via* many crosstalk mechanisms. Therefore, HBeAg affecting the host immune response also cannot exclude the role of non-canonical NF-κB pathway.

REGULATION OF HBV INFECTION BY NON-CANONICAL NF-ΚB SIGNALING PATHWAY

Abnormal host immune function and continuous HBV replication are the main causes of disease progression in patients with chronic hepatitis B (CHB) (34). Concurrent continuous HBV replication and the activation of inflammatory pathways lead to chronic liver damage (35). Immune system is very important for the elimination of HBV, but CHB patients tend to exhibit defective innate and adaptive immune function, and cannot effectively remove viral products in the liver. Previous studies indicated that non-classical NF-κB pathway in the hepatocytes and immune cells played an important role in control of HBV replication *in vitro* and clearance of HBV *in vivo* (**Figure 2**).

Hepatocytes-Intrinsic Non-Canonical NF-κB Signaling Pathway

HBV replication in hepatocytes may be related to NIK-dependent activation of the non-classical NF-κB pathway. Microarray analysis and western blotting validation suggested that mRNA and protein levels of TRAF2 and NIK in primary hepatocytes are upregulated during the early stage of HBV infection (36). Lymphotoxin beta receptor, a member of the TNF receptor superfamily, is able to activate the NIK-dependent non-canonical NF-κB pathway. Activation of this receptor could induce the expression of APOBEC3A/3B protein, which mediated deamination on the negative chain of cccDNA to degrade it (37). The above results suggested that the non-canonical NF-κB pathway activation in hepatocytes might exert a direct anti-HBV effect.

Cellular inhibitor of apoptosis proteins (cIAPs) are a family of highly conserved endogenous anti-apoptotic molecules (38). In the resting state, cIAP1/2 uses TRAF2 as an adaptor protein to connect with NIK binding protein TRAF3 to form a TRAF3-TRAF2-cIAP1/2 multi-subunit ubiquitin ligase complex, resulting in very low protein levels of cellular endogenous NIK (39). Degradation of cIAPs or loss of TRAF2 can continuously activate the NIK-dependent non-canonical NF-κB signaling

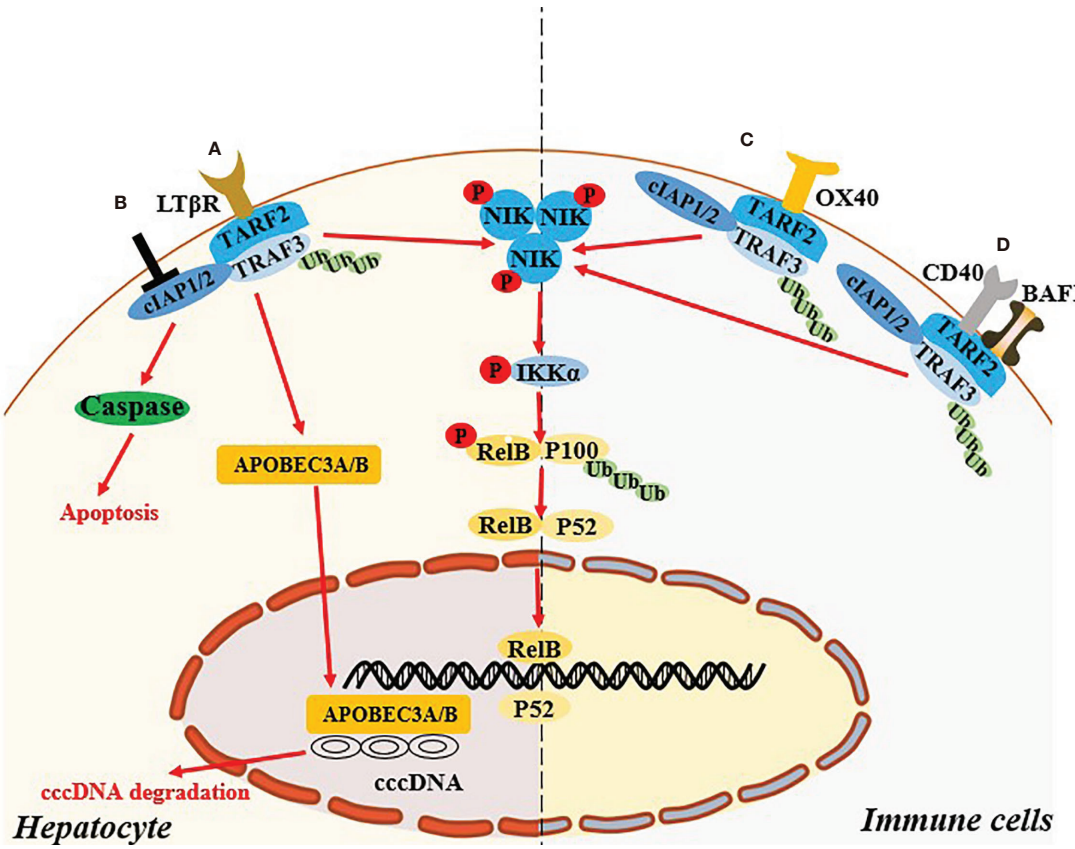

FIGURE 2 | Non-canonical NF-κB signaling pathway regulates the HBV infection. **(A)** In hepatocyte, activation of LTB receptor in hepatocyte mediates the non-canonical NF-κB signaling pathway and induce the up-regulated expression of APOBCE3A/B protein, which degrade cccDNA. **(B)** Targeting cIAPs also mediate the activating the NIK-dependent non-canonical NF-κB signaling pathway and exert the antiviral effect in hepatocyte *via* TNF-mediated death of infected cells. **(C, D)** Specific ligation of OX40, BAFFR or CD40 in immune cells might recover the exhausted immune function during HBV infection through the activation of the NIK-dependent non-canonical NF-κB signaling pathway.

pathway (39). Ebert et al. (40) reported that cIAPs can impair viral clearance by preventing TNF-mediated death of infected cells, and mice with hepatocyte-specific deficiency of cIAPs expression promoted the clearance chronic HBV infection. Moreover, birinapant, a chemical inhibitor of cIAPs, could reduce HBV DNA and hepatitis B surface antigen levels in serum, and induce hepatitis B core antigen-positive hepatocyte apoptosis in HBV persistence mouse model (41). Therefore, whether the antiviral effect mediated by targeting cIAPs is related to activation of the NIK-mediated non-canonical NF-κB signaling pathway need further investigation.

Immune Cells-Intrinsic Non-Canonical NF- κB Signaling Pathway

Abnormal expression and function of specific ligands and receptors involved in activation of the non-classical NF-κB pathway in the immune cells might be related to the chronicity of HBV infection. OX40 (also known as CD134) is an important costimulatory molecule in T cells, and its ligand OX40L (also known as CD252) is mainly expressed on antigen-presenting cells. OX40 ligation can promote T cell phenotypic transformation, maintain the activation state, and promote the proliferation of effector T cells and memory T cells, while also inhibiting the differentiation and activity of regulatory T cells (Tregs) (42, 43). Interestingly, studies suggest that the key to determining antiviral immunity is the expression of the costimulatory molecule OX40L on hepatic innate immune cells, and the expression of OX40L is positively correlated with age (44). OX40 agonists can increase the HBV clearance rate in a young mouse model of hepatitis B, as well as the strength of T cell responses in young mice and adult mice that were exposed to HBV when they were young and developed a CHB serological profile (44). Moreover, in adult humans HBV clearance is associated with increased OX40 expression in peripheral $CD4^+$ T cells (44). In a recent study OX40 was highly expressed on $CD4^+$ T cells in the immune microenvironment of HBV-related HCC (45). OX40 agonists combined with PD-1 blockers can enhance the function of HBV-specific $CD4^+$ T cells (42). The above studies suggest that in innate immune cells and T cells the OX40-mediated non-canonical NF-κB pathway may participate

in HBV clearance by affecting the function of immune cells. In a liver injury model in HBsAg transgenic mice mediated by natural killer (NK) cells induced with low or high doses of concanavalin A, the proportion of $CD4^+CD25^+FoxP3^+$ Tregs in the liver increases, and the proportion of restored Tregs continued to increase with the development of liver damage (46). The mechanism of reducing liver injury in HBs transgenic mice is related to the direct inhibition of NK cell-mediated hepatotoxicity by Tregs *via* OX40/OX40L interaction in cell-cell contact (46). In patients with CHB the immune microenvironment is characterized by the exhaustion of virus-specific T cells and an increase in negatively regulated immune cells such as Tregs. Therefore, this may also be related to the non-classical NF-κB pathway regulated by OX40/OX40L.

BAFF is an essential cytokine for the activation of B lymphocytes, and BAFF receptor is expressed on B cells (47). Interaction between BAFF and BAFF receptor can also activate the non-canonical NF-κB signaling pathway, and its mediated activation plays an important role in regulating the survival and maturation of peripheral B cells (48). Studies indicate that in CHB patients' serum BAFF is maintained at a high level, leading to excessive activation of B cells, thus changing T cell functions (upregulating PD-1, Tim-3, and Lag-3, *i.e.*, exhaustion phenotypes) and reducing reactions to PEG-IFN (49, 50). Notably however, the mechanisms by which BAFF mediates the chronicity of HBV require further clarification. Studies suggest that *in vitro* administration of CD40L signals can partially restore the function of hepatitis B surface antigen (HBsAg) -specific B cells (51). CD40-CD40L interaction can induce activation of the non-canonical NF-κB pathway in mouse splenic B cells (52). The above results suggest that non-canonical NF-κB pathway dysregulation in immune cells of patients with CHB may be related to the failure of HBV clearance and disease progression.

NIK is a key adaptor protein associated with activation of the non-classical NF-κB pathway, and may also participate in the development of CHB disease by affecting the function of immune cells. In previous studies NIK knockout in dendritic cells affected antigen presentation to $CD8^+$ T cells (53). T cell-specific NIK deficiency induces naive T cells to differentiate into effector T cells and memory T cells (54, 55). Moreover, in T cell-specific NIK-deficient mice the phosphorylation of Zap70, LAT, AKT, ERK1/2, and PLCγ is hindered, thereby blocking the T cell receptor signaling pathway (56). The continuous expression of viral antigens and the hepatic inflammatory microenvironment can downregulate the function and proportion of HBV-specific $CD4^+$ cells, $CD8^+$ T cells, dendritic cells, NK cells, and NK T cells in CHB patients. Therefore, the exhaustion of immune function in CHB patients may be related to the non-canonical NF-κB pathway dysregulation caused by downregulation of NIK in immune cells such as dendritic cells and T cells. Whether the inability of antiviral immunity in CHB patients is related to the activation of the non-canonical NF-κB pathway in these immune cells remains to be determined. In addition, IFN-γ and TNF-α produced by T cells can degrade the cccDNA through deamination, but not the cytolysis in hepatocyte, suggesting that the non-classical NF-κB pathway has a complex regulatory network in hosts with normal immunity (57).

CONCLUSION

To date studies indicate that the non-canonical NF-κB signaling pathway plays an important role in the development of the immune system and triggering inflammation, but research on the regulatory role of the HBV life cycle and host antiviral effects remains largely unknown. A variety of ligands and receptors, adaptor proteins, and regulatory factors involved in the formation of non-canonical NF-κB signaling pathway might play important roles in the establishment and development of HBV disease. Therefore, in-depth mechanistic studies investigating the interplay between HBV and non-canonical NF-κB signaling may provide potential strategies for HBV treatment.

AUTHOR CONTRIBUTIONS

XZ, XL, QC, and HL collected the data and drafted the manuscript. XZ made critical revision of the manuscript for important intellectual content. All authors contributed to the article and approved the submitted version.

FUNDING

This review was partly supported by grants from the National Natural Science Foundation of China (No. 81871664 and No.81970539).

REFERENCES

1. Zhang Q, Lenardo MJ, Baltimore D. 30 Years of NF-Kappab: A Blossoming of Relevance to Human Pathobiology. *Cell* (2017) 168:37–57. doi: 10.1016/j.cell.2016.12.012
2. Hayden MS, Ghosh S. Shared Principles in NF-kappaB Signaling. *Cell* (2008) 132:344–62. doi: 10.1016/j.cell.2008.01.020
3. Sun SC. The non-Canonical NF-kappaB Pathway in Immunity and Inflammation. *Nat Rev Immunol* (2017) 17:545–58. doi: 10.1038/nri.2017.52
4. Qu Z, Xiao G. Systematic Detection of Noncanonical NF-kappaB Activation. *Methods Mol Biol* (2015) 1280:121–54. doi: 10.1007/978-1-4939-2422-6_8
5. Sun SC. Non-Canonical NF-kappaB Signaling Pathway. *Cell Res* (2011) 21:71–85. doi: 10.1038/cr.2010.177
6. Senftleben U, Cao Y, Xiao G, Greten FR, Krahn G, Bonizzi G, et al. Activation by IKKalpha of a Second, Evolutionary Conserved, NF-Kappa B Signaling Pathway. *Science* (2001) 293:1495–9. doi: 10.1126/science.1062677
7. Thu YM, Richmond A. NF-kappaB Inducing Kinase: A Key Regulator in the Immune System and in Cancer. *Cytokine Growth Factor Rev* (2010) 21:213–26. doi: 10.1016/j.cytogfr.2010.06.002
8. Smith C, Andreakos E, Crawley JB, Brennan FM, Feldmann M, Foxwell BM. NF-kappaB-Inducing Kinase is Dispensable for Activation of NF-kappaB in Inflammatory Settings But Essential for Lymphotoxin Beta Receptor

Activation of NF-kappaB in Primary Human Fibroblasts. *J Immunol* (2001) 167:5895–903. doi: 10.4049/jimmunol.167.10.5895
9. Miyawaki S, Nakamura Y, Suzuka H, Koba M, Yasumizu R, Ikehara S, et al. A New Mutation, Aly, That Induces a Generalized Lack of Lymph Nodes Accompanied by Immunodeficiency in Mice. *Eur J Immunol* (1994) 24:429–34. doi: 10.1002/eji.1830240224
10. Koike R, Nishimura T, Yasumizu R, Tanaka H, Hataba Y, Hataba Y, et al. The Splenic Marginal Zone is Absent in Alymphoplastic Aly Mutant Mice. *Eur J Immunol* (1996) 26:669–75. doi: 10.1002/eji.1830260324
11. Franzoso G, Carlson L, Poljak L, Shores EW, Epstein S, Leonardi A, et al. Mice Deficient in Nuclear Factor (NF)-Kappa B/p52 Present With Defects in Humoral Responses, Germinal Center Reactions, and Splenic Microarchitecture. *J Exp Med* (1998) 187:147–59. doi: 10.1084/jem.187.2.147
12. Caamano JH, Rizzo CA, Durham SK, Barton DS, Raventos-Suarez C, Snapper CM, et al. Nuclear Factor (NF)-Kappa B2 (P100/P52) is Required for Normal Splenic Microarchitecture and B Cell-Mediated Immune Responses. *J Exp Med* (1998) 187:185–96. doi: 10.1084/jem.187.2.185
13. Shinkura R, Matsuda F, Sakiyama T, Tsubata T, Hiai H, Paumen M, et al. Defects of Somatic Hypermutation and Class Switching in Alymphoplasia (Aly) Mutant Mice. *Int Immunol* (1996) 8:1067–75. doi: 10.1093/intimm/8.7.1067
14. Struzik J, Szulc-Dabrowska L. Manipulation of Non-Canonical NF-kappaB Signaling by Non-Oncogenic Viruses. *Arch Immunol Ther Exp (Warsz)* (2019) 67:41–8. doi: 10.1007/s00005-018-0522-x
15. Khatiwada S, Delhon G, Nagendraprabhu P, Chaulagain S, Luo S, Diel DG, et al. A Parapoxviral Virion Protein Inhibits NF-kappaB Signaling Early in Infection. *PloS Pathog* (2017) 13:e1006561. doi: 10.1371/journal.ppat.1006561
16. Sun SC, Cesarman E. NF-kappaB as a Target for Oncogenic Viruses. *Curr Top Microbiol Immunol* (2011) 349:197–244. doi: 10.1007/82_2010_108
17. Bagneris C, Ageichik AV, Cronin N, Wallace B, Collins M, Boshoff C, et al. Crystal Structure of a Vflip-IKKgamma Complex: Insights Into Viral Activation of The IKK Signalosome. *Mol Cell* (2008) 30:620–31. doi: 10.1016/j.molcel.2008.04.029
18. Karrer U, Althage A, Odermatt B, Roberts CW, Korsmeyer SJ, Miyawaki S, et al. On the Key Role of Secondary Lymphoid Organs in Antiviral Immune Responses Studied in Alymphoplastic (Aly/Aly) and Spleenless (Hox11(-)/-) Mutant Mice. *J Exp Med* (1997) 185:2157–70. doi: 10.1084/jem.185.12.2157
19. Yu S, Chen J, Wu M, Chen H, Kato N, Yuan Z. Hepatitis B Virus Polymerase Inhibits RIG-I- and Toll-Like Receptor 3-Mediated Beta Interferon Induction in Human Hepatocytes Through Interference With Interferon Regulatory Factor 3 Activation and Dampening of the Interaction Between TBK1/IKKepsilon and DDX3. *J Gen Virol* (2010) 91:2080–90. doi: 10.1099/vir.0.020552-0
20. Yu H, Lin L, Zhang Z, Zhang H, Hu H. Targeting NF-kappaB Pathway for the Therapy of Diseases: Mechanism and Clinical Study. *Signal Transduct Target Ther* (2020) 5:209. doi: 10.1038/s41392-020-00312-6
21. Chen B, Li C, Yao J, Shi L, Liu W, Wang F, et al. Zebrafish NIK Mediates IFN Induction by Regulating Activation of IRF3 and NF-Kappab. *J Immunol* (2020) 204:1881–91. doi: 10.4049/jimmunol.1900561
22. Parvatiyar K, Pindado J, Dev A, Aliyari SR, Zaver SA, Gerami H, et al. A TRAF3-NIK Module Differentially Regulates DNA *vs* RNA Pathways in Innate Immune Signaling. *Nat Commun* (2018) 9:2770. doi: 10.1038/s41467-018-05168-7
23. Liu D, Wu A, Cui L, Hao R, Wang Y, He J, et al. Hepatitis B Virus Polymerase Suppresses NF-kappaB Signaling by Inhibiting the Activity of IKKs via Interaction With Hsp90beta. *PloS One* (2014) 9:e91658. doi: 10.1371/journal.pone.0091658
24. Suslov A, Boldanova T, Wang X, Wieland S, Heim MH. Hepatitis B Virus Does Not Interfere With Innate Immune Responses in the Human Liver. *Gastroenterology* (2018) 154:1778–90. doi: 10.1053/j.gastro.2018.01.034
25. Mutz P, Metz P, Lempp FA, Bender S, Qu B, Schoneweis K, et al. HBV Bypasses the Innate Immune Response and Does Not Protect HCV From Antiviral Activity of Interferon. *Gastroenterology* (2018) 154:1791–804. doi: 10.1053/j.gastro.2018.01.044
26. Cheng X, Xia Y, Serti E, Block PD, Chung M, Chayama K, et al. Hepatitis B Virus Evades Innate Immunity of Hepatocytes But Activates Cytokine Production by Macrophages. *Hepatology* (2017) 66:1779–93. doi: 10.1002/hep.29348
27. Chen HS, Kaneko S, Girones R, Anderson RW, Hornbuckle WE, Tennant BC, et al. The Woodchuck Hepatitis Virus X Gene is Important for Establishment of Virus Infection in Woodchucks. *J Virol* (1993) 67:1218–26. doi: 10.1128/jvi.67.3.1218-1226.1993
28. Benn J, Schneider RJ. Hepatitis B Virus HBx Protein Deregulates Cell Cycle Checkpoint Controls. *Proc Natl Acad Sci USA* (1995) 92:11215–9. doi: 10.1073/pnas.92.24.11215
29. Guo SP, Wang WL, Zhai YQ, Zhao YL. Expression of Nuclear Factor-Kappa B in Hepatocellular Carcinoma and its Relation With the X Protein of Hepatitis B Virus. *World J Gastroenterol* (2001) 7:340–4. doi: 10.3748/wjg.v7.i3.340
30. Su F, Schneider RJ. Hepatitis B Virus HBx Protein Activates Transcription Factor NF-kappaB by Acting On Multiple Cytoplasmic Inhibitors of Rel-Related Proteins. *J Virol* (1996) 70:4558–66. doi: 10.1128/jvi.70.7.4558-4566.1996
31. Kim WH, Hong F, Jaruga B, Hu Z, Fan S, Liang TJ, et al. Additive Activation of Hepatic NF-kappaB by Ethanol and Hepatitis B Protein X (HBX) or HCV Core Protein: Involvement of TNF-Alpha Receptor 1-Independent and -Dependent Mechanisms. *FASEB J* (2001) 15:2551–3. doi: 10.1096/fj.01-0217
32. Wang Y, Cui L, Yang G, Zhan J, Guo L, Chen Y, et al. Hepatitis B E Antigen Inhibits NF-kappaB Activity by Interrupting K63-Linked Ubiquitination of NEMO. *J Virol* (2019) 93:e00667-18. doi: 10.1128/JVI.00667-18
33. Yu X, Lan P, Hou X, Han Q, Lu N, Li T, et al. HBV Inhibits LPS-Induced NLRP3 Inflammasome Activation and IL-1beta Production via Suppressing the NF-kappaB Pathway and ROS Production. *J Hepatol* (2017) 66:693–702. doi: 10.1016/j.jhep.2016.12.018
34. Chen CH, Chen CY, Wang JH, Lai HC, Hung CH, Lu SN, et al. Comparison of Incidence of Hepatocellular Carcinoma Between Chronic Hepatitis B Patients With Cirrhosis Treated With Entecavir or Tenofovir in Taiwan - a Retrospective Study. *Am J Cancer Res* (2020) 10:3882–95.
35. Bertoletti A, Ferrari C. Innate and Adaptive Immune Responses in Chronic Hepatitis B Virus Infections: Towards Restoration of Immune Control of Viral Infection. *Gut* (2012) 61:1754–64. doi: 10.1136/gutjnl-2011-301073
36. Ryu HM, Park SG, Yea SS, Jang WH, Yang YI, Jung G. Gene Expression Analysis of Primary Normal Human Hepatocytes Infected With Human Hepatitis B Virus. *World J Gastroenterol* (2006) 12:4986–95. doi: 10.3748/wjg.v12.i31.4986
37. Lucifora J, Xia Y, Reisinger F, Zhang K, Stadler D, Cheng X, et al. Specific and Nonhepatotoxic Degradation of Nuclear Hepatitis B Virus cccDNA. *Science* (2014) 343:1221–8. doi: 10.1126/science.1243462
38. Liu H, Hou J, Zhang X. Targeting cIAPs, a New Option for Functional Cure of Chronic Hepatitis B Infection? *Virol Sin* (2018) 33:459–61. doi: 10.1007/s12250-018-0062-x
39. Zarnegar BJ, Wang Y, Mahoney DJ, Dempsey PW, Cheung HH, He J, et al. Noncanonical NF-kappaB Activation Requires Coordinated Assembly of a Regulatory Complex of the Adaptors Ciap1, Ciap2, TRAF2 and TRAF3 and the Kinase NIK. *Nat Immunol* (2008) 9:1371–8. doi: 10.1038/ni.1676
40. Vince JE, Wong WW, Khan N, Feltham R, Chau D, Ahmed AU, et al. IAP Antagonists Target Ciap1 to Induce TNFalpha-Dependent Apoptosis. *Cell* (2007) 131:682–93. doi: 10.1016/j.cell.2007.10.037
41. Ebert G, Preston S, Allison C, Cooney J, Toe JG, Stutz MD, et al. Cellular Inhibitor of Apoptosis Proteins Prevent Clearance of Hepatitis B Virus. *Proc Natl Acad Sci USA* (2015) 112:5797–802. doi: 10.1073/pnas.1502390112
42. Shrimali RK, Ahmad S, Verma V, Zeng P, Ananth S, Gaur P, et al. Concurrent PD-1 Blockade Negates the Effects of OX40 Agonist Antibody in Combination Immunotherapy Through Inducing T-Cell Apoptosis. *Cancer Immunol Res* (2017) 5:755–66. doi: 10.1158/2326-6066.CIR-17-0292
43. Xiao X, Balasubramanian S, Liu W, Chu X, Wang H, Taparowsky EJ, et al. OX40 Signaling Favors the Induction of T(H)9 Cells and Airway Inflammation. *Nat Immunol* (2012) 13:981–90. doi: 10.1038/ni.2390
44. Publicover J, Gaggar A, Jespersen JM, Halac U, Johnson AJ, Goodsell A, et al. An OX40/OX40L Interaction Directs Successful Immunity to Hepatitis B Virus. *Sci Transl Med* (2018) 10:eaah5766. doi: 10.1126/scitranslmed.aah5766
45. Lim CJ, Lee YH, Pan L, Lai L, Chua C, Wasser M, et al. Multidimensional Analyses Reveal Distinct Immune Microenvironment in Hepatitis B Virus-Related Hepatocellular Carcinoma. *Gut* (2019) 68:916–27. doi: 10.1136/gutjnl-2018-316510
46. Chen Y, Sun R, Wu X, Cheng M, Wei H, Tian Z. CD4+CD25+ Regulatory T Cells Inhibit Natural Killer Cell Hepatocytotoxicity of Hepatitis B Virus Transgenic Mice via Membrane-Bound TGF-Beta and OX40. *J Innate Immun* (2016) 8:30–42. doi: 10.1159/000431150

47. Claudio E, Brown K, Park S, Wang H, Siebenlist U. BAFF-Induced NEMO-Independent Processing of NF-Kappa B2 in Maturing B Cells. *Nat Immunol* (2002) 3:958–65. doi: 10.1038/ni842
48. Schiemann B, Gommerman JL, Vora K, Cachero TG, Shulga-Morskaya S, Dobles M, et al. An Essential Role for BAFF in the Normal Development of B Cells Through a BCMA-Independent Pathway. *Science* (2001) 293:2111–4. doi: 10.1126/science.1061964
49. Yang C, Li N, Wang Y, Zhang P, Zhu Q, Li F, et al. Serum Levels of B-Cell Activating Factor in Chronic Hepatitis B Virus Infection: Association With Clinical Diseases. *J Interferon Cytokine Res* (2014) 34:787–94. doi: 10.1089/jir.2014.0032
50. Khlaiphuengsin A, Chuaypen N, Hirankarn N, Avihingsanon A, Crane M, Lewin SR, et al. Circulating BAFF and CXCL10 Levels Predict Response to Pegylated Interferon in Patients With HBeAg-Positive Chronic Hepatitis B. *Asian Pac J Allergy Immunol* (2019) 39:129–35. doi: 10.12932/AP-050718-0365
51. Salimzadeh L, Le Bert N, Dutertre CA, Gill US, Newell EW, Frey C, et al. PD-1 Blockade Partially Recovers Dysfunctional Virus-Specific B Cells in Chronic Hepatitis B Infection. *J Clin Invest* (2018) 128:4573–87. doi: 10.1172/JCI121957
52. Coope HJ, Atkinson PG, Huhse B, Belich M, Janzen J, Holman MJ, et al. CD40 Regulates the Processing of NF-Kappab2 P100 to P52. *EMBO J* (2002) 21:5375–85. doi: 10.1093/emboj/cdf542
53. Lind EF, Ahonen CL, Wasiuk A, Kosaka Y, Becher B, Bennett KA, et al. Dendritic Cells Require the NF-Kappab2 Pathway for Cross-Presentation of Soluble Antigens. *J Immunol* (2008) 181:354–63. doi: 10.4049/jimmunol.181.1.354
54. Rowe AM, Murray SE, Raue HP, Koguchi Y, Slifka MK. Parker DC. A Cell-Intrinsic Requirement for NF-kappaB-Inducing Kinase in CD4 and CD8 T Cell Memory. *J Immunol* (2013) 191:3663–72. doi: 10.4049/jimmunol.1301328
55. Li Y, Wang H, Zhou X, Xie X, Chen X, Jie Z, et al. Cell Intrinsic Role of NF-kappaB-Inducing Kinase in Regulating T Cell-Mediated Immune and Autoimmune Responses. *Sci Rep* (2016) 6:22115. doi: 10.1038/srep22115
56. Lacher SM, Thurm C, Distler U, Mohebiany AN, Israel N, Kitic M, et al. NF-kappaB Inducing Kinase (NIK) is an Essential Post-Transcriptional Regulator of T-Cell Activation Affecting F-Actin Dynamics and TCR Signaling. *J Autoimmun* (2018) 94:110–21. doi: 10.1016/j.jaut.2018.07.017
57. Xia Y, Stadler D, Lucifora J, Reisinger F, Webb D, Hosel M, et al. Interferon-Gamma and Tumor Necrosis Factor-Alpha Produced by T Cells Reduce the HBV Persistence Form, cccDNA, Without Cytolysis. *Gastroenterology* (2016) 150:194–205. doi: 10.1053/j.gastro.2015.09.026

Conflict of Interest: The authors declare that the research was conducted in the absence of any commercial or financial relationships that could be construed as a potential conflict of interest.

Publisher's Note: All claims expressed in this article are solely those of the authors and do not necessarily represent those of their affiliated organizations, or those of the publisher, the editors and the reviewers. Any product that may be evaluated in this article, or claim that may be made by its manufacturer, is not guaranteed or endorsed by the publisher.

frontiers in Immunology

ORIGINAL RESEARCH
published: 04 October 2021
doi: 10.3389/fimmu.2021.745802

Agonistic Activation of Cytosolic DNA Sensing Receptors in Woodchuck Hepatocyte Cultures and Liver for Inducing Antiviral Effects

Manasa Suresh[1], *Bin Li*[1], *Xu Huang*[1], *Kyle E. Korolowicz*[1], *Marta G. Murreddu*[1], *Severin O. Gudima*[2] *and Stephan Menne*[1]*

[1] *Department of Microbiology & Immunology, Georgetown University Medical Center, Washington, DC, United States,*
[2] *Department of Microbiology, Molecular Genetics & Immunology, University of Kansas Medical Center, Kansas City, KS, United States*

OPEN ACCESS

Edited by:
Anna D. Kosinska, Helmholtz-Gemeinschaft Deutscher Forschungszentren (HZ), Germany

Reviewed by:
Sonya MacParland, University of Toronto, Canada
Baoju Wang, Huazhong University of Science and Technology, China

***Correspondence:**
Stephan Menne
Stephan.Menne@georgetown.edu

Specialty section:
This article was submitted to Viral Immunology, a section of the journal Frontiers in Immunology

Received: *22 July 2021*
Accepted: *13 September 2021*
Published: *04 October 2021*

Citation:
Suresh M, Li B, Huang X, Korolowicz KE, Murreddu MG, Gudima SO and Menne S (2021) Agonistic Activation of Cytosolic DNA Sensing Receptors in Woodchuck Hepatocyte Cultures and Liver for Inducing Antiviral Effects. Front. Immunol. 12:745802. doi: 10.3389/fimmu.2021.745802

Immune modulation for the treatment of chronic hepatitis B (CHB) has gained more traction in recent years, with an increasing number of compounds designed for targeting different host pattern recognition receptors (PRRs). These agonistic molecules activate the receptor signaling pathway and trigger an innate immune response that will eventually shape the adaptive immunity for control of chronic infection with hepatitis B virus (HBV). While definitive recognition of HBV nucleic acids by PRRs during viral infection still needs to be elucidated, several viral RNA sensing receptors, including toll-like receptors 7/8/9 and retinoic acid inducible gene-I-like receptors, are explored preclinically and clinically as possible anti-HBV targets. The antiviral potential of viral DNA sensing receptors is less investigated. In the present study, treatment of primary woodchuck hepatocytes generated from animals with CHB with HSV-60 or poly(dA:dT) agonists resulted in increased expression of interferon-gamma inducible protein 16 (IFI16) or Z-DNA-binding protein 1 (ZBP1/DAI) and absent in melanoma 2 (AIM2) receptors and their respective adaptor molecules and effector cytokines. Cytosolic DNA sensing receptor pathway activation correlated with a decline in woodchuck hepatitis virus (WHV) replication and secretion in these cells. Combination treatment with HSV-60 and poly (dA:dT) achieved a superior antiviral effect over monotreatment with either agonist that was associated with an increased expression of effector cytokines. The antiviral effect, however, could not be enhanced further by providing additional type-I interferons (IFNs) exogenously, indicating a saturated level of effector cytokines produced by these receptors following agonism. In WHV-uninfected woodchucks, a single poly(dA:dT) dose administered *via* liver-targeted delivery was well-tolerated and induced the intrahepatic expression of ZBP1/DAI and AIM2 receptors and their effector cytokines, IFN-β and interleukins 1β and 18. Receptor agonism also resulted in increased IFN-γ secretion of peripheral blood cells. Altogether, the effect on WHV replication and secretion following *in vitro* activation of IFI16, ZBP1/DAI, and AIM2 receptor pathways suggested an antiviral benefit of targeting more than one cytosolic DNA receptor. In addition, the *in vivo*

activation of ZBP1/DAI and AIM2 receptor pathways in liver indicated the feasibility of the agonist delivery approach for future evaluation of therapeutic efficacy against HBV in woodchucks with CHB.

Keywords: pattern recognition receptors, hepatitis B virus, viral DNA sensing receptors, innate immune response, woodchuck, chronic hepatitis B

INTRODUCTION

Hepatitis B virus (HBV) is the leading cause of the global hepatitis burden, with an estimated 296 million chronic carriers and an annual virus-related death toll of 820,000 (1). HBV infection acquired early in life by mother-to-child transfer or as an infant will progress to chronicity in more than 95% of cases and carriers have a high risk of developing serious liver disorders, including chronic hepatitis B (CHB), cirrhosis, and liver cancer or hepatocellular carcinoma (HCC) (2). HBV is a member of the *hepadnaviridae* family and replicates in hepatocytes by forming a reservoir of genomic DNA in the nucleus. This so-called covalently-closed circular (ccc) DNA molecule serves as the template for replication intermediate products and viral proteins. The complex HBV life cycle and the continuous replenishment of the cccDNA pool in infected hepatocytes are significant challenges for anti-HBV drug development. The current treatment options for CHB are suboptimal and rarely lead to a cure of the infection. The available nucleos(t)ide analogs are well-tolerated, but do not target the cccDNA directly, and therefore treatment cessation leads to viral rebound making their life-long administration necessary (3, 4). While systemic pegylated interferon (IFN) alpha therapy can directly target the cccDNA, it is effective only in a subset of treated patients and frequently associated with severe side effects (3, 4). In recent years, anti-HBV drug discovery has focused on direct acting antivirals and immunomodulators for targeting different steps of the HBV life cycle or for restoring the dysfunctional antiviral immune response present in patients with CHB, respectively (5).

Modulating the immune response against CHB has been explored by using several approaches, including agonistic activation of innate immune receptors, treatment with checkpoint inhibitors, adoptive transfer of T-cells, and administration of therapeutic vaccines (6–9). These approaches have demonstrated promising results in preclinical studies as they induced HBV-specific immune responses, and thus were able to overcome the impaired immunity associated with CHB. However, some of the challenges that need to be addressed in regard to immunomodulation are the systemic toxicity due to non-specific delivery of compounds and the risk of uncontrollable liver damage (i.e., acute liver failure) when breaking immune tolerance (10, 11). Furthermore, the lack of small, immunocompetent laboratory animal models for testing experimental therapeutics against HBV is an additional hurdle. The infection of the Eastern woodchuck (*Marmota monax*) with woodchuck hepatitis virus (WHV) resembles the vertical HBV transmission in humans, including immunopathogenesis and liver disease progression (12, 13). Like HBV, the outcome of WHV infection is age dependent, with 60-75% of WHV-infected neonatal woodchucks progressing to chronicity, while less than 5% of WHV-infected adult woodchucks develop CHB (14). This immunocompetent animal model is, therefore, intensively applied in the evaluation of the safety and therapeutic efficacy of novel anti-HBV drugs *in vitro* and *in vivo*.

The ability of the host immune system to fight viral infections is dependent on germline-encoded pattern recognition receptors (PRRs) that recognize unique motifs called pathogen-associated molecular patterns (PAMPs), such as viral RNA, DNA, and proteins (15). The subcellular localization of these receptors in both immune and non-immune cells is either extracellular on plasma membranes or intracellular on endosomal membranes or within the cytoplasm, but sometimes also in the nucleus. The widely studied families of PRRs include the retinoic acid-inducible gene-I like receptors (RLRs), the nucleotide-binding oligomerization domain containing protein 2 (NOD2) like receptors (NLRs), toll-like receptors (TLRs), cytosolic DNA sensors (CDSs), and inflammasomes. Stimulation of these receptors triggers their downstream signaling pathway involving adaptor molecules, transcription factors, and type-I IFNs or pro-inflammatory cytokines, and leads to an antiviral immune response (16, 17). Unlike many other viruses, HBV fails to induce a type-I IFN response immediately after infection and hence is referred to a stealth-like virus (18). While *in vitro* studies have demonstrated that HBV proteins can interfere with the receptor pathway activation (19–21), other studies have argued that the virus does not actively inhibit the function of PRRs, and that these receptors can be agonistically stimulated in the setting of CHB (22).

The safety and antiviral efficacy against HBV associated with the stimulation of mainly viral RNA sensing receptors by small agonist molecules have been investigated in preclinical studies and several compounds were subsequently tested in patients with CHB (7, 10). Within the TLR family, GS-9620 was the first-in-class TLR7 agonist that significantly suppressed viral replication in HBV-infected chimpanzees (23) and in WHV-infected woodchucks (24) as a single agent. However, this compound failed to mediate therapeutic efficacy in patients at tolerated doses (25). Monotreatment with the TLR8 agonist GS-9688 also mediated sustained antiviral effects in a subset of woodchucks (26). Other TLR7 and 9 agonists tested in the woodchuck model produced superior antiviral effects only when administered in combination with the nucleoside analog entecavir (ETV) (27–29). Apart from these TLR agonists, SB9200, a RIG-I stimulator with both immunomodulatory and direct antiviral properties (30, 31) mediated pronounced therapeutic efficacy in

woodchucks when the immune response was activated by this agonist before additional viral suppression with ETV (32). Except for TLR9, the antiviral potential of viral DNA sensing receptors against CHB, especially that of CDSs and inflammasomes, is less explored. The reason for this lack in knowledge is that many of these DNA receptors, such as interferon-gamma inducible protein 16 (IFI16), Z-DNA-binding protein 1 or DNA-dependent activator of interferon regulatory factors (ZBP1/DAI), cyclic GMP-AMP synthase (cGAS), and absent in melanoma 2 (AIM2) inflammasome, were characterized more recently for their structural properties, downstream signaling pathways, and role in infectious diseases and autoimmune disorders (33). IFI16 and ZBP1/DAI receptors recognize viral double-stranded (ds) DNA and mediate the production of type-I IFNs by recruiting the stimulator of interferon genes (STING) as adaptor molecule or by activating the TANK-binding kinase 1 (TBK1) and interferon regulatory factor 3 (IRF3) pathway, respectively (34, 35). A recent *in vitro* study further demonstrated that nucleus resident IFI16 can recognize HBV cccDNA and that receptor overexpression affects HBV replication (36). The AIM2 inflammasome recognizes viral dsDNA and initiates the formation of a multi-protein complex consisting of the receptor, the adaptor protein apoptosis-associated speck-like protein containing a CARD domain (ASC), and caspase-1 for the production of the pro-inflammatory cytokines, interleukins (IL) 1β and 18 (35). The molecular characterization of IFI16 and AIM2 receptors in woodchucks and their involvement in the control of WHV infection were described recently (37, 38). The present study reports the effects on WHV replication and secretion that are mediated by mono and combination treatment with the agonists HSV-60 and poly(dA:dT) for targeting the IFI16, ZBP1/DAI, and AIM2 receptors in primary hepatocytes generated from woodchucks with CHB. In addition, the safety and activity of a low and high dose of the poly(dA:dT) agonist for the induction of ZBP1/DAI and AIM2 receptors in the liver of WHV-uninfected woodchucks are described.

MATERIALS AND METHODS

Ethics Statement

The animal protocol # 2019-0064 entitled "Pharmacodynamic and tolerability study of innate immune receptor agonists in woodchucks" and all procedures involving woodchucks were approved by the Institutional Animal Care and Use Committee of Georgetown University on October 22, 2019 and followed the National Institutes of Health guidelines for the Care and Use of Laboratory Animals. Woodchuck were anesthetized by inhalation of isoflurane (3-5%) and by intramuscular injection of ketamine (50 mg/kg) and xylazine (5 mg/kg) for blood collection or percutaneous liver biopsy, respectively. Prior to euthanasia, woodchucks were anesthetized as described above and euthanized by an overdose of pentobarbital (80-100 mg/kg) administered by intracardiac injection, followed by bilateral intercostal thoracotomy.

Woodchuck Hepatocyte Isolation and PRR Stimulation

Primary woodchuck hepatocytes (PWHs) were generated from animals with CHB using the collagenase perfusion method and maintained for four days before treatment initiation (39). The agonists HSV-60 (Invivogen, San Diego, CA) and poly(dA:dT) (Invivogen) targeting the IFI16 or ZBP1/DAI and AIM2 receptors, respectively, were administered to PWHs at doses of 2.0 or 1.0 μg/mL, respectively, at T0 and again after 48 hours using Lipofectamine 3000 (Thermo Fisher Scientific, Waltham, MA). Lipofectamine-containing medium without agonists served as the untreated control. Cell supernatant and hepatocytes were collected every 24 hours over a 96-hour time course. Isolation of peripheral blood mononuclear cells (PBMCs) and treatment with the TLR7 agonist GS-9620 or IFN-α are described in the **Supplementary Material**.

In Vitro Receptor Pathway Activation and WHV Replication

The expression of receptors, downstream adaptor molecules, and effector cytokines (**Supplementary Table 1**) in PWHs and woodchuck hepatoma cells was determined by real-time PCR and woodchuck-specific primers and probes (**Supplementary Table 2**) as described previously (38, 40). WHV relaxed circular-(rc-) DNA was isolated from cell supernatant, while WHV pre-genomic (pg) RNA and WHV cccDNA were isolated from PWHs and quantified using real-time PCR as described previously (39, 41) and in the Supplementary Material.

Woodchuck Study Design

The two WHV-uninfected adult woodchucks, M8001 and F8003, were confirmed negative for serum WHV DNA, WHV surface antigen (WHsAg), and antibodies to WHsAg (anti-WHs antibodies) using assays described previously (29). Both animals were intravenously injected with a single dose of poly (dA:dT) (Invivogen) mixed in *in vivo*-jetPEI-Gal transfection reagent (PolyPlus Transfection, Illkirch, France), as described in the Supplementary Material. Woodchuck M8001 received a low dose (125 μg/kg), while animal F8003 received a high dose (375 μg/kg) of poly(dA:dT). Blood samples were collected into PAXGene tubes (Qiagen, Redwood City, CA) at pre-treatment, and then at 24-hours post-treatment for analyzing gene expression. Ultrasound-guided, percutaneous liver biopsies were also obtained at pre-treatment and at 24-hours post-treatment, placed immediately in liquid nitrogen, and stored at 80°C for subsequent gene expression analysis. Body weights, body temperatures, hematology, clinical chemistry, and liver histology of both woodchucks were frequently determined.

Whole Blood Assay

The effective delivery of poly(dA:dT) with the PolyPlus family of transfection reagents was first tested *in vitro* by using the jetOPTIMUS transfection reagent, and before the subsequent *in vivo* administration of the agonist to woodchucks with the *in vivo*-jetPEI-Gal transfection reagent. The jetOPTIMUS transfection reagent is specifically designed for *in vitro*

transfection of hard-to-transfect cells, including primary cells/blood cells (42). Whole blood from animals M8001 and F8003 was drawn into hirudin-coated blood collection tubes (Sarstedt, Numbrecht, Germany). A total of 185 µL of blood was then transferred into the wells of a 96-well round bottom plate (Corning, Tewksbury, MA) and incubated for 6 hours with 15 µL of jetOPTIMUS transfection reagent containing poly(dA:dT). As an untreated control, blood samples were incubated with transfection reagent only. Thereafter, blood was collected from 5 wells of treated or untreated control samples and combined, cells were lysed with RLT buffer (Qiagen) containing 1% β-mercaptoethanol, and total RNA was isolated using the QIAamp RNA Blood Mini kit (Qiagen). The mRNA was subsequently converted to complementary (c) DNA and the expression of receptors, adaptor molecules, and effector cytokines was determined by real time PCR assay, as described recently (38, 40). A fold-change of ≥2.1 from the untreated control was considered a positive result for increased gene expression after *in vitro* treatment with poly(dA:dT).

ELISpot Assay

PBMCs were isolated from woodchucks M8001 and F8003 by Ficoll-Paque density gradient centrifugation, as described in the Supplementary Material. The ELISpot assay for measuring IFN-γ secretion by blood cells was performed with a commercially available kit (Mabtech, Stockholm, Sweden) by following the manufacturer's protocol. In brief, each well of a polyvinylidene fluoride plate was pretreated with 50 µL of 70% ethanol for 2 minutes and washed with sterile water before coating with 100 µL/well of IFN-γ antibody (15 µg/mL). Following overnight incubation at 4°C, excess antibody was removed by washing five times with phosphate-buffered saline (PBS). A total of 200 µL of AIM-V cell culture medium (Thermo Fisher Scientific) was then added to each well and incubated for 30 minutes. Thereafter, PBMCs ranging from 50,000 to 125,000 cells/well were added and the plate was incubated at 37°C and 5% CO_2 for 12-48 hours. Following the incubation, cells were removed, and the plate was washed five times with PBS. The detecting antibody (255-11-biotin) was added to each well (1 µg/mL), and the plate was incubated for another 2 hours. Following washing five times with PBS, 100 µL of 1:1,000 diluted streptavidin-alkaline phosphate conjugate was added to each well and the plate further incubated for 1 hour. The plate was washed again five times with PBS and 100 µL of substrate solution was added to each well and the plate developed until spots became visible. Color development was stopped by washing extensively with tap water and the plate was air dried before spots were counted at Mabtech using an ELISpot reader.

Peripheral and Intrahepatic Expression of Receptor Pathway Molecules and Immune Cell Markers

Changes in the transcript level of ZBP1/DAI and AIM2 receptor pathway molecules (**Supplementary Table 1**) in blood and liver of woodchucks M8001 and F8003 were determined using real-time PCR assay and woodchuck-specific primers and probes (**Supplementary Table 2**), as described above under whole blood assay and previously (38, 40). A fold-change of ≥2.1 from the pre-treatment baseline was considered a positive result for increased gene expression after *in vivo* treatment with poly (dA:dT).

Statistical Analysis

Statistical comparisons were performed using unpaired Student's *t*-test with equal variance for detecting significant changes in PRR pathway activation and WHV replication and secretion in PWHs. *P* values <0.05 were considered significant.

RESULTS

Agonistic Stimulation of Viral DNA Sensing Receptors Mediates WHV Suppression

Stimulation of viral RNA sensing receptors (i.e., RIG-I, NOD2, TLR3/7/8) using small agonistic molecules has been already explored for the treatment of CHB, as described above, but the antiviral potential of viral DNA sensing receptors, except for TLR9, remains unknown. Agonistic activation of CDSs and inflammasomes within virus-infected hepatocytes, such as IFI16, ZBP1/DAI, and AIM2, could mediate an antiviral effect against HBV *via* the induced effector cytokines, such as IFN-β, IL-1β, and IL-18. For testing these receptors as potential anti-HBV drug targets, PWHs generated from the liver of five woodchucks with CHB were treated with HSV-60 and poly (dA:dT) to stimulate the CDSs IFI16 or ZBP1/DAI and the inflammasome AIM2, respectively. HSV-60 treatment (**Figure 1**) at T0 and again after 48 hours resulted in increased expression of IFI16 receptor, STING adaptor molecule, and IFN-β effector cytokine. Despite the expected variation in individual PWH cultures due to the outbred nature of donor animals, the average peak expression of receptor pathway markers was observed during 72-96 hours (fold-change: IFI16, 3.3; STING, 3.2; IFN-β, 96.0). Receptor pathway upregulation was associated with a pronounced decline in WHV replication (pgRNA and cccDNA) and secretion (rc-DNA). Compared to untreated PWHs obtained from individual animals at each timepoint, the maximum average reduction at 72-96 hours was 0.48 $\log_{10}$ for pgRNA, 1.32 $\log_{10}$ for cccDNA, and 1.21 $\log_{10}$ for rc-DNA. Poly (dA:dT) treatment (**Figure 2**) at T0 and again after 48 hours increased the expression of ZBP1/DAI DNA receptor and AIM2 inflammasome and their respective adaptor molecules TBK1 and ASC and effector cytokines IFN-β and IL-18. The average peak expression for markers of both receptor pathways was observed during 72-96 hours (fold-change: ZBP1/DAI, 36.5; AIM2, 22.3; TBK1, 99.8; ASC, 1,030.8; IFN-β, 64,406.5; IL-18, 1,497.3). Marked declines in WHV replication and secretion were obtained at 72 hours, and the maximum average reduction from untreated PWHs was 0.72 $\log_{10}$ for pgRNA, 1.56 $\log_{10}$ for cccDNA, and 1.70 $\log_{10}$ for rc-DNA. The effect on WHV secretion appeared longer-lasting, as rc-DNA continued to decline and was reduced on average by 1.72 $\log_{10}$ at 96 hours. Overall, it appeared that poly(dA:dT) at the selected dose

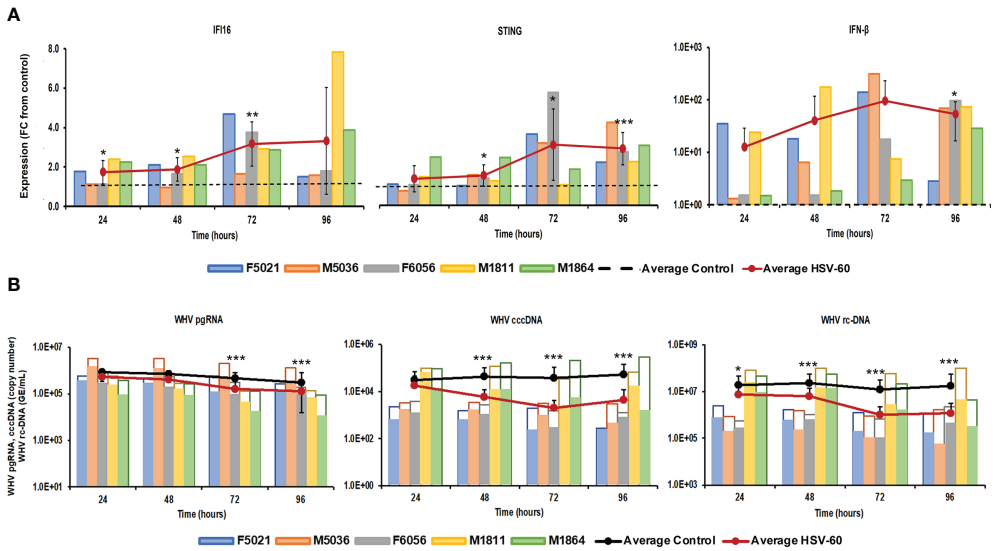

FIGURE 1 | Agonistic activation of IFI16 receptor pathway mediates WHV suppression. PWHs generated from the liver of five woodchucks with CHB were treated with HSV-60 at T0 and again at 48 hours. **(A)** The fold-changes in transcript level of IFI16, STING, and IFN-β over 96 hours are shown, when compared to their transcript level in untreated control PWHs from individual animals at each timepoint, which was set at 1.0 and is indicated by the dotted line. **(B)** The changes in WHV replication (pgRNA and cccDNA) and secretion (rc-DNA) during treatment are presented for untreated control (empty bars) and HSV-60 treated PWHs (colored bars) from individual animals at each timepoint. The average fold-change in gene transcript level or average change in WHV load of control and HSV-60-treated PWHs are presented as solid lines. Horizontal bars represent the standard error of the mean. *P* values representing statistical significance from untreated control PWHs are shown as * for <0.05, ** for <0.01, and *** for <0.001. FC, fold-change.

mediated a greater antiviral effect on WHV than HSV-60, most likely due to the activation of two receptors (ZBP1/DAI and AIM2) rather than one receptor (IFI16). Compared to IFI16 receptor stimulation by HSV-60, poly(dA:dT)-mediated activation of the ZBP1/DAI receptor resulted in a 670-fold higher IFN-β expression, in addition to IL-18 expressed by AIM2.

For controlling agonistic PRR activation by HSV-60 and poly (dA:dT) in woodchuck hepatocytes, PWHs were also treated with poly(I:C) and GS-9620 for stimulation of TLR3 (positive control) or TLR7 (negative control), respectively (**Supplementary Figure 1**). This revealed receptor pathway activation and a moderate antiviral effect against WHV by poly(I:C) but not by GS-9620. For confirming the presence of IFI16, ZBP1/DAI, and AIM2 in hepatocytes rather than in immune cells possibly contaminating the PWH cultures, woodchuck WCH-17 hepatoma cells were treated with HSV-60 and poly(dA:dT) (**Supplementary Figure 2**). This demonstrated that all three receptor pathways were inducible in the hepatoma cells, and that the upregulated expression of receptors, adaptor molecules, and effector cytokines after 24 hours, especially of ZBP1/DAI and AIM2, was fairly comparable to those obtained in PWHs.

Parallel Agonistic Stimulation of Viral DNA Sensing Receptors Enhances WHV Suppression

The distinct pathways of the IFI16, ZBP1/DAI, and AIM2 receptors, their production of different effector cytokines, and their location within the cytosol of virus-infected hepatocytes, together with the antiviral effect against WHV mediated by agonistic stimulation, may make them suitable targets for combination treatment. This concept of parallel activation of three DNA receptor pathways was tested in PWHs derived from the liver of three woodchucks with CHB, which were also utilized in the previous monotreatment experiments. Receptor agonism with HSV-60 plus poly(dA:dT) at T0 and again after 48 hours resulted in an average receptor and cytokine expression that was more pronounced than during monotreatment (**Figure 3**). The peak expression of IFI16 (fold-change: HSV-60, mono, 4.5; combo, 19.2) and ZBP1/DAI (fold-change: poly(dA:dT), mono 17.3; combo, 41.4) was observed at 96 hours. AIM2 expression peaked during 72-96 hours (fold-change: poly(dA:dT), mono 22.7; combo, 50.6), while IFN-β expression was maximal during 48-96 hours (fold-change: HSV-60, mono, 65.8; poly(dA:dT), mono, 3,188.5; combo, 10,886.9). Peak IL-18 expression was noted during 72-96 hours (fold-change: poly(dA:dT), mono, 1,497.3; combo, 33,031.0). The maximum antiviral effect of monotreatment and the added antiviral benefit of combination treatment on WHV replication and secretion was observed at 72-96 hours (reduction: pgRNA, HSV-60 mono, 0.31 $\log_{10}$; poly(dA:dT) mono, 0.40 $\log_{10}$; combo, 1.29 $\log_{10}$; cccDNA, HSV-60 mono, 1.00 $\log_{10}$; poly(dA:dT) mono, 1.33 $\log_{10}$; combo, 1.88 $\log_{10}$; rc-DNA, HSV-60 mono, 1.09 $\log_{10}$, poly(dA:dT) mono, 1.60 $\log_{10}$; combo, 2.22 $\log_{10}$). When compared to monotreatment, the increased receptor and cytokine expression during combination treatment correlated with the additional declines in WHV replication and secretion.

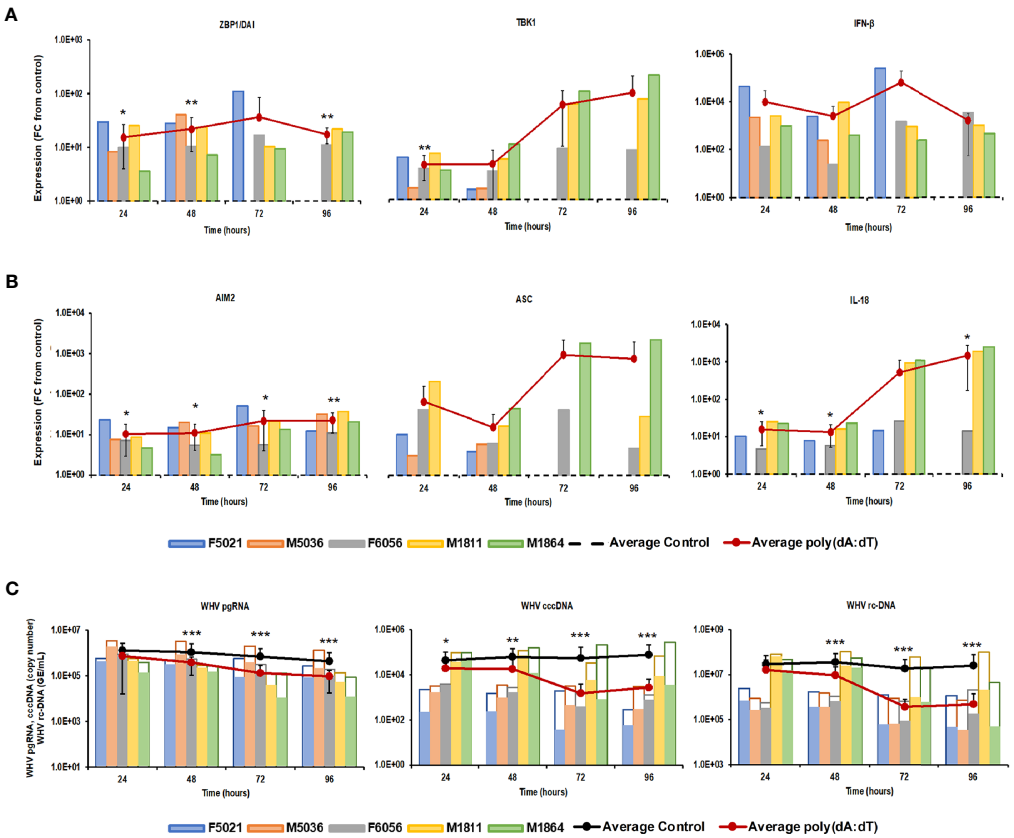

FIGURE 2 | Agonistic activation of ZBP1/DAI and AIM2 receptor pathways mediates WHV suppression. PWHs generated from the liver of five woodchucks with CHB were treated with poly(dA:dT) at T0 and again at 48 hours. The fold-changes in transcript level of **(A)** ZBP1/DAI, TBK1, and IFN-β and **(B)** AIM2, ASC, and IL-18 over 96 hours are shown, when compared to their transcript level in untreated control PWHs from individual animals at each timepoint, which was set at 1.0 and is indicated by the dotted line. **(C)** The changes in WHV replication (pgRNA and cccDNA) and secretion (rc-DNA) during treatment are presented for untreated control (empty bars) and poly(dA:dT)-treated PWHs (colored bars) from individual animals at each timepoint. The average fold-change in gene transcript level or average change in WHV load of control and poly(dA:dT)-treated PWHs are presented as solid lines. Horizontal bars represent the standard error of the mean. *P* values representing statistical significance from untreated control PWHs are shown as * for <0.05, ** for <0.01, and *** for <0.001. FC, fold-change.

Parallel Agonistic Stimulation of Viral DNA Sensing Receptors Together With Exogenously Added Type-I IFNs Fails to Enhance WHV Suppression

For determining, if the antiviral effect of combination treatment with HSV-60 and poly(dA:dT) is further enhanceable, exogenous type-I IFNs were provided *via* supernatant from woodchuck PBMCs treated with the TLR7 agonist GS-9620. It has been reported that human PBMCs derived from healthy individuals and subsequently treated with GS-9620 produce type-I IFNs and interferon stimulated genes (ISGs), and that treatment of HBV-infected PHHs with this conditioned medium (CM) results in an antiviral effect on viral replication (43). PBMCs obtained from two woodchucks with CHB were treated with GS-9620 for 8 or 24 hours (**Supplementary Figure 3**). At each timepoint, PBMCs were harvested and cell supernatant was collected and combined for subsequent treatment of PWHs with CM (i.e., GS-9620 CM), alone and in combination with HSV-60 and/or poly(dA:dT). Compared to untreated control PBMCs, a maximum expression of IFN-α, IFN-β, and ISG15 in GS-9620 treated PBMCs was observed at eight hours (fold change: M1811, IFN-α, 179.6; IFN-β, 2,098.5; ISG15, 640.3; M1864, IFN-α, 129.8; IFN-β, 87.4; ISG15, 504.7). In PWHs derived from the same two animals and treated with GS-9620 CM at T0 and again after 48 hours (**Supplementary Figure 3**), a maximum reduction of WHV replication and secretion was obtained during 72-96 hours, when compared to untreated control PWHs (reduction: pgRNA, M1811, 0.19 $\log_{10}$; M1864, 0.14 $\log_{10}$; cccDNA, M1811, 0.11 $\log_{10}$; M1864, 0.08 $\log_{10}$; rc-DNA, M1811, 0.15 $\log_{10}$; M1864, 0.09 $\log_{10}$).

Treatment of PWHs from the same two animals with the triple combination of HSV-60, poly(dA:dT), and GS-9620 CM at T0 and again after 48 hours induced a higher expression of IFI16, ZBP1/DAI, and AIM2 receptors, when compared to treatment with the double combination of HSV-60 and poly(dA:dT) (**Figure 4**). Peak receptor expression with the double and triple combination was observed at 96 hours in M1811 (fold-change: IFI16, double, 40.5, triple, 53.5; ZBP1/DAI, double, 94.8, triple, 248.7; AIM2, double, 112.1, triple, 144.1) and during 72-96 hours

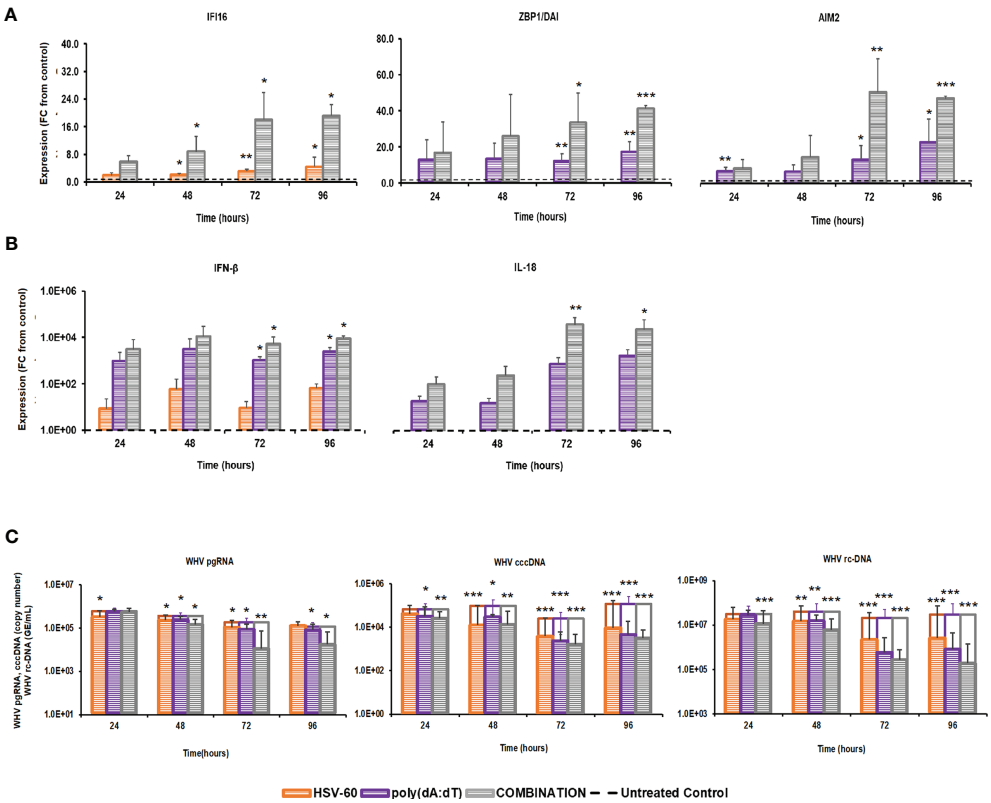

FIGURE 3 | Parallel agonistic activation of IFI16, ZBP1/DAI, and AIM2 receptor pathways enhances WHV suppression. PWHs generated from the liver of three woodchucks with CHB were treated with HSV-60 and poly(dA:dT), alone and in combination, at T0 and again at 48 hours. The fold-changes in transcript level of **(A)** IFI16, ZBP1/DAI, and AIM2 and **(B)** IFN-β and IL-18 over 96 hours are shown, when compared to their transcript level in untreated control PWHs from individual animals at each timepoint, which was set at 1.0 and is indicated by the dotted line. **(C)** The average changes in WHV replication (pgRNA and cccDNA) and secretion (rc-DNA) during mono and combination treatment are presented for untreated control (empty bars) and agonist-treated PWHs (colored bars) at each timepoint. Horizontal bars represent the standard error of the mean. *P* values representing statistical significance from untreated control PWHs are shown as * for <0.05, ** for <0.01, and *** for <0.001. FC, fold-change.

in M1864 (fold-change: IFI16, double, 10.2; triple, 12.8; ZBP1/DAI, double, 13.1, triple, 33.3; AIM2, double, 15.6, triple, 24.8). However, the triple combination failed to increase the expression of IFN-β and IL-18 beyond those obtained with the double combination, except for IFN-β in PWHs of M1864, with a relatively low expression induced by the double combination (fold-change: IFN-β, M1811, double, 31,911.8, triple,19,132.6; M1864, double, 2,375.5, triple, 4,688.3; IL-18, M1811, double, 89,600.0, triple, 27,113.1; M1864, double, 23,149.1, triple, 11,141.0). Contrary, treatment of the same PWHs with HSV-60 and GS-9620 CM resulted in a greater IFI16 receptor and effector cytokine expression, and enhanced the antiviral effect against WHV, when compared to HSV-60 monotreatment (**Supplementary Figure 4**). Treatment of these PWHs with poly(dA:dT) and GS-9620 CM resulted in a mixed expression of ZBP1/DAI and AIM2 receptors, when compared to monotreatment with poly(dA:dT), but was unable to enhance further effector cytokine expression and antiviral effect against WHV (**Supplementary Figure 5**). Thus, based on the cytokine results from triple combination treatment, it further appeared that the additional stimulus by exogenous type-I IFNs was somehow refractory for unknown reasons, since IFN-β and IL-18 expression was reduced during treatment with the triple combination, when compared to the double combination. This was consistent with the observation that the triple combination was unable to enhance the antiviral effect on WHV replication and secretion over that of the double combination in PWHs of M1811 (reduction: pgRNA, double, 1.02 $\log_{10}$, triple, 0.89 $\log_{10}$; cccDNA, double, 1.46 $\log_{10}$, triple, 1.33 $\log_{10}$; rc-DNA, double, 2.43 $\log_{10}$, triple, 2.49 $\log_{10}$) and M1864 (reduction: pgRNA, double, 1.26 $\log_{10}$, triple, 0.88 $\log_{10}$; cccDNA, double, 2.52 $\log_{10}$, triple, 2.27 $\log_{10}$; rc-DNA, double, 1.80 $\log_{10}$, triple, 1.81 $\log_{10}$). The high expression level of effector cytokines already achieved by the double combination could explain the lack of an additional antiviral effect against WHV by the triple combination. Since treatment with exogenous type-I IFNs together with poly(dA:dT) or HSV-60 and poly(dA:dT) was unable to suppress WHV further, this may indicate that the antiviral effect cannot be enhanced indefinitely during short-term treatment once hepatocytes produce and/or secrete effector cytokines at already high (i.e., saturating) levels.

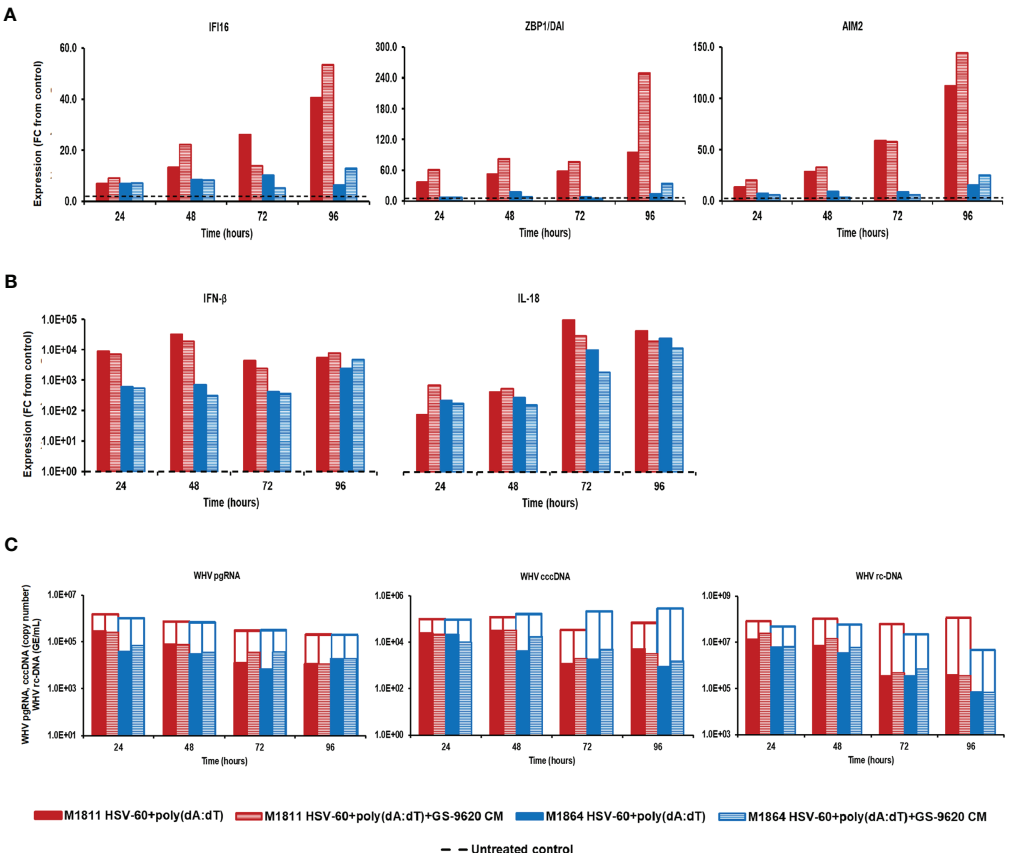

FIGURE 4 | Parallel agonistic activation of IFI16, ZBP1/DAI, and AIM2 receptor pathways together with exogenously added type-I IFNs fails to enhance WHV suppression. PBMCs and PWHs were generated from two woodchucks with CHB, GS-9620 CM was obtained from GS-9620 treated PBMCs, and used to treat PWHs from each animal at T0 and again at 48 hours together with HSV-60 and poly(dA:dT). The fold-changes in transcript level of **(A)** IFI16, ZBP1/DAI, and AIM2 and **(B)** IFN-β and IL18 over 96 hours are shown for treatment with the double (HSV-60 + poly(dA:dT)) or triple combination (HSV-60 + poly(dA:dT) + GS-9620 CM), when compared to their transcript level in untreated control PWHs from individual animals at each timepoint, which that was set at 1.0 and is indicated by the dotted line. **(C)** The changes in WHV replication (pgRNA and cccDNA) and secretion (rc-DNA) during double and triple combination treatment are presented for untreated control (empty bars) and agonist/GS-9620-treated PWHs (colored bars) from individual animals at each timepoints. FC, fold-change.

Poly(dA:dT) Treatment of WHV-Uninfected Woodchucks Stimulates ZBP1 and AIM2 Receptors in the Liver but Also in the Periphery

The results from the *in vitro* experiments in PWHs demonstrated that stimulation of more than one PRR by poly(dA:dT) produced a pronounced effect on WHV replication and secretion. For determining the activity and safety of poly(dA:dT) *in vivo*, two WHV-uninfected adult woodchucks were administered a single low (125 μg/kg in M8001) or high (375 μg/kg in F8003) dose of poly(dA:dT) mixed with *in vivo*-jetPEI-Gal transfection reagent (**Figure 5**), and the activation of ZBP1 and AIM2 receptor pathways in blood and liver was determined. The transfection reagent contains a galactose-conjugate for enhanced delivery of nucleic acids to cells expressing galactose-specific membrane lectins, including asialoglycoprotein receptor (ASGP-R) on hepatocytes (42).

Prior to administration to woodchucks M8001 and F8003, the jetOPTIMUS transfection reagent with poly(dA:dT) was tested in whole blood from these animals. Whole blood was transfected for 6 hours and blood cells were harvested thereafter. Compared to the transfection control, blood cells of both woodchucks treated with poly(dA:dT) (**Figure 6**) showed increased expression of receptors (fold-change: ZBP1/DAI, M8001, 21.3, F8003, 19.8; AIM2, M8001, 4.4, F8003, 2.7) and effector cytokines, except for IL-18 in M8001 (fold-change: IFN-β, M8001, 56.9, F8003, 44.0; IL-1β, M8001, 2.1, F8003, 2.6; IL-18, M8001, 1.2, F8003, 2.7). The expression of adaptor molecules stayed close to the transfection control baseline, expect for ASC in blood cells of M8001 (fold-change: 14.9).

After the *in vivo* administration of poly(dA:dT) in *in vivo*-jetPEI-Gal transfection reagent to both woodchucks, the intrahepatic activation of receptor pathways was determined in a liver biopsy obtained 24 hours post-treatment (**Figure 7A**). Compared to the liver biopsy obtained prior to treatment, increases in receptor expression were observed in the liver of both animals (fold-change: ZBP1/DAI, M8001 7.7, F8003, 3.0;

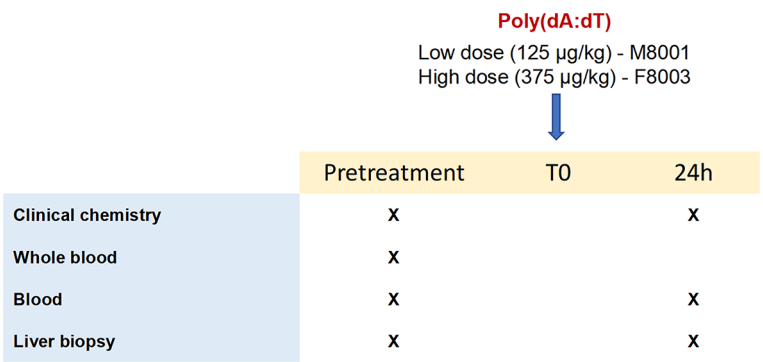

FIGURE 5 | Study design of *in vivo* poly(dA:dT) administration to woodchucks. Poly(dA:dT) mixed in *in vivo*-jetPEI-Gal transfection reagent was administered intravenously as a single dose to two WHV-uninfected adult woodchucks. Animal M8001 received a low dose (125 µg/kg), while animal F8003 received a high dose (375 µg/kg) at T0. Cross marks indicate the time of clinical chemistry measurements and sample collection.

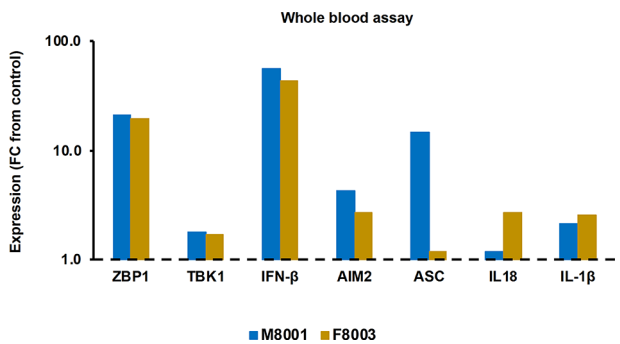

FIGURE 6 | Agonistic activation of ZBP1/DAI and AIM2 receptor pathways in woodchuck blood. Whole blood from animals M8001 and F8003 was treated with poly(dA:dT) in jetOPTIMUS transfection reagent. The fold-changes in transcript level of receptors (ZBP1/DAI and AIM2), adaptor molecules (TBK1 and ASC), and effector cytokines (IFN-β, IL-18, and IL-1β) after 6 hours are shown, when compared to their transcript level in transfection reagent treated control whole blood from individual animals, which was set at 1.0 and is indicated by the dotted line. FC, fold-change.

AIM2, M8001, 2.8, F8003, 2.4), indicating on-target receptor stimulation. However, the expression of most effector cytokines stayed relatively unchanged, expect for IFN-β in F8003 (fold-change: 4.2). The peripheral activation of receptor pathways was further tested in blood obtained 24-hours post-treatment (**Figure 7B**). Compared to blood obtained prior to treatment, increased receptor expression was noted in blood of both animals for ZBP1/DAI (fold-change: M8001, 7.9; F8003, 4.0), but for AIM2 only in M8001 (fold-change: 2.4). The expression of IFN-β and IL-1β was also increased in M8001 (fold-change: IFN-β, 3.4; IL-1β, 2.9), but remained close to the pre-treatment baseline in F8003. No comparable expression changes were observed for IL-18 in both animals.

Since it has been demonstrated that activation of inflammatory pathways can indirectly lead to IFN-γ production by T-cells *via* IL-18 (44, 45), PBMCs obtained from animals M8001 and F8003 24-hours post-treatment were subjected to an ELISpot assay and the number of IFN-γ secreting cells determined (**Figure 8A**). Compared to PBMCs obtained prior to treatment, an increase in IFN-γ secreting cells was observed that appeared dose-dependent (fold-change: M8001, 6.3; F8003, 28.3).

The administration of poly(dA:dT) in *in vivo*-jetPEI-Gal transfection reagent was well-tolerated by both woodchucks, since changes in body weight, body temperature, and hematology were not noted during the 24-hour time course (data no shown). Liver enzymes, including alanine aminotransferase (ALT), aspartate aminotransferase (AST), gamma-glutamyl transferase (GGT), and sorbitol dehydrogenase (SDH), were measured as markers of liver injury prior to treatment and 24 hours post-treatment. In agreement with the normal range of liver enzyme levels in WHV-uninfected woodchucks (46, 47), ALT levels stayed unchanged, AST levels declined somewhat, and only minor but insignificant increases in SDH and GGT levels were observed in both animals or only in one animal, respectively, (**Figure 8B**). Furthermore, when compared to pre-treatment, changes in liver histology associated with agonistic treatment were absent in both animals at 24 hours post-treatment (**Supplementary Figure 6**).

DISCUSSION

The host RNA and DNA sensing PRRs recognize viral nucleic acids and these PAMPs then trigger the receptor downstream signaling pathways to produce different effector cytokines. These effector cytokines secreted after receptor pathway activation act at the intersection of the innate and adaptive arms of the immunity, and thus influence the direction and magnitude of the adaptive immune response against viral infections (16). Induction of virus-specific adaptive immunity, including T- and B-cell responses, is considered the hallmark for the resolution of either HBV or WHV infection (48, 49). The role of innate immune cells, including natural killer (NK) cells, dendritic cells (DCs), and macrophages, and the involvement of PRRs in the resolution of HBV infection is only just emerging (50, 51). Recent studies demonstrated the *in*

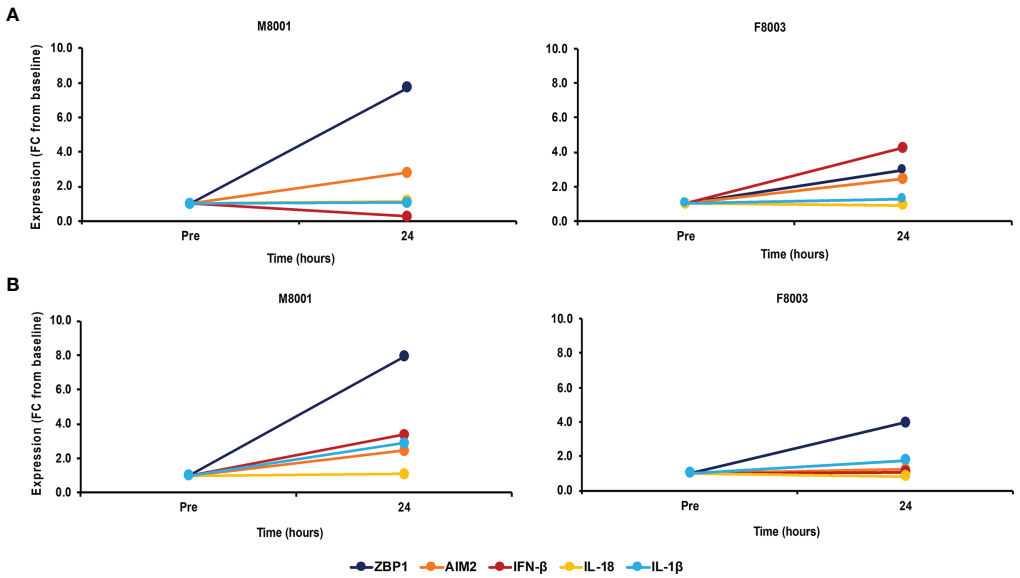

FIGURE 7 | Single dose administration of poly(dA:dT) to woodchucks results in agonistic activation of ZBP1/DAI and AIM2 receptor pathways in the liver and periphery. Liver biopsies and blood from animals M8001 and F8003 were collected 24 hours after intravenous injection of a single low (M8001) or high (F8003) dose of poly(dA:dT) in *in vivo*-jetPEI-Gal transfection reagent. The fold-changes in transcript level of receptors (ZBP1/DAI and AIM2) and effector cytokines (IFN-β, IL-18, and IL-1β) in **(A)** liver and **(B)** blood are shown, when compared to their transcript level at pre-treatment in liver biopsies and blood from the same animals, which was set at 1.0. FC, fold-change.

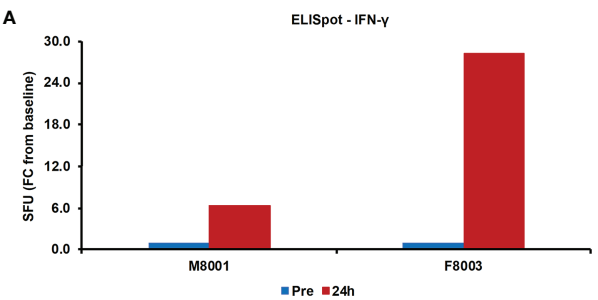

B

Liver enzymes

	Time point	ALT (IU/L)	AST (IU/L)	SDH (IU/L)	GGT (IU/L)
M8001	Pretreatment	<5	40.0	14.0	0.0
	24 hours	<5	26.0	19.0	1.0
F8003	Pretreatment	<5	25.0	11.0	2.0
	24 hours	<5	22.0	22.0	2.0

FIGURE 8 | Single dose administration of poly(dA:dT) to woodchucks results in an increased number of IFN-γ secreting blood cells and nearly unchanged liver enzymes. **(A)** PBMCs from animals M8001 and F8003 were isolated 24 hours after intravenous injection of a single low (M8001) or high (F8003) dose of poly(dA:dT) in *in vivo*-jetPEI-Gal transfection reagent and subjected to an ELISpot assay. The fold-changes in spot-forming units (SFU) are shown, when compared to the spot number at pre-treatment in PBMCs from both animals, which was set at 1.0. **(B)** The levels of ALT, AST, SDH, and GGT in serum of both animals measured prior to treatment and at 24 hours post-treatment are shown. The normal range of liver enzyme levels in WHV-uninfected woodchucks is 1-6 IU/mL for ALT, 9-55 IU/mL for AST, and 0.8-2.6 IU/mL for GGT (46). For SDH, the normal range in WHV-uninfected woodchucks is 7-31 IU/mL (47). FC, fold-change; IU, international units.

vitro recognition of HBV nucleic acids by PRRs, such as cytosolic RIG-I sensing the 5' ε structure of HBV pgRNA (52) and nucleus resident IFI16 sensing HBV cccDNA (36), thereby promoting the suppression of these key viral molecules. In addition, several viral RNA sensing receptors have been targeted for antiviral effect against CHB *in vivo* (7, 10), but the contribution of other receptors, especially of CDSs and inflammasomes, to HBV resolution and their potential as anti-HBV drug targets are less known. In a recent study, we investigated the previously unknown kinetics of 16 receptors from different families of PRRs in liver and blood of woodchucks during WHV resolution (38). The peak transcripts of these receptors and the maximum protein presence of selected receptors in the liver correlated with the decline in viremia and antigenemia, initially mediated by IFN-γ secreting NK-cells, followed by the responses of virus-specific T- and B-cells (40). Furthermore, a comparison of PRR expression and presence during viral clearance and progression to CHB indicated the involvement of CDSs and inflammasomes in the control of WHV infection during resolution and the lack thereof during persistence (38). These results supported the continued testing of pathway activation and antiviral effects associated with agonistic stimulation of viral DNA sensing receptors in the current study.

Stimulation of the DNA receptors IFI16, ZBP1/DAI, and AIM2 with HSV-60 and poly(dA:dT) agonists resulted in marked IFN-β and IL-18 expression in PWHs from woodchucks with CHB and produced pronounced effects on WHV replication and secretion, indicating that CDS and inflammasome pathways are not actively suppressed or blocked by WHV. Lack of viral interference is further supported by the antiviral effects that are mediated by RNA receptor agonism *in vitro* (TLR3) and *in vivo* (TLR3/7/8/9 or RIG-I), with the latter resulting in reduced or undetectable HBV and WHV viremia and antigenemia levels, and antibody seroconversion in at least subsets of mice and woodchucks (22, 24, 26, 27, 29, 32, 53). Future studies should focus on understanding how HBV/WHV in the setting of CHB avoids efficient detection by PRRs and induction of an innate immune response, both of which is different to the strong receptor pathway activation and antiviral immune response induction during viral resolution. However, the above studies in woodchucks using mRNA expression assays could not differentiate between the PRR location in WHV-uninfected or infected hepatocytes or in non-parenchymal and/or immune cells within the liver, except for a few receptors for which cross-reactive antibodies became available (38). Analyzing immune events in liver at the transcript level mirrors the average from all cells within the biopsy sample, while WHV-infected PWHs could contain minor numbers of non-parenchymal and immune cells. Presence of immune cells in our PWH cultures, such as DCs, could be excluded, as direct treatment with the TLR7 agonist GS-9620 did neither mediate receptor and type-I IFN upregulation nor resulted in an antiviral effect, as also shown for HBV-infected PHHs (43). Cells other than hepatocytes, such as Kupffer cells, present within our PWH cultures may have contributed to the increased IFN-β and IL-18 expression after agonistic activation of IFI16, ZBP1/DAI, and AIM2, because DNA receptor pathways in PHHs are sometimes less activatable by agonists, when compared to human blood-derived macrophages and woodchuck fibroblastoma cells (37, 54). Contrary, another study reported that cGAS levels present in PHHs are sufficient for activation by HBV-derived naked DNA (55). The above studies are in agreement with our previous observation on maximum macrophage accumulation within the liver during WHV resolution in woodchucks (40), which correlated with the peak expression of CDSs and inflammasomes (38). These studies are also in agreement with the response of woodchuck hepatoma cells to agonistic receptor stimulation in the current study. While ZBP1/DAI and AIM2 receptor, adaptor molecule, and cytokine expression was comparable to those in PWHs using poly(dA:dT), IFI16 receptor pathway upregulation with HSV-60 revealed a somewhat lower IFN-β expression in hepatoma cells, suggesting a possible difference between healthy and malignant WHV-infected hepatocytes in regard to the downstream signaling of this receptor.

Mirroring the situation of multiple PRR upregulation in woodchuck liver during WHV resolution for viral control (38), agonistic activation of more than one DNA receptor (i.e., IFI16 *versus* ZBP1/DAI and AIM2), and especially parallel activation of all three receptors, in WHV-infected PWHs increased the overall effector cytokine expression and mediated an antiviral benefit. Furthermore, poly(dA:dT) recognition by RIG-I *via* RNA-polymerase III-transcribed intermediate RNA has been reported (56) and may have contribute to this antiviral benefit. This observation justifies identifying the antiviral potential of HBV/WHV-specific DNA (and RNA) receptors within infected hepatocytes, as the intrinsic immune response induced upon agonistic stimulation will act directly at the site of viral replication. The capability of IFN-α to directly target HBV cccDNA and of type-I IFNs to inhibit HBV pgRNA transcription from cccDNA and to block HBV pgRNA packaging into nucleocapsids have been described previously (57–59). Thus, the induction of type-I IFNs within HBV/WHV-infected hepatocytes by PRR agonism can lead to a marked suppression of viral replication. Furthermore, effector cytokines produced within hepatocytes and then secreted will activate the antiviral functions of innate immune cells that are resident or accumulate in the liver for shaping the adaptive immune response. However, the *in vitro* short-term antiviral effect in WHV-infected PWHs was not enhanceable indefinitely once saturating IFN-β and IL-18 levels were produced by CDSs and inflammasomes and/or secreted, although receptor levels continued to increase. The latter is likely due to a positive feedback loop, since the induction of type-I IFNs can enhance the expression of selected PRRs and ISGs in cell culture and animal models (60). Increased PRR upregulation in the liver was also observed following systemic administration of IFN-α to woodchucks (61). The contribution of the cytokines IFN-α and IL-1β that are also produced by IFI16 and ZBP1/DAI or AIM2 receptors, respectively, to the overall antiviral effect in WHV-infected PWH cultures is unknown, and thus requires additional testing before exploring agonistic stimulation of these receptors for the treatment of CHB.

As a first step in this direction, administration of a single dose of poly(dA:dT) to WHV-uninfected woodchucks was safe, based on unchanged body weight, body temperature, hematology, and clinical chemistry 24 hours later. Furthermore, changes in liver histology were absent and no marked elevation in liver enzymes was observed, except for some minor increases in GGT and SDH in one or both animals, respectively. Following treatment, the intrahepatic expression of ZBP1/DAI and AIM2 receptors and their effector cytokines increased in the liver and periphery of both woodchucks, but the changes did not appear dose-dependent. Consistent with the role of IL-18 as a co-activator of IFN-γ production (44), a dose-dependent increase in T-cells secreting IFN-γ was observed.

The *in vivo*-jetPEI-Gal transfection reagent has been previously applied in mouse models for the liver-targeted delivery of nucleic acids (42), but cross-reactivity to the woodchuck ASGP-R has not been tested. The intrahepatic upregulation of ZBP1/DAI and AIM2 receptors after treatment with poly(dA:dT) suggests that this transfection reagent can be used for targeting woodchuck liver with DNA-based agonists. Since an increased expression of these receptors was also observed in the periphery after treatment, the efficiency of the transfection reagent in liver-specific agonist delivery may be lower than anticipated. Although ASGP-R expression is commonly described to be exclusively on liver cells, low-level expression of this receptor on the surface of activated human PBMCs and T-cells has been described (62, 63), indicating a possible ASPG-R presence on non-hepatic cells. Thus, future woodchuck studies will need to focus on improving the liver-specific transfection efficiency by testing additional transfection reagents, in addition to finding an optimal dose of the poly(dA:dT) agonist. Overall, the present study demonstrated an antiviral benefit that is associated with the agonistic activation of more than one PRR pathway. More specifically, the activation of one cytosolic DNA (i.e., ZBP1/DAI) and one inflammasome (i.e., AIM2) receptor pathway has the advantage of inducing effector cytokines with rather distinct functions that could promote an overall more suitable immune response against chronic HBV infection. The safe *in vivo* administration of poly(dA:dT) that resulted in the intrahepatic upregulation of both receptors further encourages evaluating this agonist for therapeutic efficacy against CHB.

DATA AVAILABILITY STATEMENT

The original contributions presented in the study are included in the article/**Supplementary Material**. Further inquiries can be directed to the corresponding author.

ETHICS STATEMENT

The animal study was reviewed and approved by the Institutional Animal Care and Use Committee of Georgetown University.

AUTHOR CONTRIBUTIONS

MS, BL, XH, KK, MM, SG, and SM contributed to the conception and design of the study. MS, BL, XH, KK, MM, and SM performed the experiments. MS performed the statistical analysis. MS wrote the first draft of the manuscript. All authors contributed to the article and approved the submitted version.

FUNDING

MS, MM, SG, and SM were supported in part by grant R01CA166213 of the National Institutes of Health (NIH)/National Cancer Institute (NCI). The funders had no role in the design of the study, in the collection, analyses, or interpretation of data, in the writing of the manuscript, or in the decision to publish the results.

ACKNOWLEDGMENTS

We gratefully acknowledge Dr. Bhaskar V. Kallakury of the Department of Pathology at Georgetown University for excellent assistance with the evaluation of woodchuck liver tissues. Data from the *in vitro* studies presented in this manuscript were previously included in the thesis document of MS (64).

SUPPLEMENTARY MATERIAL

The Supplementary Material for this article can be found online at: https://www.frontiersin.org/articles/10.3389/fimmu.2021.745802/full#supplementary-material

REFERENCES

1. World Health Organization. *Hepatitis B*. Geneva, Switzerland: WHO (2021).
2. Yuen MF, Chen DS, Dusheiko GM, Janssen HLA, Lau DTY, Locarnini SA, et al. Hepatitis B Virus Infection. *Nat Rev Dis Primers* (2018) 4:18035. doi: 10.1038/nrdp.2018.35
3. Fanning GC, Zoulim F, Hou J, Bertoletti A. Therapeutic Strategies for Hepatitis B Virus Infection: Towards a Cure. *Nat Rev Drug Discov* (2019) 18(11):827–44. doi: 10.1038/s41573-019-0037-0
4. Revill PA, Chisari FV, Block JM, Dandri M, Gehring AJ, Guo H, et al. A Global Scientific Strategy to Cure Hepatitis B. *Lancet Gastroenterol Hepatol* (2019) 4(7):545–58. doi: 10.1016/S2468-1253(19)30119-0
5. Bartenschlager R, Urban S, Protzer U. Towards Curative Therapy of Chronic Viral Hepatitis. *Z Gastroenterol* (2019) 57(1):61–73. doi: 10.1055/a-0824-1576
6. Kosinska AD, Bauer T, Protzer U. Therapeutic Vaccination for Chronic Hepatitis B. *Curr Opin Virol* (2017) 23:75–81. doi: 10.1016/j.coviro.2017.03.011
7. Suslov A, Wieland S, Menne S. Modulators of Innate Immunity as Novel Therapeutics for Treatment of Chronic Hepatitis B. *Curr Opin Virol* (2018b) 30:9–17. doi: 10.1016/j.coviro.2018.01.008
8. Bertoletti A, Tan AT. HBV as a Target for CAR or TCR-T Cell Therapy. *Curr Opin Immunol* (2020b) 66:35–41. doi: 10.1016/j.coi.2020.04.003
9. Hoogeveen RC, Boonstra A. Checkpoint Inhibitors and Therapeutic Vaccines for the Treatment of Chronic HBV Infection. *Front Immunol* (2020) 11:401. doi: 10.3389/fimmu.2020.00401
10. Meng Z, Chen Y, Lu M. Advances in Targeting the Innate and Adaptive Immune Systems to Cure Chronic Hepatitis B Virus Infection. *Front Immunol* (2019) 10:3127. doi: 10.3389/fimmu.2019.03127

11. Bertoletti A, Tan AT. Challenges of CAR- and TCR-T Cell-Based Therapy for Chronic Infections. *J Exp Med* (2020a) 217(5):e20191663. doi: 10.1084/jem.20191663
12. Menne S, Cote PJ. The Woodchuck as an Animal Model for Pathogenesis and Therapy of Chronic Hepatitis B Virus Infection. *World J Gastroenterol* (2007) 13(1):104–24. doi: 10.3748/wjg.v13.i1.104
13. Suresh M, Menne S. Application of the Woodchuck Animal Model for the Treatment of Hepatitis B Virus-Induced Liver Cancer. *World J Gastrointest Oncol* (2021) 13(6):509–35. doi: 10.4251/wjgo.v13.i6.509
14. Cote PJ, Korba BE, Miller RH, Jacob JR, Baldwin BH, Hornbuckle WE, et al. Effects of Age and Viral Determinants on Chronicity as an Outcome of Experimental Woodchuck Hepatitis Virus Infection. *Hepatology* (2000) 31 (1):190–200. doi: 10.1002/hep.510310128
15. Carty M, Guy C, Bowie AG. Detection of Viral Infections by Innate Immunity. *Biochem Pharmacol* (2021) 183:114316. doi: 10.1016/j.bcp.2020.114316
16. Amarante-Mendes GP, Adjemian S, Branco LM, Zanetti LC, Weinlich R, Bortoluci KR. Pattern Recognition Receptors and the Host Cell Death Molecular Machinery. *Front Immunol* (2018) 9:2379. doi: 10.3389/fimmu.2018.02379
17. Liu G, Gack MU. Distinct and Orchestrated Functions of RNA Sensors in Innate Immunity. *Immunity* (2020) 53(1):26–42. doi: 10.1016/j.immuni.2020.03.017
18. Wieland S, Thimme R, Purcell RH, Chisari FV. Genomic Analysis of the Host Response to Hepatitis B Virus Infection. *Proc Natl Acad Sci USA* (2004) 101 (17):6669–74. doi: 10.1073/pnas.0401771101
19. Revill P, Yuan Z. New Insights Into How HBV Manipulates the Innate Immune Response to Establish Acute and Persistent Infection. *Antivir Ther* (2013) 18(1):1–15. doi: 10.3851/IMP2542
20. Faure-Dupuy S, Lucifora J, Durantel D. Interplay Between the Hepatitis B Virus and Innate Immunity: From an Understanding to the Development of Therapeutic Concepts. *Viruses* (2017) 9(5):95. doi: 10.3390/v9050095
21. Megahed FAK, Zhou X, Sun P. The Interactions Between HBV and the Innate Immunity of Hepatocytes. *Viruses* (2020) 12(3):285. doi: 10.3390/v12030285
22. Suslov A, Boldanova T, Wang X, Wieland S, Heim MH. Hepatitis B Virus Does Not Interfere With Innate Immune Responses in the Human Liver. *Gastroenterology* (2018a) 154(6):1778–90. doi: 10.1053/j.gastro.2018.01.034
23. Lanford RE, Guerra B, Chavez D, Giavedoni L, Hodara VL, Brasky KM, et al. GS-9620, an Oral Agonist of Toll-Like Receptor-7, Induces Prolonged Suppression of Hepatitis B Virus in Chronically Infected Chimpanzees. *Gastroenterology* (2013) 144(7):1508–1517, 1517 e1501-1510. doi: 10.1053/j.gastro.2013.02.003
24. Menne S, Tumas DB, Liu KH, Thampi L, AlDeghaither D, Baldwin BH, et al. Sustained Efficacy and Seroconversion With the Toll-Like Receptor 7 Agonist GS-9620 in the Woodchuck Model of Chronic Hepatitis B. *J Hepatol* (2015) 62 (6):1237–45. doi: 10.1016/j.jhep.2014.12.026
25. Gane EJ, Lim YS, Gordon SC, Visvanathan K, Sicard E, Fedorak RN, et al. The Oral Toll-Like Receptor-7 Agonist GS-9620 in Patients With Chronic Hepatitis B Virus Infection. *J Hepatol* (2015) 63(2):320–8. doi: 10.1016/j.jhep.2015.02.037
26. Daffis S, Balsitis S, Chamberlain J, Zheng J, Santos R, Rowe W, et al. Toll-Like Receptor 8 Agonist GS-9688 Induces Sustained Efficacy in the Woodchuck Model of Chronic Hepatitis B. *Hepatology* (2020) 73(1):53–67. doi: 10.1002/hep.31255
27. Meng Z, Zhang X, Pei R, Zhang E, Kemper T, Vollmer J, et al. Combination Therapy Including CpG Oligodeoxynucleotides and Entecavir Induces Early Viral Response and Enhanced Inhibition of Viral Replication in a Woodchuck Model of Chronic Hepadnaviral Infection. *Antiviral Res* (2016) 125:14–24. doi: 10.1016/j.antiviral.2015.11.001
28. Korolowizc KE, Li B, Huang X, Yon C, Rodrigo E, Corpuz M, et al. Liver-Targeted Toll-Like Receptor 7 Agonist Combined With Entecavir Promotes a Functional Cure in the Woodchuck Model of Hepatitis B Virus. *Hepatol Commun* (2019) 3(10):1296–310. doi: 10.1002/hep4.1397
29. Korolowicz KE, Suresh M, Li B, Huang X, Yon C, Leng X, et al. Treatment With the Immunomodulator AIC649 in Combination With Entecavir Produces Antiviral Efficacy in the Woodchuck Model of Chronic Hepatitis B. *Viruses* (2021b) 13(4):648. doi: 10.3390/v13040648
30. Iyer RP, Roland A, Jin Y, Mounir S, Korba B, Julander JG, et al. Anti-Hepatitis B Virus Activity of ORI-9020, a Novel Phosphorothioate Dinucleotide, in a Transgenic Mouse Model. *Antimicrob Agents Chemother* (2004) 48(6):2318–20. doi: 10.1128/AAC.48.6.2318-2320.2004
31. Korolowicz KE, Iyer RP, Czerwinski S, Suresh M, Yang J, Padmanabhan S, et al. Antiviral Efficacy and Host Innate Immunity Associated With SB 9200 Treatment in the Woodchuck Model of Chronic Hepatitis B. *PloS One* (2016) 11(8):e0161313. doi: 10.1371/journal.pone.0161313
32. Suresh M, Korolowicz KE, Balarezo M, Iyer RP, Padmanabhan S, Cleary D, et al. Antiviral Efficacy and Host Immune Response Induction During Sequential Treatment With SB 9200 Followed by Entecavir in Woodchucks. *PloS One* (2017) 12(1):e0169631. doi: 10.1371/journal.pone.0169631
33. Jeffries AM, Marriott I. Cytosolic DNA Sensors and CNS Responses to Viral Pathogens. *Front Cell Infect Microbiol* (2020) 10:576263. doi: 10.3389/fcimb.2020.576263
34. Kuriakose T, Kanneganti TD. ZBP1: Innate Sensor Regulating Cell Death and Inflammation. *Trends Immunol* (2018) 39(2):123–34. doi: 10.1016/j.it.2017.11.002
35. Zheng D, Liwinski T, Elinav E. Inflammasome Activation and Regulation: Toward a Better Understanding of Complex Mechanisms. *Cell Discov* (2020) 6 (1):36. doi: 10.1038/s41421-020-0167-x
36. Yang Y, Zhao X, Wang Z, Shu W, Li L, Li Y, et al. Nuclear Sensor Interferon-Inducible Protein 16 Inhibits the Function of Hepatitis B Virus Covalently Closed Circular DNA by Integrating Innate Immune Activation and Epigenetic Suppression. *Hepatology* (2020) 71(4):1154–69. doi: 10.1002/hep.30897
37. Yan Q, Li M, Liu Q, Li F, Zhu B, Wang J, et al. Molecular Characterization of Woodchuck IFI16 and AIM2 and Their Expression in Woodchucks Infected With Woodchuck Hepatitis Virus (WHV). *Sci Rep* (2016) 6:28776. doi: 10.1038/srep28776
38. Suresh M, Li B, Murreddu MG, Gudima SO, Menne S. Involvement of Innate Immune Receptors in the Resolution of Acute Hepatitis B in Woodchucks. *Front Immunol* (2021) 12:713420. doi: 10.3389/fimmu.2021.713420
39. Murreddu MG, Suresh M, Gudima SO, Menne S. Measurement of Antiviral Effect and Innate Immune Response During Treatment of Primary Woodchuck Hepatocytes. *Methods Mol Biol* (2017) 1540:277–94. doi: 10.1007/978-1-4939-6700-1_24
40. Suresh M, Czerwinski S, Murreddu MG, Kallakury BV, Ramesh A, Gudima SO, et al. Innate and Adaptive Immunity Associated With Resolution of Acute Woodchuck Hepatitis Virus Infection in Adult Woodchucks. *PloS Pathog* (2019) 15(12):e1008248. doi: 10.1371/journal.ppat.1008248
41. Freitas N, Lukash T, Rodrigues L, Litwin S, Kallakury BV, Menne S, et al. Infection Patterns Induced in Naive Adult Woodchucks by Virions of Woodchuck Hepatitis Virus Collected During Either the Acute or Chronic Phase of Infection. *J Virol* (2015) 89(17):8749–63. doi: 10.1128/JVI.00984-15
42. PolyPlus. Available at: https://www.polyplus-transfection.com.
43. Niu C, Li L, Daffis S, Lucifora J, Bonnin M, Maadadi S, et al. Toll-Like Receptor 7 Agonist GS-9620 Induces Prolonged Inhibition of HBV *via* a Type I Interferon-Dependent Mechanism. *J Hepatol* (2018) 68(5):922–31. doi: 10.1016/j.jhep.2017.12.007
44. Dinarello CA. Immunological and Inflammatory Functions of the Interleukin-1 Family. *Annu Rev Immunol* (2009) 27:519–50. doi: 10.1146/annurev.immunol.021908.132612
45. Nakanishi K. Unique Action of Interleukin-18 on T Cells and Other Immune Cells. *Front Immunol* (2018) 9:763. doi: 10.3389/fimmu.2018.00763
46. Bellezza CAC, Hornbuckle WE, Roth L, Tennant BC. Woodchucks as Laboratory Animals. In *Laboratory Animal Medicine*, 2nd Ed. Amsterdam, The Netherlands Elsevier Science (2002). p. 309–28. doi: 10.1016/B978-012263951-7/50011-9
47. Korolowicz KE, Suresh M, Li B, Huang X, Yon C, Kallakury BV, et al. Combination Treatment With the Vimentin-Targeting Antibody hzVSF and Tenofovir Suppresses Woodchuck Hepatitis Virus Infection in Woodchucks. *Cells* (2021a) 10(9):2321. doi: 10.3390/cells10092321
48. Menne S, Cote PJ, Butler SD, Toshkov IA, Gerin JL, Tennant BC. Immunosuppression Reactivates Viral Replication Long After Resolution of Woodchuck Hepatitis Virus Infection. *Hepatology* (2007) 45(3):614–22. doi: 10.1002/hep.21558
49. Bertoletti A, Ferrari C. Adaptive Immunity in HBV Infection. *J Hepatol* (2016) 64(1 Suppl):S71–83. doi: 10.1016/j.jhep.2016.01.026
50. Maini MK, Gehring AJ. The Role of Innate Immunity in the Immunopathology and Treatment of HBV Infection. *J Hepatol* (2016) 64(1 Suppl):S60–70. doi: 10.1016/j.jhep.2016.01.028

51. Chiale C, Marchese AM, Robek MD. Innate Immunity and HBV Persistence. *Curr Opin Virol* (2021) 49:13–20. doi: 10.1016/j.coviro.2021.04.003
52. Sato S, Li K, Kameyama T, Hayashi T, Ishida Y, Murakami S, et al. The RNA Sensor RIG-I Dually Functions as an Innate Sensor and Direct Antiviral Factor for Hepatitis B Virus. *Immunity* (2015) 42(1):123–32. doi: 10.1016/j.immuni.2014.12.016
53. Wu J, Huang S, Zhao X, Chen M, Lin Y, Xia Y, et al. Poly(I:C) Treatment Leads to Interferon-Dependent Clearance of Hepatitis B Virus in a Hydrodynamic Injection Mouse Model. *J Virol* (2014) 88(18):10421–31. doi: 10.1128/JVI.00996-14
54. Cheng X, Xia Y, Serti E, Block PD, Chung M, Chayama K, et al. Hepatitis B Virus Evades Innate Immunity of Hepatocytes But Activates Cytokine Production by Macrophages. *Hepatology* (2017) 66(6):1779–93. doi: 10.1002/hep.29348
55. Lauterbach-Riviere L, Bergez M, Monch S, Qu B, Riess M, Vondran FWR, et al. Hepatitis B Virus DNA is a Substrate for the cGAS/STING Pathway But is Not Sensed in Infected Hepatocytes. *Viruses* (2020) 12(6):592. doi: 10.3390/v12060592
56. Ablasser A, Bauernfeind F, Hartmann G, Latz E, Fitzgerald KA, Hornung V. RIG-I-Dependent Sensing of Poly(Da:Dt) Through the Induction of an RNA Polymerase III-Transcribed RNA Intermediate. *Nat Immunol* (2009) 10(10):1065–72. doi: 10.1038/ni.1779
57. Wieland SF, Guidotti LG, Chisari FV. Intrahepatic Induction of Alpha/Beta Interferon Eliminates Viral RNA-Containing Capsids in Hepatitis B Virus Transgenic Mice. *J Virol* (2000) 74(9):4165–73. doi: 10.1128/jvi.74.9.4165-4173.2000
58. Lucifora J, Xia Y, Reisinger F, Zhang K, Stadler D, Cheng X, et al. Specific and Nonhepatotoxic Degradation of Nuclear Hepatitis B Virus cccDNA. *Science* (2014) 343(6176):1221–8. doi: 10.1126/science.1243462
59. Liu Y, Nie H, Mao R, Mitra B, Cai D, Yan R, et al. Interferon-Inducible Ribonuclease ISG20 Inhibits Hepatitis B Virus Replication Through Directly Binding to the Epsilon Stem-Loop Structure of Viral RNA. *PloS Pathog* (2017) 13(4):e1006296. doi: 10.1371/journal.ppat.1006296
60. Michalska A, Blaszczyk K, Wesoly J, Bluyssen HAR. A Positive Feedback Amplifier Circuit That Regulates Interferon (IFN)-Stimulated Gene Expression and Controls Type I and Type II IFN Responses. *Front Immunol* (2018) 9:1135. doi: 10.3389/fimmu.2018.01135
61. Fletcher SP, Chin DJ, Gruenbaum L, Bitter H, Rasmussen E, Ravindran P, et al. Intrahepatic Transcriptional Signature Associated With Response to Interferon-Alpha Treatment in the Woodchuck Model of Chronic Hepatitis B. *PloS Pathog* (2015) 11(9):e1005103. doi: 10.1371/journal.ppat.1005103
62. Park JH, Kim KL, Cho EW. Detection of Surface Asialoglycoprotein Receptor Expression in Hepatic and Extra-Hepatic Cells Using a Novel Monoclonal Antibody. *Biotechnol Lett* (2006) 28(14):1061–9. doi: 10.1007/s10529-006-9064-0
63. Harris RL, van den Berg CW, Bowen DJ. ASGR1 and ASGR2, the Genes That Encode the Asialoglycoprotein Receptor (Ashwell Receptor), Are Expressed in Peripheral Blood Monocytes and Show Interindividual Differences in Transcript Profile. *Mol Biol Int* (2012) 2012:283974. doi: 10.1155/2012/283974
64. Suresh M. *Immune Responses During Resolution of Acute Hepatitis B in Woodchucks and Their Modulation for Treatment of Chronic Hepatitis B* (2020). Washington, DC: Georgetown University Dissertation Document.

Conflict of Interest: SM serves occasionally as a paid scientific consultant to Northeastern Wildlife, Inc. (Harris, ID, USA), the only commercial source for woodchucks within the United States, from which the animals of the current study were purchased.

The remaining authors declare that the research was conducted in the absence of any commercial or financial relationships that could be construed as a potential conflict of interest.

Publisher's Note: All claims expressed in this article are solely those of the authors and do not necessarily represent those of their affiliated organizations, or those of the publisher, the editors and the reviewers. Any product that may be evaluated in this article, or claim that may be made by its manufacturer, is not guaranteed or endorsed by the publisher.

frontiers in Immunology

ORIGINAL RESEARCH
published: 06 October 2021
doi: 10.3389/fimmu.2021.734246

Depletion of T cells *via* Inducible Caspase 9 Increases Safety of Adoptive T-Cell Therapy Against Chronic Hepatitis B

Alexandre Klopp[1,2,3], *Sophia Schreiber*[1,2], *Anna D. Kosinska*[1,2,3], *Martin Pulé*[4], *Ulrike Protzer*[1,2,3] *and Karin Wisskirchen*[1,2,3]*

[1] School of Medicine, Institute of Virology, Technical University of Munich, Munich, Germany, [2] Institute of Virology, Helmholtz Zentrum München, Munich, Germany, [3] German Center for Infection Research (DZIF), Munich Partner Site, Munich, Germany, [4] Department of Haematology, Cancer Institute, University College London, London, United Kingdom

OPEN ACCESS

Edited by:
Nilu Goonetilleke, University of North Carolina at Chapel Hill, United States

Reviewed by:
Anthony Tanoto Tan, Duke-NUS Medical School, Singapore
Rachel Rutishauser, University of California, San Francisco, United States

***Correspondence:**
Karin Wisskirchen
Karin.wisskirchen@helmholtz-muenchen.de

Specialty section:
This article was submitted to Viral Immunology, a section of the journal Frontiers in Immunology

Received: *30 June 2021*
Accepted: *17 September 2021*
Published: *06 October 2021*

Citation:
Klopp A, Schreiber S, Kosinska AD, Pulé M, Protzer U and Wisskirchen K (2021) Depletion of T cells via Inducible Caspase 9 Increases Safety of Adoptive T-Cell Therapy Against Chronic Hepatitis B. Front. Immunol. 12:734246. doi: 10.3389/fimmu.2021.734246

T-cell therapy with T cells that are re-directed to hepatitis B virus (HBV)-infected cells by virus-specific receptors is a promising therapeutic approach for treatment of chronic hepatitis B and HBV-associated cancer. Due to the high number of target cells, however, side effects such as cytokine release syndrome or hepatotoxicity may limit safety. A safeguard mechanism, which allows depletion of transferred T cells on demand, would thus be an interesting means to increase confidence in this approach. In this study, T cells were generated by retroviral transduction to express either an HBV-specific chimeric antigen receptor (S-CAR) or T-cell receptor (TCR), and in addition either inducible caspase 9 (iC9) or herpes simplex virus thymidine kinase (HSV-TK) as a safety switch. Real-time cytotoxicity assays using HBV-replicating hepatoma cells as targets revealed that activation of both safety switches stopped cytotoxicity of S-CAR- or TCR-transduced T cells within less than one hour. *In vivo*, induction of iC9 led to a strong and rapid reduction of transferred S-CAR T cells adoptively transferred into AAV-HBV-infected immune incompetent mice. One to six hours after injection of the iC9 dimerizer, over 90% reduction of S-CAR T cells in the blood and the spleen and of over 99% in the liver was observed, thereby limiting hepatotoxicity and stopping cytokine secretion. Simultaneously, however, the antiviral effect of S-CAR T cells was diminished because remaining S-CAR T cells were mostly non-functional and could not be restimulated with HBsAg. A second induction of iC9 was only able to deplete T cells in the liver. In conclusion, T cells co-expressing iC9 and HBV-specific receptors efficiently recognize and kill HBV-replicating cells. Induction of T-cell death via iC9 proved to be an efficient means to deplete transferred T cells *in vitro* and *in vivo* containing unwanted hepatotoxicity.

Keywords: T-cell therapy, chronic hepatitis B, safeguard molecules, inducible caspase 9, suicide switch, chimeric antigen receptor (CAR)

INTRODUCTION

Worldwide, about 257 million humans are chronically infected with the hepatitis B virus (HBV) (1). Around one third of those will develop secondary diseases such as liver cirrhosis or hepatocellular carcinoma. The currently available treatments for chronic hepatitis B suppress viral replication but in most of the cases do not lead to eradication of the virus (2). In acute hepatitis B a strong immune response develops, in which $CD8^+$ T cells are key to clearing the virus. By contrast, the T-cell response against the virus in patients with chronic hepatitis B is inefficient because it is weak and oligoclonal (3). Hence, adoptive T-cell therapy with HBV-specific T cells represents a promising therapeutic strategy in order to eliminate HBV and induce functional cure (4).

T cells can be genetically engineered to express either an HBV-specific chimeric antigen receptor (S-CAR) (5, 6) or a natural T-cell receptor (TCR) (7, 8). The S-CAR contains an antibody fragment that is directed against HBV surface proteins present on cells, in which the virus replicates (9). Upon binding to HBsAg on cells, the S-CAR T cell becomes activated through its CD28 and CD3 signaling domains. The natural TCRs recognize either HBV core- or S-peptides presented on HLA-A2 and their engagement leads to physiological activation of the T cell (7, 8). Previous *in vitro* experiments in our laboratory have demonstrated that both, S-CAR T cells and TCR T cells are very efficient effector cells, capable of eliminating up to 100% of HBV-replicating target cells and secreting high amounts of antiviral cytokines such as IFN-γ (5–7). *In vivo*, specific killing of HBV-replicating hepatocytes leads to a transient and moderate increase of alanine amino transferase (ALT) levels after transfer of S-CAR T cells into HBV-transgenic (6) or TCR T cells into HBV-infected uPA-SCID mice (8).

Since adoptive transfer of functionally active HBV-specific T cells intends to eliminate infected hepatocytes, the benefits of resolving persistent HBV infection may come along with risks of inducing a hepatitis flare. Furthermore, although S-CAR T cells only seem to be sensitive to cell- or plate-bound HBsAg *in vitro* and did not cause any severe liver damage *in vivo* (5, 6), soluble HBsAg in the serum of infected patients still poses a theoretical risk of off-site activation of the cells and an unwanted cytokine release. Hence, the evaluation of strategies to increase the safety of adoptively transferred HBV-specific T cells is an important step to prevent and overcome these potential threats.

Several clinical cancer trials using T-cell therapy have reported a morbidity and occasionally mortality resulting from T-cell toxicity (10). These include on-target, off-tumor effects because some target antigens are also expressed on healthy tissues (11, 12), or off-target effects due to unintentionally or deliberately (e.g. to increase affinity) inserted mutations in the sequence of a particular TCR or CAR (13–15). The most frequent side effect observed after CAR T-cell therapy is a cytokine release syndrome (CRS), which is believed to be an indirect consequence of an excessive expansion and activation of CAR T cells. It may even have a fatal outcome for the respective patient (16, 17), although clinicians in the meantime have gained ample experience how to handle CRS and prevent severe consequences (16).

To increase safety of adoptive cell transfer, various safeguard systems have been developed to allow depletion of transferred T cells on demand. Safeguard mechanisms can be expressed either intra- or extracellularly and, when activated, induce "suicide" of the transferred T cell. The most commonly tested mechanisms in the clinics are an inducible caspase 9 (iC9) (18) and a thymidine kinase of herpes simplex virus (HSV-TK) (19). iC9 consists of a part of the human caspase 9 and a domain that can bind the small molecules AP1903 and AP20187 with high affinity. These molecules act as chemical inducers of dimerization (CID) of the iC9 which then rapidly activates downstream executing caspases resulting in apoptosis of the cell carrying iC9. HSV-TK phosphorylates the prodrug ganciclovir (GCV) that is then incorporated into host DNA and terminates the elongation of DNA strands leading to cell death (20). Its effect, however, is not strictly limited to the HSV-TK positive cells and can also affect neighbouring cells (21).

In this study, we expressed either iC9 or HSV-TK in HBV-specific-TCR and S-CAR T cells. We investigated the effect of induction of these safeguard mechanisms on cytotoxicity and cytokine release of redirected T cells and the consequences of T-cell depletion for the antiviral effect *in vitro* in cell culture. Furthermore, depletion of S-CAR T-cells via iC9 was studied *in vivo* in a preclinical model of chronic HBV infection.

MATERIALS AND METHODS

Cloning

All constructs (HBV-specific receptors and safeguard molecules) used were codon-optimized. iC9 or HSV-TK were linked to the respective receptors via a T2A element. The HBV-specific receptors were amplified from constructs previously described for the S-CAR (5) or the HBV-specific TCRs (7). Plasmids coding for the safeguard mechanisms [iC9 and HSV-TK (22)] were obtained from Martin Pulé. PCRs of safeguard and receptor genes were performed with the Phusion Hot Start Flex 2x Master Mix (New England Biolabs) according to the manufacturer's instructions. The primers linking both fragments were designed with an overlap of ~ 18 bp. The fusion of two equimolar PCR fragments (total of 300 ng) was performed with 15 initial cycles without the primers followed by additional 15 cycles after addition of the primers. Plasmids were purified with the GeneJET Plasmid Miniprep Kit (Thermo Fisher Scientific) or the Plasmid *Plus*Midi Kit (Qiagen) depending on the desired quantity of purified plasmid, following the manufacturer's instructions.

Retroviral Transduction of Human PBMCs

24-well non-tissue culture plates (Falcon) were coated with human anti-CD3 (eBioscience) (5 µg/mL) and anti-CD28 (eBioscience) (0.05 µg/mL) antibodies (2 hours, 37°C) and blocked for 30 minutes at 37°C with 2% bovine serum albumin (BSA) in PBS. Freshly isolated or thawed human PBMCs were counted and adjusted to $0.6\text{-}0.8x10^6$ cells/mL human T cell medium (hTCM) [RPMI, 10% fetal calf serum (FCS), 1% glutamine, 1% penicillin and streptomycin, 1% sodium pyruvate, 1% non-essential amino acids (NEAA) and 0.01 M

HEPES (all from Thermo Fisher Scientific)] supplemented with 300 U/mL IL-2 (Novartis) and 1.5 mL of the cell suspension was seeded per well (day one). Cells were incubated for 48 hours at 37°C. After incubation, two transduction rounds on two consecutive days (day three and four) were performed. Before transduction, non-tissue 6- or 24-well-plates were coated with RetroNectin (20 µg/mL in PBS, 2 hours at RT; Takara) and blocked for 30 minutes at 37°C with 2% BSA in PBS. Retroviral supernatants were obtained from RD114 packaging cells (293GP-R30 (23), Biovec pharma) that had been transfected (Lipofectamine 2000 from Invitrogen) with MP71 retroviral plasmids [as previously described (7)] containing the respective sequences, filtered (0.45 µm sterile filter from Sarstedt) and added to the wells. Plates were centrifuged (2000 g, 2 hours, 32°C). During centrifugation, the PBMCs were counted, washed and adjusted to $1x10^6$ cells per mL fresh hTCM supplemented with 300 U/mL IL-2. After centrifugation, the cell suspension was added to the plates containing the supernatants. The plates were centrifuged once again (1000 g, 10 minutes, 32°C) and incubated at 37°C overnight. On day five and six, the T cells were collected, washed and counted. They were then adjusted to $0.5x10^6$ cells/mL supplement with 180 U/mL IL-2 for expansion. On day ten, the transduction rate of the T cells was determined by flow cytometry (see below) and they were either frozen or subsequently used for functional assessment.

Co-Culture Experiments

For functionality assessment, transduced T cells were co-cultured with target cells. For all co-culture experiments, unless otherwise stated, $5x10^4$ HepG2.2.15 cells [stable HBV-producing human hepatoma cell line derived from HepG2 (24, 25)] were seeded in 200 µL DMEM full medium (10% FCS, 1% penicillin and streptomycin, 1% glutamine, 1% NEEA and 1% sodium pyruvate) per well on a collagen-coated (Collagen R (Serva) 1:10 in H_2O for 30 minutes at 37°C) 96-well electronic microtiter plates (ACEA Biosciences) seven to ten days prior start of the co-culture. The following day, medium was changed to Diff medium [DMEM full medium + 2.5% DMSO (Sigma)], allowing the differentiation of target cells. Transduced T cells were either taken from an expansion culture or thawed one day prior to starting the co-culture and kept in culture with 30 U/mL IL-2. On the day of the co-culture, transduced T cells were washed and resuspended in the appropriate amount of fresh hTCM without IL-2. Medium was changed on the plates with target cells to DMEM full medium with 2% DMSO, 100 µL/well. Transduced T cells were added to the wells in an indicated E:T ratio in 100 µL/well (final concentration of 1% DMSO in co-culture). The number of effector T cells/well was adjusted according to the transduction efficiency of each receptor to identical numbers of receptor-expressing cells. Real-time viability of target cells was determined using an xCELLigence SP Real-Time Cell Analyzer (ACEA Biosciences) allowing the quantitative and continuous monitoring of adherent target cells, through the measurement of electrical impedance every 15 minutes. The electrical impedance displayed as cell index (CI) and determining the target cell viability was normalized to the start of the co-culture. Experiments were performed in triplicates. For addition of CID [B/B Homodimerizer (AP20187) from Takara; 0.5 mM in 100% ethanol] or ganciclovir (Invivogen; 10 mg/mL in distilled water adjusted with NaOH 1M and HCl 1M to pH 11), 100 µL medium was removed per well. The respective substance was diluted in DMEM full medium to achieve the desired concentration and 100 µL were added per well.

The concentration of human IFN-γ in the supernatant to assess the activation of T cells was determined using MaxiSorb ELISA 96-well plates (Thermo Fisher Scientific) and commercially available ELISA kits (Invitrogen) according to manufacturer's instructions. The conversion of TMB substrate was determined by measurement of OD_{450} subtracted by OD_{560} on an ELISA-Reader infinite F200 (Tecan).

Flow Cytometry

For the staining of surface proteins, cells were resuspended in FACS buffer (0.1% BSA in PBS) with the respective antibodies and incubated for 30 minutes on ice and in the dark. The following antibodies were used: mCD4 (eBioscience), mCD8 (BD Biosciences), mCD45.1 (eBioscience), mCD45.2, mIFN-γ, mTNF-α (all from BD Biosciences); hCD4 (Thermo Fisher Scientific), hCD8 (Dako). Viability of cells was determined using a live/dead cell marker (LIVE/DEAD Fixable Green Dead Cell Stain Kit, Thermo Fisher Scientific). For intracellular cytokine staining, cells were permeabilized by resuspending them in Cytofix/Cytoperm (BD Biosciences) prior to the antibody staining, following the manufacturer's instructions. In order to determine the absolute cell count by flow cytometry, CountBright™ Absolute Counting Beads (Thermo Fisher Scientific) were added to the cell suspension shortly before measurement. If CAR expression was analyzed together with other surface proteins such as CD8, stainings were performed sequentially. The CAR was first stained with an anti-human IgG antibody (Abcam) followed by the staining of the other surface proteins with the respective antibody. The samples were then analyzed on a CytoFLEX S flow cytometer (Beckman Coulter). The obtained data was evaluated with FlowJo 10.4.

Retroviral Transduction of Murine Splenocytes

24-well non-tissue culture plates were coated with murine anti-CD3 and anti-CD28 antibodies (kindly provided by R. Feederle, Helmholtz Zentrum München) at a concentration of 10 µg/mL each in PBS for 2 hours at 37°C and blocked for 30 minutes at 37°C with 2% BSA in PBS. Freshly isolated murine splenocytes from donor mice were enriched for $CD8^+$ by magnetic activated cell sorting (MACS) using CD8a (Ly2) Microbeads (Miltenyi). $CD8^+$ T cells were separated according to manufacturer's instructions. They were counted, washed and adjusted to $0.8x10^6$ cells per 1.5 mL mouse T cell medium (mTCM) (RPMI Dutch modified, 10% FCS, 1% glutamine, 1% penicillin and streptomycin, 1% sodium pyruvate, and 50 µM β-mercaptoethanol all from Thermo Fisher Scientific) and supplemented with 5 ng/mL IL-12 (kindly provided by E. Schmitt, University of Mainz). 1.5 mL of the cells were then seeded on the antibody-coated 24-well plates and incubated at 37°C overnight. On the following day, retroviral supernatant from Platinum-E packaging cells (based on the 293T

cell line) transfected with MP71 retroviral plasmids containing the respective coding sequence was collected and filtered (0.45 µm sterile filter). Protamine sulfate (2 µg/mL; Leo Pharma) was added to the activated $CD8^+$ T cells and the retroviral supernatants. The retroviral supernatant was then added to the wells and the plates were centrifuged (2500 rpm, 90 minutes, 32°C). Cells were incubated overnight at 37°C. On the next day, a second transduction round similar to the first round was performed. Here, 2 mL of supernatant per well was collected from the plates and stored at 37°C. It was re-added after the centrifugation step and supplied with 2 µg/mL protamine sulfate. On day four, the transduction rate was determined by flow cytometry. The cells were counted, washed and resuspended in the appropriate volume of PBS to allow injection of $2x10^6$ transduced T cells in 200 µL PBS per mouse.

Animal Experiments

Mouse experiments were conducted in accordance with the German Law for the Protection of Animals and were approved by the local authorities (Regierung von Oberbayern). $Rag2^{-/-}$IL-$2Rgc^{-/-}$ recipient mice and $CD45.1^+$ C57BL/6J donor mice were bred and kept in-house in specific pathogen-free animal facilities. AAV serotype 2 containing the genome of HBV genotype D was packed with an AAV serotype 8 capsid, as previously reported (26). In both mouse experiments shown in this paper (**Figures 3–6**) male and female mice were used. Based on the previous observation that HBV replicates better in AAV-HBV-infected male mice, the AAV-titer was adjusted accordingly: male mice were infected with $1x10^{10}$ and female mice with $3x10^{10}$ viral genomes, each in 100 µL PBS injected in the tail vein. For T-cell transfer, $2x10^6$ freshly transduced murine T cells were injected in 200 µL PBS intraperitoneally per mouse ($Rag2^{-/-}$IL-$2Rgc^{-/-}$, 14-20 weeks old). Both, the virus stock solution as well as the T cells were kept on ice until shortly before injection. CID (AP20187 from Takara) was prepared according to the manufacturer's recommendation using the prepared stock solution (lyophilized dimerizer in 100% ethanol), PEG-400 (100%; Sigma-Aldrich) and Tween (2%; Roth). CID was administered via intraperitoneal injection within 30 min after preparation in a dosage of 10 mg/kg and was kept on ice until shortly before injection. Four similar iC9 depletion experiments were performed and two representative experiments are shown (**Figures 3–5**).

Serological Analyses

Peripheral blood was collected into Microvette 500 LH-Gel tubes (Sarstedt) and centrifuged to separate serum (10 minutes, 5000 g, RT). For measurement of ALT levels, serum was diluted 1:4 with PBS and the Reflotron ALT test was used (Roche Diagnostics). Serum HBs- and HBe-antigen levels were determined on an Architect™ platform using the quantitative HBsAg test (6C36-44; cut-off, 0.25 IU/mL) and the HBeAg Reagent Kit with HBeAg Quantitative Calibrators (7P24-01; cut-off, 0.20 PEI U/mL) (Abbott Laboratories). Serum levels of IFN-γ, TNF-α, IL-6 and MCP-1 were detected via the cytometric bead array mouse inflammation kit (BD) according to the manufacturer's instructions and measured on a CytoFLEX S flow cytometer (Beckman Coulter). Data analysis was done with the Prism 8 software.

Isolation of Human and Murine PBMCs, Murine Splenocytes and Murine Liver-Associated Lymphocytes

For the isolation of human PBMCs, blood was collected from healthy donors using a syringe containing heparin. The PBMCs were purified by diluting the blood 1:2 with wash medium (RPMI + 1% Pen/Strep) and layering it on top of Biocoll separating solution (Biochrom) for centrifugation (1200 g, 20 minutes at RT without breaks). For the isolation of murine splenocytes, spleens from donor mice were mashed through a 100 µm cell strainer (Falcon), washed and resuspended in 2 mL of ACK lysis buffer (8 g NH_4Cl, 1 g $KHCO_3$, 37 mg Na_2EDTA, add to 1 l H_2O, pH 7.2-7.4) and incubated for 2 minutes at RT to lyse the erythrocytes. The reaction was stopped by addition of 48 mL of mTCM, the splenocytes were pelleted (350 g, 5 minutes, 4°C) and resuspended in the appropriate medium and volume. For isolation of mouse PBMCs, 15 µL of heparinized whole blood from Microvette 500 LH-Gel tubes was incubated with 250 µL ACK lysis buffer for 2 minutes at RT. Cells were then pelleted and resuspended with 200 µL of FACS buffer. For isolation of liver-associated lymphocytes (LAL), livers were collected from mice after perfusion with PBS to remove non-liver associated lymphocytes. The livers were mashed through a 100 µm cell strainer and washed. The cell strainer was repeatedly washed with wash medium followed by additional mashing steps. The flow through including the cells was then pelleted (350 g, 5 minutes, 4°C), resuspended in 12.5 mL collagenase medium [4500 U collagenase type 4 (Worthington) in Williams Medium E (Thermo Fisher Scientific) supplemented with 8.75 µL $CaCl_2$ (2,5M)] and incubated at 37°C for 20 min with repeated stirring. After centrifugation, liver leukocytes were purified using an 80%/40% Percoll (GE Healthcare) gradient (1400 g, 20 minutes, RT, without brake).

Ex Vivo Antigen Stimulation

Flat-bottom 96-well non-tissue-plates were coated with HBsAg (2.5 µg/mL in PBS; Roche Diagnostics) or anti-CD3 and anti-CD28 antibodies (10 µg/mL in PBS) for two hours at 37°C and blocked for 30 minutes at 37°C with 2% BSA in PBS. After incubation, transduced T cells, freshly isolated splenocytes or LALs were added in appropriate number ($2x10^5$ cells/well) to the plate. Cells were incubated for the indicated time at 37°C. For the analysis of intracellular cytokine expression by ICS, Brefeldin A (1 µg/mL; Sigma-Aldrich) was added to cells two hours after start of stimulation and cells were incubated for additional 14 hours at 37°C.

Immunohistochemistry

Liver pieces were fixed in 4% paraformaldehyde (PFA; Santa Cruz Biotechnology) for 24 hours and then transferred into PBS until paraffin embedding for histological analyses. After antigen retrieval at 100°C for 30 minutes with EDTA, liver sections (2 µm) were stained with rabbit anti-HBcAg (Diagnostic Biosystems, 1:50 dilution) as primary antibody and appropriate

horseradish peroxidase-coupled secondary antibodies. Immunohistochemistry was performed using a Leica Bond MAX system (Leica Biosystems). For analysis, tissue slides were scanned using an Aperio AT2 slide scanner (Leica Biosystems). HBcAg-positive hepatocytes were manually counted after defining cut-offs for the localization, intensity and distribution of the signal in 10 random view fields (20x magnification) per tissue and the mean numbers of HBcAg-positive hepatocytes were quantified per mm^2.

Statistical Analysis

Statistical analyses were done with the Prism 8 software. Statistical differences were calculated using the Mann-Whitney test. P-values < 0.05 were considered significant.

RESULTS

Induction of iC9 in HBV-Specific T Cells Rapidly Stops Their Effector Function *In Vitro*

First, the inducible caspase safeguard system iC9 was cloned into a retroviral vector encoding for HBV-specific receptors. iC9 was linked either to the S-CAR (env-specific), the TCR $4G_{S20}$ (S-specific) or the TCR $6K_{C18}$ (core-specific) via a 2A element (**Figure 1A**). All HBV-specific receptors were successfully expressed in 52-75% of T cells after retroviral transduction as quantified by flow cytometry analysis (**Figure 1B**). Co-expression of the safeguard molecule reduced the transduction efficiency of HBV-specific receptors by around 10-40% depending on the receptor and experiment (**Supplementary Figure 1A**). The expression level as determined by the MFI was reduced only in iC9-S-CAR T cells compared to S-CAR T cells not co-expressing iC9. Consequently, S-CAR T-cell killing was slightly delayed, while effector functions of TCR-expressing T cells remained unaltered (**Supplementary Figures 1B–G**). Next, we investigated the effect of inducing the iC9 safeguard mechanism in T cells. To this end, the transduced T cells were co-cultured with HBV^+ HepG2.2.15 cells and the viability of the HBV-replicating target cell line was measured using a real-time cytotoxicity assay. When around 40% of HBV^+ target cells were killed, CID was added in different concentrations to induce the iC9 safeguard system. Killing by iC9-S-CAR T cells was reduced within one hour (**Supplementary Figure 2A**), even when the lowest concentration of CID (1 ng/mL) was used (**Figure 1C**). In addition, the HBV-specific production of IFN-γ measured 96 hours later, was reduced by 10-fold (**Figure 1D**). Likewise, cytotoxicity and cytokine production of T cells expressing HBV-specific TCRs were rapidly stopped (**Figures 1E–H** and **Supplementary Figures 2B, C**). Interestingly, compared to TCR-grafted T cells (**Figures 1E, G**) killing by S-CAR T cells was slower (**Figure 1C**). This led to an overall longer duration of the co-culture with S-CAR or mock T cells and probably caused a generally reduced target cell viability after 90 hours (**Figure 1C**). Taken together, induction of the iC9 safeguard mechanism rapidly halted effector functions of HBV-specific T cells.

Ganciclovir Treatment of HBV-Specific T Cells Expressing the HSV Thymidine Kinase Abrogates their Effector Function *In Vitro*

In analogy to iC9, the safety switch HSV-TK was first cloned into the vector encoding HBV-specific receptors (**Figure 2A**). After retroviral transduction, the rate of T cells expressing an HBV-specific receptor was around 80% for the three constructs (**Figure 2B**). In contrast to iC9, co-expression of HSV-TK in T cells did not alter expression rates of S-CAR or TCRs (**Supplementary Figure 3A**). Nevertheless, HSV-TK co-expression delayed T-cell killing by ten hours (**Supplementary Figures 3B, D, F**) while cytokine production was only slightly reduced in T cells expressing the S-specific TCR $4G_{S20}$ (**Supplementary Figures 3C, E, G**). Next, HSV-TK T cells were co-cultured with HBV^+ target cells and GCV was added to induce effector cell death. A titration of GCV was performed including the manufacturer's recommendation of 10 mg/mL. Depletion of HBV-specific HSV-TK^+ T cells after administration of ≥ 10 mg/mL GCV halted cytotoxicity (**Figures 2C, E, G**) within less than one hour (**Supplementary Figures 4A–C**) and stopped production of IFN-γ (**Figures 2D, F, H**). Although a concentration of 1 mg/mL GCV was sufficient to stop T-cell effector functions, it was not as efficient as higher concentrations of GCV and occurred only ten hours later (**Figures 2C, E, G**). Overall, we concluded that HSV-TK worked as a very potent safeguard system to stop the effector function of HBV-specific T cells *in vitro*.

In Vivo Induction of iC9 Prevents Toxicity of S-CAR T Cells

Based on the *in vitro* results, both safeguard systems tested seemed equally suitable for depletion of HBV-specific T cells. However, in our hands application of GCV was more difficult as it needs to be kept at very alkaline conditions (approximately pH11) to prevent precipitation. In a first *in vivo* experiment (data not shown), GCV induced tissue irritation at the injection site causing distress for the animals and thereby rendered GCV delivery unreliable.

Hence, we selected iC9 as the more promising and convenient safeguard system for further evaluation *in vivo*. More specifically, we aimed to adapt our model of chronic hepatitis B (27) to resemble a clinical scenario that might require on-demand depletion of adoptively transferred T cells. To this end, a high titer HBV infection was established in $Rag2^{-/-}$IL-$2Rgc^{-/-}$ mice, resulting in high amounts of circulating HBsAg and infected hepatocytes. The lack of T, B, and NK cells provided "space" for the high number of adoptively transferred T cells to engraft and expand most efficiently. Murine $CD45.1^+$ $CD8^+$ T cells were engineered to co-express iC9 and the S-CAR since it functions independently of human MHC molecules and is hence easier to apply. CID was administered on day four and 13 post T-cell transfer and one group of mice was sacrificed on day seven, when hepatotoxicity was expected to peak (6, 27) and one group on day 14 (**Figure 3A**). Cells expressing a decoy-CAR (SΔ-CAR) that can bind HBsAg but does not carry signaling domains served as a control for unspecific effects of CID towards T-cell survival or

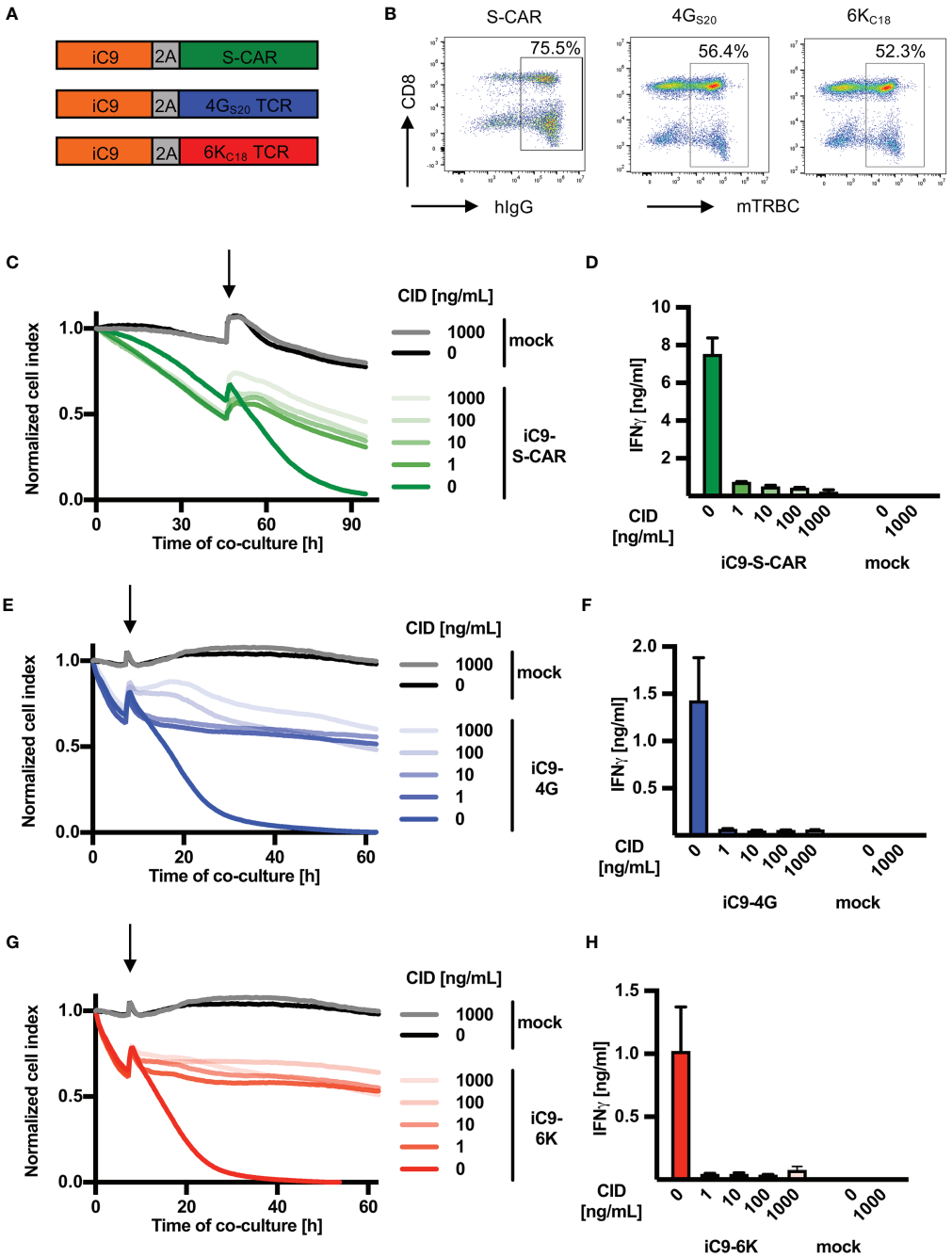

FIGURE 1 | Depletion of HBV-specific T cells via iC9 *in vitro*. **(A)** Schematic representation of the safeguard molecule inducible caspase 9 (iC9) linked to HBV-specific receptors through a T2A element to allow equimolar expression of the proteins. The S-CAR consists of an antibody fragment, which binds to the viral envelope proteins on infected cells, a human IgG1 spacer and CD28/CD3 signaling domains. The TCRs 4G$_{S20}$ (specific for the envelope peptide S20) and 6K$_{C18}$ (specific for the core peptide C18) contain murine constant domains (mTRBC) for better pairing of TCR chains (arranged as beta chain-P2A-alpha chain). **(B)** On day ten after retroviral transduction, cells were stained for hIgG (CAR) or mTRBC (TCRs) and the respective receptor expression was quantified by flow cytometry. **(C–H)** 1.25x10^4 receptor$^+$ T cells co-expressing iC9 were co-cultured with HBV$^+$ HepG2.2.15 target cells at an effector to target ratio of 1:4. CID was added (highlighted by an arrow) after the first day in different concentrations ranging from 1 to 1000 ng/mL to activate the inducible caspase 9 cascade leading to T-cell death. **(C, E, G)** Cell viability of target cells was determined with the xCELLigence RTCA in real-time and is displayed as normalized cell index (normalized to the start of co-culture). **(D, F, H)** IFN-γ determined in cell culture medium on day four of the co-culture. This experiment was repeated twice and one representative example is shown. Co-cultures were done in technical triplicates and mean, or mean +/- SEM are shown, respectively.

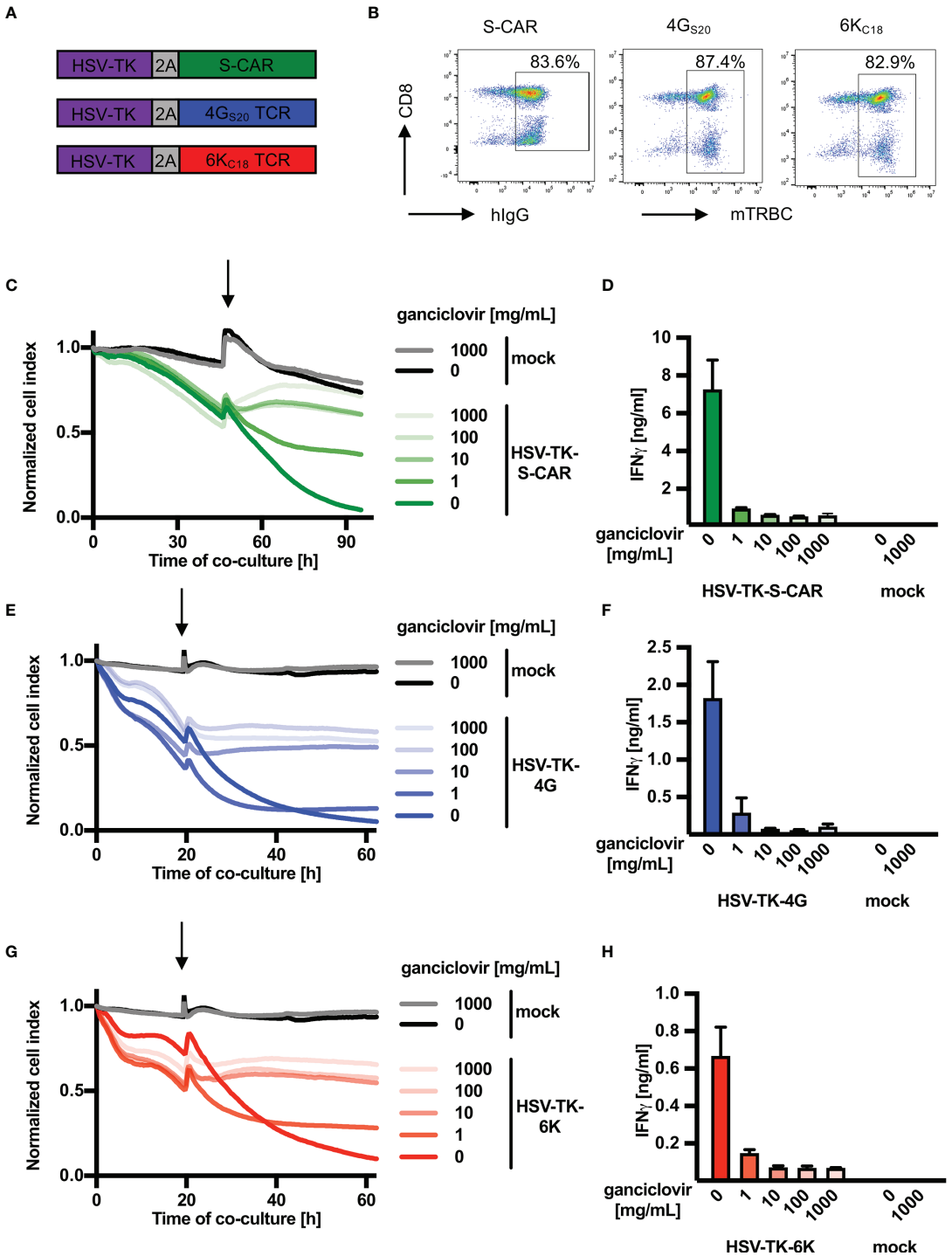

FIGURE 2 | Depletion of HBV-specific T cells via HSV-TK *in vitro*. **(A)** Schematic representation of the safeguard molecule herpes simplex virus thymidine kinase (HSV-TK) linked to either S-CAR or TCR 4G$_{S20}$ or 6K$_{C18}$ through a T2A element. **(B)** Receptor expression of transduced T cells assessed by flow cytometry on day ten after retroviral transduction. **(C–H)** 1.25x10^4 receptor$^+$ T cells co-expressing HSV-TK were co-cultured with HBV$^+$ HepG2.2.15 target cells at an effector to target ratio of 1:4. Ganciclovir was added (highlighted by an arrow) after the first day in different concentrations ranging from 1 to 1000 mg/mL to interrupt DNA synthesis and inducing T-cell death **(C, E, G)** Killing of target cells was measured using the xCELLigence real-time cell analyzer and is reported as the normalized cell index relative to the starting point of the co-culture. **(D, F, H)** IFN-γ determined in cell culture medium on day four of the co-culture. This experiment was repeated twice and one representative example is shown. Co-cultures were done in technical triplicates and mean, or mean +/- SEM are shown, respectively.

HBV replication (**Figure 3B**). All mice of the group that had received S-CAR T cells, but no CID, died between day eight and day twelve, while those mice, in which S-CAR T cells were depleted, survived (**Figure 3C**). The death of the animals was not preceded by a loss in body weight (**Figure 3D**) and ALT levels had only slightly increased to on average of 150 U/l (**Figure 3E**), indicating that rather a general and not a liver-directed immune reaction caused the fatalities. Mice, in which S-CAR T cells were depleted, lost around 15% of their body weight by day 14 (**Figure 3D**) and induction of the iC9 safeguard mechanism prevented the moderate hepatotoxicity (**Figure 3E**).

To evaluate a potential cytokine release syndrome (28), we measured the serum concentration of inflammatory cytokines over the course of the experiment. The cytokines IFN-γ, TNF-α, IL-6 and MCP-1 were slightly elevated four days post transfer of HBV-specific T cells but not of control T cells (**Figures 3F–I**) and IFN-γ, TNF-α and IL-6 further increased significantly in the mice without T-cell depletion (**Figures 3F–H**). However, three days after injection of CID all cytokines had returned to background levels (**Figures 3F–I**). Interestingly, this effect was only temporary and cytokine levels rose again one week after T-cell depletion. A second injection of CID reduced IFN-γ and IL-6 levels within one day (**Figures 3F, H**) but not TNF-α and MCP-1 (**Figures 3G, I**). Taken together, induction of the iC9 safeguard system in HBV-specific T cells efficiently prevented liver damage and stopped systemic presence of inflammatory cytokines. This pointed to an efficient depletion of iC9-S-CAR T cells.

In Vivo Induction of iC9 Reduces Numbers of Transferred T Cells and Renders Them Non-Functional

In order to quantify the depletion of transferred T cells in blood, but also spleen and liver, mice were sacrificed on day seven and 14. The congenic marker CD45.1/2 allowed for easy differentiation of transferred $CD45.1^+$ cells from endogenous $CD45.2^+$ immune cells (**Figure 4A**). Although $CD45.1^+$ cells were not completely depleted after CID injection (**Figure 4A**, lower row), additional staining for the S-CAR revealed that especially T cells with a high S-CAR expression were targeted and had completely vanished from all examined compartments (**Figure 4B**). On day seven, numbers of transferred T cells in the blood and the spleen were reduced by $1.5\log_{10}$ and in the liver by $2\text{-}3\log_{10}$ in comparison to mice in which suicide of HBV-specific T cells had not been induced (**Figure 4C**). The number of transferred cells that remained after depletion was comparable to the number of SΔ-CAR T cells, which did not get a specific stimulus for proliferation. A second CID administration on day 13, with the idea to eliminate the remaining cells that had not been depleted by the first CID administration, was most effective in the liver but did not lead to the complete elimination of cells (**Figure 4C**).

In addition, the isolated T cells were assessed for their functionality. To this end, LALs and splenocytes were incubated on HBsAg-coated plates and stained for secretion of IFN-γ, TNF-α and IL-2 (**Supplementary Figure 5A**). Sixty percent of $CD45.1^+$ T cells retrieved from the spleen, i.e. most of the S-CAR T cells, exhibited HBsAg-specific production of cytokines, with IFN-γ being most prominent (**Figure 4D**). This expression was almost completely abrogated in three out of four mice that had received CID and in line with the observation that mostly $S\text{-}CAR^{hi}$ T cells had been depleted (**Figure 4B**). Nevertheless, the $CD45.1^+$ T cells could still be activated non-specifically by anti-CD3/anti-CD28 stimulation, further indicating that only the transduced HBV-specific T cells had been depleted (**Supplementary Figure 5**). Interestingly, in this experiment the functional profile of LALs differed from that of splenocytes. Despite a high expression of the S-CAR in the group without depletion (**Figure 4B**), only an average of 15% secreted cytokines upon restimulation with HBsAg (**Figure 4E**). Injection of CID successfully depleted HBV-specific cells in half of the mice. Despite a second injection of CID, few HBV-specific T cells remained detectable in spleen and liver (**Figures 4F, G**). Taken together, depletion of iC9-S-CAR T cells was very efficient, albeit not complete, and their functionality was diminished.

Specific Depletion of S-CAR T Cells Reduces the Antiviral Effect of the Adoptive T-Cell Transfer

Given the successful depletion of HBV-specific T cells (**Figure 4**) accompanied by a lack of cytotoxic T-cell activity in the liver and cytokine secretion (**Figure 3**), we set out to quantify how much this safety measure would come at the cost of the therapeutic, antiviral efficacy of adoptive T-cell transfer. Histological analysis of liver tissue revealed that upon CID injection immune cells did not accumulate near the central veins anymore (**Figure 5A**) and concomitantly the number of $HBcAg^+$ hepatocytes remained as high as in control groups (**Figures 5A, B**). Similarly, the effect of S-CAR T cells on levels of circulating HBsAg was completely abrogated three days after the first CID injection (**Figure 5C**). In contrast to that, the second CID injection that had also spared some remaining HBV-specific T cells (**Figures 4F, G**), still allowed S-CAR T cells to reduce HBsAg by 50% between day 7 and day 14 (**Figure 5C**). Levels of HBeAg remained unaltered throughout the treatment in all groups (**Figure 5D**). Taken together, delayed reduction of HBsAg and steady levels of HBcAg suggested that S-CAR T-cell depletion hampered not only the side effects of T-cell therapy but also their antiviral effect.

Suicide of HBV-Specific T Cells Can Be Induced Within One Hour *In Vivo*

From our *in vitro* experiments, we had learned that induction of the iC9 safeguard immediately prevented further cytotoxicity of HBV-specific T cells. We next asked, whether this would also hold true *in vivo*. Six days post transfer of iC9-S-CAR T cells, CID was injected 16, six and one hour before analyzing blood, spleen and liver of the mice (**Figure 6A**). The number of transferred T cells in blood was reduced by around 1 $\log_{10}$ already one hour after induction of the safeguard system (**Figure 6B**). In contrast to that, in spleen and liver the reduction of transferred T cells was more profound six and 16 hours post CID injection (**Figures 6C, D**). After one hour, the

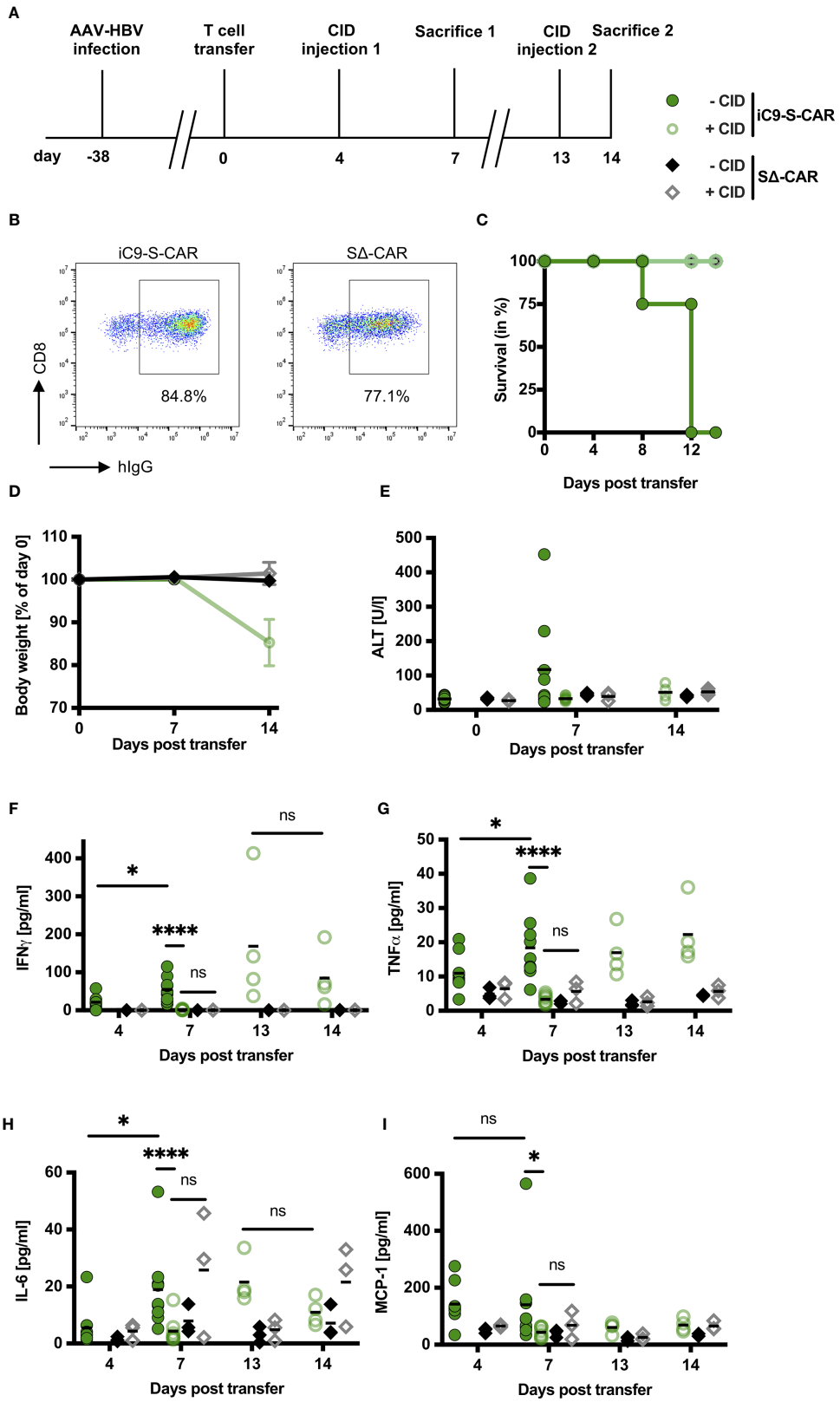

FIGURE 3 | Continued

FIGURE 3 | Impact of iC9 induction on side effects of adoptive T-cell transfer *in vivo*. **(A)** Scheme of the experimental procedure. Rag2$^{-/-}$IL-2Rgc$^{-/-}$ mice were infected with HBV using an adeno-associated vector. 1x10^{10} viral genomes for male and 3x10^{10} viral genomes for female mice were injected intravenously per mouse. After establishment of a stable infection around five weeks later, 2x10^{6} iC9-S-CAR T cells (n = 17) or SΔ-CAR T cells (n = 6) were administered i.p. per mouse. The SΔ-CAR, containing the same extracellular domains to bind HBsAg but exchanged intracellular domains rendering it incapable of activating T cells, served as a control for the antiviral effect of T cells and unspecific effects of CID injection. CID or a negative control (preparation identical to CID but without the active substance) was injected i.p. on day four and day 13. Nine mice of the iC9-S-CAR group were sacrificed on day seven, the rest of the mice were sacrificed on day 14. **(B)** Receptor expression of retrovirally transduced T cells assessed by flow cytometry on the day of adoptive T-cell transfer. **(C)** Survival analysis of the mice between transfer of the T cells and sacrifice. **(D)** Change in body weight of the different groups. Individual weights for each mouse on day zero were set to 100%. **(E)** ALT activity measured in mouse sera on day zero, seven and 14 after T-cell transfer. **(F–I)** Cytokines in mouse sera on day four, seven, 13 and 14 after T-cell transfer were determined by cytometric bead array and flow cytometry. Blood on day four and 13 was collected just before CID injection. **(D–I)** Data points represent individual animals and mean values are indicated. Mann-Whitney test: ns, not significant, *p < 0.05, ****p < 0.0001.

depletion rate was only around 50% in both organs compared to the cell numbers at earlier time points of depletion. Regardless of the time point, HBV-specific T cells in the spleen were efficiently depleted from around 30% to 5% of cytokine secreting cells (**Figure 6E**). In the liver, the rate of HBV-reactive T cells was reduced from around 40% to 10% already one hour after induction of T-cell suicide (**Figure 6F**). Surprisingly, the number of HBV-specific T cells in the liver was higher when CID had been injected 16 hours, before sacrifice compared to an exposure time of six or one hour. In summary, the velocity of T-cell suicide via iC9 dimerization was high and comparable *in vitro* and *in vivo*.

DISCUSSION

Adoptive T-cell therapy for the treatment of chronic hepatitis B aims to overcome the scarce and narrow T-cell response (3, 29, 30) by applying highly potent, genetically engineered HBV-specific T cells that are able to clear HBV infection via cytotoxicity and cytokine secretion (5, 8). In this study, we evaluated iC9 and HSV-TK as safeguard systems in the context of adoptive T-cell transfer for treatment of persistent HBV infection. *In vitro*, induction of iC9 or HSV-TK co-expressed in HBV-specific-TCR and S-CAR T cells immediately halted T-cell cytotoxicity and cytokine production. *In vivo*, induction of iC9 in S-CAR T cells led to a strong and fast depletion of transferred T cells and prevented liver toxicity and cytokine release. This, however, came at the costs of a loss of antiviral efficacy.

The concept of equipping cells with a safeguard before adoptive transfer originates from stem cell transfer to counteract side effects such as graft-versus-host disease (31). HSV-TK (19, 32), iC9 (33, 34) and a truncated form of the epidermal growth factor receptor (EGFR, targeted by the antibody Cetuximab) (35) are the most clinically advanced and especially iC9 and tEGFR have since been adapted in adoptive T-cell therapy to deplete CAR- or TCR-redirected T cells on demand (36, 37). Given that EGFR has been reported to be expressed on regenerative clusters of hepatocytes (38) and that we were seeking a safeguard that prevents excessive liver damage, we did not select tEGFR but focused on HSV-TK and iC9.

So far, suicide switches have been mostly applied for CAR T cells (36, 37) and the usage for iC9 has only been described for one TCR (39). In our study, co-expression of either suicide switch *per se* did not alter the expression or functionality of HBV-specific T cells considerably. This was also true for the TCR, which as a heterodimer might be more sensitive to additional genes being expressed from the same transgene. Both, induction of HSV-TK and iC9, was equally fast and effective in stopping HBV-specific T cells from executing their designated effector functions. Others have characterized HSV-TK as being as potent as iC9 but rather slow in inducing T-cell death *in vitro* (22) and requiring multiple GCV injections in patients (40). A reason why HSV-TK induction was faster in our system could be that T cells were in a highly active state when treated with GCV and were potentially more prone to DNA incorporation of GCV. Nevertheless, we decided against a further *in vivo* evaluation of the HSV-TK suicide switch because of its reported immunogenicity (41), the side and bystander effects of GCV (21, 42, 43), and the technical difficulty of injecting the alkaline GCV solution into the thin murine veins (43).

The iC9 system provides an interesting alternative because it is poorly immunogenic as it only contains human-derived domains, the dimerizer for its induction is biologically inert and was proven to be safe in healthy volunteers (44). The mechanism of dimerizer activation is independent of the cell cycle and iC9 was shown to be highly effective and very fast in both preclinical and clinical studies (18, 45), which prompted us to evaluate iC9 also in our *in vivo* model.

We have previously shown that application of S-CAR T cells in HBV-replicating mice is safe. In immune competent HBV transgenic mice (6) and tolerized AAV-HBV infected mice (27), and likewise in the present study, the grafted T cells only induced a moderate liver damage while slowly reducing viral loads. Here, in order to simplify testing of the iC9 safety switch, we adjusted the model to allow exuberant S-CAR T-cell activation risking non-liver specific side effects. To this end, the S-CAR used in this study was codon-optimized and carried the natural IgG1-spacer, leading to a higher expression and most powerful activation (data not shown) including potential off-target activation via binding to Fc-receptor bearing cells, as opposed to the non-codon-optimized S-CAR with an immune-silenced IgG1-spacer (46) used previously (27). Furthermore, a high dosage of 2x10^{6} S-CAR-CD8^{+} T cells (equivalent to approx. 6x10^{9} per 75 kg patient) was injected into immune incompetent mice allowing rapid T cell expansion. These modifications of the model resulted in 20-fold higher T cell numbers in the blood and likely facilitated a strong, systemic T cell activation, which was unforeseen and unfortunately let to the fatalities observed in this study. These high numbers of engrafted T cells allowed for better quantification of T cell depletion on a logarithmic scale, which was not feasible when we aimed at quantifying T cell depletion in above mentioned immune

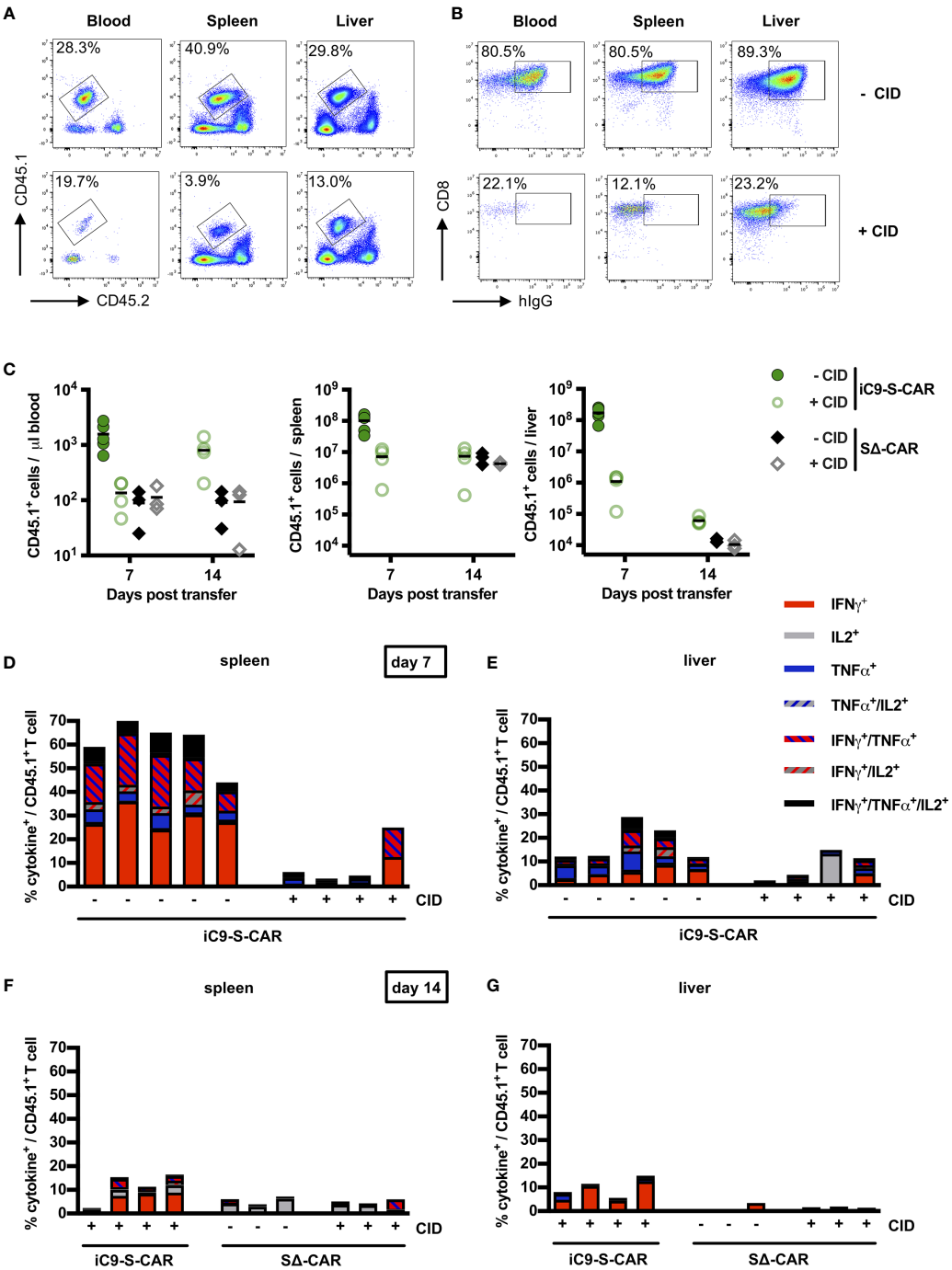

FIGURE 4 | Depletion of transduced T cells via iC9 *in vivo*. **(A)** Exemplary flow cytometry plot of transferred CD45.1$^+$ T cells found in peripheral blood, in the spleen and in the liver. Both, a mouse which did not receive CID (upper row) and a mouse which received CID (lower row), were sacrificed on day seven post T-cell transfer. The congenic marker CD45.1 allowed to differentiate transferred cells from the endogenous CD45.2$^+$ cells of the recipient mice. **(B)** Exemplary flow cytometry plot of CD8$^+$ and CAR T cells in peripheral blood, in the spleen and in the liver of the same mice as shown in **(A)**. **(C)** Count of transferred CD45.1$^+$ T cells in the peripheral blood, the spleen and the liver on day seven and day 14 after T-cell transfer. Absolute count of cells was determined by flow cytometry using Counting Beads. The result was extrapolated to the concentration in blood or to the whole organ considering the proportion that was used to isolate splenocytes or LALs. Data for the iC9-S-CAR group on day 14 are not available because the animals died between day seven and 14. **(D–G)** *Ex-vivo* functionality of transferred CD45.1$^+$ T cells collected from spleen (**D** day seven, **F** day 14) or liver (**E** day seven, **G** day 14). Intracellular cytokine expression (TNF-α, IFN-γ and IL-2) was determined after overnight-culture on plate-bound HBsAg. **(C)** Data points represent individual animals and mean values are indicated. **(D–G)** Each column represents an individual animal.

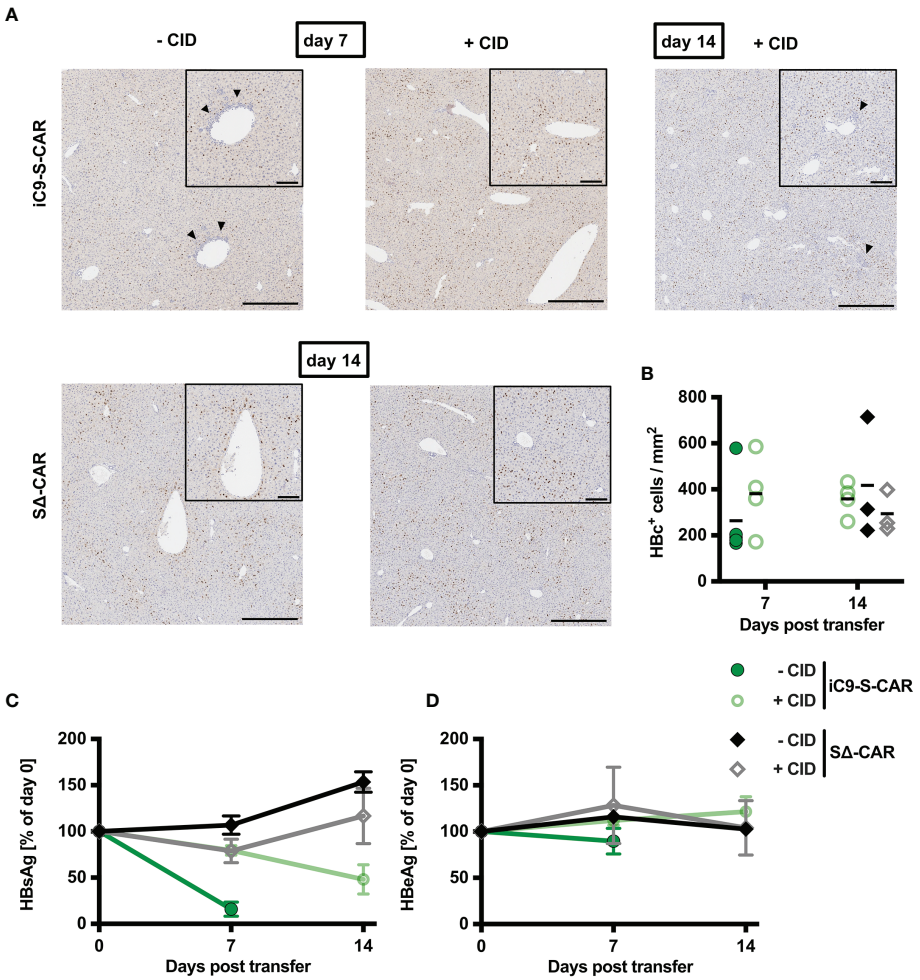

FIGURE 5 | Antiviral effect of iC9-S-CAR T cells *in vivo*. **(A)** Exemplary (1 mouse per group) liver immunohistochemistry stainings for HBcAg-positive hepatocytes. Bars represent 200 µm in the overview and 80 µm in the inlay of the central vein. Arrows indicate lymphocyte infiltrates. **(B)** Quantification of histological analysis of HBcAg expression including all the mice from all the different groups. **(C, D)** HBsAg and HBeAg levels in the serum over time relative to day zero determined by diagnostic assays. **(B)** Data points represent individual animals and mean values are indicated. **(C, D)** Data are given as mean values +/- SD.

competent mouse models (data not shown). For the assessment of side effects of T-cell therapies, preclinical *in vivo* models should mimic the clinical setting as precisely as possible. By using a mouse model lacking T, B and NK cells we cannot fully investigate the interactions of the transferred T cells with the endogenous immune cells and how this might possibly impact on the safety of T-cell therapy. In fact, although CAR T cells are known to initate a possible CRS, the endogenous immune system plays a key role in its clinical manifestation (47).

In our set-up, we were able to rescue mice from excessive S-CAR T-cell activation by a single CID injection preventing moderate hepatotoxicity and halting cytokine release. One CID administration led to a reduction of transferred T cells by over 90% in blood and spleen and over 99% in the liver. This is in line with the depletion rates in blood that other studies in mice (48–51), macaques (52) and men (53–55) have reported. In fact, considering that most of the remaining transferred cells had no or at best a low expression of the S-CAR and showed low *ex vivo* reactivity towards HBsAg, the specific depletion of iC9-S-CAR T cells was presumably even higher than 99% in our setting.

Nevertheless, transferred T cells were not completely eliminated. The escape of T cells with low receptor expression or little activation even from repeated CID (55) has been observed in other models and several reasons have been discussed. It has been proposed, for example, that activation positively influences transgene expression and T cells were shown to be susceptible again to CID when they had been stimulated *ex vivo* (51, 55). This would explain why depletion after CID was in our model most effective in the liver, the site where S-CAR T cells encountered their cellular target. Furthermore, in the setting of hematopoietic stem cell transplantation with iC9-expressing T cells, virus-specific T cells recovered more easily than alloreactive T cells (54). It was suggested that they are more resistant to apoptotic signals (54)

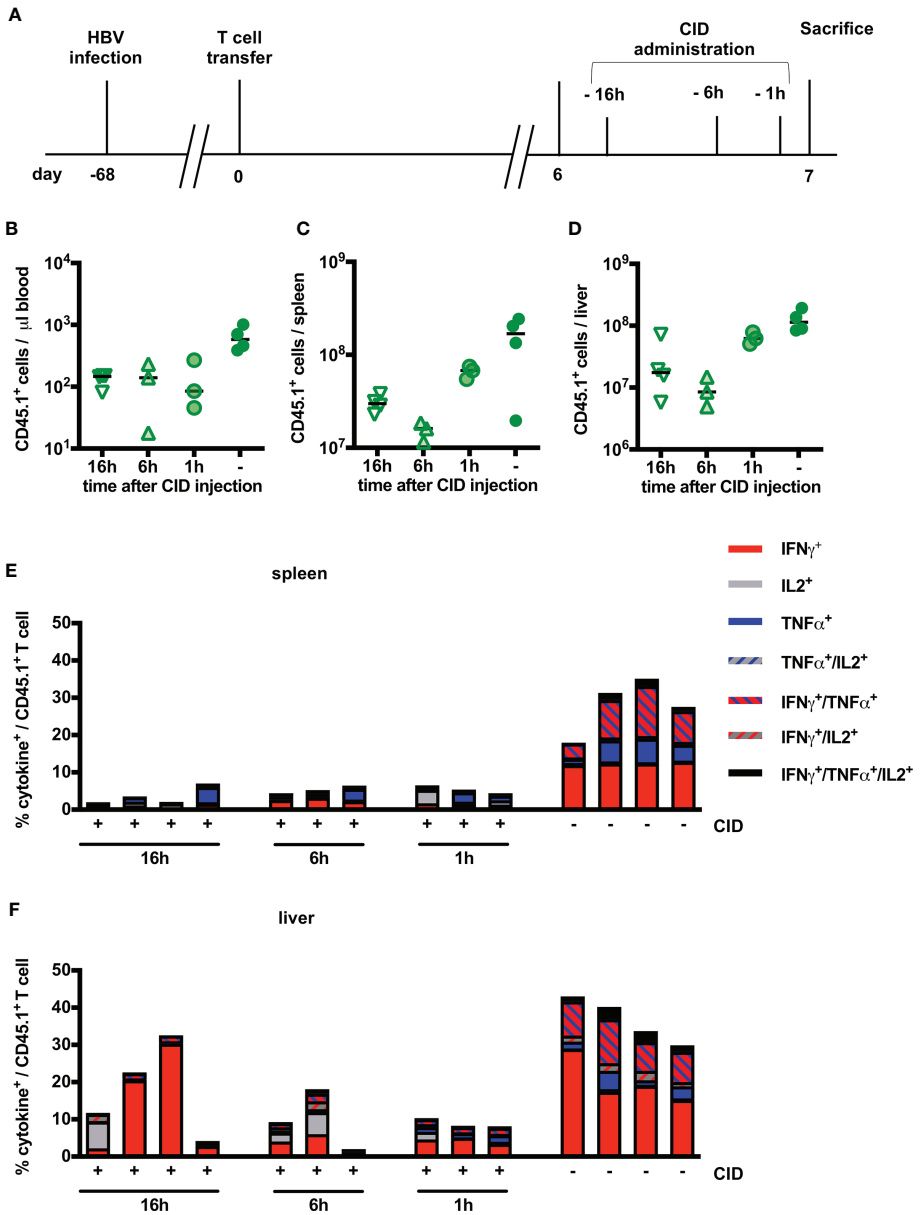

FIGURE 6 | Kinetics of iC9-mediated T-cell depletion *in vivo*. **(A)** Scheme of the experimental procedure. Infection of Rag2$^{-/-}$IL-2Rgc$^{-/-}$ mice with HBV was achieved using an adeno-associated vector. Similar to **Figure 3**, 1x10^{10} viral genomes for male and 3x10^{10} viral genomes for female mice were injected intravenously per mouse. After establishment of a stable infection around 5 weeks later, 2x10^{6} iC9-S-CAR T cells (n = 14) were administered i.p. per mouse. CID was administered between day six and seven and mice were sacrificed on the same day but at different timepoints after CID administration 1h (n = 3), 6h (n = 3) and 16h (n = 4). 4 additional mice received no CID. **(B–D)** Count of transferred CD45.1^{+} T cells in the peripheral blood **(B)**, the spleen **(C)** and the liver **(D)** on different timepoints after CID administration. Count of transferred CD45.1^{+} T cells in the peripheral blood, the spleen and the liver on day seven and day 14 after T-cell transfer. Absolute count of cells was determined by flow cytometry using Counting Beads. The result was extrapolated to the concentration in blood or to the whole organ considering the proportion that was used to isolate splenocytes or LALs. **(E, F)** *Ex vivo* functionality of transferred CD45.1^{+} T cells in the spleen **(E)** and the liver **(F)** via measurement of intracellular cytokine expression (TNF-α, IFN-γ and IL-2) determined after overnight-culture on plate-bound HBsAg. **(B–D)** Data points represent individual animals and mean values +/- SD are indicated. **(E, F)** Each column represents an individual animal.

and the addition of antiapoptotic agents could increase sensitivity towards CID (56). Indeed, it was reported that cells that are resistant to CID have upregulated levels of B-cell lymphoma 2 (Bcl-2) protein, which as a target of caspase 3 could prevent a lower threshold for apoptosis (52). Interestingly, HBV-specific T cells have been shown to differ in their Bcl-2 levels depending on their antigen-specificity, with polymerase-specific T cells expressing significantly less Bcl-2 than core-specific T cells (57). Assuming that this phenomenon was dependent on the site of antigen encounter, i.e. presumably the

liver for polymerase-specific T cells and lymphoid organs for core-specific T cells due to circulating HBeAg, this could explain why iC9-S-CAR T cells were particularly susceptible towards CID. Intriguingly, a second CID on day 13 seemed to spare iC9-S-CAR T cells in blood and spleen but not in the liver, supporting the notion that the liver environment induced a special T-cell phenotype.

Most studies so far have been performed in xenograft models or in humans, relying only on blood analyses. By contrast, our model is a syngeneic one using murine T cells that can interact with murine tissue and might be the reason for the particular depletion kinetics observed. In human studies, many of the iC9-expressing T cells were depleted as fast as 30 minutes after CID (53, 55). In our experiments, depletion of iC9-S-CAR T cells was at its maximum one hour after CID while numbers in spleen and liver were further reduced six hours after CID, which could be a result of the pharmacokinetics of the dimerizer. Interestingly, T-cell numbers were higher in spleen and liver when CID was done 16 hours compared to six hours before sacrifice. We can only speculate that the remaining T cells had started proliferating again, and that the reported short cell cycle durations of activated T cells of around six hours (58) reflected on the retrieved T-cell numbers. There is no doubt that some of the iC9-S-CAR T cells were still active after the first CID on day seven, since we observed reduced levels of HBsAg, loss of body weight and an increase in inflammatory cytokines in this group. This might differ from other studies, in which iC9-CD19-CAR T cells, once depleted, remained steady at low levels (50, 51) maybe due to a lack of stimulus in these xenograft models.

Not surprisingly, depletion of iC9-S-CAR T cells came at the cost of delaying any antiviral activity as HBsAg only started to drop by day 14 and $HBcAg^+$ hepatocytes and HBeAg remained unchanged. Using S-CAR T cells to treat AAV-HBV infection, we have previously observed a fast drop of HBsAg and an up to two week delay in HBeAg decrease (27), which can be explained by HBsAg being bound by S-CAR T cells leading to a decrease of free, measurable HBsAg. A lack of tumor cells being controlled after CID has also been observed in lymphoma models (51, 59). This reflects the principal dilemma of adoptive T-cell therapy, in which T cell-related safety and efficacy are inherently linked together.

Apart from the iC9 suicide switch, other strategies to manage acute toxicities can be considered. The IL-6 receptor blocking antibody tocilizumab is very efficient in reverting CRS symptomology (16). However, during CRS, IL-6 is mostly produced by monocytes (60) and blocking its activity will not directly affect T-cell effector function and hence not prevent T-cell-related toxicity. Another therapeutic option is the administration of corticosteroids that have strong immuno suppressive properties. They have been shown to be effective in the management of CRS that occurred after T-cell therapy (16, 47, 61). Nonetheless, the long-term use of systemic corticosteroids has side effects and can lead to a reactivation of HBV infection or enhance the viral replication (62) and would thus diminish the chances of the host´s endogenous HBV-specific immune response to be reinvigorated by adoptive T-cell therapy. *Mestermann et al.* recently proposed an elegant way to switch T-cell functionality on and off on demand by using the tyrosine kinase inhibitor Dasatinib. In their system, Dasatinib rapidly paused complete T-cell functionality while dexamethasone had only a partial effect on cytotoxicity and IFN-γ secretion (63). However, in the end, when adoptively transferred T cells have cleared the infection, it would also be desirable to have a safeguard at hand that targets and eliminates specifically only the genetically modified T cells. In our hands, iC9 seems to be a convenient and reliable safeguard mechanism to do so as proven by its fast and effective T cell depletion and prevention of toxicity in our model of adoptive T-cell therapy of chronic hepatitis B.

DATA AVAILABILITY STATEMENT

The raw data supporting the conclusions of this article will be made available by the authors, without undue reservation.

ETHICS STATEMENT

The animal study was reviewed and approved by the District Government of Upper Bavaria (permission number: 02-17-227).

AUTHOR CONTRIBUTIONS

AK and SS conducted the *in vitro* experiments. AK and ADK performed the *in vivo* experiments. AK, UP, and KW designed the experiments. AK and KW analyzed the data. MP provided essential material. UP provided critical infrastructure. AK and KW wrote the manuscript. All authors contributed to the article and approved the submitted version.

FUNDING

The work was funded by the German Research Foundation (DFG) *via* TRR36 as a stipend to AK and by the German Center for Infection Research (DZIF) as a young investigator grant (05.812) to KW.

ACKNOWLEDGMENTS

We thank the Comparative Experimental Pathology (CEP) of TUM (PD Dr. Katja Steiger, Anne Jacob) for excellent technical support. We thank Theresa Asen and Philip Hagen for excellent technical assistance.

SUPPLEMENTARY MATERIAL

The Supplementary Material for this article can be found online at: https://www.frontiersin.org/articles/10.3389/fimmu.2021.734246/full#supplementary-material

REFERENCES

1. *Global Hepatitis Report 2017*. Geneva, Switzerland: World Health Organization (2017).
2. Trépo C, Chan HL, Lok A. Hepatitis B Virus Infection. *Lancet* (2014) 384 (9959):2053–63. doi: 10.1016/S0140-6736(14)60220-8
3. Rehermann B, Fowler P, Sidney J, Person J, Redeker A, Brown M, et al. The Cytotoxic T Lymphocyte Response to Multiple Hepatitis B Virus Polymerase Epitopes During and After Acute Viral Hepatitis. *J Exp Med* (1995) 181 (3):1047–58. doi: 10.1084/jem.181.3.1047
4. Tan AT, Schreiber S. Adoptive T-Cell Therapy for HBV-Associated HCC and HBV Infection. *Antiviral Res* (2020) 176:104748. doi: 10.1016/j.antiviral.2020.104748
5. Bohne F, Chmielewski M, Ebert G, Wiegmann K, Kürschner T, Schulze A, et al. T Cells Redirected Against Hepatitis B Virus Surface Proteins Eliminate Infected Hepatocytes. *Gastroenterology* (2008) 134(1):239–47. doi: 10.1053/j.gastro.2007.11.002
6. Krebs K, Böttinger N, Huang LR, Chmielewski M, Arzberger S, Gasteiger G, et al. T Cells Expressing a Chimeric Antigen Receptor That Binds Hepatitis B Virus Envelope Proteins Control Virus Replication in Mice. *Gastroenterology* (2013) 145(2):456–65. doi: 10.1053/j.gastro.2013.04.047
7. Wisskirchen K, Metzger K, Schreiber S, Asen T, Weigand L, Dargel C, et al. Isolation and Functional Characterization of Hepatitis B Virus-Specific T-Cell Receptors as New Tools for Experimental and Clinical Use. *PloS One* (2017) 12(8). doi: 10.1371/journal.pone.0182936
8. Wisskirchen K, Kah J, Malo A, Asen T, Volz T, Allweiss L, et al. T Cell Receptor Grafting Allows Virological Control of Hepatitis B Virus Infection. *J Clin Invest* (2019) 129(7):2932–45. doi: 10.1172/JCI120228
9. Zhao L, Chen F, Quitt O, Festag M, Ringelhan M, Wisskirchen K, et al. Hepatitis B Virus Envelope Proteins Can Serve as Therapeutic Targets Embedded in the Host Cell Plasma Membrane. *bioRxiv* (2020). doi: 10.1101/2020.12.21.423802
10. Santomasso B, Bachier C, Westin J, Rezvani K, Shpall EJ. The Other Side of CAR T-Cell Therapy: Cytokine Release Syndrome, Neurologic Toxicity, and Financial Burden. *Am Soc Clin Oncol Educ Book* (2019) 39:433–44. doi: 10.1200/EDBK_238691
11. Morgan RA, Yang JC, Kitano M, Dudley ME, Laurencot CM, Rosenberg SA. Case Report of a Serious Adverse Event Following the Administration of T Cells Transduced With a Chimeric Antigen Receptor Recognizing ERBB2. *Mol Ther* (2010) 18(4):843–51. doi: 10.1038/mt.2010.24
12. Morgan RA, Chinnasamy N, Abate-Daga DD, Gros A, Robbins PF, Zheng Z, et al. Cancer Regression and Neurologic Toxicity Following Anti-MAGE-A3 TCR Gene Therapy. *J Immunother (Hagerstown Md: 1997)* (2013) 36(2):133. doi: 10.1097/CJI.0b013e3182829903
13. Linette GP, Stadtmauer EA, Maus MV, Rapoport AP, Levine BL, Emery L, et al. Cardiovascular Toxicity and Titin Cross-Reactivity of Affinity-Enhanced T Cells in Myeloma and Melanoma. *Blood J Am Soc Hematol* (2013) 122 (6):863–71. doi: 10.1182/blood-2013-03-490565
14. van Loenen MM, de Boer R, Amir AL, Hagedoorn RS, Volbeda GL, Willemze R, et al. Mixed T Cell Receptor Dimers Harbor Potentially Harmful Neoreactivity. *Proc Natl Acad Sci* (2010) 107(24):10972–7. doi: 10.1073/pnas.1005802107
15. Johnson LA, Morgan RA, Dudley ME, Cassard L, Yang JC, Hughes MS, et al. Gene Therapy With Human and Mouse T-Cell Receptors Mediates Cancer Regression and Targets Normal Tissues Expressing Cognate Antigen. *Blood* (2009) 114(3):535–46. doi: 10.1182/blood-2009-03-211714
16. Maude SL, Barrett D, Teachey DT, Grupp SA. Managing Cytokine Release Syndrome Associated With Novel T Cell-Engaging Therapies. *Cancer J (Sudbury Mass)* (2014) 20(2):119. doi: 10.1097/PPO.0000000000000035
17. Shimabukuro-Vornhagen A, Gödel P, Subklewe M, Stemmler HJ, Schlößer HA, Schlaak M, et al. Cytokine Release Syndrome. *J Immunother Cancer* (2018) 6(1):56. doi: 10.1186/s40425-018-0343-9
18. Di Stasi A, Tey S-K, Dotti G, Fujita Y, Kennedy-Nasser A, Martinez C, et al. Inducible Apoptosis as a Safety Switch for Adoptive Cell Therapy. *N Engl J Med* (2011) 365(18):1673–83. doi: 10.1056/NEJMoa1106152
19. Bonini C, Ferrari G, Verzeletti S, Servida P, Zappone E, Ruggieri L, et al. HSV-TK Gene Transfer Into Donor Lymphocytes for Control of Allogeneic Graft-Versus-Leukemia. *Science* (1997) 276(5319):1719–24. doi: 10.1126/science.276.5319.1719
20. Ciceri F, Bonini C, Stanghellini MTL, Bondanza A, Traversari C, Salomoni M, et al. Infusion of Suicide-Gene-Engineered Donor Lymphocytes After Family Haploidentical Haemopoietic Stem-Cell Transplantation for Leukaemia (the TK007 Trial): A Non-Randomised Phase I–II Study. *Lancet Oncol* (2009) 10 (5):489–500. doi: 10.1016/S1470-2045(09)70074-9
21. Kuriyama S, Nakatani T, Masui K, Sakamoto T, Tominaga K, Yoshikawa M, et al. Bystander Effect Caused by Suicide Gene Expression Indicates the Feasibility of Gene Therapy for Hepatocellular Carcinoma. *Hepatology* (1995) 22(6):1838–46. doi: 10.1016/S1470-2045(09)70074-9
22. Marin V, Cribioli E, Philip B, Tettamanti S, Pizzitola I, Biondi A, et al. Comparison of Different Suicide-Gene Strategies for the Safety Improvement of Genetically Manipulated T Cells. *Hum Gene Ther Methods* (2012) 23 (6):376–86. doi: 10.1089/hgtb.2012.050
23. Ghani K, Wang X, de Campos-Lima PO, Olszewska M, Kamen A, Riviere I, et al. Efficient Human Hematopoietic Cell Transduction Using RD114-And GALV-Pseudotyped Retroviral Vectors Produced in Suspension and Serum-Free Media. *Hum Gene Ther* (2009) 20(9):966–74. doi: 10.1089/hum.2009.001
24. Hirschman SZ, Price P, Garfinkel E, Christman J, Acs G. Expression of Cloned Hepatitis B Virus DNA in Human Cell Cultures. *Proc Natl Acad Sci* (1980) 77 (9):5507–11. doi: 10.1073/pnas.77.9.5507
25. Sells MA, Chen ML, Acs G. Production of Hepatitis B Virus Particles in Hep G2 Cells Transfected With Cloned Hepatitis B Virus DNA. *Proc Natl Acad Sci* (1987) 84(4):1005–9. doi: 10.1073/pnas.84.4.1005
26. Dion S, Bourgine M, Godon O, Levillayer F, Michel M-L. Adeno-Associated Virus-Mediated Gene Transfer Leads to Persistent Hepatitis B Virus Replication in Mice Expressing HLA-A2 and HLA-DR1 Molecules. *J Virol* (2013) 87(10):5554–63. doi: 10.1128/JVI.03134-12
27. Festag MM, Festag J, Fräßle SP, Asen T, Sacherl J, Schreiber S, et al. Evaluation of a Fully Human, Hepatitis B Virus-Specific Chimeric Antigen Receptor in an Immunocompetent Mouse Model. *Mol Ther* (2019) 27(5):947–59. doi: 10.1016/j.ymthe.2019.02.001
28. Teachey DT, Rheingold SR, Maude SL, Zugmaier G, Barrett DM, Seif AE, et al. Cytokine Release Syndrome After Blinatumomab Treatment Related to Abnormal Macrophage Activation and Ameliorated With Cytokine-Directed Therapy. *Blood J Am Soc Hematol* (2013) 121(26):5154–7. doi: 10.1182/blood-2013-02-485623
29. Bertoletti A, Sette A, Chisari FV, Penna A, Levrero M, De Carli M, et al. Natural Variants of Cytotoxic Epitopes Are T-Cell Receptor Antagonists for Antiviral Cytotoxic T Cells. *Nature* (1994) 369(6479):407–10. doi: 10.1038/369407a0
30. Maini MK, Boni C, Ogg GS, King AS, Reignat S, Lee CK, et al. Direct Ex Vivo Analysis of Hepatitis B Virus-Specific CD8+ T Cells Associated With the Control of Infection. *Gastroenterology* (1999) 117(6):1386–96. doi: 10.1016/S0016-5085(99)70289-1
31. Jones BS, Lamb LS, Goldman F, Di Stasi A. Improving the Safety of Cell Therapy Products by Suicide Gene Transfer. *Front Pharmacol* (2014) 5:254. doi: 10.3389/fphar.2014.00254
32. Greco R, Oliveira G, Stanghellini MTL, Vago L, Bondanza A, Peccatori J, et al. Improving the Safety of Cell Therapy With the TK-Suicide Gene. *Front Pharmacol* (2015) 6:95. doi: 10.3389/fphar.2015.00095
33. Straathof KC, Pule MA, Yotnda P, Dotti G, Vanin EF, Brenner MK, et al. An Inducible Caspase 9 Safety Switch for T-Cell Therapy. *Blood* (2005) 105 (11):4247–54. doi: 10.1182/blood-2004-11-4564
34. Gargett T, Brown MP. The Inducible Caspase-9 Suicide Gene System as a "Safety Switch" to Limit on-Target, Off-Tumor Toxicities of Chimeric Antigen Receptor T Cells. *Front Pharmacol* (2014) 5:235. doi: 10.3389/fphar.2014.00235
35. Wang X, Chang W-C, Wong CW, Colcher D, Sherman M, Ostberg JR, et al. A Transgene-Encoded Cell Surface Polypeptide for Selection, *In Vivo* Tracking, and Ablation of Engineered Cells. *Blood J Am Soc Hematol* (2011) 118 (5):1255–63. doi: 10.1182/blood-2011-02-337360
36. Andrea AE, Chiron A, Bessoles S, Hacein-Bey-Abina S. Engineering Next-Generation CAR-T Cells for Better Toxicity Management. *Int J Mol Sci* (2020) 21(22):8620. doi: 10.3390/ijms21228620

37. Yu S, Yi M, Qin S, Wu K. Next Generation Chimeric Antigen Receptor T Cells: Safety Strategies to Overcome Toxicity. *Mol Cancer* (2019) 18(1):1–13. doi: 10.1186/s12943-019-1057-4
38. Hattoum A, Rubin E, Orr A, Michalopoulos GK. Expression of Hepatocyte Epidermal Growth Factor Receptor, FAS and Glypican 3 in EpCAM-Positive Regenerative Clusters of Hepatocytes, Cholangiocytes, and Progenitor Cells in Human Liver Failure. *Hum Pathol* (2013) 44(5):743–9. doi: 10.1016/j.humpath.2012.07.018
39. Orlando D, Miele E, De Angelis B, Guercio M, Boffa I, Sinibaldi M, et al. Adoptive Immunotherapy Using PRAME-Specific T Cells in Medulloblastoma. *Cancer Res* (2018) 78(12):3337–49. doi: 10.1158/0008-5472.CAN-17-3140
40. Tiberghien P, Ferrand C, Lioure B, Milpied N, Angonin R, Deconinck E, et al. Administration of Herpes Simplex–Thymidine Kinase–Expressing Donor T Cells With a T-Cell–Depleted Allogeneic Marrow Graft. *Blood J Am Soc Hematol* (2001) 97(1):63–72. doi: 10.1182/blood.V97.1.63
41. Berger C, Flowers ME, Warren EH, Riddell SR. Analysis of Transgene-Specific Immune Responses That Limit the *In Vivo* Persistence of Adoptively Transferred HSV-TK–modified Donor T Cells After Allogeneic Hematopoietic Cell Transplantation. *Blood* (2006) 107(6):2294–302. doi: 10.1182/blood-2005-08-3503
42. Matsumoto K, Shigemi A, Ikawa K, Kanazawa N, Fujisaki Y, Morikawa N, et al. Risk Factors for Ganciclovir-Induced Thrombocytopenia and Leukopenia. *Biol Pharm Bull* (2015) 38(2):235–8. doi: 10.1248/bpb.b14-00588
43. European Medicines Agency. *Cymevene: Summary of Product Characteristics, Labelling and Package Leaflet: European Medicines Agency*. Available at: https://www.ema.europa.eu/en/documents/referral/cymevene-article-30-referral-annex-iii_en.pdf.
44. Iuliucci JD, Oliver SD, Morley S, Ward C, Ward J, Dalgarno D, et al. Intravenous Safety and Pharmacokinetics of a Novel Dimerizer Drug, AP1903, in Healthy Volunteers. *J Clin Pharmacol* (2001) 41(8):870–9. doi: 10.1177/00912700122010771
45. Tey S-K, Dotti G, Rooney CM, Heslop HE, Brenner MK. Inducible Caspase 9 Suicide Gene to Improve the Safety of Allodepleted T Cells After Haploidentical Stem Cell Transplantation. *Biol Blood Marrow Transplant* (2007) 13(8):913–24. doi: 10.1016/j.bbmt.2007.04.005
46. Hombach A, Hombach A, Abken H. Adoptive Immunotherapy With Genetically Engineered T Cells: Modification of the IgG1 Fc 'Spacer'domain in the Extracellular Moiety of Chimeric Antigen Receptors Avoids 'Off-Target'activation and Unintended Initiation of an Innate Immune Response. *Gene Ther* (2010) 17(10):1206–13. doi: 10.1038/gt.2010.91
47. Lee DW, Gardner R, Porter DL, Louis CU, Ahmed N, Jensen M, et al. Current Concepts in the Diagnosis and Management of Cytokine Release Syndrome. *Blood J Am Soc Hematol* (2014) 124(2):188–95. doi: 10.1182/blood-2014-05-552729
48. Budde LE, Berger C, Lin Y, Wang J, Lin X, Frayo SE, et al. Combining a CD20 Chimeric Antigen Receptor and an Inducible Caspase 9 Suicide Switch to Improve the Efficacy and Safety of T Cell Adoptive Immuno therapy for Lymphoma. *PloS One* (2013) 8(12):e82742. doi: 10.1371/journal.pone.0082742
49. Warda W, Larosa F, Da Rocha MN, Trad R, Deconinck E, Fajloun Z, et al. CML Hematopoietic Stem Cells Expressing IL1RAP Can Be Targeted by Chimeric Antigen Receptor–Engineered T Cells. *Cancer Res* (2019) 79(3):663–75. doi: 10.1158/0008-5472.CAN-18-1078
50. Hoyos V, Savoldo B, Quintarelli C, Mahendravada A, Zhang M, Vera J, et al. Engineering CD19-Specific T Lymphocytes With Interleukin-15 and a Suicide Gene to Enhance Their Anti-Lymphoma/Leukemia Effects and Safety. *Leukemia* (2010) 24(6):1160–70. doi: 10.1038/leu.2010.75
51. Diaconu I, Ballard B, Zhang M, Chen Y, West J, Dotti G, et al. Inducible Caspase-9 Selectively Modulates the Toxicities of CD19-Specific Chimeric Antigen Receptor-Modified T Cells. *Mol Ther* (2017) 25(3):580–92. doi: 10.1016/j.ymthe.2017.01.011
52. Barese CN, Felizardo TC, Sellers SE, Keyvanfar K, Di Stasi A, Metzger ME, et al. Regulated Apoptosis of Genetically Modified Hematopoietic Stem and Progenitor Cells Via an Inducible C Aspase-9 Suicide Gene in R Hesus M Acaques. *Stem Cells* (2015) 33(1):91–100. doi: 10.1002/stem.1869
53. Zhang P, Raju J, Ullah MA, Au R, Varelias A, Gartlan KH, et al. Phase I Trial of Inducible Caspase 9 T Cells in Adult Stem Cell Transplant Demonstrates Massive Clonotypic Proliferative Potential and Long-Term Persistence of Transgenic T Cells. *Clin Cancer Res* (2019) 25(6):1749–55. doi: 10.1158/1078-0432.CCR-18-3069
54. Zhou X, Dotti G, Krance RA, Martinez CA, Naik S, Kamble RT, et al. Inducible Caspase-9 Suicide Gene Controls Adverse Effects From Alloreplete T Cells After Haploidentical Stem Cell Transplantation. *Blood* (2015) 125(26):4103–13. doi: 10.1182/blood-2015-02-628354
55. Zhou X, Naik S, Dakhova O, Dotti G, Heslop HE, Brenner MK. Serial Activation of the Inducible Caspase 9 Safety Switch After Human Stem Cell Transplantation. *Mol Ther* (2016) 24(4):823–31. doi: 10.1038/mt.2015.234
56. Minagawa K, Jamil MO, Al-Obaidi M, Pereboeva L, Salzman D, Erba HP, et al. In Vitro Pre-Clinical Validation of Suicide Gene Modified Anti-CD33 Redirected Chimeric Antigen Receptor T-Cells for Acute Myeloid Leukemia. *PloS One* (2016) 11(12):e0166891. doi: 10.1371/journal.pone.0166891
57. Schuch A, Alizei ES, Heim K, Wieland D, Kiraithe MM, Kemming J, et al. Phenotypic and Functional Differences of HBV Core-Specific Versus HBV Polymerase-Specific CD8+ T Cells in Chronically HBV-Infected Patients With Low Viral Load. *Gut* (2019) 68(5):905–15. doi: 10.1136/gutjnl-2018-316641
58. Yoon H, Kim TS, Braciale TJ. The Cell Cycle Time of CD8+ T Cells Responding *In Vivo* Is Controlled by the Type of Antigenic Stimulus. *PloS One* (2010) 5(11):e15423. doi: 10.1371/journal.pone.0015423
59. Quintarelli C, Vera JF, Savoldo B, Giordano Attianese GM, Pule M, Foster AE, et al. Co-Expression of Cytokine and Suicide Genes to Enhance the Activity and Safety of Tumor-Specific Cytotoxic T Lymphocytes. *Blood J Am Soc Hematol* (2007) 110(8):2793–802. doi: 10.1182/blood-2007-02-072843
60. Norelli M, Camisa B, Barbiera G, Falcone L, Purevdorj A, Genua M, et al. Monocyte-Derived IL-1 and IL-6 Are Differentially Required for Cytokine-Release Syndrome and Neurotoxicity Due to CAR T Cells. *Nat Med* (2018) 24(6):739–48. doi: 10.1038/s41591-018-0036-4
61. Brudno JN, Kochenderfer JN. Toxicities of Chimeric Antigen Receptor T Cells: Recognition and Management. *Blood J Am Soc Hematol* (2016) 127(26):3321–30. doi: 10.1182/blood-2016-04-703751
62. KIM TW, KIM MN, KWON JW, KIM KM, KIM SH, Kim W, et al. Risk of Hepatitis B Virus Reactivation in Patients With Asthma or Chronic Obstructive Pulmonary Disease Treated With Corticosteroids. *Respirology* (2010) 15(7):1092–7. doi: 10.1111/j.1440-1843.2010.01798.x
63. Mestermann K, Giavridis T, Weber J, Rydzek J, Frenz S, Nerreter T, et al. The Tyrosine Kinase Inhibitor Dasatinib Acts as a Pharmacologic On/Off Switch for CAR T Cells. *Sci Trans Med* (2019) 11(499). doi: 10.1126/scitranslmed.aau5907

Conflict of Interest: KW and UP are co-founders and shareholders of SCG Cell Therapy Pte. Ltd.

KW is partially employed by SCG Cell Therapy GmbH.

The remaining authors declare that the research was conducted in the absence of any commercial or financial relationships that could be construed as a potential conflict of interest.

Publisher's Note: All claims expressed in this article are solely those of the authors and do not necessarily represent those of their affiliated organizations, or those of the publisher, the editors and the reviewers. Any product that may be evaluated in this article, or claim that may be made by its manufacturer, is not guaranteed or endorsed by the publisher.

frontiers in Immunology

ORIGINAL RESEARCH
published: 15 October 2021
doi: 10.3389/fimmu.2021.767000

Identification and Mapping of HBsAg Loss-Related B-Cell Linear Epitopes in Chronic HBV Patients by Peptide Array

Shuqin Gu[1†], Zhipeng Liu[1†], Li Lin[2†], Shihong Zhong[1], Yanchen Ma[1], Xiaoyi Li[1], Guofu Ye[1], Chunhua Wen[1], Yongyin Li[1] and Libo Tang[1*]*

[1] State Key Laboratory of Organ Failure Research, Guangdong Provincial Key Laboratory of Viral Hepatitis Research, Department of Infectious Diseases, Nanfang Hospital, Southern Medical University, Guangzhou, China, [2] Department of Oncology, Nanfang Hospital, Southern Medical University, Guangzhou, China

OPEN ACCESS

Edited by:
Jia Liu,
Huazhong University of Science and Technology, China

Reviewed by:
Chaohong Liu,
Huazhong University of Science and Technology, China
Jin Hou,
Second Military Medical University, China

***Correspondence:**
Yongyin Li
yongyinli@foxmail.com
Libo Tang
tanglibosmu@foxmail.com

[†]These authors have contributed equally to this work and share first authorship

Specialty section:
This article was submitted to Viral Immunology, a section of the journal Frontiers in Immunology

Received: 30 August 2021
Accepted: 29 September 2021
Published: 15 October 2021

Citation:
Gu S, Liu Z, Lin L, Zhong S, Ma Y, Li X, Ye G, Wen C, Li Y and Tang L (2021) Identification and Mapping of HBsAg Loss-Related B-Cell Linear Epitopes in Chronic HBV Patients by Peptide Array. Front. Immunol. 12:767000. doi: 10.3389/fimmu.2021.767000

Identification of immunogenic targets against hepatitis B virus (HBV)-encoded proteins will provide crucial advances in developing potential antibody therapies. In this study, 63 treatment-naïve patients with chronic HBV infection and 46 patients who achieved hepatitis B surface antigen loss (sAg loss) following antiviral treatment were recruited. Moreover, six patients who transitioned from the hepatitis B e antigen-positive chronic infection phase (eAg^+CInf) to the hepatitis phase (eAg^+CHep) were enrolled from real-life clinical practice. Additionally, telbivudine-treated eAg^+CHep patients and relapsers or responders from an off-treatment cohort were longitudinally studied. The frequencies and function of B cells were assessed by flow cytometry. We devised a peptide array composed of 15-mer overlapping peptides of HBV-encoded surface (S), core (C), and polymerase (P) proteins and performed a screening on B-cell linear epitopes with sera. Naïve B cells and plasmablasts were increased, whereas total memory, activated memory (AM), and atypical memory (AtM) B cells were reduced in sAg^- patients compared with sAg^+ patients. Importantly, longitudinal observations found that AtM B cells were associated with successful treatment withdrawal. Interestingly, we identified six S-specific dominant epitopes (S33, S34, S45, S76, S78, and S89) and one C-specific dominant epitope (C37) that reacted with the majority of sera from sAg^- patients. Of note, more B-cell linear epitopes were detected in CHep patients with alanine aminotransferase (ALT) flares than in nonflare CInf patients, and five B-cell linear epitopes (S4, S5, S10, S11, and S68) were overwhelmingly recognized by ALT flare patients. The recognition rates of epitopes on C and P proteins were significantly increased in CHep patients relative to CInf patients. Strikingly, a statistically significant elevation in the number of positive epitopes was observed when ALT nonflare patients shifted into the flare phase. Moreover, S76 identified at baseline was confirmed to be associated with a complete response after 48 weeks of telbivudine therapy. Taken together, we identified several functional cure-related B-cell linear epitopes of chronic HBV infection, and these epitopes may serve as vaccine candidates to elicit neutralizing antibodies to treat HBV infection.

Keywords: B-cell linear epitopes, hepatitis B virus, HBsAg loss, peptide array, atypical memory B cells

INTRODUCTION

Although an effective preventative vaccine has successfully protected newborns from hepatitis B virus (HBV) infection, approximately 300 million people with persistent positivity of hepatitis B surface antigen (sAg) are at high risk of developing HBV-related liver diseases worldwide (1). Currently, widespread application of interferon and nucleos(t)ide analogs (NUCs) attains significant improvement in restraining HBV replication, decreasing the rates of hepatocellular carcinoma and hepatic failure in patients with chronic hepatitis B (CHB); however, achieving sAg loss as an optimal endpoint is still burdensome and challenging (2, 3). Therapeutic vaccine development is needed to accelerate the goal of "the elimination of viral hepatitis as a public health threat by 2030" proposed by the World Health Organization.

HBV is a member of the family *Hepadnaviridae* with an appropriate 3.2 kb genome encoding four open reading frames, which are translated into the viral surface (S), core (C), polymerase (P), and X proteins; each can elicit specific immune responses against HBV (4). Cumulative data have highlighted the critical role of antibodies specific against the S, C, and P proteins triggered by HBV-specific B cells. The detection of hepatitis B surface antibody (sAb) is associated with virus control and disease resolution, and hepatitis B core antibody (cAb), a marker of past or current HBV exposure, is associated with acute liver damage. Meanwhile, antibodies against the P protein were reported to exert antiviral effects (5–7). The large S protein is further divided into 3 domains, $PreS_1$, $PreS_2$, and S, in which the chief immunogenic target, "a determinant region" is located (8). Epitope-based therapeutic vaccines and corresponding neutralizing antibodies have shown unique advantages in suppressing virus replication and decreasing sAg levels (9–12). However, the persistent existence of sAg and apparent discrepancies between animal models and clinical patients limit their clinical application. In addition, a recent phase 2, randomized, controlled open-label study showed that a designed therapeutic vaccine targeting HBV-encoded S, C, and X proteins failed to decrease the levels of sAg, despite inducing robust immunologic enhancement (13). Therefore, promising alternative novel epitopes urgently need to be identified as immunotherapeutic targets to eradicate HBV.

Chronic HBV infection is a long-term dynamic process of the interaction between the virus and host immunity. This infection is systematically divided into five phases based on alanine aminotransferase (ALT), HBV DNA level, the presence or absence of hepatitis B e antigen (eAg) and liver inflammation (2). High viremia and antigen load hamper both adaptive and innate immunity (14, 15). Persistent exposure to high sAg loading is associated with a dysfunctional HBV-specific immune response (16, 17). Conversely, patients who achieve sAg loss following antiviral treatment always have a satisfactory off-treatment response and a low incidence of hepatocellular carcinoma (18–20). Hence, it is necessary to explore the dominant B-cell epitopes on HBV proteins among patients in different phases and evaluate the association between dominant epitopes and powerful immune responses or favorable treatment responses. The dominant B-cell epitopes in sAg loss patients may be a more promising candidate to boost the HBV-specific immune response and achieve a functional cure. Unfortunately, to date, there is a lack of comprehensive investigation of B-cell epitopes in patients with different natural histories.

In this study, using a peptide array composed of 15-mer overlapping peptides of HBV-encoded S, C, and P proteins and screening with sAg loss sera, we identified 6 S-specific dominant epitopes (S33, S34, S45, S76, S78, and S89) and one C-specific dominant epitope (C37) that reacted with the majority of sera from patients with a functional cure. These data provide information for developing novel epitope candidates to elicit neutralizing antibodies to treat HBV infection.

MATERIALS AND METHODS

Study Subjects

The participants who provided written informed consent in this study consisted of 4 groups. In the first group, a total of 109 chronic HBV infection patients and 18 sAg-negative healthy individuals with normal ALT levels were enrolled for a cross-sectional study. Sixty-three treatment-naïve patients were classified into eAg-positive chronic infection (eAg^+CInf, n=21), eAg^+ chronic hepatitis (eAg^+CHep, n=21), and eAg^-CInf (n=21) based on an issued clinical practice guideline (2). Forty-six CHB patients who achieved sAg loss following antiviral treatment were recruited. The second group enrolled six patients who transitioned from the ALT nonflare phase to the flare phase from real-life clinical practice. The third group recruited twelve eAg^+ CHB patients treated with NUCs and fulfilled the criteria by the stopping rule of APASL from a prospective observational cohort. In this off-treatment cohort, six patients were sustained responders. The other six patients were defined as relapsers who experienced clinical relapse (HBV DNA > 2000 IU/mL and ALT > 2 times the upper limit of normal during follow-up discontinuing therapy). In the fourth group, eAg^+ CHB patients who participated in a clinical trial of telbivudine (trial number: CLDT600ACN07T) were longitudinally studied. Three telbivudine-treated subjects were defined as the complete response (CR) group (with normal ALT, HBeAg seroconversion, and HBV DNA level < 1000 copies/mL) at week 48, and the other subjects were classified as the noncomplete response (NCR, n=2) group. Patients who suffered from autoimmune diseases, other active diseases, or coinfection with HAV, HCV, HDV, or HIV were excluded. All subjects were recruited at Nanfang Hospital (Guangzhou, China). This study was conducted in compliance with the Declaration of Helsinki and approved by the Ethical Committee of Nanfang Hospital.

Serological Assays and HBV DNA Assays

The levels of human serum sAg, sAb, eAg, and eAb were quantitatively determined using the Roche COBAS® 6000 analyzer (Roche Molecular Diagnostics, Rotkreuz, Switzerland). The sAg had a lower limit of detection of 0.05 IU/mL. For the cross-sectional cohort, the levels of serum HBV DNA were quantified by the Roche LightCycler® 480 II (Roche Molecular

Diagnostics, Pleasanton, CA) with a Hepatitis B Viral Quantitative Fluorescence Diagnostic Kit (Sansure Biotech, Hunan, China), with a lower limit of quantitation of 100 IU/mL. For detection in the longitudinal cohort, serum HBV DNA was quantified by a Roche Cobas Amplicor PCR assay (Roche Molecular Systems, Branchburg, NJ, USA). The detection limit of HBV DNA was no lower than 300 copies/mL. The normal ranges for ALT and AST levels were 9–50 U/L and 15–40 U/L, respectively.

Phenotype Analysis and Intracellular Cytokine Staining (ICS)

Peripheral blood mononuclear cells (PBMCs) were isolated from fresh heparinized blood by Ficoll-Hypaque density gradient centrifugation, and some cells were cryopreserved in liquid nitrogen for further analysis. After staining with a Live/Dead Fixable Near-IR Dead Cell Stain kit (Life Technologies), thawed PBMCs (5×10^5 cells/tube) were stained with fluorescence phenotype antibodies (CD19-BV510, 562947, BD; CD10-PE-CF594, 562396; CD21-BV421, 562966, BD; CD27-Per-Cy5.5, 560612, BD; CD38-PE-Cy7, 560677, BD; or CD150-BV421, 562875, BD) at 4°C for 30 minutes and analyzed on a BD Aria III flow cytometer (BD Bioscience). To assess the function of B cells, PBMCs were stimulated with PMA (50 ng/mL), ionomycin (0.75 μg/mL), CPG (10 μg/mL, InvivoGen), CD40L (1 μg/mL, PeproTech), and BFA (1 μg/mL). The ICS was performed as previously described (21). Briefly, cells were stained with CD19-BV510, fixed and permeabilized using a Cytofix/Cytoperm kit (BD Bioscience), and then staining was performed with the corresponding intracellular antibody (IFN-γ-PE/Dazzle^{TM} 594, 562875, Biolegend). All flow cytometric analyses were performed using FlowJo V10.0.7 software (Treestar).

Peptide Array and Serum Screening

Ninety-eight 15-mer peptides overlapping by 11 residues covering large surface (S) proteins ($PreS_1$, $PreS_2$, and S region) were selected for the assay (**Supplementary Table 1**). In addition, the top response rates of 15-mer peptides in the C protein (top 18) and P protein (top 16) from our previous cultured T-cell enzyme-linked immunospot assay (ELISpot) were also included for the assay (**Supplementary Table 1**). The peptides covering the entire sequence of HBV genotypes B and C were gifts from Johnson & Johnson. The peptide array was manufactured by Suzhou Epitope Biotechnology Co., Ltd. (Suzhou, China). Approximately 0.6 nL of each peptide with a concentration of 0.1 mg/mL was printed onto activated nanomembranes by SmartArrayer 48 as previously described (22, 23). Serum was immediately withdrawn and frozen at -20°C until use. Sera were diluted (1:100) and incubated with a peptide array at 37°C for 30 minutes. Diluted sera without precoated peptide (buffer dot) in each microarray were used as a negative control. After washing, the peptide arrays were incubated with horseradish peroxidase (HRP)-conjugated goat anti-human IgG. Dots were visualized by Super Signal Femto Maximum Sensitivity Substrate for Chemiluminescence (Thermo Fisher), and images were captured by a cool CCD. The mean +3 SD of the buffer dot was used as the background intensity. A signal above 1500 was considered positive. Positive peptide coverage was defined as the ratio of the number of peptides recognized by at least one serum sample to the total number of peptides in each subpartition. The average recognition rate was generated to define the average peptide reaction capacity of patients in subpartitions.

Statistical Analysis

Data are expressed as median (interquartile range). The Mann–Whitney *U* test or Wilcoxon signed-rank test was used when two groups were compared. For multiple group comparisons, the Kruskal–Wallis H test and *post hoc* test (Dunn's test) were performed. Correlations between variables were assessed with Spearman's rank-order correlation coefficient. Categorical variables were compared by the chi-square test. SPSS Statistics 20.0 (Chicago, IL) and GraphPad Prism 8 software were used for statistical analysis. All statistical analyses were based on two-tailed hypothesis tests, and a P value < 0.05 was considered statistically significant.

RESULTS

B-Cell Subsets Varied in sAg Loss and Were Associated With Successful Treatment Withdrawal

First, we investigated the percentage of total B cells, naïve B cells, plasmablasts, total memory, resting memory (RM), activated memory (AM), and atypical memory (AtM) B-cell subsets in patients with different immune statuses of HBV infection as well as healthy controls (HCs) (**Table 1** and **Supplementary Figure 1A**). The frequency of total $CD19^+$ B cells in PBMCs was significantly higher in sAg^+ patients than in HCs (**Figure 1A**). The frequency of naïve B cells and plasmablasts was preferentially increased, whereas total memory B cells were significantly reduced in sAg^- patients compared with sAg^+ patients (**Figure 1A**). In addition, a decreased proportion of AM or AtM B cells was observed in patients who achieved sAg loss, and RM B cells were the dominant phenotype in all phases (**Figure 1B** and **Supplementary Figure 1B**). We next examined whether the frequency of AtM B cells was correlated with virological parameters. The frequency of AtM B cells was positively correlated with serum sAg and HBV DNA levels (**Figure 1C**). In addition, a similar positive correlation was detected between the expression of SLAM on $CD19^+$ B cells and serum eAg levels. In contrast, inverse correlations were found between IFN-γ-expressing $CD19^+$ B cells and eAg and HBV DNA levels (**Figure 1D**). The expression of SLAM on $CD19^+$ B cells was similar among all phases, but IFN-γ-expressing $CD19^+$ B cells were expanded in eAg^-CInf patients (**Supplementary Figure 1C**). An increased frequency of $CD19^+$ B cells and naïve B cells within the cohort studied was found in responders at week 48 after NUCs discontinuation (**Table 2** and **Figure 1E**). Notably, AtM B cells were dramatically enriched in responders 8 and 12 weeks after stopping treatment compared to relapsers (**Figure 1F**). Together, these results indicated that

TABLE 1 | Clinical characteristics of the cross-sectional study subjects.

Group	eAg+ chronic infection	eAg+ chronic hepatitis	eAg- chronic infection	sAg loss	Healthy controls
No. of patients (M/F)	21 (12/9)	21 (17/4)	21 (14/7)	46 (41/5)	18 (8/10)
Age (year)	30.00 (24.75-36.00)	30.00 (25.50-33.50)	37.00 (33.75-46.00)	41.00 (35.00-53.00)	24.00 (23.00-27.00)
HBV DNA (lg IU/mL)	8.23 (7.78-8.53)	7.91 (7.62-8.24)	2.00[a]	T.N.D	n.d.
ALT (ULN)	0.45 (0.37-0.59)	3.14 (1.90-6.34)	0.40 (0.24-0.53)	0.44 (0.31-0.61)	0.28 (0.18-0.30)
AST (ULN)	0.56 (0.51-0.57)	2.20 (1.23-3.40)	0.50 (0.41-0.64)	0.50 (0.45-0.58)	0.35 (0.37-0.67)
sAg (P/N)	21/0	21/0	21/0	0/46	0/18
sAb (P/N)	0/21	0/21	0/21	22/24	18/0
eAg (P/N)	21/0	21/0	0/21	2/44	0/18
eAb (P/N)	0/21	0/21	21/0	27/19	0/18

Data were shown as median (25-75% percentile).

[a]Eighteen subjects were lower than 2.0 in HBeAg- chronic infection.

ALT, alanine aminotransferase; AST, aspartate aminotransferase; eAb, hepatitis B e antibody; eAg, hepatitis B e antigen; sAb, hepatitis B surface antibody; sAg, hepatitis B surface antigen; n.d., not determined; P/N, positive or negative; T.N.D, target not detected; ULN, the upper limit of normal.

alteration of the distribution and function of B-cell subsets might be associated with the outcome of HBV infection.

Identification of Dominant S-Specific Linear B-Cell Epitopes of Chronic HBV Infection by a Peptide Array

Detection of sAbs produced by B cells is associated with disease resolution and virus control in chronic HBV infection. To map the dominant linear B-cell epitopes of sAbs recognized by these patients, a peptide array composed of 98 overlapping 15-mer peptides covering the large S protein was conducted (**Figure 2A**). According to the classical regions of the large S protein, these peptides were classified into 8 subpartitions: $PreS_1$ (S1–31), $PreS_1$-S_2 (S28–31), $PreS_2$ (S28–44), $PreS_2$-S (S41–44), S (S41–98), Pre a (S72–75), a (S72–80), and Suf a (S78–80). Then, we used this peptide array to perform serum screening for a total of 59 serum samples from patients with chronic HBV infection, including 17 sAg loss patients. The design of the 5*5 peptide array and representative results were shown in **Figure 2B**. In summary, the positive peptide coverage of each subpartition varied from 47.1% to 100%, although the recognition rate of each peptide was low (**Figure 2C**).

sAg Loss Patients Have Fewer B-Cell Linear Epitopes but a Higher Recognition Rate

Then, we attempted to identify the dominant B-cell epitopes shared by patients in different immune phases. The peptide array showed that the dominant linear B-cell epitopes mainly lay in the S subpartition in all stages. An increasing recognition rate of the $PreS_1$ subpartition was also observed in eAg^+CHep and sAg loss patients (**Figure 3A** and **Supplementary Figure 2**). We next compared the recognition rate and positive peptide coverage of subpartitions between patients with sAg^+ and sAg^-. The subpartition recognition rate was comparable in these two groups; however, the positive peptide coverage of the total large S protein and S subpartition was lower in sAg^- patients (**Figure 3B**). In contrast, six peptides (S33, S34, S45, S76, S78, and S89) reacted with the majority of sera from patients who achieved sAg loss (**Figure 3C**). Overall, these data implied that the dominant linear B-cell epitopes appear to be associated with the prognosis of chronic HBV infection.

A Specific Linear Epitope on the "A Determinant Region" Identified by sAg Loss Sera Is Associated With a Favorable Treatment Response

Considering the pivotal role of antibodies against the "a determinant region" during vaccination, we then investigated the dominant linear B-cell epitopes in "a" subpartition (**Figure 4A**). Relative to patients with sAg^+, the recognition rates of S76 and S78 were significantly increased in patients with sAg^- (**Figure 4B**). In addition, the proportion of sAg^- patients in the S76- or S78-positive group was significantly higher than that in the S76- or S78-negative group (**Figure 4C**). Intriguingly, the longitudinal analysis showed an expansive tendency of positive epitopes in patients who achieved complete response (CR) after 48 weeks of telbivudine treatment. In addition, all patients with S76 positivity at baseline achieved CR after therapy (**Table 3** and **Figure 4D**). These results suggested that the S76 linear B-cell epitope may be a good marker to predict a favorable treatment response to telbivudine.

Dominant Linear B-Cell Epitopes Are Expanded in Chronic HBV-Infected Patients With Liver Inflammation

Chronic HBV infection is an extremely complicated dynamic process, especially in the hepatitis phase, in which elevated ALT reflects inflammatory activity accompanied by immune activation. We further characterized the distribution of linear B-cell epitopes between patients with CInf and CHep. We found that more linear B-cell epitopes of sAbs were detected in CHep patients, and five linear B-cell epitopes (S4, S5, S10, S11, and S68) were overwhelmingly recognized by CHep patients (**Figure 5A**). Strikingly, the results also showed an elevated intensity of linear epitope signals in CHep patients (**Figure 5B**). Subsequently, we explored linear B-cell epitopes from six eAg^+CInf patients with normal ALT levels who shifted into the eAg^+CHep phase with ALT flares during the follow-up. As shown in **Figure 5C**, new epitopes appeared in the flare phase of these patients. Of note, there was a statistically significant elevation in the number of positive epitopes when patients shifted into the ALT flare phase (**Figure 5C**). Collectively, these results showed that dominant linear B-cell epitopes could reflect immune activation in CHB.

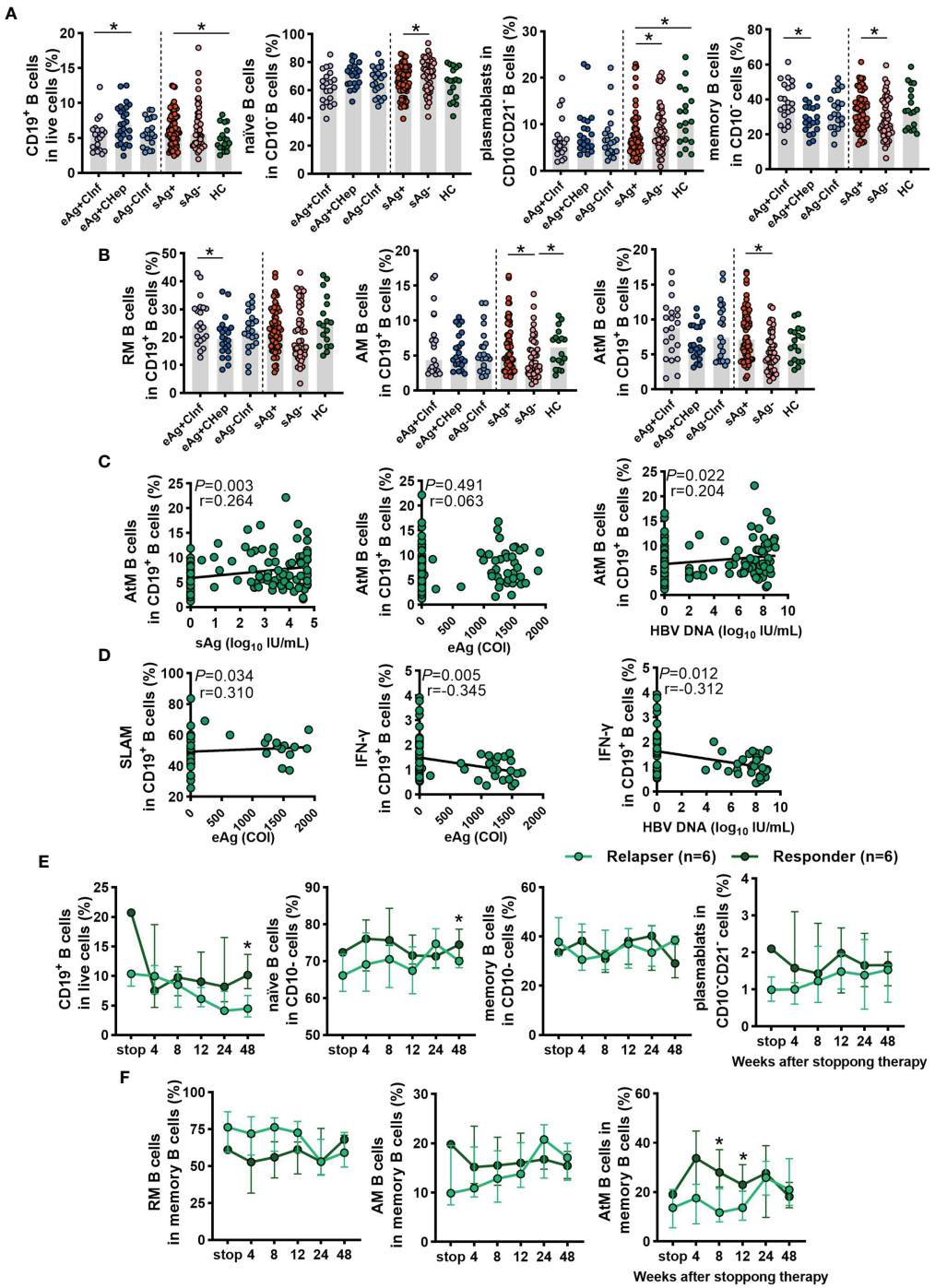

FIGURE 1 | Analyses of the B-cell subsets in the cross-sectional cohort and NUCs withdrawal cohort. **(A)** Comparison of the frequencies of total CD19$^+$ B cells, naïve B cells, plasmablasts, and memory B cells in patients with chronic HBV infection and HCs. According to the EASL clinical practice guideline, these subjects were classified into 4 groups: hepatitis B e antigen-positive chronic infection (eAg$^+$CInf, n=21), eAg-positive chronic hepatitis (eAg$^+$CHep, n=21), eAg$^-$CInf (n=21), and hepatitis B surface antigen-negative (sAg-, n=46). **(B)** Frequency of resting memory (RM), activated memory (AM), and atypical memory (AtM) B cells among CD19$^+$ B cells in HBV patients and HCs. **(C)** Spearman's correlation between the frequency of AtM B cells among CD19$^+$ B cells and the levels of serum virological parameters. **(D)** The correlation between the expression of SLAM and IFN-γ on CD19$^+$ B cells and the levels of serum virological parameters. **(E, F)** Longitudinal analysis of B-cell subsets after stopping NUCs therapy. **(A, B)** Kruskal–Wallis H test and Dunn's multiple comparisons test. **(C, D)** Spearman's rank correlation test. **(E, F)** Mann–Whitney *U* test. $^*P < 0.05$.

TABLE 2 | Clinical characteristics of responders and relapsers with chronic HBV infection at the end of treatment.

Group	responder	relapser
No. of patients (M/F)	6 (6/0)	6 (5/1)
Age (year)	32.00 (29.25-37.50)	42.00 (37.00-48.25)
ALT (ULN)	0.40 (0.37-0.57)	0.44 (0.36-0.84)
Quantitative sAg (IU/mL)	232.50 (20.91-1787.00)	1553.00 (76.20-5325.00)
eAg (P/N)	0/6	0/6
eAb (P/N)	6/0	6/0
HBV DNA (lg IU/mL)	T.N.D	T.N.D
Median duration of medication (weeks)	188.00 (107.00-264.00)	290.00 (200.00-374.00)
Median time to virological relapse (weeks)	NA	107.00 (12.00-150.00)

Data were shown as median (25-75% percentile).
ALT, alanine aminotransferase; eAb, hepatitis B e antibody; eAg, hepatitis B e antigen; sAg, hepatitis B surface antigen; NA, not applicable; P/N, positive or negative; T.N.D, target not detected; ULN, the upper limit of normal.

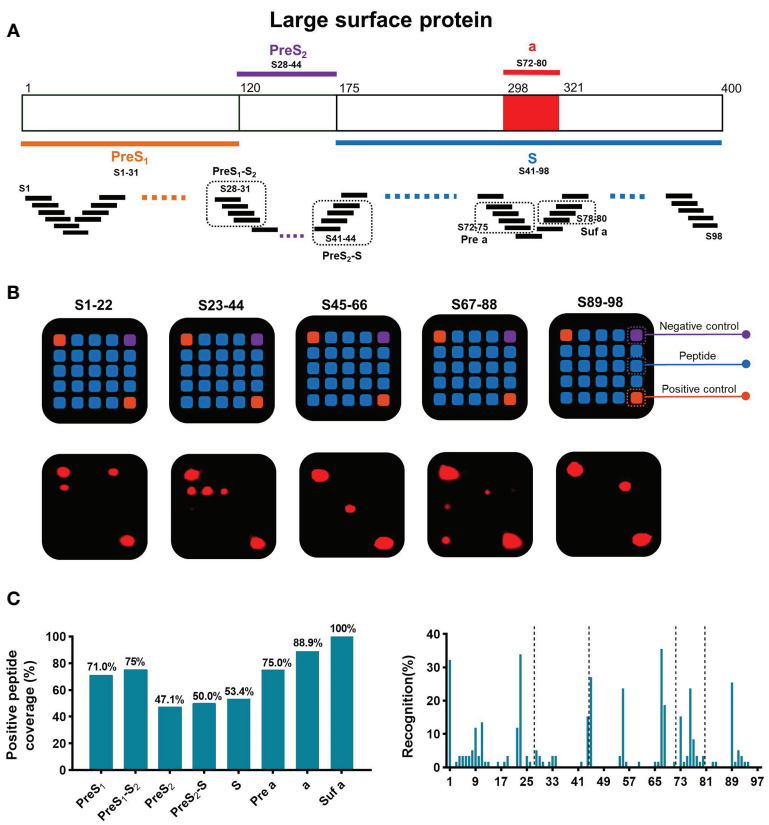

FIGURE 2 | General recognition of linear B-cell epitopes on S protein by peptide array. **(A)** Schematic of the large surface proteins $PreS_1$, $PreS_2$, and S. In the diagram of S, the "a determinant region" is red. Design of peptide array. Fifteen-mer overlapping peptides covering the entire S protein were shown. According to the classical regions of the large S protein, these peptides were classified into 8 subpartitions: $PreS_1$ (S1–31), $PreS_1$-S_2 (S28–31), $PreS_2$ (S28–44), $PreS_2$-S (S41–44), S (S41–98), Pre a (S72–75), a (S72–80), and Suf a (S78–80). **(B)** Representative peptide array. Design of the 5*5 peptide array; for each subarray, there were negative and positive controls (top). Five representative subarrays with positive results (bottom). **(C)** Positive peptide coverage in subpartitions and recognition rate of each peptide in patients with chronic HBV infection.

A Higher Linear B-Cell Epitope Recognition Rate on C and P Proteins in CHep

Additionally, we tested the dominant linear B-cell epitopes of the C and P proteins in chronic HBV infection. The top 18 response rates of 15-mer peptides in the C protein and the top 16 in the P protein from our earlier cultured T-cell ELISpot were selected, and all can be identified in the array (**Supplementary Figures 3A, B**). An increasing number of positive epitopes on the P protein were shown in eAg^+CHep patients relative to patients with sAg loss (**Supplementary Figure 3C**). Patients carrying sAg displayed a higher recognition rate of the selected peptides on the P protein

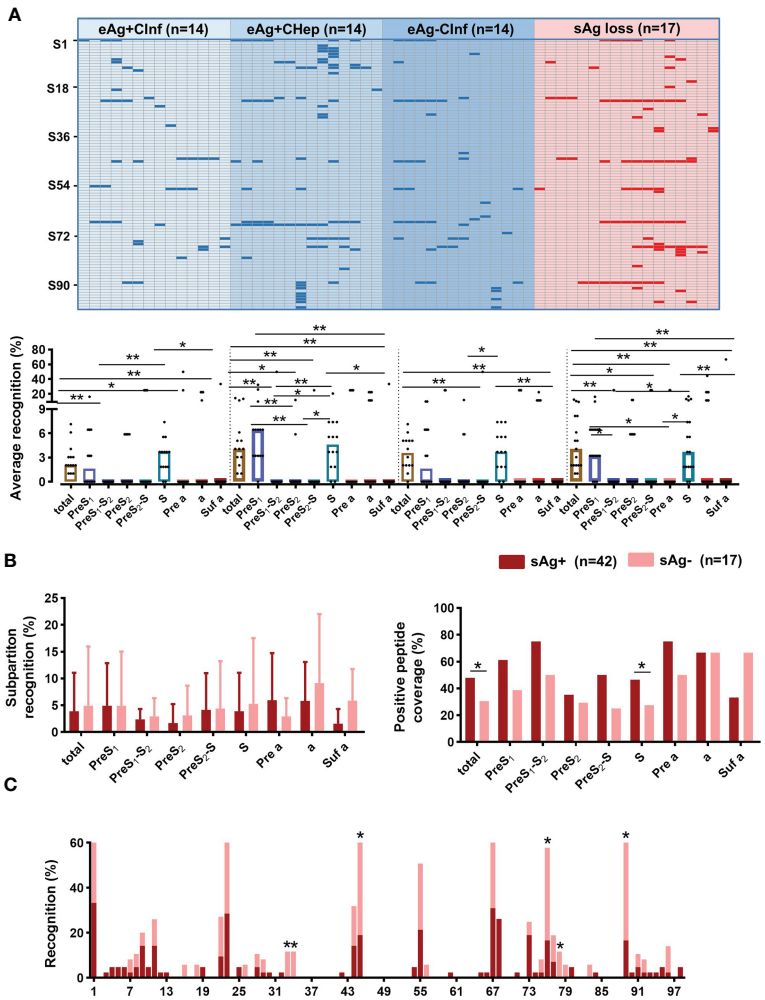

FIGURE 3 | Screening sera from patients with chronic HBV infection. **(A)** Sera from patients with chronic HBV infection were diluted (1:100) and incubated with a peptide array, followed by incubation with HRP-conjugated anti-human IgG. The peptide array was visualized by chemiluminescent reagents, scanned, and quantified. Peptides with a signal above 1500 (mean +3 SD of the negative control) were counted as positive (blue and red bars). The positive peptides for each subject were plotted. Comparing the average recognition rate of each peptide in subpartitions in patients with chronic HBV infection. **(B)** Comparison of the subpartition recognition rate (a set of recognition rates in the subpartition of each patient) and positive peptide coverage between the sAg^+ and sAg^- groups. **(C)** Comparison of the recognition rate of each peptide between sAg^+ and sAg^- groups. **(A)** Kruskal–Wallis H test and Dunn's multiple comparisons test. **(B)** Mann–Whitney *U* test (left) and Chi-square test (right). **(C)** Chi-square test. $^*P < 0.05$, $^{**}P < 0.01$.

than those with sAg^-; correspondingly, the positive peptide coverage of the C and P proteins in sAg^+ patients was higher than that in sAg^- patients (**Figure 6A**). Strikingly, C37 on the C protein stood out from the selected peptides; its recognition rate was significantly increased in patients with sAg^-; moreover, the proportion of sAg^- patients in the C37-positive group was significantly higher than that in the C37-negative group (**Figures 6B, C**). We also examined the variation in linear B-cell epitopes between CInf patients and CHep patients. A higher recognition rate of the selected peptides on C and P proteins was observed in CHep patients, along with higher positive peptide coverage (**Figure 6D**). Compared with CInf patients, the recognition rate of C15 on C protein and P167 on P protein were significantly increased in CHep patients (**Figure 6D**). The proportion of CHep patients in the C15- or P167-positive group was significantly higher than that in the C15- or P167-negative group (**Figures 6E, F**). Notably, a remarkable decrease in the proportion of P188 was found in the flare phase compared to the nonflare stage in these six patients during follow-up (**Figure 6G**). These findings indicated a broad value of linear B-cell epitopes on HBV proteins to evaluate the prognoses of patients.

DISCUSSION

Previous studies have identified several neutralizing antibodies against HBV protein from a small number of HBV vaccinees or controllers (9, 24). In contrast, we screened sera from 59 patients with chronic HBV infection, including 17 patients who achieved

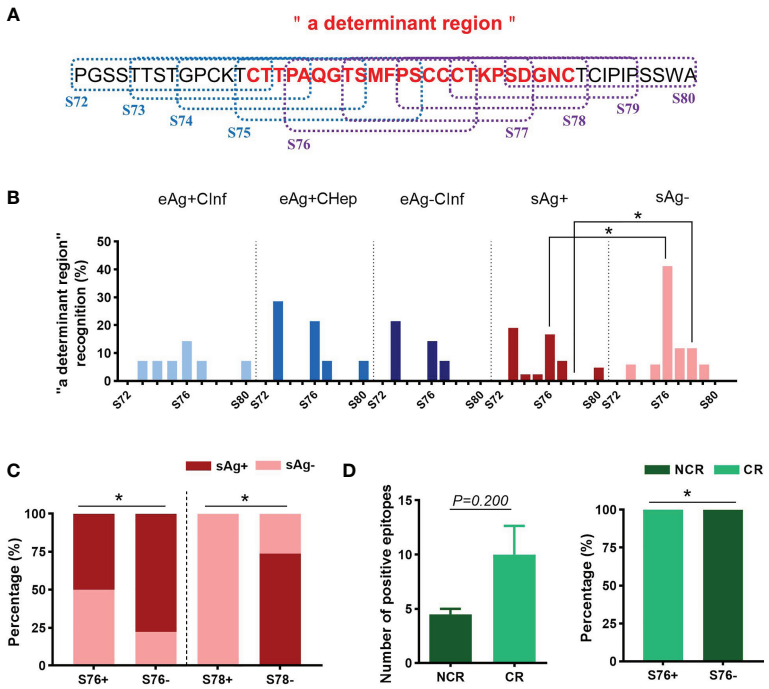

FIGURE 4 | Distribution of linear B-cell epitopes on "a determinant region". **(A)** The amino acid sequence of "a determinant region". The dotted boxes indicate the corresponding peptides. The "a determinant region" was in red. **(B)** The recognition rate of each peptide in "a determinant region". **(C)** The proportion of patients with detectable sAg or sAg loss in the S76+/- or S78+/- groups. **(D)** Comparison of the number of positive peptides between the complete response (CR) and noncomplete response (NCR) groups (left). The proportion of patients with different treatment responses in the S76+/- group (right). **(B–D)** Chi-square test. *$P < 0.05$.

TABLE 3 | Clinical characteristics of the study subjects with telbivudine therapy for the longitudinal study.

Group		CR	NCR	*P* value
No. of patients (M/F)		3 (1/2)	2 (2/0)	0.136[a]
Age (year)		34.00 (24.00-35.00)	25.50 (25.00-26.00)	0.800[b]
0 weeks	HBV DNA (lg copies/mL)	8.63 (8.38-8.88)	8.18 (8.04-8.32)	0.800[b]
	ALT (U/L)	253.00 (159.00-256.00)	258.00 (222.00-294.00)	0.983[b]
	eAg (P/N)	3/0	2/0	
48 weeks	HBV DNA (lg copies/mL)	n.d.	n.d.	
	ALT (U/L)	14.00 (10.00-18.00)	19.00 (15.00-23.00)	0.400[b]
	eAg (P/N)	0/3	2/0	0.025[a]

Data were shown as median (25-75% percentile).
[a]*Chi-squared test.*
[b]*Mann-Whitney U test.*
ALT, alanine aminotransferase; CR, complete response; eAg, hepatitis B e antigen; NCR, non-complete response; P/N, positive or negative.

sAg loss by a peptide array. The same strategy has been used to identify dominant epitopes in other infectious diseases (22, 23, 25, 26). To learn the profile of the B-cell linear epitopes recognized by chronic HBV infection for guiding vaccine design, we devised a peptide array composed of 15-mer overlapping peptides of HBV-encoded S, C, and P proteins and performed a screening on B-cell linear epitopes with sera from patients in different phases of the natural history. The data presented in this study provide information for developing novel epitope candidates to potentially elicit neutralizing antibodies to treat chronic HBV infection. First, the proportion of dysfunctional AtM B cells was decreased in patients who achieved sAg loss and was associated with successful treatment withdrawal. Second, we identified seven dominant epitopes recognized by sAg loss patients (S33, S34, S45, S76, S78, S89, and C37), and a specific epitope, S76, at baseline was associated with a favorable treatment response to telbivudine therapy. Third, dominant linear B-cell epitopes are expanded in chronic hepatitis B. Future studies are needed to further comprehend the role and neutralization capacity of antibodies against these epitopes.

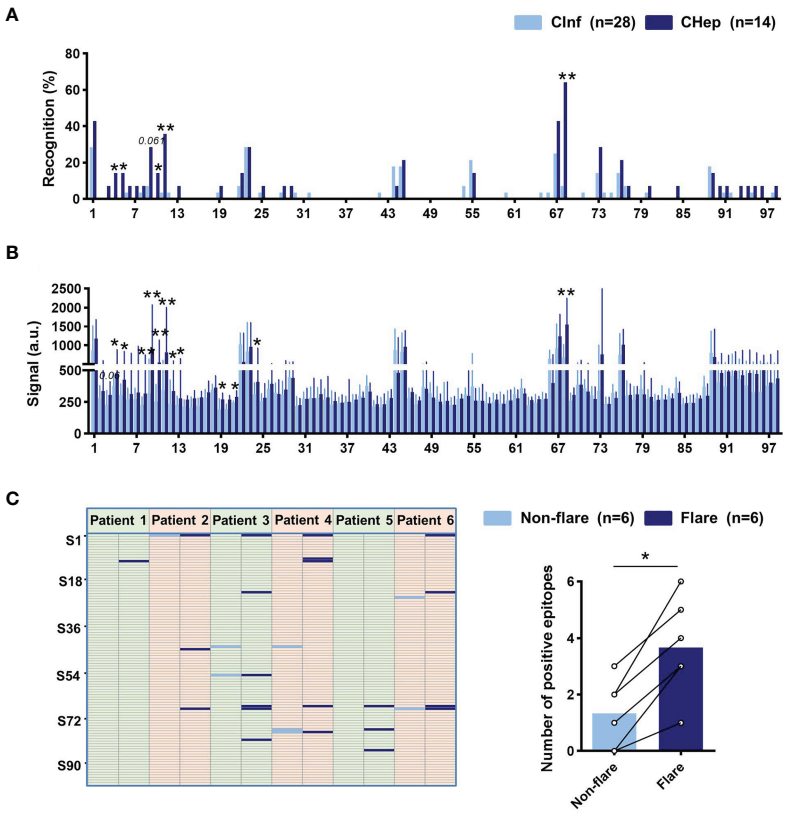

FIGURE 5 | Linear B-cell epitope variation between chronic HBV infection (CInf) and chronic hepatitis B (CHep). **(A)** Comparison of the recognition rate of each peptide between CInf and CHep patients. **(B)** The original signal change of each peptide between CInf and CHep patients. **(C)** Distribution of linear B-cell epitopes of six patients who transitioned from the nonflare eAg^+CInf phase to the eAg^+CHep phase with ALT flares. Positive epitopes were plotted in the nonflare (light blue bar) and flare (dark blue bar) phases (left). Comparing the number of positive peptides between ALT nonflare and flare phases (right). **(A)** Chi-square test. **(B)** Mann–Whitney *U* test. **(C)** Wilcoxon signed-rank test. $^*P < 0.05$, $^{**}P < 0.01$.

Clinically, sAg is a sensitive diagnostic marker for HBV infection. Serum sAg titers are highly correlated with reactivity to antiviral therapy and prognosis. Moreover, the incapacitated immune system induced by overwhelming sAg was the real culprit for the unsatisfactory effect of anti-HBV therapy (27, 28). Therefore, sAg is becoming the most promising target for epitope-based therapy to achieve a functional cure. Three forms of HBV S protein were displayed on HBV virions: the large S ($PreS_1$+$PreS_2$+S), the middle S ($PreS_2$+S), and the small S (S). Antibodies against the prime target "a determinant region" in the S domain, the antigenic loop and central immunodominant region for HBV prevention and therapy, conferred efficient viremia suppression: E6F6-like mAbs targeted epitope on "a determinant region" (recognize aa 119–125 of S) strikingly suppressed HBV DNA and HBsAg levels in an HBV mouse model (10). To attain more aggressive HBV-specific immune responses and therapeutic effects, they further designed S-aa 119–125-containing B cell epitope-based therapeutic vaccines. The remarkable and prolonged suppression effects on sAg and viral loading in HBV carrier mice confirmed its potential in therapeutic vaccine design for CHB treatment (11). However, antibodies against a similar recognition site were not found in a human counterpart (12). In the present study, we demonstrated that the recognition rates of S76 and S78 on "a determinant region" were distinctly higher in sAg loss patients despite decreased positive peptide coverage of the S domain. Total memory B cells and AtM B cells, the main component of sAg-specific B cells (29–31), were reduced in sAg loss, which mainly resulted from the decline of sAg and eAg. Combined with the findings that an increasing proportion of plasmablasts in sAg loss could differentiate into antibody-producing cells and an inverse association between the frequency of immunoregulatory IFN-γ-producing B cells and virological parameters, it is reasonable to speculate that fewer defective B cells in sAg loss may produce effective neutralizing antibodies against these two epitopes in conquering sAg seroclearance. To further investigate the relationship between these epitopes and treatment response, we longitudinally analyzed the dominant linear B-cell epitope in patients treated with telbivudine for 48 weeks. Notably, patients identified as S76, S1, or S9 at baseline were more likely to achieve CR after the entire therapy (**Figure 4D** and **Supplementary Figure 4**). It should be emphasized that small quantity of longitudinal participants and patients with sAg loss might cause potential bias, which makes it difficult to match all

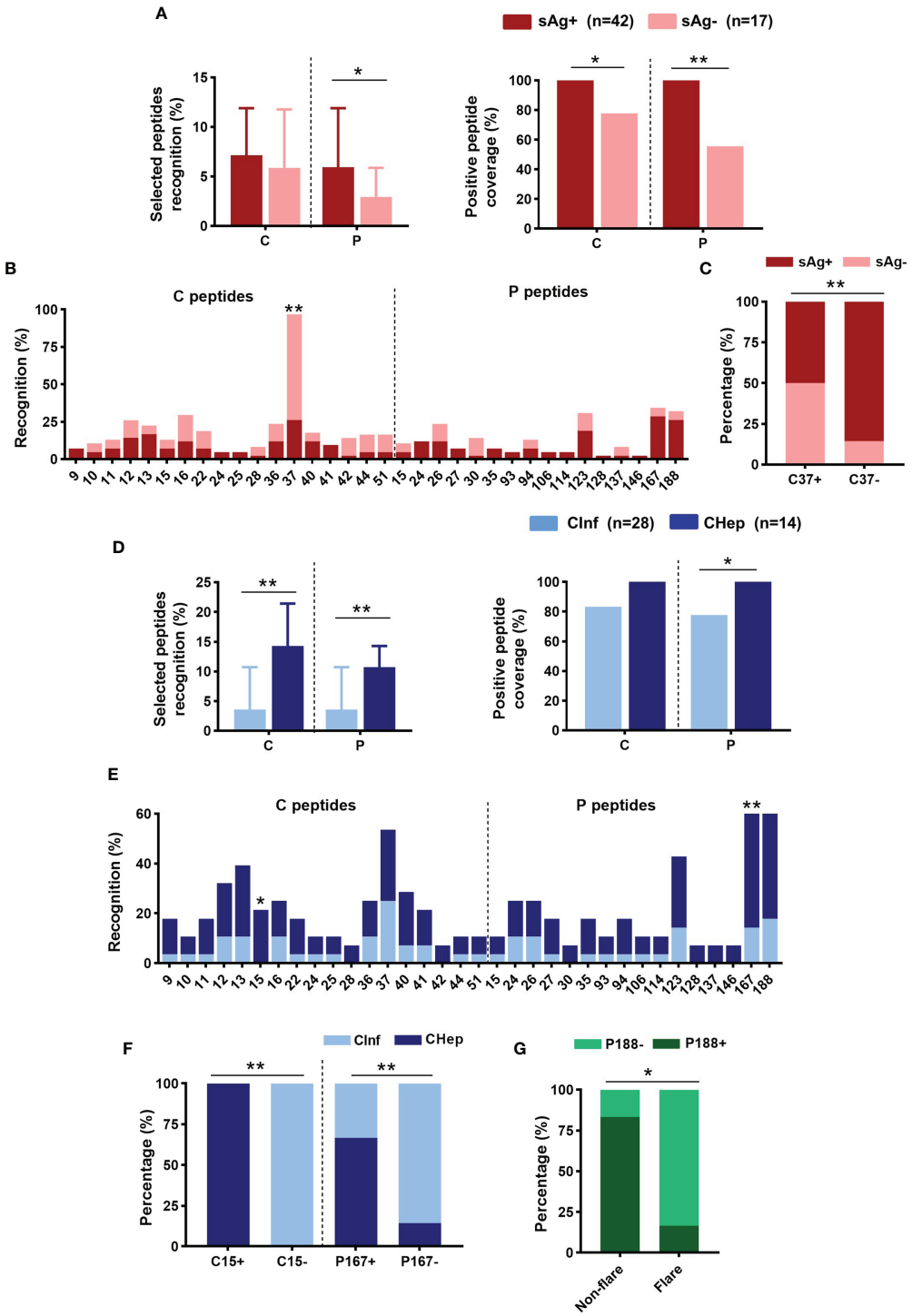

FIGURE 6 | Distribution of linear B-cell epitopes on core (C) and polymerase (P) proteins. **(A)** Comparison of the recognition rate and positive peptide coverage on C or P between sAg^+ and sAg^- groups. **(B)** The recognition rate of the selected peptide on C or P. **(C)** Proportion of patients with detectable sAg or sAg loss in the C37+/- group. **(D)** Comparison of the recognition rate and positive peptide coverage on C or P proteins between CInf and CHep patients. **(E)** Comparison of the recognition rate of the selected peptides between CInf and CHep patients. **(F)** The proportion of patients with CInf or CHep in the C15+/- or P167+/- groups. **(G)** The proportion of P188 was positive or negative in the ALT nonflare and flare phases of those six patients. **(A, D)** Mann–Whitney *U* test (left) and Chi-square test (right). **(B, C, E–G)** Chi-square test. $^*P < 0.05$, $^{**}P < 0.01$.

comparisons; further investigation is warranted to verify this preliminary conclusion.

Recently, an increasing number of publications identified several epitopes besides S76 or S78 that play a pivotal role in inducing the HBV-specific immune response. Further *in vivo* preclinical experiments also confirmed the neutralizing ability of epitope-corresponding antibodies (9, 12, 32). However, the persistent existence of sAg restricted their clinical application. The discrepancies possibly resulted from the various natural histories of selected individuals. In this study, we focused on pursuing candidate epitopes that drove the transformation to sAg seroclearance. The straightforward comparison between sAg loss and sAg-positive patients may make it easier to identify the pivotal epitopes that may play critical roles in achieving a functional cure while neglected under various alternative epitopes in other studies. Of note, the dominant epitopes on the C protein in patients who achieved a functional cure were also consistent with our previous finding that HBV C-specific T-cell responses played an essential role in HBV control (33). To our knowledge, few studies have documented sAg loss-related dominant epitopes, which would have potentially far-reaching ramifications for immunotherapy of chronic HBV infection. Further experiments are needed to clarify this hypothesis, and the therapeutic effect of antibodies against nominated epitopes remains to be elucidated.

Dozens of resources and efforts have been devoted to developing anti-HBV therapy; nevertheless, progress is still tortuous due to the difficulty of overcoming immune tolerance in chronic HBV infection. The natural history of chronic HBV infection is a long-term dynamic process and consists of five discontinuous phases. HBV-specific adaptive immunity can also change from immune tolerance to progressive immune activation, inactivation, reactivation, and exhaustion (34). Emerging evidence has shown that "immune tolerant" CInf patients tend to develop hepatocellular carcinoma compared with "immune active" CHep patients (12% *vs.* 6% per 10 years) (34, 35). In addition, the diverse immune status may be a consequence of the abundance of dominant epitopes, which may strongly influence immune activation signaling (36). Hence, it is essential to explore the epitope variation between CInf and CHep patients. Our peptide array data demonstrated that S4, S5, S10, S11, S68, C15, and P167 were the most distinguishable dominant epitopes in CHep patients relative to CInf patients. Additionally, we longitudinally analyzed the dynamic variation of epitopes in six patients who transitioned from the ALT nonflare eAg^+CInf phase to the flare eAg^+CHep phase. Emerging epitopes in the ALT flare phase of these patients further confirmed that dominant linear B-cell epitopes could reflect immune activation in CHB. Interestingly, we found that the majority of dominant epitopes in immune-active CHep patients were located in the $PreS_1$ domain. Antibodies against S regions are believed to elicit neutralizing infectivity. Meanwhile, the $PreS_1$ domain interacts with the HBV receptor NTCP on hepatocytes (37, 38). Thus, it is reasonable to speculate that the abundance of epitopes reflecting immune activation during chronic HBV infection may activate the HBV-specific immune response, elicit neutralizing antibodies, inhibit virus replication, and disrupt susceptibility to NTCP for HBV entry, which should be elucidated in future studies.

In summary, we identified the dominant B-cell linear epitopes of chronic HBV infection by a peptide array. These results will be essential to guide the therapeutic vaccine design for chronic HBV infection.

DATA AVAILABILITY STATEMENT

The raw data supporting the conclusions of this article will be made available by the authors, without undue reservation.

ETHICS STATEMENT

The studies involving human participants were reviewed and approved by Ethical Committee of Nanfang Hospital. The patients/participants provided their written informed consent to participate in this study.

AUTHOR CONTRIBUTIONS

SG, LT, and YL designed the study. SG, ZL, and LL performed the experiments and analyses. SG, ZL, SZ, YM, XL, GY, and CW collected samples and laboratory data. SG, ZL, LT, and YL wrote the manuscript. LT and YL supervised the study. All authors contributed to the article and approved the submitted version.

FUNDING

This work was supported by grants from the National Natural Science Foundation of China (81971933 and 81770592), National Science and Technology Major Project of China (2018ZX10301202), and the Outstanding Youth Development Scheme of Nanfang Hospital, Southern Medical University (2020J003).

ACKNOWLEDGMENTS

The authors would like to express their gratitude to all the patients and healthy volunteers who participated and the staff who helped with recruitment.

SUPPLEMENTARY MATERIAL

The Supplementary Material for this article can be found online at: https://www.frontiersin.org/articles/10.3389/fimmu.2021.767000/full#supplementary-material

Supplementary Table 1 | The amino acid sequences of HBV peptides.

Supplementary Figure 1 | Cross-sectional analysis of B-cell subsets. **(A)** Gating strategy for total $CD19^+$ B cells and their distribution into naïve B cells ($CD19^+CD10^-CD21^+CD27^-$), memory B cells ($CD19^+CD10^-CD21^-$ and $CD19^+CD10^-CD21^+CD27^+$),

plasmablasts ($CD19^+CD10^-CD21^-CD27^+CD38^+$), resting memory (RM, $CD21^+CD27^+$), activated memory (AM, $CD21^-CD27^+$), and atypical memory (AtM, $CD21^-CD27^-$) B-cell subsets. **(B)** Frequency of RM, AM, and AtM B cells among $CD19^+$ B cells in patients with chronic HBV infection. **(C)** The expression of SLAM and IFN-γ on $CD19^+$ B cells within patients with chronic HBV infection and HCs. **(B, C)** Kruskal–Wallis H test and Dunn's multiple comparisons test. $^*P < 0.05$, $^{**}P < 0.01$.

Supplementary Figure 2 | Comparing the number of positive epitopes in patients with chronic HBV infection in different subpartitions.

Supplementary Figure 3 | General recognition of linear B-cell epitopes on C and P proteins. **(A)** The recognition rate of the selected peptide on C and P proteins in patients with chronic HBV infection. **(B)** Positive peptide coverage on C and P. **(C)** Comparison of the number of positive epitopes on the C or P protein in patients with chronic HBV infection. **(B)** Chi-square test. **(C)** Mann–Whitney *U* test. $^*P < 0.05$.

Supplementary Figure 4 | The proportion of patients with different treatment responses in the S1+/- or S9+/- groups. Chi-square test. $^*P < 0.05$.

REFERENCES

1. Polaris Observatory Collaborators. Global Prevalence, Treatment, and Prevention of Hepatitis B Virus Infection in 2016: A Modelling Study. *Lancet Gastroenterol Hepatol* (2018) 3:383–403. doi: 10.1016/s2468-1253(18)30056-6
2. European Association for the Study of the Liver. EASL 2017 Clinical Practice Guidelines on the Management of Hepatitis B Virus Infection. *J Hepatol* (2017) 67:370–98. doi: 10.1016/j.jhep.2017.03.021
3. Fanning GC, Zoulim F, Hou J, Bertoletti A. Therapeutic Strategies for Hepatitis B Virus Infection: Towards a Cure. *Nat Rev Drug Discov* (2019) 18:827–44. doi: 10.1038/s41573-019-0037-0
4. Gerlich WH. Medical Virology of Hepatitis B: How it Began and Where We are Now. *Virol J* (2013) 10:239. doi: 10.1186/1743-422X-10-239
5. Hoofnagle JH, Gerety RJ, Barker LF. Antibody to Hepatitis-B-Virus Core in Man. *Lancet* (1973) 2:869–73. doi: 10.1016/s0140-6736(73)92004-7
6. Farci P, Diaz G, Chen Z, Govindarajan S, Tice A, Agulto L, et al. B Cell Gene Signature With Massive Intrahepatic Production of Antibodies to Hepatitis B Core Antigen in Hepatitis B Virus-Associated Acute Liver Failure. *Proc Natl Acad Sci USA* (2010) 107:8766–71. doi: 10.1073/pnas.1003854107
7. Hu S, Xiong H, Kang X, Wang S, Zhang T, Yuan Q, et al. Preparation and Functional Evaluation of Monoclonal Antibodies Targeting Hepatitis B Virus Polymerase. *Virulence* (2021) 12:188–94. doi: 10.1080/21505594.2020.1869391
8. Urban S, Bartenschlager R, Kubitz R, Zoulim F. Strategies to Inhibit Entry of HBV and HDV Into Hepatocytes. *Gastroenterology* (2014) 147:48–64. doi: 10.1053/j.gastro.2014.04.030
9. Hehle V, Beretta M, Bourgine M, Ait-Goughoulte M, Planchais C, Morisse S, et al. Potent Human Broadly Neutralizing Antibodies to Hepatitis B Virus From Natural Controllers. *J Exp Med* (2020) 217:e20200840. doi: 10.1084/jem.20200840
10. Zhang TY, Yuan Q, Zhao JH, Zhang YL, Yuan LZ, Lan Y, et al. Prolonged Suppression of HBV in Mice by a Novel Antibody That Targets a Unique Epitope on Hepatitis B Surface Antigen. *Gut* (2016) 65:658–71. doi: 10.1136/gutjnl-2014-308964
11. Zhang TY, Guo XR, Wu YT, Kang XZ, Zheng QB, Qi RY, et al. A Unique B Cell Epitope-Based Particulate Vaccine Shows Effective Suppression of Hepatitis B Surface Antigen in Mice. *Gut* (2020) 69:343–54. doi: 10.1136/gutjnl-2018-317725
12. Wang Q, Michailidis E, Yu Y, Wang Z, Hurley AM, Oren DA, et al. A Combination of Human Broadly Neutralizing Antibodies Against Hepatitis B Virus HBsAg With Distinct Epitopes Suppresses Escape Mutations. *Cell Host Microbe* (2020) 28:335–49.e6. doi: 10.1016/j.chom.2020.05.010
13. Boni C, Janssen HLA, Rossi M, Yoon SK, Vecchi A, Barili V, et al. Combined GS-4774 and Tenofovir Therapy Can Improve HBV-Specific T-Cell Responses in Patients With Chronic Hepatitis. *Gastroenterology* (2019) 157:227–41.e7. doi: 10.1053/j.gastro.2019.03.044
14. Shin EC, Sung PS, Park SH. Immune Responses and Immunopathology in Acute and Chronic Viral Hepatitis. *Nat Rev Immunol* (2016) 16:509–23. doi: 10.1038/nri.2016.69
15. Tsai KN, Kuo CF, Ou JJ. Mechanisms of Hepatitis B Virus Persistence. *Trends Microbiol* (2018) 26:33–42. doi: 10.1016/j.tim.2017.07.006
16. Fisicaro P, Barili V, Rossi M, Montali I, Vecchi A, Acerbi G, et al. Pathogenetic Mechanisms of T Cell Dysfunction in Chronic HBV Infection and Related Therapeutic Approaches. *Front Immunol* (2020) 11:849. doi: 10.3389/fimmu.2020.00849
17. Kim JH, Ghosh A, Ayithan N, Romani S, Khanam A, Park JJ, et al. Circulating Serum HBsAg Level is a Biomarker for HBV-Specific T and B Cell Responses in Chronic Hepatitis B Patients. *Sci Rep* (2020) 10:1835. doi: 10.1038/s41598-020-58870-2
18. Kim GA, Lim YS, An J, Lee D, Shim JH, Kim KM, et al. HBsAg Seroclearance After Nucleoside Analogue Therapy in Patients With Chronic Hepatitis B: Clinical Outcomes and Durability. *Gut* (2014) 63:1325–32. doi: 10.1136/gutjnl-2013-305517
19. Yip TC, Wong GL, Chan HL, Tse YK, Lam KL, Lui GC, et al. HBsAg Seroclearance Further Reduces Hepatocellular Carcinoma Risk After Complete Viral Suppression With Nucleos(T)Ide Analogues. *J Hepatol* (2019) 70:361–70. doi: 10.1016/j.jhep.2018.10.014
20. Wu S, Luo W, Wu Y, Chen H, Peng J. HBsAg Quantification Predicts Off-Treatment Response to Interferon in Chronic Hepatitis B Patients: A Retrospective Study of 250 Cases. *BMC Gastroenterol* (2020) 20:121. doi: 10.1186/s12876-020-01263-6
21. Ma SW, Huang X, Li YY, Tang LB, Sun XF, Jiang XT, et al. High Serum IL-21 Levels After 12 Weeks of Antiviral Therapy Predict HBeAg Seroconversion in Chronic Hepatitis B. *J Hepatol* (2012) 56:775–81. doi: 10.1016/j.jhep.2011.10.020
22. Lu Y, Li Z, Teng H, Xu H, Qi S, He J, et al. Chimeric Peptide Constructs Comprising Linear B-Cell Epitopes: Application to the Serodiagnosis of Infectious Diseases. *Sci Rep* (2015) 5:13364. doi: 10.1038/srep13364
23. Xue Q, Xu H, Liu H, Pan J, Yang J, Sun M, et al. Epitope-Containing Short Peptides Capture Distinct IgG Serodynamics That Enable Differentiating Infected From Vaccinated Animals for Live-Attenuated Vaccines. *J Virol* (2020) 94:e01573–19. doi: 10.1128/JVI.01573-19
24. Wang W, Sun L, Li T, Ma Y, Li J, Liu Y, et al. A Human Monoclonal Antibody Against Small Envelope Protein of Hepatitis B Virus With Potent Neutralization Effect. *mAbs* (2015) 8:468–77. doi: 10.1080/19420862.2015.1134409
25. Zhang H, Song Z, Yu H, Zhang X, Xu S, Li Z, et al. Genome-Wide Linear B-Cell Epitopes of Enterovirus 71 in a Hand, Foot and Mouth Disease (HFMD) Population. *J Clin Virol* (2018) 105:41–8. doi: 10.1016/j.jcv.2018.06.001
26. Yi Z, Ling Y, Zhang X, Chen J, Hu K, Wang Y, et al. Functional Mapping of B-Cell Linear Epitopes of SARS-CoV-2 in COVID-19 Convalescent Population. *Emerg Microbes Infect* (2020) 9:1988–96. doi: 10.1080/22221751.2020.1815591
27. Mak LY, Seto WK, Fung J, Yuen MF. Use of HBsAg Quantification in the Natural History and Treatment of Chronic Hepatitis B. *Hepatol Int* (2020) 14:35–46. doi: 10.1007/s12072-019-09998-5
28. Hoogeveen RC, Boonstra A. Checkpoint Inhibitors and Therapeutic Vaccines for the Treatment of Chronic HBV Infection. *Front Immunol* (2020) 11:401. doi: 10.3389/fimmu.2020.00401
29. Burton AR, Pallett LJ, McCoy LE, Suveizdyte K, Amin OE, Swadling L, et al. Circulating and Intrahepatic Antiviral B Cells are Defective in Hepatitis B. *J Clin Invest* (2018) 128:4588–603. doi: 10.1172/jci121960
30. Le Bert N, Salimzadeh L, Gill US, Dutertre CA, Facchetti F, Tan A, et al. Comparative Characterization of B Cells Specific for HBV Nucleocapsid and Envelope Proteins in Patients With Chronic Hepatitis B. *J Hepatol* (2020) 72:34–44. doi: 10.1016/j.jhep.2019.07.015
31. Salimzadeh L, Le Bert N, Dutertre CA, Gill US, Newell EW, Frey C, et al. PD-1 Blockade Partially Recovers Dysfunctional Virus-Specific B Cells in Chronic Hepatitis B Infection. *J Clin Invest* (2018) 128:4573–87. doi: 10.1172/jci121957
32. Yato K, Onodera T, Matsuda M, Moriyama S, Fujimoto A, Watashi K, et al. Identification of Two Critical Neutralizing Epitopes in the Receptor Binding Domain of Hepatitis B Virus Pres1. *J Virol* (2020) 95:e01680–20. doi: 10.1128/JVI.01680-20. 10.1128/JVI.01680-20.

33. Chen C, Jiang X, Liu X, Guo L, Wang W, Gu S, et al. Identification of the Association Between HBcAg-Specific T Cell and Viral Control in Chronic HBV Infection Using a Cultured ELISPOT Assay. *J Leukoc Biol* (2021) 109:455–65. doi: 10.1002/JLB.5MA0620-023RR
34. Chen Y, Tian Z. HBV-Induced Immune Imbalance in the Development of HCC. *Front Immunol* (2019) 10:2048. doi: 10.3389/fimmu.2019.02048
35. Kim GA, Lim YS, Han S, Choi J, Shim JH, Kim KM, et al. High Risk of Hepatocellular Carcinoma and Death in Patients With Immune-Tolerant-Phase Chronic Hepatitis B. *Gut* (2018) 67:945–52. doi: 10.1136/gutjnl-2017-314904
36. Kuipery A, Gehring AJ, Isogawa M. Mechanisms of HBV Immune Evasion. *Antiviral Res* (2020) 179:104816. doi: 10.1016/j.antiviral.2020.104816
37. Yan H, Zhong G, Xu G, He W, Jing Z, Gao Z, et al. Sodium Taurocholate Cotransporting Polypeptide is a Functional Receptor for Human Hepatitis B and D Virus. *eLife* (2012) 1:e00049. doi: 10.7554/eLife.00049
38. Bertoletti A, Ferrari C. Adaptive Immunity in HBV Infection. *J Hepatol* (2016) 64:S71–83. doi: 10.1016/j.jhep.2016.01.026

Conflict of Interest: The authors declare that the research was conducted in the absence of any commercial or financial relationships that could be construed as a potential conflict of interest.

frontiers in Immunology

ORIGINAL RESEARCH
published: 27 October 2021
doi: 10.3389/fimmu.2021.710528

Baseline Quantitative Hepatitis B Core Antibody Titer Is a Predictor for Hepatitis B Virus Infection Recurrence After Orthotopic Liver Transplantation

Bin Lou[1,2,3†], Guanghua Ma[1†], Feifei LV[1], Quan Yuan[4], Fanjie Xu[1], Yuejiao Dong[1], Sha Lin[1], Yajun Tan[1], Jie Zhang[1] and Yu Chen[1,2,3]*

[1] Department of Laboratory Medicine, The First Affiliated Hospital, College of Medicine, Zhejiang University, Hangzhou, China, [2] Key Laboratory of Clinical In Vitro Diagnostic Techniques of Zhejiang Province , Hangzhou, China, [3] Institute of Laboratory Medicine, Zhejiang University, Hangzhou, China, [4] National Institute of Diagnostics and Vaccine Development in Infectious Disease, School of Life Science, Xiamen University, Xiamen, China

OPEN ACCESS

Edited by:
Zhongji Meng,
Hubei University of Medicine, China

Reviewed by:
Qian Zhou,
The First Affiliated Hospital of Sun Yat-Sen University, China
Baoju Wang,
Huazhong University of Science and Technology, China

***Correspondence:**
Yu Chen
chenyuzy@zju.edu.cn

[†]These authors have contributed equally to this work

Specialty section:
This article was submitted to Viral Immunology, a section of the journal Frontiers in Immunology

Received: *16 May 2021*
Accepted: *08 October 2021*
Published: *27 October 2021*

Citation:
Lou B, Ma G, LV F, Yuan Q, Xu F, Dong Y, Lin S, Tan Y, Zhang J and Chen Y (2021) Baseline Quantitative Hepatitis B Core Antibody Titer Is a Predictor for Hepatitis B Virus Infection Recurrence After Orthotopic Liver Transplantation. Front. Immunol. 12:710528. doi: 10.3389/fimmu.2021.710528

Objective: Hepatitis B virus (HBV) reinfection is a serious complication that arise in patients who undergo hepatitis B virus related liver transplantation. We aimed to use biomarkers to evaluate the HBV reinfection in patients after orthotopic liver transplantation.

Methods: Seventy-nine patients who underwent liver transplantation between 2009 and 2015 were enrolled, and levels of biomarkers were analyzed at different time points. Cox regression and receiver operating characteristic (ROC) curves of different markers at baseline were used to analyze sustained hepatitis B surface antigen (HBsAg) loss. The Kaplan-Meier method was used to compare the levels of the biomarkers.

Results: Among the 79 patients, 42 sustained HBsAg loss with a median time of 65.2 months (12.0-114.5, IQR 19.5) after liver transplantation and 37 patients exhibited HBsAg recurrence with a median time of 8.8 (0.47-59.53, IQR 19.47) months. In the ROC curve analysis, at baseline, 4.25 $\log_{10}$ IU/mL qHBcAb and 2.82 $\log_{10}$ IU/mL qHBsAg showed the maximum Youden's index values with area under the curves (AUCs) of 0.685and 0.651, respectively. The Kaplan-Meier method indicated that qHBsAg and quantitative antibody against hepatitis B core antigen (qHBcAb) levels in the two groups were significantly different (p = 0.031 and 0.006, respectively). Furthermore, the Cox regression model confirmed the predictive ability of qHBcAb at baseline (AUC = 0.685).

Conclusion: Lower pretransplantation qHBcAb is associated with HBV infection. The baseline concentration of qHBcAb is a promising predictor for the recurrence of HBV in patients undergoing liver transplantation and can be used to guide antiviral treatment for HBV infection.

Keywords: qHBcAb, liver transplantation, HBV recurrence, sustained HBV loss, qHBsAg

INTRODUCTION

Hepatitis B virus (HBV) infection is a global health problem. Chronic hepatitis B (CHB) is a major disease that threatens human health, especially in southeast Asia and Africa. According to clinical statistics, the global prevalence of hepatitis B surface antigen (HBsAg) was 3.9% in 2016, corresponding to 291 million infections (1). Additionally, nearly 25% of chronic HBV carriers develop terminal stage liver-related diseases including chronic hepatitis, cirrhosis, and primary hepatocellular carcinoma, causing 0.8 million deaths annually (2, 3). Liver transplantation (LT) is an established treatment option for serious liver disease caused by HBV infection. The data from the European Liver Transplant Registry database (ELTR) verified that viral hepatitis B was the most common indication (9.8%) of LT from 2007 to 2017 (4). HBV recurrence is a risk factor for patients who have undergone LT and leads to grievous failure of treatment and poor prognosis (5, 6). The HBV reinfection rate was higher than 90% (7) and the 2-year survival rate was only 50% (8) before the application of immune globulin and antiviral drugs. In recent years, the therapeutic strategy of nucleos(t)ide analogs (NAs) combined with immune globulin has proven useful in preventing HBV reinfection after LT (9, 10). However, this strategy does not completely protect against future recurrence of HBV infection. HBV reinfection is not only dependent on residual viral infection in extrahepatic organs, but also individual immune responses. Therefore, it is necessary to find satisfactory biomarkers that reflect specific immune responses to HBV to predict the recurrence of HBsAg.

Antibody against hepatitis B core antigen (HBcAb) is a widespread biomarker in patients with HBV infection and can be present in current or previous infections. Routine serum screening for HBcAb and other HBV-related biomarkers has been performed in some countries with a high HBV infection rate. Nevertheless, for some patients, HBcAb may be the only serological marker of HBV infection in serum (11, 12), and "HBcAb only" status may reflect occult HBV infection (13). Additionally, HBcAb alone can be used to evaluate the risk for HBV reactivation in patients who have received antiviral treatment that may lead to immunosuppression, patients with human immunodeficiency virus (HIV) infection or chronic hepatitis C virus (HCV) infection (14, 15).

One study revealed that HBcAb plays a valuable role in CHB disease by inhibiting or clearing HBV (16). Thus, patients with a high titer of HBcAb before therapy had a stronger acquired immune response that was related to a satisfactory outcome after antiviral treatment (17).

Owing to the inferior performance of the competitive immunoassay, current commercially available HBcAb assays have a narrow linearity range. A novel immunoassay for qualitative HBcAb based on the double-antigen sandwich enzyme-linked immunosorbent assay method has demonstrated sensitivity and specificity (18).

In this retrospective longitudinal study, we aimed to analyze the clinical value of qHBcAb, qHBsAg and other viral marker concentrations, focusing on the outcome of patients who underwent LT.

MATERIALS AND METHODS

Patients

Overall, 363 patients who underwent HBV-related LT between 2009 and 2015 at the First Affiliated Hospital, College of Medicine, Zhejiang University were enrolled in this study. The patients selected were also negative for HCV infection, HIV infection, and other chronic diseases. Serum samples were collected and stored at -80°C until use. This study was reviewed and approved by the Ethics Committees of the First Affiliated Hospital, College of Medicine, Zhejiang University. This study followed the 1964 Helsinki Declaration and its later amendments. Prior informed consent was obtained from the enrolled patients or their legal guardians.

Post-Transplant Therapy

Antiviral prophylaxis was administered to all recipients, and they were treated with NAs in combination with low-dose hepatitis B immunoglobulin (HBIG). Briefly, 2000 IU HBIG was intravenously injected during the anhepatic phase, followed by 800 IU daily intramuscular administration for the first week and then weekly for 3 weeks, and monthly thereafter.

All patients received a Tacrolimus based steroid-sparing or steroid-free immunosuppression regimen. Tacrolimus and mycophenolate mofetil (750 mg every 12 h) were administered from the first post-operative day. The target blood trough level of tacrolimus was 7-10 ng/mL for the first postoperative month and was aimed at 5-7 ng/mL thereafter.

Measurement of qHBcAb Concentration in Serum

The qHBcAb level in serum was measured using a newly developed double-sandwich immunoassay (100–100 000 IU/mL; Wantai, China), calibrated using the World Health Organization standard (NIBSC, UK) (19, 20). QHBcAb was measured at baseline, with the sought time of HBsAg-positive status before LT being at least two weeks, and then at different time points after LT.

Measurement of qHBsAg, qHBeAg, HBcAb and HBV DNA Concentrations in the Serum

Serum levels of qHBsAg, qHBeAg and HBcAb were measured using a chemiluminescence microparticle immunoassay (CMIA) on an Abbott Architect I4000 automated analyzer (Abbott Laboratories, Chicago, IL, USA). HBV DNA levels in serum were measured using Qiagen PCR kits (Hilden, Germany) on ABI 7500 qRT-PCR System (ABI Laboratories, USA) according to the manufacturer's instructions. The linear detection range was 3 - 7 $\log_{10}$ IU/mL, with a correlation coefficient of the standard curve >0.995. Biomarkers were measured before LT and at different time points after LT.

Statistical Analysis

Chi–squared and Mann–Whitney U tests were performed as appropriate. The accuracy of serum qHBcAb and qHBsAg levels

predicting HBsAg recurrence was determined by applying the receiver operating characteristic (ROC) curve analysis. HBV reinfection was assessed using Kaplan-Meier survival analysis. The risk of HBV reinfection after LT was determined using the Cox regression model. Statistical significance was set at $p < 0.05$. Statistical analysis and presentation were performed using SPSS software (version 23.0; SPSS, Chicago, IL, USA). Graphical analysis and data presentation were performed using GraphPad Prism version 5.0 and R version 4.0 (R Foundation).

RESULTS

Characteristics of Patients

A total of 363 patients were enrolled in this study, 79 patients were selected retrospectively, and 284 patients were excluded including 44 patients with HBsAg-negative status, 53 patients with underlying diseases or other infectious diseases, 18 patients receiving an HBV-positive graft, 17 patients who died post LT, 5 patients who underwent retransplantation and 147 patients without sufficient serum samples or integrated follow-up time points (**Supplementary Figure 1**). Among the 79 enrolled patients, 37 exhibited HBsAg recurrence with a median time of 8.8 (0.47 - 59.53, IQR 19.47) months, and 42 sustained HBsAg loss with a median follow-up time of 65.2 months (12.0 - 114.5, IQR 19.5) after LT.

The clinical characteristics of patients at baseline are shown in **Table 1** for patients who retained sustained HBsAg loss or achieved HBsAg recurrence during the follow-up period. There were no significant differences in sex, age and treatment received between the two groups ($p = 0.672$, 0.089 and 0.515, respectively). The characteristics of qHBcAb and qHBsAg were significantly different between the groups ($p = 0.037$ and 0.023, respectively). Compared with HBcAb measured by Abbott Architect CMIA (indirect method), the difference in qHBcAb measured by double-sandwich immunoassay was more significant between the observed groups ($p = 0.023$ vs 0.743). The titers of HBV DNA, qHBeAg, alanine aminotransferase (ALT) and aspartate aminotransferase (AST) were not significantly different among the compared groups ($p = 0.394$, 0.732, 0.453 and 0.146, respectively).

Kinetics of qHBcAb and qHBsAg in HBsAg Recurrence and Sustained HBsAg Loss Groups

As shown in **Figure 1**, during baseline to 1 week after LT, both qHBsAg and qHBcAb were significantly decreased in both sustained HBsAg loss group and HBsAg recurrence group ($p < 0.001$ and $p < 0.05$). However, the changes in qHBcAb and qHBsAg in the two groups were not significantly different after 1 week. At each time point between baseline and 24 weeks after LT, the titer of qHBcAb in the sustained HBsAg loss group was higher than that in the HBsAg recurrence group.

Comparison of Potential Risk Factors at Baseline Using the Cox Regression Model

To further evaluate the potential risk factors associated with HBV recurrence after LT, Cox regression analysis was performed for age, sex, ALT, HBV DNA, qHBsAg, qHBeAg and qHBcAb. As shown in **Table 2** and **Supplementary Figure 2**, the qHBcAb level at baseline was a strong predictor for HBsAg recurrence after LT, with both the univariate and multivariate analyses (crude HR: 0.40; 95% CI: 0.20-0.78; $p = 0.01$ vs adjusted HR 0.42; 95% CI: 0.19-0.94; $p = 0.04$).

TABLE 1 | Characteristics of enrolled patients at baseline.

Characteristics	HBsAg recurrence in follow-up time (n = 37)	Sustained HBsAg loss after LT (n = 42)	*p*
Male, n (%)	33 (89%)	37 (88%)	*0.672*[a]
Age (years) at baseline before liver transformation, median (range)	54 (28 - 67)	48 (29 - 66)	*0.089*[b]
Treatment received			*0.515*[a]
LAM/HBIG	17 (45.95%)	22 (52.38%)	
ADV/LAM/HBIG	10 (27.03%)	8 (19.05%)	
ETV/HBIG	6 (16.22%)	4 (9.52%)	
ETV/LAM/HBIG	4 (10.81%)	8 (19.05%)	
HBV related disease before LT			*0.293*[a]
HCC	22 (59.46%)	20 (47.62%)	
Non-HCC	15 (40.54%)	22 (52.38%)	
qHBsAg (log_{10} IU/mL), median (range)	2.80 (-0.31 - 3.95)	2.34 (-0.89 - 4.22)	*0.037*[c]*
qHBeAg (log_{10} 0.18 PEIU/mL), median (range)	-0.36 (0-1.57)	-0.39 (0-1.46)	*0.732*[c]
HBcAb (S/CO)	10.38 (0.22 - 47.27)	10.73 (1.88 - 14.16)	*0.743*[c]
qHBcAb (log_{10} IU/mL), median (range)	3.51 (1.06 - 4.85)	4.01 (2.12 - 5.12)	*0.023*[c]*
HBV DNA (positive%)	12 (32.43%)	10 (23.81%)	*0.394*[a]
ALT (IU/mL), median (range)	39 (14 - 1149)	43 (17 - 221)	*0.453*[c]
AST (IU/mL), median (range)	59 (22 - 1535)	53 (21 - 355)	*0.146*[c]

LAM, lamivudine; ADV, adefovir; ETV, entecavir; HBIG, hepatitis B immunoglobulin; ALT, alanine aminotransferase; AST, aspartate aminotransferase; HCC, hepatocellular carcinoma.
*[a]Chi-Square test. [b]Independent samples t test. [c]Mann-Whitney U test. *p < 0.05.*

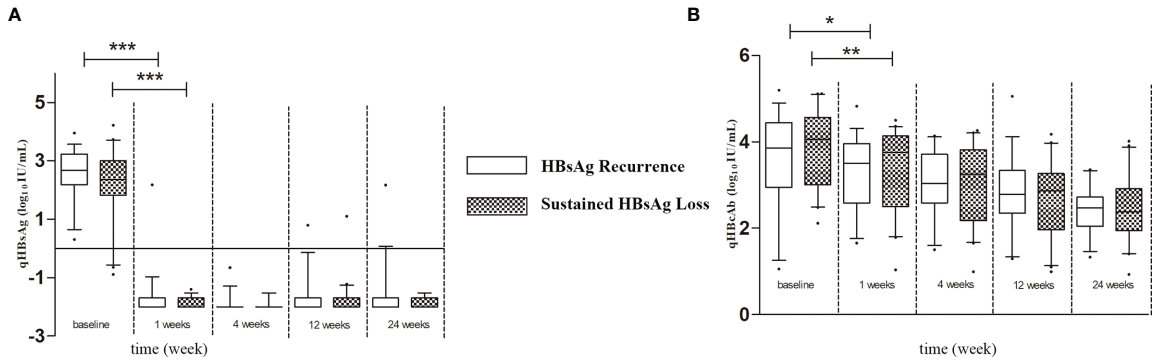

FIGURE 1 | **(A)** The Kinetics of qHBsAg in HBsAg recurrence and sustained HBsAg loss groups. **(B)** The Kinetics of qHBcAb in HBsAg recurrence and sustained HBsAg loss groups. Box plots showing the median, interquartile range and absolute range of qHBcAb and qHBsAg at baseline and at 1 week, 4 weeks, 12 weeks and 24 weeks in groups (blank box plots: HBsAg recurrence group; latticed box: sustained HBsAg loss group. *p<0.05; **p<0.01; ***p<0.001).

TABLE 2 | Risk factors for HBV recurrence after liver transplantation.

Variable	Univariate analysis				Multivariate analysis			
	B	SE	*p*	Crude HR	B	SE	*p*	Adjusted HR
qHBsAg[a,d]	0.70	0.33	0.03*	2.01 (1.05-3.86)	0.59	0.37	0.11	1.80 (0.87-3.72)
qHBcAb[b,d]	-0.92	0.35	0.01*	0.40 (0.20-0.78)	-0.87	0.41	0.04*	0.42 (0.19-0.94)
Age[e]	0.03	0.02	0.07	1.03 (1.00-1.06)	0.02	0.02	0.35	1.02 (0.98-1.05)
Sex[c]	0.13	0.42	0.76	1.13 (0.50-2.59)	-0.37	0.47	0.44	0.69 (0.28-1.74)
ALT[e]	0.00	0.00	0.18	1.00 (1.00-1.01)	0.00	0.00	0.83	0.99 (0.98-1.00)
AST[e]	0.00	0.00	0.09	1.00 (1.00-1.01)	0.00	0.00	0.17	1.00 (0.99-1.02)
HBV DNA[c,d]	0.26	0.35	0.47	1.29 (0.65-2.57)	0.59	0.43	0.17	1.79 (0.77-4.23)
qHBeAg[e]	0.02	0.02	0.38	1.02 (0.97-1.07)	0.01	0.02	0.77	1.01 (0.96-1.06)

The variables included in the Cox regression analysis were age, sex (female vs male), and baseline ALT, HBV DNA, qHBsAg, qHBeAg and qHBcAb levels.
*[a]qHBsAg ≤ 2.82 vs > 2.82 log10 IU/mL, [b]HBcAb < 4.25 vs ≥ 4.25 log10 IU/mL, [c]HBV DNA ≤ 3.0 vs > 3.0 log10 IU/mL, [d]Categorical variable, [e]Continuous variable, *p < 0.05.*

QHBcAb and qHBsAg as Predictors of HBsAg Recurrence

The ability of qHBcAb and qHBsAg at baseline to predict HBsAg recurrence was analyzed using ROC curves to compare HBsAg recurrence and sustained HBsAg loss groups (**Figures 2A, C**). The area under the curves (AUCs) of qHBcAb and qHBsAg were 0.685 (95% confidence interval, 0.577 - 0.799) and 0.651 (95% confidence interval, 0.538 - 0.763), respectively. Using the Youden index (**Figures 2B, D**), we predicted that when qHBcAb was higher than 4.25 $\log_{10}$ IU/mL and qHBsAg was lower than 2.82 $\log_{10}$ IU/mL, sustained HBsAg loss would occur more readily after LT.

Combined qHBcAb With qHBsAg as Predictors of HBsAg Recurrence

As shown in **Figure 3**, the combination of qHBsAg and qHBcAb was a stronger predictor of HBsAg recurrence than individual biomarkers at baseline. The cutoff values of 1.81 log10 IU/mL and 3.68 log10 IU/mL at baseline for qHBsAg and qHBcAb, respectively, had sensitivity of 72.0%, specificity of 62.2%, PPV of 72.0% and NPV 62.2%, with an AUC value of 0.727 (0.621, 0.833; 95% CI) (**Supplementary Table 1**).

Comparison of qHBcAb and qHBsAg at Baseline Using Kaplan-Meier Method

Figures 4A, B show the comparison of HBsAg recurrence rates at the time of the last follow-up by Kaplan-Meier method. Patients who experienced high a risk of HBsAg recurrence had lower qHBcAb (qHBcAb < 4.25 $\log_{10}$ IU/mL) and higher qHBsAg (qHBsAg > 2.82 $\log_{10}$ IU/mL) levels than those who achieved sustained HBsAg loss (p = 0.006 and 0.031, respectively) (**Figure 4**).

DISCUSSION

HBV infection is associated with progression to hepatocellular carcinoma or other end-stage liver diseases, and LT is the only curative therapeutic method (21). However, increased liver transplantation failure rate and decreased patient survival rate in these patients are correlated with HBV reinfection and recurrence of hepatocellular carcinoma (22). HBIG and antiviral treatments are administered alone or in combination to prevent reinfection with HBV after LT (23). HBIG and nucleos(t)ide analogs can prevent reinfection with HBV

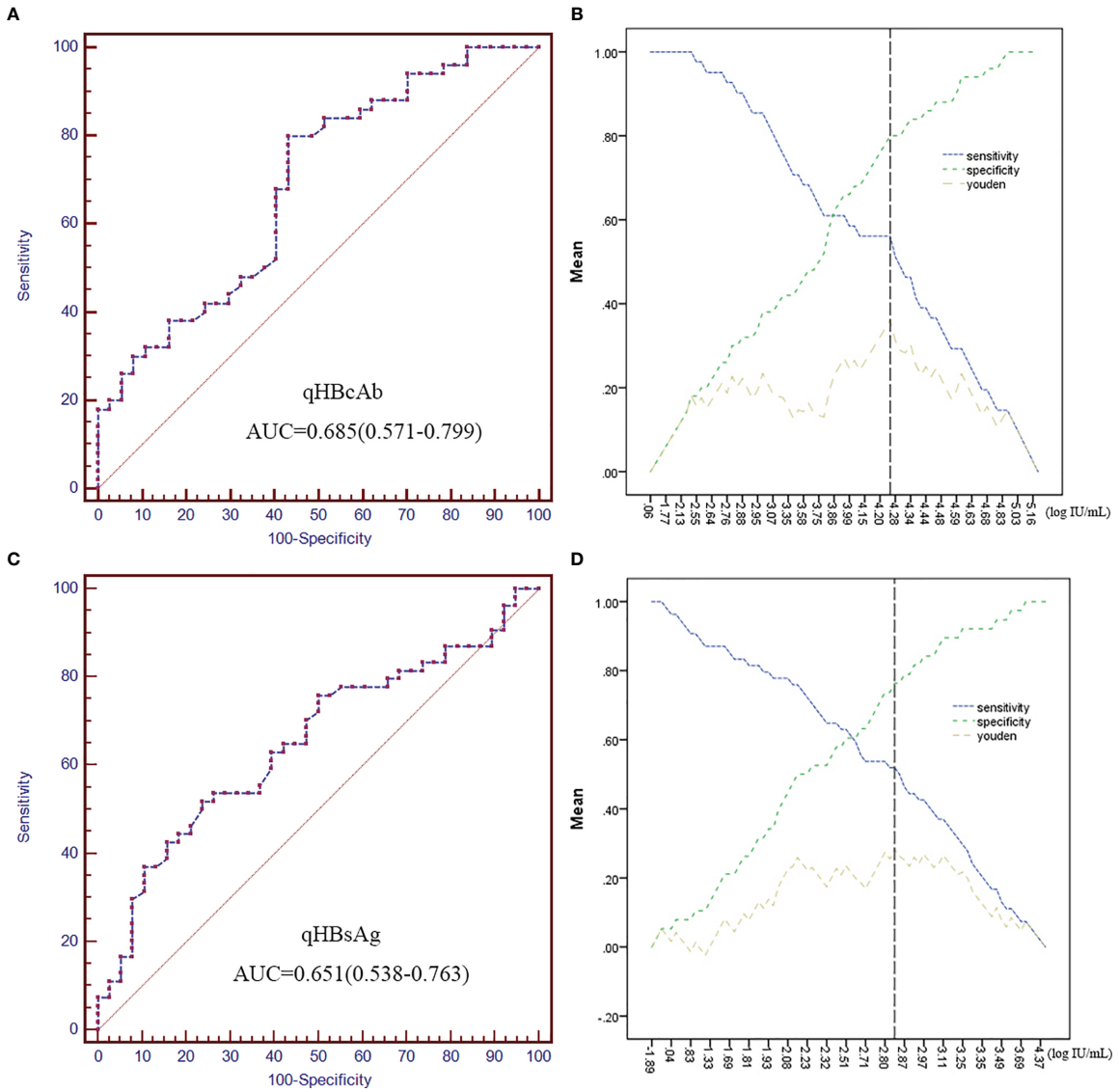

FIGURE 2 | QHBcAb and qHBsAg as predictors of HBsAg recurrence. **(A, C)**. Receiver operating characteristic (ROC) analyses of qHBcAb and qHBsAg as predictors of HBsAg recurrence at baseline. **(B, D)**. Curves of the specificity, sensitivity and Youden index for qHBcAb and qHBsAg. The position of the black vertical dotted line shows the maximum Youden index that was used to predict HBsAg recurrence.

through different mechanisms. HBIG eliminates circulating virus particles and induces antiviral and immune-mediated functions (24), while nucleos(t)ide analogs directly inhibit the process of viral reverse transcription, thus reducing viral load (25). The treatment of such patients aims to increase the "sustained HBsAg loss" rate during the period of follow-up. The HBV reinfection rate in patients post-LT was approximately 10% after they received combined prophylactic treatment with HBIG and NAs (26).

A newly developed assay based on double-sandwich immunoassay technology to measure qHBcAb showed higher sensitivity and specificity than those based on competitive/inhibitory principles (19, 27). Several studies have focused on the use of qHBcAb to evaluate the antiviral therapeutic effect in patients with CHB disease. Yuan et al. revealed that qHBcAb was closely correlated with hepatic inflammatory activities and can serve as a new marker of antiviral treatment response in CHB patients (17, 28). However, the measurement of qHBcAb to determine the risk of HBsAg recurrence after LT has not been reported. This study aimed to analyze qHBcAb and other serological viral markers to identify the predictors of HBsAg recurrence after LT.

Here, ROC curve was used to predict HBsAg recurrence, we found that qHBcAb was a stronger predictor than qHBsAg of HBsAg recurrence after LT due to its larger AUC value. In addition, Cox regression analysis was performed to identify the

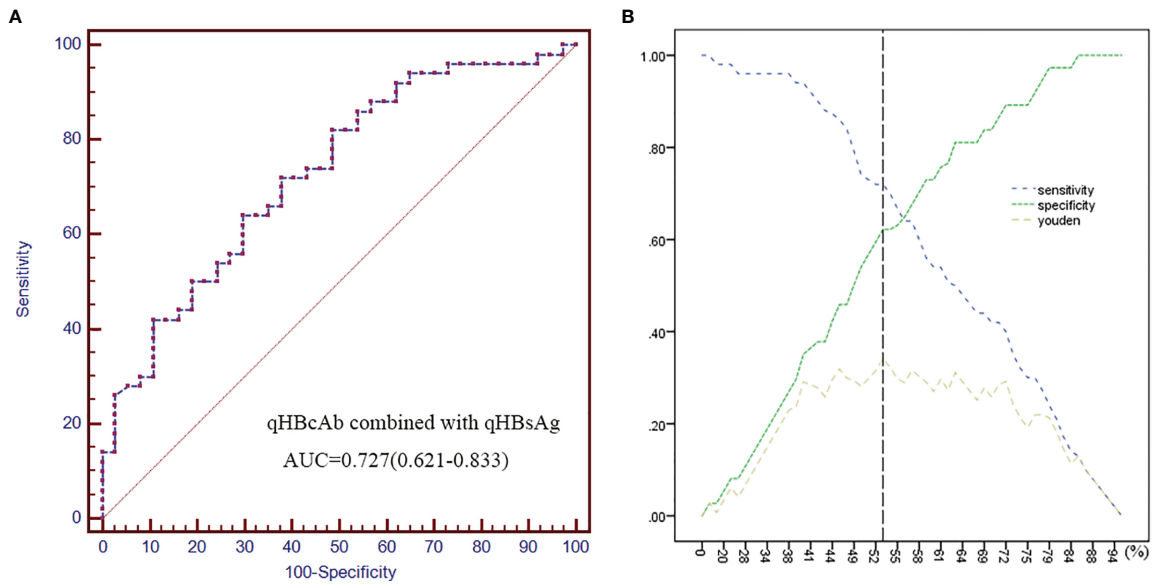

FIGURE 3 | Combined qHBcAb with qHBsAg as predictors of HBsAg recurrence. **(A)** The ROC curve of combined qHBcAb and qHBsAg at baseline. **(B)** Curves of the specificity, sensitivity and Youden index. The position of the black vertical dotted line shows the maximum Youden index that was used to predict HBsAg recurrence.

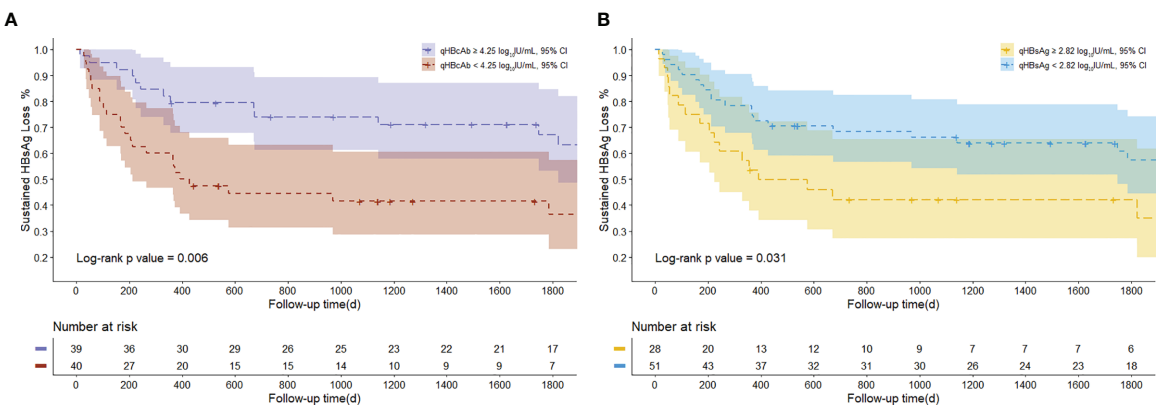

FIGURE 4 | The Kaplan-Meier curve of HBsAg conversion rates at the last time of follow-up. **(A)** The proportion of patients with sustained HBsAg loss according to qHBcAb at baseline. **(B)** The proportion of patients with sustained HBsAg loss according to qHBsAg at baseline.

potential risk factors for HBsAg recurrence after LT; qHBcAb and qHBsAg levels at baseline had more satisfactory HR scores than other markers, confirming the predictive ability of qHBcAb and qHBsAg for HBsAg recurrence after LT.

Furthermore, on the basis of cutoff values obtained from the ROC analysis at baseline, we used the different ranges of qHBcAb and qHBsAg levels to evaluate the sustained HBsAg loss rate by Kaplan-Meier analysis. We found that low qHBcAb and high qHBsAg levels were associated with HBV reinfection.

Circulating HBsAg correlates with the presence of covalently closed circular DNA (cccDNA) (29), and is a key marker of infection, a high HBsAg level indicates a high hepatitis B viral load *in vivo*. Therefore, patients with high serum qHBsAg titers are associated with high a probability of HBsAg recurrence after LT. However, the mechanism underlying the predictive value of HBcAb titer remains unclear. Chan et al. revealed that hepatitis B core antigen (HBcAg), a viral nucleocapsid protein, is the most immunogenic component of HBV (30). Zgair et al. demonstrated that HBcAb plays an important role in inhibiting HBV through the hepatocytotoxic effect of anti-HBc-secreting B cells (16). Thus, a high qHBcAb level can represent a strong immune response to HBV and may be the reason for sustained HBsAg loss in patients with a high titer of qHBcAb at baseline.

In this study, some novel results were obtained in LT patients from baseline to the last follow-up period, and a higher qHBcAb level before LT corresponded with sustained HBsAg loss. These conclusions may be meaningful for adjusting the duration of antiviral medicine usage after LT in patients with different qHBcAb and qHBsAg levels. However, this study has some limitations. First, the results were based on a small sample size, possibly limiting the accuracy of results. Second, related data on HBV genotype and mutation were not acquired; this may play potential roles during treatment (31–33). Third, the markers mentioned in this study were only serum markers, while other immunological markers and liver tissues were not analyzed. In summary, this is the first study to describe qHBcAb as a marker to predict the treatment response of LT patients. The measurement of qHBcAb could potentially assist surgeons in identifying patients who might benefit from specific antiviral treatments after LT.

DATA AVAILABILITY STATEMENT

The original contributions presented in the study are included in the article/**Supplementary Material**. Further inquiries can be directed to the corresponding author.

ETHICS STATEMENT

The studies involving human participants were reviewed and approved by Ethics Committees of the First Affiliated Hospital, College of Medicine, Zhejiang University and 1964 Helsinki declaration and its later amendments. The patients/participants provided their written informed consent to participate in this study.

AUTHOR CONTRIBUTIONS

YC and QY planned and designed the study. BL and GM performed the experiments and wrote the paper. FL and FX performed serum qHBsAg, qHBeAg, HBcAb, and HBV DNA measurement experiments. YD, YT, and JZ performed the serum qHBcAb measurement. All authors contributed to the article and approved the submitted version.

FUNDING

This work was supported by the National 863 Program for the Biological and medical technology (no. 2011AA02A100) and the National Key Programs for Infectious Diseases of China (no. 2012ZX10002005).

SUPPLEMENTARY MATERIAL

The Supplementary Material for this article can be found online at: https://www.frontiersin.org/articles/10.3389/fimmu.2021.710528/full#supplementary-material

REFERENCES

1. Polaris Observatory Collaborators. Global Prevalence, Treatment, and Prevention of Hepatitis B Virus Infection in 2016: A Modelling Study. *Lancet Gastroenterol Hepatol* (2018) 3(6):383–403. doi: 10.1016/S2468-1253(18)30056-6
2. Urabe A, Imamura M, Tsuge M, Kan H, Fujino H, Fukuhara T, et al. The Relationship Between HBcrAg and HBV Reinfection in HBV Related Post-Liver Transplantation Patients. *J Gastroenterol* (2016) 52:366–75. doi: 10.1007/s00535-016-1240-y
3. McNaughton AL, D'Arienzo V, Ansari MA, Lumley SF, Littlejohn M, Revill P, et al. Insights From Deep Sequencing of the HBV Genome-Unique, Tiny, and Misunderstood. *Gastroenterology* (2019) 156(2):384–99. doi: 10.1053/j.gastro.2018.07.058
4. Belli LS, Perricone G, Adam R, Cortesi PA, Strazzabosco M, Facchetti R, et al. Impact of DAAs on Liver Transplantation: Major Effects on the Evolution of Indications and Results. An ELITA Study Based on the ELTR Registry. *J Hepatol* (2018) 69(4):810–7. doi: 10.1016/j.jhep.2018.06.010
5. Xi ZF, Xia Q. Recent Advances in Prevention of Hepatitis B Recurrence After Liver Transplantation. *World J Gastroenterol* (2015) 21(3):829–35. doi: 10.3748/wjg.v21.i3.829
6. Chauhan R, Lingala S, Gadiparthi C, Lahiri N, Mohanty SR, Wu J, et al. Reactivation of Hepatitis B After Liver Transplantation: Current Knowledge, Molecular Mechanisms and Implications in Management. *World J Hepatol* (2018) 10(3):352–70. doi: 10.4254/wjh.v10.i3.352
7. Karliova M, Malago M, Trippler M, Valentin-Gamazo C, Rothaar T, Broelsch CE, et al. Seroconversion in Patients With Acute Hepatitis B Reinfection After Liver Transplantation With a Combined Treatment of Lamivudine and Hepatitis B Immune Globulin. *Transplant Proc* (2002) 34(8):3319–22. doi: 10.1016/S0041-1345(02)03558-3
8. Starzl TE, Demetris AJ, Van Thiel D. Liver Transplantation. *N Engl J Med* (1989) 321(16):1092–9. doi: 10.1056/NEJM198910193211606
9. Angus PW, Patterson SJ, Strasser SI, Valentin-Gamazo C, Rothaar T, Broelsch CE. A Randomized Study of Adefovir Dipivoxil in Place of HBIG in Combination With Lamivudine as Post-Liver Transplantation Hepatitis B Prophylaxis. *Hepatology* (2008) 48(5):1460–6. doi: 10.1002/hep.22524
10. Steinmuller T, Seehofer D, Rayes N, Müller AR, Settmacher U, Jonas S, et al. Increasing Applicability of Liver Transplantation for Patients With Hepatitis B-Related Liver Disease. *Hepatology* (2002) 35(6):1528–35. doi: 10.1053/jhep.2002.33681
11. Grob P, Jilg W, Bornhak H, Gerken G, Gerlich W, Günther S, et al. Serological Pattern "Anti-HBc Alone": Report on a Workshop. *J Med Virol* (2000) 62(4):450–5. doi: 10.1002/1096-9071(200012)62:4<450::AID-JMV9>3.0.CO;2-Y
12. Weber B, Melchior W, Gehrke R, Doerr HW, Berger A, Rabenau H. Hepatitis B Virus Markers in Anti-HBc Only Positive Individuals. *J Med Virol* (2001) 64(3):312–9. doi: 10.1002/jmv.1052
13. Vitale F, Tramuto F, Orlando A, Vizzini G, Meli V, Cerame G, et al. Can the Serological Status of Anti-HBc Alone Be Considered a Sentinel Marker for Detection of Occult HBV Infection? *J Med Virol* (2008) 80:577–82. doi: 10.1002/jmv.21121
14. Pérez-Rodríguez MT, Sopeña B, Crespo M, Rivera A, González del Blanco T, Ocampo A, et al. Clinical Significance of "Anti-HBc Alone" in Human Immunodeficiency Virus-Positive Patients. *World J Gastroenterol* (2009) 15:1237–41. doi: 10.3748/wjg.15.1237
15. Wedemeyer H, Cornberg M, Tegtmeyer B, Frank H, Tillmann HL, Manns MP, et al. Isolated Anti-HBV Core Phenotype in Anti-HCV-Positive Patients is Associated With Hepatitis C Virus Replication. *Clin Microbiol Infect* (2004) 10(1):70–2. doi: 10.1111/j.1469-0691.2004.00771.x
16. Zgair AK, Ghafil JA, Al-Sayidi RH. Direct Role of Antibody-Secreting B Cells in the Severity of Chronic Hepatitis B. *J Med Virol* (2015) 87(3):407–16. doi: 10.1002/jmv.24067

17. Fan R, Sun J, Yuan Q, Xie Q, Bai X, Ning Q, et al. Baseline Quantitative Hepatitis B Core Antibody Titre Alone Strongly Predicts HBeAg Seroconversion Across Chronic Hepatitis B Patients Treated With Peginterferon or Nucleos(T)Ide Analogues. *Gut* (2016) 65:313–20. doi: 10.1136/gutjnl-2014-308546
18. Li A, Yuan Q, Huang Z, Fan J, Guo R, Lou B, et al. Novel Double-Antigen Sandwich Immunoassay for Human Hepatitis B Core Antibody. *Clin Vaccine Immunol* (2010) 17(3):464–9. doi: 10.1128/CVI.00457-09
19. World Health Organization. *WHO International Standard: First International Standard for Anti-Hepatitis B Core Antigen*. Available at: http://www.nibsc.ac.uk/documents/ifu/95-522.pdf.
20. Song LW, Liu PG, Liu CJ, Zhang TY, Cheng XD, Wu HL, et al. Quantitative Hepatitis B Core Antibody Levels in the Natural History of Hepatitis B Virus Infection. *Clin Microbiol Infect* (2015) 21(2):197–203. doi: 10.1016/j.cmi.2014.10.002
21. Terrault NA, Bzowej NH, Chang KM, Hwang JP, Jonas MM, Murad MH, et al. AASLD Guidelines for Treatment of Chronic Hepatitis B. *Hepatology* (2016) 63:261–83. doi: 10.1002/hep.28156
22. Saab S, Yeganeh M, Nguyen K, Durazo F, Han S, Yersiz H, et al. Recurrence of Hepatocellular Carcinoma and Hepatitis B Reinfection in Hepatitis B Surface Antigen-Positive Patients After Liver Transplantation. *Liver Transplant* (2009) 15(11):1525–34. doi: 10.1002/lt.21882
23. Katz LH, Tur-Kaspa R, Guy DG, Paul M. Lamivudine or Adefovir Dipivoxil Alone or Combined With Immunoglobulin for Preventing Hepatitis B Recurrence After Liver Transplantation. *Cochrane Database Syst Rev* (2010) 7):CD006005. doi: 10.1002/14651858.CD006005.pub2
24. Buti M, Mas A, Prieto M, Casafont F, González A, Miras M, et al. Adherence to Lamivudine After an Early Withdrawal of Hepatitis B Immune Globulin Plays an Important Role in the Long-Term Prevention of Hepatitis B Virus Recurrence. *Transplantation* (2007) 84(5):650–4. doi: 10.1097/01.tp.0000277289.23677.0a
25. Schreibman IR, Schiff ER. Prevention and Treatment of Recurrent Hepatitis B After Liver Transplantation: The Current Role of Nucleoside and Nucleotide Analogues. *Ann Clin Microbiol Antimicrob* (2006) 5:8. doi: 10.1186/1476-0711-5-8
26. Faria LC, Gigou M, Roque-Afonso AM, Sebagh M, Roche B, Fallot G, et al. Hepatocellular Carcinoma Is Associated With an Increased Risk of Hepatitis B Virus Recurrence After Liver Transplantation. *Gastroenterology* (2008) 134 (7):1890–9. doi: 10.1053/j.gastro.2008.02.064
27. Lou B, Fan J, Yuan Q, Yajun T, Li T, Jie Z, et al. Performance Evaluation of Three Different Immunoassays for Detection of Antibodies to Hepatitis B Core. *Clin Chem Lab Med* (2013) 51(2):e23–5.
28. Yuan Q, Song LW, Liu CJ, Li Z, Liu PG, Huang CH, et al. Quantitative Hepatitis B Core Antibody Level may Help Predict Treatment Response in Chronic Hepatitis B Patients. *Gut* (2013) 62:182–4. doi: 10.1136/gutjnl-2012-302656
29. Tout I, Loureiro D, Mansouri A, Soumelis V, Boyer N, Asselah T. Hepatitis B Surface Antigen Seroclearance: Immune Mechanisms, Clinical Impact, Importance for Drug Development. *J Hepatol* (2020) 73(2):409–22. doi: 10.1016/j.jhep.2020.04.013
30. Chan TT, Chan WK, Wong GL, Chan AW, Nik Mustapha NR, Chan SL, et al. Positive Hepatitis B Core Antibody Is Associated With Cirrhosis and Hepatocellular Carcinoma in Nonalcoholic Fatty Liver Disease. *Am J Gastroenterol* (2020) 115(6):867–75. doi: 10.14309/ajg.0000000000000588
31. Brunetto MR, Oliveri F, Colombatto P, Moriconi F, Ciccorossi P, Coco B, et al. Hepatitis B Surface Antigen Serum Levels Help to Distinguish Active From Inactive Hepatitis B Virus Genotype D Carriers. *Gastroenterology* (2010) 139 (2):483–90. doi: 10.1053/j.gastro.2010.04.052
32. Martinot-Peignoux M, Lapalus M, Laouénan C, Lada O, Netto-Cardoso AC, Boyer N, et al. Prediction of Disease Reactivation in Asymptomatic Hepatitis B E Antigen-Negative Chronic Hepatitis B Patients Using Baseline Serum Measurements of HBsAg and HBV-DNA. *J Clin Virol* (2013) 58(2):401–7. doi: 10.1016/j.jcv.2013.08.010
33. Betz-Stablein BD, Töpfer A, Littlejohn M, Yuen L, Colledge D, Sozzi V, et al. Single-Molecule Sequencing Reveals Complex Genome Variation of Hepatitis B Virus During 15 Years of Chronic Infection Following Liver Transplantation. *J Virol* (2016) 90(16):7171–83. doi: 10.1128/JVI.00243-16

Conflict of Interest: The authors declare that the research was conducted in the absence of any commercial or financial relationships that could be construed as a potential conflict of interest.

Publisher's Note: All claims expressed in this article are solely those of the authors and do not necessarily represent those of their affiliated organizations, or those of the publisher, the editors and the reviewers. Any product that may be evaluated in this article, or claim that may be made by its manufacturer, is not guaranteed or endorsed by the publisher.

frontiers in Immunology

REVIEW
published: 29 October 2021
doi: 10.3389/fimmu.2021.766534

In Vivo Mouse Models for Hepatitis B Virus Infection and Their Application

*Yanqin Du[1], Ruth Broering[2], Xiaoran Li[3], Xiaoyong Zhang[3], Jia Liu[4], Dongliang Yang[4] and Mengji Lu[1]**

[1] Institute for Virology, University Hospital Essen, University of Duisburg-Essen, Essen, Germany, [2] Department of Gastroenterology and Hepatology, University Hospital Essen, University of Duisburg-Essen, Essen, Germany, [3] State Key Laboratory of Organ Failure Research, Guangdong Provincial Key Laboratory of Viral Hepatitis Research, Department of Infectious Diseases, Nanfang Hospital, Southern Medical University, Guangzhou, China, [4] Department of Infectious Diseases, Union Hospital, Tongji Medical College, Huazhong University of Science and Technology, Wuhan, China

Despite the availability of effective vaccination, hepatitis B virus (HBV) infection continues to be a major challenge worldwide. Research efforts are ongoing to find an effective cure for the estimated 250 million people chronically infected by HBV in recent years. The exceptionally limited host spectrum of HBV has limited the research progress. Thus, different HBV mouse models have been developed and used for studies on infection, immune responses, pathogenesis, and antiviral therapies. However, these mouse models have great limitations as no spread of HBV infection occurs in the mouse liver and no or only very mild hepatitis is present. Thus, the suitability of these mouse models for a given issue and the interpretation of the results need to be critically assessed. This review summarizes the currently available mouse models for HBV research, including hydrodynamic injection, viral vector-mediated transfection, recombinant covalently closed circular DNA (rc-cccDNA), transgenic, and liver humanized mouse models. We systematically discuss the characteristics of each model, with the main focus on hydrodynamic injection mouse model. The usefulness and limitations of each mouse model are discussed based on the published studies. This review summarizes the facts for considerations of the use and suitability of mouse model in future HBV studies.

Keywords: hydrodynamic injection, viral vector, transgenic mouse, liver humanized mouse, hepatitis B virus

OPEN ACCESS

Edited by:
Hung-Chih Yang,
National Taiwan University, Taiwan

Reviewed by:
Masanori Isogawa,
National Institute of Infectious Diseases (NIID), Japan
Jia-Horng Kao,
National Taiwan University, Taiwan

***Correspondence:**
Mengji Lu
mengji.lu@uni-due.de

Specialty section:
This article was submitted to Viral Immunology, a section of the journal Frontiers in Immunology

Received: *29 August 2021*
Accepted: *14 October 2021*
Published: *29 October 2021*

Citation:
Du Y, Broering R, Li X, Zhang X, Liu J, Yang D and Lu M (2021) In Vivo Mouse Models for Hepatitis B Virus Infection and Their Application. Front. Immunol. 12:766534. doi: 10.3389/fimmu.2021.766534

INTRODUCTION

Hepatitis B virus (HBV) is a prototypical member of the *Hepadnaviridae* family (1). Despite the availability of an effective vaccine, HBV infection remains a global health issue that affects approximately 3.5% of the global population, with around 257 million chronically infected people worldwide (2). These patients have a high risk of developing into end-stage liver diseases such as cirrhosis and hepatocellular carcinoma (HCC). Current treatment options of chronic HBV infection include antiviral cytokine pegylated interferon (IFN) alpha, and the HBV polymerase inhibitors nucleos(t)ide analogues (NAs). However, the available treatment regimens rarely clear HBV in chronically infected patients.

The host spectrum of HBV is very narrow; only few primates such as chimpanzees (3) and Mauritian cynomolgus monkeys (4) are susceptible to HBV infection. Tree shrews (*Tupaia belangeri*)

have also been reported to be susceptible to HBV infection, but it is transient and mild (5). Other members of the *Hepadnaviridae* family, such as duck hepatitis virus and woodchuck hepatitis virus have been used for studies on HBV replication and pathogenesis in their own hosts (6–9). However, such specific virus-host systems are significantly different from the situation in humans with HBV infection (10). Moreover, the lack of essential reagents for studies in these hosts, ethical restrictions, and high costs for animal maintenance and care strongly limit the use of these animal models. Therefore, easy-to-handle HBV models based on laboratory mouse strains are important animal models for HBV research.

HBV mouse models have evolved and greatly improved research progress. In this review, we summarize the currently available mouse models for HBV research, including hydrodynamic injection (HDI), viral vector-mediated transfection, HBV recombinant covalently closed circular DNA (rc-cccDNA), transgenic, and liver humanized mouse models. We systematically discuss the characteristics, usefulness, and limitation for each model.

HDI MOUSE MODEL

HDI is an efficient procedure for delivering genetic materials to the mouse liver. During this procedure, a large volume of liquid containing HBV DNA plasmid is injected through the mouse tail vein by pressure within few seconds. The high pressure permeabilizes the capillary endothelium and generates "pores" in the plasma membrane of surrounding hepatocytes, through which DNA may reach the intracellular space (11). Then the retained HBV plasmid DNA initiates HBV replication by transcription of pregenomic RNA and other HBV mRNAs, followed by the formation of HBV replication intermediates and expression of HBV proteins. The standard procedure of HDI requires injection of liquid equal to 8–10% mouse weight (g) within 5–8 s (12, 13). Different vectors containing replication-competent HBV genomes could be used for this purpose, including an adeno-associated virus/HBV 1.2 plasmid (pAAV/HBV1.2) with a 1.2-fold overlength HBV genotype A genome (13), pcDNA 3.1(+)-HBV1.3C with a 1.3-fold HBV genotype C genome (14), and pSM2 plasmid with a head-to-tail tandem dimeric HBV genome (15).

Factors Influencing HBV Persistence in the HDI Mouse Model

The HDI HBV mouse model can be used to establish transient or persistent HBV replication with HBsAg secretion into the peripheral circulation from 1 week to more than 6 months. HBV persistence in this model is determined by different factors, including the genetic background of mouse strains, age, gender, plasmid backbone, and the dosage of plasmid (**Table 1**). The genetic background plays a key role in HBV exposure outcome. It has been reported that 40–60% C3H/HeH and C57BL/6 mice

TABLE 1 | Factors influence HBV persistence in HDI mouse model.

Authors	Mouse background/ gender/age	Plasmid backbone, dosage	Persistent of HBV antigens or replicative intermediates
Yang et al. (12)	B10.D2 and CB17 NOD/Scid (6-9 weeks)	13.5 μg pT-MCS-HBV1.3 and 4.5 μg pCMV-SB	HBsAg, HBeAg disappeared at 7 dpi; HBcAg 1 dpi (6%), 7 dpi (4%)
Huang et al. (13)	C57BL/6 (male, 6-8 weeks)	10 μg, pAAV/HBV1.2	80% mice HBsAg positive at week 5; 40% HBsAg positive > 6 month; replicative intermediates remained detectable at 22 dpi
	BALB/c (male, 6-8 weeks)	10 μg, pAAV/HBV1.2	HBsAg disappeared from week 2; replicative intermediates decreased from 14 dpi
	C57BL/6 (male, 6-8 weeks)	10 μg, pGEM4Z/HBV1.2,	HBsAg disappeared within 3 weeks
Li et al. (14)	C57BL/6 (male, 6-8 weeks)	15 μg pAAV/HBV1.3, pcDNA3.1(+)-HBV1.3	HBsAg disappeared within 8 weeks after injection of 15 μg pAAV/HBV1.3; 60% mice were HBsAg-positive at week 20 after injection of 15 μg pcDNA3.1(+)-HBV1.3
Li et al. (16)	C57BL/6 (male, 6-8 weeks)	5, 10, or 100 μg pAAV/ HBV1.2	80% mice were HBsAg positive for more than 6 months (5 μg); 40% mice were HBsAg positive for more than 6 months (10 μg); HBsAg was cleared at week 5 (100 μg);
	BALB/c (male, 6-8 weeks)	1 or 5 μg, pAAV/HBV1.2	20% HBsAg positive > 3 month (1μg); 60% HBsAg positive > 3 month (5 μg)
Wang et al. (17)	C57BL/6 (male, 5-6 weeks)	6 or 20 μg, pAAV/ HBV1.2	100% HBsAg positive at 6 wpi (6 μg); HBsAg disappeared at 4 wpi (20 μg);
		6 μg pAAV/HBV1.2 + 14 μg pAAV/control	HBsAg disappeared at 4 wpi
Chou et al. (18)	BALB/cJ, FVB/NJ, NOD/ShiLtJ, 129×1/SvJ (male, 6 weeks)	10 μg pAAV/HBV1.2	HBsAg rapidly disappeared within 4 weeks after injection
	C3H/HeN, C57BL/6, DBA/2J, CBA/caJ (male, 6 weeks)	10 μg pAAV/HBV1.2	40% C57BL/6, 90% C3H/HeN, 75% DBA/2J, 100% CBA/caJ remained HBsAg-poitive at 8 wpi
	C3H/HeN, C57BL/6, DBA/2J, CBA/caJ (male, 12 weeks)	10 μg pAAV/HBV1.2	HBsAg disappeared at 5 wpi in C3H and DBA/2J mice; 12-week-old C57BL/6 mice accelerated HBsAg clearance compared to younger mice
Peng et al. (19)	C3H/HeN (male, 5-6 weeks)	10 μg pAAV/HBV1.2	HBsAg persisted for up to 46 weeks
Yuan et al. (20)	AAVS1 (female and male, 6-8 weeks)	10 μg pAAV/HBV1.2	Male mice express higher levels of HBsAg, HBeAg than female mice
Kosinska et al. (15)	C57BL/6 (female and male, 9-10 weeks)	10 μg pSM2	Male mice express higher levels of HBsAg, HBeAg than female mice

Dpi, days post injection; wpi, weeks post injection.

remain HBV-positive up to 6 months after HDI of 10 μg pAAV/HBV1.2 (13, 18–20). In contrast, BALB/cJ, FVB/NJ, NOD/ShiLtJ, and 129×1/SvJ mice that received the same plasmid injection rapidly clear HBV within 3-5 weeks post injection (wpi). Even mice with the same background but different substrains display different outcomes after HDI of HBV plasmid. In C57BL/6N mice, HBsAg and HBV DNA rapidly decline below the limit of detection within 8 weeks, while HBsAg remains detectable in C57BL/6J mice at 26 wpi (21).

HBV persistence differs in mice of different ages or gender after HDI. 12-week-old adult C3H/HeN mice have been shown to clear HBV within 6 wpi; however, 50% of their younger counterparts (6-week-old) remain HBsAg-positive at 26 wpi (18). The same study suggested that adult mice possess mature gut microbiota that stimulates liver immunity, resulting in rapid HBV clearance, while younger mice are immune-tolerant through the Toll-like receptor (TLR)-4 dependent pathway (18). Another study using AAVS1 mice demonstrated that male AAVS1 mice receiving 10 μg pAAV/HBV1.2 express higher HBsAg and HBeAg levels than female mice (20). Similarly, male C57BL/6 mice that received 10 μg pSM2 plasmid expressed higher levels of HBV proteins than their female counterparts (15). Mechanistically, it is due to high frequency of regulatory T cells and low response of HBV-specific T cells in male mice (15).

The plasmid backbone also affects HBV persistence in mice after HDI. In contrast to pAAV/HBV1.2, injection of pGEM4Z with the same 1.2-fold HBV genotype A genome into C57BL/6 mice produces only transient antigenemia, and HBsAg rapidly disappears within 3 weeks (13). In line with this, mice injected with 15 μg pAAV/HBV1.3 containing 1.3-fold HBV genotype C genome clear the HBsAg within 8 weeks while 60% mice remain HBsAg-positive at week 20 post HDI of pcDNA3.1 (+)-HBV1.3 (14).

Finally, the doses of plasmid backbone or HBV genome also greatly impact HBV persistence in HDI model. Approximately 40-80% C57BL/6 mice that receive 5 or 6 μg pAAV/HBV1.2 develop HBsAg persistence up to 6 months, while a high dose of 100 μg pAAV/HBV1.2 results in HBsAg clearance within 4-5 weeks (16, 17). Similarly, 20 μg pAAV/HBV1.2 or 6 μg pAAV/HBV1.2 plus 14 μg pAAV/control plasmid also results in HBV clearance within 4 weeks (17).

These data highlight the need for researchers to carefully choose mouse strains and plasmid doses when using this model in HBV research.

Application of the HDI Mouse Model for Studies on Immune Responses During Virus Clearance

There is a consensus that adaptive immune responses, especially those of virus-specific T cells, play an essential role in mediating intrahepatic HBV clearance (22). In acute HBV infection in humans, viral clearance is associated with the development of a vigorous multispecific CD8+ T cell response and an acute necroinflammatory liver disease; it was therefore assumed that HBV clearance is principally mediated by virus-specific major histocompatibility complex class I-restricted cytotoxic T lymphocytes (CTLs) (23). The immune effectors required for HBV clearance were screened in an HBV HDI mouse model, which also demonstrated that CD8+ T cells are the key cellular effectors mediating hepatic HBV clearance (24). Consistent with these findings, chronic HBV infection is characterized by weak or undetectable HBV-specific CD8+ T cell responses and the presence of functionally exhausted HBV-specific CD8+ T cells that are unable to clear the virus (25–27).

The use of mouse models allows detailed analysis of immune responses to HBV *in vivo*. Several studies employed HDI mouse models to investigate immune responses to HBV and their relationship with HBV clearance. An acute HBV replication mouse model was established by HDI of pT-MCS-HBV1.3 and pCMV-SB. A variety of immunodeficient mouse strains have been used to determine the roles of different types of immune cells in HBV clearance in this model; the results showed that natural killer (NK) cell, type I IFN, CD4, and CD8, but not B cells, contribute to HBV clearance (24). Similarly, Tseng et al. showed that the molecules involved in innate immunity, including IFN-α/β receptor (IFNAR), RIG-I, MDA5, Myd88, NLRP3, ASC, and interleukin-1 receptor (IL-1R), are not essential for HBV clearance in the mouse model (28). Another study using a panel of mouse strains lacking specific innate immunity components demonstrated that HBV-specific T cell responses are functionally impaired in TLR signaling-deficient mice, thus allowing enhanced and prolonged HBV replication and expression (29). In line with this, when blocking the type I IFN receptor or TLR7 signaling pathway, $CD8^+$ T cell activation and HBV clearance are significantly impaired (30).

The immune factors that suppress or contribute to HBV persistence could be also found by comparing HBV HDI mouse models that mimic acute-resolving and chronic HBV infection. By comparing C57BL/6N and C57BL/6J mice, Wang et al. found that regulatory T (Treg) cells suppress the follicular helper T (Tfh) cells response to HBsAg in C57BL/6J mice and thus lead to persistent HBV infection (21). Importantly, this is consistent with the impaired Tfh-cell response to HBsAg in patients with chronic HBV infection (21). Consistently, depletion of Tregs or inhibition of their function with a blocking antibody against cytotoxic T-lymphocyte-associated protein 4 (CTLA4) restored the Tfh-cell response to HBsAg both in the HBV-persistent mice and patients with chronic HBV infection (21). In line with this, our group demonstrated that intrahepatic HBV replication resulted in increased intrahepatic Treg infiltration and thus limited intrahepatic anti-HBV CD8+ T cell responses (31). We further demonstrated that the suppression of anti-HBV CTL function by Tregs is gender related, which nicely explains the gender-related differences in HBV infection outcomes in humans (15). It has also been reported that the chronic HBV replication mouse model established by HDI of pAAV/HBV1.2 is unable to respond to HBsAg vaccination, which is attributed to IL-10 secretion by Kupffer cells (KCs) (32). Moreover, extracellular vesicles secreted by HBV-infected cells from patients with HBV exert immunosuppressive functions and lead to HBV persistence in the HDI model (33). Recently, we demonstrated that during acute-

resolving HBV infection in HDI model using pSM2 plasmid, the liver produces increased amounts of matrix metalloprotease (MMP) 2, which, together with MMP9, mediate membrane CD100 shedding from the surface of T cells and NK cells in the secondary lymphoid organs and increase serum soluble CD100 levels (34). By interacting with CD72, sCD100 induces the activation of antigen-presenting cells in the spleen and liver in the HDI mice, thus promoting the intrahepatic anti-HBV CD8 T cell response and virus clearance (34).

Other Applications of the HDI Mouse Model

Immune therapeutic strategies that aim to restore the antiviral function of HBV-specific $CD8^+$ T cells have been intensively examined in HBV HDI mouse models that mimic chronic HBV infection. To mimic patients with chronic hepatitis B, the persistent HBV replication mouse models are usually established by HDI of 6-10 μg pAAV/HBV1.2 plasmid into 5-to-6-week-old male C57BL/6 or C3H mice (35, 36). Our group previously demonstrated that intravenous administration of TLR3 ligand Polyinosinic:polycytidylic acid [poly(I:C)] led to HBV clearance, which was associated with increased $CD8^+$ T cell infiltration in the liver in an IFN-γ- and CXCR-3-dependent manner (37). Furthermore, we also showed that the NOD1 ligand, D-glutamyl-meso-diaminopimelic acid, enhanced the antigen-presenting function of liver sinusoidal endothelial cells to promote HBV-specific $CD8^+$ T cells and HBV clearance in an HBV-persistent HDI mouse model (35). Therapeutic strategies targeting immune checkpoint programmed death-1/programmed death ligand-1 to restore the antiviral function of HBV-specific $CD8^+$ T cells were also examined in an HBV persistent HDI mouse model (38).

HDI mouse models are also widely used to test antiviral agents such as lamivudine (14), RNA interference targeting HBV replicative intermediates (39), and the HBV genome-specific guide RNA-mediated clustered regularly interspaced short palindromic repeats (CRISPR)/Cas9 system (40). Anti-HBV vaccines such as cytomegalovirus-based vaccines (41) were also tested in this model.

Another advantage of the model is that plasmids of different HBV genotypes and variants or mutants can be constructed and injected into the mice. Therefore, they can be used for testing antiviral effects against mutated HBV (42) and exploring the influence of HBV genome strain on HBV persistence, as well as its underlying mechanisms (14, 43).

Limitations of the HDI Mouse Model

Although HDI mouse models are widely used to investigate immune responses and evaluate antiviral compounds, the limitations should be carefully considered. Firstly, the HDI method is stressful for animals as it involves injecting a large volume of liquid, and it also causes significant liver damage in the first few days after injection (10). Secondly, the non-HBV immune response elicited by the plasmid backbone should also be considered. Thirdly, mouse hepatocytes are extremely inefficient in forming cccDNA from rcDNA, resulting in a general absence of cccDNA (44). Fourthly, intrahepatic transfection efficiency is only ~6% in this model (12), much lower than in HBV-infected patients in the real world. Finally, due to the lack of the entry receptor in mice, this is not a natural infection model, so it cannot be used to study the entire infection process. Considering the huge differences between HDI mouse model and patients with HBV infection, researchers should be careful when evaluating the findings about the therapeutic value of immunological and pharmacological interventions against acute and chronic HBV infection in hydrodynamic transfection systems.

There are other aspects to consider when interpreting results from HDI mouse models. When modeling acute HBV infection, the levels of HBsAg and HBV DNA decline quickly in the initial phase. This also occurs under treatment with various of immunosuppressive agents (45), suggesting that this process is not immune-related and that the results obtained in such a situation should be interpreted with care. Although HBV can persist in the host and maintain its replication over a prolonged period, the immunological mechanisms leading to persistence are primarily related to lack of recruitment and intrahepatic accumulation of activated T cells to HBV. Intrahepatic immune activation by TLR ligands result in immune cell infiltration and HBV clearance (37). A major issue is the lack of inflammation in mice with persistent HBV replication, resulting in insufficient recruitment of immune cells into the liver. Thus, HDI mouse models may be useful for investigating host immune responses and viral clearance or persistence; however, a direct comparison with acute and chronic HBV infection in humans is not always possible.

VIRAL VECTOR-MEDIATED TRANSFECTION MOUSE MODEL

Viral vector-mediated transfection mouse model is based on viral transduction by intravenous injection hepatotropic viral vectors containing 1.2- to 1.3-fold HBV genomes, including Adenovirus (Ad) (46–48), and Adeno-associated virus (AAV) (49–51). In this model, HBV genome is inserted to the genome of viral vectors, which initiates HBV replication and secretion of infectious HBV virions. Both vector models express HBV replication intermediates, and the dose of Ad-HBV directly correlates with the outcome of HBV persistence (52). AAV belongs to the family *Parvoviridae*, which is characterized by site-specific integration, natural deficiency, and low immunogenicity. AAV has a variety of serotypes, each of which has organ specificity, making it an ideal gene-targeting vector. Studies have shown that the liver transduction efficiency of AAV8 is stronger than that of AAV1, 5, and 6 serotypes, indicating that AAV8 is highly hepatotropic (53). This feature is favorable for the application of AAV8 in HBV-related studies.

Applications of the Viral Vector-Mediated Transfection Mouse Model

Both Ad-HBV and AAV-HBV transfection mouse models can establish persistent HBV replication for more than 3 months or

even more than 1 year (46, 52, 54). Notably, only low doses of Ad-HBV have been reported to establish such persistent HBV replication (46). The high doses of Ad-HBV can induce acute-resolving hepatitis, which is partially due to strong non-HBV immune responses induced by the vector itself (55, 56). Nevertheless, this permits the investigation of mechanisms of immune-mediated viral clearance, including the role of NK cells (57) and intrahepatic CTLs (58).

Compared with Ad-HBV, AAV-HBV vectors have minimal AAV genomes with only the essential AAV inverted terminal repeat sequence that is responsible for viral packaging and does not encode any AAV viral proteins. Thus, this vector has a clean background and does not induce an obvious non-HBV immune response (59), making it a more suitable tool to establish persistent HBV infection (10). More importantly, the AAV-HBV mouse model allows more efficient and homogeneous HBV transduction than the HDI model with ~60% of hepatocytes expressing HBcAg 12 weeks after injection (49).Serum HBsAg in AAV-HBV mice remains at relative high levels even in 3 or 4 month (**Table 2**). Therefore, the AAV-HBV mouse model is preferred to evaluate therapeutic vaccines for chronic infection (61) and the antiviral effects of TLR agonists like the TLR9 ligand CpG (50). It is worth mentioning that Prof. Xiaobing Wu's group in Shanghai developed a persistent HBV replication mouse model by transduction of recombinant AAV8 (rAAV8)-HBV 1.3 into C57BL/6 mice (62). This model is also used to evaluate antiviral effects of NAs such as entecavir and lamivudine (63). Moreover, two studies reported fibrosis in HBV mice transfected with AAV8-HBV1.2, which is one of the few replicative models that can be used to study the mechanism of liver fibrosis in the course of chronic hepatitis B (64, 65). Lucifora et al. reported that cccDNA can be detected by Southern blot in an AAV-HBV model (66). However, it remains uncertain whether AAV-HBV generates cccDNA in murine hepatocytes through rcDNA, the natural precursor of cccDNA.

Limitations of the Viral Vector-Mediated Transfection Mouse Model

As adenoviral vectors have large genomes and encode numerous non-HBV viral products, it is technically challenging to interpret the HBV-related immune response and pathogenesis in the Ad-HBV transfection model (55, 56). Moreover, except for the observed liver fibrosis in AAV8-HBV1.2-transfected mice mentioned above, Ad-HBV and AAV-HBV mice do not usually develop pathological changes in the liver. Although rAAV8-HBV1.3 can to some extent achieve persistent HBV replication after transfection, it cannot stimulate HBV-specific humoral immunity (67). This may be due to immune tolerance induced by the AAV8 vector (67). Moreover, similar to the HDI approach, this model does not represent real infection. For these reasons, it is controversial whether this model can be used to study HBV immunology, which limits its application.

HBV RC-cccDNA MOUSE MODEL

The stable cccDNA pool is a barrier to HBV eradication in patients. However, one common disadvantage of the HDI injection and virus-vector transduction mouse models is that HBV cccDNA is rarely and not convincingly detected, suggesting that the intracellular recycling pathway is severely impaired in mouse hepatocytes (68). To address cccDNA related issues, a recombinant cccDNA (rc-cccDNA) mouse model was developed. In 2014, Qiang Deng's group first reported that coinjection of a plasmid containing double-LoxP flanked HBV DNA sequence and a plasmid expressing Cre recombinase induced rc-cccDNA

TABLE 2 | Serum HBsAg levels among different chronic HBV mouse model.

Authors	Mouse background	Mouse model	HBsAg positive rate	HBsAg levels
Huang et al. (13)	C57BL/6 (male, 6-8 weeks)	HDI model 10 μg pAAV/HBV1.2	80% at 5 wpi	10000 ng/ml at 1 wpi; 100-1000ng/ml at 5 wpi
Li et al. (14)	C57BL/6 (male, 6-8 weeks)	HDI model 15 μg pcDNA3.1(+)-HBV1.3	60% at 20 wpi	OD450: 3.0-3.5 at 1 wpi; ~1.5 at 20 wpi
Li et al. (16)	C57BL/6 (male, 6-8 weeks)	HDI model 5μg pAAV/HBV1.2	80% at 24 wpi	OD450: 2.5-3.0 at 1 wpi 1.0-2.5 at 24 wpi
Wang et al. (17)	C57BL/6 (male, 5-6 weeks)	HDI model 6 μg pAAV/HBV1.2,	100% at 6 wpi	1000 ng/ml at 1 wpi; 100-1000 ng/ml at 6 wpi
Peng et al. (19)	C3H/HeN (male, 5-6 weeks)	HDI model 10 μg pAAV/HBV1.2	90% at 46 wpi	2000-3000 IU/ml at beginning; 60-100 IU/ml at 46 wpi
Huang et al. (46)	n.a	Ad-HBV vector Infected with 10^8 infectious unites of Ad-HBV	n.a	10000-100000 S/CO at 1 wpi; ~ 100 S/CO at day 100 after infection
Dion et al. (49)	HLA-A2/DR1 mice (male, 6-8 weeks)	AAV2/8-HBV vector Infected with 5×10^{10}vg	n.a	~ 100 μg/ml at 2 wpi ~ 80 μg/ml at 16 wpi
Yang et al. (50)	C57BL/6 (male, 6-8 weeks)	AAV-HBV vector Infected with 1×10^{11}vg	n.a	2000-3000 ng/ml at 2 wpi and 12 wpi
Yan et al. (60)	C3H (male, 4-6 weeks)	Rc-ccc DNA model HDI of 10 μg of HBVcircle	100% at 7 wpi	10000 ng/ml at 1 wpi; 1000-10000 ng/ml at 7 wpi

*HDI, hydrodynamic injection; HLA-A2/DR1, HLA-A*0201/DRB1*0101-transgenic, H-2 class I/class II knockout (KO) mice; n.a, not available; S/CO, signal to control ratio; wpi, weeks post injection.*

generation in the murine liver (69). This rc-cccDNA is similar to the real HBV cccDNA that acts as the template producing mature HBV virus. However, the plasmid backbone after excision remained in the mouse liver and evoked a non-HBV immune response, which critically influenced rc-cccDNA stability and HBV antigenemia *in vivo* (69). To overcome this issue, the same group developed an improved version of the cccDNA mouse using a replication-defective recombinant adenoviral vector to deliver linear HBV genome into Cre transgenic mice (70). HBV persists more than 62 weeks in this model, and sustained necroinflammatory response and fibrosis can be observed in the liver, which is analogous to the progressive pathology of clinical hepatitis (70).

Alternatively, a hydrodynamic-injected recombinant HBV minicircle cccDNA generated from a genetically engineered *Escherichia coli* strain also formed authentic cccDNA-like molecules in murine hepatocytes and achieved high-level, persistent HBV replication in C3H mice (60). Another group recently developed rc-cccDNA to mimic cccDNA using HDI of a Cre/LoxP-HBV plasmid into NOD-scid IL1Rg^{null} mice (71). In their system, HBx-mutant and green fluorescent protein reporter plasmids are created by these cis-Cre/LoxP-HBV plasmids to further probe cccDNA biology and develop antiviral strategies against cccDNA (71).

In the rc-cccDNA mice, HBV replication and observed phenotypes are entirely driven by cccDNA-like viral genome, making it a more biologically relevant model for testing antiviral agents targeting cccDNA, such as CRISPR/Cas9 nuclease, as well as small molecules specifically silencing or destabilizing cccDNA (72, 73). Nevertheless, the rc-cccDNA does not have the fully identical characteristics of cccDNA formed from rcDNA. These rc-cccDNA systems also do not overcome the limitation of impaired intracellular recycling pathway in mouse hepatocytes. Therefore, the application of this system is still limited.

TRANSGENIC MOUSE MODELS

In the 1980s, HBV transgenic mouse models were generated with embryo microinjection technology. These transgenic lineages express one of the HBV gene products under the control of the native viral regulatory elements or cell-specific promoters (74). The insertion of overlength HBV genomes supports viral replication, including particle production and infectious virion release (3, 75, 76). Transgenic models have substantially contributed to the understanding of molecular virus-host interactions and the biology of HBV-related immunology and pathogenesis. They can be separated into single HBV-protein transgenic mice and full-genome transgenic mice.

Single-Protein Transgenic Mice

The HBV protein-transgenic mice express HBV proteins such as HBsAg (77, 78), HBcAg (79), HBeAg (80), or HBx (81). These models can be used to study the virology and oncogenic potential of these HBV proteins.

In 1985, Chisari et al. developed the first HBV transgenic mice that express HBsAg (77). It was initially suggested that this model did not exhibit signs of pathology. Later, the same group described that increased expression of large HBsAg, rather than the small and middle HBsAg proteins, inhibits the secretion of HBsAg-containing particles (78). Furthermore, HBsAg accumulation in the endoplasmic reticulum of hepatocytes leads to continuous inflammation and liver injury, followed by HCC development (82). The same HBs-transgenic mice were crossed to C57BL/6 and BALB/c, which revealed that HBsAg protein-induced liver injury depends on host genetic background (83). It was recently shown that methylation of specific CpG sites controls gene expression in these HBs-transgenic mice, resulting in decreased cell stress and improved liver integrity (84). Although pathological aspects of HBsAg could be revealed with this model, the intracellular accumulation does not reflect the natural function of HBsAg in HBV-infected humans.

To address HBV biology and immunological aspects, HBeAg-transgenic mice were generated to investigate the role of immunological tolerance in chronic infection of newborns (80). Both HBeAg and HBcAg are expressed in this model. It has been suggested that HBeAg secretion may be one of the viral strategies for HBV persistence after perinatal infection (80). Another HBcAg-transgenic mouse model was used to examine factors that influence the intracellular localization of nucleocapsid particles in hepatocytes; it demonstrated that nucleocapsids can form *de novo* within the nucleus, and the reformed nucleocapsid cannot be transported across the intact nuclear membrane (79). Knowledge about the functional and structural significance of HBcAg and HBeAg could be gained with these models.

Mice transgenic for HBx protein have yielded controversial results regarding its oncogenic potential. Early reports showed that HBx-expressing mice develop HCC (81, 85, 86). However, others reported contradicting findings that HBx alone is not sufficient for inducing HCC development (87–89). Hepatocarcinogenesis has been directly compared in HBsAg and HBx knock-in transgenic mice. HBsAg and HBx genes were integrated into the mouse p21 locus using homologous recombination. Although p21-HBx transgenic mice developed HCC at the age of 18 months, p21-HBsAg transgenic mice have developed HCCs 3 months earlier. Herein, the expression of genes related to metabolism and genomic instability largely resembled the molecular changes during HCC development in humans (90). However, hepatocarcinogenesis in HBV-transgenic mice occurs in a cirrhosis-free condition and does not reflect the common situation in HCC-developing patients with chronic hepatitis B infection.

Full-Genome Transgenic Mice

Single-HBV protein transgenic mice facilitated investigation of the assembly, secretion, immune responses, and functionality of these proteins *in vivo*. However, HBV-full genome transgenic mice support the whole HBV life cycle *in vivo*. The integrated HBV genome includes terminally redundant DNA representing a 1.3 overlength HBV genome leading to efficient viral replication, including rcDNA synthesis from pregenomic RNA, viral assembly, and production of infectious HBV particles that are morphologically indistinguishable from human-derived virions (76). Due to self-tolerance, full-genome transgenic mice do not suffer from T cell-related liver injury. The lack of hepatitis

indicates that HBV viral proteins or HBV itself is not cytopathic in transgenic mice. Adoptive transfer of HBV-specific cytotoxic T cells caused acute liver disease and thus resulted in temporal clearance of HBsAg (91, 92). These HBV replication-competent transgenic mice have been extensively used to evaluate antiviral drugs that hinder HBV replication, including small interfering RNAs (93, 94); cytokines (95, 96); and various polymerase inhibitors such as adefovir dipivoxil (97), lamivudine (98), and entecavir (99). Thus, cellular, molecular pathogenic, and antiviral mechanisms occurring in acute viral hepatitis have been recapitulated in full-genome transgenic mice.

Limitation of Transgenic HBV Models

All lineages of HBV transgenic mice generated to date are immunologically tolerant to viral antigens, particularly at the T-cell level, and they do not develop acute or chronic hepatitis. Therefore, these models do not develop HBV-related liver diseases including liver injury and progressive fibrosis and cirrhosis. Due to the transgenic origin of HBV replication, these mice do not have the potential of viral clearance (100). Another restriction is the lack of cccDNA in these full-genome transgenic mice, suggesting that species-specific differences may play a role in determining the host range of this virus (74). Still, the full-genome transgenic mice are absent of the HBV entry factor NTCP. Although infectious particles are produced, hepatocyte infection does not occur. Furthermore, in human NTCP-expressing transgenic mice, HBV infection in mouse hepatocytes is also limited due to the lack of a host cell dependency factor (100). For these reasons, studies examining HBV entry, mechanisms underlying infection, compounds interfering with the infection process, and cccDNA synthesis are not suitable in full-genome transgenic mice.

LIVER-HUMANIZED MOUSE MODEL

Although mice are not the natural host for HBV, a human liver chimeric mouse model makes it possible to study the entire infection process (from viral entry to cccDNA synthesis and intrahepatic spread). The human liver chimeric mouse model is generated by engraftment of primary human hepatocytes in highly immunodeficient mice. The success of this model is based on the principle of inducing murine hepatocellular damage and abolishing adaptive immune responses to allow survival of the transplanted xenogeneic hepatocytes (10). Three different liver humanized mouse models are currently available for studying HBV infection.

The first kind of liver humanized mouse is the urokinase-type plasminogen activator/severe combined immunodeficiency (alb-uPA/Scid) mouse, in which overexpression of uPA transgene driven by the murine albumin (alb) promoter results in hypofibrinogenemia and severe hepatotoxicity (101). After backcrossing alb-uPA mice with immunodeficient mice (e.g., Scid, $RAG2^{-/-}$ and Scid/beige mice), human hepatocytes are introduced *via* intrasplenic injection and reach the injured liver, where they begin to proliferate to replace the diseased mouse hepatocytes (102). Human hepatocytes can reconstitute up to 70% of liver in this model (103), but it has several drawbacks including kidney and hematologic disorders, potentially fatal bleeding, low breeding efficiency, and narrow time range for liver manipulation (103, 104).

To circumvent these challenges, an alternative human liver chimeric mouse model was generated: the triple knockout $FAH^{-/-}$ $RAG2^{-/-}IL2RG^{-/-}$ (FRG) mouse. This mouse model was produced by crossing fumaryl acetoacetate hydrolase (Fah) knockout mice with double immunodeficient $RAG2^{-/-}$IL-2 receptor γ chain (IL2RG) mice (105). The Fah gene encodes the last enzyme in the tyrosine catabolism pathway, and its deficiency leads to accumulation of toxic tyrosine metabolic intermediates and subsequent liver failure (106, 107). However, liver injury in this model can be prevented with 2-(2-nitro-4-trifluoromethylethylbenzoyl)-cyclohexane-1,3-dione (NTBC) (105). This model requires continuous cycling of NTBC to sustain human hepatocyte engraftment for extended periods of time, but this can achieve ~97% human liver chimerism (105).

The third mouse model is generated based on TK-NOG mice, which carry the transgene of the herpes simplex virus 1(HSV1) thymidine kinase (TK) in triple immune defect Nod/Scid/$IL2rg^{-/-}$ (NOG) mice (108, 109). Similar to FRG mice, liver injury can be induced in a controlled manner by ganciclovir that selectively destroy TK-expressing murine hepatocytes (108, 109). The liver repopulation rate in this model is ~70%, which is comparable to the alb-uPA/Scid mouse. However, a major drawback is that male TK-NOG mice are sterile.

In contrast to transgenic HBV mice, liver humanized mice are susceptible to HBV infection (110) and cccDNA is formed in transplanted hepatocytes. These models can be used to study viral infection, the nature of cccDNA, and interactions between HBV and its host (111), as well as test novel antiviral agents (112, 113). However, immunodeficiency makes these mice unsuitable for studying immune responses. The high cost and technical difficulties also pose great challenges for the availability of this mouse model.

IMMUNOCOMPETENT HUMAN LIVER CHIMERIC MICE

Liver humanized mice have complete immunodeficiency, which does not allow the study of adaptive immune responses and immunotherapeutic strategies. To circumvent this limitation, immunocompetent human liver-chimeric mice dually reconstituted with both immune cells and hepatocytes of human origin were developed by transplantation of human hematopoietic stem cells or fetal liver cells (114–117). Another approach to study immune responses in chimeric mice is adoptive transfer of human immune cells into previously infected mice (118). However, the generation of double chimeric systems is still a major challenge; both the source of human cells and mouse background massively influence the outcomes of cell engraftment and maturation.

THE APPLICATION OF MOUSE MODELS TARGETING HBV CURE

Three categories of HBV cure, complete cure, functional cure and partial cure, have been defined according to clinical

parameters and the corresponding underlying molecular mechanisms. Complete cure is defined as the loss of HBsAg and the complete elimination of all forms of replicating HBV, including cccDNA while functional cure only refers to HBsAg loss or HBsAg seroconversion (119). Complete cure is an ideal goal; however, current available agents can not completely eradicate the cccDNA in infected hepatocytes. Therefore, a functional cure is the currently accepted goal for new HBV therapies. CHB patients achieving functional cure have a very benign prognosis and the negligible risk of progression to liver cirrhosis and HCC (120).

Current novel treatment options under development targeting HBV functional cure or even HBV eradication included direct antivirals that aim at inhibiting virus entry, degrading cccDNA or preventing cccDNA formation, silencing viral transcripts, modulating nucleocapsid assembly, preventing HBsAg secretion, and immune modulators that aim to restore effective HBV-specific immune responses (121). The liver-humanized mice and immunocompetent human liver chimeric mice allow *de novo* HBV infection and thus maintain the cccDNA pool. Therefore, these two models can be used to test agents targeting HBV entry, cccDNA synthesis, virus assembly and secretion. The rc-cccDNA mouse model is particularly useful for evaluating efficacy of cccDNA-targeting agents. The HDI, Ad-vector and full-genome HBV transgenic mice could be used to evaluate the efficacy of nucleoside analogues and siRNA silencing viral transcripts. Moreover, the immunocompetent mice in HDI system and human liver chimeric mice allows to investigate the restoration of HBV-specific immunity by the treatment with novel immune modulators. As discussed in the previous sections, therapeutic vaccines, toll-like receptor agonists, polymerase inhibitors, small interfering RNAs, and HBV entry inhibitors have been tested as single agents or in combinations in these mouse models. The major advantages of working with mouse models are the ease by which *in vivo* target engagement and the mechanism of actions can be assessed. The wealth of historical data and reagents tested in a great number of diverse mouse studies can be drawn upon to understand the downstream effects on viral infection or the host immunity (122). However, whether success of new treatments in the mouse models could be translated to the human setting remains to be analyzed in each case.

A last critical issue for achieving HBV cure is HBV integration. Unfortunately, this aspect of HBV cure is not yet considered in the investigation in HBV mouse models. Though the transgenic HBV mouse models contain integrated viral genomes in the host genome, the consequence for viral control is not analyzed in an appropriate context and needs attention in the future studies.

CONCLUSION

This review discussed the *in vivo* mouse models for HBV research. Each has its own strengths and weaknesses (**Table 3**), offering good opportunities to choose between different models based on the specific research questions addressed. The HDI model can establish both acute and chronic HBV replication in immunocompetent mice, so it is extensively used to investigate immune responses during virus clearance and evaluate novel antiviral agents. When using this model, the mouse background, age, gender, and HBV plasmid dose should be carefully

TABLE 3 | Characteristics of different types of HBV mouse model.

Mouse models	Advantages	Applications	Limitations
Hydrodynamic injection	Immunocompetent Transient and persistent replication model	Investigate immune responses Testing novel antiviral agents HBV variants or mutants	No cccDNA; No infection; Relatively lower efficiency; Liver damage
Viral vector-mediated transfection model			
Ad-HBV transduction	Immunocompetent	Immune-mediated viral clearance	No cccDNA; No infection; High non-HBV immune response; Transient replication
AAV-HBV transduction	Immunocompetent Higher transfection efficiency Persistent replication	Test antiviral agents Study mechanism of fibrosis(?)	cccDNA rarely observed; No infection; immune tolerance
rc-cccDNA mouse model	cccDNA formation	Antiviral agents targeting cccDNA	No infection; not the physical DNA formed by rcDNA
HBV transgenic mouse model			
Single protein-transgenic mice	Express single HBV protein	Virology and oncogenic potential of HBV proteins	No infection; No cccDNA No HBV replication
Full genome-transgenic mice	Whole HBV life cycle Effective viral replication	Antiviral drugs interfering HBV replication	No infection; No cccDNA Self-tolerance; Not cytopathic
Liver humanized mouse model	Susceptible to HBV infection cccDNA formation	Study viral infection Interaction between HBV and host	Immune deficient High cost Technical challenging
Immunocompetent human liver chimeric mice	Immunocompetent Susceptible to HBV infection cccDNA formation	Study viral infection Immune responses	High cost Technical challenging

considered. The AAV transduction-mediated replicon delivery model can also establish persistent HBV replication and is used to investigate antiviral compounds. However, due to the non-HBV immunity elicited by the vector, it is still controversial whether this model could be used to study HBV immunology. The development of transgenic mouse models enables elucidation of molecular virus-host interactions and the biology of HBV-related immunology and pathogenesis. The human liver chimeric mouse model also makes it possible to study the entire infection process, but the high cost and technical difficulties limit the wide applicability of this model. In summary, the development of HBV mouse models has opened a new era in HBV research. Together with *in vitro* cell culture models, these mouse models will provide great insight for developing novel therapeutic strategies to cure HBV.

AUTHOR CONTRIBUTIONS

YD and ML conceptualized this review. RB, XL, XZ, and JL wrote parts of the review. YD and ML drafted the layout for the review and wrote the discussion. DY edited the review. All authors contributed to the article and approved the submitted version.

FUNDING

This work was supported by a scholarship of Medical Faculty of University of Duisburg-Essen, a grant of Deutsche Forschungsgemeinschaft (RTG 1949/2), and grants of National Natural Science Foundation of China (81871664, 81861138044, 91742114 and M-0060).

REFERENCES

1. Seeger C, Mason WS. Molecular Biology of Hepatitis B Virus Infection. *Virology* (2015) 479-480:672–86. doi: 10.1016/j.virol.2015.02.031
2. Hutin Y, Nasrullah M, Easterbrook P, Nguimfack BD, Burrone E, Averhoff F, et al. Access to Treatment for Hepatitis B Virus Infection - Worldwide, 2016. *MMWR Morb Mortal Wkly Rep* (2018) 67:773–7. doi: 10.15585/mmwr.mm6728a2
3. Guidotti LG, Rochford R, Chung J, Shapiro M, Purcell R, Chisari FV. Viral Clearance Without Destruction of Infected Cells During Acute HBV Infection. *Science* (1999) 284:825–9. doi: 10.1126/science.284.5415.825
4. Dupinay T, Gheit T, Roques P, Cova L, Chevallier-Queyron P, Tasahsu SI, et al. Discovery of Naturally Occurring Transmissible Chronic Hepatitis B Virus Infection Among Macaca Fascicularis From Mauritius Island. *Hepatology* (2013) 58:1610–20. doi: 10.1002/hep.26428
5. Walter E, Keist R, Niederost B, Pult I, Blum HE. Hepatitis B Virus Infection of Tupaia Hepatocytes *In Vitro* and *In Vivo*. *Hepatology* (1996) 24:1–5. doi: 10.1053/jhep.1996.v24.pm0008707245
6. Roggendorf M, Kosinska AD, Liu J, Lu M. The Woodchuck, a Nonprimate Model for Immunopathogenesis and Therapeutic Immunomodulation in Chronic Hepatitis B Virus Infection. *Cold Spring Harb Perspect Med* (2015) 5:a021451. doi: 10.1101/cshperspect.a021451
7. Reaiche GY, Le Mire MF, Mason WS, Jilbert AR. The Persistence in the Liver of Residual Duck Hepatitis B Virus Covalently Closed Circular DNA Is Not Dependent Upon New Viral DNA Synthesis. *Virology* (2010) 406:286–92. doi: 10.1016/j.virol.2010.07.013
8. Yang Q, Zhao X, Zang L, Fang X, Zhao J, Yang X, et al. Anti-Hepatitis B Virus Activities of Alpha-DDB-FNC, A Novel Nucleoside-Biphenyldicarboxylate Compound in Cells and Ducks, and Its Anti-Immunological Liver Injury Effect in Mice. *Antiviral Res* (2012) 96:333–9. doi: 10.1016/j.antiviral.2012.10.003
9. D'Ugo E, Argentini C, Giuseppetti R, Canitano A, Catone S, Rapicetta M. The Woodchuck Hepatitis B Virus Infection Model for the Evaluation of HBV Therapies and Vaccine Therapies. *Expert Opin Drug Discovery* (2010) 5:1153–62. doi: 10.1517/17460441.2010.530252
10. Allweiss L, Dandri M. Experimental *In Vitro* and *In Vivo* Models for the Study of Human Hepatitis B Virus Infection. *J Hepatol* (2016) 64:S17–31. doi: 10.1016/j.jhep.2016.02.012
11. Suda T, Liu D. Hydrodynamic Gene Delivery: Its Principles and Applications. *Mol Ther* (2007) 15:2063–9. doi: 10.1038/sj.mt.6300314
12. Yang PL, Althage A, Chung J, Chisari FV. Hydrodynamic Injection of Viral DNA: A Mouse Model of Acute Hepatitis B Virus Infection. *Proc Natl Acad Sci U.S.A.* (2002) 99:13825–30. doi: 10.1073/pnas.202398599
13. Huang LR, Wu HL, Chen PJ, Chen DS. An Immunocompetent Mouse Model for the Tolerance of Human Chronic Hepatitis B Virus Infection. *Proc Natl Acad Sci U.S.A.* (2006) 103:17862–7. doi: 10.1073/pnas.0608578103
14. Li X, Liu G, Chen M, Yang Y, Xie Y, Kong X. A Novel Hydrodynamic Injection Mouse Model of HBV Genotype C for the Study of HBV Biology and the Anti-Viral Activity of Lamivudine. *Hepat Mon* (2016) 16:e34420. doi: 10.5812/hepatmon.34420
15. Kosinska AD, Pishraft-Sabet L, Wu W, Fang Z, Lenart M, Chen J, et al. Low Hepatitis B Virus-Specific T-Cell Response in Males Correlates With High Regulatory T-Cell Numbers in Murine Models. *Hepatology* (2017) 66:69–83. doi: 10.1002/hep.29155
16. Li L, Li S, Zhou Y, Yang L, Zhou D, Yang Y, et al. The Dose of HBV Genome Contained Plasmid has a Great Impact on HBV Persistence in Hydrodynamic Injection Mouse Model. *Virol J* (2017) 14:205. doi: 10.1186/s12985-017-0874-6
17. Wang X, Zhu J, Zhang Y, Li Y, Ma T, Li Q, et al. The Doses of Plasmid Backbone Plays a Major Role in Determining the HBV Clearance in Hydrodynamic Injection Mouse Model. *Virol J* (2018) 15:89. doi: 10.1186/s12985-018-1002-y
18. Chou HH, Chien WH, Wu LL, Cheng CH, Chung CH, Horng JH, et al. Age-Related Immune Clearance of Hepatitis B Virus Infection Requires the Establishment of Gut Microbiota. *Proc Natl Acad Sci USA* (2015) 112:2175–80. doi: 10.1073/pnas.1424775112
19. Peng XH, Ren XN, Chen LX, Shi BS, Xu CH, Fang Z, et al. High Persistence Rate of Hepatitis B Virus in a Hydrodynamic Injection-Based Transfection Model in C3H/HeN Mice. *World J Gastroenterol* (2015) 21:3527–36. doi: 10.3748/wjg.v21.i12.3527
20. Yuan L, Wang T, Zhang Y, Liu X, Zhang T, Li X, et al. An HBV-Tolerant Immunocompetent Model That Effectively Simulates Chronic Hepatitis B Virus Infection in Mice. *Exp Anim* (2016) 65:373–82. doi: 10.1538/expanim.16-0013
21. Wang X, Dong Q, Li Q, Li Y, Zhao D, Sun J, et al. Dysregulated Response of Follicular Helper T Cells to Hepatitis B Surface Antigen Promotes HBV Persistence in Mice and Associates With Outcomes of Patients. *Gastroenterology* (2018) 154:2222–36. doi: 10.1053/j.gastro.2018.03.021
22. Chisari FV, Ferrari C. Hepatitis B Virus Immunopathogenesis. *Annu Rev Immunol* (1995) 13:29–60. doi: 10.1146/annurev.iy.13.040195.000333
23. Thimme R, Wieland S, Steiger C, Ghrayeb J, Reimann KA, Purcell RH, et al. CD8(+) T Cells Mediate Viral Clearance and Disease Pathogenesis During Acute Hepatitis B Virus Infection. *J Virol* (2003) 77:68–76. doi: 10.1128/JVI.77.1.68-76.2003
24. Yang PL, Althage A, Chung J, Maier H, Wieland S, Isogawa M, et al. Immune Effectors Required for Hepatitis B Virus Clearance. *Proc Natl Acad Sci USA* (2010) 107:798–802. doi: 10.1073/pnas.0913498107
25. Wang Q, Pan W, Liu Y, Luo J, Zhu D, Lu Y, et al. Hepatitis B Virus-Specific CD8+ T Cells Maintain Functional Exhaustion After Antigen Reexposure in an Acute Activation Immune Environment. *Front Immunol* (2018) 9:219. doi: 10.3389/fimmu.2018.00219
26. Rehermann B. Pathogenesis of Chronic Viral Hepatitis: Differential Roles of T Cells and NK Cells. *Nat Med* (2013) 19:859–68. doi: 10.1038/nm.3251

27. Rehermann B, Nascimbeni M. Immunology of Hepatitis B Virus and Hepatitis C Virus Infection. *Nat Rev Immunol* (2005) 5:215–29. doi: 10.1038/nri1573
28. Tzeng HT, Tsai HF, Chyuan IT, Liao HJ, Chen CJ, Chen PJ, et al. Tumor Necrosis Factor-Alpha Induced by Hepatitis B Virus Core Mediating the Immune Response for Hepatitis B Viral Clearance in Mice Model. *PloS One* (2014) 9:e103008. doi: 10.1371/journal.pone.0103008
29. Ma Z, Liu J, Wu W, Zhang E, Zhang X, Li Q, et al. The IL-1r/TLR Signaling Pathway Is Essential for Efficient CD8(+) T-Cell Responses Against Hepatitis B Virus in the Hydrodynamic Injection Mouse Model. *Cell Mol Immunol* (2017) 14:997–1008. doi: 10.1038/cmi.2017.43
30. Lan P, Zhang C, Han Q, Zhang J, Tian Z. Therapeutic Recovery of Hepatitis B Virus (HBV)-Induced Hepatocyte-Intrinsic Immune Defect Reverses Systemic Adaptive Immune Tolerance. *Hepatology* (2013) 58:73–85. doi: 10.1002/hep.26339
31. Dietze KK, Schimmer S, Kretzmer F, Wang J, Lin Y, Huang X, et al. Characterization of the Treg Response in the Hepatitis B Virus Hydrodynamic Injection Mouse Model. *PloS One* (2016) 11:e151717. doi: 10.1371/journal.pone.0151717
32. Xu L, Yin W, Sun R, Wei H, Tian Z. Kupffer Cell-Derived IL-10 Plays a Key Role in Maintaining Humoral Immune Tolerance in Hepatitis B Virus-Persistent Mice. *Hepatology* (2014) 59:443–52. doi: 10.1002/hep.26668
33. Kakizaki M, Yamamoto Y, Otsuka M, Kitamura K, Ito M, Kawai HD, et al. Extracellular Vesicles Secreted by HBV-Infected Cells Modulate HBV Persistence in Hydrodynamic HBV Transfection Mouse Model. *J Biol Chem* (2020) 295:12449–60. doi: 10.1074/jbc.RA120.014317
34. Yang S, Wang L, Pan W, Bayer W, Thoens C, Heim K, et al. MMP2/MMP9-Mediated CD100 Shedding Is Crucial for Inducing Intrahepatic Anti-HBV CD8 T Cell Responses and HBV Clearance. *J Hepatol* (2019) 71:685–98. doi: 10.1016/j.jhep.2019.05.013
35. Huang S, Zou S, Chen M, Gao X, Chen L, Yang X, et al. Local Stimulation of Liver Sinusoidal Endothelial Cells With a NOD1 Agonist Activates T Cells and Suppresses Hepatitis B Virus Replication in Mice. *J Immunol* (2018) 200:3170–9. doi: 10.4049/jimmunol.1700921
36. Du Y, Yan H, Zou S, Khera T, Li J, Han M, et al. Natural Killer Cells Regulate the Maturation of Liver Sinusoidal Endothelial Cells Thereby Promoting Intrahepatic T-Cell Responses in a Mouse Model. *Hepatol Commun* (2021) 5:865–81. doi: 10.1002/hep4.1676
37. Wu J, Huang S, Zhao X, Chen M, Lin Y, Xia Y, et al. Poly(I:C) Treatment Leads to Interferon-Dependent Clearance of Hepatitis B Virus in a Hydrodynamic Injection Mouse Model. *J Virol* (2014) 88:10421–31. doi: 10.1128/JVI.00996-14
38. Tzeng HT, Tsai HF, Liao HJ, Lin YJ, Chen L, Chen PJ, et al. PD-1 Blockage Reverses Immune Dysfunction and Hepatitis B Viral Persistence in a Mouse Animal Model. *PloS One* (2012) 7:e39179. doi: 10.1371/journal.pone.0039179
39. McCaffrey AP, Nakai H, Pandey K, Huang Z, Salazar FH, Xu H, et al. Inhibition of Hepatitis B Virus in Mice by RNA Interference. *Nat Biotechnol* (2003) 21:639–44. doi: 10.1038/nbt824
40. Lin SR, Yang HC, Kuo YT, Liu CJ, Yang TY, Sung KC, et al. The CRISPR/Cas9 System Facilitates Clearance of the Intrahepatic HBV Templates In Vivo. *Mol Ther Nucleic Acids* (2014) 3:e186. doi: 10.1038/mtna.2014.38
41. Huang H, Ruckborn M, Le-Trilling V, Zhu D, Yang S, Zhou W, et al. Prophylactic and Therapeutic HBV Vaccination by an HBs-Expressing Cytomegalovirus Vector Lacking an Interferon Antagonist in Mice. *Eur J Immunol* (2021) 51:393–407. doi: 10.1002/eji.202048780
42. Qin B, Budeus B, Cao L, Wu C, Wang Y, Zhang X, et al. The Amino Acid Substitutions Rtp177g and Rtf249a in the Reverse Transcriptase Domain of Hepatitis B Virus Polymerase Reduce the Susceptibility to Tenofovir. *Antiviral Res* (2013) 97:93–100. doi: 10.1016/j.antiviral.2012.12.007
43. Shen Z, Yang H, Yang S, Wang W, Cui X, Zhou X, et al. Hepatitis B Virus Persistence in Mice Reveals IL-21 and IL-33 as Regulators of Viral Clearance. *Nat Commun* (2017) 8:2119. doi: 10.1038/s41467-017-02304-7
44. Ortega-Prieto AM, Cherry C, Gunn H, Dorner M. *In Vivo* Model Systems for Hepatitis B Virus Research. *ACS Infect Dis* (2019) 5:688–702. doi: 10.1021/acsinfecdis.8b00223
45. Wang J, Wang B, Huang S, Song Z, Wu J, Zhang E, et al. Immunosuppressive Drugs Modulate the Replication of Hepatitis B Virus (HBV) in a Hydrodynamic Injection Mouse Model. *PloS One* (2014) 9:e85832. doi: 10.1371/journal.pone.0085832
46. Huang LR, Gabel YA, Graf S, Arzberger S, Kurts C, Heikenwalder M, et al. Transfer of HBV Genomes Using Low Doses of Adenovirus Vectors Leads to Persistent Infection in Immune Competent Mice. *Gastroenterology* (2012) 142:1447–50. doi: 10.1053/j.gastro.2012.03.006
47. Suzuki M, Kondo S, Yamasaki M, Matsuda N, Nomoto A, Suzuki T, et al. Efficient Genome Replication of Hepatitis B Virus Using Adenovirus Vector: A Compact Pregenomic RNA-Expression Unit. *Sci Rep* (2017) 7:41851. doi: 10.1038/srep41851
48. Sprinzl MF, Oberwinkler H, Schaller H, Protzer U. Transfer of Hepatitis B Virus Genome by Adenovirus Vectors Into Cultured Cells and Mice: Crossing the Species Barrier. *J Virol* (2001) 75:5108–18. doi: 10.1128/JVI.75.11.5108-5118.2001
49. Dion S, Bourgine M, Godon O, Levillayer F, Michel ML. Adeno-Associated Virus-Mediated Gene Transfer Leads to Persistent Hepatitis B Virus Replication in Mice Expressing HLA-A2 and HLA-DR1 Molecules. *J Virol* (2013) 87:5554–63. doi: 10.1128/JVI.03134-12
50. Yang D, Liu L, Zhu D, Peng H, Su L, Fu YX, et al. A Mouse Model for HBV Immunotolerance and Immunotherapy. *Cell Mol Immunol* (2014) 11:71–8. doi: 10.1038/cmi.2013.43
51. Huang YH, Fang CC, Tsuneyama K, Chou HY, Pan WY, Shih YM, et al. A Murine Model of Hepatitis B-Associated Hepatocellular Carcinoma Generated by Adeno-Associated Virus-Mediated Gene Delivery. *Int J Oncol* (2011) 39:1511–9. doi: 10.3892/ijo.2011.1145
52. Tzeng H, Hsu P, Chen P. Immunocompetent Nontransgenic Mouse Models for Studying Hepatitis B Virus Immune Responses. *J Gastroen Hepatol* (2013) 28:116–9. doi: 10.1111/jgh.12035
53. Paneda A, Vanrell L, Mauleon I, Crettaz JS, Berraondo P, Timmermans EJ, et al. Effect of Adeno-Associated Virus Serotype and Genomic Structure on Liver Transduction and Biodistribution in Mice of Both Genders. *Hum Gene Ther* (2009) 20:908–17. doi: 10.1089/hum.2009.031
54. von Freyend MJ, Untergasser A, Arzberger S, Oberwinkler H, Drebber U, Schirmacher P, et al. Sequential Control of Hepatitis B Virus in a Mouse Model of Acute, Self-Resolving Hepatitis B. *J Viral Hepat* (2011) 18:216–26. doi: 10.1111/j.1365-2893.2010.01302.x
55. Cavanaugh VJ, Guidotti LG, Chisari FV. Inhibition of Hepatitis B Virus Replication During Adenovirus and Cytomegalovirus Infections in Transgenic Mice. *J Virol* (1998) 72:2630–7. doi: 10.1128/JVI.72.4.2630-2637.1998
56. Hartman ZC, Kiang A, Everett RS, Serra D, Yang XY, Clay TM, et al. Adenovirus Infection Triggers a Rapid, MyD88-Regulated Transcriptome Response Critical to Acute-Phase and Adaptive Immune Responses in Vivo. *J Virol* (2007) 81:1796–812. doi: 10.1128/JVI.01936-06
57. Zeissig S, Murata K, Sweet L, Publicover J, Hu Z, Kaser A, et al. Hepatitis B Virus-Induced Lipid Alterations Contribute to Natural Killer T Cell-Dependent Protective Immunity. *Nat Med* (2012) 18:1060–8. doi: 10.1038/nm.2811
58. Huang LR, Wohlleber D, Reisinger F, Jenne CN, Cheng RL, Abdullah Z, et al. Intrahepatic Myeloid-Cell Aggregates Enable Local Proliferation of CD8(+) T Cells and Successful Immunotherapy Against Chronic Viral Liver Infection. *Nat Immunol* (2013) 14:574–83. doi: 10.1038/ni.2573
59. Mingozzi F, Liu YL, Dobrzynski E, Kaufhold A, Liu JH, Wang Y, et al. Induction of Immune Tolerance to Coagulation Factor IX Antigen by *In Vivo* Hepatic Gene Transfer. *J Clin Invest* (2003) 111:1347–56. doi: 10.1172/JCI200316887
60. Yan Z, Zeng J, Yu Y, Xiang K, Hu H, Zhou X, et al. HBVcircle: A Novel Tool to Investigate Hepatitis B Virus Covalently Closed Circular DNA. *J Hepatol* (2017) 66:1149–57. doi: 10.1016/j.jhep.2017.02.004
61. Moshkani S, Chiale C, Lang SM, Rose JK, Robek MD. A Highly Attenuated Vesicular Stomatitis Virus-Based Vaccine Platform Controls Hepatitis B Virus Replication in Mouse Models of Hepatitis B. *J Virol* (2019) 93:e01586-18. doi: 10.1128/JVI.01586-18
62. Dong XY, Yu CJ, Wang G, Tian WH, Lu Y, Zhang FW, et al. Establishment of Hepatitis B Virus Chronic Infection Mouse Model by *In Vivo* Transduction With a Recombinant Adeno-Associated Virus 8 Carrying 1.3 Copies of HBV Genome. *Chin J Virol* (2010) 26:425–31.
63. Wang GJ, Wang G, Dong XY, Tian WH, Yu CJ, Wei GC, et al. Anti-HBV Effect of Nucleotide Analogues on Mouse Model of Chronic HBV Infection

Mediated by Recombinant Adeno-Associated Virus 8. *Chin J Biotechnol* (2013) 29:95–106.
64. Kan F, Ye L, Yan T, Cao J, Zheng J, Li W. Proteomic and Transcriptomic Studies of HBV-Associated Liver Fibrosis of an AAV-HBV-Infected Mouse Model. *BMC Genomics* (2017) 18:641. doi: 10.1186/s12864-017-3984-z
65. Ye L, Yu H, Li C, Hirsch ML, Zhang L, Samulski RJ, et al. Adeno-Associated Virus Vector Mediated Delivery of the HBV Genome Induces Chronic Hepatitis B Virus Infection and Liver Fibrosis in Mice. *PloS One* (2015) 10: e130052. doi: 10.1371/journal.pone.0130052
66. Lucifora J, Salvetti A, Marniquet X, Mailly L, Testoni B, Fusil F, et al. Detection of the Hepatitis B Virus (HBV) Covalently-Closed-Circular DNA (cccDNA) in Mice Transduced With a Recombinant AAV-HBV Vector. *Antiviral Res* (2017) 145:14–9. doi: 10.1016/j.antiviral.2017.07.006
67. Ziegler RJ, Cherry M, Barbon CM, Li C, Bercury SD, Armentano D, et al. Correction of the Biochemical and Functional Deficits in Fabry Mice Following AAV8-Mediated Hepatic Expression of Alpha-Galactosidase a. *Mol Ther* (2007) 15:492–500. doi: 10.1038/sj.mt.6300066
68. Li F, Wang Z, Hu F, Su L. Cell Culture Models and Animal Models for HBV Study. *Adv Exp Med Biol* (2020) 1179:109–35. doi: 10.1007/978-981-13-9151-4_5
69. Qi Z, Li G, Hu H, Yang C, Zhang X, Leng Q, et al. Recombinant Covalently Closed Circular Hepatitis B Virus DNA Induces Prolonged Viral Persistence in Immunocompetent Mice. *J Virol* (2014) 88:8045–56. doi: 10.1128/JVI.01024-14
70. Li G, Zhu Y, Shao D, Chang H, Zhang X, Zhou D, et al. Recombinant Covalently Closed Circular DNA of Hepatitis B Virus Induces Long-Term Viral Persistence With Chronic Hepatitis in a Mouse Model. *Hepatology* (2018) 67:56–70. doi: 10.1002/hep.29406
71. Kruse RL, Legras X, Barzi M. Cre/LoxP-HBV Plasmids Generating Recombinant Covalently Closed Circular DNA Genome Upon Transfection. *Virus Res* (2021) 292:198224. doi: 10.1016/j.virusres.2020.198224
72. Dong C, Qu L, Wang H, Wei L, Dong Y, Xiong S. Targeting Hepatitis B Virus cccDNA by CRISPR/Cas9 Nuclease Efficiently Inhibits Viral Replication. *Antiviral Res* (2015) 118:110–7. doi: 10.1016/j.antiviral.2015.03.015
73. Kennedy EM, Kornepati AV, Cullen BR. Targeting Hepatitis B Virus cccDNA Using CRISPR/Cas9. *Antiviral Res* (2015) 123:188–92. doi: 10.1016/j.antiviral.2015.10.004
74. Chisari FV. Hepatitis B Virus Transgenic Mice: Insights Into the Virus and the Disease. *Hepatology* (1995) 22:1316–25. doi: 10.1016/0270-9139(95)90645-2
75. Araki K, Miyazaki J, Hino O, Tomita N, Chisaka O, Matsubara K, et al. Expression and Replication of Hepatitis B Virus Genome in Transgenic Mice. *Proc Natl Acad Sci* (1989) 86:207–11. doi: 10.1073/pnas.86.1.207
76. Guidotti LG, Matzke B, Schaller H, Chisari FV. High-Level Hepatitis B Virus Replication in Transgenic Mice. *J Virol* (1995) 69:6158–69. doi: 10.1128/jvi.69.10.6158-6169.1995
77. Chisari F, Pinkert C, Milich D, Filippi P, McLachlan A, Palmiter R, et al. A Transgenic Mouse Model of the Chronic Hepatitis B Surface Antigen Carrier State. *Science* (1985) 230:1157–60. doi: 10.1126/science.3865369
78. Chisari FV, Filippi P, McLachlan A, Milich DR, Riggs M, Lee S, et al. Expression of Hepatitis B Virus Large Envelope Polypeptide Inhibits Hepatitis B Surface Antigen Secretion in Transgenic Mice. *J Virol* (1986) 60:880–7. doi: 10.1128/jvi.60.3.880-887.1986
79. Guidotti LG, Martinez V, Loh YT, Rogler CE, Chisari FV. Hepatitis B Virus Nucleocapsid Particles do Not Cross the Hepatocyte Nuclear Membrane in Transgenic Mice. *J Virol* (1994) 68:5469–75. doi: 10.1128/jvi.68.9.5469-5475.1994
80. Milich DR, Jones JE, Hughes JL, Price J, Raney AK, McLachlan A. Is a Function of the Secreted Hepatitis B E Antigen to Induce Immunologic Tolerance *in Utero*? *Proc Natl Acad Sci* (1990) 87:6599–603. doi: 10.1073/pnas.87.17.6599
81. Kim C, Koike K, Saito I, Miyamura T, Jay G. HBx Gene of Hepatitis B Virus Induces Liver Cancer in Transgenic Mice. *Nature* (1991) 351:317–20. doi: 10.1038/351317a0
82. Chisari FV, Klopchin K, Moriyama T, Pasquinelli C, Dunsford HA, Sell S, et al. Molecular Pathogenesis of Hepatocellular Carcinoma in Hepatitis B Virus Transgenic Mice. *Cell* (1989) 59:1145–56. doi: 10.1016/0092-8674(89)90770-8
83. Churin Y, Roderfeld M, Stiefel J, Wurger T, Schroder D, Matono T, et al. Pathological Impact of Hepatitis B Virus Surface Proteins on the Liver Is Associated With the Host Genetic Background. *PloS One* (2014) 9:e90608. doi: 10.1371/journal.pone.0090608
84. Graumann F, Churin Y, Tschuschner A, Reifenberg K, Glebe D, Roderfeld M, et al. Genomic Methylation Inhibits Expression of Hepatitis B Virus Envelope Protein in Transgenic Mice: A Non-Infectious Mouse Model to Study Silencing of HBV Surface Antigen Genes. *PloS One* (2015) 10:e146099. doi: 10.1371/journal.pone.0146099
85. Yu D, Moon H, Son J, Jeong S, Yu S, Yoon H, et al. Incidence of Hepatocellular Carcinoma in Transgenic Mice Expressing the Hepatitis B Virus X-Protein. *J Hepatol* (1999) 31:123–32. doi: 10.1016/S0168-8278(99)80172-X
86. Koike K, Moriya K, Iino S, Yotsuyanagi H, Endo Y, Miyamura T, et al. High-Level Expression of Hepatitis B Virus HBx Gene and Hepatocarcinogenesis in Transgenic Mice. *Hepatology* (1994) 19:810–9. doi: 10.1002/hep.1840190403
87. Lee TH, Finegold MJ, Shen RF, DeMayo JL, Woo SL, Butel JS. Hepatitis B Virus Transactivator X Protein Is Not Tumorigenic in Transgenic Mice. *J Virol* (1990) 64:5939–47. doi: 10.1128/jvi.64.12.5939-5947.1990
88. Perfumo S, Amicone L, Colloca S, Giorgio M, Pozzi L, Tripodi M. Recognition Efficiency of the Hepatitis B Virus Polyadenylation Signals Is Tissue Specific in Transgenic Mice. *J Virol* (1992) 66:6819–23. doi: 10.1128/jvi.66.11.6819-6823.1992
89. Quetier I, Brezillon N, Revaud J, Ahodantin J, DaSilva L, Soussan P, et al. C-Terminal-Truncated Hepatitis B Virus X Protein Enhances the Development of Diethylnitrosamine-Induced Hepatocellular Carcinogenesis. *J Gen Virol* (2015) 96:614–25. doi: 10.1099/vir.0.070680-0
90. Wang Y, Cui F, Lv Y, Li C, Xu X, Deng C, et al. HBsAg and HBx Knocked Into the P21 Locus Causes Hepatocellular Carcinoma in Mice. *Hepatology* (2004) 39:318–24. doi: 10.1002/hep.20076
91. Ando K, Moriyama T, Guidotti LG, Wirth S, Schreiber RD, Schlicht HJ, et al. Mechanisms of Class I Restricted Immunopathology. A Transgenic Mouse Model of Fulminant Hepatitis. *J Exp Med* (1993) 178:1541–54. doi: 10.1084/jem.178.5.1541
92. Moriyama T, Guilhot S, Klopchin K, Moss B, Pinkert CA, Palmiter RD, et al. Immunobiology and Pathogenesis of Hepatocellular Injury in Hepatitis B Virus Transgenic Mice. *Science* (1990) 248:361–4. doi: 10.1126/science.1691527
93. Klein C, Bock CT, Wedemeyer H, Wustefeld T, Locarnini S, Dienes HP, et al. Inhibition of Hepatitis B Virus Replication *In Vivo* by Nucleoside Analogues and siRNA. *Gastroenterology* (2003) 125:9–18. doi: 10.1016/S0016-5085(03)00720-0
94. Marimani MD, Ely A, Buff MC, Bernhardt S, Engels JW, Scherman D, et al. Inhibition of Replication of Hepatitis B Virus in Transgenic Mice Following Administration of Hepatotropic Lipoplexes Containing Guanidinopropyl-Modified siRNAs. *J Control Release* (2015) 209:198–206. doi: 10.1016/j.jconrel.2015.04.042
95. Wieland SF, Guidotti LG, Chisari FV. Intrahepatic Induction of Alpha/Beta Interferon Eliminates Viral RNA-Containing Capsids in Hepatitis B Virus Transgenic Mice. *J Virol* (2000) 74:4165–73. doi: 10.1128/JVI.74.9.4165-4173.2000
96. McClary H, Koch R, Chisari FV, Guidotti LG. Relative Sensitivity of Hepatitis B Virus and Other Hepatotropic Viruses to the Antiviral Effects of Cytokines. *J Virol* (2000) 74:2255–64. doi: 10.1128/JVI.74.5.2255-2264.2000
97. Julander JG, Sidwell RW, Morrey JD. Characterizing Antiviral Activity of Adefovir Dipivoxil in Transgenic Mice Expressing Hepatitis B Virus. *Antiviral Res* (2002) 55:27–40. doi: 10.1016/S0166-3542(01)00223-6
98. Weber O, Schlemmer KH, Hartmann E, Hagelschuer I, Paessens A, Graef E, et al. Inhibition of Human Hepatitis B Virus (HBV) by a Novel Non-Nucleosidic Compound in a Transgenic Mouse Model. *Antiviral Res* (2002) 54:69–78. doi: 10.1016/S0166-3542(01)00216-9
99. Julander JG, Colonno RJ, Sidwell RW, Morrey JD. Characterization of Antiviral Activity of Entecavir in Transgenic Mice Expressing Hepatitis B Virus. *Antiviral Res* (2003) 59:155–61. doi: 10.1016/S0166-3542(03)00109-8

100. Lempp FA, Mutz P, Lipps C, Wirth D, Bartenschlager R, Urban S. Evidence That Hepatitis B Virus Replication in Mouse Cells Is Limited by the Lack of a Host Cell Dependency Factor. *J Hepatol* (2016) 64:556–64. doi: 10.1016/j.jhep.2015.10.030
101. Dandri M, Burda MR, Torok E, Pollok JM, Iwanska A, Sommer G, et al. Repopulation of Mouse Liver With Human Hepatocytes and *In Vivo* Infection With Hepatitis B Virus. *Hepatology* (2001) 33:981–8. doi: 10.1053/jhep.2001.23314
102. Meuleman P, Libbrecht L, De Vos R, de Hemptinne B, Gevaert K, Vandekerckhove J, et al. Morphological and Biochemical Characterization of a Human Liver in a uPA-SCID Mouse Chimera. *Hepatology* (2005) 41:847–56. doi: 10.1002/hep.20657
103. Sun S, Li J. Humanized Chimeric Mouse Models of Hepatitis B Virus Infection. *Int J Infect Dis* (2017) 59:131–6. doi: 10.1016/j.ijid.2017.04.002
104. Brezillon NM, DaSilva L, L'Hote D, Bernex F, Piquet J, Binart N, et al. Rescue of Fertility in Homozygous Mice for the Urokinase Plasminogen Activator Transgene by the Transplantation of Mouse Hepatocytes. *Cell Transplant* (2008) 17:803–12. doi: 10.3727/096368908786516800
105. Azuma H, Paulk N, Ranade A, Dorrell C, Al-Dhalimy M, Ellis E, et al. Robust Expansion of Human Hepatocytes in Fah-/-/Rag2-/-/Il2rg-/- Mice. *Nat Biotechnol* (2007) 25:903–10. doi: 10.1038/nbt1326
106. Grompe M, Al-Dhalimy M, Finegold M, Ou CN, Burlingame T, Kennaway NG, et al. Loss of Fumarylacetoacetate Hydrolase Is Responsible for the Neonatal Hepatic Dysfunction Phenotype of Lethal Albino Mice. *Genes Dev* (1993) 7:2298–307. doi: 10.1101/gad.7.12a.2298
107. Bissig KD, Le TT, Woods NB, Verma IM. Repopulation of Adult and Neonatal Mice With Human Hepatocytes: A Chimeric Animal Model. *Proc Natl Acad Sci USA* (2007) 104:20507–11. doi: 10.1073/pnas.0710528105
108. Hasegawa M, Kawai K, Mitsui T, Taniguchi K, Monnai M, Wakui M, et al. The Reconstituted 'Humanized Liver' in TK-NOG Mice Is Mature and Functional. *Biochem Biophys Res Commun* (2011) 405:405–10. doi: 10.1016/j.bbrc.2011.01.042
109. Kosaka K, Hiraga N, Imamura M, Yoshimi S, Murakami E, Nakahara T, et al. A Novel TK-NOG Based Humanized Mouse Model for the Study of HBV and HCV Infections. *Biochem Biophys Res Commun* (2013) 441:230–5. doi: 10.1016/j.bbrc.2013.10.040
110. Tsuge M, Hiraga N, Takaishi H, Noguchi C, Oga H, Imamura M, et al. Infection of Human Hepatocyte Chimeric Mouse With Genetically Engineered Hepatitis B Virus. *Hepatology* (2005) 42:1046–54. doi: 10.1002/hep.20892
111. Lutgehetmann M, Volz T, Kopke A, Broja T, Tigges E, Lohse AW, et al. *In Vivo* Proliferation of Hepadnavirus-Infected Hepatocytes Induces Loss of Covalently Closed Circular DNA in Mice. *Hepatology* (2010) 52:16–24. doi: 10.1002/hep.23611
112. Petersen J, Dandri M, Mier W, Lutgehetmann M, Volz T, von Weizsacker F, et al. Prevention of Hepatitis B Virus Infection *In Vivo* by Entry Inhibitors Derived From the Large Envelope Protein. *Nat Biotechnol* (2008) 26:335–41. doi: 10.1038/nbt1389
113. Lutgehetmann M, Mancke LV, Volz T, Helbig M, Allweiss L, Bornscheuer T, et al. Humanized Chimeric uPA Mouse Model for the Study of Hepatitis B and D Virus Interactions and Preclinical Drug Evaluation. *Hepatology* (2012) 55:685–94. doi: 10.1002/hep.24758
114. Washburn ML, Bility MT, Zhang L, Kovalev GI, Buntzman A, Frelinger JA, et al. A Humanized Mouse Model to Study Hepatitis C Virus Infection, Immune Response, and Liver Disease. *Gastroenterology* (2011) 140:1334–44. doi: 10.1053/j.gastro.2011.01.001
115. Bility MT, Zhang L, Washburn ML, Curtis TA, Kovalev GI, Su L. Generation of a Humanized Mouse Model With Both Human Immune System and Liver Cells to Model Hepatitis C Virus Infection and Liver Immunopathogenesis. *Nat Protoc* (2012) 7:1608–17. doi: 10.1038/nprot.2012.083
116. Irudayaswamy A, Muthiah M, Zhou L, Hung H, Jumat N, Haque J, et al. Long-Term Fate of Human Fetal Liver Progenitor Cells Transplanted in Injured Mouse Livers. *Stem Cells* (2018) 36:103–13. doi: 10.1002/stem.2710
117. Bility MT, Cheng L, Zhang Z, Luan Y, Li F, Chi L, et al. Hepatitis B Virus Infection and Immunopathogenesis in a Humanized Mouse Model: Induction of Human-Specific Liver Fibrosis and M2-Like Macrophages. *PloS Pathog* (2014) 10:e1004032. doi: 10.1371/journal.ppat.1004032
118. Okazaki A, Hiraga N, Imamura M, Hayes CN, Tsuge M, Takahashi S, et al. Severe Necroinflammatory Reaction Caused by Natural Killer Cell-Mediated Fas/Fas Ligand Interaction and Dendritic Cells in Human Hepatocyte Chimeric Mouse. *Hepatology* (2012) 56:555–66. doi: 10.1002/hep.25651
119. Likhitsup A, Lok AS. Understanding the Natural History of Hepatitis B Virus Infection and the New Definitions of Cure and the Endpoints of Clinical Trials. *Clin Liver Dis* (2019) 23:401–16. doi: 10.1016/j.cld.2019.04.002
120. Wedemeyer H. The Widespread Rarity of HBsAg Loss in Chronic Hepatitis B. *Lancet Gastroenterol Hepatol* (2019) 4:190–2. doi: 10.1016/S2468-1253(18)30384-4
121. Lok AS, Zoulim F, Dusheiko G, Ghany MG. Hepatitis B Cure: From Discovery to Regulatory Approval. *J Hepatol* (2017) 67:847–61. doi: 10.1016/j.jhep.2017.05.008
122. Fanning GC, Zoulim F, Hou J, Bertoletti A. Therapeutic Strategies for Hepatitis B Virus Infection: Towards a Cure. *Nat Rev Drug Discovery* (2019) 18:827–44. doi: 10.1038/s41573-019-0037-0

Conflict of Interest: The authors declare that the research was conducted in the absence of any commercial or financial relationships that could be construed as a potential conflict of interest.

frontiers in Immunology

ORIGINAL RESEARCH
published: 21 January 2022
doi: 10.3389/fimmu.2021.757379

Murine CXCR3$^+$CXCR6$^+$γδT Cells Reside in the Liver and Provide Protection Against HBV Infection

Yanan Wang[1†], Yun Guan[1,2†], Yuan Hu[1], Yan Li[3], Nan Lu[4] and Cai Zhang[1*]*

[1] Institute of Immunopharmaceutical Sciences, School of Pharmaceutical Sciences, Cheeloo College of Medicine, Shandong University, Jinan, China, [2] Jining No. 1 People's Hospital, Jining, China, [3] Institute of Biomedical Sciences, College of Life Sciences, Shandong Normal University, Jinan, China, [4] Institute of Diagnostics, School of Medicine, Cheeloo College of Medicine, Shandong University, Jinan, China

OPEN ACCESS

Edited by:
Mengji Lu,
Essen University Hospital, Germany

Reviewed by:
Yongyan Chen,
University of Science and Technology of China, China
Sivasankaran M. Ponnan,
Fred Hutchinson Cancer Research Center, United States

***Correspondence:**
Cai Zhang
caizhangsd@sdu.edu.cn
Nan Lu
lunan@sdu.edu.cn

[†]These authors have contributed equally to this work

Specialty section:
This article was submitted to Viral Immunology, a section of the journal Frontiers in Immunology

Received: 12 August 2021
Accepted: 28 December 2021
Published: 21 January 2022

Citation:
Wang Y, Guan Y, Hu Y, Li Y, Lu N and Zhang C (2022) Murine CXCR3$^+$CXCR6$^+$γδT Cells Reside in the Liver and Provide Protection Against HBV Infection. Front. Immunol. 12:757379. doi: 10.3389/fimmu.2021.757379

Gamma delta (γδ) T cells play a key role in the innate immune response and serve as the first line of defense against infection and tumors. These cells are defined as tissue-resident lymphocytes in skin, lung, and intestinal mucosa. They are also relatively abundant in the liver; however, little is known about the residency of hepatic γδT cells. By comparing the phenotype of murine γδT cells in liver, spleen, thymus, and small intestine, a CXCR3$^+$CXCR6$^+$ γδT-cell subset with tissue-resident characteristics was found in liver tissue from embryos through adults. Liver sinusoidal endothelial cells mediated retention of CXCR3$^+$CXCR6$^+$ γδT cells through the interactions between CXCR3 and CXCR6 and their chemokines. During acute HBV infection, CXCR3$^+$CXCR6$^+$ γδT cells produced high levels of IFN-γ and adoptive transfer of CXCR3$^+$CXCR6$^+$ γδT cells into acute HBV-infected TCRδ$^{-/-}$ mice leading to lower HBsAg and HBeAg expression. It is suggested that liver resident CXCR3$^+$CXCR6$^+$ γδT cells play a protective role during acute HBV infection. Strategies aimed at expanding and activating liver resident CXCR3$^+$CXCR6$^+$ γδT cells both *in vivo* or *in vitro* have great prospects for use in immunotherapy that specifically targets acute HBV infection.

Keywords: liver, γδT cells, residency, liver-resident γδT cells, chemotaxis, HBV infection

INTRODUCTION

The liver is not only involved in regulating metabolism but also has important immunological characteristics (1, 2). Liver tissue is enriched with innate immune cells that can effectively and quickly defend against invading microorganisms and tumor transformation (3–5). Lymphocytes are classically viewed as continuously circulating in peripheral organs; however, recent studies demonstrate the existence of tissue-resident lymphocytes in the skin, lung, and intestinal mucosa and other peripheral organs, where they exert protective immunity to infection and malignancy (6–9). Notably, the liver contains multiple resident lymphocytes including memory CD8$^+$ T (T_{RM}) cells, invariant natural killer T (iNKT) cells, mucosal-associated invariant T (MAIT) cells, and natural killer (NK) cells (10, 11). Liver-resident lymphocytes have a similar distribution, phenotype, and method of transcriptional regulation and function (12–15).

γδT cells are a unique subset of innate-like T lymphocytes with diverse structural and functional heterogeneity. Unlike αβT cells, γδT cells recognize antigens independent of MHC restriction and do not require antigen processing and presentation (16, 17). Murine γδT cells constitute only a small proportion of lymphocytes in peripheral organs—such as spleen and lymph nodes—but are abundant in the liver, accounting for 3%–5% of all intrahepatic lymphocytes. In an acute HBV infection model, the number of hepatic γδT cells significantly increases and exhibits elevated expression of the activation marker, CD69 (18). However, the role of γδT cells during the early stages of acute HBV infection is not well defined. γδT cells are present in high numbers in epithelial and mucosal barriers and several γδT-cell subsets naturally establish residency at barrier sites, as illustrated by the presence of $V\gamma5^+$ and $V\gamma3V\delta1^+$ T-cell subsets in the intestinal epithelium and epidermis, respectively (19–22). Tian's group reported a liver-resident γδT population maintained by gut commensal microbes through CD1d/lipid antigens. This liver-resident γδT-cell population predominantly produced IL-17A and accelerated the progression of nonalcoholic fatty liver disease (23). However, there is a limited understanding of the resident characteristics of γδT cells in the hepatic immune microenvironment. A deeper and more comprehensive understanding of liver-resident γδT cells will inform the development of novel treatments for diverse liver diseases.

MATERIALS AND METHODS

Animals

Five to 8-week-old male C57BL/6J, BALB/c, and nude mice were purchased from Beijing Hua Fukang Bioscience Co., Ltd. (Beijing, China). $TCR\delta^{-/-}$ mice were a gift from Dr. Zhinan Yin (Nankai University). $CD45.1^+$ mice were a gift from Dr. Zhigang Tian (University of Science and Technology of China). All mice were housed in a specific pathogen-free facility under ethical conditions. Experiments were performed with age- and sex-matched animals according to the guidelines for experimental animals from Shandong University and were approved by the Committee on the Ethics of Animal Experiments of Shandong University (Jinan, China) (2017-D023).

Acute HBV Infection Model

The pAAV plasmid and the pAAV-HBV1.2 plasmid containing the full-length HBV DNA were kindly provided by Dr. Peijer Chen (National Taiwan University College of Medicine, Taipei, China). An acute HBV infection model was established by hydrodynamic injection of 20 μg pAAV-HBV1.2 plasmid in 1× phosphate buffer solution (PBS) equivalent to 10% of the mouse body weight by way of the tail veil into wild-type (WT) C57BL/6J and $TCR\delta^{-/-}$ mice (24).

Parabiosis

Parabiosis was established as described previously (25). In brief, 5- to 6-week-old male $CD45.1^+$ and $CD45.2^+$ C57BL/6J mice were matched for body weight and anaesthetized prior to surgery. An incision along the lateral aspect was performed from 0.5 cm above the elbow to 0.5 cm below the knee joint, and the skin was gently detached from the subcutaneous fascia. The knee joints and skins of the paired mice were attached from the elbow to the knee with nonabsorbable silk. Neomycin was added to the drinking water for 7 days. Two weeks after parabiosis, two mice shared the blood circulation.

Cell Isolation

Mice were sacrificed, and the bone marrow (BM), inguinal lymph node (iLN), spleen, liver, thymus, intestine, and skin were collected. MNCs from each organ were separated and mononuclear cells (MNCs) were collected. In brief, iLN and thymus were passed through a 200-gauge steel mesh and centrifuged at 400×*g* for 5 min in 1 × PBS. Spleens were first passed through a 200-gauge steel mesh, lysed with red blood cell (RBC) lysis buffer and washed with 1 × PBS. Bone marrows were washed by syringe, and MNCs were harvested after RBC lysis and washing. Livers were passed through a 200-gauge steel mesh, and the cell pellets were collected. MNCs were isolated by gradient centrifugation with 40% Percoll at 800×*g* for 25 min and harvested after RBC lysis and washing. Skins were excised and minced into small pieces, then digested with 0.04% collagenase I (Gibco, Carlsbad, CA, USA) for 2 h at 37°C. The large pieces were removed by filtration, and the MNCs were obtained by gradient centrifugation with 40% and 70% Percoll. IELs were isolated from the small intestine as previously described (26, 27). Peyer's patches (PP) were surgically removed from the intestines and excised into small pieces. The specimens were then digested with prewarmed IEL digestive juice and incubated with stirring for 40 min at 37°C and passed over two nylon wool columns to remove undigested tissue debris. IELs were isolated by gradient centrifugation with 40% and 70% Percoll (GE Healthcare, Uppsala, Sweden).

The mice were anesthetized prior to a laparotomy to obtain the LSECs. The liver was perfused with EGTA/HBSS solution through the portal vein. The inferior vena cava was rapidly cut after the liver turned completely pale. Next, the liver was perfused with 37°C prewarmed Collagenase IV (Gibco) solution for 5 min, excised, and digested in collagenase solution for 15 min in a 37°C incubator. LSECs were obtained by gradient centrifugation with 25% and 50% Percoll. The cellular precipitate was resuspended in 1 ml DMEM+10% FBS medium and seeded into 24-well plates at a density of 1×10^5 cells/well. After 4 h, the supernatant was gently removed and replaced with 500 μl fresh DMEM medium.

Flow Cytometry

MNCs in a single-cell suspension were blocked with anti-CD16/32 (eBioscience, San Diego, CA, USA) and stained with a cocktail of antibodies specific for different cell types for 30 min at 4°C. The foxp3 staining kit (eBioscience) was used to stain the nucleus transcription factor. To detect expression of IL-17A and IFN-γ, the cells were stimulated with phorbol 12-myristate 13-acetate (PMA, 30 ng/ml, Sigma-Aldrich Co., St. Louis, MO, USA) and ionomycin (1 μg/ml, Sigma-Aldrich) for 4 h and treated with monensin (1 μg/ml, Sigma-Aldrich) and brefeldin A (BFA, 1 μg/ml, Biolegend, San Diego, CA, USA) after 1 h of stimulation. After surface staining, cells were fixed, permeabilized, and

stained with the indicated intracellular antibodies. Flow cytometry was performed using a fluorescence-activated cell sorter (FACS) Aria III (BD Biosciences, San Jose, CA, USA), and data were analyzed with FlowJo software (TreeStar Inc., Ashland, OR, USA). At least 3×10^5 total events were needed for the FACS analysis. Data are presented in **Supplementary Table S1**.

Cell Sorting and Adoptive Transfer

Hepatic MNCs were stained with anti-CD3e, anti-TCRγ/δ, anti-CXCR3, and anti-CXCR6 antibodies to sort $CXCR3^+CXCR6^+$ γδT cells using a FACS Aria III (BD Biosciences). The purity of the sorted cell populations was >95%. Approximately 50,000 purified $CXCR3^+CXCR6^+$ γδT cells in 200 μl 1 × PBS were intravenously injected into sublethally irradiated $TCR\delta^{-/-}$ mice (6.5 Gy given 1 day before adoptive transfer). An acute HBV infection model was established in WT, $TCR\delta^{-/-}$, and $TCR\delta^{-/-}$ mice after adoptive transfer of $CXCR3^+CXCR6^+$ γδT cells.

RNA Isolation and Real-Time PCR

Total γδT-cell RNA from the indicated tissues was extracted using TRIZOL reagent (Invitrogen, Carlsbad, CA, USA) according to the manufacturer's instructions. The RNA concentration was quantified using Nanodrop 2000 (Thermo Fisher, Waltham, MA, USA). cDNA was generated using a FastQuant RT Kit (Tiangen Biotech Co. Ltd., Beijing, China) and real-time polymerase chain reaction was performed using a SYBR Green SuperMix (Roche, Basel, Switzerland) on a LightCycler 480 platform (Roche). Relative mRNA levels were normalized to β-actin mRNA levels. The primers are described in **Supplementary Table S2**.

Transwell Assay

Hepatic MNCs were seeded at 5×10^5 in 100 μl serum-free RPMI-1640 media in the above inserts with a pore size of 0.4 μm. The lower chamber contained 500 μl DMEM medium with untreated LSECs or LSECs incubated with neutralizing chemokine-targeting antibodies at 37°C for 2 h. After a 2-h incubation, absolute numbers of the migrated cells were detected by FACSAria III.

Chemokine Detection by ELISA

The LSECs were inoculated into 24-well plates (1×10^5 cells/well). After culturing for 4 h, the supernatant was absorbed, washed three times with 1 × PBS, and replaced with fresh DMEM medium (500 μl). Cell culture supernatants were collected at 24 h. CXCL9, CXCL10, CXCL11, and CXCL16 chemokine levels were detected in the LSEC culture supernatants by ELISA (PeproTech, East Windsor, New Jersey, USA) according to the manufacturers' instructions.

Serum HBV Ag Assays

Serum hepatitis B surface Ag (HBsAg) and hepatitis BeAg (HBeAg) from mice with acute HBV infection were assayed using the HBsAg and HBeAg detection kits (Autobio, Zhengzhou, China) according to the manufacturer's instructions.

HBV DNA Detection

Serum HBV DNA copies were extracted from 50 μl serum and detected by quantitative PCR using a diagnostic kit for HBV DNA (Da An Gene, Guangzhou, China) according to the manufacturer's instructions.

Statistical Analysis

The data were analyzed using GraphPad Prism 7 software (GraphPad Software Inc., San Diego, CA, USA). Data are presented as the mean ± standard error of the mean (SEM). Differences between more than two groups were statistically analyzed by one-way analysis of variance (one-way ANOVA). A two-way ANOVA test was used to determine differences in HBsAg, HBeAg, and HBV DNA tests. A p-value <0.05 was considered statistically significant ($^*p < 0.05$; $^{**}p < 0.01$; $^{***}p < 0.001$).

RESULTS

$CXCR3^+CXCR6^+$ γδT Cells Only Exist in Liver

IELs and skin are rich in γδT cells, where they regulate inflammation, pathogen invasion, and tumor surveillance (22, 28, 29). In this study, the liver also had a higher proportion of γδT cells than other immune organs and tissues, including the BM, inguinal LN, spleen, and thymus (**Supplementary Figure S1** and **Figures 1A, B**). This finding correlates with results from a recent study (23).

This study also assessed the phenotype of γδT cells in liver, first by analyzing molecules associated with γδT-cell-induced cytokine production. Hepatic γδT cells expressed low levels of CD27, which is a fate determinant of γδT cells to express IFN-γ but not IL-17A. The expression was similar in γδT cells from the IEL but significantly lower than γδT cells from the spleen and thymus (30) (**Figure 1C**). Hepatic γδT cells also expressed higher levels of IL-2 receptor beta CD122, which is expressed on IFN-γ^+ γδT cells, compared with γδT cells from other immune organs and tissues (31) (**Figure 1C**). Hepatic γδT cells exhibited higher NKG2D expression, indicating that these cells may be involved in immune defense and tissue protection in the liver (**Figure 1D**). γδT cells induce effector–target cell apoptosis through the Fas–FasL pathway (32, 33). Hepatic γδT cells have a higher expression of Fas (CD95) than intestinal epithelial γδT cells but lower expression than thymic γδT cells (**Figure 1D**). Importantly, hepatic γδT cells expressed a high level of the adhesion and retention molecule, CD44, and a low level of the lymph node homing molecule, CD62L (**Figure 1E**). Overall, these data indicate that hepatic γδT cells exhibited a unique phenotype that was distinct from γδT cells found in other organs.

Chemokines and chemokine receptors regulate the trafficking and accumulation of lymphocytes in homeostasis and disease. The mRNA level of chemokine receptors in γδT cells was measured in multiple organs. As shown in **Figure 2A**, CXCR3, CXCR6, and CCR2 mRNA levels were higher in hepatic γδT cells than in other tissues and organs. Hepatic γδT cells from nude mice still retained high CXCR3 and CXCR6 expression

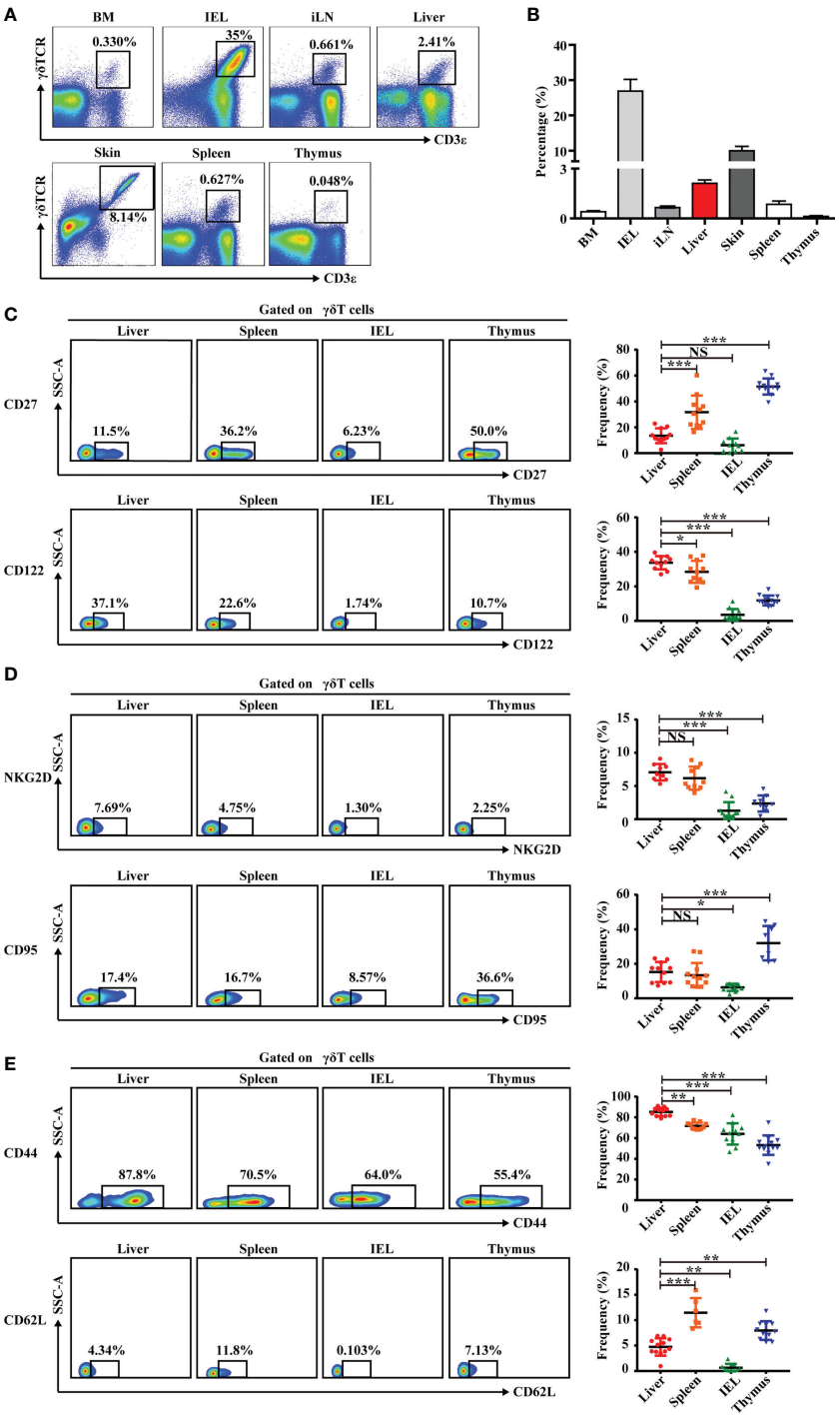

FIGURE 1 | Liver contains abundant γδT cells that exhibit a unique phenotype. **(A)** Representative FACS plots of γδT cells (CD3^{+}TCRγδ^{+}) in BM, IEL, iLN, liver, skin, spleen, and thymus of C57BL/6J mice. **(B)** Statistical analysis of γδT-cell percentages in the indicated organs. **(C–E)** Representative FACS plots (left) and percentage (right) of γδT surface markers on cells in indicated organs. Each dot represents a mouse. Data are shown as mean ± SEM. (*$p < 0.05$; **$p < 0.01$; ***$p < 0.001$. One-way ANOVA with *post-hoc* test). BM, bone marrow; IEL, intraepithelial lymphocyte; iLN, inguinal lymph node; NS, not significant.

(**Figure 2B**), indicating that thymus deficiency did not impact expression. CXCR3 and CXCR6 expression was further examined by flow cytometry. Results showed that hepatic γδT cells expressed higher levels of CXCR3 and CXCR6 than those from spleen, IEL, and thymus in C57BL/6J mice (**Supplementary Figure S2** and **Figure 2C**). Furthermore, the CXCR3^{+}CXCR6^{+}

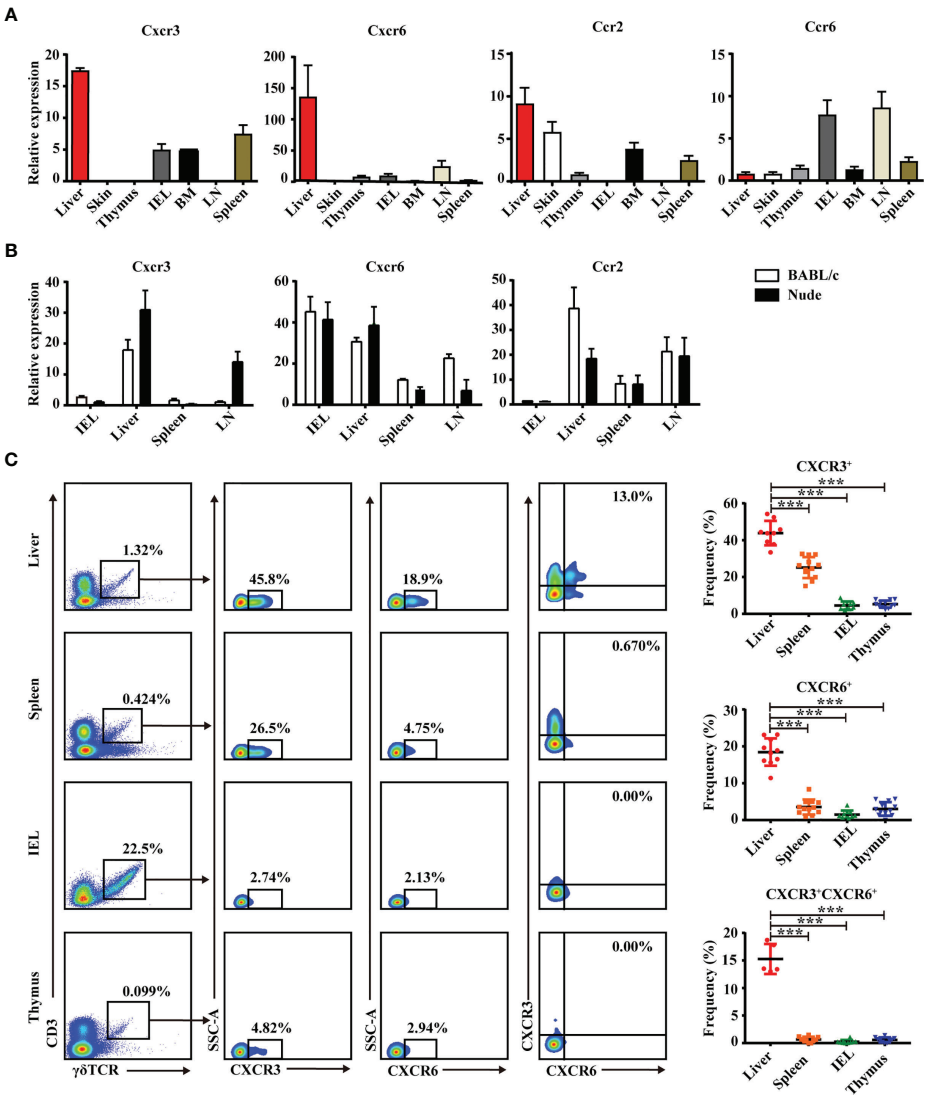

FIGURE 2 | Liver contains a specific CXCR3$^+$CXCR6$^+$ γδT subset. **(A)** CXCR3, CXCR6, CCR2, and CCR6 mRNA expression in γδT cells from indicated organs of C57BL/6J mice. **(B)** CXCR3, CXCR6, and CCR2 mRNA expression in γδT cells from IEL, liver, spleen, and iLN of BALB/c and nude mice. **(C)** Representative FACS plots and percentage of γδT cells expressing CXCR6 or CXCR3 in liver, spleen, IELs, and thymus of C57BL/6J mice. Each dot represents a mouse. Data are shown as mean ± SEM. (***$p < 0.001$. One-way ANOVA with *post-hoc* test).

γδT-cell subset was found in liver but not in the spleen, IEL, or thymus (**Figure 2C**). These data indicate that hepatic γδT cells exhibited a unique phenotype and the CXCR3$^+$CXCR6$^+$ γδT subset specifically exists in liver.

CXCR3$^+$CXCR6$^+$ γδT Cells Have Tissue-Resident Characteristics and Specifically Reside in Liver

Tissue-resident lymphocytes often express CD103, CD69, CD44, and CD49a, which mediate adhesion and retention, and lack the lymphoid homing markers, CD62L and CCR7 (6, 34). In this study, hepatic CXCR3$^+$CXCR6$^+$ γδT cells expressed high levels of CD69, CD103, CD44, and CD49a (**Figure 3A**) and low levels of CD62L and CCR7 (**Figure 3B** and **Supplementary Figure S3**). These cells also expressed a high level of the transcription factor, PLZF, which is important for innate tissue-resident lymphocytes like iNKT cells and MAIT cells (35), and a low level of BlIMP1, which correlates with diverse tissue-resident lymphocyte populations such as T_{RM} and NKT cells (**Figure 3C**). These data indicate that hepatic CXCR3$^+$CXCR6$^+$ γδT cells have tissue-resident characteristics.

To further confirm whether these cells specifically reside in liver, CD45.1$^+$ and CD45.2$^+$ mice were surgically joined by parabiosis (**Figure 3D**). After 2 weeks, the percentages of CD45.1$^+$ or CD45.2$^+$ cells in peripheral blood lymphocytes (PBLs) were equivalent, indicating that the parabiosis models were successfully established

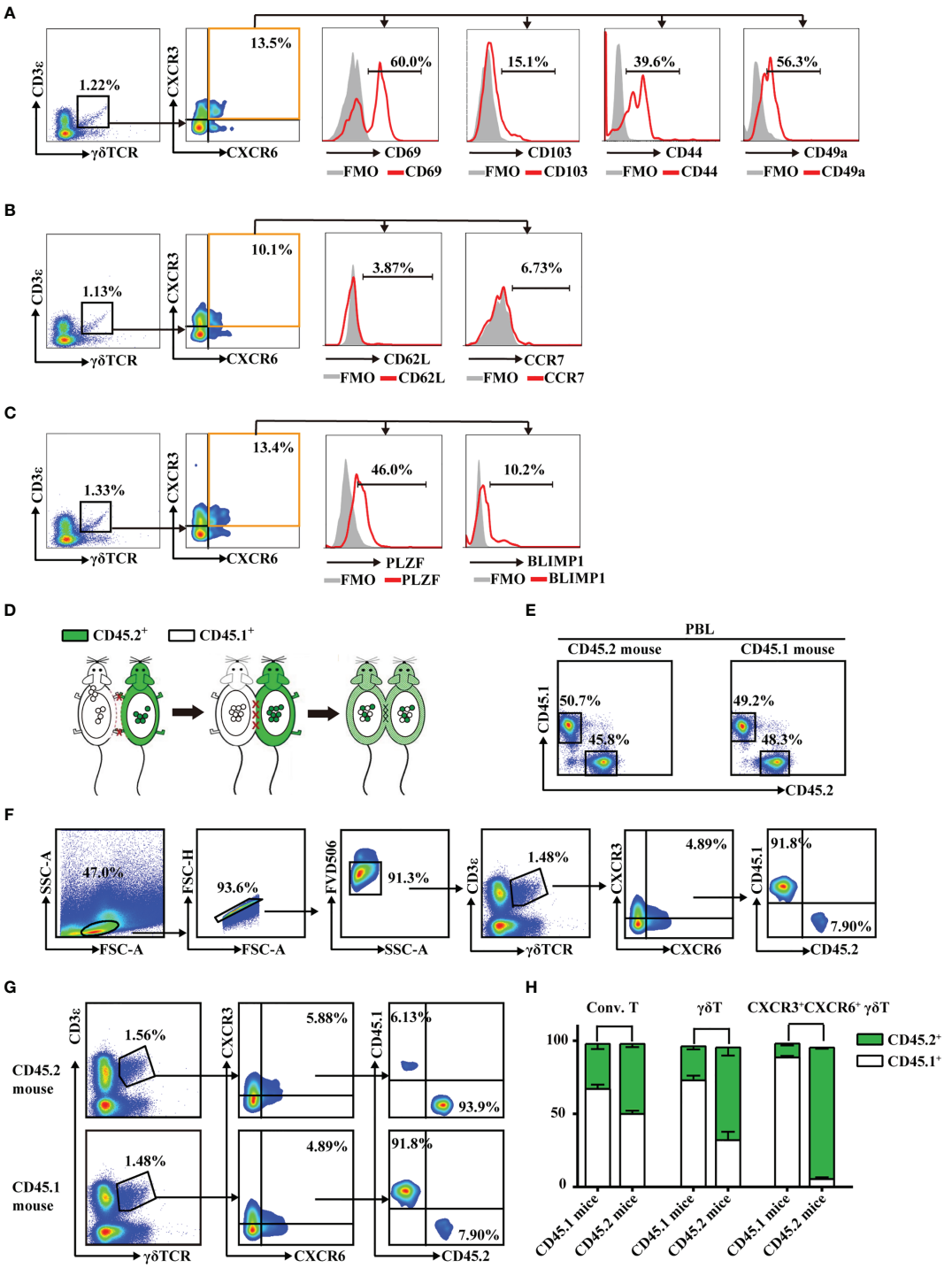

FIGURE 3 | CXCR3$^+$CXCR6$^+$ γδT cells have tissue-resident characteristics and specifically reside in liver. **(A–C)** FACS analysis of CD69, CD103, CD44, and CD49a **(A)**, CD62L and CCR7 **(B)**, and PLZF and Blimp1 **(C)** expression on hepatic CXCR3$^+$CXCR6$^+$ γδT cells from C57BL/6J mouse livers. **(D)** Parabiotic joining of CD45.1 and congenic CD45.2 mice led to the development of a shared circulatory system 2 weeks after surgery. **(E)** The percentages of CD45.1$^+$ and CD45.2$^+$ cells in peripheral blood lymphocytes (PBLs) in parabiosis models. **(F)** Gating strategy of CD45.1$^+$ or CD45.2$^+$ expression on hepatic CXCR3$^+$CXCR6$^+$ γδT cells. **(G)** The host origin (CD45.1$^+$ or CD45.2$^+$) of hepatic CXCR3$^+$CXCR6$^+$ γδT cells was identified by FACS analysis in each mouse in the CD45.1/CD45.2 parabiotic mouse pairs at 14 days postsurgery. **(H)** The percentage of CD45.1$^+$ or CD45.2$^+$ conventional T cells (CD3$^+$TCRγδ$^-$NK1.1$^-$), γδT cells (CD3$^+$TCRγδ$^+$), and CXCR3$^+$CXCR6$^+$ γδT cells from the liver of CD45.1/CD45.2 parabiotic B6 mouse.

(**Figure 3E**). The redistribution of γδT cells in each mouse in the CD45.1/CD45.2 parabiotic mouse pairs was assessed (**Figure 3F**). While conventional T cells were mutually exchanged, hepatic $CXCR3^+CXCR6^+$ γδT cells from the $CD45.1^+$ parabiont mice were almost entirely $CD45.1^+$, with very few $CD45.2^+$, while $CXCR3^+CXCR6^+$ γδT cells from the $CD45.2^+$ parabiont mice were primarily $CD45.2^+$ (**Figures 3G, H**). These data suggest that hepatic $CXCR3^+CXCR6^+$ γδT cells were seldom exchanged between $CD45.1^+$ and $CD45.2^+$ parabiont mice. In addition, 70%–80% $CXCR3^+CXCR6^-$ γδT cells and $CXCR3^-CXCR6^+$ γδT cells were $CD45.1^+$ in $CD45.1^+$ parabiont mice, whereas the reverse was observed in $CD45.2^+$ parabiont mice (**Supplementary Figure S4**). In summary, the parabiosis assay indicated that $CXCR3^+CXCR6^+$ γδT cells were predominantly retained in the liver, while $CXCR3^+CXCR6^-$ γδT cells and $CXCR3^-CXCR6^+$ γδT cells have less liver-resident features.

Liver-Resident $CXCR3^+CXCR6^+$ γδT Cells Exist in Liver From Embryo to Adulthood

In general, γδT cells are exported from the thymus at defined periods of fetal and neonatal development, and then migrate to and populate different peripheral tissues in adult animals (36). However, intestinal γδT cells can also develop in intestinal crypts and reside in the gut (37). To explore whether the existence of hepatic γδT cells was dependent on the thymus, the proportion of γδT cells in athymic nude and WT BALB/c mice were assessed. The proportion of intestinal γδT cells in nude mice was nearly identical to the proportion of intestinal γδT cells in WT BALB/c mice. Importantly, the liver still contained γδT cells in athymic nude mice despite the lack of γδT cells in the spleen (**Supplementary Figures S5A, B**). These data suggest that some hepatic γδT cells are not dependent on the thymus. Assessment of γδT cells during different stages of growth showed that they are found in liver and thymus from embryo to adulthood. As the mice grew, the percentage of γδT cells decreased in the thymus and increased in the liver (**Figure 4A** and **Supplementary Figure S6**). More importantly, $CXCR3^+CXCR6^+$ γδT cells were present in the liver from embryo to adulthood and the proportion increased as the mice aged; however, they were absent in the thymus during particular stages of growth (**Figure 4B**).

$CXCR3^+CXCR6^+$ γδT cells expressed high levels of the IFN-γ-associated transcriptional factor, T-bet, from embryo to adulthood, while rarely expressing the IL-17A-associated transcriptional factor, RORγt (**Figure 4C**). In addition, hepatic $CXCR3^+CXCR6^+$ γδT cells expressed a high level of tissue-resident-associated molecules like CD103 and CD69 and the transcription factor, PLZF, but rarely expressed CD62L during development (**Figure 4D** and **Supplementary Figure S7**).

In summary, these data collectively indicate that $CXCR3^+CXCR6^+$ γδT cells are retained in liver from embryo to adulthood and have tissue-resident characteristics during mouse development.

Liver Sinusoidal Endothelium Cells Mediate Retention of Liver-Resident $CXCR3^+CXCR6^+$ γδT Cells

LSECs secrete a variety of chemokines that promote the recruitment of immune cells (38, 39). Results from the present study showed that the liver-resident γδT-cell subset specifically expressed the chemokine receptors, CXCR3 and CXCR6. Thus, we hypothesized that chemotaxis may play an important role in the recruitment and retention of $CXCR3^+CXCR6^+$ γδT cells in the liver. LSECs were isolated and chemokines, including the ligands of CXCR3 (CXCL9, CXCL10, CXCL11) and the ligand of CXCR6 (CXCL16), were measured in the culture supernatants. LSECs produced high levels of CXCL9, CXCL11, and CXCL16 (**Figure 5A**). To further demonstrate the recruitment function of LSECs, a transwell assay was performed to test the chemotactic ability of chemokines secreted by LSECs on $CXCR3^+CXCR6^+$ γδT cells (**Figure 5B**). When the lower chamber contained untreated LSECs, $CXCR3^+CXCR6^+$ γδT cells were recruited from the above inserts. Chemotaxis was significantly reduced when CXCL9 and CXCL11 were neutralized, indicating that the chemokines, CXCL9 and CXCL11, play important roles in the retention of $CXCR3^+CXCR6^+$ γδT cells (**Figure 5C**). When CXCL16 was neutralized, the level of chemotaxis between the LSECs and $CXCR3^+CXCR6^+$ γδT cells was also weakened (**Figure 5C**). These findings indicate that the chemokines, CXCL9, CXCL11, and CXCL16, are all required for the retention of $CXCR3^+CXCR6^+$ γδT cells. Taken together, these results indicate that LSECs play an important role in retaining liver-resident $CXCR3^+CXCR6^+$ γδT cells through the interaction between the chemokine receptors, CXCR3 and CXCR6, and their ligands.

Liver-Resident $CXCR3^+CXCR6^+$ γδT Cells Play a Protective Role During Acute HBV Infection

Liver-resident $CXCR3^+CXCR6^+$ γδT cells produced high levels of IFN-γ and expressed a high level of the IFN-γ transcription factor, T-bet (**Supplementary Figure S8** and **Figures 6A, B**). However, these cells produced very little IL-17A and expressed low levels of the IL-17A transcription factor, RORγt (**Figures 6A, B**). The production of IFN-γ indicated that liver-resident $CXCR3^+CXCR6^+$ γδT cells may be involved in protective immunity against viruses and intracellular pathogens. In an acute HBV infection model, the proportion and absolute numbers of $CXCR3^+CXCR6^+$ γδT cells increased on day 7 and returned to normal levels as the infection progresses (**Figure 6C**). The expression of Ki67 was measured at different time points. On the third day after infection, $CXCR3^+CXCR6^+$ γδT cells showed significantly higher expression of Ki67, indicating that the proliferative capacity of $CXCR3^+CXCR6^+$ γδT cells was enhanced postinfection (**Figure 6D**). Notably, IFN-γ levels increased after 7 days postinfection (**Figure 6E**). These results indicate that liver-resident $CXCR3^+CXCR6^+$ γδT cells proliferate during acute HBV infection and IFN-γ from these cells may be involved in eliminating HBV. IL-17A secretion increased at the early stage of infection, and decreased after 10 days, and was then maintained at a low level (**Figure 6E**).

To further investigate the role of $CXCR3^+CXCR6^+$ γδT cells during HBV infection, the acute HBV infection model was established in WT, $TCR\delta^{-/-}$ mice, and $TCR\delta^{-/-}$ mice that were adoptively transferred with $CXCR3^+CXCR6^+$ γδT cells. HBsAg, HBeAg, and HBV DNA levels were measured in serum at

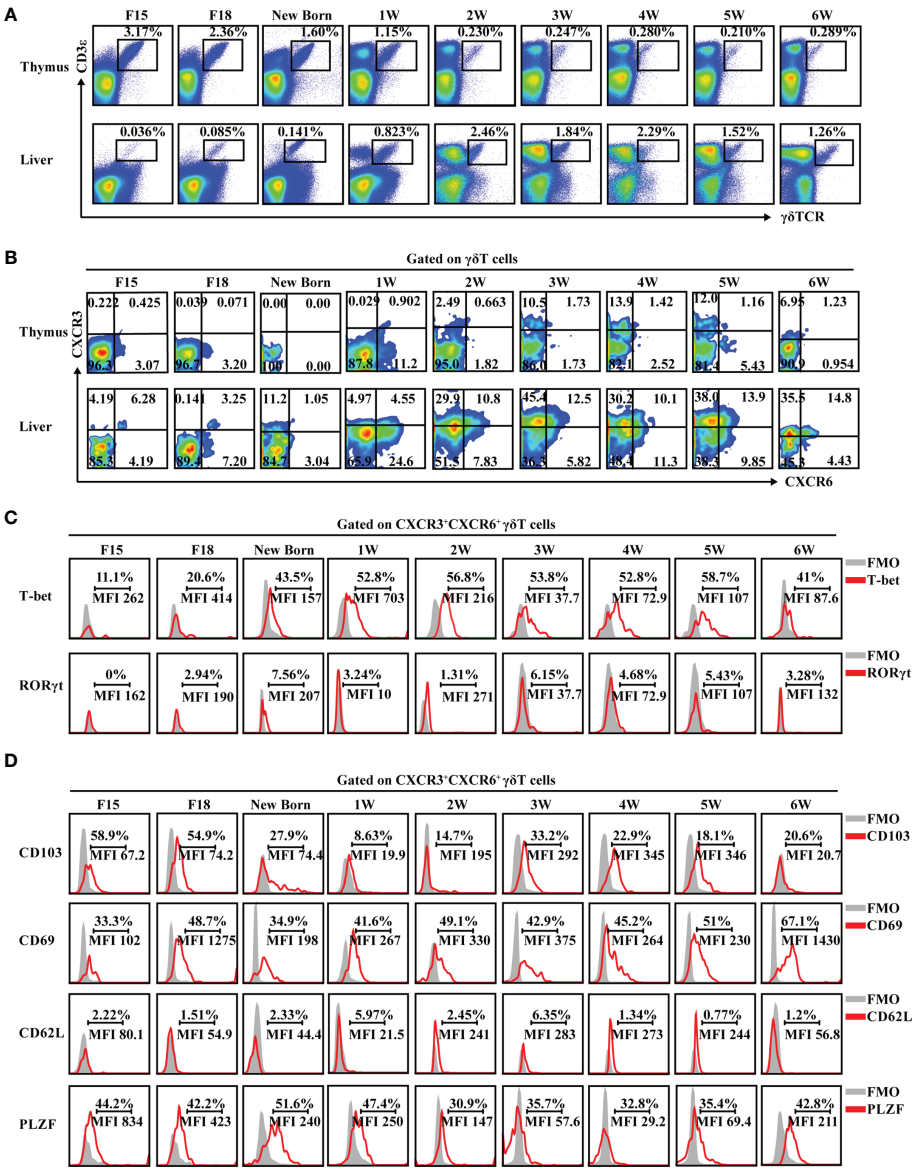

FIGURE 4 | CXCR3⁺CXCR6⁺ γδT cells exist in liver and express tissue-resident markers from embryo to adulthood. **(A)** FACS analysis of γδT cells in thymus (top) and liver (bottom) at different developmental stages of C57BL/6J mice. **(B)** FACS analysis of CXCR3⁺CXCR6⁺ γδT cells in the thymus and liver at the different developmental stages of C57BL/6J mice. **(C, D)** FACS analysis of T-bet and RORγt **(C)** and CD103, CD69, CD62L, and PLZF expression **(D)** in hepatic CXCR3⁺CXCR6⁺ γδT cells at the indicated ages over time.

different time points. TCRδ$^{-/-}$ mice that had received CXCR3⁺CXCR6⁺ γδT cells exhibited markedly lower serum HBsAg, HBeAg, and HBV DNA levels than TCRδ$^{-/-}$ mice that did not receive CXCR3⁺CXCR6⁺ γδT cells (**Figure 6F**). These data suggest that liver-resident CXCR3⁺CXCR6⁺ γδT cells may be involved in the clearance of HBV. Interestingly, TCRδ$^{-/-}$ mice had lower serum HBsAg, HBeAg, and HBV DNA than WT mice, suggesting that other subsets of γδT cells may have different or even opposing effects during acute HBV infection. The roles of other subsets of γδT cells in acute HBV infection deserved further research.

These findings demonstrate that liver-resident CXCR3⁺CXCR6⁺ γδT cells exert a protective role during acute HBV infection through production of IFN-γ.

DISCUSSION

In the present study, a unique γδT-cell subset characterized by CXCR3⁺CXCR6⁺ expression was specifically found to reside in murine liver. Moreover, these cells existed from embryo to adult and exhibited tissue-resident characteristics. LSECs promoted

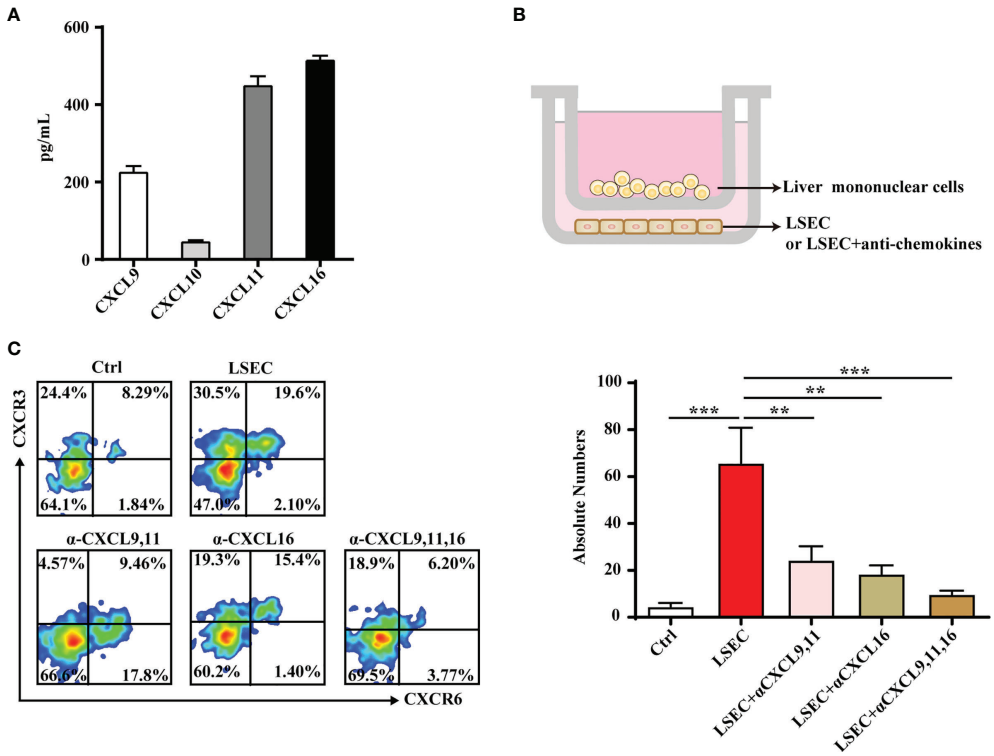

FIGURE 5 | LSECs promote the recruitment of CXCR3$^+$CXCR6$^+$ γδT cells to the liver. **(A)** Freshly isolated LSECs (1 × 10^5 per well) were seeded into 24-well plates and incubated at 37°C. The culture supernatant of each well was collected at 24 h and CXCL9, CXCL10, CXCL11, and CXCL16 levels in the culture supernatant were detected by ELISA. **(B)** Transwell was performed to test the chemotactic effect of LSECs to CXCR3$^+$CXCR6$^+$ γδT cells. The inserts were seeded with 5 × 10^5 liver mononuclear cells in 100 μl serum-free RPMI-1640 media. The lower chamber contained 500 μl DMEM medium with untreated LSECs or LSECs incubated with neutralizing antibodies specific for indicated chemokines at 37°C for 2 h. **(C)** FACS analysis (left) and absolute numbers (right) of CXCR3$^+$CXCR6$^+$ γδT cells in the lower chamber migrated from the upper insert after a 2-h incubation. Data are shown as mean ± SEM. (**$p < 0.01$; ***$p < 0.001$. One-way ANOVA with *post-hoc* test).

the recruitment and retention of CXCR3$^+$CXCR6$^+$ γδT cells by secreting CXCL9, CXCL11, and CXCL16. Importantly, liver-resident CXCR3$^+$CXCR6$^+$ γδT cells secreted high levels of IFN-γ and provided protection against acute HBV infection.

Tissue-resident lymphocytes share similar phenotypes, functional properties, and transcriptional regulation (10, 34). CXCR3 and CXCR6 are present in liver-resident NK cells and CD8$^+$ T cells (40–42). The engagement of chemokines and chemokine receptors is required for lymphocyte trafficking and retention in the liver. CXCR3 and its ligands mediate T-cell and TRAIL$^+$ liver-resident NK cell chemotaxis toward the liver (43, 44). Liver-resident NK cells, NKT cells, and CD8$^+$ T cells are selectively retained in liver in response to the chemotactic stimuli provided through the CXCR6 and CXCL16 interaction (45–47). Results from the present study provide the first evidence that CXCR3, CXCR6, and their ligands are critical for the accumulation and residency of γδT cells. Hepatic CXCR3$^+$CXCR6$^+$ γδT cells express PLZF, which is involved in a transcriptional network that promotes liver residency of human NK cells (48). A parabiosis model, one of the most common methods for assessing tissue residency (25), was used to further verify that CXCR3$^+$CXCR6$^+$ γδT cells specifically reside in the liver.

Similar to the intestine, the liver still contained γδT cells in athymic nude mice (**Supplementary Figure S5**), indicating that hepatic γδT cells do not dependent on the thymus. Furthermore, CXCR3$^+$CXCR6$^+$ γδT cells were not present in the thymus at all stages of growth, these cells were present in the liver from embryo to adulthood and the percentage increased as mice aged (**Figure 4**). These findings indicated that liver-resident CXCR3$^+$CXCR6$^+$ γδT cells may have a unique development pathway. While the thymus provides an inductive environment for the development of T cells from hematopoietic progenitor cells, prior studies have shown that γδT cells can develop extrathymically. Intestinal γδT cells, for example, can develop in intestinal crypts and reside in the gut (37, 49, 50). In addition, the adult liver contains hematopoietic stem and progenitor cells (HSPCs) and is believed to be an extramedullary hematopoietic organ (51–53). Hepatic heterogeneous Lin$^-$Sca-1$^+$c-Kit$^+$ (LSK, contains hematopoietic stem cells and multipotent progenitors) cells can differentiate into both myeloid cells and lymphocytes, including γδT cells, and type 1 innate lymphoid cells (ILC1s) (54–56). Our recent findings showed that liver hematopoietic progenitor Lin$^-$Sca-1$^+$Mac-1$^+$ (LSM) cells can differentiate into γδT-cell precursor (pre-γδT) cells and functionally mature IFN-

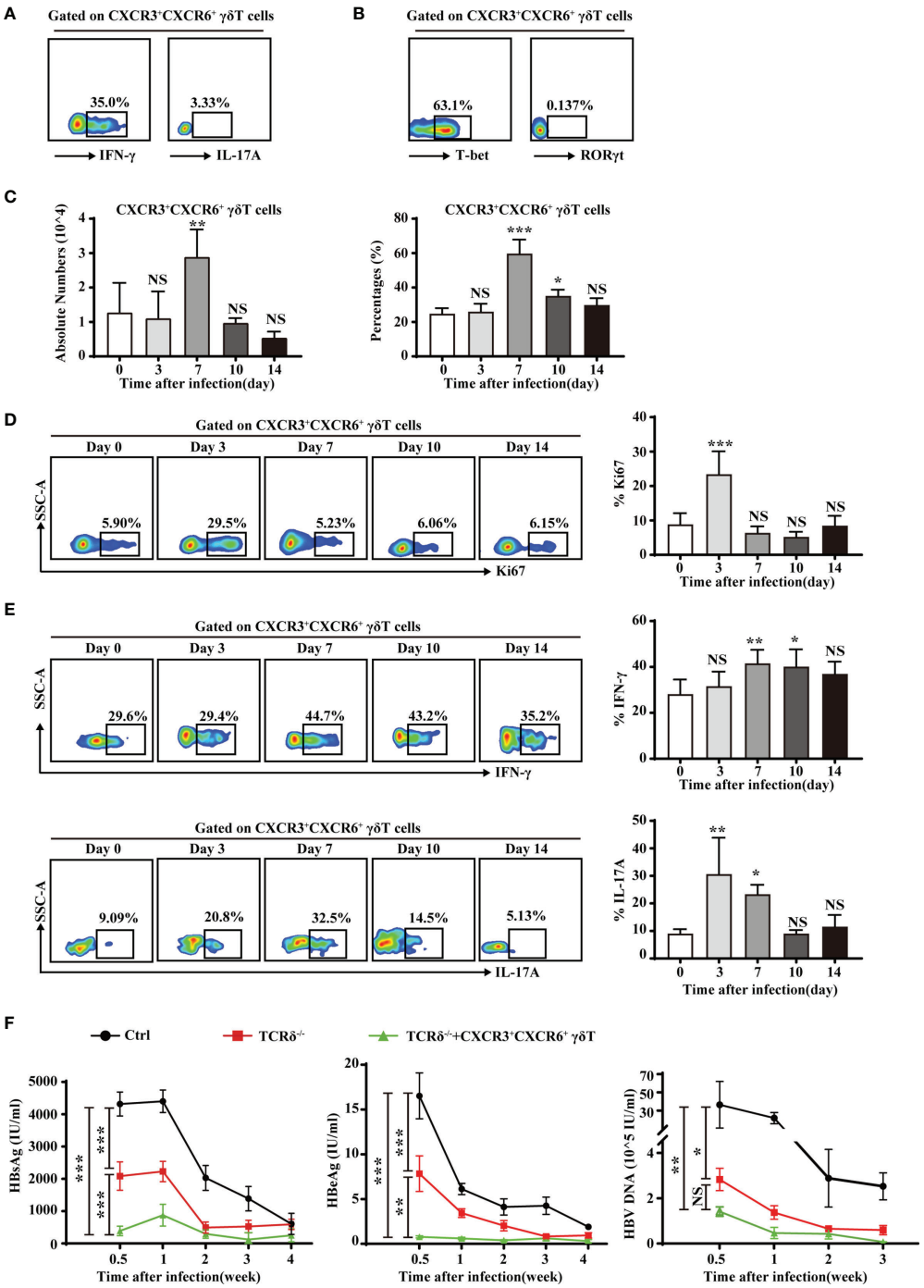

FIGURE 6 | Liver-resident CXCR3$^+$CXCR6$^+$ γδT cells contribute to the clearance of HBV. **(A)** IFN-γ and IL-17A expression on PMA/ionomycin-stimulated CXCR3$^+$CXCR6$^+$ γδT cells in the liver of C57BL/6J mice. **(B)** T-bet and RORγt expression in hepatic CXCR3$^+$CXCR6$^+$ γδT cells. **(C)** An acute HBV infection model was established by hydrodynamic injection of pAAV-HBV1.2 plasmid into the tail veil. The absolute numbers (left) and percentages (right) of liver-resident CXCR3$^+$CXCR6$^+$ γδT cells after acute HBV infection at the indicated time points. **(D)** FACS analysis (left) and statistical analysis (right) of Ki67 on CXCR3$^+$CXCR6$^+$ γδT cells after acute HBV infection at the indicated time points. **(E)** FACS analysis (left) and statistical analysis (right) of IFN-γ (top) and IL-17 (bottom) secreted by PMA/ionomycin-stimulated CXCR3$^+$CXCR6$^+$ γδT cells after acute HBV infection at the indicated time points. **(E)** HBsAg, HBeAg, and HBV DNA detection in serum at the indicated time points of an HBV acute infection model in WT, TCRδ$^{-/-}$, and TCRδ$^{-/-}$ mice after adoptive transfer of CXCR3$^+$CXCR6$^+$ γδT cells. Data are shown as mean ± SEM. [*$p < 0.05$; **$p < 0.01$; ***$p < 0.001$. One-way ANOVA with *post-hoc* test **(C–E)**, two-way ANOVA test **(F)**]. NS, not significant.

γ$^+$ γδT cells but not IL-17a$^+$ γδT cells in a thymus-independent manner. This research suggests that γδT cells are involved in a distinct developmental pathway that is independent of the thymus (57). More evidence is required to better understand how liver-resident CXCR3$^+$CXCR6$^+$ γδT cells develop.

γδT cells can establish long-lived memory and resident populations in response to local inflammation or pathogen invasion and exert long-term protective roles (19–21, 58). Circulating γδT cells participate in lymphoid stress surveillance during HBV infection with differential activation and differentiation (59). However, the role of liver-resident γδT cells during acute HBV infection remains unknown. In the current study, CXCR3$^+$CXCR6$^+$ γδT cells produced more IFN-γ and were associated with reduced disease severity after adoptive transfer into HBV-infected TCRδ$^{-/-}$ mice (**Figure 6**). These findings suggest that liver-resident CXCR3$^+$CXCR6$^+$ γδT cells inhibit acute HBV infection; however, the precise mechanism and memory characteristics of these cells require further study. In recent years, γδT cells have attracted more attention for potential use during tumor immunotherapy because of their strong cytotoxic effect on tumor cells, lack of MHC restriction on antigen recognition, and easy expansion both *in vitro* and *in vivo* (60–62). γδT cells are used for immunotherapy through *in vivo* stimulation with synthetic phosphoantigens like BrHPP, aminodicarbonates such as zoledronate, and glycolipid antigens presented by CD1d or adoptive transfer after expansion *ex vivo* (63–65). Current research is focused on combining direct antiviral agents and immunotherapy to treat HBV infection. Targeting the host immune system to strengthen innate and specific adaptive immune responses may help to eliminate this virus. DC vaccines, cytokine-induced killer (CIK) cells, immune checkpoint inhibitors, and genetically edited T cells (CAR/TCR-T) are used in the treatment of chronic viral infections and related cancers (66–68). In view of the antiviral effect of liver-resident CXCR3$^+$CXCR6$^+$ γδT cells, stimulation of these cells *in vivo* or adoptive transfer of liver-resident CXCR3$^+$CXCR6$^+$ γδT cells after *ex vivo* expansion may be a new therapeutic strategy for acute HBV infection.

Similar to mice, human livers also contain a liver-resident CD27^{lo}CD45RA^{lo} subset of Vδ1$^+$ γδT cells expressing high levels of CXCR3 and CXCR6. They produce significantly more of the pro-inflammatory cytokines, IFN-γ and TNF-α, and may be involved in responding to CMV infection (69). It is also worth noting that serum HBsAg, HBeAg, and HBV DNA levels are significantly lower in TCRδ$^{-/-}$ mice than WT mice (**Figure 6F**). This may be related to the heterogeneity of γδT cells. γδT cells are a heterogeneous population and consist of different subsets including IFN-γ-producing γδ T cells, IL-17-producing γδ T cells, γδ NKT cells, and so on (57, 70). The TCRδ$^{-/-}$ mice were systemic TCRδ gene deletion, and all γδT-cell subsets are deficient. Other γδT-cell subsets in liver may have different, even opposite, effects during acute HBV infection. The roles of other subsets of γδT cells in acute HBV infection deserved further research.

In summary, the current study was the first to demonstrate that CXCR3$^+$CXCR6$^+$ γδT cells are a liver-resident γδT-cell subset with a unique phenotype and tissue-resident characteristics. LSECs mediated the retention of CXCR3$^+$CXCR6$^+$ γδT cells through the interaction between the chemokine receptor, CXCR3, and its ligands, CXCL9 and CXCL11, as well as CXCR6 and its ligand, CXCL16. Liver-resident CXCR3$^+$CXCR6$^+$ γδT cells were protective against acute HBV infection. While additional research is required to better define the exact mechanism by which CXCR3$^+$CXCR6$^+$ γδT cells exert their protective role, findings from the current study provide more insight into liver-resident lymphocytes and provide novel strategies for the treatment of diverse liver diseases.

DATA AVAILABILITY STATEMENT

The raw data supporting the conclusions of this article will be made available by the authors, without undue reservation.

ETHICS STATEMENT

The animal study was reviewed and approved by the Committee on the Ethics of Animal Experiments of Shandong University.

AUTHOR CONTRIBUTIONS

YW performed the experiments, analyzed the data, and wrote the manuscript. YG performed and designed the experiments and analyzed the data. YH and YL performed the experiments and analyzed the data. NL provided guidance for the experiment design and contributed to analyzing and discussing the data. CZ directed the research program, provided guidance and suggestions for the experimental design, analyzed the data, and wrote the manuscript. All authors contributed to the article and approved the submitted version.

FUNDING

This work was supported by grants from the National Natural Science Foundation of China (91842305, 81771686), the Shandong Provincial Natural Science Foundation (ZR2020MH260), and the Shandong Provincial Key Research and Development Program (Major Scientific and Technological Innovation Project) (2019JZZY021013).

ACKNOWLEDGMENTS

We thank Translational Medicine Core Facility of Advanced Medical Research Institute, Shandong University for consultation and instrument availability that supported this work.

SUPPLEMENTARY MATERIAL

The Supplementary Material for this article can be found online at: https://www.frontiersin.org/articles/10.3389/fimmu.2021.757379/full#supplementary-material

REFERENCES

1. Kubes P, Jenne C. Immune Responses in the Liver. *Annu Rev Immunol* (2018) 36:247–77. doi: 10.1146/annurev-immunol-051116-052415
2. Gao B, Jeong WI, Tian Z. Liver: An Organ With Predominant Innate Immunity. *Hepatology* (2008) 47(2):729–36. doi: 10.1002/hep.22034
3. Feng D, Gao B. From Basic Liver Immunology to Therapeutic Opportunities for Liver Diseases. *Cell Mol Immunol* (2021) 18(1):1–3. doi: 10.1038/s41423-020-00607-2
4. Chen Y, Tian Z. Innate Lymphocytes: Pathogenesis and Therapeutic Targets of Liver Diseases and Cancer. *Cell Mol Immunol* (2021) 18(1):57–72. doi: 10.1038/s41423-020-00561-z
5. Ruf B, Heinrich B, Greten TF. Immunobiology and Immunotherapy of HCC: Spotlight on Innate and Innate-Like Immune Cells. *Cell Mol Immunol* (2021) 18(1):112–27. doi: 10.1038/s41423-020-00572-w
6. Fan X, Rudensky AY. Hallmarks of Tissue-Resident Lymphocytes. *Cell* (2016) 164(6):1198–211. doi: 10.1016/j.cell.2016.02.048
7. Brownlie D, Scharenberg M, Mold JE, Hard J, Kekalainen E, Buggert M, et al. Expansions of Adaptive-Like NK Cells With a Tissue-Resident Phenotype in Human Lung and Blood. *Proc Natl Acad Sci U S A* (2021) 118(11): e2016580118. doi: 10.1073/pnas.2016580118
8. Sun H, Sun C, Xiao W, Sun R. Tissue-Resident Lymphocytes: From Adaptive to Innate Immunity. *Cell Mol Immunol* (2019) 16(3):205–15. doi: 10.1038/s41423-018-0192-y
9. Wu B, Zhang G, Guo Z, Wang G, Xu X, Li JL, et al. The SKI Proto-Oncogene Restrains the Resident CD103(+)CD8(+) T Cell Response in Viral Clearance. *Cell Mol Immunol* (2021) 18(10):2410–21. doi: 10.1038/s41423-020-0495-7
10. Wang Y, Zhang C. The Roles of Liver-Resident Lymphocytes in Liver Diseases. *Front Immunol* (2019) 10:1582. doi: 10.3389/fimmu.2019.01582
11. Sung CC, Horng JH, Siao SH, Chyuan IT, Tsai HF, Chen PJ, et al. Asialo GM1-Positive Liver-Resident CD8 T Cells That Express CD44 and LFA-1 are Essential for Immune Clearance of Hepatitis B Virus. *Cell Mol Immunol* (2021) 18(7):1772–82. doi: 10.1038/s41423-020-0376-0
12. Peng H, Jiang X, Chen Y, Sojka DK, Wei H, Gao X, et al. Liver-Resident NK Cells Confer Adaptive Immunity in Skin-Contact Inflammation. *J Clin Invest* (2013) 123(4):1444–56. doi: 10.1172/JCI66381
13. Fernandez-Ruiz D, Ng WY, Holz LE, Ma JZ, Zaid A, Wong YC, et al. Liver-Resident Memory CD8(+) T Cells Form a Front-Line Defense Against Malaria Liver-Stage Infection. *Immunity* (2016) 45(4):889–902. doi: 10.1016/j.immuni.2016.08.011
14. Swadling L, Pallett LJ, Maini MK. Liver-Resident CD8+ T Cells: Learning Lessons From the Local Experts. *J Hepatol* (2020) 72(6):1049–51. doi: 10.1016/j.jhep.2020.02.001
15. Peng H, Tian Z. Tissue-Resident Natural Killer Cells in the Livers. *Sci China Life Sci* (2016) 59(12):1218–23. doi: 10.1007/s11427-016-0334-2
16. Hayday AC. Gammadelta T Cell Update: Adaptate Orchestrators of Immune Surveillance. *J Immunol* (2019) 203(2):311–20. doi: 10.4049/jimmunol.1800934
17. Chien YH, Meyer C, Bonneville M. Gammadelta T Cells: First Line of Defense and Beyond. *Annu Rev Immunol* (2014) 32:121–55. doi: 10.1146/annurev-immunol-032713-120216
18. Chang L, Wang L, Ling N, Peng H, Chen M. Increase in Liver Gammadelta T Cells With Concurrent Augmentation of IFN-Beta Production During the Early Stages of a Mouse Model of Acute Experimental Hepatitis B Virus Infection. *Exp Ther Med* (2020) 19(1):67–78. doi: 10.3892/etm.2019.8197
19. Cheng M, Hu S. Lung-Resident Gammadelta T Cells and Their Roles in Lung Diseases. *Immunology* (2017) 151(4):375–84. doi: 10.1111/imm.12764
20. Woodward Davis AS, Bergsbaken T, Delaney MA, Bevan MJ. Dermal-Resident Versus Recruited Gammadelta T Cell Response to Cutaneous Vaccinia Virus Infection. *J Immunol* (2015) 194(5):2260–7. doi: 10.4049/jimmunol.1402438
21. Romagnoli PA, Sheridan BS, Pham QM, Lefrancois L, Khanna KM. IL-17A-Producing Resident Memory Gammadelta T Cells Orchestrate the Innate Immune Response to Secondary Oral Listeria Monocytogenes Infection. *Proc Natl Acad Sci U S A* (2016) 113(30):8502–7. doi: 10.1073/pnas.1600713113
22. Nielsen MM, Witherden DA, Havran WL. Gammadelta T Cells in Homeostasis and Host Defence of Epithelial Barrier Tissues. *Nat Rev Immunol* (2017) 17(12):733–45. doi: 10.1038/nri.2017.101
23. Li F, Hao X, Chen Y, Bai L, Gao X, Lian Z, et al. The Microbiota Maintain Homeostasis of Liver-Resident gammadeltaT-17 Cells in a Lipid Antigen/CD1d-Dependent Manner. *Nat Commun* (2017) 7:13839. doi: 10.1038/ncomms13839
24. Zheng M, Sun R, Wei H, Tian Z. NK Cells Help Induce Anti-Hepatitis B Virus CD8+ T Cell Immunity in Mice. *J Immunol* (2016) 196(10):4122–31. doi: 10.4049/jimmunol.1500846
25. Kamran P, Sereti KI, Zhao P, Ali SR, Weissman IL, Ardehali R. Parabiosis in Mice: A Detailed Protocol. *J Vis Exp* (2013) (80):50556. doi: 10.3791/50556
26. Li Z, Zhang C, Zhou Z, Zhang J, Zhang J, Tian Z. Small Intestinal Intraepithelial Lymphocytes Expressing CD8 and T Cell Receptor Gammadelta are Involved in Bacterial Clearance During Salmonella Enterica Serovar Typhimurium Infection. *Infect Immun* (2012) 80(2):565–74. doi: 10.1128/IAI.05078-11
27. Li Y, Liu M, Zuo Z, Liu J, Yu X, Guan Y, et al. TLR9 Regulates the NF-kappaB-NLRP3-IL-1beta Pathway Negatively in Salmonella-Induced NKG2D-Mediated Intestinal Inflammation. *J Immunol* (2017) 199(2):761–73. doi: 10.4049/jimmunol.1601416
28. Losurdo G, Piscitelli D, Ierardi E, Di Leo A. Intraepithelial Lymphocytes: Bystanders or Causative Factors in Functional Gastrointestinal Disorders? *Cell Mol Immunol* (2021) 18(7):1620–1. doi: 10.1038/s41423-020-00614-3
29. Kabelitz D, Serrano R, Kouakanou L, Peters C, Kalyan S. Cancer Immunotherapy With Gammadelta T Cells: Many Paths Ahead of Us. *Cell Mol Immunol* (2020) 17(9):925–39. doi: 10.1038/s41423-020-0504-x
30. Ribot JC, deBarros A, Pang DJ, Neves JF, Peperzak V, Roberts SJ, et al. CD27 is a Thymic Determinant of the Balance Between Interferon-Gamma- and Interleukin 17-Producing Gammadelta T Cell Subsets. *Nat Immunol* (2009) 10(4):427–36. doi: 10.1038/ni.1717
31. Shibata K, Yamada H, Nakamura R, Sun X, Itsumi M, Yoshikai Y. Identification of CD25+ Gamma Delta T Cells as Fetal Thymus-Derived Naturally Occurring IL-17 Producers. *J Immunol* (2008) 181(9):5940–7. doi: 10.4049/jimmunol.181.9.5940
32. Tramonti D, Rhodes K, Martin N, Dalton JE, Andrew E, Carding SR. gammadeltaT Cell-Mediated Regulation of Chemokine Producing Macrophages During Listeria Monocytogenes Infection-Induced Inflammation. *J Pathol* (2008) 216(2):262–70. doi: 10.1002/path.2412
33. Li H, Xiang Z, Feng T, Li J, Liu Y, Fan Y, et al. Human Vgamma9Vdelta2-T Cells Efficiently Kill Influenza Virus-Infected Lung Alveolar Epithelial Cells. *Cell Mol Immunol* (2013) 10(2):159–64. doi: 10.1038/cmi.2012.70
34. Mackay LK, Kallies A. Transcriptional Regulation of Tissue-Resident Lymphocytes. *Trends Immunol* (2017) 38(2):94–103. doi: 10.1016/j.it.2016.11.004
35. Thomas SY, Scanlon ST, Griewank KG, Constantinides MG, Savage AK, Barr KA, et al. PLZF Induces an Intravascular Surveillance Program Mediated by Long-Lived LFA-1-ICAM-1 Interactions. *J Exp Med* (2011) 208(6):1179–88. doi: 10.1084/jem.20102630
36. Carding SR, Egan PJ. Gammadelta T Cells: Functional Plasticity and Heterogeneity. *Nat Rev Immunol* (2002) 2(5):336–45. doi: 10.1038/nri797
37. Nonaka S, Naito T, Chen H, Yamamoto M, Moro K, Kiyono H, et al. Intestinal Gamma Delta T Cells Develop in Mice Lacking Thymus, All Lymph Nodes, Peyer's Patches, and Isolated Lymphoid Follicles. *J Immunol* (2005) 174(4):1906–12. doi: 10.4049/jimmunol.174.4.1906
38. Shetty S, Lalor PF, Adams DH. Liver Sinusoidal Endothelial Cells - Gatekeepers of Hepatic Immunity. *Nat Rev Gastroenterol Hepatol* (2018) 15(9):555–67. doi: 10.1038/s41575-018-0020-y
39. Xie X, Luo J, Broering R, Zhu D, Zhou W, Lu M, et al. HBeAg Induces Liver Sinusoidal Endothelial Cell Activation to Promote Intrahepatic CD8 T Cell Immunity and HBV Clearance. *Cell Mol Immunol* (2021) 18(11):2572–4. doi: 10.1038/s41423-021-00769-7
40. Dudek M, Pfister D, Donakonda S, Filpe P, Schneider A, Laschinger M, et al. Auto-Aggressive CXCR6(+) CD8 T Cells Cause Liver Immune Pathology in NASH. *Nature* (2021) 592(7854):444–9. doi: 10.1038/s41586-021-03233-8
41. Holz LE, Chua YC, de Menezes MN, Anderson RJ, Draper SL, Compton BJ, et al. Glycolipid-Peptide Vaccination Induces Liver-Resident Memory CD8(+) T Cells That Protect Against Rodent Malaria. *Sci Immunol* (2020) 5(48): eaaz8035. doi: 10.1126/sciimmunol.aaz8035
42. Harmon C, Jameson G, Almuaili D, Houlihan DD, Hoti E, Geoghegan J, et al. Liver-Derived TGF-Beta Maintains the Eomes(hi)Tbet(lo) Phenotype of Liver

Resident Natural Killer Cells. *Front Immunol* (2019) 10:1502. doi: 10.3389/fimmu.2019.01502
43. Marra F, Tacke F. Roles for Chemokines in Liver Disease. *Gastroenterology* (2014) 147(3):577–94 e1. doi: 10.1053/j.gastro.2014.06.043
44. Yano T, Ohira M, Nakano R, Tanaka Y, Ohdan H. Hepatectomy Leads to Loss of TRAIL-Expressing Liver NK Cells *via* Downregulation of the CXCL9-CXCR3 Axis in Mice. *PloS One* (2017) 12(10):e0186997. doi: 10.1371/journal.pone.0186997
45. Geissmann F, Cameron TO, Sidobre S, Manlongat N, Kronenberg M, Briskin MJ, et al. Intravascular Immune Surveillance by CXCR6+ NKT Cells Patrolling Liver Sinusoids. *PloS Biol* (2005) 3(4):e113. doi: 10.1371/journal.pbio.0030113
46. Zhao J, Zhang S, Liu Y, He X, Qu M, Xu G, et al. Single-Cell RNA Sequencing Reveals the Heterogeneity of Liver-Resident Immune Cells in Human. *Cell Discovery* (2020) 6(1):22. doi: 10.1038/s41421-020-0157-z
47. Hudspeth K, Donadon M, Cimino M, Pontarini E, Tentorio P, Preti M, et al. Human Liver-Resident CD56(bright)/CD16(neg) NK Cells are Retained Within Hepatic Sinusoids *via* the Engagement of CCR5 and CXCR6 Pathways. *J Autoimmun* (2016) 66:40–50. doi: 10.1016/j.jaut.2015.08.011
48. Hess LU, Martrus G, Ziegler AE, Langeneckert AE, Salzberger W, Goebels H, et al. The Transcription Factor Promyelocytic Leukemia Zinc Finger Protein Is Associated With Expression of Liver-Homing Receptors on Human Blood CD56(bright) Natural Killer Cells. *Hepatol Commun* (2020) 4(3):409–24. doi: 10.1002/hep4.1463
49. Laky K, Lefrancois L, Lingenheld EG, Ishikawa H, Lewis JM, Olson S, et al. Enterocyte Expression of Interleukin 7 Induces Development of Gammadelta T Cells and Peyer's Patches. *J Exp Med* (2000) 191(9):1569–80. doi: 10.1084/jem.191.9.1569
50. Oida T, Suzuki K, Nanno M, Kanamori Y, Saito H, Kubota E, et al. Role of Gut Cryptopatches in Early Extrathymic Maturation of Intestinal Intraepithelial T Cells. *J Immunol* (2000) 164(7):3616–26. doi: 10.4049/jimmunol.164.7.3616
51. Kotton DN, Fabian AJ, Mulligan RC. A Novel Stem-Cell Population in Adult Liver With Potent Hematopoietic-Reconstitution Activity. *Blood* (2005) 106 (5):1574–80. doi: 10.1182/blood-2005-03-1017
52. Crane GM, Jeffery E, Morrison SJ. Adult Haematopoietic Stem Cell Niches. *Nat Rev Immunol* (2017) 17(9):573–90. doi: 10.1038/nri.2017.53
53. Wang XQ, Lo CM, Chen L, Cheung CK, Yang ZF, Chen YX, et al. Hematopoietic Chimerism in Liver Transplantation Patients and Hematopoietic Stem/Progenitor Cells in Adult Human Liver. *Hepatology* (2012) 56(4):1557–66. doi: 10.1002/hep.25820
54. Meng D, Qin Y, Lu N, Fang K, Hu Y, Tian Z, et al. Kupffer Cells Promote the Differentiation of Adult Liver Hematopoietic Stem and Progenitor Cells Into Lymphocytes *via* ICAM-1 and LFA-1 Interaction. *Stem Cells Int* (2019) 2019:4848279. doi: 10.1155/2019/4848279
55. Qin Y, Fang K, Lu N, Hu Y, Tian Z, Zhang C. Interferon Gamma Inhibits the Differentiation of Mouse Adult Liver and Bone Marrow Hematopoietic Stem Cells by Inhibiting the Activation of Notch Signaling. *Stem Cell Res Ther* (2019) 10(1):210. doi: 10.1186/s13287-019-1311-0
56. Bai L, Vienne M, Tang L, Kerdiles Y, Etiennot M, Escaliere B, et al. Liver Type 1 Innate Lymphoid Cells Develop Locally *via* an Interferon-Gamma-Dependent Loop. *Science* (2021) 371(6536):eaba4177. doi: 10.1126/science.aba4177
57. Hu Y, Fang K, Wang Y, Lu N, Sun H, Zhang C. Single-Cell Analysis Reveals the Origins and Intrahepatic Development of Liver-Resident IFN-Gamma-Producing Gammadelta T Cells. *Cell Mol Immunol* (2021) 18(4):954–68. doi: 10.1038/s41423-021-00656-1
58. Khairallah C, Chu TH, Sheridan BS. Tissue Adaptations of Memory and Tissue-Resident Gamma Delta T Cells. *Front Immunol* (2018) 9:2636. doi: 10.3389/fimmu.2018.02636
59. Chang KM, Traum D, Park JJ, Ho S, Ojiro K, Wong DK, et al. Distinct Phenotype and Function of Circulating Vdelta1+ and Vdelta2+ gammadeltaT-Cells in Acute and Chronic Hepatitis B. *PloS Pathog* (2019) 15(4):e1007715. doi: 10.1371/journal.ppat.1007715
60. Sebestyen Z, Prinz I, Dechanet-Merville J, Silva-Santos B, Kuball J. Translating Gammadelta (Gammadelta) T Cells and Their Receptors Into Cancer Cell Therapies. *Nat Rev Drug Discovery* (2020) 19(3):169–84. doi: 10.1038/s41573-019-0038-z
61. Liu Y, Zhang C. The Role of Human Gammadelta T Cells in Anti-Tumor Immunity and Their Potential for Cancer Immunotherapy. *Cells* (2020) 9 (5):1206. doi: 10.3390/cells9051206
62. Duan Y, Li G, Xu M, Qi X, Deng M, Lin X, et al. CFTR is a Negative Regulator of Gammadelta T Cell IFN-Gamma Production and Antitumor Immunity. *Cell Mol Immunol* (2021) 18(8):1934–44. doi: 10.1038/s41423-020-0499-3
63. Lo Presti E, Pizzolato G, Gulotta E, Cocorullo G, Gulotta G, Dieli F, et al. Current Advances in Gammadelta T Cell-Based Tumor Immunotherapy. *Front Immunol* (2017) 8:1401. doi: 10.3389/fimmu.2017.01401
64. Wada I, Matsushita H, Noji S, Mori K, Yamashita H, Nomura S, et al. Intraperitoneal Injection of *In Vitro* Expanded Vgamma9Vdelta2 T Cells Together With Zoledronate for the Treatment of Malignant Ascites Due to Gastric Cancer. *Cancer Med* (2014) 3(2):362–75. doi: 10.1002/cam4.196
65. Xu Y, Xiang Z, Alnaggar M, Kouakanou L, Li J, He J, et al. Allogeneic Vgamma9Vdelta2 T-Cell Immunotherapy Exhibits Promising Clinical Safety and Prolongs the Survival of Patients With Late-Stage Lung or Liver Cancer. *Cell Mol Immunol* (2021) 18(2):427–39. doi: 10.1038/s41423-020-0515-7
66. Gehring AJ, Protzer U. Targeting Innate and Adaptive Immune Responses to Cure Chronic HBV Infection. *Gastroenterology* (2019) 156(2):325–37. doi: 10.1053/j.gastro.2018.10.032
67. Meng Z, Chen Y, Lu M. Advances in Targeting the Innate and Adaptive Immune Systems to Cure Chronic Hepatitis B Virus Infection. *Front Immunol* (2019) 10:3127. doi: 10.3389/fimmu.2019.03127
68. Zhang C, Hu Y, Xiao W, Tian Z. Chimeric Antigen Receptor- and Natural Killer Cell Receptor-Engineered Innate Killer Cells in Cancer Immunotherapy. *Cell Mol Immunol* (2021) 18(9):2083–100. doi: 10.1038/s41423-021-00732-6
69. Hunter S, Willcox CR, Davey MS, Kasatskaya SA, Jeffery HC, Chudakov DM, et al. Human Liver Infiltrating Gammadelta T Cells are Composed of Clonally Expanded Circulating and Tissue-Resident Populations. *J Hepatol* (2018) 69 (3):654–65. doi: 10.1016/j.jhep.2018.05.007
70. Paul S, Singh AK, Shilpi, Lal G. Phenotypic and Functional Plasticity of Gamma-Delta (Gammadelta) T Cells in Inflammation and Tolerance. *Int Rev Immunol* (2014) 33(6):537–58. doi: 10.3109/08830185.2013.863306

Conflict of Interest: The authors declare that the research was conducted in the absence of any commercial or financial relationships that could be construed as a potential conflict of interest.

Publisher's Note: All claims expressed in this article are solely those of the authors and do not necessarily represent those of their affiliated organizations, or those of the publisher, the editors and the reviewers. Any product that may be evaluated in this article, or claim that may be made by its manufacturer, is not guaranteed or endorsed by the publisher.

Advantages of publishing in Frontiers

OPEN ACCESS
Articles are free to read for greatest visibility and readership

FAST PUBLICATION
Around 90 days from submission to decision

HIGH QUALITY PEER-REVIEW
Rigorous, collaborative, and constructive peer-review

TRANSPARENT PEER-REVIEW
Editors and reviewers acknowledged by name on published articles

Frontiers
Avenue du Tribunal-Fédéral 34
1005 Lausanne | Switzerland

Visit us: www.frontiersin.org
Contact us: frontiersin.org/about/contact

REPRODUCIBILITY OF RESEARCH
Support open data and methods to enhance research reproducibility

DIGITAL PUBLISHING
Articles designed for optimal readership across devices

FOLLOW US
@frontiersin

IMPACT METRICS
Advanced article metrics track visibility across digital media

EXTENSIVE PROMOTION
Marketing and promotion of impactful research

LOOP RESEARCH NETWORK
Our network increases your article's readership